Relationships between sediment, moisture and soil crust characteristics in arid environments.

Kirk, Alastair James

Relationships between sediment, moisture and soil crust characteristics in arid environments

Alastair James Kirk

Doctor of Philosophy

University of Durahm

Department of Geography

1997

Relationships between sediment, moisture and soil crust characteristics in arid environments

Alastair Kirk

From a geomorphological point of view, arid environments are characterised by complex process interactions and suites of landforms which can be sensitive to their controlling parameters. Relationships between sediment, moisture and soil crust characteristics are no exception. Field research and a programme of laboratory study were undertaken between 1993 and 1995 on the soils of the northern Badia of Jordan to advance knowledge on aspects of arid zone soil dynamics, with a particular emphasis on crusting.

The research focuses primarily on the effect soil crusts have upon the equilibrium of sediment dynamics at a hillslope scale and a ridge-furrow scale. The implications of the crust upon moisture storage within the surface layers of the soil are examined and the spatial characteristics which arise due to management practices and climate variables considered. A new, non-destructive dielectric technique to investigate moisture content in dryland soils has been developed and tested.

Monitoring has taken place to examine the effects of irrigation upon the surface characteristics of the surrounding soil, with special reference to evaporation fluxes within a furrow and the associated precipitation of salts. The role of small-scale topography tends to be underestimated. Different types of crust have been studied from various topographic locations. Soil fabric and porosity have been studied, to increase understanding of micro-scale depositional and erosional processes. A new method of tracing fine material through the upper soil profile has been developed. As crusts form, the tracer can be used to monitor the movement of fines, permitting a much clearer understanding of soil and water dynamics as a result of rainfall events.

TABLE OF CONTENTS

LIST OF FIGURES

LIST OF TABLES

LIST OF PLATES

I confirm that no part of the material offered in this thesis has previously been submitted by me or any other person for a degree in this or any other university. In all cases, where it is relevant, material from the work of others has been acknowledged. Quotations and paraphrases are suitably indicated.

Signed: .....

Date: 14th November 1997

ACKNOWLEDGEMENTS

> *You care for the land and water it, you enrich it abundantly. The streams of God are filled with water to provide people with corn, for so you have ordained it. You drench its furrows and level its ridges; you soften it with showers and bless its crops. You crown the year with your bounty and your carts overflow with abundance. The grasslands of the desert overflow; the hills are clothed with gladness. The meadows are covered with flocks and the valleys are mantled with corn; they shout for joy and sing.*
> Psalm 65 vv.9-13

First of all, I must thank and praise the LORD my God, for guiding me through the last four years, for protecting me, especially at the time of my car crash in Jordan, and for his abundant grace and intimacy during my time in the desert. Our beautiful creation constantly reveals the hand of the LORD and that is no more clearly demonstrated by the intricate nature and processes which occur at the interface between soil, water and atmosphere. This thesis seeks to look into the storehouse of God's knowledge in order to gain His true wisdom.

Second, I must thank my parents and sister Louise, who have supported me with their overwhelming love, in both prayer and financial sacrifice, throughout the past four years. They have funded the majority of my doctoral studies and it is therefore my great joy to dedicate this work to them.

I thank my supervisors, Drs Bob Allison and Nick Cox. Bob has encouraged and driven me towards my goal. He has supported me financially and even given me supervisory sessions in the Philippines next to the South China Sea! He has become a friend, a mentor and has put up with my many idiosyncrasies which is a feat in itself. Nick has been instrumental in the production of the thesis with his fine eye for my many mistakes in earlier drafts. He has also encouraged me to use statistics in an inspirational fashion!

There are many people and organisations who have been very helpful during the course of my doctoral studies. I will endeavour to pick out those who have been most influential.

I cannot go any further before acknowledging the role of the Royal Geographical Society in London and the Higher Council for Science and Technology in Amman. Without the Badia Research and Development Programme there would have been no opportunity to study the fascinating landscape of the black basalt desert. They have provided financial support in the field as well as an infrastructure at Safawi which has been invaluable even if, at times, it seemed more of a hindrance than a help. In terms of personalities, I thank Dr Roderic Dutton, Dr Fataftah and Mr Shahbaz as the directors of the Programme, the Safawi team and the CORD personal assistants, Patrick Miller and Rodney Stobbs. Working in the desert alone was a lonely existence, but my heartfelt thanks goes to Darius Campbell, Alan Roe and Karen Jones for lending support in the field and giving me the necessary encouragement to carry on. Karen especially needs a gold medal for the many mornings she got up at 5 to go out to the field to help me with the rainfall simulation experiments. Thanks also must go to the farmers with whom I worked. They were most welcoming and I hope that some of the work presented here might become useful in making irrigated agriculture more sustainable in their environment.

Gratitude must be shown to the Institute of Hydrology for generously providing the Automatic Weather station and the Surface Capacitance Probe. These two items have been instrumental in the direction of the research and I hope that the SCIP data will be especially useful for further use in arid soils. Special thanks must go to David Cooper and David Robinson.

Various people from different academic departments have given advice and helped with technical aspects of laboratory work. .Dr Abu-Sharar from the University of Jordan is one of the best Arab soil scientists and I am grateful to him for his help and hospitality while in Jordan. Mervyn Jones and his assistant Anne, who co-ordinate the micromorphology preparation at the Faculty of Agriculture at the University of Newcastle, have spent many hours helping me. Mervyn is the only man I know who

asks for payment in Crystic resin! My thanks also goes to Dr Nicholas Pepin in Portsmouth for putting me on the right track with my climate data. Alex Koh from Bath should be commended for his hours of help trying to improve the method of using digital photography on my thin sections.

Communication is one of the most important aspects of research and I have valued discussions with research staff in Durham, especially Dr David Higgitt and Dr Eric Brouwer and fellow postgraduates, Edward Twiddy, Neil Coe, Christoph Puhr, Helen Dunsford and Owen Kimber.

Thanks must go to the staff at St John's College. David Day, Margaret Masson and Gillian Boughton have all lent their heartfelt support reinforcing the fact that St John's is a loving community, which is rare to find these days.

Finally, and with great fondness, I would like to thank the technicians for all their hard work, patience and encouragement. The laboratories would not be the same without Derek Coates, Brian Priestley and Frank Davies who put up with my mess and often disorganised work schedule. Thanks also to Ron Hardy in geology for his help and encouragement with regard to all the X-ray work. A big thank-you must go to Michele Johnson who has helped me with all the thin-section photography and has often developed photographs at short notice.

Dedicated to my dear Mum, Dad and Sister

1. INTRODUCTION

The degradation and irreversible destruction of soil have reached alarming proportions. Every year worldwide 5-7 million ha of agricultural land are lost, and the productivity of even more land is steadily decreasing. A quarter of agricultural land is badly damaged, i.e. its productivity is significantly impaired. (Steiner, 1996, p. vi)

1.1 RESEARCH AIMS

This study arises from the need to gain a better understanding of the processes of soil degradation in arid environments. The underlying motive for such work lies in the fact that the soil and water of the northern Badia are not being used in a sustainable manner, because the bedouin are generally unaware of the need to conserve them. From a scientific point of view arid environments are poorly understood and the processes involved in soil crusting are no exception.

The research framework needed to undertake such work inevitably embraces methodologies and expertise from both the geomorphological and the soil science communities. The former brings a truly spatial and topographical element to the study and the latter provides many of the techniques and methods of classification.

Within this multidisciplinary approach, a number of primary research aims were recognised:

1. To sample soil crusts in order to monitor their effect upon the equilibrium of sediment dynamics at a hillslope and ridge-furrow scale.

2. To observe the effect that the crust has upon moisture storage within the surface layers of the soil and to explain the spatial characteristics which arise due to management practices and climatic variables.

3. To monitor the effectiveness of a new, non-destructive, dielectric technique to examine moisture content in dryland soils.

4. To examine the effect of irrigation upon the surface characteristics of the surrounding soil, with special reference to the evaporation fluxes within the furrow and the associated precipitation of salts.

5. To investigate the role of small-scale topography upon the type of crust which forms in terms of both fabric and porosity.

6. To develop a new method of tracing fine material through the upper soil profile during crust formation using rainfall simulation and use it to monitor the movement of fines during crust formation and development.

1.2 THE NORTHERN BADIA

For the purpose of this research, the term *northern Badia* will be used to define an area on the southern and western slopes of the Jebal Hâuran. The Jebal Hâuran is distinct, from a climatic perspective, from areas further south and east towards Azraq and Safawi respectively.

A large number of farms, supported by irrigation water from a basalt aquifer, have become established between Mafraq and Umm el Quttayyn over the last twenty years. As the search for new agricultural land has continued in the 1990s, land to the east of Umm el Quttayyn has been brought into production. As the bedouin extend the eastern boundary of irrigated agriculture, opportunities to monitor the effect of the irrigation techniques upon the soil have arisen. The field sites have, therefore, been primarily chosen to represent the present eastern boundary of irrigation.

The area has attracted geological attention, notably from Huntings Technical Services (1965); van den Boom & Suwwan (1966); Bender (1968); Barberi *et al.* (1979); Abed *et al.* (1985); Dwairi (1987); Guba & Mustafa (1988); Moffat (1988); Andrews (1992) and Ibrahim (1993a,1993b). However, until the formation of the

Badia Research and Development Programme at the end of 1992, there had been little work pertaining to the geomorphology or soils of the area. The Programme, a joint venture between the Royal Geographical Society, London and the Higher Council for Science and Technology, Amman, was primarily set up to examine how sustainable development could take place within the fragile Badia environment. The work presented here represents the first major in depth research carried out on the soils of the northern Badia.

1.3 Related research on soil crusts from other arid environments

Although there has been much work on soil crusts over the past fifty years, much of it has been laboratory-based. Field-based research has generally concentrated upon arid sandy soils (Valentin, 1986; Bresson & Valentin, 1990; Valentin, 1991; Bielders *et al.*, 1996) or temperate fine-grained soils (Mücher & De Ploey, 1977; Mücher *et al.*, 1981; Poesen & Govers, 1986; Mermut *et al.*, 1995; Mermut *et al.*,1997). The Badia soils, therefore, represent a good opportunity to study arid fine-grained soils.

Much of the literature is dominated by soil scientists and so the topographic component is largely ignored: yet it is of vital importance to the understanding of spatial differences in crust morphology (Bielders *et al.*, 1996). There are obvious benefits in combining the two approaches to aid understanding of the surface processes and their effect on soil structure.

1.4 The organisation of the thesis

The following is a summary of the thesis layout. The first half of the thesis, from chapter 2 to chapter 5, researches the underpinning assumptions, theories and methods which are used for data collection and analysis and provide a necessary foundation to the data presented and discussed in chapters 6 to 8.

Chapter 2 provides the reader with an essential understanding of the characteristics of the northern Badia environment. It is an area unknown to many, and therefore it is

appropriate to outline the geological formations, the hydrogeology and the climate as well as to summarise some of the past and present human impact on the landscape. Chapter 3 reviews the principal research which has been carried out on soil crust formation, concentrating upon the physical and chemical processes which contribute to their development, before looking at the way in which water moves through the crust, by both infiltration and evaporation. Areas of further soil crust research are highlighted to show how this thesis fits into the broader patterns and questions of the discipline. This is followed in chapter 4 by an examination of the techniques used to determine the material properties of the crusts collected in Jordan. The chapter outlines the significance of well-designed spatial sampling and discusses methods which have had to be adapted for the specific problems inherent in the Jordan samples. Chapter 5 introduces an integrated set of climate data from different spatial and temporal scales to show the importance of contemporary data as a foundation to rainfall modelling. Methodological considerations are presented for the setting up of rainfall simulation studies.

Chapter 6 examines the use of a capacitance probe in measuring the moisture content of the surface soil layers. This is a new technique, not previously used in an arid environment, which requires calibration for the specific soil type. Data are provided which link wind direction, rainfall and the extent of crust formation with the final moisture content of the soil. The physical and chemical properties of the soil are drawn together in chapter 7, in order to look at local redistribution of sediment within the ridge-furrow sequence. The effect of irrigation upon secondary development or destruction of crust structure is then considered. The data presented in chapter 7, which predominantly concerns soil material properties, are reinterpreted in chapter 8 using micromorphology to examine the effect of erosional and depositional processes on soil fabric. Rainfall simulation experiments and discussion on the movement of fines into the soil profile complete chapter 8. Finally, chapter 9 summarises the original contribution made by this research and explains how it integrates with the general trends of soil crust research, before recommending possible avenues for further research.

2. PHYSICAL AND ANTHROPOGENIC CHARACTERISTICS OF THE NORTHERN BADIA

"A little later we turned to the right, off the pilgrim road, and took a short cut across gradually rising ground to flat basalt ridges, buried in sand till only their topmost piles showed above the surface. It held moisture enough to be well grown over with hard wiry grass and shrubs up and down the slopes, on which a few sheep and goats were pasturing." (T.E. Lawrence, 1926 p.84)

2.1 INTRODUCTION

Many developing countries, especially those with a considerable environmental diversity, tend to concentrate economic development in regions which have a good propensity to give a positive rate of return. In many countries, however, population pressure has caused people to settle in more marginal areas. In the Hashemite Kingdom of Jordan, past economic concentration in the prosperous Jordan Valley and the Jordanian hills has led to over-population. There is now an increasing urgency to examine potential for development in the desert areas or Badia of eastern Jordan (Allison *et al.*, 1992). While arid lands can be resource-rich, this is not the case in eastern Jordan. The fact that the area suffers from a large water deficit compounds the human and ecological hardship. Betts (1992) suggests that the imbalance between east and west Jordan has always been the case: '*Throughout history, the resources of the environmentally rich Mediterranean zone have been plentiful and numerous, but limited choice and scarcity of resources has characterised the semi-arid and arid regions further* east' (p.111). Increasing anthropogenic activity in such a fragile environment gives rise to land degradation which is epitomised by the reduction of soil quality. The removal of the vegetation cover, associated with population pressure and more specifically over-grazing, is held to be the major cause of land degradation in Jordan (Farhan & Mikbel, 1986)

and in arid lands in general (Agnew & Anderson, 1992). The natural response of most human groups, such as the Bedouin of Jordan, to harsh and fragile environmental conditions is to diversify, to rely on a variety of different agricultural and economic livelihoods, so that if one fails there will always be another (Betts, 1992). It is in just such a precarious environment in northern Jordan that agricultural development is being encouraged, providing the context and indeed the necessity for research into the physical environment.

Jordan, along with its neighbours Syria, Lebanon and Israel, lies on the narrow strip of land, often called the Levant, which connects the two largest continents of Asia and Africa (Phillips, 1954). Jordan occupies the position of a transitional state, separating Israel to the west, with its predominantly Mediterranean climate, from the northern part of the Arabian desert to the east. Despite its small size, Jordan is diverse both culturally and physically, epitomising its transitional nature. The precipitation gradient is marked, changing from well over 500 mm a^{-1} in the northwest in the area surrounding Irbid, to under 50 mm a^{-1} in the southeast beyond Azraq, El-Jafr and Ma'an, a distance little more than 100 kilometres. The desert area or Badia includes the whole of the eastern part of Jordan, making up over 80% of the total land area (Al-Homoud *et al.*, 1995). The Badia is classed as a semi-arid to arid steppe environment and falls almost exclusively in the arid climate zone, with rainfall less than 100 mm a^{-1} in most areas (Figure 2.1).

The reason why the northern Badia, otherwise known as the Haurân, can be taken as a geographical entity, distinct from the rest of the Badia further south, is primarily its geology. The stratigraphy and structure, in particular, determine the individual surface and groundwater characteristics. Much of the northern Badia lies on a Tertiary basalt pavement, which gives rise to a very specific environment. The area is a complex collage of basalt flows which differ in age and have been extruded from volcanic cones lying along large fault and dyke sequences (Ibrahim, 1993a). Basalt boulders of differing size currently dominate the ground surface. The age, mineralogy and material properties of the basalts are the major factors influencing boulder size, drainage density, wadi morphology, slope form and slope angle (Allison & Higgitt, in press).

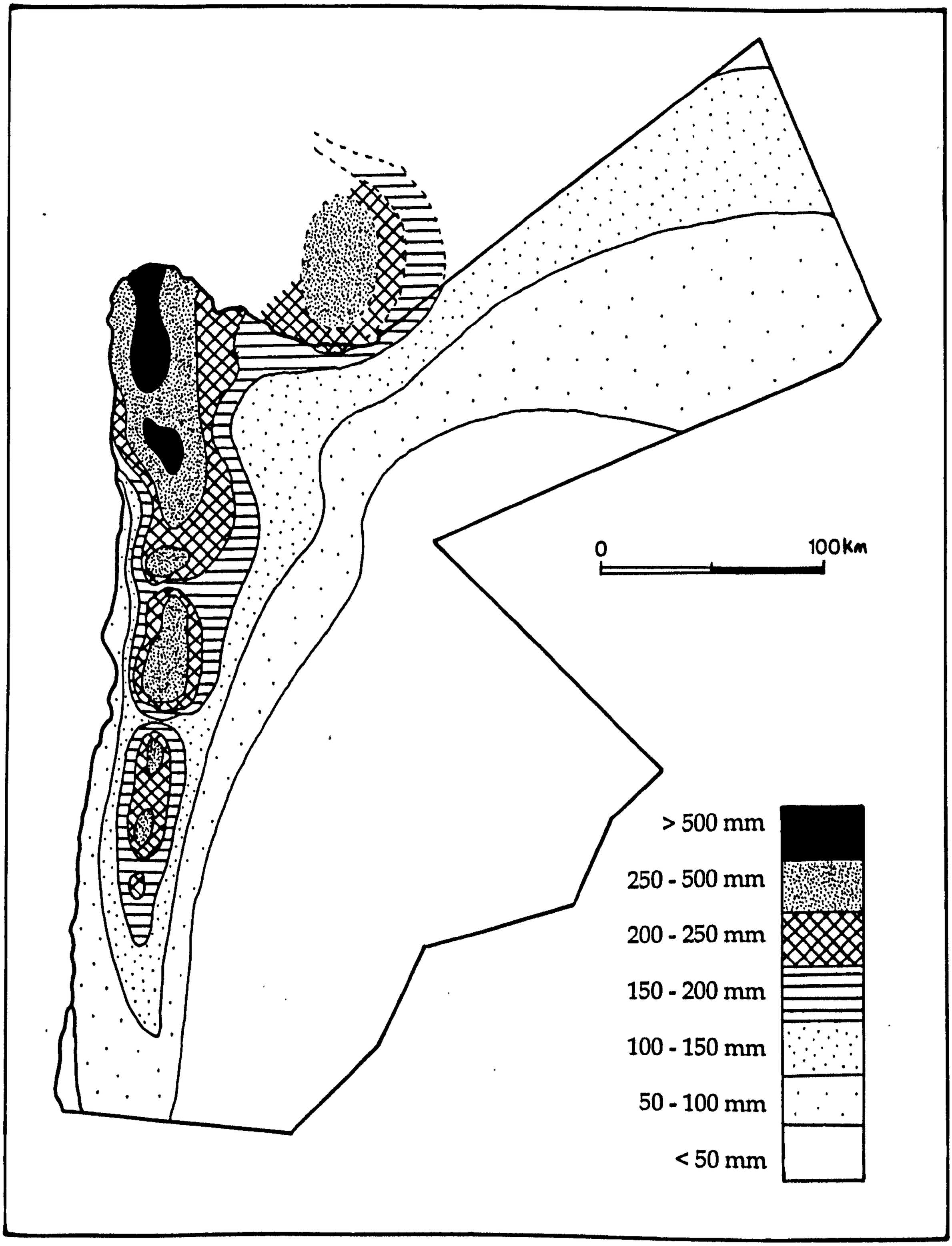

Figure 2.1: Mean annual rainfall distribution map of Jordan

Figure 2.2: The northern Badia and the Jebal Haurân

1400
1200
1000
SYRIA
UMM EL QUTTAIN
DEIR AL KAHF
AL RAFAI'AT
UMM HUSSEIN
ASH RAFIA
MENARA
Jabal al Asfar
AL BISIRIYYA
AS SAFAWI
Jabal al Aritayn
AL ARITAYN
Qa Be'gawier
800
600
Jabal al Mukeizin
AL AZRAQ
AZRAQ SHISHAN
Qa Azraq
Wadi Rajil
0 5 10 15
Km

The northern Badia has an altitudinal variation of approximately 1 000 metres. The central sections of the Jebal Haurân reach over 1 400 metres in southern Syria, while the Azraq basin and Sirhan depression to the southwest of Azraq on the border with Saudi Arabia are just over 400 metres (Figure 2.2). The ground surface is one of undulating topography where small wadis have slowly cut down 25 to 30 metres through the basalt flows (Al-Homoud *et al.*, 1995). Only in the most well developed wadis does there seem to be any evidence of incision. The relative relief is very low. Gradients above 2% are rare except in the vicinity of volcanic cones and dykes.

2.2 THE GEOLOGICAL SETTING OF THE NORTHERN BADIA

The geology of the northern Badia is the key to interpreting much of the geomorphology, hydrogeology and pedology. The basalts of the Ash Shamah plateau, an area which extends from the north Jordan Valley through southern Syria, the north eastern part of Jordan and a small section of north western Saudi Arabia (Figure 2.3), have dominated landscape evolution since the mid-Pleistocene. Because of the importance of the plateau formation within the geological history of the whole of Jordan, it is essential to understand the structural geology of the wider region.

2.2.1 The geological history of Jordan

On a continental scale, many of the sedimentary geological sequences originate from the narrowing and eventual closure of the Tethys Sea to the north. The northward progression of the Arabian plate with respect to the African plate caused crustal downwarping, attenuation and considerable faulting. In terms of vulcanicity, the two main fissure systems, which trend east-west and northwest-southeast, refer to the main periods of activity during the early Miocene and Pliocene-Holocene respectively. The palaeomagnetic data suggest that there has been a two-stage movement of the Arabian plate causing the two distinct periods of vulcanicity along the Dead Sea Rift and, more importantly, in the northern Badia (Barberi, 1979).

There was little terrestrial sedimentation until the Late Jurassic when the eolian Kurnub Sandstone was laid down over the whole of what is now Jordan. Shaw (1947) was the first to identify these Nubian-type, poorly consolidated sandstones in the exposures in Wadi Hathira (Kurnub). Their existence in the eastern part of Jordan was later corroborated by Quennell (1951). A gradual marine transgression during the Cretaceous resulted in the laying down of various bedded limestone facies interbedded with marls, called the Ajlun series. The Ajlun is thickest in the north and west, gradually thinning to the south and east. The Belqa series overlies the Ajlun series and is made up predominantly of marls and chalks. The Belqa series was continuously sedimented throughout the Upper Cretaceous, Palaeocene, Eocene and into the Oligocene, when there was terrestrial emergence (Burdon, 1959). The continuation of sedimentation between the Mesozoic and Cainozoic is largely unknown in Europe but in Jordan there is no sedimentation break within the chalk-marl facies. The transition can only be identified by the micropalaeontological record.

A combination of the closure of the Tethys Sea, more specifically the Bitlis Ocean, and the relative movement of the Arabian Peninsula during the Late Cretaceous, caused the opening of the Red Sea forming the present Jordan-Arava graben. The large-scale rifting and the associated sinistral strike-slip faulting which developed along the eastern edge of the Jordan Valley rift are the most important developments in the formation of the present Jordanian landscape. The Oligocene saw the uplifting and tilting to the east of the marine sediments, to produce a peneplained surface which originated on the edge of the newly formed rift valley and dipped into Arabia in the east. As the land emerged from its final transgressive phase, there was rejuvenation of the drainage feeding the Jordan Valley. Each successive opening and downward movement of the Jordan Rift Valley has lowered the base-level and captured drainage patterns which would have originally flowed parallel to dip, east towards Wadi Sirhan.

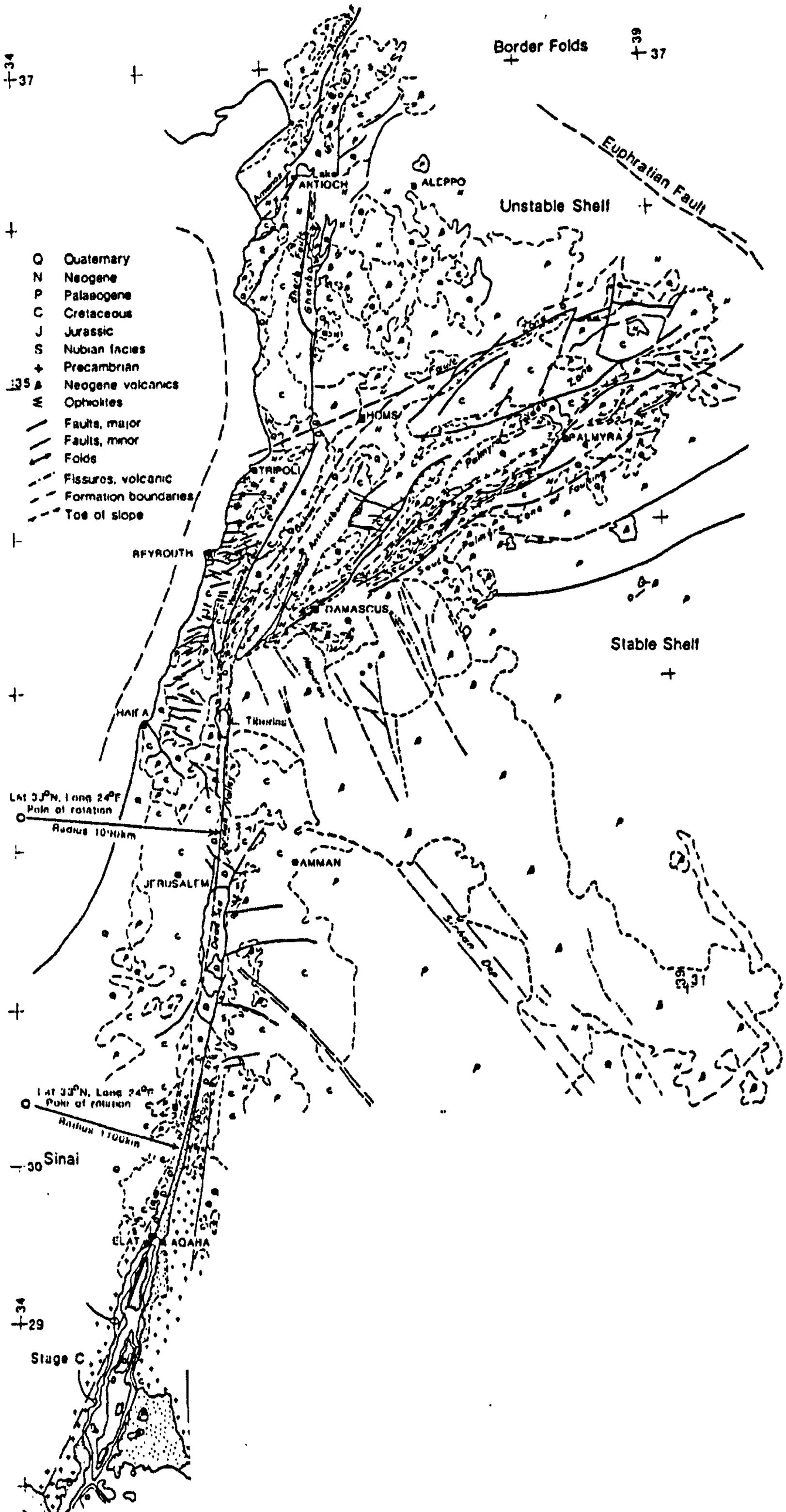

Figure 2.3: The structural geology of the Western Arabia rift system

(Quennell, 1984, p. 777)

Quennell's 1956 reconstruction has shown seven low-level surfaces, which suggests that it was the repeated lowering of the valley rather than the uplifting and tilting of the block that has been instrumental in encouraging drainage rejuvenation. The Wadi Mujeb and Wadi Hasa, which descend into the deepest part of the rift valley, have cut through over 1 750 metres of strata. The other important aspect of the rifting has been the considerable faulting, which has occurred across the whole of Jordan as a result of the down-throw of the rift valley. Faulting has encouraged the location of drainage networks in the west and provided weak points for volcanic activity in the east and north. The watershed divides the drainage into the rift valley to the west and an inland into the string of topographic depressions including the Azraq depression to the north, Wadi Sirhan and the El-Jafr depression to the south (Beheiry, 1969). The marine Belqa sequences have been eroded, mainly by eolian processes, leaving flint on the ground surface. The occasional inselbergs, such as those at Qatafi, are made up of harder limestone, chalk or flint inliers.

2.2.2 The evolution of the Ash Shamah basalts

The term Ash Shamah basalts originating from the nomenclature of Barberi *et al.* (1979) and Quennell (1984) was adopted by Ibrahim (1993a) to refer to the exposed group of basalts of northern Jordan and termed the Harrat Ash Shaam Basaltic Super-Group (Table 2.1). The Miocene and Pliocene saw limited sediment deposition except for lacustrine deposition in the Rift Valley. However, from as early as 13.7 ± 0.7 Ma, until less than 0.5 Ma, there were major extrusive flows of basalt throughout southern Syria and northern Jordan (Moffat, 1988). The flows covered an area of approximately 45 000 km^2 of which a quarter is in present Jordanian territory (Bender, 1975). The western boundary of the plateau is on the rift itself in the Golan, which stretches eastwards around the southern edge of the Damascus Basin. However, the majority of volcanism occurred well within the Arabian Plate (Barberi *et al.*, 1979). Alkali olivine basalts (Ibrahim, 1993a) originated along fissures and were laid down in thin horizontal beds. The beds were later covered by more viscous mountain building flows which built up the Jebal Haurân, emanating from fissures with a south-southeast to north-northwest strike (340°), an angle almost normal to the south Palmyra zone of faulting (Quennell, 1984, Figure 2.3).

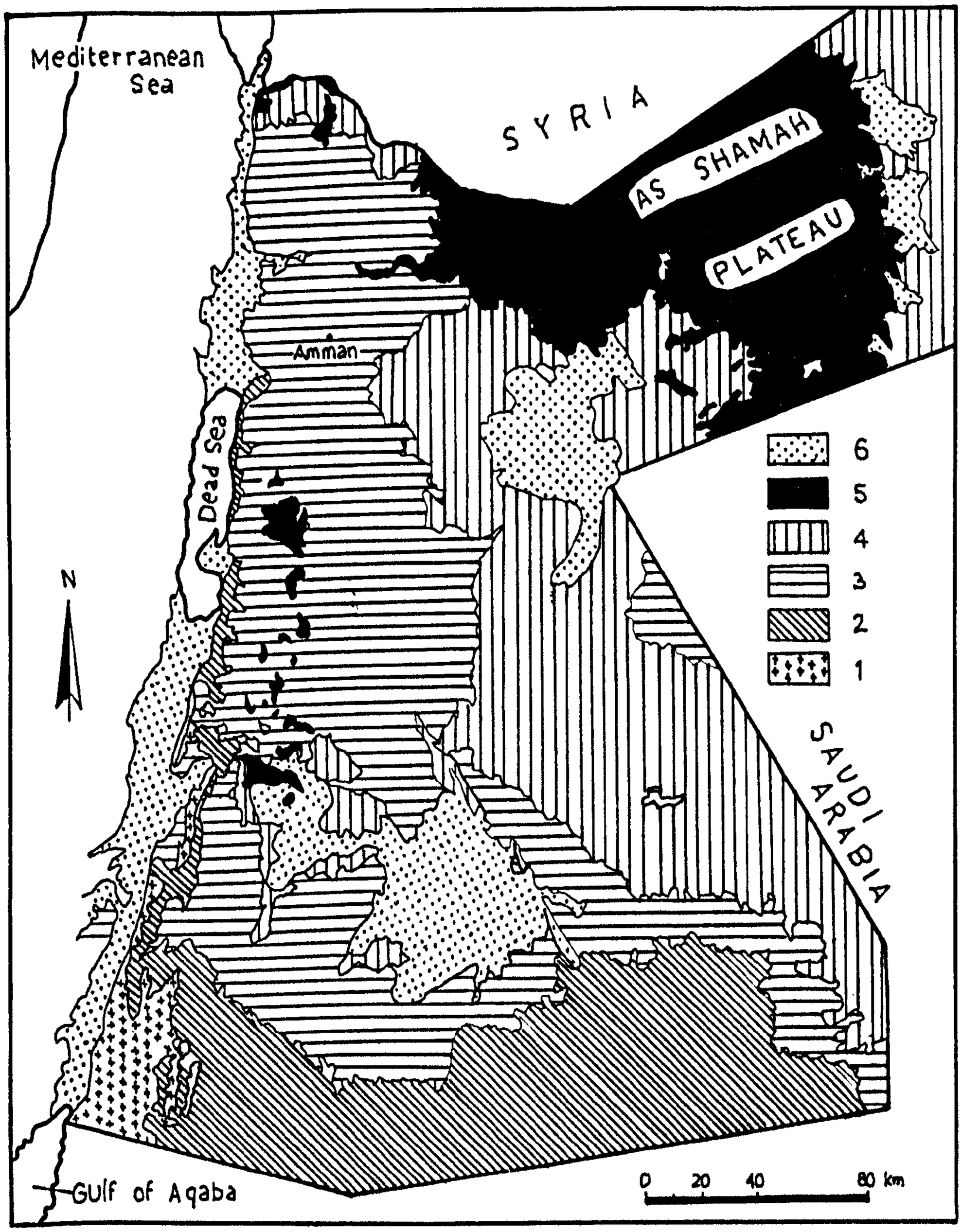

Figure 2.4: A simplified geology of Jordan. Source: Barberi *et al.* (1979)

Key: 1 = Precambrian Basement; 2 = Palaeozoic to Triassic sediments; 3 = Jurassic and Cretaceous sediments; 4 = Tertiary sediments; 5 = Tertiary and Quaternary volcanics; 6 = Quaternary sediments

Some of the cones are geologically young; the youngest flows in Syria in the northwestern Jebal Haurân have been dated at 4 000 B.P. (De Vries & Barendsen, 1954). The resulting basalt wedge is approximately 1 500 metres thick in southern Syria, thinning southwards until it pinches out just north of Azraq. Such a loading on the crust is considerable and may have encouraged underthrusting (Quennell, 1984). The basalts are petrographically very similar and can be classified as either alkali basalts or basenites/nephaline basenites (Barberi *et al.*, 1979), consisting of labradorite (60-70% anorthite), olivine, clinopyroxene, augite and magnetite-ilmenite. Although Burdon (1959) denies the existence of zeolites, large quantities of zeolite and palagonitized tuff have been found in certain of the volcanic cones especially around Jebal Aritain and Jebal al-Asfar (Dwairi, 1987; Ibrahim, 1993b).

During the earliest geological surveys of the northern part of Jordan, the so-called Nordostjordanische Deckenbasalte (Bender, 1968), six separate phases of vulcanism were identified (van den Boom & Suwwan, 1966). The first three (B1-B3) were not exposed, but were known for their hydrogeological properties as aquifers (Hunting Technical Services, 1965). They were thought to constitute a total thickness of up to 150 metres separated by paleosols approximately 5 metres thick. Between 6 and 20 metres of deposition was found below a fourth layer of basalt (B4), which has an exposure of some 60 metres in the Wadi Dhuleil, between Safawi and Ruwaishid (Hunting Technical Services, 1965). While the oldest basalts are laid down upon Middle Eocene Limestone, the fourth phase is covered by a Miocene interbedded sand- and limestone. Bender (1968) dated the four lower basalts to between the Upper Eocene and Miocene. The fifth basalt (B5) was regarded as the most important and most extensive extrusion. It was measured at 25 metres thick and overlaid an unconformable layer of older basalts, tuff, palagonitic sediments and clay horizons, as well as the calcic sandstones and marls of the Miocene.

Harrat Ash Shaam Basaltic Super Group			
Formation	Group	Bender (1968)	Moffat (1988) K-Ar ages
Fahda Vesicular Basalt (FA)	BISHRIYA	B6/5	0.1-1.45 Ma
Wadi Manasif Basalt (WMF)	(BY)	B6	
Aritayn Volcaniclasics (AT)	RIMAH	Bt	2.01-2.94 Ma
Hassan Scoriaceous (HN)	(RH)	Bt	
Mahadda Basalt (M)		B5	
Madhala olivine Pyric Basalt (MOB)		B5/4	
Hasimyya Aphanitic Basalt (HAB)	ASFAR	B5	1.96-3.41 Ma
Ushayib Olivine Pyroxene Pyric Basalt (UB)	(A)	B5	
Ufayhim Xenolithic Basalt (UM)		B6/5	
Salaman Flood Basalt (SN)	SAFAWI	B5/4	8.45-9.3 Ma
Abed Olivine Pyric Basalt (AOB)	(SW)	B5	mean 8.91 Ma
Ali Doleritic Trachytic Basalt (AI)		B5	
Continental / Marine Sedimentation	(QCS)	tt4	
Quirma Calcareous Sandstone Formation			
	WISAD	B4	9.37-10.53 Ma
	(WD)		

Table 2.1: A summary of the geology of Harrat Ash Shaam Basaltic Super Group

Source: adapted from Ibrahim (1993a)

The B5 basalts were found to correlate well with the basalt extrusions overlying the limestone plateau to the north of the Yarmouk river, which were dated to coincide with the tectonic mountain building phases of the upper Pleistocene (Bender, 1968). Between the fifth and sixth phases of vulcanicity observed by Bender (1968), there was a tuff phase (Bt) in which a thin layer of tuff and lapilli became incorporated into the upper part of the fifth layer (B5). The final basalt extrusion (B6) was characterised by kilometre-long flows from north to south which covered all the older basalt phases.

Plate 2.1: A False Colour Composite Landsat TM image of part of the northern Badia close to Safawi

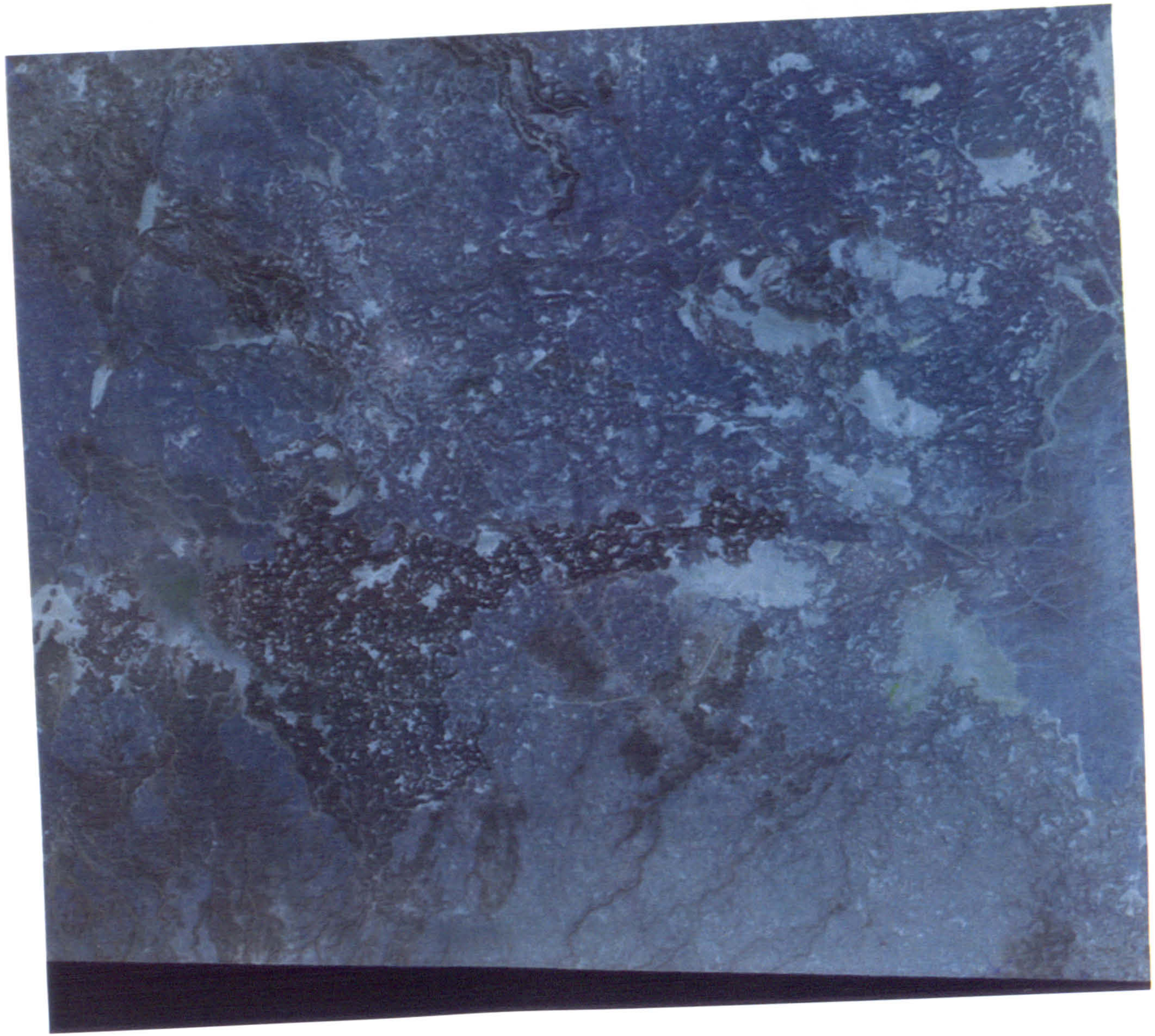

Again these flows can be correlated with the basalt flows flowing westwards between Mukheiba and the confluence of the Yarmouk and Jordan rivers (Bender, 1968).

The more recent classifications of the exposed basalt phases, Table 2.1, shows that the classification of Bender (1968) is more complicated. While the B4 correlates with the Wisad, the Upper layers described by Bender (1968) as B5 and B6 are less well correlated. The more recent research by Barberi *et al.* (1979), Moffat (1984) and the work of the Jordan Geological Survey (Ibrahim, 1993a) indicates that there are various formations, each with a different mineralogy (Barberi *et al.*, 1979; Ibrahim, 1993a). One consequence is different boulder size at the ground surface (Allison & Higgitt, in press), this being important in understanding the present landscape. The Landsat Thematic Mapper image (Plate 2.1) shows part of the basalt plateau around Safawi. A recent flow dominates the centre of the image showing minimal drainage connectivity and a large number of qa. Older basalts, such as the Abed basalt can be distinguished in the western section of the image in the wadi beds just to the west of Safawi as well as in the wadi beds in the east. A clear line of dykes can be seen running west-northwest in the northeastern corner of the image. The field sites used in the research are located to the east of this image.

2.3 Hydrogeology

There are three major aquifer systems which underlie the northern area of the Badia. The lower two are charged from the west of Jordan and the upper by precipitation falling on the Jebal Haurân. The aquifers are separated by aquitards, but there is considerable leakage in different areas of the Azraq Basin (Gibbs, 1993). The lowest aquifer is constrained within the braided river sands of the Kurnub sandstone and is as deep as 3.4 kilometres in the Azraq area (Andrews, 1992). The late Cretaceous limestones of the lower Ajlun group separate the lowest and middle aquifers. Due to the chemical change of the groundwater during its movement through the aquifer, there is an increase in the amounts of salts adsorbed with distance from the source and hence the water found in both the lower and the middle aquifers is partially

saline and of inferior quality when compared with the water from the upper aquifer, which is contained within the Pleistocene basalts of the Harrat Ash-Shaam Basaltic Super Group.

The water contained in the upper aquifer, which recharges in the Jebal Haurân above 800 metres (Dottridge, 1998), is extremely pure (Lloyd, 1965; Drury, 1993). With increasing distance south from the recharge source there is metasomatism which is enhanced by the over-extraction of water in the Azraq area. This results in a rapid degradation of water quality (Table 2.2)

Site	Northing	Total Dissolved Salt (mg/l)	Sodium Adsorption Ratio	Electrolyte Conductivity (mmho/cm)
J01	184875	221	2.35	300
J07	180850	229	2.06	340
J05	152443	374	3.46	610
J14	144350	846	4.89	1520
Rain water	n/a	123	0.22	190

Table 2.2: A transect of water quality in the basalt aquifer: Source: Drury, 1993

J01: Upper farm; J07: Lower farm; J05: 10 km N. of Azraq; J14: 10 km W. of Azraq (the farms are shown on Figure 2.8)

The Jebal Haurân is the most important recharge area east of the Jordan Valley. It is the only region with a higher rainfall that can sustain a recharge to groundwater (Burdon, 1982). At present abstraction is in excess of 60 million m^3 a^{-1} which compares unfavourably with current recharge estimates of 22-36 million m^3 a^{-1} (Dottridge, 1998). The drying up of the Azraq springs in 1987 and 1992 and the consequent drying of the lake at Azraq are clear signs of the unsustainability (Al-Jayyousi & Shatanawi, 1995).

2.4 GEOMORPHOLOGY

The geomorphology of the Ash Shamah basaltic plateau is dependent upon the characteristics of the individual lava flows which make up the basaltic super group.

As has already been seen in section 2.2.2, the most recent geological surveys indicate that the super group can be split into five major groups and fifteen formations. The older basalts, for example from the Safawi Group (Table 2.1), have developed much more mature landscape characteristics. The older basalts in the east around Safawi are generally of the Abed (AOB) and Salaman (SN) type; and their corresponding slope development is that of convex and concavo-convex slopes (Allison & Higgitt, in press), while the wadi channels and corresponding drainage density is well developed (Al-Homoud *et al.*, 1995). The geomorphology of the younger basalts, such as the Bishriya (BY), is characterised by concave slopes and a poorly developed drainage pattern (Allison & Higgitt, in press).

The other significant geomorphological features on the plateau are the Qa (Arabic for low place - Plate 2.2). These pans develop over a long period of time which means that the largest Qa can be found on the older basalts (Plate 2.1). The Qa and Marab are local names given to sediment pans which often cover several square kilometres. The Qa are topographic lows where sediment is deposited either from in-flowing wadis or by slope wash from the surrounding hillslopes. The distinctive hydrological feature which characterises Qa is the lack of significant outflow. As water and sediment are transported into the closed depressions, deposition leaves a build-up of fine silt layers. The surface is relatively impervious, except for the desiccation cracks, and the resulting infiltration capacity is very low (Allison *et al.*, 1993; Warburton, in press).

The Marab usually make up sections of wadis where the gradient has become so reduced as to create large areas of silt deposition. Most of the Qa and Marab deposits are made up of fine-grained sediments and usually display low salinity. Although most sediment-filled depressions fall into the categories of Marab or Qa, there is, in reality, a spectrum of distinct features, which display slightly different depositional and transport regimes.

Plate 2.2: Looking north over Qa Sbeika from a row of dykes

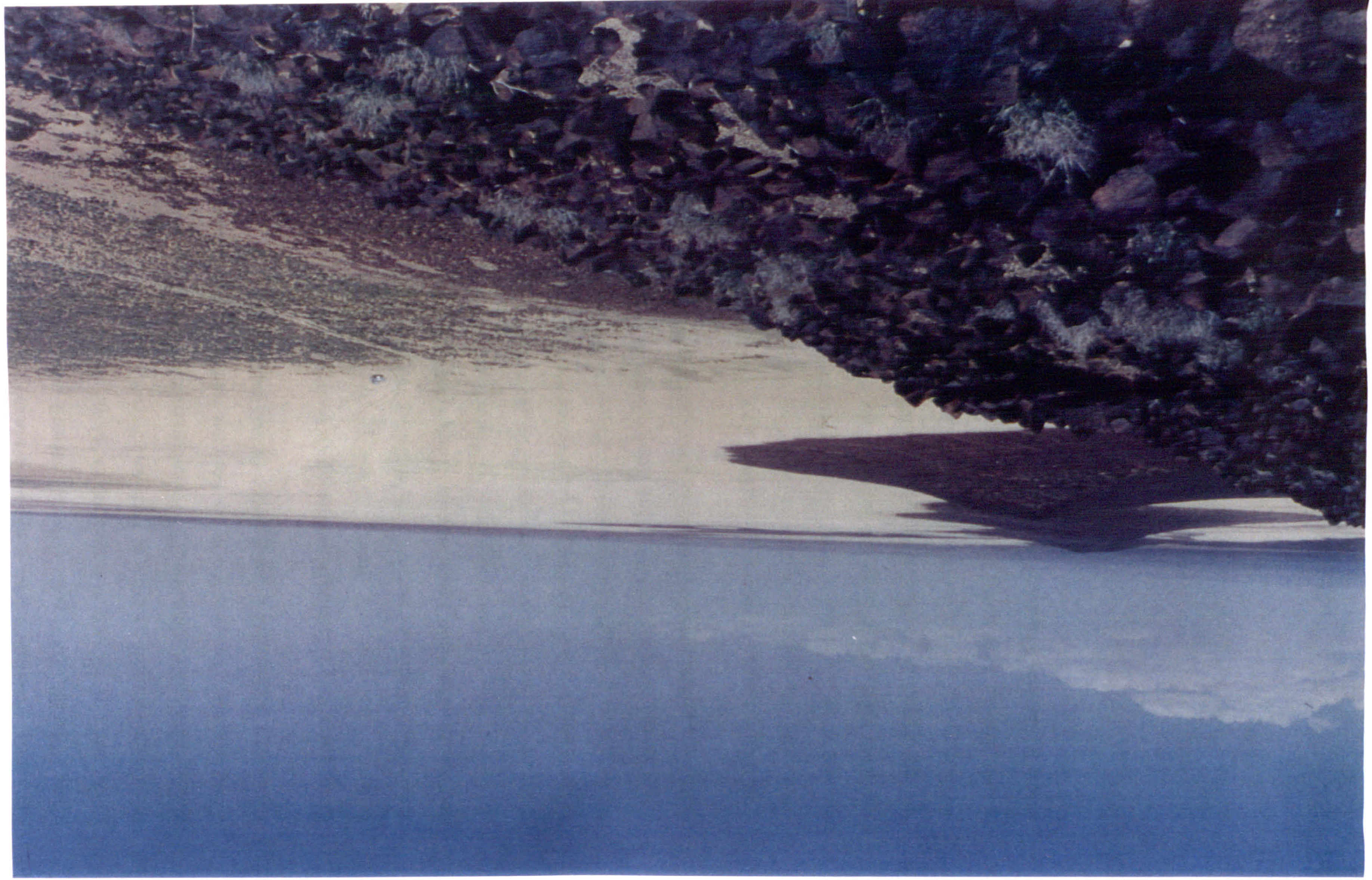

The typical desert pavement, which covers much of the landscape with its individual clasts of basalt, has a good potential for soil water and dew retention during the cooler parts of the year in comparison with the areas further east and south, where there is only a small covering of flints and chert (Garrard *et al.*, 1975). The moisture, although limited, is often enough to encourage the growth of small annuals, including cereal grasses. Towards the north west the basalt boulders become progressively covered by lichens, due to the greater moisture availability.

Each type of basalt, although petrographically similar (Barberi *et al.*, 1979), displays differing clast size and shape. Clast morphology plays an important part in determining certain slope processes including raindrop impact, infiltration, erosion and runoff. The Abed basalt consists of large clasts often measuring about 30 cm in diameter. The Salaman basalt has weathered into small basalt chips, which are elongate and rarely measure more than a few centimetres. The difference in sediment cover is considerable. The large Abed blocks have large spaces between one another which allows a significant amount of sediment to be moved by water. The basalt chips of the Salaman, on the other hand, cover the sediment almost completely, acting as a mulch and therefore reduce the possibility of erosion.

The wadi systems are extensive (Figure 2.2), although few of the channels are well developed. The general direction of water flow is from north to south, from the Jebal Haurân to the Azraq Basin. Much of the drainage pattern in the east is dominated by the Wadi Rajil, which flows down the eastern side of the Jebal Haurân, through the Qa and Marab at Sbeika. The wadi then flows southwards and eventually flows westwards into Qa Azraq. Much of the western drainage is dominated by a few large wadis, such as wadi Safawi, which drain the Jebal Haurân from the south and flow through Marab at Khanna or Be'gawier before entering Qa Azraq.

2.5 THE SOILS OF JORDAN

The soils of Jordan are closely associated with the geomorphology, tectonic activity and the underlying geology. The Jordan Valley, which is undergoing considerable tectonic activity, has soils which are dominated by highly weathered colluvial material and fan deposits from the valley sides. In addition, there is an inlux of alluvial material from the extensive wadi systems which have cut down, against the regional isostatic and tectonic movements, from the interior of Jordan.

In the west and north of Jordan along the East Bank highlands, plentiful rainfall has allowed relatively deep soils to develop. Terra rossa soils tend to be associated with the hard crystalline limestone beds of the Ajlun Series, while the brown chert soils form on the much more siliceous and cherty limestones of the Belqa Series (Beaumont & Atkinson, 1969). Both soil types range from clay loams to silty clays, with upward of 50% clay and 30% silt, and tend to be slightly alkaline (Fisher *et al.*, 1966).

Further eastwards in the Badia as a whole, the soils become lighter in colour, usually taking a light brownish-red hue associated with the arid climate. Only small areas of the desert steppe contain sandy soil because of the limited outcropping of sandstone. More regular are the limestone and chert soils which are thin, stony and mixed with loess material originating further east in Arabia (Bruins & Yaalon, 1979).

2.5.1 The soils of the northern Badia

The soils of the northern Badia should be considered separately from the rest of the Badia because they have developed and are considerably affected by the underlying basalts. The soils are deep reddish brown in colour (10-5YR 4/4-6/6) and are largely covered by basalt boulders. Soil depth is spatially variable, depending on the surface topography (Allison & Higgitt, in press). On topographic highs soil depth will usually be less than half a metre and in places bedrock is exposed, but in basins of high sedimentation from the surrounding slopes, soil depth can be more than two metres. The data presented in Table 2.3 are taken from the survey of the whole of the Wadi Rajil region, which includes most of the basalt plateau to the east and south of

the Jebal Haurân, carried out by Huntings Technical Services in 1992 and 1993. It can be seen that there is relatively little variability between soil types. Most of the soils which fall under the Camborthid classification are fine grained. One of the sub-groups, the *Typic Calciorthid*, contains considerable amounts of caliche and carbonate nodules.

Soil taxonomic Subgroups	Soil description	Colour	Location and geomorphology
Typic Camborthid	Deep silty-sandy clay loam, compacted at depth with basalt stones and gravel at about 50 cm, often with hard capped vesicular surface	7.5-5YR 5/6-4/6 or 10-9YR 5/6	Throughout region
Xerertic Camborthid	Heavy silty clay loam to clay. Strong platy to wedge structure but lacking slickensides. Often compacted at depth	7.5-5YR 4/6-4/4	Flat to gently sloping Qa and alluvial plains around Qa Be'gawier and Qa Sbeika
Xerochreptic Camborthid	Silty clay loam to silty clay, often with moderate sub-angular blocky structure. Developed from limestone alluvium, becoming sandy and gravelly with depth	7.5-10YR 5/6-4/6	Found in small blocks in the northern and middle parts of the Wadi Rajil. More extensive around the southern limits of the basalt
Typic Calciorthid	Deep very gravelly silt loam to sandy clay loam to clay loam. Large soft to moderately hard calcareous concentration producing a calcic horizon from about 20 cm depth. Common Mn concentrations	7.5-5YR 5/6-4/6	Flat wide wadis and Qa with gravelly gritty surface, sometimes with caliche. Found north of Qa Be'gawier
Typic Torriorthent	Unstructured, extremely gravelly coarse sand to sandy clay loam, poorly sorted	7.5-5YR 5/6-4/6	Northern edge of Wadi Rajil

Table 2.3: An overview of soils found on the basalt plateau of northern Jordan,

Source: unpublished data from Huntings Technical Services

It has been suggested that the soils of the region are a result of weathering of the basalt (Al-Homoud *et al.*, 1995), especially in past pluvial environments. However, a micromorphological study of the soil fabric and mineralogy suggests that the pedogenesis is more complex (Kirk, in press). The occurrence of calcareous nodules and a preponderance of silt-sized quartz grains within the fabric suggest a mixture of origins. There is no doubt that some physical and chemical weathering is presently

acting on the basalt to provide a sediment source because at depth, basalt core stones are well weathered. The inclusion of calcareous material would suggest a limestone source, indicating either wind-blown sediment from the south or east, or a local remnant from pre-basaltic erosion of the underlying limestones. Since quartz is not found in basalt, the quartz within the soil cannot be derived from basalt weathering. A more likely source is the Arabian loess deposits. If Bruins & Yaalon (1979) and Issar & Bruins (1983) are correct in their theories concerning deposition in the Negev and Sinai, then it is likely that some sedimentation in the Ash Shameh plateau has a similar origin.

2.6 CLIMATE

The climate of the northern Badia can be classified as Mediterranean Saharan because, although it is arid, it is less arid than the Arabian or North African deserts and has a smaller seasonal and diurnal temperature range, with the sparse rainfall concentrated in the winter months. Air temperature is highly variable and although the average is only 17.5 °C, the minimum and maximum temperatures are -5 °C and 46 °C respectively (Al-Homoud *et al.*, 1995).

2.6.1 Climate in the Eastern Mediterranean region

The general pattern of climate which controls much of the Levant and the Gulf is dominated by large-scale atmospheric circulation conditions. The patterns would have been present in the past, although they could have been geographically displaced and changed in intensity over time (Wigley & Farmer, 1982), dependent on factors such as the North Atlantic Oscillation (Cullen, 1997). Winter is characterised by cyclonic disturbances and low mean pressure in the Mediterranean, with higher pressure further east associated with the Siberian high. Unsettled weather in the Mediterranean basin is especially prevalent when the westerlies are in their low-index or blocked stages and the Polar Front Jetstream exhibits a strong oscillatory pattern allowing meridional transport of cold air (Perry, 1981). The lower position of

the Polar Front Jetstream over central Europe brings with it substantial amounts of rain. During spring the Sub-tropical Jetstream begins to move northwards from its location over the Tropic of Cancer and as the Polar Front Jetstream is pushed northward, precipitation is reduced.

In the winter and spring, the Cyprus lows are an important key to precipitation over the Levant (Krown, 1966; Lamb, 1968). Eastern penetration depends on the zonality of the upper flow and the strength of the Siberian High. There is some debate whether the position of the European Trough in the Mediterranean gives more or less rainfall in the Levant. It is generally believed that if cyclonic conditions stagnate over Cyprus, dry winter conditions will tend to prevail over the Middle East. If the surface cyclonic conditions move to the east, westerly winds predominate and precipitation occurs, especially over higher ground (FAO, 1962). Lamb (1968) believes that wetter conditions between the fifth and third millennium B.P. were primarily due to the easterly position of the trough. Krown (1966), however, relates wetter conditions in the Levant to a more westerly position of the trough in the Mediterranean.

By May, the influence of the Polar front and its associated westerlies is negligible. They are replaced with sub-tropical ridges of high pressure. It is during the summer months that the contracted circum-polar vortex ensures that the Mediterranean is a region of subsidence associated with a sub-tropical, upper tropospheric high (Perry, 1981). The effect of the Indian Monsoon is considerable. As it advances northwards during June, the easterly jet strengthens due to pressure differentials over continental Asia. The resulting complex set of jets extends over southern Arabia. The intensity of the jets is directly proportional to the rainfall received by the Upper Nile catchment. The jet system is also associated with upper air convergence causing widespread subsidence characteristic of the Middle Eastern desert areas. Although during most summer seasons there is consistent high pressure, the northerly expression of the jets can have an occasional effect in the northern Badia.

It is during the transitional seasons, especially in early autumn, that year-to-year variation in the general circulation is greatest, causing widely unsettled weather in

the Mediterranean. The combination of the irregular southerly movement of the Sub-tropical Jetstream from its summer position over Turkey down to northern Sudan and the subsequent increase in surface pressure over the Levant causes a pulsatory seasonal transition (Perry, 1981).

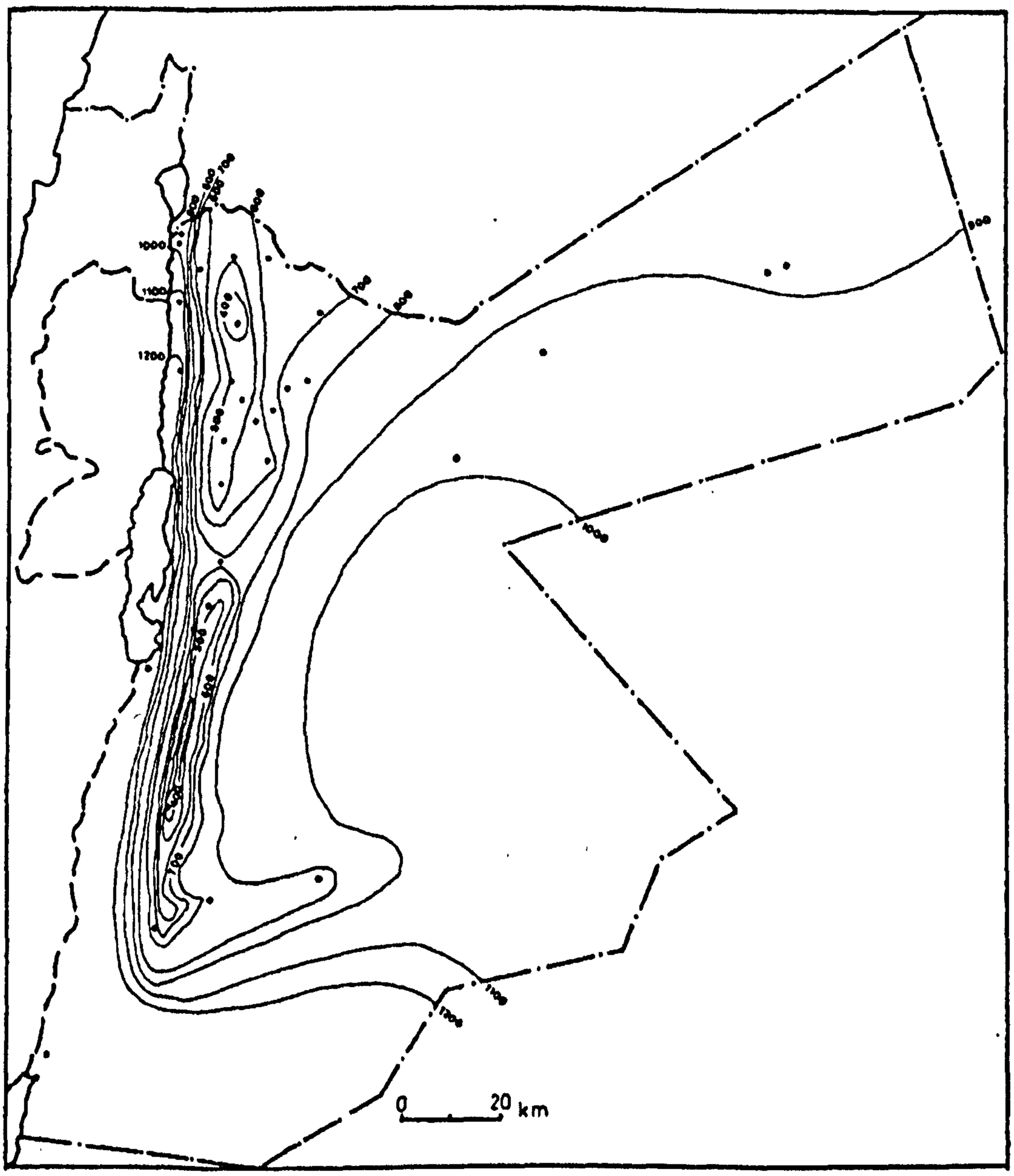

Figure 2.5: Mean water need or potential evaporation (mm) between 1966-1980 using Thornthwaite's model (1955) - Source: Shehadeh (1985), p. 34

2.6.2 Precipitation and mass water balance in Jordan

With the exception of the Jordan Valley, rainfall decreases from west to east and from north to south. The eastward precipitation decrease is mainly caused by the adiabatic heating of the moist winds on the lee slopes of the mountains bordering the east side of the Jordan Valley. The variation from north to south is attributed to the increased distance from the main tracks of Mediterranean depressions and the small number of depressions which travel along the southern Mediterranean track (Shehadeh, 1985). The two maps (Figure 2.5 & Figure 2.6), taken from Shehadeh (1985), show various average data for the evaporative fluxes for the whole of Jordan.

The potential evaporation map and moisture deficiency map (Shehadeh, 1985) are based on the moisture budget equations of Thornthwaite & Mather (1955). Both use data from the period 1966 to 1980. Although potential evaporation is as low as 400 mm a^{-1} around Irbid and Ajlun, giving an overall annual positive water balance, in the Badia the figure is above 900 mm a^{-1} and more recent data estimates a potential evapotranspiration rate of between 1 800 and 2 000 mm a^{-1} (Dottridge, 1998), which is much higher than the annual rainfall. The average moisture deficiency map corroborates the potential evaporation, indicating minimum moisture deficiency in the mountains and considerable deficits in the Badia and the Arava with maxima of 1 827 mm in Ghor Safi and 1 646 mm in Aqaba.

2.6.3 Climate factors affecting the northern Badia

The specific control on climate, in particular the precipitation, is the Jebal Haurân. The mountain range rises over 1 400 metres in southern Syria and is a significant orographic barrier to the air masses travelling from the Mediterranean. In the winter months, although much of the moisture is deposited on the hills as precipitation either side of the Jordan Valley, there is a significant amount of precipitation in the northern Badia as the air masses are forced to rise over the Jebal Haurân. The precipitation gradient is such that the amount of rainfall at the summit is up to five times greater than the mean figure for the northern Badia. This not only affects the availability of water on the foot-slopes of the Jebal Haurân but is important for wadi flow throughout the region (Dottridge, 1998).

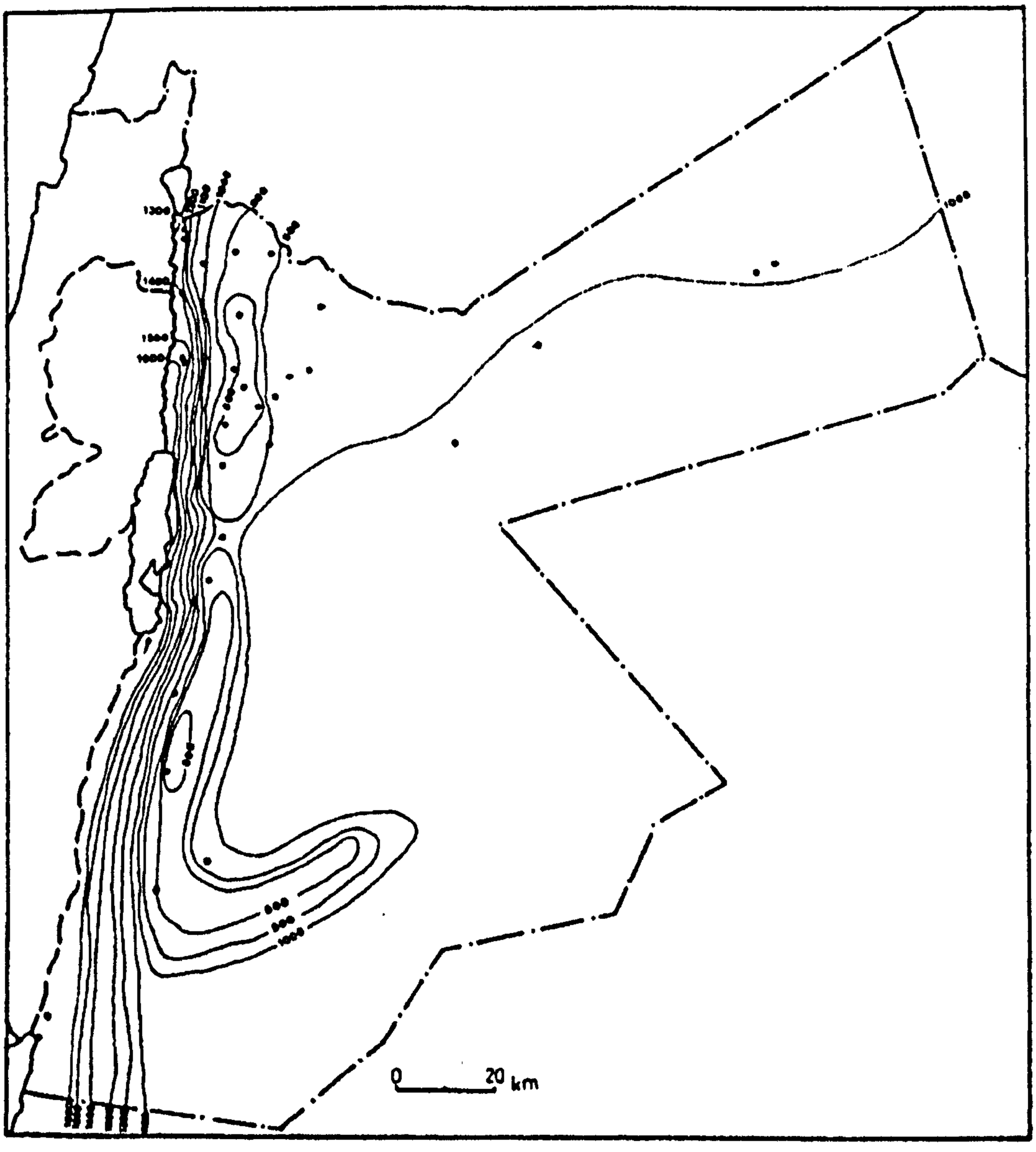

Figure 2.6: Mean moisture deficiency (mm) between 1966-1980

Source: Shehadeh (1985), p. 35

2.7 HOLOCENE CLIMATE CHANGE

Climate change research in recent decades has largely focused upon the higher latitudes of Europe and America, rather than on the low to middle latitudes of the Middle East. The situation reflects the relative ease of finding suitable datable sediments in the higher latitudes, while similar indicators in the lower latitudes are difficult to find (Baruch, 1994). For example, Roberts (1982), in his survey of Near Eastern Lake level dates, found only 154 ^{14}C dates from 31 sites which covered Arabia, the Levant, Egypt and North Sudan as well as Greece, Turkey, Iran and the Caucasus. Remarkably few stratigraphic events have been radiometrically fixed outside Israel and the Nile Valley (Butzer, 1975). Many of the dates which do exist are taken from the Jordan Valley and Lake Lissan (Dead Sea), but it is often argued that these should be considered as a special case, because the whole rift valley floor has dropped between 150 and 200 metres due to down-faulting at around 20 000 B.P. (Neev and Emery, 1967). More recently, with the development of thermo-luminesescence dating, there has been an increase in the study of the effect of climate change on Paleolithic sites (Valladas, 1992; Goldberg, 1994; Mercier & Valladas, 1994).

A key debate in the environmental and climatic histories of the Middle East centres on the correlation of pluvial events with the glaciation events of northern Europe and the extent to which specific events can be defined as being pluvial or interpluvial. It has been suggested that the periods between 17-10 ka and 10-6 ka show strong evidence of being pluvial (Neev & Emery, 1967; Horowitz, 1979), but the intervening period is contested and some think that 10-6 should also be considered as pluvial (Bar-Mathews, 1997). Using planktonic foraminiferal faunas, Thiede (1978) suggests that winter and summer water temperatures on the Levantine coast during the height of the last glaciation (ca. 18 000 B.P.) were approximately 18°C and 25°C respectively. Butzer (1975), on the other hand, suggests that the Holocene climatic variations do not neatly fit into those of the higher latitude glaciations, varying considerably from region to region within the Mediterranean and North Africa.

Issar and Bruins (1983) attempt to use a combination of aquifer geochemistry and changes in the depositional pluvial-eolian regime to consider what they see as a series of multi-annual cycles, bringing about fluctuations between periods of drought and periods of higher humidity. Looking at the ^{2}H composition in the Kurnub sandstone aquifers in the Sinai and the Negev, Issar & Bruins (1983) identified periods when a lower deuterium excess in the palaeowater occurred, which could be interpreted as either an increase in sea surface temperature or an equivalent increase in humidity. In addition, the plains of the northern part of the Negev, as well as the valley systems of the southern Negev and Sinai, are covered in a 14 metre layer of loess, the Neviot series, which is thought to be pluvio-eolian in origin (Bruins & Yaalon, 1979). The composition of the sediment is similar to that of contemporary dust which is transported during the early and late summer Hamseen winds, which come from Arabia. There are alternating silty and clayey bands which have been attributed to moister and drier conditions in the Upper Pleistocene and Holocene (Bruins & Yaalon, 1979). The upper Holocene layers of this loess have a low clay content (25%), but further down there is an increase in the clay to 40-60%. Ganor (1975) associates the sedimentological and meteorological conditions optimal for dust deposition and found that dust falling without rain consists of less than 20% clay, but pluvio-eolian deposition can contain between 50 and 60% clay. Hence the Neviot sequence would seem to suggest that rainfall has been 50-100% more than present levels during the Pleistocene. This adds weight to the work done on aquifer recharge (Issar & Bruins, 1983), as they suggest that between 20 000 and 70 000 B.P. there was twice the level of precipitation relative to the period after 20 000 B.P. More recent evidence from the study of pedogenic carbonate nodules has shown that there were periods at 13 000, 28 000 and 37 000 which were significantly wetter than present (Goodfriend & Magoritz, 1988).

Old marsh deposits have been found in the Sinai at Wadi Feiran with silt and clay sequences. The age of the uppermost layers of marsh deposits is about 20 000 B.P. (Carmi *et al.*, 1971), which suggests a considerable reduction in the water supply and a corresponding disappearance of the lake and marsh. Although these paleo-geomorphological data are useful in pin-pointing a likely threshold in the magnitude

of precipitation, the lack of dates for the area constrains the utility of the datasets, especially in trying to understand smaller fluctuations within the cycle.

The closest location to the northern Badia where paleo-environmental research has been carried out, is at El Jafr, 120 kilometres south of Azraq (Huckriede & Wiesemann, 1968). They date the end of the sedimentation phase of pluvial limestone in the El Jafr depression at 27 700 ± 870 B.P., which occurs in the middle of the Late Pleistocene Glacial. They suggest that the pluvial period was followed by a much drier climate until the Late Pleistocene when wetter conditions returned, although without significant further sedimentation.

Although it has been possible to place the end of the last Pluvial in the late Pleistocene, there has been little attempt to suggest a chronological sequence for more recent smaller-scale changes. Unlike the threshold change from Pluvial to Interpluvial, which leaves significant markers in the stratigraphy, smaller variations can often only be detected in the historical record using alternative sources of information. The only attempt to link such smaller changes in climate and precipitation over the Late Pleistocene and Holocene periods has been that of Butzer (1958). He uses historical, archaeological and geomorphological sources to produce a chronology of what he calls postpluvials and subpluvials (Table 2.4). He also tries to illustrate the relative fluctuations in rainfall (Figure 2.7).

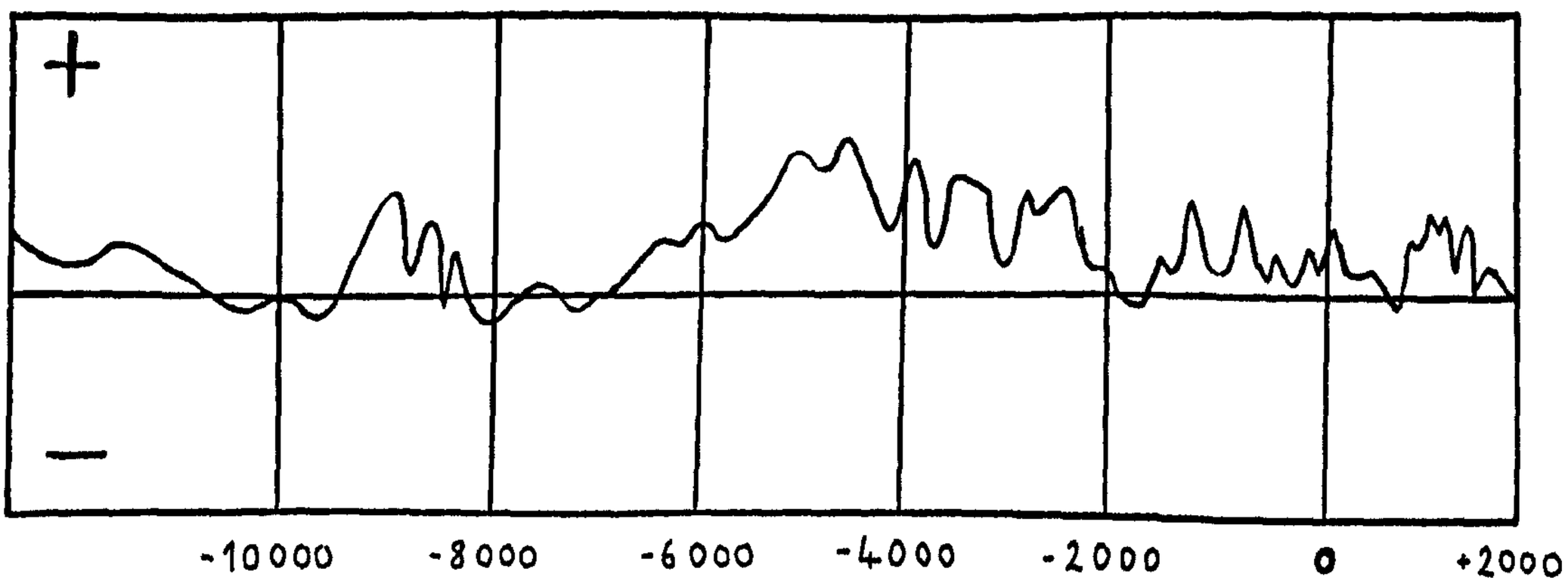

Figure 2.7: Relative trends of Near Eastern precipitation during the Late Glacial and Postglacial periods - Source: Butzer (1958).

POSTPLUVIAL I. During the period following the close of the Pleistocene Pluvial about 16 000 B.P., wind erosion was particularly pronounced. Temperatures and rainfall of the Near East were somewhat less than that of present, probably reaching a minimum during the 14 000 B.P.
SUBPLUVIAL I. (12 000 B.P.) A moderate and likewise temporary improvement of rainfall conditions. A last readvance of the disappearing Pleistocene glaciers took place, accompanied by lower temperatures effective to at least as far south as 33° N.
POSTPLUVIAL IIa. (10 500 - 8 800 B.P.) Following the humid relapse associated with the last glacial advance, temperatures rose. Typical conditions included a rainfall slightly less than present.
POSTPLUVIAL IIb. (8 800 - 7 000 B.P.) A marked improvement in precipitation.
SUBPLUVIAL II. (7 000 - 4 400 B.P.) The Neolithic moist interval which enjoyed a somewhat higher rainfall than the present, despite indications of higher local temperatures. If evaporation was high then conditions were part-way to being fully Pluvial. Sudden decreases in rainfall seem to have occurred shortly after 5 600 and 4 850 B.P.
POSTPLUVIAL III. (4 400 - 2 850 B.P.) Renewed decrease in precipitation during the fifth millennium B.P. led to a longer period of variable conditions. Average rainfall was a little below that of today, but interrupted by at least one moist spell in around 3 200 B.P.
POSTPLUVIAL IVa. (2 850 - 1 200 B.P.) Characterised by rainfall conditions similar to that of today but with small scale fluctuations. Periods of higher humidity occurred around 1 800 B.P. and 1 500 B.P., but these were juxtaposed with drought conditions in between and especially around 1 400 B.P.
POSTPLUVIAL IVb. (1 300 B.P. to the present day) Short term fluctuations continue with rainfall on average slightly higher than that of present. Colder conditions caused the Black Sea and the Nile to freeze during the around 1 000 B.P. Only in the last century has there been a marked climatic deterioration, with a 1% to 15% decrease in rainfall, a fall in interior-draining lake levels and a decrease in the Nile volume.

Table 2.4: Classification of climatic fluctuations since the last Pluvial - adapted from Butzer (1958)

2.8 ANTHROPOGENIC CONSIDERATIONS IN THE NORTHERN BADIA

The area named by archaeologists the southern Haurân (Butler, 1919) has been irregularly populated since prehistory (Garrard *et al.*, 1975). Evidence for human groups has been found as early as the Neolithic, indicating that a highly mobile and diversified nomadic population lived in northern Jordan (Homès-Fredericq & Hennessy, 1989). Jawa, one of the oldest known walled cities in the world, is situated on an island in the Wadi Rajil (Helms, 1981; Betts, 1991) on the eastern slopes of the Jebal Haurân: it is here that water catchment and harvesting schemes dating back to 3200 BC have been discovered. The Bible talks of the giant cities of Bashan, the capital of which was the city of Edrei (Num. 21:33; Deut. 3:1,10; Josh. 13:31). The main building phase which is visible today is Nabataean, Roman and Byzantine, with considerable later modification by the Muslims. From a geographical point of view, given the fragile environment which exists in the northern Badia, it is important to ascertain how large settlements could have been built and how they survived. If a large population was maintained in the past it is interesting to consider what effects the earlier generations had in modifying the landscape.

> *The study of settlement patterns in arid areas can provide a highly sensitive indication of the climate, of the delicate balance between human populations and environmental resources and of the mechanisms of human adaption to a marginal climate. Furthermore, because of their very marginal nature and therefore lack of agricultural disturbance, such regions are eminently suitable to study the past* (Garrard *et al.*, 1975, p.109).

The Nabatean settlements, dating back to circa 2 050 B.P., are mostly covered by the Roman re-building but inscriptions, especially on family tombs, can be found. The main Roman period of building began in the time of Trajan and is said to have flourished until the time of Constantine. The greatest period of building was that of the Byzantine stretching from the second quarter of the fourth century until the seventh (Butler, 1919). The Romans were always keen to protect their realm and road networks from bedouin attack (Issac, 1992) and so the regular scattering of forts

such as the one at Deir al kahf is not so surprising. The large towns of Umm al-Jimal and Bosra, however, pose a problem. If the climate was similar to the present, then how could such a fragile environment support large Roman towns. Umm al-Jimal, translated as 'mother of camels', lying about 20 km east of modern-day Mufraq, was a walled city, covering more than a third of a square kilometre and had a probable population of 10,000 (De Vries, 1981). The city in the sixth century probably had more than twenty churches, a Praetorium and many grand two- and three- storey mansions (Lankester Harding, 1959). What is most important, with regard to this study, is that the city has no natural wells or springs, but was situated just to the east of a wadi and 400 metres northwest of the city wall there was a masonry dam. From this dam, a sub-surface aqueduct can be traced to the east wall with several tributary aqueducts flowing from it before turning into the city and flowing into a large Roman reservoir situated in the centre of the city. The wadi, which probably only flowed a few times during the winter season, would have been dammed up and water would have flowed through the various sealed conduits and filled at least four reservoirs, as well as separate cisterns. It was not lack of water which caused the city's decline, but an earthquake in 747 AD (De Vries, 1981) which destroyed many of the settlements in the southern Haurân region. It was a geological catastrophe, with perhaps upwards of a thousand year return interval, which devastated the cities of the northern Badia rather than the fragile environment.

Butler's expedition early in this century came to the conclusion that there had been a considerable change in climate over the last fifteen hundred years. He says in his description of Deir al-Kahf:

> *"It is quite certain that the region was not desert in ancient times; for all the way from Iᶜ nât there are remains of ancient walls that divided fields and the traces of furrows still remain as evidence of former cultivation. These signs of former fertility extend farther to the south and southeast, as far as the eye can reach"* (Butler, 1919, p.145)

Butzer (1955) confirms that there were periods between 1-180 AD, 390-415 AD and 670-925 when the whole of Jordan was wetter than it is today. Whether or not the

climate was wetter during the six hundred years after Christ, what is important is that agriculture was widely practised as far east as Deir al-Kahf. The basalt-covered ground would have been cleared and the blocks used to enclose fields around the various settlements. The removal of the basalt blocks would have reduced infiltration, encouraged the erosion of fine material by the wind, and, as a consequence, reduced the fertility of the top soil. In other words, the modern geomorphological landscape has been sculpted by anthropogenic behaviour, not of the recent past, but of the ancient past.

The geography of the southern Haurân and the rest of the Harra has probably changed little since the dispersion of the population after the earthquake in the eighth century. Most of the villages have grown up during the twentieth century, often upon sites of the earlier Christian settlements. The population is heavily concentrated near Mufraq and is situated either on the Mufraq to Safawi road or on a parallel road which runs just south of the Syrian border. There are no settlements east of Al-Bishriya, except for a small cluster of houses between Jebal Aritain and Jebal al-Asfar, until the road joins the Amman-Baghdad highway at Safawi. Both Safawi and Al-Ruwaishid, which is a further 90 kilometres east, grew up earlier this present century around pumping stations for the Baghdad-Haifa oil pipeline, but since its demise in the 1940s, they have become service centres for travellers driving between Jordan and Iraq. The population in the villages has more than tripled over the last twenty years from 5,161 in 1976 to 16,267 in 1994 (215% increase) as the government has actively tried to settle the Bedouin, but there is still a large semi-nomadic population which travels throughout the year looking for pasture over the whole region (Maani *et al.*, 1995).

2.9 PASTORALISM AND IRRIGATED AGRICULTURE

The majority of the Bedouin living in the northern Badia rely on small-scale, speculative rain-fed growing of wheat and barley and keeping of sheep and goats. In the north, around villages like Deir al-Kahf (Figure 2.2), there is often enough rainfall for a reasonable annual crop. Further south the risks associated with rain-fed farming are much greater. One factor which has made rain-fed agriculture less viable

in recent years is the construction of dams on the Jebal Haurân in Syria. Formerly, there was regular wadi flow down from the mountains and through the foothills of the southern Haurân. Now the only flow in the wadis is generated by the much lower rainfall totals which fall on the Jordanian foothills of the Jebal Haurân. In the last decade, irrigation agriculture has been encouraged by loans from the government to drill private wells. As the population has settled, land cleared by earlier generations has been used. The new generation of entrepreneurial farmers has also moved eastward. New land has been brought into use by clearing the basalt boulders. Removal is almost complete near Mufraq and gradually reduces until it fades out about 65 km east of Mufraq.

The choice of the farms (Figure 2.8) used in the research was twofold. First, they occupy the current eastern fringe of irrigated agriculture over the area as a whole and therefore represent the threshold between desert and land utilisation. Second, they form a transect up the foothills of the Jebal Haurân and so lie on a gradient of considerable change in altitude and rainfall. Each farm has been granted loans to drill wells which reach down to the upper basalt aquifers. The depth of the aquifer below the surface declines from 450 metres at the most northerly farm to 292 metres at the southerly farm (Drury, 1993). Such figures represent very deep wells and considerable financial investment in the region of £60,000. The rate of water extraction is approximately 60 m^3s^{-1}, which is fed onto the fields using a series of pipes. Irrigation lines called *laterals* draw off the main pipes and are submerged under plastic sheeting. Water is delivered to the plants by means of drippers or emitters at a rate of between 2 $\ell\ h^{-1}$ and 8 $\ell\ h^{-1}$. The emitters are placed at selected intervals (0.5 - 1 metres) along the irrigation laterals depending on the planting distance, the type of crop to be irrigated and the type of soil (Goldberg *et al.*, 1976). The soil in the immediate vicinity becomes saturated during irrigation, but the moisture level drops away from the emitter.

Irrigation begins in April (Plate 2.5) and continues throughout the summer until October. The usual crops are tomatoes, chillies, okra and water melon. Other methods of irrigation are used for forage crops and fruit trees, but these are less abundant because of the lower short-term return that they give to the farmer. At the

PAGE
MISSING
IN
ORIGINAL

Plate 2.3: Ploughing the land for the following season's cultivation - often encouraging large deflation of fines.

Plate 2.4: The laying down of irrigation laterals and urea on newly ploughed land

Plate 2.5: Irrigation begins in April. Black plastic sheeting reduces evaporation

end of the season, the plastic and the irrigation pipes are all rolled up and stored and the plant residue is left as forage until the farmer decides to plough and plant wheat, barley, shallots or cauliflower as rain-fed crops for the winter season. Once the winter crops have been gathered in the following March, the fields are left bare, while other fields are prepared for the next year's irrigation. A three or four year rotation is adhered to, so that after three years of being bare, a field will once again be ploughed and prepared for another season of irrigated crops.

In preparation for irrigation, the land will be cleared of basalt if it is the first year of cultivation and ploughed before the winter rains (Plate 2.3). The land will then be left for four or five months, during which time a crust will have formed. In late March or early February the soil will be ploughed once again and then rolled before laying the irrigation pipes and planting (Plate 2.4). Urea fertiliser is then applied in strips parallel to the irrigation lines, which are spaced at two metre intervals, and covered in black plastic. Soil is then heaped on to the edge of the plastic from the intervening area which produces a ridge and furrow effect (Plate 2.5).

2.10 Conclusion

The Jordan Badia constitutes a zone of anthropogenic and environmental transition. At the human level, it constitutes the interface between the sedentarised populations of the west to the nomadic bedouin of the east. From an environmental point of view, the arid steppe of the Syrian desert lies on the transitional agro-climatological zone which divides the semi-arid Mediterranean basin from the hyper-aridity of Arabia. Due to the area's lack of economically exploitable resources, harsh climate and shortage of water, past human occupation has been sporadic and often associated with either pluvial climatic conditions or territorial conquest. Until recently, the area has been inhabited by nomadic bedouin who have made their livelihood by the herding of sheep, goats and speculative planting of wheat in areas of known water flow. In the last two decades sedentarisation has begun. Coinciding with the growth

of village populations, there has been an increase in land clearance, enclosure and intensified agricultural activity. The changing use of such a fragile environment will inevitably have many consequences, including anthropogenic effects on physical parameters such as soil quality.

3. PROCESSES AFFECTING SOIL CRUST FORMATION AND THE SUBSEQUENT ALTERATIONS IN THE MOVEMENT OF WATER AND SEDIMENT AT THE SOIL SURFACE

"The upper few millimetres of soil is the gateway to the soil below, and thus it has a direct and dramatic influence on the world around us." (Poesen & Nearing, 1993, p. v)

3.1 INTRODUCTION

Soil crusting defines a set of mechanisms which have long been observed in soil science (Duley, 1939). Because the surface soil layers provide the interface between the atmosphere and the regolith, they have an important role in determining the movement of water and the transport of mineral and organic materials over the land surface. A soil crust controls, to a large extent, the flux of nutrients, water, gases and heat to and from the underlying soil (Poesen & Nearing, 1993). Sumner & Stewart (1992) assert the profound influence of crusts upon the soil-air interface: '*As a result of particle sorting by [the] water, crusts are formed which determine all future allocation of precipitation to infiltration and runoff*' (p. iii). Indeed, the soil crust plays such an important boundary role that it has aroused the interest of many widely differing disciplines.

This chapter will discuss the processes which cause the formation and development of different sorts of soil crusts, using examples from both field and laboratory. The intrinsic properties of soil which give it a propensity to crust will be investigated. The effects of surface crusts upon runoff, erosion, infiltration, solute movement and evaporation need to be considered, especially with regard to soil and water chemistry. The morphology and classification of crusts will be reviewed. Soil crusting will be put into context with soil degradation processes acting in arid environments and plant, soil and water interactions.

3.2 HISTORICAL DEVELOPMENTS IN SOIL CRUST RESEARCH

The importance of soil crusts has long been recognised (Duley, 1939). His observations of the surface factors affecting the rate of intake of water by soils provide the basis on which soil crust research now rests.

> *'It has been observed in the present studies that the rapid reduction in the rate of intake of water by bare soils as rain falls on the surface is accompanied by the formation of a thin compact layer at the surface of the soil. Through this layer the water seems to pass very slowly. This layer is apparently the result of a severe structural disturbance due in part to the beating effect of the raindrops and in part to an assorting action as water flows over the surface and the fine particles are fitted around the larger ones to form a relatively non-pervious seal, giving the soil a slick appearance on the surface'* (Duley, 1939, p. 62)

The formation of the surface seal was seen by Duley (1939) not as an increase in fine material at the soil surface, but rather as a movement of fine material into the pores which surround the larger particles, thus producing a compact and dense surface layer.

The first systematic laboratory tests carried out on soil crusts, measuring permeability (McIntyre, 1958a) and raindrop impact effects (McIntyre, 1958b), involved the formation of crusts in small cups using simulated rainfall. The experiments were designed to test the effect of washing-in of fine material and the compaction of the surface by drop impact. It was noticed that as the soil surface aggregates dispersed fine particles were released, washed into and filled the sub-surface pores (McIntyre, 1958b). Coincident with the relocation of fines to produce the surface seal, there was a considerable reduction in permeability of the crusted material from 144 mm h^{-1} for non-crusted soil to 1.8×10^{-2} mm h^{-1} (McIntyre, 1958a). It was considered that the structural sealing caused by raindrop impact was two-layered, with a thin 0.1 mm skin and a washed-in zone extending down a further 2 mm to 3 mm. Both of the layers reduced permeability, the skin by an order of 2000 and the washed-in zone by an order of 200 compared with the undisturbed soil beneath. Despite inaccuracies in the measurement of hydraulic head gradient, work by McIntyre laid the blueprint for many of the soil crust concepts, such as skin and washed-in layer, as well as drawing a

general scheme of crust formation emphasising the role of compaction by raindrops (Mualem *et al.*, 1990).

By the mid- to late 1960s research had shifted to look at the intrinsic nature of the soil undergoing seal formation (Tackett & Pearson, 1965). The formation of soil crusts was related to particular particle-size distributions within the soil. However, it was suggested that the skin might not be related to compaction effects. In order to discover the nature of the washing-in of particles and the necessary effect of inter-aggregate clogging, it was observed that there was a gradual change in the bulk density ρ_b of the upper two centimetres of the soil profile from 1.32 g cm^{-3} to 1.61 g cm^{-3}. It can thus be deduced that the disturbed layer is considerably thicker than previously assumed by McIntyre (1958a) and that particles that are washed-in down the profile are permeating deeper. The results cast doubt upon the observational identification of the exact nature of the seal and washed-in layers. The concept of a two-layer crust, comprising skin and washed-in zone, was challenged by Evans & Buol (1968). Whereas Duley (1939) and McIntyre (1958a) examined low magnification micrographs (x15), more recent work concentrated on micrographs of soil crusts taken by a petrographic microscope, at magnifications up to x100. These micrographs showed that, in some soils, particles in the layer immediately below the surface skin were preferentially orientated, while for others orientation of silt and sand particles occurred in deeper layers of the crust only. As microscope technology has improved, more detailed studies have been undertaken to analyse the structure of soil crusts.

With the advent of scanning electron microscopy (SEM), the high-resolution study of the micromorphological aspects of crust form has increased knowledge of the washed-in layer. It has been possible to identify thin seals measuring less than 0.1 mm (Epstein & Grant, 1973; Chen *et al.* 1980; Tarchitzky *et al.*, 1984). Although no distinct visual layers were identified beneath the seal which corresponded to the washed-in zone observed by McIntyre (1958a), there was a 2-3 mm layer with a higher density than bulk soil, within which aggregates had been destroyed (Chen *et al.* 1980; Tarchitzky *et al.*, 1984). A reduced porosity would be expected during the formation of the seal. It was found that the upper 0.1 mm of the soil was devoid of large pores. In the 0.1 mm to 0.5 mm zone such pores represented just 1% of the total volume and in the 1 mm to

2 mm layer they occupied 10-13% (Epstein & Grant, 1973). It was also observed that there was little difference in the proportion of clay in the top 0.22 mm of the soil, when compared with the underlying material, suggesting that the finer particles were not being washed down the profile, but rather being transported away by runoff (Epstein & Grant, 1973). This view was supported by Eigel & Moore (1983), who found that the main effect of rainfall was an increase in bulk density near the surface. There was an observed gradual decrease in bulk density with depth from 1.95 g cm^{-3} at the surface to 1.35 g cm^{-3} at a depth of 10 mm (Eigel & Moore 1983). However, neither rainfall duration nor intensity was found to have an effect on the particle size distribution in the top layer of the soil.

Much early work concentrated upon the physical processes causing aggregate breakdown, namely raindrop impact. However, research in the late 1970s and 1980s began to investigate the role of soil chemistry in clay dispersion mechanisms. It was shown that it was possible to have a well-developed washed-in zone without the occurrence of a surface skin seal (Gal *et al.*, 1984; Shainberg, 1985). If conditions are favourable for clay dispersion, i.e. high sodicity and a low electrolyte content in the water, then it is possible for naked sand grains to be held loosely at the surface while the fine silts and clays are redeposited in pores in the subsurface, thus clogging them and making the washed-in zone less porous. The surface sand grains can easily be eroded by subsequent runoff water. The washed-in layer is then exposed and the surface seal never develops.

Field studies have observed crust layers of up to 20 mm, which is considerably thicker than those observed in the laboratory (Hillel, 1959; Hadas & Frenkel, 1982; Boiffin, 1984; West *et al.*, 1992). The term natural crust has been used to describe thick, naturally occurring crusts which are made up of a seal and numerous in-washing events. Thick natural crusts were characterised by a slow build-up of bulk density down through the top 20 mm (Hillel, 1959) or several distinct layers (Hadas & Frenkel, 1982; Boiffin, 1984). It is conceivable that relatively minor changes in soil texture or structure, not noticeable by microscope observations, may significantly affect the hydraulic conductivity (Mualem & Assouline, 1989) and therefore be a sign of reduced infiltration (Edwards & Larson, 1969; Sharma *et al.*, 1981). In the upper layer of the

soil profile there was an abrupt decrease of hydraulic head at the upper layer to a depth of 10 mm and only at 20 mm did it reach its equilibrium value (Sharma *et al.*, 1981). The hydraulic gradient profile is therefore an important source of information about the actual seal layer (Mualem *et al.*, 1990).

In recent years there have been attempts to model the different physical and chemical processes together (Le Bissonnais, 1990; Römkens *et al.*, 1990). The initial structure (Chiang *et al.*, 1993), particle-size distribution (Onofiok & Singer, 1984) and antecedent moisture content (Le Bissonnais & Bruand, 1993) are important factors influencing aggregate slaking and crust development. A study of three Californian soils with very different physical characteristics showed that the coarser-textured sandy loam soil showed no evidence of a washed-in zone, but the finer silt and clay loam soils had a distinct washed-in layer (Onofiok & Singer, 1984). In conjunction with the physical processes, however, is the chemistry of the soil or applied water. High levels of exchangeable sodium in the soil (E.S.P.) or in the soil water (S.A.R.) have been shown to be responsible for a significant washed-in zone and subsequent reduction in infiltration rate (Agassi *et al.*, 1981; Kazman *et al.*, 1983; Gal *et al.*, 1984). The levels of sodium are offset, to a certain extent, by the electrolyte concentration of the applied water and the presence or absence of swelling clays such as montmorillonite. Together these factors allow chemical dispersion of soil particles to take place and free them to move downwards through the soil profile and clog the pores in the sub-surface.

3.3 PROCESSES INVOLVED IN THE FORMATION OF SEALS AND CRUSTS

3.3.1 Surface sealing vs. surface crusting

A distinction is usually made between surface sealing and crusting. The Soil Science Society of America (1984) define surface sealing as the orientation and packing of dispersed soil particles in the immediate surface layer of the soil, rendering it relatively impermeable to water. Römkens *et al.* (1990) define the surface seal as the

structural degradation of a thin layer at the soil surface during a rainstorm or irrigation event. The seal is therefore critical for short-term rates of erosion and determines hydraulic properties. The surface crust, on the other hand, refers to the hardening and increase in strength of the surface layer during subsequent drying. Similarly, Bradford & Huang (1992) state that the seal represents the breakdown of clods and aggregates, due to chemical and physical variables, upon wetting by precipitation or irrigation. The inter-aggregate pores become filled with detached material and, with the reorientation of particles, forms a dense layer. The soil crust can only be said to form as the soil dries (Remley & Bradford, 1989). In summary, the seal refers to the moist condition and crust refers to the resulting dry hard surface layer (Mualem *et al.*, 1990).

3.3.2 Aggregate stability and the condition of soil erosivity

Aggregate stability, a measure of soil aggregate resistance to breakdown, influences many soil physical and hydraulic characteristics including surface sealing, soil surface roughness, infiltration and hydraulic conductivity. Much of the soil erosion process research focuses on erosion sub-processes such as aggregate stability (De Ploey & Poesen, 1985; Farres, 1987; Imeson & Kwaad, 1990). Soil aggregate stability is of key importance, not only in constraining the magnitude of soil erosion during rainstorms (Bryan 1968, 1969; Farmer, 1973) and determining the amount of rainsplash (Parsons *et al.*, 1994; Mermut *et al.*, 1997), but also to the formation of structural crusts (Farres, 1978; Bradford *et al.*, 1986; Norton, 1987) and depositional crusts (Morin & Van Winkel, 1996). The instability of aggregates is essential for crusting to occur. However, for most soils, wash and splash amounts decrease once a seal is established (Bradford *et al.*, 1986a, 1986b; Norton, 1987). A positive correlation was found between the aggregate stability of four American soils, infiltration and clay content, and a negative correlation with strength (Table 3.1).

Soil Series	% Sand 2-0.05 mm	% Silt 2 - 50 μm	% Clay < 2 μm	MWD† mm	D_{50}‡ mm	>250μm %	Strength $\Delta\tau$ kPa	Infiltration ΔI mm h^{-1}
Vicksburg	8	85	7	0.65	0.05	39.2	36.5	3.9
Miami	10	60	30	1.15	0.68	85.4	6.2	12.2
Sharpsburg	4	63	33	2.00	1.39	89.2	1.7	32.8
Brooksville	4	59	37	2.15	1.51	92.5	16.4	15.7

Table 3.1: Indices of seal formation, aggregate stability (2-8 mm aggregates) and infiltration rates on four soils after rainfall simulation for 30 minutes. All slopes have steepness of 9 %. Adapted from Bradford & Huang (1992) p.60
†MWD: mean weight diameter (Kemper & Rosenau, 1986) ‡D_{50}: median aggregate diameter of prewetted aggregates

Sand %	Silt %	Clay %	Soil identification	Location	Source
80	15	5	Loamy fine sand	Niono, Mali	Hoogmoed (1986)
83	2	15	Loamy sand	Coastal plain, Israel	Ben-Hur *et al.* (1985)
84	5	11	Ferralitic sandy soil	Adiopodoumé, Ivory Coast	Lafforgue & Naah (1976)
84	6	10	Loamy sand soil	Jodhpur, India	Sharma *et al.* (1983)
84	10	6	Loamy sand soil	Owerri, Nigeria	Boers *et al.* (1988)
85	2	13	Loamy sand soil	Sharon Plain, Israel	Morin *et al.* (1981)
86	6	8	Sverdrup sandy soil	Minnesota, USA	Young & Onstad (1976)
89	2	9	Fine sandy soil	Tongeren, Belgium	Poesen (1984)
89	7	4	Princeton Loamy fine soil	Indiana, USA	Mannering (1967)
90	6	5	Sand	Agadez, Niger	Valentin (1986)
92	5	3	Sand	Sadore, Niger	Hoogmoed (1986)
94	4	2	Sand	Indiana, USA	Mannering (1967)

Table 3.2: Textural composition of sandy soils reported to be susceptible to surface sealing. Source: Poesen (1992)

The two key variables which affect aggregate stability are the textural attributes of the soil (Kheyrabi & Monnier, 1968; Bradford *et al.*, 1987b; Poesen, 1992 - Table 3.2; Le Bissonnais & Arrouays, 1997) and antecedent moisture (Cousen & Farres, 1984; Le Bissonnais *et al.*,1989; Le Bissonnais, 1990; Truman *et al.*, 1990; Levy *et al.*, 1997). The physical composition of the soil has important implications for seal development and strength, which reach a threshold of <200 g kg^{-1} clay, 30 g kg^{-1} organic C and 2.0 % CBD-extractable Al and Fe (Le Bissonnais & Singer, 1993). The presence of swelling clays is especially important, during intense rainfall, for rapidly reducing the infiltration rate (Mermut *et al.*, 1995). The *rainfall component* (Le Bissonnais, 1990) will change according to the initial structural state of the soil (Figure 3.1). If aggregates are saturated before rainfall, breakdown intensity is closely related to the kinetic energy of raindrops. If the aggregates are dry, breakdown intensity is independent of kinetic energy and only depends on raindrop size and rain intensity.

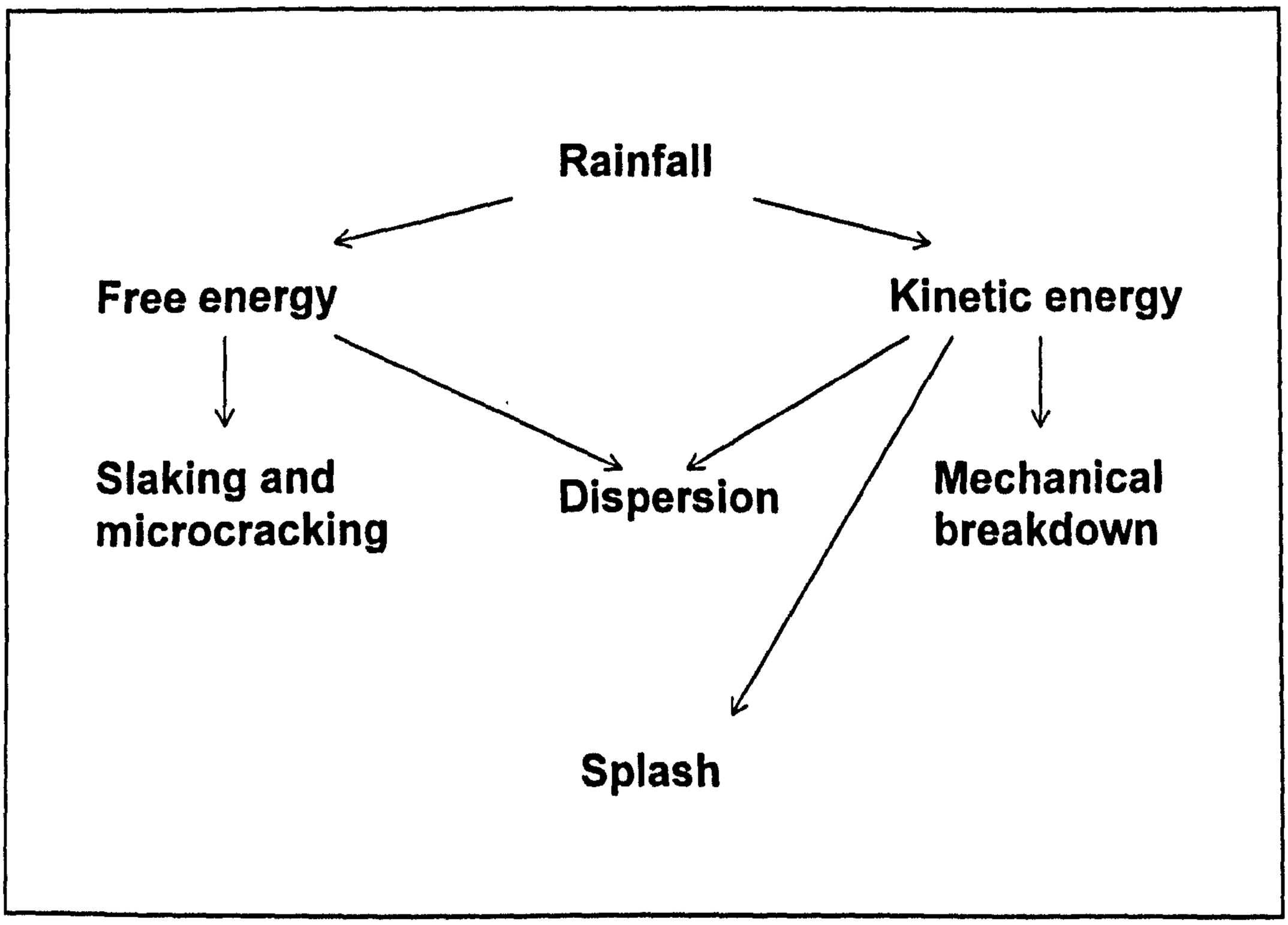

Figure 3.1: The two rainfall components controlling aggregate stability.

Source: Le Bissonnais (1990)

The processes involved in aggregate stability change spatially and temporally. For example, the aggregate stability of tropical soils is more dependent upon rainfall energy than antecedent moisture condition (Watung *et al.*, 1996), while different crust forms can often be identified depending on the season in which they developed (Le Bissonnais & Bruand 1993). Winter crusts, due to high antecedent moisture conditions, are formed by individual particle detachment producing a single layer of packed individual particles. In the spring, the dominant slaking mechanism is microcracking and the resulting crusts are formed by the coalescence of micro-aggregates.

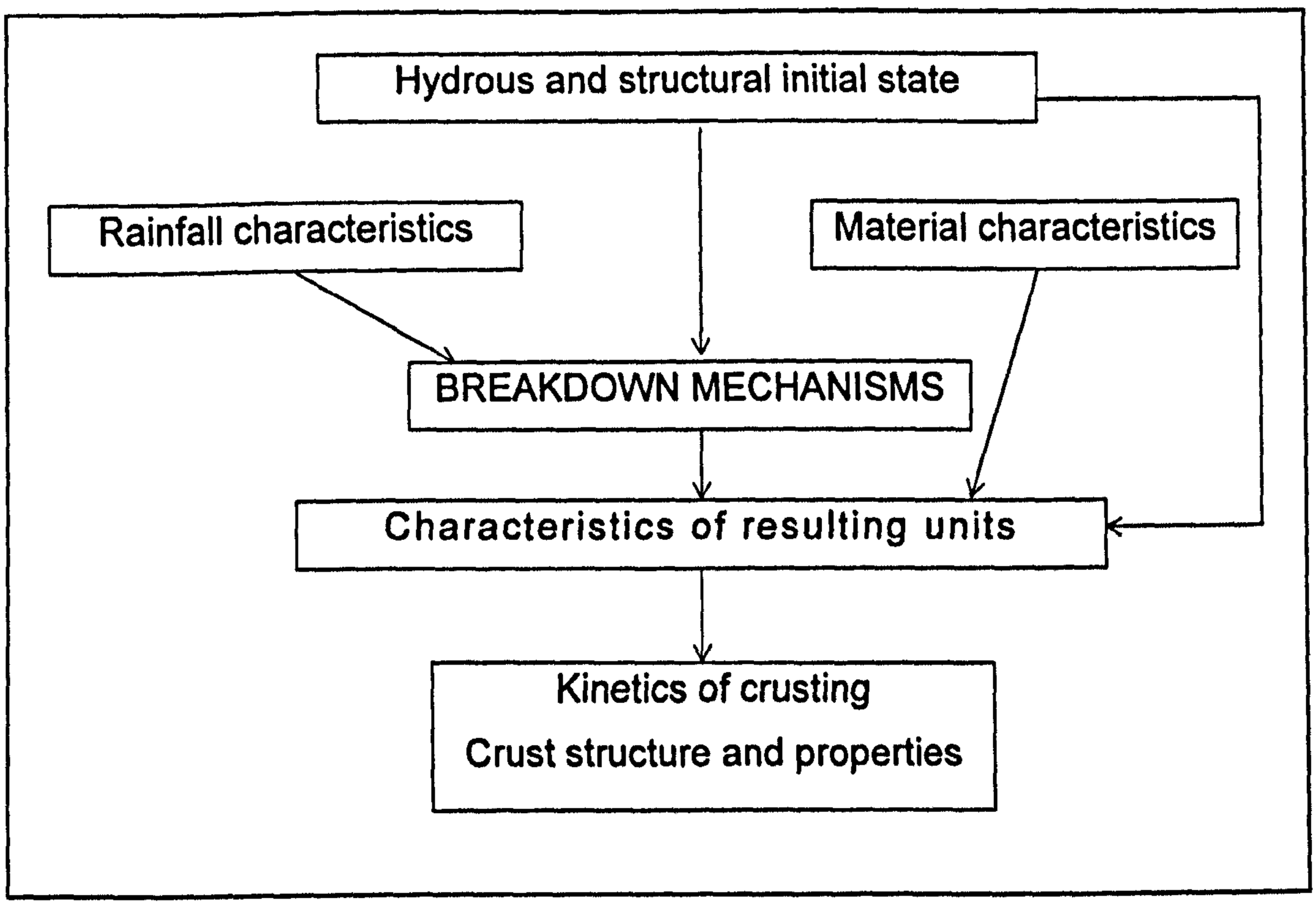

Figure 3.2: The relation between the crusting parameters

Source: Le Bissonnais (1990)

When the processes of aggregate breakdown, particle displacement, and compaction under raindrop impact combine, structural evolution takes place. This structural evolution, in turn, determines the infiltration capacity and roughness (Figure 3.2). There is no unique relationship between rainfall characteristics and soil surface

behaviour. A soil with characteristics which make it prone to crusting will do so even if the rainfall is not aggressive. Conversely, if the soil is very permeable, then the most aggressive rainstorm will not cause crusting.

Having argued that the stability of the soil aggregates is fundamental to the process of surface crusting, its measurement remains a problem. The fact that many methods have been used for measuring aggregate stability reflects the importance of the process and the lack of a reliable standardised methodology (Table 3.3). Many tests for erodibility do not reflect the mechanisms involved and other measures give contradictory results. For example, there is no standardisation in the drop characterisation used for calculating the time to breakdown (Farres & Cousen, 1985). Hence a standardised method for the study of aggregate stability would be of great interest for predicting erosion and crust formation on cultivated soils (Le Bissonnais, 1996a).

Type of treatment	**Form of sample**	**Expression of the result**	**Authors**
Wet sieving	3-5 mm	MWD	Yoder (1936)
	<2 mm	% > 200	Hénin *et al.* (1958)
	whole soil	change in MWD	De Leenheer & De Boodt (1959)
	1-2 mm	% > 250	Kemper & Rosenau (1986)
	2-3.4 mm	MWD	Churchman & Tate (1987)
	1-2 mm	% > 250	Pojasok & Kay (1990)
Raindrops or rainfall	4-5 mm	time to breakdown	Low (1967)
	2-9 mm	MWD	Young (1984)
	5-8 mm	time to breakdown	Farres (1987)
	whole soil	% > 125	Loch (1994)
Ultrasonic dispersion	4-5 mm	dispersion rate	Edwards & Bremner (1967)
	4-5 mm	inter-aggregate pore volume	Grieve (1980)
Immersion	3-5 mm	qualitative	Emerson (1967)
Dry sieving	< 4 mm	MWD	Kemper & Chepil (1965)

Table 3.3: Characteristics of some of the main methods for testing aggregate stability

Note: several of these methods include various pretreatments

Source: Le Bissonnais (1996b). MWD: Mean Weight Diameter

In response to this call for a standard method, a multi-faceted approach which combines much of the existing research (Yoder, 1936; Hénin et al., 1958; Grieve, 1980; Kemper & Rosenau, 1986) has been suggested in order to distinguish between the different breakdown mechanisms (Le Bissonnais, 1996b). It combines three treatments, which test for different wetting conditions and energies: fast wetting, dry wetting and stirring after pre-wetting, and measures the resulting fragment size distribution after each treatment (Le Bissonnais, 1996b; Le Bissonnais & Arrouays, 1997).

3.3.3 The relationship between rainfall intensity and crust development

Various investigations have taken place, often experimental in nature, to determine the importance of raindrop impact on surface crust development and soil detachment often by describing distinct phases of detachment (Al-Durrah & Bradford, 1981; 1982). In stage I, a crater is formed in the soil under the drop, simultaneously creating a bulge around the depression as the vertical strain of the drop is released. In stage II, the compressive stresses are converted into a shear stress because of the development of a radial jet. Stage III represents the complete development of a lateral jet. The pressure exerted upon the soil during impact is one of the most important variables in the modelling of aggregate stability and soil crust development. The energy required to detach *in situ* particles is considerably greater than that needed to entrain loose sediment (Nearing *et al.*, 1994) and so the rainfall intensity is of ultimate importance. Differences in the breakdown of soil crumbs are associated with the duration of application of the stress and to the concentration of stress around the periphery of the raindrop (Ghadiri & Payne, 1977). Similarly, drop shape has an important role to play in causing deformation of the soil surface and erosion of the surface aggregates (Riezebos and Epema, 1985).

However, it is not only the forces of the rain drop which are responsible for the soil crust and detachment processes. The texture of the soil and the clay lattice properties are paramount in determining the amount of interrill erosion: soil detachability is inversely related to clay content and sediment transport increases linearly with clay

content (Sharma *et al.*, 1995). Swelling smectite-type clays cause the highest rates of splash (Mermut *et al.*, 1997).

Various attempts to model the response of surfaces in terms of detachment to raindrop impact, drop size and rainfall velocity distributions have been carried out, using both semi-empirical models (Gilley *et al.*, 1985b) and purely numerical relationships (Huang *et al.* 1982; Nearing *et al.*, 1986). The best functions for the evaluation of potential detachment rates seem to be based on measures that combine two or more of the rainfall characteristics: for example, kinetic energy multiplied by drop circumference (Gilley *et al.*, 1985a), or the velocity of rainfall impact and the size of the raindrop, producing drop momentum, which correlates well with the resulting seal formation and final infiltration rate (Betzalel *et al.*, 1995). Such an initial condition can be approximated to a soil crust as drop impact has a much more limited deformation effect on the soil surface (Nearing *et al.*, 1987). Peak stresses of between 0.5 MPa and 1.5 MPa occurred within 13 to 21 μs of initial contact, with a general reduction to about 100 kPa after 50 μs depending on droplet size (Nearing *et al.*, 1987).

In attempting to classify the effect of raindrops on individual soil particles, Alder (1979) listed four primary damage modes associated with the impact of liquid drops on a solid surface. At the start of an impact event, there is mechanical deformation of the surface which generates a series of stress waves moving out from the contact zone. Dilational, distortional and finally Rayleigh surface waves develop. After a threshold in pressure build-up, deformation of the droplet causes a lateral outflow sheet to form which can cause shearing in the local aggregates. In the case of a porous surface, water jets associated with the drop will travel into the subsurface pores and cracks, thus activating further potential physical breakdown mechanisms. Examining the effect the pressures have on the reorganisation of particles into a seal, Moss (1991a) found that the pressure of a droplet, falling at or near to terminal velocity, is enough to propagate through a plastic shield and cause the reorganisation and compaction of surface soil particles. It is clear that the pressure of raindrops induces a strain within the top few millimetres of the soil and as a result there is the formation of pores and a process of strain-induced segregation (Bielders and Baveye, 1995a). As the soil becomes partly saturated there are strong cohesive forces which limit the percolation of particles into

the profile. However, the drop pressure is great enough to overcome the cohesive forces and encourage downward movement of fine particles to form a washed-out layer which accumulates at a depth related to the average momentum of the raindrops (Bielders and Baveye, 1995b).

3.3.4 The importance of rainfall intensity and duration

Seal development is not uniquely related to cumulative rainfall energy (Valentin, 1986), but rainfall intensity also has an important role to play (Römkens *et al.*, 1986; Mermut *et al.*, 1995). Seal hydraulic conductance rapidly decreases with increased rainfall energy but then levels-off to a near constant value. The degree of seal development, determined by the final hydraulic conductance values, depends on rainfall intensity. Paradoxically, looking at the response to two rainstorms separated by 16 hours, it was concluded that seal development was reduced as rainfall intensity increased and *vice versa* (Römkens *et al.*, 1985). This anomalous result is probably due to greater turbulence in the thicker surface water films at larger rainstorm intensity regimes and the eroding action of impacting raindrops. Turbulence tends to keep fine sediment particles and colloidal material in suspension and prevents clogging of the soil pores. Soil crusting should be studied over a series of wetting and drying events (Falayi & Bouma, 1975; Bresson & Valentin, 1990). It is clear that the amount and rate of aggregate pre-wetting and the ageing duration after wetting are influential in the overall aggregate stability during subsequent rainfall events and therefore the susceptibility to seal (Le Bissonnais & Singer, 1992; Levy *et al.*, 1997). Very little information is currently available on changes of seal properties during subsequent rainfall events. The information that is available is contradictory, ranging from no significant effect (Morin and Benyamini, 1977), to increasing infiltration (Ben-Hur *et al.*, 1985) and decreasing crust strength (Bradford & Huang, 1992). Others have denied the positive effect on infiltration (Roth & Helming, 1992) and found increasing runoff and decreased infiltration in pre-crusted soils. On highly stable agricultural soil, where over a third of clods were larger than 100 mm, clods reacted in different ways depending on the number of rainfall events (Mellis *et al.*, 1996). It is likely that the apparent differences of opinion relate to the soil properties under investigation and, to a degree, some over-simplification of the issue. What is

probably closer to the truth is a model of continuous destruction and recreation of surface crusts during successive storms (Hardy *et al.*, 1986). Such a view has been reiterated by Remley & Bradford (1989) and Luk & Cai (1990), who indicate that seal development is a complex interaction of contradictory processes, with sub-processes of both seal formation and seal destruction induced by raindrop compaction and detachment. The abrasion of particles during wind erosion processes can also influence the state of the crust between rain events, often breaking it up entirely if the initial crust is weak enough (Rice *et al.*, 1996).

3.3.5 Effect of rock fragments on infiltration and surface seal formation

Desert hillslopes, especially those of the Badia, are often characterised by a mantle of stony debris, which may reflect a relict transport process or current redistribution of surface material (Allison and Higgitt, in press). Similar characteristics have been identified in the Negev (Amit & Gerson, 1986). It has been recently recognised that soil crusts and rock fragments have significant roles to play in determining infiltration (Valentin, 1994) and overland flow (Yair & Lavee, 1976). Rock fragments will cause increases and decreases in infiltration rate under different conditions and it is likely that contradictory data sets occur because there is no adequate methodology for describing stone cover (Dunkerley, 1995). The position of the rock fragment within the surface layer exerts a strong control on infiltration (Poesen, 1986a, 1986b; Poesen *et al.*, 1990). The sealing index (S.I.), which is the rate of change of the percolation of water through the seal during a rainfall event, equalled only 5.4 mm h^{-2} for rocks resting on the surface, while for partly embedded rocks it was 9.0 mm h^{-2}. Field evidence investigating the role of rock fragments on raindop-soil interactions has been contradictory. Rock fragments can reduce raindrop impact and therefore seal formation, with the additional factor that water can infiltrate along the interfaces between rock and soil surfaces. Rock fragments also act as a mulch to reduce raindrop impact and hence sealing (Meyer *et al.*, 1972; Kochenderfer & Helvey, 1987). However, a negative correlation between rock fragment cover and infiltration can also occur (Blackburn, 1975; Casenave & Valentin, 1992). Valentin (1994) shows, from field studies undertaken in West Africa, that the vesicular porosity of the surface seal is inversely proportional to free

rock fragment percentage, and increased with embedded rock fragments. Wilcox *et al.* (1988) postulate that stone pavement evolution in arid and semi-arid regions is due entirely to surface lowering, intensified by lack of vegetation. It is therefore not the blocks themselves which promote or reduce infiltration, but the soil crusting and compaction resulting from raindrop impact.

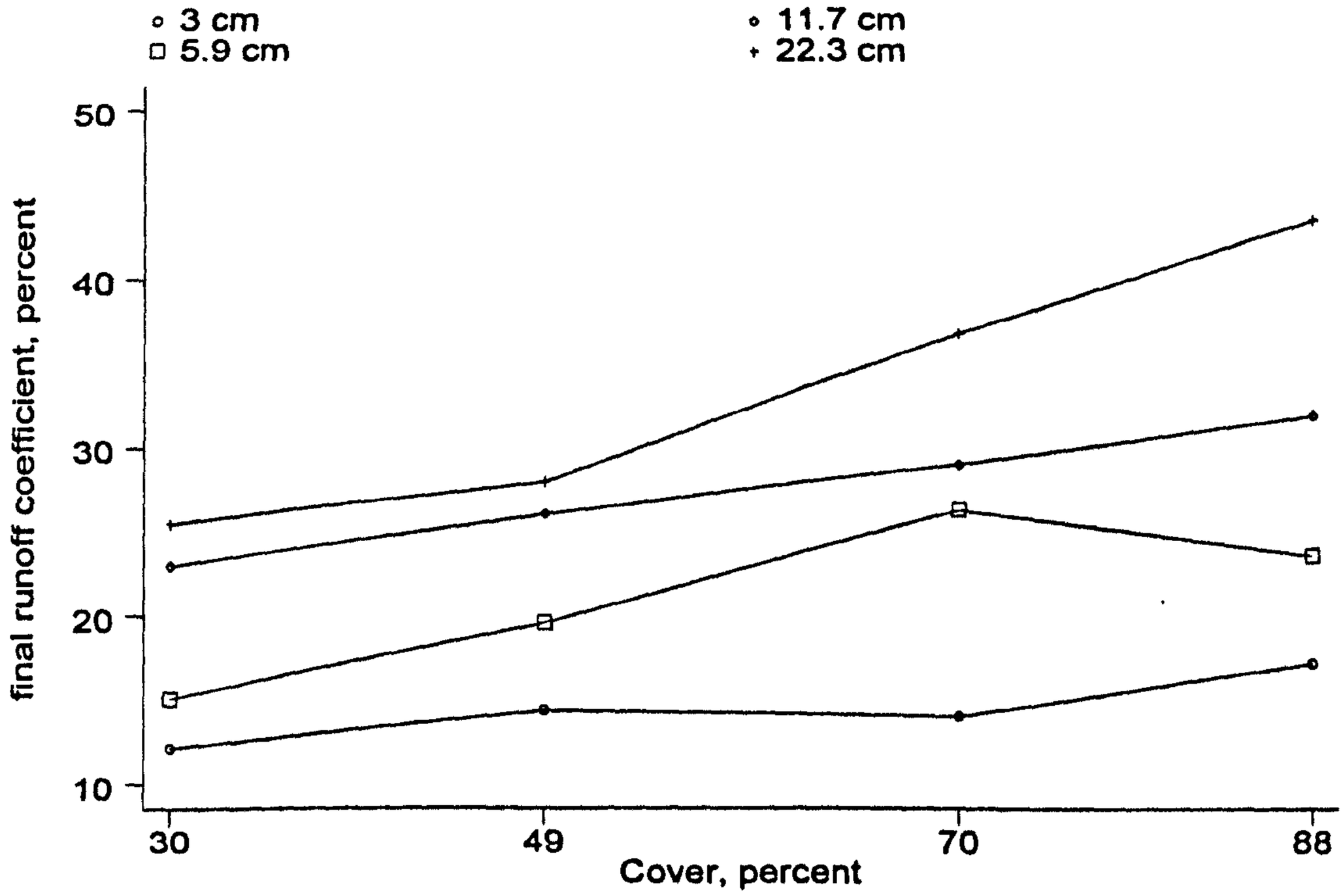

Figure 3.3: Effects of rock-fragment size and cover on final runoff coefficient. Rock fragments rest on the soil surface. Adapted from Poesen (1992)

The three key variables affecting the influence of rock fragments upon seal development and infiltration are size, percentage cover and the embeddedness of the rock fragments (Bunte & Poesen, 1994). Smaller clasts will tend to reduce the infiltration, while larger ones (>26 mm) encourage infiltration (Wilcox *et al.*, 1988; Brakensiek & Rawls, 1994). If the fragment is not embedded, the soil surface could absorb part of the rock flow and part of the Horton overland flow created on the soil seal surface. In addition, the reduction in raindrop impact means that the S.I. will be

low. However, if the rocks are embedded, the sealed surface is bonded strongly onto the edges of the fragment, resulting in a higher S.I. (Poesen, 1992). Lavee & Poesen (1991) and Poesen & Lavee (1991) give results on the combination of size and cover of fragments upon infiltration and the trend is obviously positive concerning both variables (Figure 3.3).

3.3.6 Influence of slope angle upon sealing and infiltration characteristics

Various authors have suggested negative linkages between surface seal development and slope angle. Unit area runoff volume, on a loamy soil, decreases with increasing slope gradient to a threshold of 12° (Poesen, 1984; Poesen & Govers, 1986). Poesen (1987) uses seal strength, as measured with a torvane, and seal index (S.I.) as two indicators to propose that increase in slope can be related to weaker and thinner crusts. He explains this by suggesting that the increase in surface wash, as slope angle increases, obstructs the full development of the seal. For short duration rainfall events there is a high negative correlation between runoff and slope, with a minimum value occurring at around 10°. As rainfall duration increases, runoff and slope angle take on a positive correlation (Luk *et al.*, 1993). Likewise on surfaces which are highly susceptible to sealing, infiltration rates generally increase, while crust strength decreases between 9% (5.1°) and the 20% (11.3°) slopes (Bradford & Huang, 1992). This was seen to be a result of several factors including increasing rill activity and stronger erosional influences (Bradford & Huang, 1992), smaller raindrop impact per unit area and associated reduction in the normal component of rainfall (assuming vertical fall) and a higher frequency of surface ponding on lower-angled slopes which increase the compactive energy of raindrops (Poesen, 1984; 1986). Differential cracking may also play a significant role in controlling runoff at different slope angles (Govers, 1991). If the distribution and strength of the surface crust vary downslope as it becomes more concave or convex, then that will affect the way in which runoff is generated and where infiltration will take place (Gascuel-Odoux *et al.*, 1996).

3.4 THE INFLUENCE OF SOIL CHEMISTRY UPON SEAL DEVELOPMENT AND INFILTRATION

Permeability of soil is a function of the square of the pore radius and the porosity or cross-sectional area available for flow. It follows that any process or treatment which reduces the overall porosity will have a dramatic effect on soil permeability and hence infiltration of rain or irrigation water. There is a set of physico-chemical processes which play a role in reducing the permeability of the surface soil layers. Under certain conditions clays will disperse and clog the pore space as the pressures between the silicate clay sheets increase due to chemical imbalance. The most important ion is exchangeable sodium (E.S.P.), which has a high propensity to develop in semi-arid and arid environments due to inadequate leaching, and causes repulsive interparticle forces within clays. Similarly, at low electrolyte levels (EC), of either the soil or the applied water, dispersion will take place. All are important considerations when determining how aggregates have broken down and the amount of pore clogging which has taken place during seal formation to create a distinct layer of reduced permeability. Consequently, consideration of clay dispersion and flocculation under different chemical regimes is necessary.

3.4.1 Dispersion of clay minerals and its effect upon infiltration

Flocculation and dispersion are vitally important in determining the physical behaviour of the colloidal fractions of soils and therefore implicitly affect the physical properties which soils exhibit, the chemical details of which are covered by van Olphen (1977). For many soils the dominant ion balancing the lattice charge is calcium. However, soils developed in semi-arid or arid environments may have appreciable quantities of sodium ions balancing the charge. The predominance of exchangeable sodium ions may adversely affect the physical attributes of the soil, including permeability (Quirk, 1986). The Exchangeable Sodium Percentage (E.S.P.) of the soil and the Electrolyte Concentration (E.C.) of the applied water have a considerable effect on the propensity for clay minerals within the soil fabric to disperse. Such a dispersion and re-orientation of the clay material within the available pore spaces causes the plugging of pore networks, the subsequent reduction in hydraulic conductivity and hence a permeability drop of the near-surface layers.

The crystals of clay minerals are composed of elementary silicate sheets stacked in the direction of the *c*-axis. The mica-illite and kaolinite crystals do not expand in water and therefore have a fixed *c*-axis. Montmorillonite and related smectite minerals swell as a result of hydration of the cations balancing the charge of the elementary silicate sheets.

The threshold concentration concept, which was initially developed by Quirk & Schofield (1955), has been used to determine the structural stability and permeability of the soil (Shainberg & Letey, 1984; Quirk, 1986). It is defined as the concentration in the percolating solution that would give rise to a 10-15% decrease in hydraulic conductivity at a given E.S.P. The difference in the observed threshold concentration between a sodium-saturated and a calcium-saturated soil is considerable. For the sodium-saturated soil only an EC of greater than 250 meq dm^{-3} is enough to keep it above the threshold limit. If concentrations as low as 50 meq dm^{-3} are used, permeability is reduced by over 60%. On the other hand, if the soil is saturated with calcium, then even the addition of distilled water would not reduce permeability more than 25%. The threshold in such a case occurs at about 0.2 meq dm^{-3} and at concentrations over 2 meq dm^{-3} the clays flocculate. However, there has been a lack of consensus among soil scientists on the limit for reduction in HC below which soil structure is adversely affected. Suggestions for an adequate limit include 15% (Quirk & Schofield, 1955), 25% (McNeal & Coleman, 1966) and 50% (Shainberg & Letey, 1984). Using a method of optical transmission (%T) to identify the stability of aggregates Abu-Sharar (1988) suggested that for a given S.A.R. there would be a critical concentration (CC) corresponding to maximum clay dispersion (minimum %T = 10) and a threshold concentration (TC) where there was very little dispersion (maximum %T = 20).

The difference between sodium and calcium in their capacity to cause flocculation is illustrated in Table 3.4. More recently, the whole concept of using the critical threshold as a measure of soil degradation has been challenged (Crescimanno *et al.*, 1995), because soil instability often takes place at lower values of E.S.P. This has led to suggestions that infiltration rates alone are a better and more sensitive indicator of E.S.P. than hydraulic conductivity (Shainberg & Letey, 1984). Furthermore,

Crescimanno *et al.* (1995) point out that the behaviour of soils at increasing E.S.P. appears to be a continuum rather than having any threshold values. In addition, Curtin *et al.* (1994) found that it was only with the input of high mechanical energy that distinct thresholds occurred, whereas with reduced energy, as would be expected in field conditions, the thresholds were absent.

Mineral	Background electrolyte	pH	CFC mol m^{-3}
Georgia kaolinite	NaCl	7	5.0
	$NaHCO_3$	8.3	245.0
	$CaCl_2$	7	0.4
Vermiculite	NaCl	7	38.0
	$NaHCO_3$	8.3	58.0
	$CaCl_2$	7	0.8
Illite 36	NaCl	7	9.0
	$NaHCO_3$	8.3	185.0
	$CaCl_2$	7	0.13

Table 3.4: Critical flocculation concentrations (CFC) for some clay minerals at a suspension strength of 0.6 g kg^{-1}. Source: Arora & Coleman (1979)

3.4.2 Dispersion versus mechanical processes

It is generally accepted that a high Sodium Adsorption Ratio (S.A.R.) and a low Electrolyte Concentration (Quirk & Schofield, 1955; Shainberg *et al.*, 1981) in the soil and soil water are associated with soil structural instability, seal development and degradation (Agassi *et al.*, 1981; Shainberg, 1985). Clay dispersion at the soil surface under the influence of impacting raindrops has been seen as playing a major role in the formation of a soil crust (Miller, 1987; Miller & Scifres, 1988; Shainberg *et al.*, 1989). Some consider that it is the clogging of pores immediately below the surface which gives rise to the washed-in zone (McIntyre, 1958; Gal *et al.*, 1984).

However, much of the research has looked at the indirect effect of S.A.R. and E.C. on infiltration rates, rather than focusing upon the different interactions of the physico-chemical processes involved (Rhoades, 1972). The properties of the seal are determined, in the most part, by the dispersion of clays which in turn constrains the final rate of infiltration. Abu-Sharar *et al.* (1987) state that *'At present we still do not have reliable criteria and standards for predicting a priori how these parameters quantitatively affect structural stability and hydraulic conductivity of soils'* (p. 309). The processes involved are the swelling of clays, clay dispersion with the subsequent plugging of connecting pores, and slaking of the aggregates.

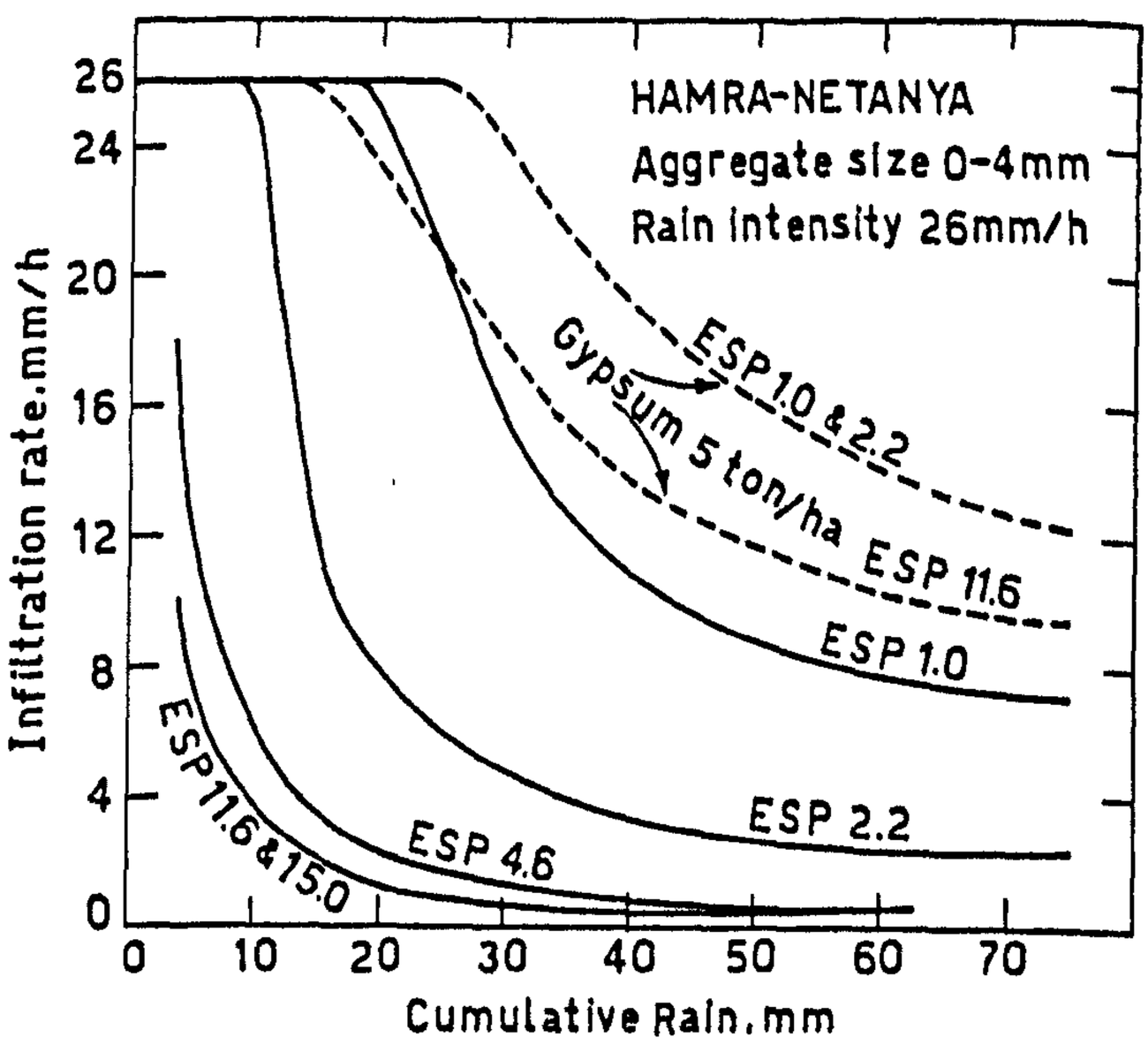

Figure 3.4: The infiltration rate of the Natanya soil as a function of cumulative rain: The effects of soil E.S.P. and phosphogypsum application.
Source: Kazman *et al.* (1983)

The EC of the applied water plays a significant role in the degree of crusting (Oster & Schroer 1979; Agassi *et al.*, 1981). Infiltration rates increase markedly as the EC of the water from the rainfall simulator increases from distilled to 5.6 dS m^{-1}. When low concentrations are applied, dispersion is the main process forming the crust, resulting in an almost complete reduction in final infiltration rate (FIR), whereas if concentrations are high, dispersion is reduced and the crust forms entirely by aggregate slaking, resulting in the maintenance of the FIR at 8-15 mm h^{-1} (Agassi *et*

al., 1981). By keeping EC and raindrop impact energy constant, that there is a considerable change in FIR as E.S.P. increases (Kazman *et al.*, 1983 - Figure 3.4) Even at very low levels of sodicity (E.S.P. = 1.0) crusting occurs causing the infiltration rate to drop from over 100 mm h^{-1} to a final infiltration rate (FIR) of only 7 mm h^{-1}.

A total of 2 g kg^{-1} dispersed clay (i.e. less than 0.8% of the total soil clay) is sufficient to decrease the hydraulic conductivity of the soil by 72% (Amézketa & Aragüés, 1995). In addition there are significant decreases in HC at higher ECs, which are explained by an osmotic explosion effect caused by steep gradients in EC between macro- and micropores (Shainberg *et al.*, 1981a).

Although clay dispersion is often upheld as the dominant physico-chemical mechanism, there is a body of opinion which suggests that other processes are equally important. For example, McNeal & Coleman (1966), Jayawardene & Beattie (1978) and Jayawardene (1979) concluded that swelling of soils was the dominant mechanism by which hydraulic conductivity (HC) is reduced. An alternative view, first proposed by Emerson (1964), is that soil aggregates when immersed in water often break down into discrete units. This process of slaking, which can proceed without prior clay dispersion, has been argued by Abu-Sharar *et al.* (1987) to be more important. At an S.A.R. of zero there is no ≤2 μm clay dispersion until the EC is reduced to 3.19 mol m^{-3} and none at the ≤1 μm level until the EC is as low as 0.28 mol m^{-3}. As EC is reduced, there is extensive slaking of larger into smaller aggregates along with a release of clay. Abu-Sharar *et al.* (1987) repudiate the mechanism proffered by Emerson & Bakker (1973), who suggest that clay is only dispersed from the periphery of aggregates, and instead propose that larger aggregates begin to slake along planes of weakness prior to dispersion. By measuring the optical transmission (%T) of suspensions of a Jordanian soil, Abu-Sharar (1988) concludes that slaking of soil aggregates into fine aggregates (2-5 μm) takes place without any clay dispersion. This means that the deterioration in soil structure and consequent reductions in HC could be attributed to the failure of aggregates, rather than the clay dispersion mechanism proposed by Shainberg *et al.* (1981a, 1981b).

3.4.3 Effect of conditioners and water quality on dispersion and crust formation

In order to reduce soil structural degradation and to retard the rate of both structural and depositional crust formation (Le Souder *et al.*, 1989), ways have to be found to overcome the mechanisms of seal formation and crust development, therefore maintaining a high infiltration rate. The main method is the use of conditioners, which are mixed in with the surface soil layers before or during irrigation and cultivation. These conditioners take on various forms including mineral conditioners, mulches, organic polymers and sewage sludge. In the past, large amounts of conditioner were applied at high cost, to improve soil structure. New strategies of application using various mixtures in smaller amounts have revived interest in controlling the development of crusts (Norton *et al.*, 1993).

Phosphogypsum applied at 5 Mg ha^{-1} , in order to release electrolytes into the percolating and runoff water and hence reduce clay dispersion, results in maintaining soil aggregate stability (Agassi *et al.*, 1990). Runoff is reduced by 75%, while erosion is reduced to only 1-3% of the original rate. Application of gypsum to the soil during tillage causes a considerable reduction in crust strength (Frenkel & Hadas, 1981), although the effect is exponential with the greatest differences occurring as strength increases. Others have disagreed suggesting that, due to a greater retention of clay in the surface layers, surface crust development increases (Borselli *et al.*, 1996a) and therefore seedling emergence reduces due to fewer cracks (Borselli *et al.*, 1996b).

Comparing the dissolution coefficients of mined and industrial gypsum and their relative effects upon infiltration into a sodic soil, Keren & Shainberg (1981) observe that industrial gypsum dissolves an order of magnitude faster than mined gypsum. The subsequent FIR using the mined gypsum is unable to counteract the effect of the sodic soil, except if the gypsum is ground to powder. However, for the industrial gypsum the infiltration rate increases between two and four times compared with the soil without gypsum. Le Souder *et al.* (1989) use an aluminium polycation which is sprayed onto the soil and adsorbs on negative clay sites to modify clay reorganisation and flocculation. Using micromorphological analysis, it can be observed that the

formation of the seal takes longer to develop with the conditioner and depositional crusts are absent.

While the addition of gypsum and mineral or organic polymers modifies the soil by protecting clays against the propensity to disperse, thus reducing crust formation and increasing hydraulic conductivity, mulches are used to protect the soil surface aggregates from raindrop impact. Mulches are effective in reducing raindrop splash by more than 92% and interrill erosion by 76% (Singer *et al.*, 1981). The preventing of raindrop impact by mulching maintains a relatively high permeability at the soil surface (Agassi *et al.*, 1985), although the best results come when mulching is combined with chemical amendments (Zhang & Miller, 1996a).

Organic polymers such as 'Super Slurper' (Hemyari & Nofziger, 1981), which is a hydrolysed starch polyacrylonitrile graft copolymer, more commonly Polyacrylamide (PAM) (Levy *et al.*, 1995; Trout *et al.*, 1995; Zhang & Miller, 1996b), as well as cationic polymers (Ben-Hur *et al.*, 1990), have all been used to increase permeability in soil crust conditions. The application of PAM is intended to stabilise soil aggregates by flocculating the clay particles. Its adsorption by clay minerals is therefore highly dependent upon the molecular size, conformation, charge characteristics of the polymer and the nature of the soil colloids such as external surface area and pore sizes (Letey, 1994). Polymers have been shown to be effective in increasing hydraulic conductivity (Helalia *et al.*, 1988) and porosity (Shanmuganathan & Oades, 1982). They also encourage flocculation (Helalia & Letey, 1988), which increases aggregate stability and therefore reduces runoff and erosion (Zhang & Miller, 1996b). PAM is widely used on arid soils where past irrigation with poor quality water has led to an increase in ESP and a reduction in soil stability. The addition of PAM to low EC water triples FIR, but when added to saline water its effectiveness is reduced to 35% (Levy *et al.*, 1995). PAM is able to control the development of runoff at low ESPs (<4), but is ineffectual at higher ESPs, but erosion is reduced at all levels. Trout *et al.* (1995) record a mean reduction in erosion of 70% and an increase in infiltration of 30%. Ben-Hur *et al.* (1990) reviewed the effectiveness of non-ionic, anionic and cationic polymers and found that the first two had little effect, but that the cationic polymer had a flocculating

action which compensated for the disruption of aggregates by raindrop impact. Hemyari & Nofziger (1981) measured the effect such polymers had on crust strength and found reductions of 84%, 75% and 54% for a sandy loam, a loamy sand and a clay loam soil, indicating that the largest reductions in strength occurred on the soils with the highest clay contents. Similarly, it was found that in sandy soils conditioned with gel, there were improvements in the soil hydraulic properties (Al-Darby, 1996) and a small decrease in crust strength, but only with saline application waters (Al-Omran *et al.*, 1991).

Both Shainberg *et al.* (1990) and Stern *et al.* (1991) compared the different effects of polymers, mulches and phosphogypsum (PG) and came to similar conclusions: PAM is more effective than PG. When they are mixed together infiltration is further improved (Figure 3.5).

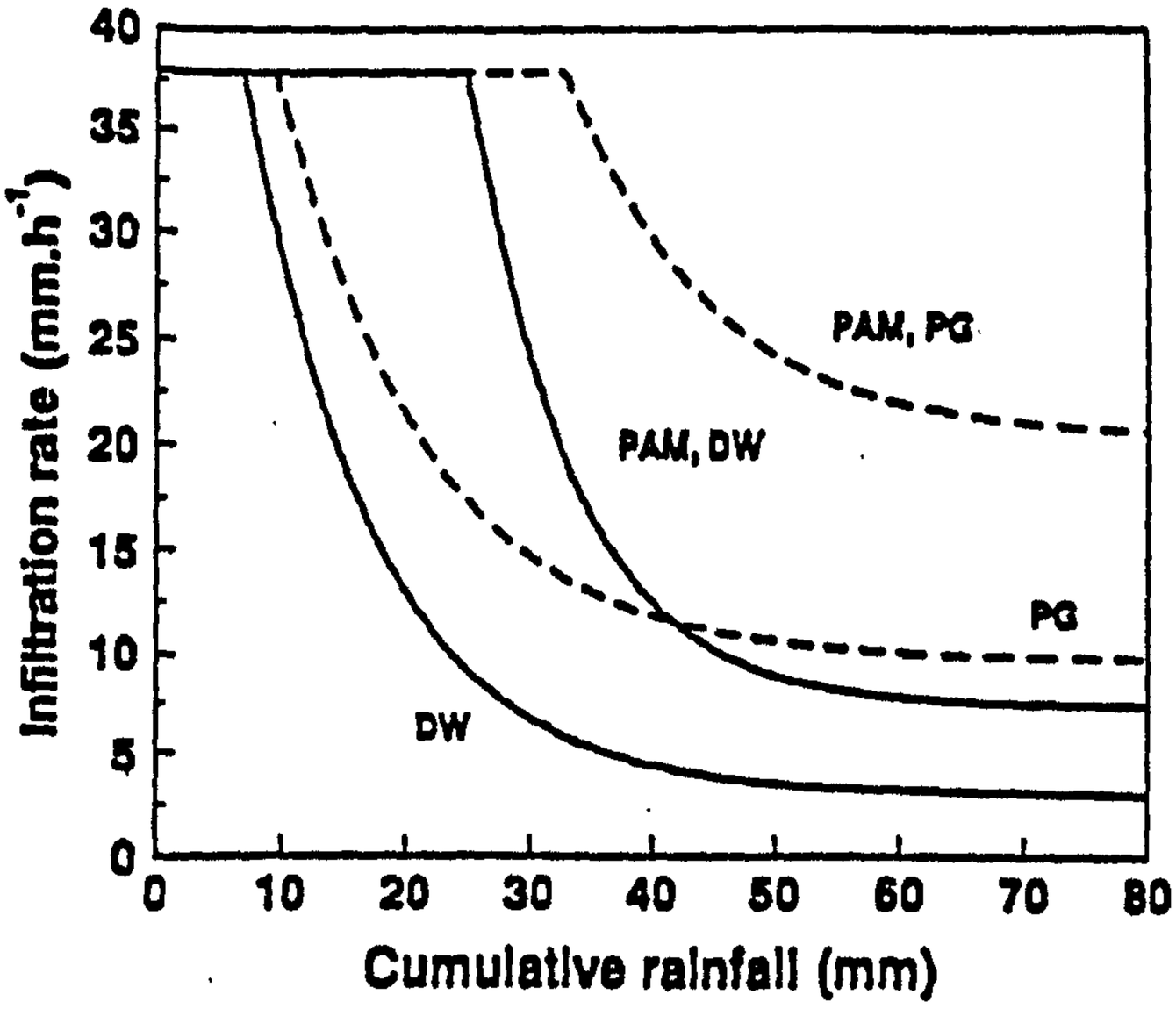

Figure 3.5: Infiltration rate of a grumusol as a function of cummulative rainfall, phosphogypsum treatment (PG, at 5 Mg ha^{-1}), and PAM application (at 20 kg ha^{-1}). DW = distilled water. Source: Shainberg *et al.* (1990)

Sewage sludge is another, rather underused method of increasing the aggregate stability of soils and reducing the propensity to seal (Pagliai *et al.*, 1983), although there has been evidence of toxicity and contamination if the sludge is enriched in heavy metals. However, municipal waste can be used effectively to increase the stability of soil aggregates by reducing clay dispersion (Abu-Sharar, 1993 - Figure 3.6.)

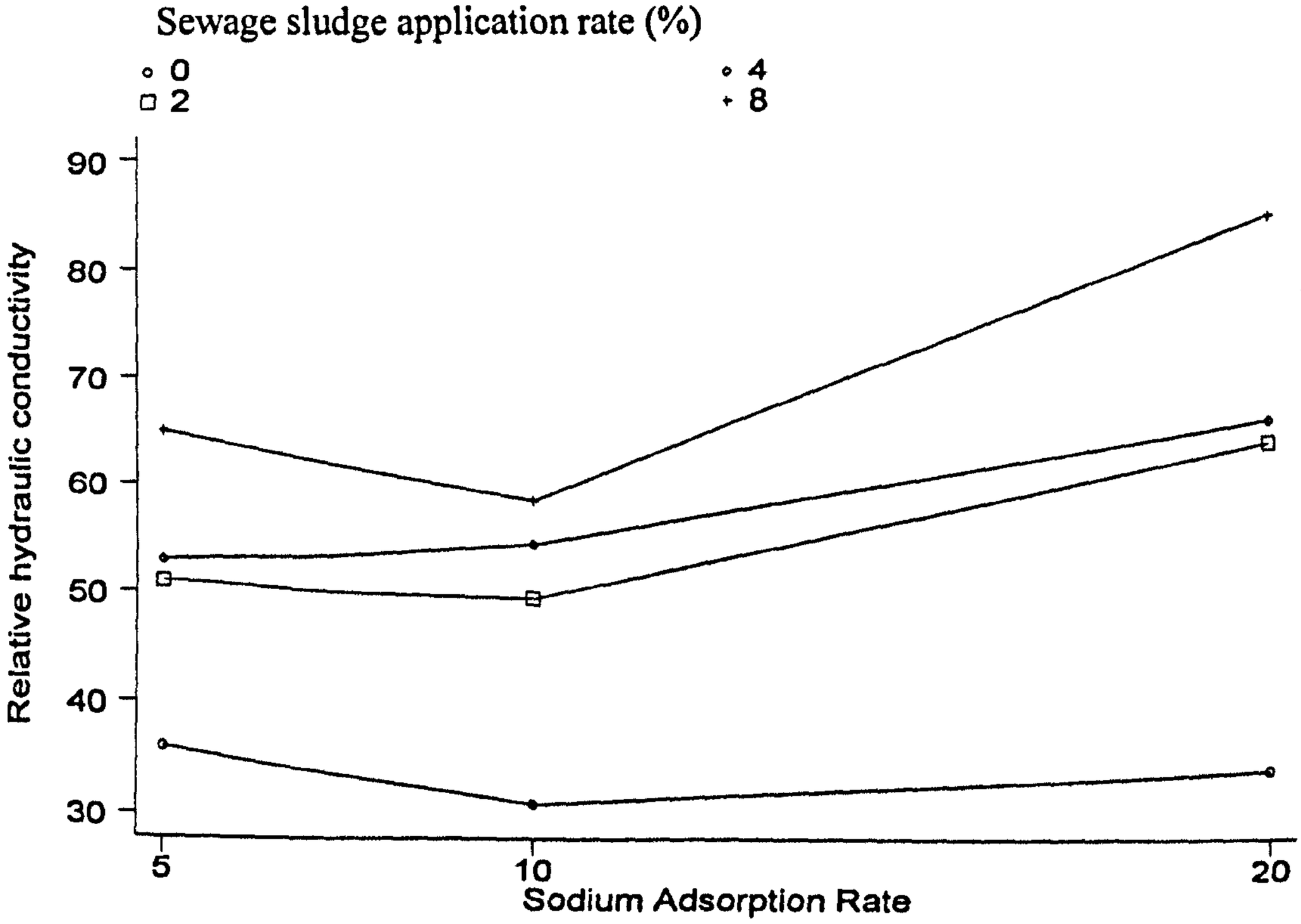

Figure 3.6: Relative hydraulic conductivity[a] associated with the clay threshold concentration at the respective SAR for sludge-amended soil samples from Jordan. Source: Abu-Sharar (1993).

[a] Percent of the corresponding maximum value obtained when initially permeating the most concentrated electrolyte solution.

The improvement in permeability is highly dependent on the type of conditioner applied (Abu-Sharar, 1996). Sewage sludge causes a greater increase in infiltration than gypsum, which in turn is better than cement dust while the application of phosphate rock has least effect (Abu-Sharar, 1996 - Table 3.5).

Treatment	Plot 1	Plot 2	Plot 3	Average
Control	4.86±0.13	3.29±0.15	3.75±0.19	3.97±0.68
Phosphate rock	5.03±0.27	5.68±0.00	5.03±0.66	5.25±0.51
Cement dust	10.54±0.49	10.96±0.00	9.86±0.28	10.47±0.56
Gypsum	22.05±0.18	21.11±0.04	19.51±0.54	20.89±1.10
Sewage sludge	42.61±0.00	39.91±0.45	38.48±0.23	40.33±1.74

Table 3.5: Steady state infiltration rate (mm h^{-1}) for the treatment plots as measured in summer 1992 using distilled water and a constant head device (average of 10 replicates), Jordan. Source: Abu-Sharar (1996)

3.5 SOIL CRUST FORM AND MICROMORPHOLOGY

Although the factors which combine to produce a soil crust are well known, the processes acting within the surface layers can usually only be identified by observing the morphological changes. Morphological analysis has been used from the very earliest research (Duley, 1939; McIntyre, 1958a, 1958b; Evans & Buol, 1968). However, because there is considerable variability in soil and rainfall characteristics in addition to methodological differences between scientists, there have often been divergent interpretations of the imagery. Any micromorphological description has the important limitation of scale. Spatial relationships that occur on a greater scale than the area of the sample (mm to cm) cannot be appreciated, which puts more responsibility on the sample collector. In addition, with such a dynamic process, it is impossible to make statements about processes if samples are only taken at the end of rainfall events. Changes in morphology occurring during earlier stages of rainfall are lost, such as the formation of microlayers which are later eroded (West *et al.*, 1992).

Theories involving the formation of soil crusts fall into two major categories, first properly defined by Chen *et al.* (1980), who defined soil crusts as either structural or

depositional. Structural crusts are formed by water drop impact and associated rapid wetting of the soil surface. Depositional crusts are formed by the translocation of fine particles and their deposition at a certain distance from their original location (Valentin & Bresson, 1992). More recently other terminology has been developed: disruptional rather than structural crust, because this type of crust is formed by structural disruption, and sedimentational rather than depositional, because this term has been used as a possible synonym to washed-in zone (Arshad & Mermud, 1988; Moore & Singer, 1990; Slattery & Bryan, 1994). Alternative terms such as lamellar crust have been defined to correspond with McIntyre's skin seal. However, the skin seal, which is often dominated by a strong continuous orientation of clay particles, is extremely thin (< 50 μm) and is probably better defined as an afterflow seal (Slattery & Bryan, 1994), as it forms over depositional and structural crusts by fine particle deposition after rainfall cessation rather than by raindrop impact. The processes leading to the formation of structural crusts may well act simultaneously with those leading to depositional crusts. However, in order to investigate one particular process, the processes have often been treated separately. While most research has focused upon the formation of structural crusts, some have recently questioned such a focus: Morin & Van Winkel (1996) argue that all the processes involved in forming a structural crust increase the sediment availability in sheet wash, so that depositional crusts will subsequently form downslope. The most comprehensive classification to date is that of Valentin & Bresson (1992 - Table 3.6).

3.5.1 Comparative micromorphologies of temperate and arid soil crusts

Certain types of crust are more likely to develop in temperate environments (Mücher & De Ploey, 1977), while others will have a tendency to occur only in arid ones (Chen *et al.*, 1980) (Table 3.6 & Figure 3.7). Arid topsoils, dominated by silt and clay, are very similar to those which occur under temperate conditions. In sandy soils, several specific crusts develop, which occur almost exclusively in arid conditions (Bresson & Valentin, 1990).

Table 3.6: Classification of soil crusts according to morphology, genesis and environment. Source: adapted from Valentin & Bresson (1992)

Group	Type	Description of the crust	Environment
Structural crusts	Slaking	Thin layered, porous with a weak void interconnection. No clear textural disjunction. Aggregate slaking and microcracking are the dominant processes.	Soils with low aggregate stability, loamy cultivated soils, arid soils.
(Disruptional)	Infilling	Bare silt grains which clog the interaggregate interstices and form a net-like filling. The silt grains are deposited deeper into the packing voids, thus reducing infiltration.	Indicative of slow erosion of the surface aggregates creating a large amount of illuvial silt. Usually in temperate areas with low rainfall intensities.
	Coalescing	Thick crusts with increasing void convexity towards the soil surface. The result of gradual compaction due to aggregate coalescence by deformation under plastic conditions.	Observed in wet soils under rainfall with high kinetic energy.
	Sieving or filtration	Layers of loose skeleton grains overlying a plasmic layer. A gradual fining downwards from coarse to fine particles.	These develop in sandy soils under tropical climatic conditions.
Depositional crusts	Runoff	Typically apedal, very compact and characterised by a microbedded layer. Fine beds of alternating particle size are contrasted in texture and unconformable with the soil beneath.	Often overlay structural crusts. Regularly found in poorly sorted soils. In topographic lows where energy is rapidly dissipated.
(Sedimentation)	Still or puddle	Consists of densely packed and well-sorted particles, the size of which gradually increases with depth. The fine upper layers break up into curled-up plates upon drying.	Crusts that form in standing water, where the particles have been able to sediment out of solution.
Erosional crusts	Skin seals or plasmic layer	One rigid, thin and smooth surface layer enriched in fine particles. Voids are generally restricted to cracks and vesicles.	Eroded structural crusts by wind or overland flow where a dense plasmic layer has first been formed.
Biological crusts	Cryptogamic	The strengthening of soil aggregates or existing soil crusts by certain algae or fungi which stabilise the soil by exuding mucilaginous material, often forming pedestal features.	Can occur anywhere where there are micro-organisms.

Source: adapted from Valentin & Bresson (1992)

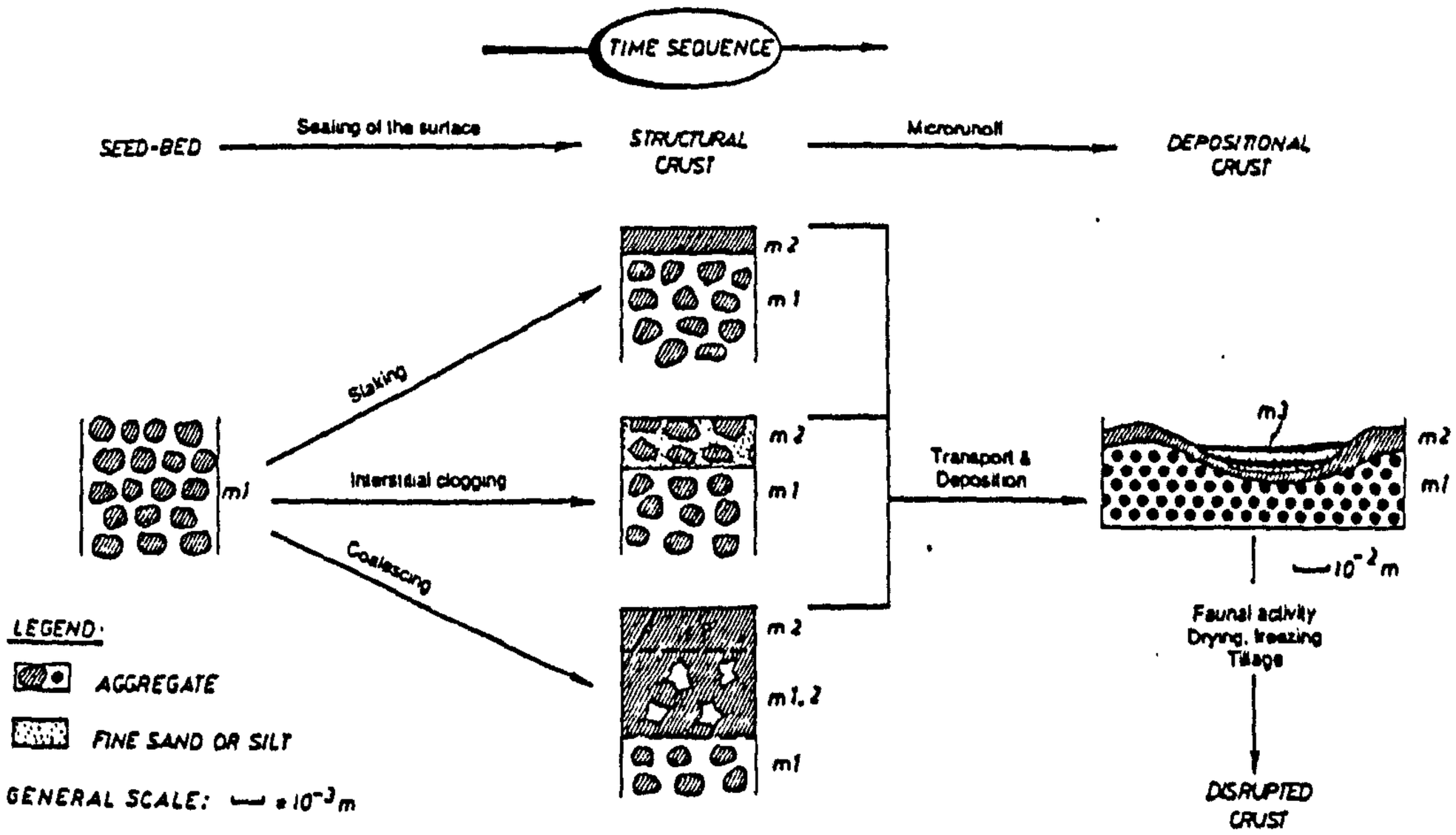

Fig 1: Crusting pattern in temperate areas (loamy cultivated soils)

Fig 2: Crusting pattern in arid areas: sandy pasture soils

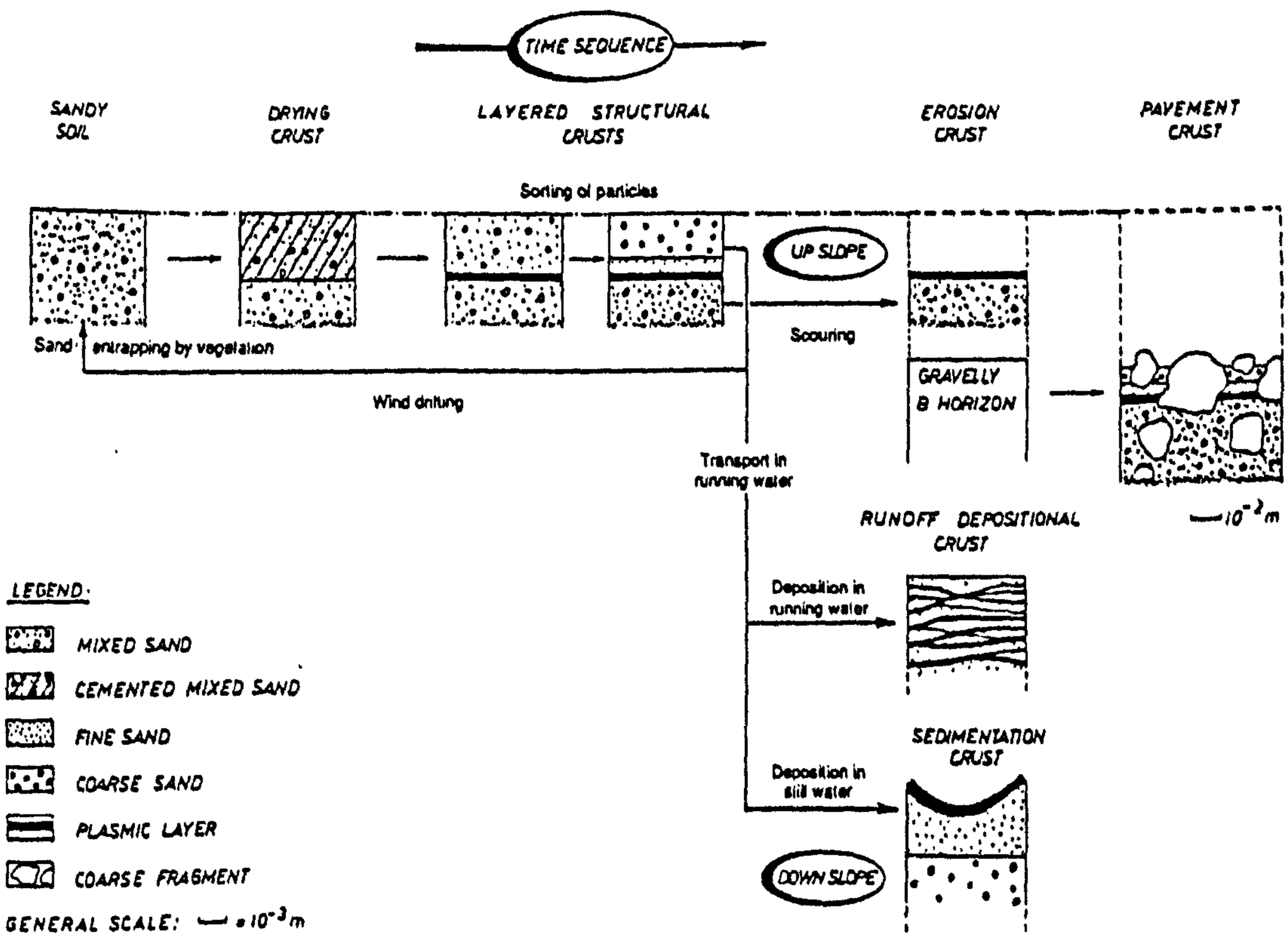

Figure 3.7: Crusting patterns in temperate and arid regions.

Source Bresson & Valentin (1990)

The drying crust occurs on soils where the surface is protected from raindrop impact by vegetation. Surface structural changes are restricted to a slight cementation of the upper millimetres due to repeated wetting and drying. The layered structural crust consists of a layer of loose grains overlaying a plasmic seal which, in its most advanced form, Valentin (1991) categorises as filtration pavement (three layer crust). The uppermost layer consists of loose, coarse grains, the middle layer is made up of fine, cemented grains with vesicular voids, and the lower layer is a plasmic seal which is finer, more oriented material with a much reduced porosity (Valentin, 1981). The erosion crust refers to the plasmic layer remaining after the removal of sandy layers by wind and water erosion. The fourth category of arid sandy crust formations is the runoff depositional crust (Bresson & Valentin, 1990). These consist of several alternate sorted micro-beds, with a more or less inter-bedded orientation. They are often a few centimetres thick and often lie above structural crusts in the base of furrows. Sedimentation crusts consist of densely-packed, well-sorted particles, the size of which progressively increases with depth.

3.5.2 Biological crusts

Whatever the type of crust, whether it be erosional or depositional, it may be strengthened by certain algae or fungi. Microphytes are often associated with soil surface crusts (West, 1990) and have been seen to play a major role in the initiation of crust development (Johansen, 1993). Soil scientists have largely ignored or played down the role of organisms in the formation process, despite the importance attributed to them by biologists and ecologists. Some microphytic crust organisms, particularly the cyanobacteria (e.g. *Microcoleus vaginatus, Chlamydomonas acidophilia*), exude mucilaginous materials that glue the organisms, organic matter and soil physical particles in place (Campbell *et al.*, 1989), but destroy alumino-silicates (Kovda, 1980). Others are more filamentous (e.g. *Nostoc commune and Lyngbya* sp.) and bind particles by entanglement (McKenna Neuman *et al.*, 1996). Because microphytic crusts variously cover landscapes with generally sparse vascular plant growth and litter, but high rates of natural erosion, it has been appealing to assume that soil surface microphytes slow down both wind and water erosion. There have indeed been numerous qualitative statements which suggest such a connection (Mücher, 1988;

Campbell *et al.*, 1989), but much of the research has not been supported by evidence from well-designed experiments (West, 1990). Recent work has begun to quantify the importance of different microphytic species on interrill erosion, infiltration capacity (Williams *et al.*, 1995) and wind erosion (McKenna Neuman *et al.*, 1996). The research suggests that microphytic crusts are vital in the stabilisation of the finer soil fractions (Williams *et al.*, 1995), while McKenna Neuman *et al.* (1996) conclude that on sandy soils only the filamentous algae can protect the soil surface against wind erosion. The formation of pedestal features in areas colonised by microphytic crusts confirms that surrounding uncolonised crust will be more prone to erosion (Casenave and Valentin, 1989). Such crusts consist of either mineral layers with a small amount of associated algae or cryptogamic crusts which are made up of continuous cryptogam mats (Mücher *et al.*, 1988).

The influence of microphytic crusts has often been overlooked and yet, especially in the case of arid zone soils, they are a very important natural mechanism for protecting the soil surface. An almost negligible amount of water is needed for their colonisation and yet they are fragile and very susceptible to tillage, grazing and vehicle compaction, taking many years to recover from disturbance.

3.5.3 Changes in the soil surface characteristics

Most of the soil crusting literature has concentrated either on the processes involved in the formation and development of the seal or on its effects on infiltration, runoff and erosion. Much less attention has been given to the change in morphology of the soil surface as a result of the formation of a seal or the micro-scale spatial distribution of surface crusts. Various scientists have attempted to divide seal formation into distinct periods, each defining a specific stage of the process and consequently a specific morphology (Chen *et al.*, 1980; Moore & Singer, 1990; Le Bissonnais & Singer 1992; Le Bissonnais & Singer 1993). Stage I refers to the time period from the beginning of rainfall to the initiation of runoff. Stage II lasts until runoff has reached steady state. Stage III defines the period after steady state runoff has been established (Chen *et al.*, 1980). The stages will be profoundly affected by

the initial water content (Le Bissonnais & Singer 1992) and it is possible that soils under experimentation will not reach Stage III (Le Bissonnais & Singer 1993).

Changes in surface roughness during rainfall events have long been identified and correlated with changes in infiltration (Steichen, 1984), runoff (Cogo *et al.*, 1983), erosion (Johnson *et al.*, 1979) and more recently with antecedent soil water content (Rudolph *et al.*, 1997). Surface roughness controls the spatial surface processes and in return, the surface processes also change the surface topography, displaying an inseparable interaction (Bradford and Huang, 1992). Changes in surface roughness have an important impact upon water and wind erosion (Saleh *et al.*, 1997). As the surface changes microtopographic highs and lows change, allowing an evolving spatial distribution of different crust types (Bielders *et al.*, 1996). With new instruments that can measure down to the millimetre scale, such as laser scanners (Römkens *et al.*, 1988; Huang & Bradford, 1990; Magunda *et al.*, 1997) and close-range photogrammetry (Jeschke, 1990; Helming *et al.*, 1993; Merel, in press), it has been possible to identify precisely changes taking place as the crust forms over single or multiple rainfall events. Such equipment gives a height resolution of approximately 0.2 mm (Helming *et al.* 1993; Huang & Bradford, 1990).

The initial change in microtopography causes the surface roughness to increase with rainfall. The fine material consolidates in the interstices, while the larger scale roughness produced by the larger clods remains unchanged. As the soil aggregates continue to slake on the impact of raindrops (Le Bissonnais *et al.*, 1989), and as clay dispersion takes place due to the low electrolyte content of the rainwater (Norton *et al.*, 1993), the small micro-aggregates and primary particles become oriented and organised into a crust (Farres, 1978) by interstitial filling (Boiffin, 1986). Microtopographic highs tend to be lowered over time, so that the locations and potential for ponding decrease and therefore infiltration becomes more indistinct and eventually disappears, thus increasing overall runoff (Magunda *et al.*, 1997). Zobeck and Onstad (1987) reported a positive correlation between random roughness and cumulative precipitation.

Results obtained by Helming *et al.* (1993) suggest that the random roughness coefficient (RRC) decreased by about 12% after rainfall for an initially rough relief, but there was a 43% decrease in RRC for a surface which was initially finer. The propensity of a soil to crust also depends upon the initial clod size (Rudolph, 1997). Farres (1978) found that a clod of 3.3 mm diameter takes much longer to crust than one of 6.7 mm, although Zobeck and Popham (1992) found that aggregate size and crust cover were not affected by geometric aggregate diameter. Although under high energy raindrop impact conditions most aggregates will eventually break down, large surface aggregates and primary particles (>1000 μm) actually reduce the possibility of crusting by allowing surface pores to persist, and consequently encouraging hydraulic penetration (Moss, 1991b). Bradford & Huang (1992) disagree that decreasing roughness automatically follows from an increase in rainfall. They suggest that the initial surface condition and controlling processes are more important. For example, if there is a flat surface, surface roughness will always decrease, but for soil on 9% and 20% slopes there is progressively more roughness because erosion is more important than crusting. For soils containing rock fragments, surface roughness changes become more complex still (van Wesemael *et al.*, 1996), with an overall increase in RRC for all sizes of rock block, although for the smallest (1.7-2.7 cm) fragments an initial decrease was observed.

The importance of surface roughness for soil crust research is that it has implications for agricultural management, with specific reference to tillage methodologies (Allmaras *et al.*, 1967; Römkens & Wang, 1984). If the soil preparation involves creating a rough surface, then infiltration will continue to be high, even on steeper slopes, but if the method creates a fine flat surface, then crusting will dominate. Linden & Van Doren (1986) introduced two surface configuration parameters of clod inclination and average relief to determine the importance of roughness on transport and erosion.

3.6 THE EFFECT OF SOIL CRUSTING UPON WATER FLUXES AND HYDRAULIC CONDUCTIVITY

3.6.1 Physical properties affecting infiltration

In soils displaying stable surface aggregates, there is an inevitable decrease in the infiltration capacity as a result of the reduction in the matric suction gradient that occurs as infiltration proceeds (Hillel, 1980). Generally, the infiltration rate (IR) is high during the early stages of infiltration, particularly when the soil is initially dry, but decreases to approach a constant rate asymptotically, due to a reduction in the matric suction gradient which occurs as infiltration proceeds (Shainberg & Levy, 1996). In the initial wetting, the surface becomes saturated, while the sub-surface layers remain dry and hence the matric suction gradient is great. As the wetting zone deepens, the gradient is reduced. However, the infiltration of water into bare soils will be vastly reduced if a seal forms on the soil surface (Morin & Benyamini, 1977; Ben-Hur *et al.*, 1987; Morin *et al.*, 1989; Morin & Kosovsky, 1995). The nature of the soil surface will be the main control upon the reduction in infiltration through the particle size distribution (Poesen, 1984; Moss, 1991a), porosity (Ela *et al.*, 1992), soil chemistry, stability of the soil aggregates (Farres, 1978), the roughness of the surface (Falayi & Bouma, 1975; Steichen, 1984), bulk density of the resulting crust (Saleh, 1993), and dominant clay mineralogy (Sumner, 1992; Mermut *et al.*, 1997), although the chemistry of the applied water is also important (section 3.4).

3.6.2 Modelling approaches to infiltration through crusted soils

Infiltration of water, whether it be rain or irrigation water, through the top few millimetres of the soil has always been at the forefront of soil crust research. The infiltrating water acts as the medium in which dispersed aggregates are taken down the profile to provide a washed-in layer. During this century various scientists have attempted to model infiltration into soils and more recently into crusted soils. Models have tended to revolve around analytical and empirical approaches (Horton, 1940) and numerical solutions (Green & Ampt, 1911; Richards, 1954; Philip, 1957). Analytical difficulties in solving the Richards equation for composite domains have limited studies to numerical solutions on the one hand or solutions based on drastic

simplifications of the original problem on the other. The problem arises because infiltration begins at time zero with a simple 3-dimensional movement of water through the profile, but with small increases in time there is a considerable change in the boundary conditions as a seal develops. As has been discussed previously, this change is gradual and highly dependent upon intrinsic and extrinsic factors. Hydraulic conductivity (K) of the near surface-pores is rapidly reduced creating a two-layered medium, with the surface FIR tending to 0, but with the subsoil FIR remaining high. Ponding follows the decrease in K, causing a distortion in the energy impact of raindrops and affecting the pressure of water on the surface.

The Green-Ampt approach with flux conditions through the seal has been used to acquire an analytical solution for infiltration, assuming hydraulic resistance of the seal increased exponentially with time (Farrell & Larson, 1972). However, soil water suction and hydraulic conductivity were assumed to be temporally constant below the seal. Similar assumptions were used by Brakensiek & Rawls (1982), who used a weighted average conductivity in the Green-Ampt formulation, rather than a flux condition. For a high rainfall rate and certain other assumptions, a similarity of wetted profiles exists in the early stages of infiltration through a seal (Ahuja & Römkens, 1974). Hortonian approaches to infiltration were found to be more closely matching to laboratory and field experiments under simulated rainfall by using an exponential decay equation (Morin & Benyamini, 1977; Morin & Cluff, 1980). The increasing resistance is a function of cumulative kinetic energy of impacting rainfall. A Green-Ampt type solution for infiltration through a stable crust was obtained, but again soil water suction and hydraulic conductivity had to be assumed constant (Hillel & Gardner, 1970). Only in 1983 was a model developed in which these two parameters were incorporated when Ahuja (1983) developed two new Green-Ampt type equations for predicting infiltration through a stable crust. More recently Aboujaoudé *et al.* (1991) looked at a finite-difference numerical solution of the Richards equation for one- and two-dimensional flow. In the first of their two models the crust is assumed to be instantaneously saturated and has an impedance characterized by a hydraulic resistance. The second model considers the underlying soil as well as the crust in a

two-layered system. Most of the above studies assumed that the crust was initially saturated and subsequently Hillel and Gardner (1969) modeled the infiltration by

$$q = -K\left(\frac{h_{ex} - h_N + e}{e}\right),$$

where q [ms^{-1}] is the infiltration flux density through the crust,

K [ms^{-1}] is the hydraulic conductivity of the crust,

e [m] is the crust thickness and

h_N and h_{ex} [m] are the effective pressure at the interface, and at the crust surface.

In the field, crust thickness need not be constant. In fact microtopography studies have shown that crust thickness even at the scale of a furrow can have significant spatial variability (Bielders *et al.*, 1996). At such a scale, use of a one-dimensional flow model to describe infiltration is questionable.

3.6.3 The evaporation of water from soils

The study of water movement in soils has generally focused upon infiltration and although it is known that much water is lost through evaporation, especially in semi-arid and arid environments, little research has been carried out (Rose, 1996). The vapour pressure of water in moist soil differs little from that of free water (Marshall & Holmes, 1988). Accordingly, the rate of evaporation from initially saturated soils is constant under given atmospheric conditions (Bond & Willis, 1969). Laboratory experiments using soil columns (Gardner & Hillel, 1962; Gardner & Gardner, 1969) have been shown to be in agreement with the non-linear desorptive diffusion equation proposed by Gardner (1962),

$$E_t = -\frac{dS}{dt} = \frac{D(S/L)S\pi^2}{4L^2}, \qquad \frac{Dt}{L^2} > 0.3,$$

where S is the depth of stored water between the soil surface and some depth L,

E_t is the evaporation rate and

D is the soil diffusivity, which itself is a non-linear function of soil water content.

Despite the difficulties in the natural spatial variability in soil water content (Nielsen *et al.*, 1973; Biggar and Nielsen, 1976), it has been seen that the simple model described the field-scale water transport well (Parlange *et al.*, 1993). However, the only field experiments looking at the simultaneous redistribution and evaporation of water after its application either concentrate on one soil (Gardner *et al.*, 1970) or use non-destructive techniques for measuring water content, which are unable to define adequately the fine resolution changes in soil moisture (Gardner *et al.*, 1970; Parlange *et al.*, 1993).

The upward movement of water through soil is easier on one level to conceptualise than infiltration because issues of ponding and changes in the soil surface characteristics avoided. However, just as the presence of a mulch (Bond & Willis, 1969; Gill & Jalota, 1996) reduces evaporation, then it is likely that a surface crust also helps to retain water in the soil (Bresler & Kemper, 1970). Just as the presence of a crust complicates the numerical and analytical modelling of infiltration (Section 3.6.2), the same is likely for evaporation from a multi-layered soil column as similar changes in boundary conditions have to be imagined. Although water in the crust itself will evaporate quickly because of an increase in its conducting capacity, water cannot be drawn up to the surface from under the crust because of the destruction of the soil structure and specifically the conducting pores (Bresler & Kemper, 1970).

3.7 CONCLUSION

It is apparent that there is still much which is not known about infiltration processes into soils and that, despite many different approaches to the problem, there is no one convincing model.

There are differing opinions which relate to the formation of seal and crust development. It can be seen as a highly complex set of mechanisms which relate to the geomorphological context, the climate, hydrological attributes and the pedological, as well as human influence through conditioner use and agricultural practice. It is important that the methods of data collection and analysis are appropriate to the process that is to be elucidated. As the research in this thesis includes a large amount of soil micromorphology, it is important to get the temporal and spatial scales correct. It is also important to consider how to constrain specific variables during field measurements. Much of the work reviewed in this chapter refers to laboratory simulations rather than work in the field. Such factors as the water chemistry used in a rainfall simulator, not to mention the actual methods of rainfall simulation, are easy to overlook. The following chapter seeks to address such problems discussing the methodology which underpins the research.

4. FIELD AND LABORATORY TECHNIQUES

The intensity with which a soil must be sampled to estimate with given accuracy some characteristic will depend on the magnitude of the variation within the soil population under consideration. (Petersen & Calvin, 1986)

4.1 INTRODUCTION

In recent years, attention in geomorphology has been turning from a more traditional form - process understanding of earth surface properties to material properties (Allison, 1996). While geomorphology has concentrated significantly on explanations of process-form interactions, other disciplines, such as soil science, civil engineering, engineering geology and geology, have been focusing on either material-form or material-process relationships. Such philosophical assumptions in each subject area lead to an inability for interdisciplinary communication which is sorely needed if scientists are going to be able to understand landscape processes. There is pressure upon geomorphologists to take material properties into account and likewise there is pressure exerted by geomorphologists, which can be seen in Allison's (1997) recent argument that process-form interactions are vitally important to the engineering geology community. It is no longer enough to say that a certain process working at a certain scale in the landscape will produce a specific form. It is therefore simplistic to suggest that the process of mechanical impact of raindrops upon a soil surface will produce a smoother, denser soil surface layer or form, which will in turn affect other processes such as infiltration, ponding, runoff and erosion. Chapter 3 has sought to identify many of the complex material properties, both physical and chemical, which are important temporally and spatially in producing different types of crust.

It is important when studying soil crust sediments to carry out a series of analyses to examine the material physical and chemical attributes. In many cases standard methods of analysis can be adopted. For the purpose of this study new techniques have been developed to examine specific phenomena. Finally, there are some situations where standard methods have been adapted to meet specific needs associated with this research.

4.2 Field Surveying and Sampling Framework

The most northerly farm known as High Farm (section 2.9 and Figure 2.10), which lies on the eastern edge of Al-Rafai'at, has the most complex geomorphology of the three studied (Figure 4.1). Drainage is to the north and west with the highest part of the farm lying in the south-east. There is a complicated basin in the middle of the farm which encourages some internal drainage. Slope angles are small, which means that the different aspects have little appreciable effect upon wind and water erosion. The Middle Farm lies on the outskirts of Umm Hussein and is about 5 km south of Al-Rafai'at. The well is situated at the top of a small hillock and drainage tends to radiate from the summit (Figure 4.2). The slopes are more clearly defined than on High Farm with steeper gradients, but they are also complex. The Low Farm, which lies on the Mafraq - Safawi road in the village of Ashrafia, is the simplest in slope form, with the main fields sloping from the east and west into a small wadi (Figure 4.3). The High and Middle Farm soils were classified as *Xerocreptic Camborthids* and the Low Farm soil was classified as a *Typic Calciorthid* (El-Rihani *et al.*, 1993). A detailed field survey was undertaken to establish the precise topography of each site and decide on the level of detail needed for sampling and analysis. One site had to be selected for particular plot experiments and therefore a site with simple slope characteristics needed to be established. Hence, Low Farm was chosen for more detailed sampling framework, while the Middle and High Farms were used to corroborate and reinforce the data collected from Low Farm.

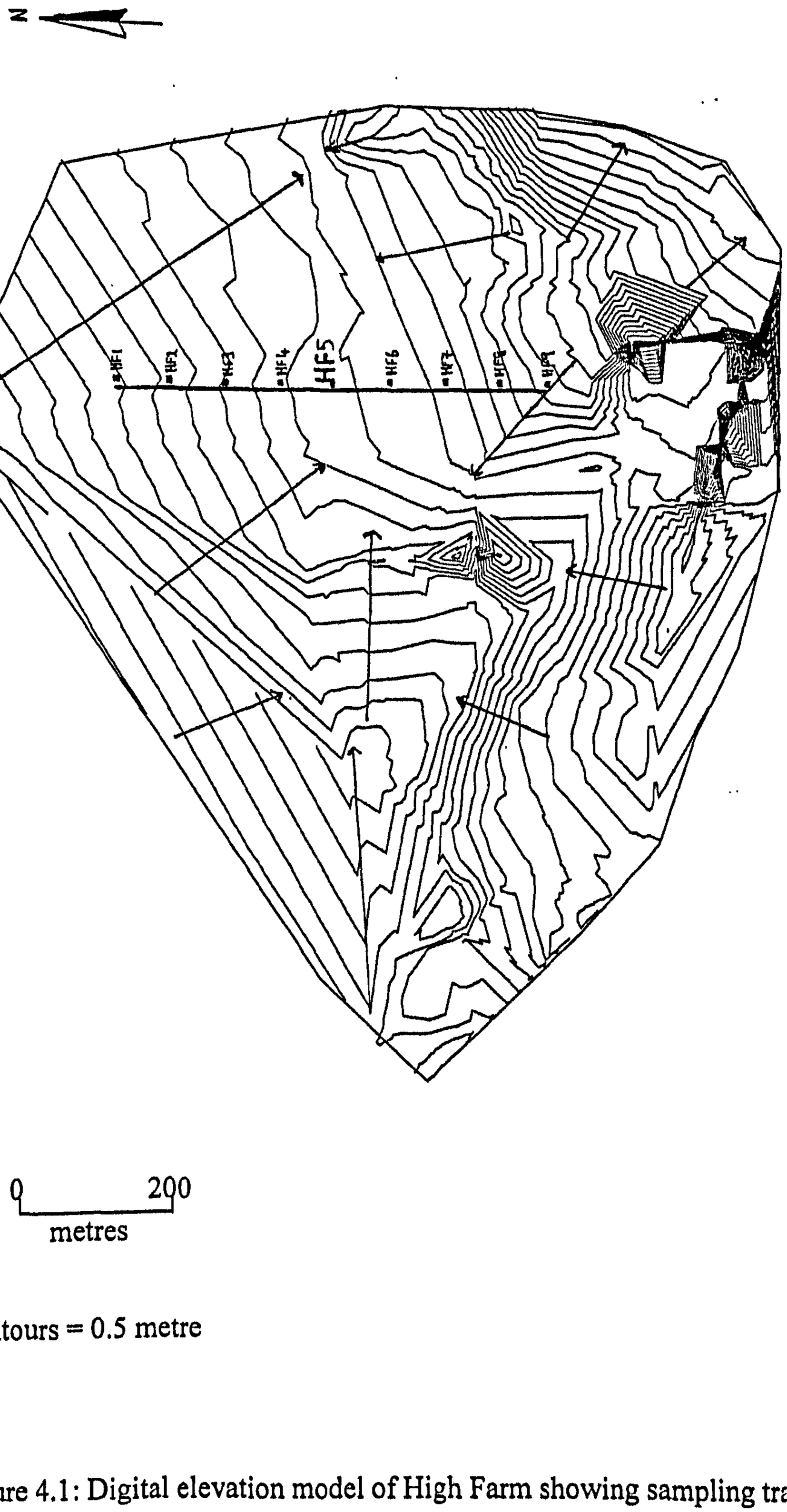

Contours = 0.5 metre

Figure 4.1: Digital elevation model of High Farm showing sampling transect

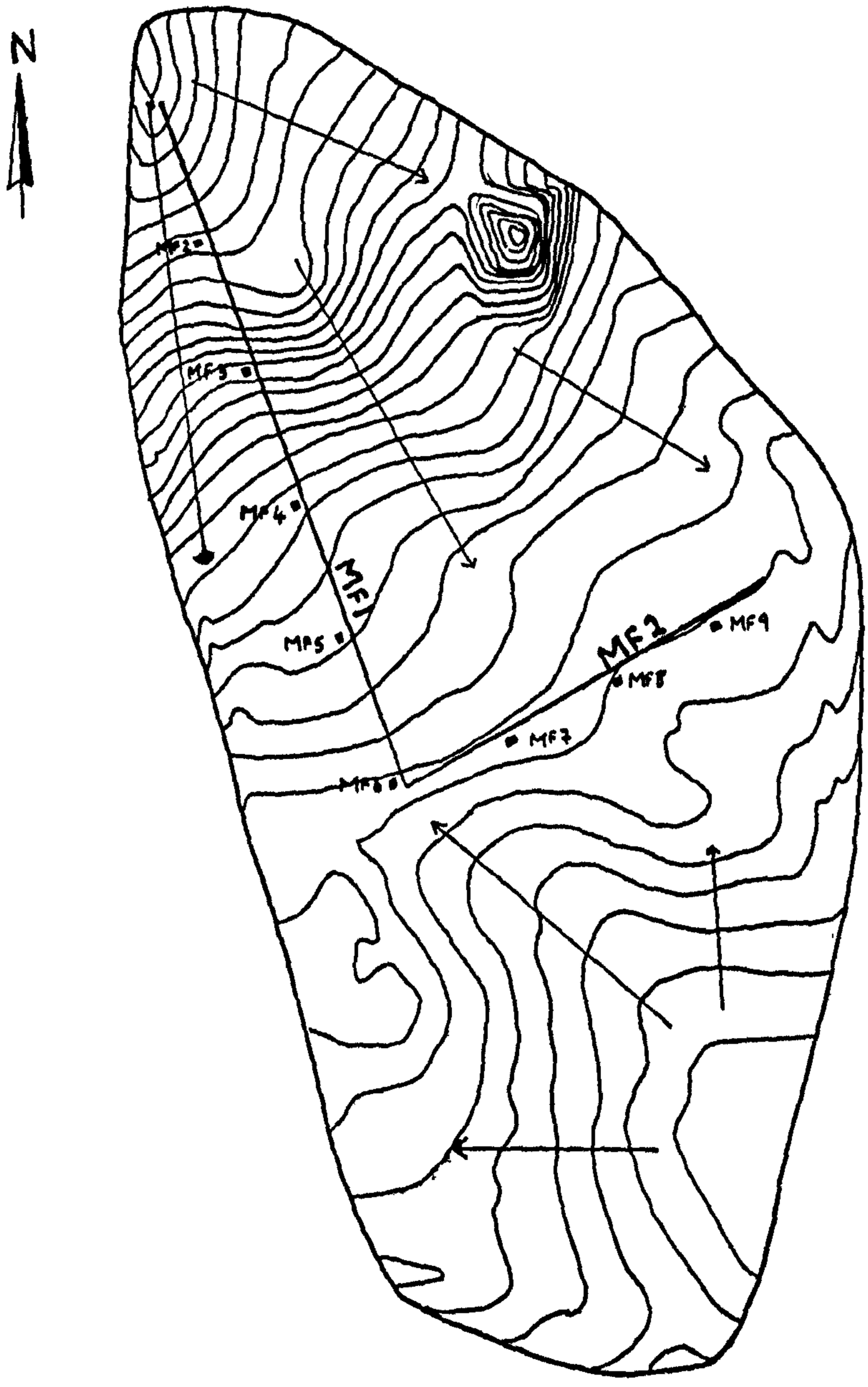

Figure 4.2: Digital elevation model of Middle Farm showing sampling transect

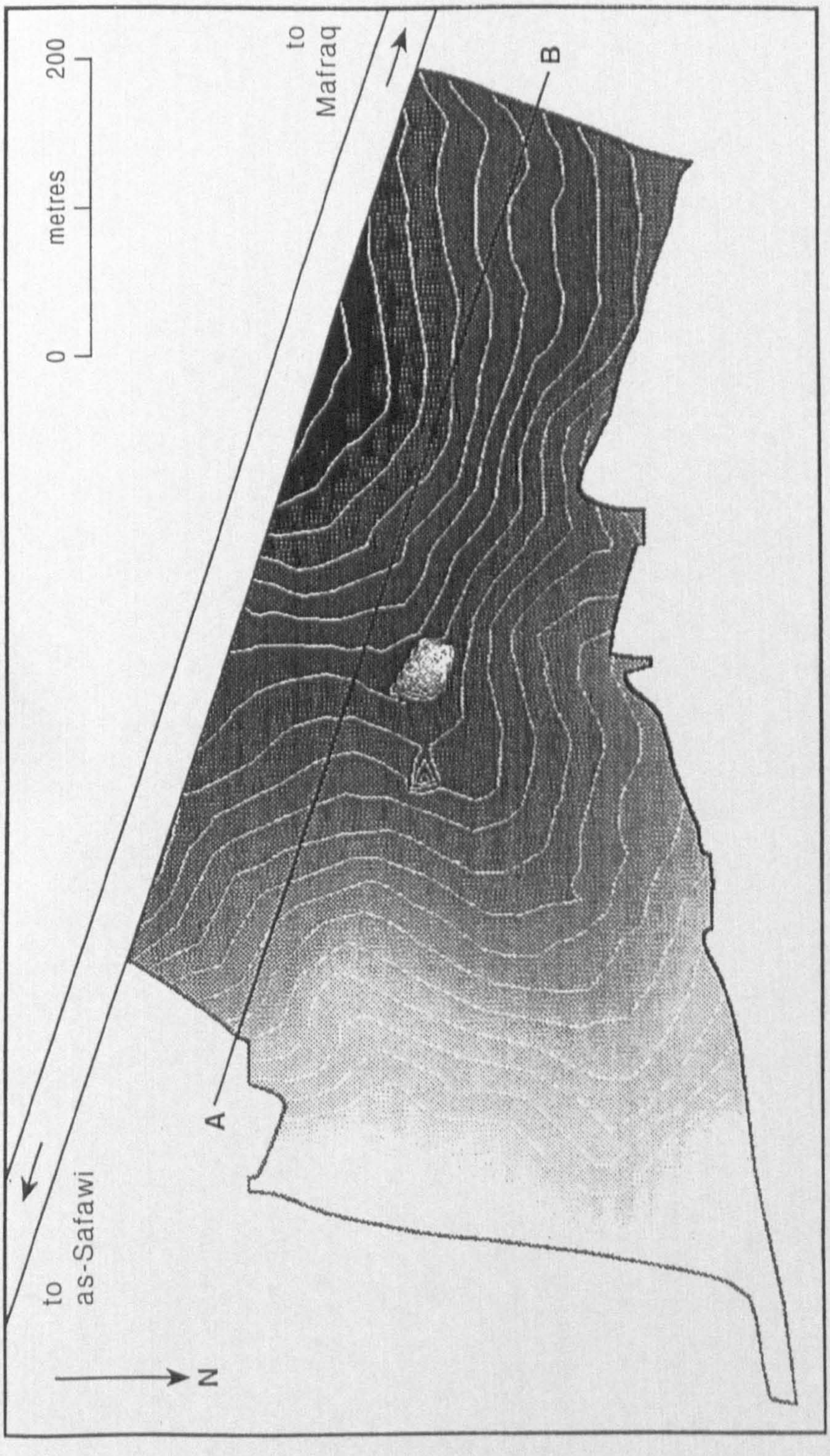

Contours = 0.5 metre

Figure 4.3: Digital elevation model of Low Farm showing sampling transect

4.2.1 Field survey

Almost without exception in the soil crust literature, there is little consideration of where samples are taken with respect to controls such as slope position, despite clear evidence that soil physical and chemical properties are profoundly affected by topography (Malo *et al.*, 1974; Gregorich & Anderson, 1985; Pierson & Mulla, 1990; Brubaker *et al.*, 1993; Brown & Dunkerley, 1996). All three farms were surveyed using a Leica Wild TC1010 total station level. The perimeter of each farm, field boundaries and several random transects were surveyed to establish spot heights. The accuracy of the data were tested by comparing results for a benchmark at the beginning and end of each survey session. On each occasion work was found to be accurate to one millimetre. The results were inputed in a C++ program to translate the measured data into *x*, *y* and *z* co-ordinates. The co-ordinates were transferred to an Arc-Info TIN coverage in order to produce detailed topographic maps (DEMs).

4.2.2 Soil sampling

On many occasions soil scientists collect large bulk samples (Chartres & Mücher, 1989). Others take soil from the surface 250 mm or less for use in laboratory plots (Al-Durrah & Bradford, 1981; Shainberg & Singer, 1986; Abu-Sharar, 1988; Le Bissonnais *et al.*, 1989; Ben Hur *et al.*, 1990; Moss, 1991a). The key to successful sampling is scale. Most processes are scale-specific and interact with other processes acting at different scales and so the sampling strategy needs to account for these relationships. For example, aggregate breakdown is fundamental to the formation of a soil crust. However, the breakdown of one specific aggregate is not going to have much effect on the amount of erosion taking place in a ridge-furrow sequence and still less on the general erosion taking place on a whole field. Likewise, the erosion processes acting on one agricultural field are not going to explain the general landscape characteristics of a whole catchment. Many of the processes related to soil crusting are best observed using plots, in both the field and the laboratory. Plots used in other studies vary in size from less than 1 m^2 (Bradford *et al.*, 1986; Farres & Muchena, 1996) through 1 m^2 and 2 m^2 (Morin *et al.*, 1981; Agassi *et al.*, 1990; Abu-Sharar, 1996), up to large plots such as 10 m x 20 m (van der Watt & Claassens,

1990) and 70 m x 100 m (Baumhardt *et al.*, 1992). The choice of plot can determine the scale of the process which is being observed. On occasions the scale problem is overcome by having interlocking plots of increasing size (Abrahams *et al.*, 1995).

From initial observation of the sites, it became clear that there were two levels of scale by which processes could be observed: the field and the ridge-furrow sequence. Few studies take a more holistic view of landscape position (Govers & Poesen, 1986; Gascuel-Odoux *et al.*, 1996; Ternan *et al.*, 1996). Many prefer, instead, to sample several soils from different regions in order to understand differences in soil physical characteristics (Bradford *et al.*, 1990; Le Bissonnais & Singer, 1993; Valentin, 1994). A similar lack of awareness of the role of micro-topography occurs at the ridge-furrow scale, because many scientists use level plots rather than looking at actual changes within a field ridge-furrow sequence, despite evidence suggesting distinct changes in crust properties (Bielders *et al.*, 1996) and infiltration (Aboujaoudé *et al.*, 1991; Trout *et al.*, 1995).

In order to try to gain an understanding at the various scales, a diversity of sampling was undertaken. Initially a random stratified sample was taken at the field scale. Each farm was stratified into distinct areas, depending on agricultural usage. First, the newly ploughed land which was being used for irrigation for the first time during the summer of 1994. Second, the land which had previously been irrigated. Third, partially cleared land which had not been irrigated before (Plate 4.1). At this level of investigation, infiltration characteristics and soil bulk density were measured and bulk samples were taken from the top 150 mm. The second level of sampling involved a transect across the whole of a farm taking in the topographic changes at each farm (Loague, 1992; Perrolf & Sandsrom, 1995) in order to identify erosional and depositional dynamics at the scale of a whole slope. Points were chosen along a line at 50 metre intervals. At each 50 metre point a crust sample was taken and the top 150 mm was augered. The third sampling level involved taking up to eight crust samples from the ridge-furrow sequence around one point on the 50 metre transects. This allowed the sampling of different types of crust within a 1 metre area, to investigate small-scale salinity changes and variations in erosion and sedimentation which were identified

Plate 4.1: A view of Low Farm across land which has not yet been used for irrigation towards an area which is presently undergoing irrigation

in the crust development. Finally, 1 m^2 plots were prepared for rainfall simulation experiments. Samples were taken from the plots at a time sequence during rain to investigate the processes of seal formation under experimentally constrained conditions.

A significant problem with sampling the surface characteristics of arid soils is their friable and unstable nature. It is difficult to take a standard sample with a Kubiëna tin or similar technique. If the soil is wetted, the surface characteristics are disturbed and the density of the sample makes it even more problematic. To overcome these problems, the surface layer was divided from the subsurface soil. The top layer often lifted off easily and samples were placed in a plastic sample bag. A 15 cm auger sample was then taken from the same location. At some locations pieces of crust were needed for thin section analysis and so the sample was wrapped in tissue to ensure safe transportation.

4.2.3 Plot simulation studies

Several weeks before the rainfall experiments were due to start, ten plots were selected on Low Farm at Ash-rafiyya. Plots were located, using the DEM, in an area with a small 0.5° - 1° east-west slope (Stern *et al.*, 1991; Ternan *et al.*, 1996). In order to reduce the variability of aggregate and clod sizes across a plot and to limit preferential water movement or storage within the soil, most scientists coarsely sieve the soil in the plot (Morin *et al.*, 1981; Bradford *et al.*, 1986; Shiel & Yuniwo, 1993). Each area, of about 1.5 m^2, was ploughed manually so that all the soil from the top 10 cm had been overturned and all the large clods were broken up. The finely aggregated soil was then flattened and constrained on the up-slope and side-slope positions by 1 m x 0.15 m planks which were buried to about 8 -10 cm depth (Luk & Morgan, 1981; Sidiras & Roth, 1987; Stern *et al.*, 1991). The plots were given the dimensions of 1 m^2 to correlate with the area over which the simulated rainfall fell. They were left without disturbance for two weeks before commencing the experiments.

4.2.4 An investigation to relate climatic variables to crust development and strength

One of the important features of crust development during the winter on ploughed fields is the spatial variability of crust formation due to the predominant wind direction during rain events (Sharon *et al.*, 1983; Sharon *et al.*, 1989). To investigate the intra-furrow variation, a series of shear vane tests were carried out at High Farm at Al-rafai'at. Two transects, one at 50 m and the other at 5 m intervals, were sampled along a north-south trending ridge-furrow sequence, from a topographic high point to the base of the slope. At each point along the transect, an approximate profile was measured from one ridge to the next and shear vane data were obtained for five points: eastern ridge summit, eastern flank, base, western flank, and finally the western ridge summit.

4.2.5 Infiltration tests

Infiltration of water, whether it be rain or irrigation water, has always been a key component of soil crust research (Section 3.6). The infiltrating water acts as the medium in which dispersed soil aggregates and primary soil particles are taken down into the soil profile to provide a washed-in layer. Field infiltration experiments usually take the form of either rainfall simulation tests or single / multi-ring infiltrometers (Roth *et al.*, 1985; Sidiras & Roth, 1987; Youngs, 1991; Boers *et al.*, 1992). There are certain limitations to each method as a way of modelling actual infiltration during a rainfall event. A rainfall simulator can reproduce rainfall in a reasonably accurate manner, but it is extremely difficult to constrain the plot in order to collect the runoff in order to calculate the total infiltration.

Infiltration tests were undertaken in the field using a double ring infiltrometer. The outside ring, with a radius of 153 mm, was used to reduce the amount of lateral water movement from the inside infiltrometer. The inner ring, with a radius of 118 mm, from which measurements were taken, was kept at a constant head with a depth of 170-180 mm (Sidiras & Roth, 1987). A test should last until the steady state infiltration rate has been reached (Bowyer-Bower, 1993). That time is determined by the nature of the land system under study (Warburton, in press) and large variations can exist over small distances (Merzougui & Gifford, 1987). From pilot studies it was seen that steady state

occurs after approximately an hour to an hour and a half. Each test was therefore conducted for two hours.

In each of the stratified sampling areas (Section 4.2.2), four infiltration tests were carried out. Both rings were pushed into the soil to a depth of between 3 cm and 7 cm to avoid piping. The outer ring was filled to 15 cm and then left to drop of its own accord. A piece of sackcloth was laid in the inner ring to reduce the amount of disturbance of the soil aggregates as the water was poured in. The constant head of water was maintained using a simple siphon from a 1000 ml cylinder and regulated by a small clamp (Figure 4.4). Readings were taken at 60 second intervals for the first fifteen minutes because the initial infiltration rate was often high. After the first fifteen minutes, readings were taken at two minute intervals. After an hour, the readings were taken every four minutes. After each infiltration test the ground was excavated to measure the wetted perimeter.

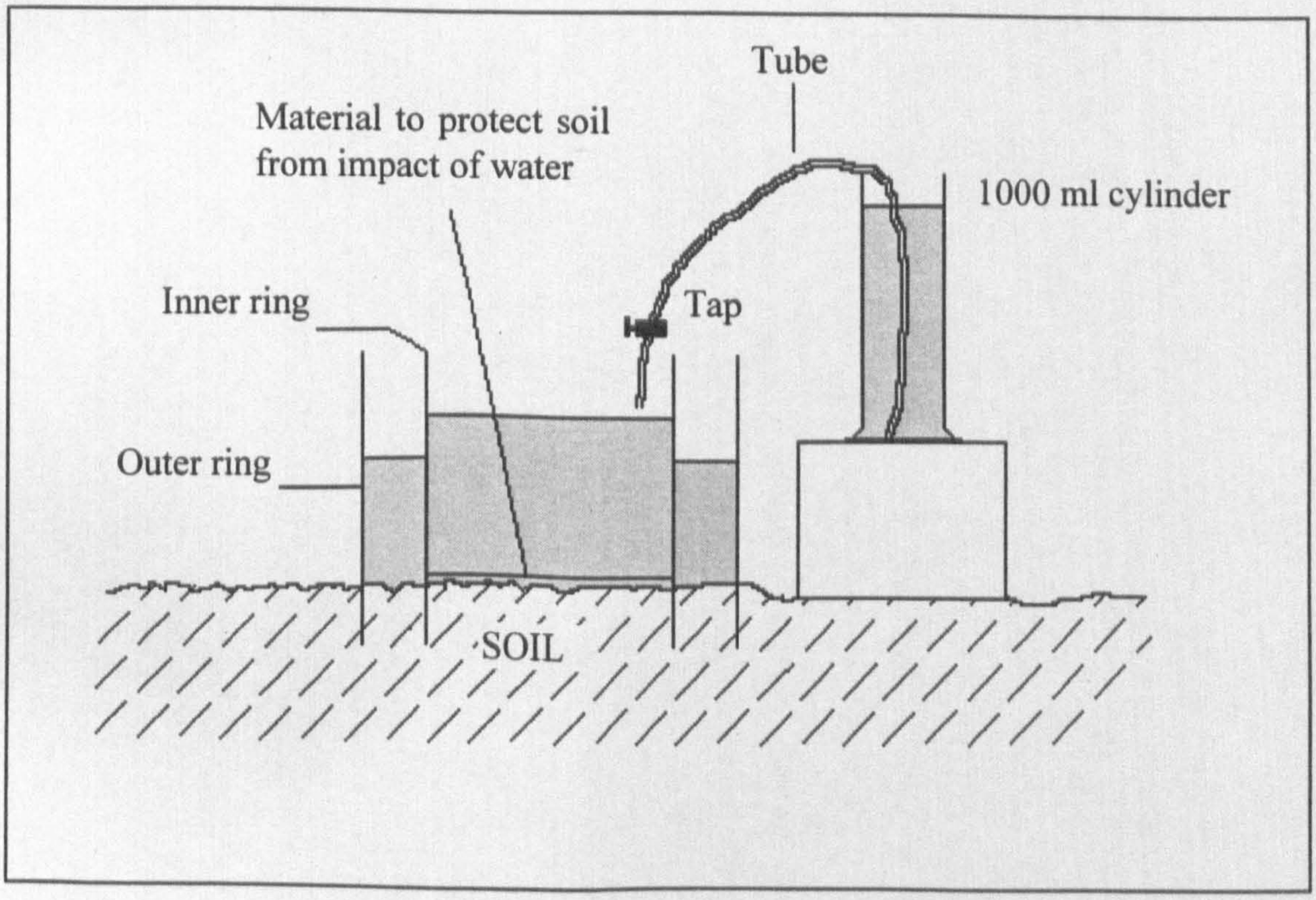

Figure 4.4: Double ring infiltrometer used in the field

There is limited knowledge concerning the dynamics of two and three dimensional flow into soil media (Philip, 1986), especially in the case of soil crusts where there are different layers of permeability (Hillel & Gardner, 1970). It is important to be aware that the infiltration ring size affects the infiltration rate. The bigger the ring, the greater the accuracy since there is a more representative area of soil within the ring, and therefore a smaller likelihood of getting too many large or small pores. Bouwer (1986) recommends a ring of at least 1 m in diameter but that is not necessarily practical, especially with regard to the water usage. Generally the infiltration rate measured using smaller rings will be higher than in larger rings (Youngs, 1987). Another potential source of error is lateral water movement beneath the ring. Normally a second or double ring can compensate for this phenomenon, but it is almost impossible to judge its effectiveness (Youngs, 1987) and indeed Swartzendruber & Olsen (1961) concluded that it is in fact wrong to use a second ring to buffer for edge effects and lateral flow. Another problem that arises with the use of a double ring is the question of water levels. While it is clear that a constant head should be maintained in the inner ring, what is not so clear is whether it is important to keep the water level in the outer ring at that same constant head. Lastly, there is a question concerning the level of the constant head in the inner ring. It has been suggested that a head such as 170 mm is much too large and causes a situation where there is viscous flow in the upper centimetres of the soil column (Abu-Sharar, pers. comm.). The view taken for this work was that the head level should remain constant throughout all the experiments so that values can be compared.

4.3 LABORATORY WORK

4.3.1 Particle size analysis

One of the key controls upon the formation and development of soil seals and crusts is particle size (Tackett and Pearson, 1965; Moss, 1991a). Whether the washed-in formation of thick structural crusts (McIntyre, 1958a) or the formation of depositional puddle crusts (Farres, 1978; Valentin, 1992) is being investigated, the

most important variable will be the preferential movement of different sediment size fractions either over the surface as surface wash or down into the sub-soil and into the pore spaces. It is only by looking at the three-dimensional spatial changes in particle size distribution that one can become familiar with the processes taking place in the field. In determining the particle size distribution certain experimental limitations must be considered.

Several possibilities of grain size measurement are available to the geomorphologist. If the particles are larger than silt size, the grains can be measured using sieves. Material smaller than 2 mm can be measured manually under a microscope (Folk, 1966). Such a method is accurate, despite being somewhat subjective, but takes a great amount of time. Most scientists use methods of sedimentation for the smaller fraction (<63 μm). More recently, electrical sensing and laser defraction techniques have been developed. These are not without problems (Goudie *et al.*, 1990). The method adopted in this work follows the British Standards methodology (BS 1377, 1990). The >63 μm fraction is dry sieved with mesh sizes of 63 μm, 212 μm and 600 μm. The silt and clay fractions are then separated using sedimentation by the pipette method (Gee & Bauder, 1986).

Material which has previously been air-dried is disaggregated with a pestle and mortar and passed through a 2 mm sieve to remove the gravel fraction. A sub-sample of approximately 10 g is placed into a beaker before 10 ml of dispersing agent, sodium metaphosphate, is added along with 100 ml of distilled water. The mixture is then left to stand overnight. Prior to wet sieving the material on a 63 μm sieve, the mixture is agitated by placing the beaker into an ultrasonic bath for 15 minutes (Edwards & Bremner, 1967). The soil solution is poured onto the 63 μm sieve and a gardening sprayer containing distilled water is used to break up any remaining aggregated particles. The sub-63 μm fraction is collected in a tray placed underneath the sieve and then washed into a 500 ml sedimentation tube. The remaining material on the sieve is then washed into an evaporating basin and left in a drying oven overnight at 105 °C. When a set of sedimentation tubes have been filled, they are placed into a water bath which is set at 25 °C. Using Stokes' Law, it is possible to work out, at a given water temperature, the rate of settling-out of any

grain size fraction. After shaking the tubes a 10 ml pipette is placed down into the sample at a depth of 10 cm. At 4 minutes and five seconds a sample is taken and placed into a pre-weighed vial. The material collected should represent a sample of the medium to fine silt and clay. The procedure is repeated with the pipette after 46 minutes and then 6 hours and 54 minutes to get samples of the fine silt and clay and then just the clay respectively. The vials are left in a drying oven overnight at 105 °C and then reweighed. Meanwhile, the >63 μm sample, which has been dried, is shaken through a nest of three sieves (63, 212 and 600 μm) and the sediment remaining on each sieve represents the total coarse, medium and fine sand fractions. The sand fractions can be worked out directly by comparing their weights with the initial sub-sample. The silt and clay samples are calculated by taking the clay and subtracting the clay and fine silt and then multiplying out to get a percentage of the original sample. This procedure is repeated with the weights from the other vials to obtain percentages for each fraction. The only fraction which is not directly determined is the coarse silt (20 - 63 μm) which is calculated as a remainder of the total.

One of the problems of the above procedure is that two methods are being used to look at the whole particle size range and this leads to the question of what exactly is being measured as grain size (Komar & Cui, 1984). A sieve of a certain diameter assumes that all grains are spherical and that any grain with a diameter no greater than the length of the size of the sieve openings will fall through. Such a preconception is not associated with the sedimentation method because measurements are made on an equivalent sedimentation diameter. Irregular grains will have the same settling rate as near-spherical particles. Natural grains typically have angular shapes which roughly approximate to triaxial ellipsoids (Sahu, 1965). Ideally, the sedimentation method should be used for the whole size range, but the sands would settle out much too quickly to secure an accurate measurement. The sedimentation method uses a general equation which was first obtained by Stokes (1851), who noted that a sphere or cylinder will pass through water at a certain rate, depending not only on the density of the liquid and mass of the particle but also on the internal friction of the liquid itself. Such a resistance proves to be proportional,

for a given fluid and velocity, not to the surface but to the radius of the sphere (Stokes, 1851). Of the two techniques, sedimentation is more accurate because the probability of a particle passing through a sieve in a given time of shaking depends on the nature of the particle, the number of particles of that size and the properties of the sieve (Day, 1965). In the case of the Jordanian Badia soils, most variability in particle size is in the silt and clay fractions and so it is being measured almost entirely by sedimentation which should give accurate data.

4.3.2 Soil chemistry

The soil crust represents the interface between the main body of soil and the atmosphere. It is instrumental in controlling the flow of water in and out of the soil. In an arid environment, a majority of water entering the soil is stored in the upper centimetres and is gradually drawn back to the surface by evapotranspiration, diffusivity or capillary action caused by evaporative forces. In a non-irrigated landuse system, there is an equilibrium between the amount of water and vegetation. If water is artificially introduced into the system, upward non-transpirational water flow increases and consequently salts are absorbed, transported and precipitated at the soil surface. A soil crust may be more or less affected by salt precipitation over small spatial scales and this can lead to preferential secondary soil detachment and transport. It is therefore important to study the change of salt accumulations over both time and space. Soil samples were tested for the four major exchangeable soil cations, Na, Mg, Ca and K, using atomic absorption spectrometry (Hesse, 1971; Page, 1982).

To obtain a useable solution from the soil, NH_4Ac was leached through 5 g of the sample. The leachate contains the exchangeable cations which have been replaced by the ammonium. The leachate is reduced to a spray by a nebulizer, and drawn into a cloud chamber, where the larger drops condense and drain out. The smaller drops mix with the acetylene fuel and continue into the burner. The drops and fuel are completely mixed by the time they reach the burner and are ignited to form a flame that burns at 2300 °C. Standard solutions in diluted extracts (NH_4Ac) are introduced

in the same way to calibrate the machine for each cation over its likely concentration range.

The wavelengths at which individual elements absorb are well defined and each element has an optimum range between x20 and x200 of its specific sensitivity which represents the threshold at which the element reaches its atomic phase (Table 4.1). For example, in the case of magnesium, which has a quoted sensitivity of 0.015 p.p.m., the optimum range of absorption is between 0.3 and 3 p.p.m. Absorption is only linear in this range so if the concentration of the sample lies outside this range, two options are available. First, the initial sample can be diluted by a known quantity of NH_4Ac, although there may well be more inaccuracy in diluting the sample than there would have been from using the more concentrated solution. The alternative is to increase the sensitivity range of the machine by rotating the burner by 30^{o}. This, in effect, limits the area over which the lamp beam interacts with the flame, which reduces the sensitivity and gives a tenfold increase in the range.

Element	Wavelength nm	Slit width (mm)	Sensitivity (mg ℓ^{-1})	Sensitivity check (mg ℓ^{-1})	Linear range (mg ℓ^{-1})
Calcium	442.7	0.7	0.092	4.0	5.0
Magnesium	285.2	0.7	0.0078	0.3	0.5
Sodium	589.0	0.4	0.012	0.5	1.0
Potassium	766.5	1.4	0.043	2.0	2.0

Table 4.1: Element sensitivity during A.A.S. operation - Source: Perkin Elmer (1982)

When measuring the concentration of elements in solution to the accuracy of 0.1 p.p.m., there is always the possibility of error. The main sources of error occur in the sample preparation, variations in the fuel flow, fluctuations in the flame and inconsistent sample nebulization and atomisation. Other sources of error can arise because standard solutions may degrade in quality. There is a possibility of chemical

interference, where the resonance wavelength of one element is somehow dependent on the presence of another (Cooke, 1969). In order to reduce such errors various steps were taken. First, the machine was set to take five readings of the leachate from which it calculated a mean. In addition, several samples from each batch of 30 were randomly retested to check the reliability of the data being collected. To reduce any errors in the standard solutions, the machine was recalibrated after every five samples. If there was a noticeable difference (± 1 p.p.m.) in the second run, all the samples were tested again. If the standards were old, new standards were made. Sodium was the only element which could be tested directly from the leachate. It was necessary when measuring potassium to add 0.03 ml of 15,000 p.p.m. sodium solution because this increased the sensitivity of the AAS to the potassium. In addition, 0.4 ml of lanthanum chloride solution had to be added per 4 ml of leachate when testing for calcium and magnesium in order to overcome interference problems.

4.3.3 Soil fingerprinting

One of the questions in the northern Badia is the origin of the soil. While microscopic fabric analysis can provide information on the mineralogy of the soil its use as a quantitative tool is limited, especially in the identification of clay minerals. XRD (X-ray diffraction) is a technique which can characterise and evaluate the mineralogy and therefore help to explain how the soil has formed (Whittig & Allardice, 1986). It is a fast and precise method of characterising the mineralogy of fine-grained sediments (Hardy & Tucker, 1988). X-ray radiation beams hitting the sample will be diffracted depending on the minerals in the sample. The sample rotates so that different minerals will diffract at different degrees of rotation. The output appears as a series of peaks at different intervals which denote the type of clay. The height of the peak gives the relative magnitude of clay in the sample. The initial hypothesis (Al-Homoud *et al.*, 1995) was that the soils of the northern Badia are derived primarily from the weathering of local basalt. To test the hypothesis samples of unweathered basalt, weathered basalt and soil from Low Farm were compared using X-ray diffraction and fluorescence.

For X-ray diffraction analysis a sample of the finest material (<5 μm) is needed. For the weathered basalt and unweathered basalt samples, this was obtained by breaking down the rock with a tungsten carbide ball mill and an agate pestle and mortar. For the soil, a sample was left in a sedimentation tube for approximately seven hours until only the finest silts and clays remained in suspension. Material was taken from the tube and placed in a beaker with three small glass slides in the base. The beaker was left several days to allow the water to evaporate leaving the sediment to settle on the slides. Many geologists have tried to make slides which have no interference from the non-clay fraction, but settling of particles is problematic and the < 2 μm classification for clays can be unhelpful. If there is too large a proportion of quartz, feldspar and calcite the task of identification becomes more difficult because of overlapping diffraction maxima (Towe, 1974). One slide was used directly without further treatment. One was heated in a furnace to 375 °C. The third was soaked in ethylene glycol. Under treatment, the clay diffraction pattern will change allowing better distinguishing between clays. Measuring the actual amounts of different clays has caused some disagreement. Some prefer to compare the magnitudes against set standards (Gibbs, 1967). Others have calculated formulae which take into account different crystallinity indices (Hooton & Giorgetta, 1977). For the analysis of the Jordanian samples exact magnitudes were considered unnecessary as only one sample of each type was being used. Approximations were taken using the relative areas under the diffractogram peaks.

4.3.3.1 X-ray fluorescence

X-ray fluorescence records the chemistry of the complete mineralogical component of the rock or soil being measured. In trying to fingerprint the soil to understand its possible source material and how it was moved to its present location, it is valuable to obtain a good idea of the mineralogical chemistry and compare it with that of the underlying rock.

In order to measure any material, whether soil or rock, it has to be initially ground down to silt-sized components. To grind large particles an ordinary rock crusher is used, but once the material is in small enough pieces, it can be placed in a tungsten

carbide ball mill. Grinding requires cleanliness to avoid contamination between samples.

X-ray fluorescence requires a small pellet of the material for investigation, made using a hydraulic press. The sample is mixed with a single drop of Mowoil which acts as an adhesive. The mixture is placed into a chamber, flattened and white boric acid powder is used as a backing to the sample. A SPECAC hydraulic press operating at 7 tons of pressure is used to bind the material into a small round disk which can then be used for analysis.

4.4 MICROMORPHOLOGICAL FABRIC ANALYSIS

Micromorphological investigation of a soil fabric is an important procedure to look at the processes and forms produced by raindrop impact, salt precipitation and the effects of irrigation. It is an important way of characterising crusts and has been used extensively by soil scientists and to a lesser extent by geomorphologists (Evans & Buol, 1968; Mücher *et al.*, 1981, 1988; Boiffin & Bresson, 1987; Norton, 1987; Arshad & Mermut, 1988; Valentin *et al.*, 1992). Of interest in this project was the relationship between micro-topography and soil crust micromorphological attributes over small areas. By studying the changes in soil crust fabric, the processes of erosion and deposition could be elucidated. In addition, the use of rainfall simulation and tracers was developed to identify how particles penetrated the sub-crust layer and how surface silts became reorganised as a result of rainsplash and seal development.

4.4.1 Polyester versus epoxy resins

Many materials have been used to impregnate soil samples with differing success. The most suitable resins have the following properties (Murphy, 1986): low viscosity; miscible with acetone or a styrene monomer to lower its viscosity; able to be cured without requiring extreme conditions; not to change the physical structure of the soil sample or itself be changed by contact with soil material; to be totally isotropic and colourless in thin section, with a refractive index of about 1.54.

No resins are perfectly suitable for all soil types. Only Carbowax 6000 is miscible with water and has been used with wet clay and peat soils. However, it has the major disadvantage of being too soft when cured and is therefore difficult to cut (Murphy, 1986). Epoxy (Norton, 1987) and polyester (Mücher *et al.*, 1981; Bresson & Boiffin, 1990; Bielders *et al.*, 1996) resins have become the usual media within which soils are impregnated. Each has specific advantages and disadvantages.

The most significant advantage epoxy resins have over polyester resin is that they can be added to the sample and cured overnight. In comparison polyester resins take about six weeks to cure. Epoxy resins will cause little shrinkage, have resistance to other solvents and chemicals, have no volatile loss during curing, will adhere to almost any surface and are extremely tough when cured (Bouma, 1969). On the other hand, they will not mix with acetone to reduce the viscosity and their viscosity will usually only decrease with temperatures in excess of 70 °C. The resin, as it cures, goes through a very intense exothermic reaction and there are potential problems with regard to mineral transformations and structural rearrangements. Epoxy resins have been used successfully by various authors (Martin *et al.*, 1979; Chiou *et al.*, 1983), but in general soil scientists prefer to use polyester resins.

Polyester resins are readily available and usually considerably cheaper than their epoxy counterparts. A considerable amount of time and careful supervision is needed for the completion of the process. Shrinkage can occur if the resin cures too fast or if any of the solvent is trapped in the sample upon curing. The final disadvantage is that the resin is not as strong as epoxy resin once cured, but it should allow cutting and grinding without releasing mineral grains. The main advantage of polyester is that of viscosity. Polyester resins, with a viscosity usually around 6 - 20 poise at 20 °C, can be diluted to the viscosity of water by adding acetone. This factor alone, added to the fact that there is a long residence time in the sample before curing, means that the impregnation quality is superior to that produced using epoxy (FitzPatrick, 1984, Tippkötter & Ritz, 1996).

4.4.2 Preparation for sample impregnation

In order to look at soil under a microscope, samples first have to be impregnated so that they can be cut and ground to 30 μm to allow mineral identification (Gribble & Hall, 1992). To ensure that samples will fully impregnate, it is vital to remove as much water as possible. Virtually all polyester and epoxy resins, being hydrophobic, require complete removal of water from the samples (Murphy, 1986). This can be a problem for soils with high levels of organic material, which have to go through freeze drying or acetone replacement in order to remove the water without shrinking the sample (Chiou *et al.*, 1983; Murphy, 1982). For arid soils, however, there is generally a low organic matter content and the soils are almost completely dry.

4.4.3 Problems of impregnation in arid soils

One problem, revealed by this research, is that samples with low organic matter have a great propensity to slake. In preparation for impregnation acetone must be added to reduce the viscosity of the resin to allow full impregnation. It should be added slowly, causing it to soak into the sample from the base until only the top of the sample is left out of the acetone to allow air to be released as the acetone rises through the sample through capilliary action. The beakers containing the sample are sealed for three days in order to force air out from the pore spaces as the acetone rises up through the sample by capillary action.

Because the crust samples are fragile, the acetone caused some of the crust samples to slake and within minutes the structure had completely collapsed. An alternative way of adding the acetone without disruption had to be found. Slaking can only occur if air is in the sample when the acetone is added because the mechanism relies on the fact that the air is forced to escape on impact of a drop of liquid causing disintegration of the soil aggregates. If the air within the soil could be extracted beforehand, the risk of slaking would be minimised.

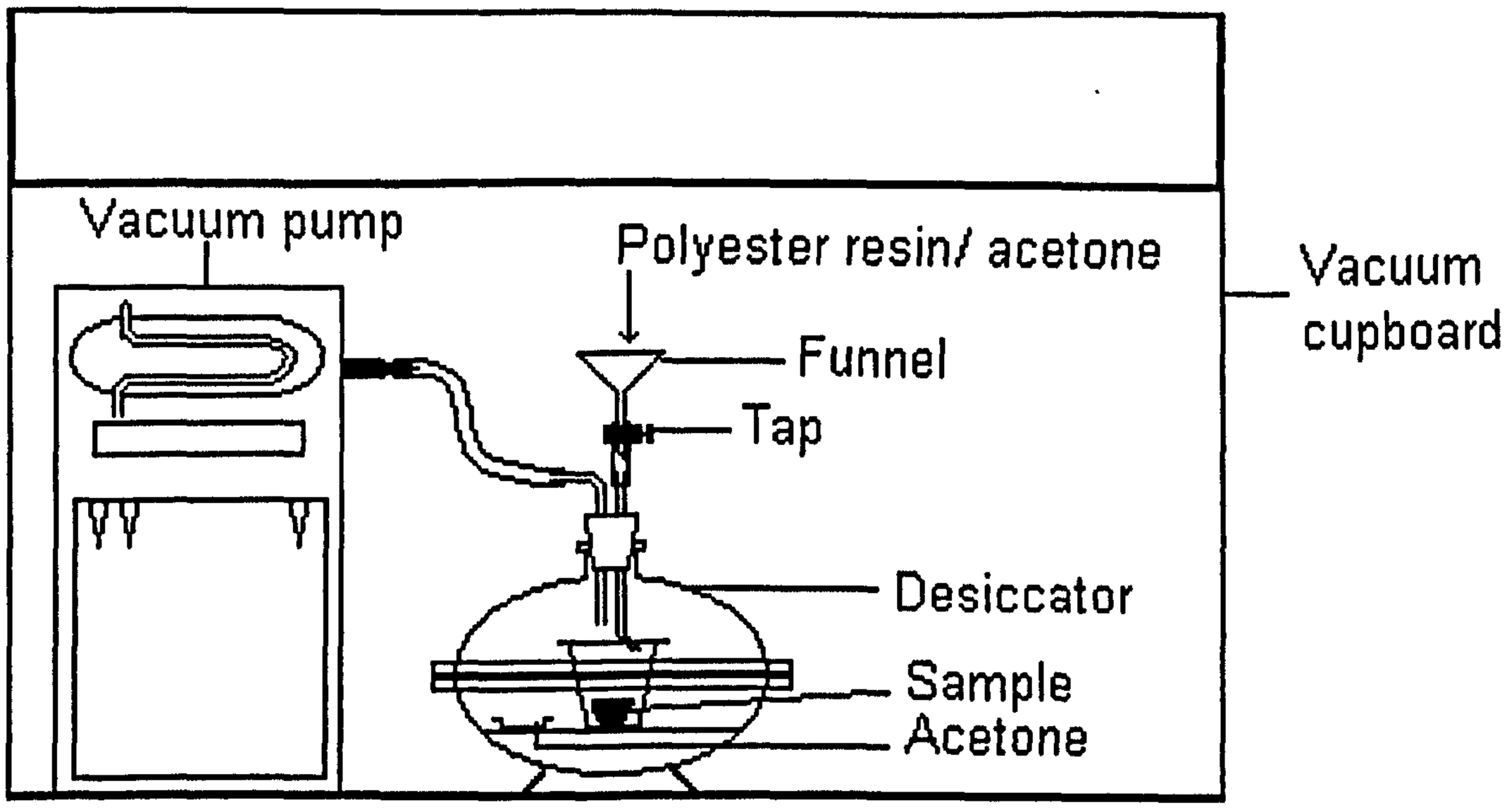

Figure 4.5: Apparatus for adding acetone under vacuum

The sample was therefore placed into a desiccator alongside a small beaker of acetone and then closed. Two glass tubes, descending down into the desiccator through a rubber bung (Figure 4.5), were attached to a vacuum pump and a clamped funnel respectively. The vacuum pump was turned on and 1 bar of pressure was reached forcing the air to be evacuated and allowing the acetone to vaporise and fill the chamber. Once the vacuum had been in place for ten minutes, the clamp on the second tube was released very slowly, allowing acetone to drop into the base of the beaker. Once the acetone had reached the top of the sample, the clamp was shut off and the vacuum slowly released. The sample with acetone could then be taken out of the desiccator and wrapped in aluminium foil to stop acetone evaporation (FitzPatrick, 1984). Using this method, it was found that slaking was avoided.

4.4.4 Resin impregnation

Once the samples are thoroughly wetted with the acetone, the foil is removed from the plastic beakers and the remaining acetone removed by suction. It is important to make sure that the samples themselves do not dry out. Meanwhile, the polyester resin is mixed with the hardening catalyst before diluting the whole mixture with acetone to lower the viscosity. The initial dilution is about 10 % resin + catalyst : 90 % acetone. The mixture is poured into the beakers completely covering the samples and the beakers are resealed to stop evaporation. The solution has such a low viscosity that it will permeate all the pore spaces and channels, replacing the acetone. This is of utmost importance when dealing with a very fine-grained soil matrix. The samples are sealed for a week to ensure full saturation before the foil is removed to allow the acetone to evaporate. As evaporation takes place, the liquid level falls rapidly due to the high quantity of acetone in the beakers concomitant with resin replacement and polymerisation. After 10 to 14 days resin polymerisation is complete and the sample is put in the soil oven at 40 °C. When it is almost set, the temperature is raised to 60 °C and then 80 °C at four day intervals, after which it is kept at 100 °C overnight to cure the resin completely. Cooling should be done over three to four days slowly reducing the temperature by 20 °C per day to avoid cracking. The whole method should take between five and six weeks.

When the sample is cut and the thin section made, it is possible to lose tiny fragments of resin or a single mineral grain during the grinding process which could subsequently be interpreted as a pore space. To avoid this problem dyes are used in the resin to distinguish pore spaces from holes in the section. In all the samples from Jordan, an ultra-violet dye, Uvitex OB, was used. It cannot be seen under a polarising microscope, but can be identified under ultra-violet light (Bresson & Boiffin, 1990). Such a dye is invaluable when analysing pore space, because all the pore spaces will reflect the UV light while the soil mass and any holes will be anisotropic.

4.4.5 Thin section preparation and mounting

Once the impregnated sample block is cured it is ready to be cut and ground down to 30 μm. For certain purposes, such as image analysis, the cut polished block is all that is required (Chartres, 1994) and it can be more accurate than thin sections for pore analysis. However, for fabric, microstructure and mineralogical analysis thin sections are required. All cutting and grinding must be done using a coolant to reduce the heat of the cutting action and to remove particles from the cutting edge of the blade. Water should never be used for soil thin sectioning, because it will cause the sediment on the slide to buckle due to the expansion of clay particles even when the impregnation is complete (Dalrymple, 1957; Murphy, 1986).

The block needs to be sliced down to about 4 mm using a thin, disk saw-blade made with a diamond bearing bronze rim. Then one side of the slice is polished, using a set of diamond plates and petroleum spirit as a lubricant. Two coarse diamond plates are used to get the section completely level and then the fine diamond plate is used to obtain a highly polished surface. It is vital to get a completely level surface because otherwise at the stage of grinding down to 30 μm the area of the section not level will pull off the slide. Immediately the section is polished it should be stuck on to a slide to avoid buckling as the section absorbs atmospheric moisture. The glass slide is cleaned with petroleum spirit and the polished soil surface is adhered using a glass bond glue. The slide and sample are then put under an air-compressed jig which can apply up to 160 mm Hg pressure. After ten minutes, a UV lamp is turned on underneath the samples for a further ten minutes. The glue normally sets in daylight over a period of hours due to natural UV. The time can be significantly reduced if an artificial light source is introduced to increase the bond. The glue has probably reached 90% of its strength in an hour and can be cut, but it is better to leave the sample overnight to allow the bond to reach full strength.

The next stage is the cutting and grinding of the sample on the slide. The slide is attached to a vacuum plate, which in turn is fixed to a circular arm which rotates downwards on to the cutting and grinding wheels in the instrument. The arm has a highly accurate micrometer affixed so that small μm increments can be made. Once

the edge of the slide is calibrated with the cutting wheel, the sample is moved by approximately 250 μm so that once the saw is rotating, it will cut most of the sample off the slide leaving only 250 μm on the slide. The arm is then moved along to the grinding wheel which has a more accurate micrometer (± 1μm) and the process is repeated. The sample is gradually cut down to about 35 μm. The exact thickness can only really be judged by looking at the quartz under the laboratory microscope, but with experience it is possible to see the thickness while still fixed on the machine. The final grinding and polishing has to be done on the diamond plate to get it down to the correct thickness (usually between 25 and 30 μm). Lastly, a cover slip is placed on top of the sample for protection following the same method as before using the glass bond.

4.5 Conclusion

Much of the soil crust literature has concentrated upon the soil processes which lead to a specific micromorphological form or state of land degradation and much less emphasis has been laid upon the geomorphological context. The sampling framework of this research has attempted to focus upon the spatial variability of soil crusts, from within a ridge-furrow sequence to the whole field. Although most scientists have identified different crust forms on widely differing soil textures (Bresson & Valentin, 1990; Valentin & Bresson, 1992), it is unusual to find explanations of variability over a single soil type and indeed within the scale of an agricultural field (Bielders *et al.*, 1996; Brown & Dunkerley, 1996).

The techniques described above allow the analysis of fine resolution changes in soil characteristics, which will increase understanding of the classification of spatial differences in crust formation. In addition, with a multiple-scale approach, it should be possible to observe how spatial variations in crusts at a ridge-furrow scale affect the overall erosion and deposition regimes within the whole field.

5. THE USE OF LOCAL CLIMATE DATA FOR ESTABLISHING RAINFALL SIMULATION PARAMETERS.

"For rainfall simulator data to be of wide use, some uniformity of equipment and test procedures is needed, and the data must be obtained under relatively standard conditions that closely simulate natural rainfall intensity and energy." (Robinson, 1979, p. 1)

"Rainfall simulation, the technique of applying water to plots in a manner similar to natural rainfall." (Neff, 1979, p. 3)

5.1 INTRODUCTION

To model and simulate rainfall it is necessary to have a clear idea of normal winter rainfall. To examine the sedimentary processes involved during raindrop impact and to understand moisture residency, it is important to measure the frequency of rainstorms and the characteristics of individual rainfall events. While most field scientists who use rainfall simulation provide some background rainfall data, it is usually only in terms of mean annual precipitation (Agassi *et al.*, 1990; Ben Hur *et al.*, 1990). Only rarely is rainfall intensity measured (Gascuel-Odoux *et al.*, 1996). In addition, it is important to measure other climatic parameters such as the rate of evaporation, to elucidate the moisture fluxes at the soil surface.

5.2 CLIMATE CONSIDERATIONS

Good climate data must be a foundation not only for rainfall simulation experiments, but also for research into soil-water interactions. It is necessary to take data from a number of different temporal scales and resolutions to gain a thorough understanding

Plate 5.1: The Automatic Weather Station at Menara

of climate conditions in an area such as the Badia, where data points are few. The majority of data used in this study come from stations monitored by either the Water Authority of Jordan or the Jordanian Department of Meteorology (Table 5.2). Some of the stations monitor daily rainfall totals and others record hourly rainfall data. The most important short-term high resolution data have been obtained from an Automatic Weather Station (AWS) installed specifically for this study. The AWS was placed close to Lower farm at Menara in order to establish a good climate link with the rainfall simulation and the soil-water experiments. The station was operational from the middle of August 1994 until the summer of 1996. The weather station (Plate 5.1) has six sensors: solar radiation, net radiation, wet- and dry-bulb temperature, wind direction and wind run, in addition to a rain gauge. Each sensor samples every ten seconds and produces an hourly mean. The rain gauge works as a tipping bucket mechanism whereby the rainfall is measured at a resolution of 0.5 mm and summed hourly. All the data are collected on a data logger which is powered by a small solar panel fixed to the main mast of the weather station. The data logger must be downloaded every month onto a portable data-unit which connects to the serial port on the back of a personal computer.

5.2.1 Temperature

The climate of the western area of the Badia has a marked, but not extreme, variation in daily and annual temperature. Summer temperatures rarely rise above 40 °C while winter temperatures seldom dip below 0 °C. This reflects the fact that the area lies close to the transition between Mediterranean conditions and a more continental climate, characterised by greater extremes, further east.

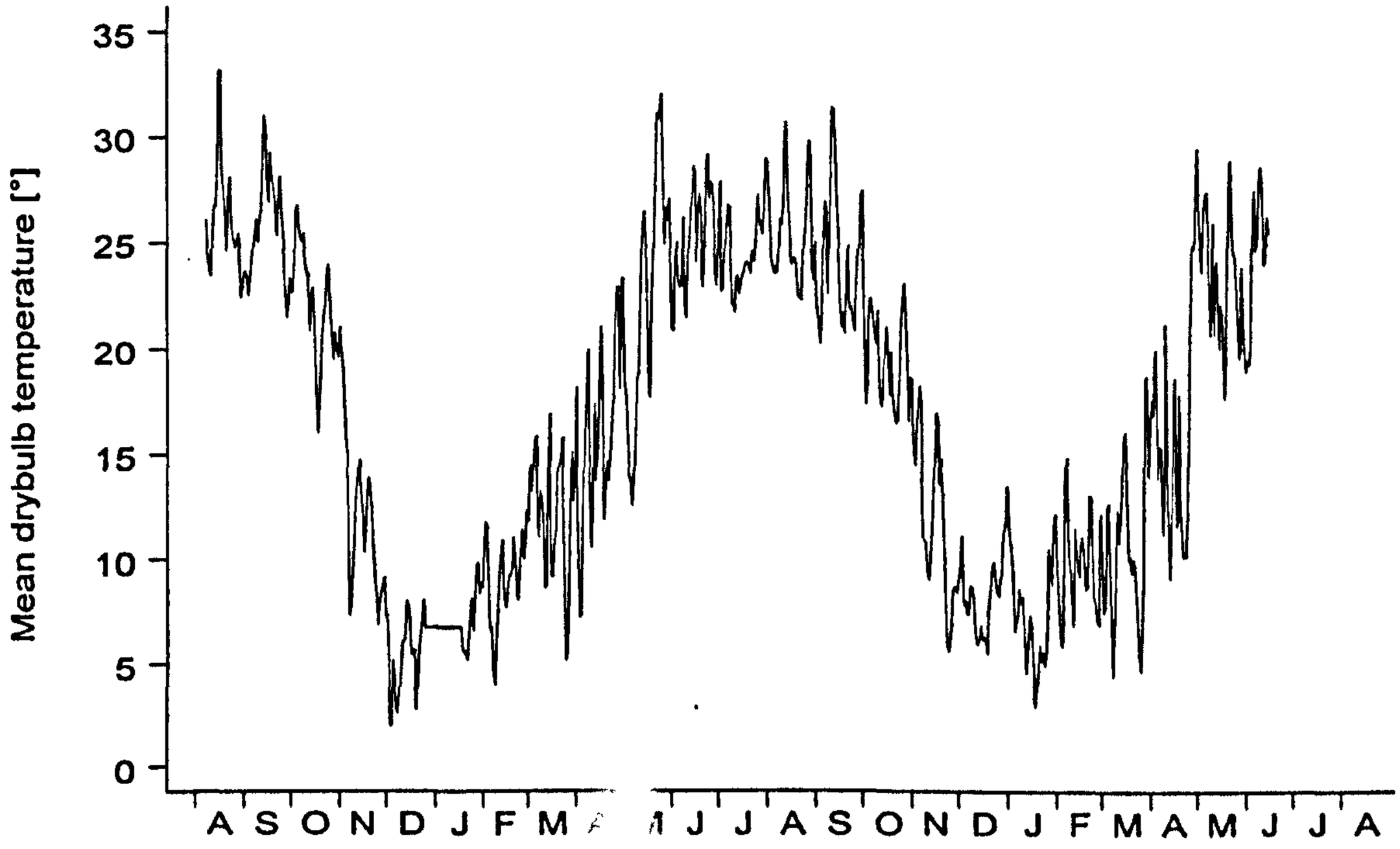

Figure 5.1: Mean daily temperature between August 1994 and June 1996

The mean daily temperature for 1994 ranged between 26.2 °C in August and 5.2 °C in December, but in the following year the range was less extreme with a mean daily temperature of 25.5 °C in August and 7.3 °C in January 1996 (Figure 5.1.). Concomitantly, there is a reduction the variability of the mean temperature from summer to winter. The highest in urnal variability of mean daily temperatures occurred in late spring and early s ner. May 1995 was the highest with 7.5 °C. This is likely to be associated with the hot chamseen winds which blow from Arabia in late spring and cause rapid warming. Generally, the cool months of December through to February have low inter-diurnal variability of between 3 and 4 °C. It should be noted that there is a three week gap in the dataset during January 1995, due to operation failure.

The diurnal temperature range is also seasonally dependent, with the greatest ranges during late spring and early summer (Figure 5.2). The lowest temperatures occur between 4 and 6 a.m. while the highest occur between 2 and 4 p.m. The lowest diurnal variation occurs in December and January where the mean range stays

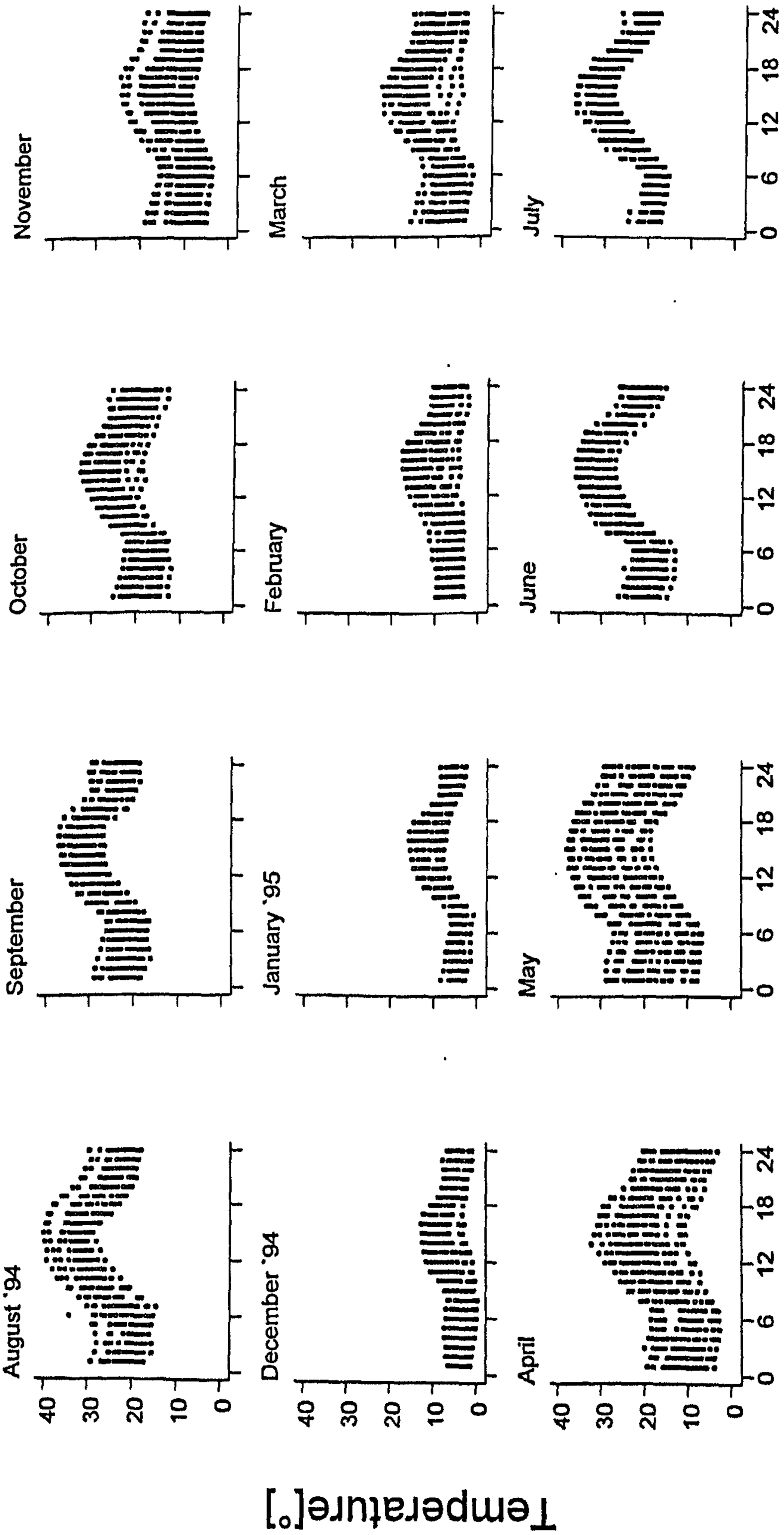

Figure 5.2: The change in diurnal temperature ranges for the year August 1994 to July 1995

between 0 °C and 20 °C. The range increases in April because the lowest night temperatures remain below 5 °C but the maximum daytime temperatures are in excess of 32 °C.

5.2.2 Wind run and direction

Wind is an important factor influencing micro-topographic variation in rainfall (Sharon *et al.*, 1989) and evaporation in the Badia. Wind data show a high diurnal variation in both speed and direction. There is a fairly consistent pattern to these features illustrating a summer-winter contrast. During summer (Figure 5.3), there is a prevailing north-easterly wind during the evening and night. However, in association with an increase in air temperature between 5 a.m. and 3 p.m. there is a significant shift to a north-westerly wind direction, which seems to follow one of two patterns. Usually the wind shifts slightly via the north, but occasionally there is a systematic veer via the south. The shifts of around 270° from north-east to north-west via south indicate periods of meteorological instability and often there is a risk of rainfall.

The pattern of wind direction differs considerably during the winter as seen in Figure 5.3 for the months October to April. The wind during the night predominantly comes from the east to south-east, although there are occasions when there is more of a northerly to north-westerly wind. As with the summer pattern, there is a movement towards the north-west as the daytime temperature increases, although unlike the summer pattern, the majority of the shift occurs via the south. The mid-day wind direction commonly comes from the south, the south-west, west and north-west. In the evening there is a shift back via the south. Obviously this simplified summary generalises about the summer and winter positions. In reality only June to August fit completely into the summer pattern and November through to February fit the winter pattern; the intervening months are inevitably evolving from one pattern to the other.

Five circular plots, Figure 5.4a-e, show the wind direction data in a form which is easier to interpret, although it must be noted that they represent a mean for the two years of data rather than for specific months. When the data were originally plotted, there was a large spike at north which did not correspond to the rest of the wind data

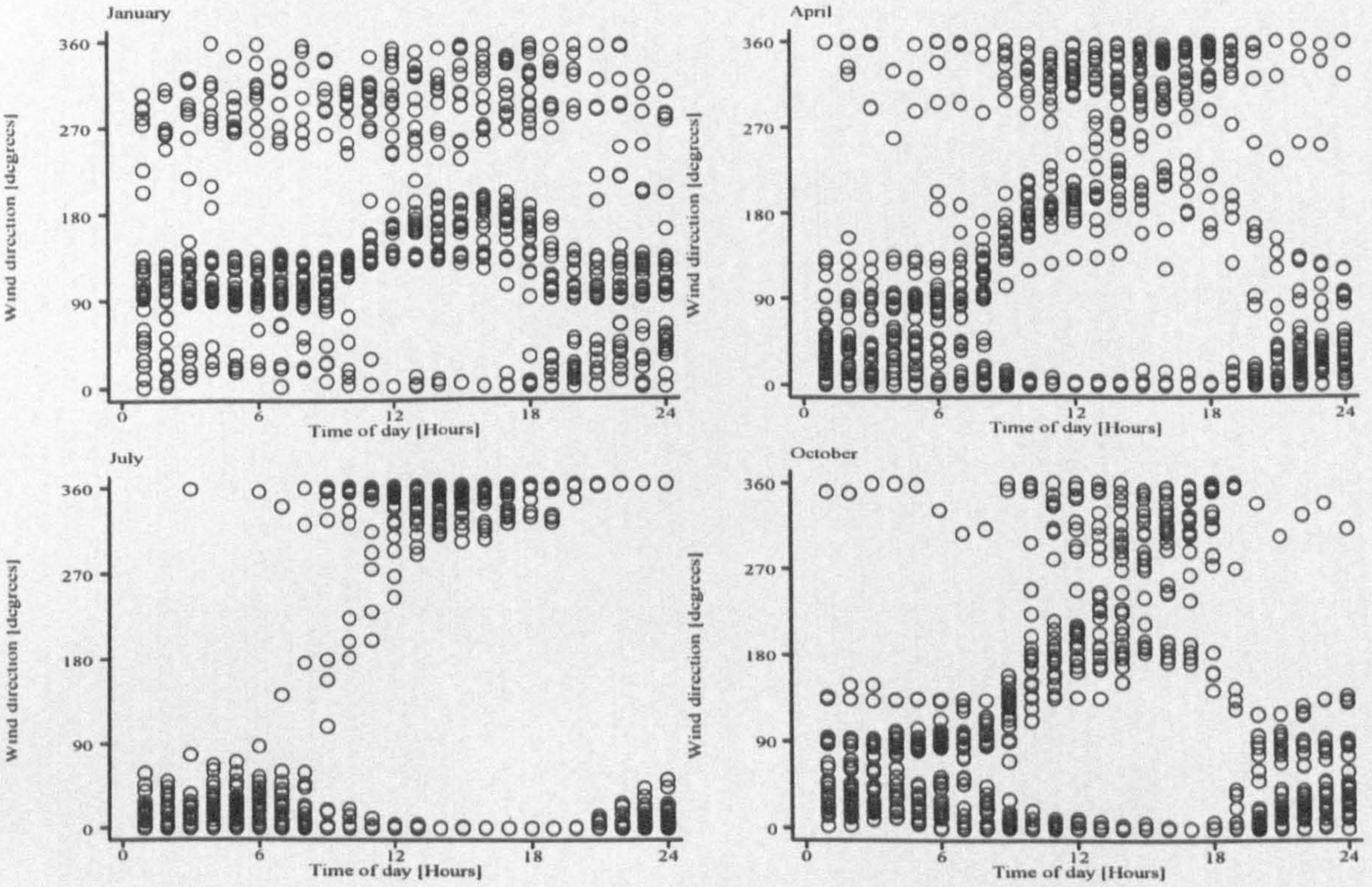

Figure 5.3: The relationship between diurnal wind direction and time of year

and was thus considered an artefact introduced by the data-logger. The inclusion of the spike subdued the remainder of the data and therefore the plots display data from 0.8° to 359.2°. The arrow shows the direction of the vector mean, that is the direction of the resultant vector (Cox, pers. comm.).

On the one hand, the plots indicate that there is a systematic shift in wind direction during the day and on the other hand, show that there is a strong correlation between wind direction and rain events. During the period between midnight and 06.00 in the morning, when the wind speed is relatively low, the mean wind direction is from the north-east (55.5°) and the high vector mean suggests that there is little standard deviation. As the morning continues there is a shift in the wind direction, but no particular dirction is favoured resulting in a very low vector strength. However, in the afternoon, as the wind speed increases, there is a significant shift to a north-westerly wind (316.5°). Such a change probably indicate katabatic airflows descending from the Jebal Haurân due to differences in pressure. In the evening, between 18.00 and midnight, there is evidence of a strong shift back to north-easterly

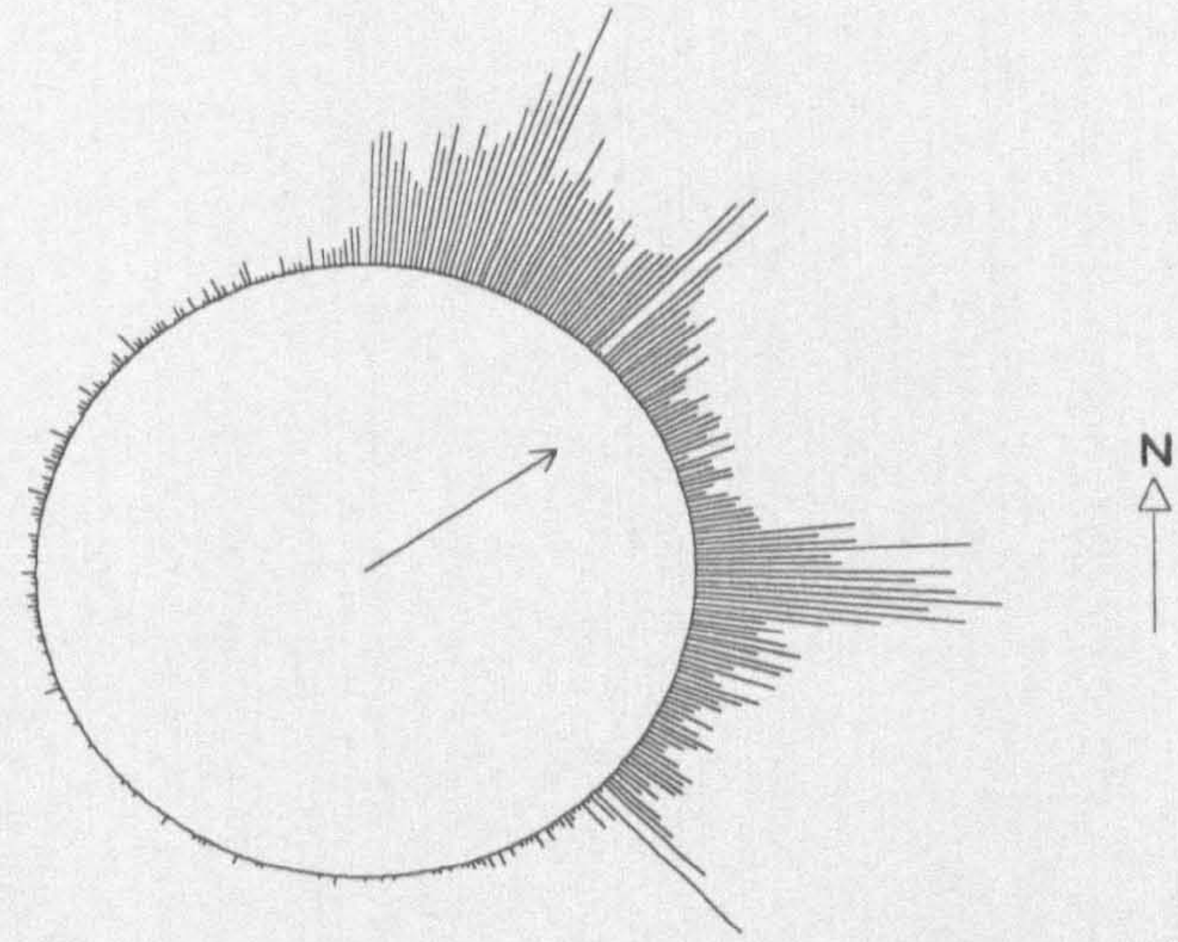

Figure 5.4a: Wind direction between midnight and 06.00 (mean direction 53.6°)

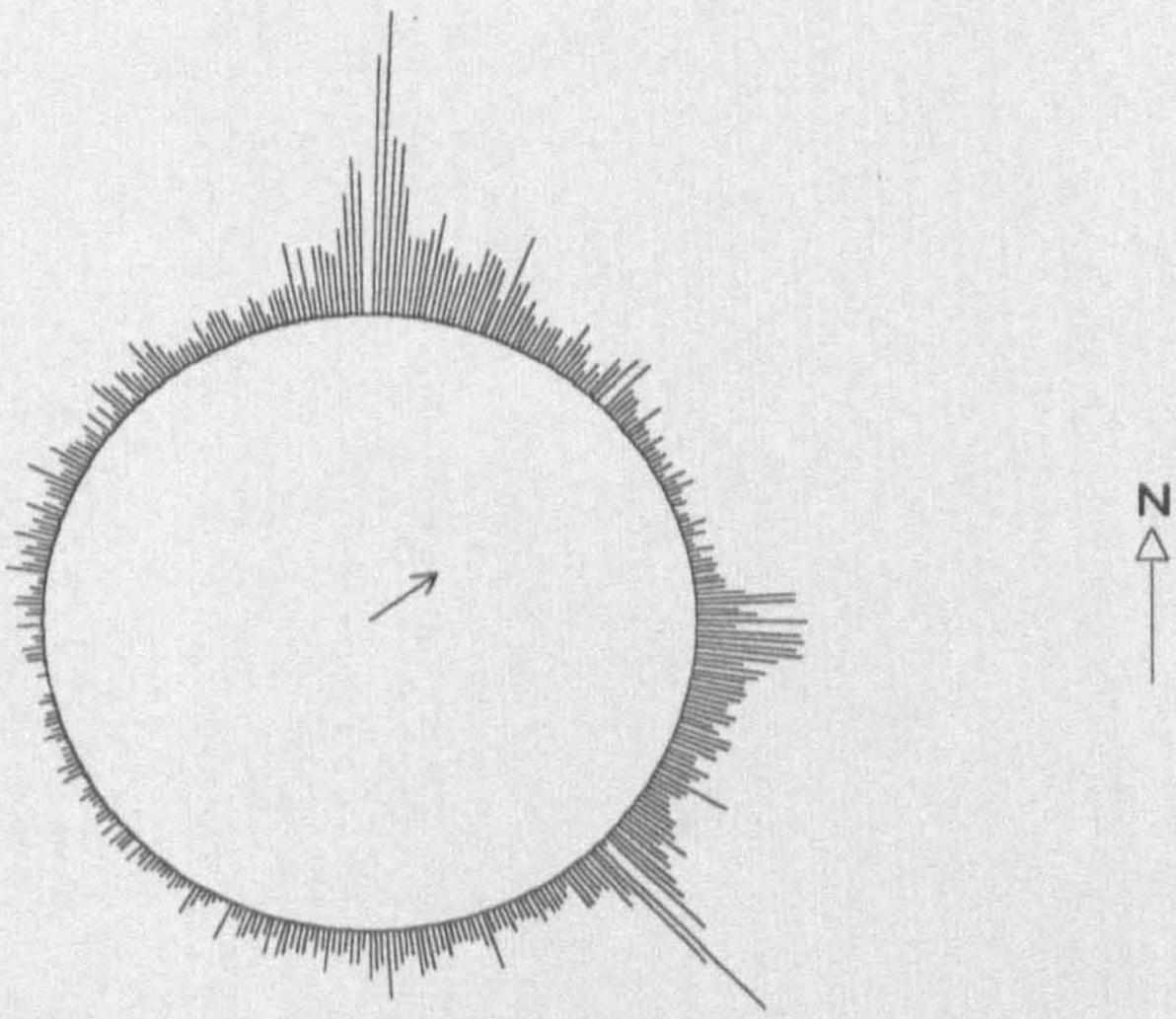

Figure 5.4b: Wind direction between 06.00 and midday (mean direction 52.8°)

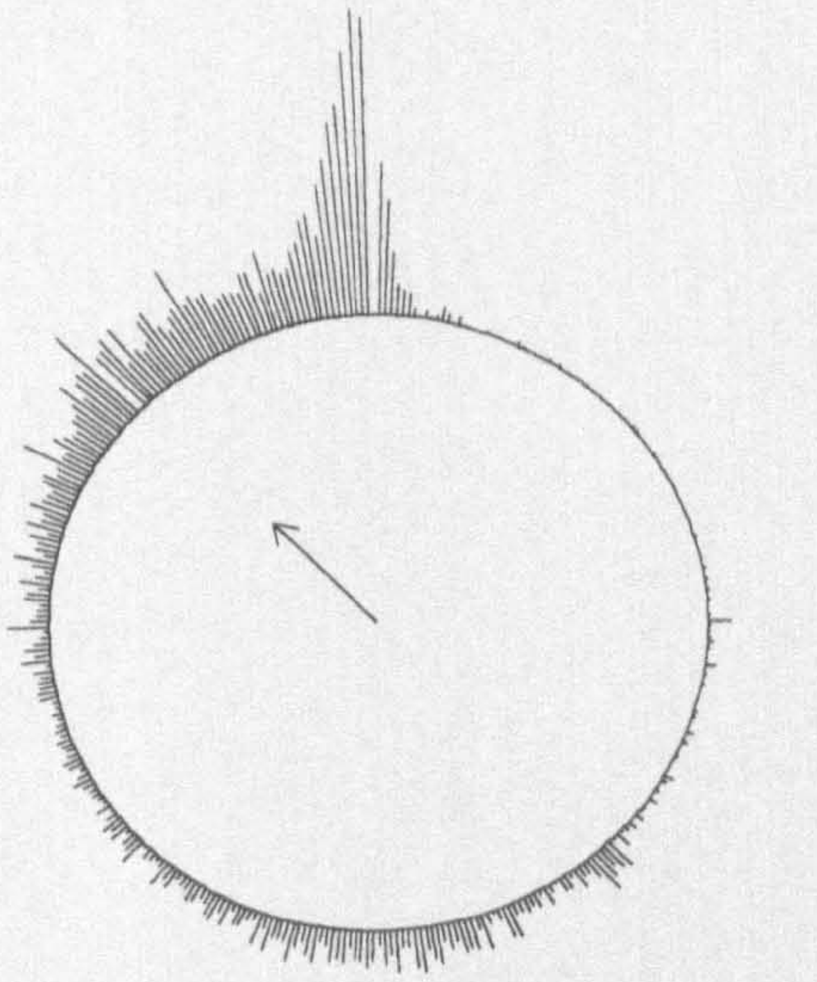

Figure 5.4c: Wind direction between midday and 18.00 (mean direction 316.5°)

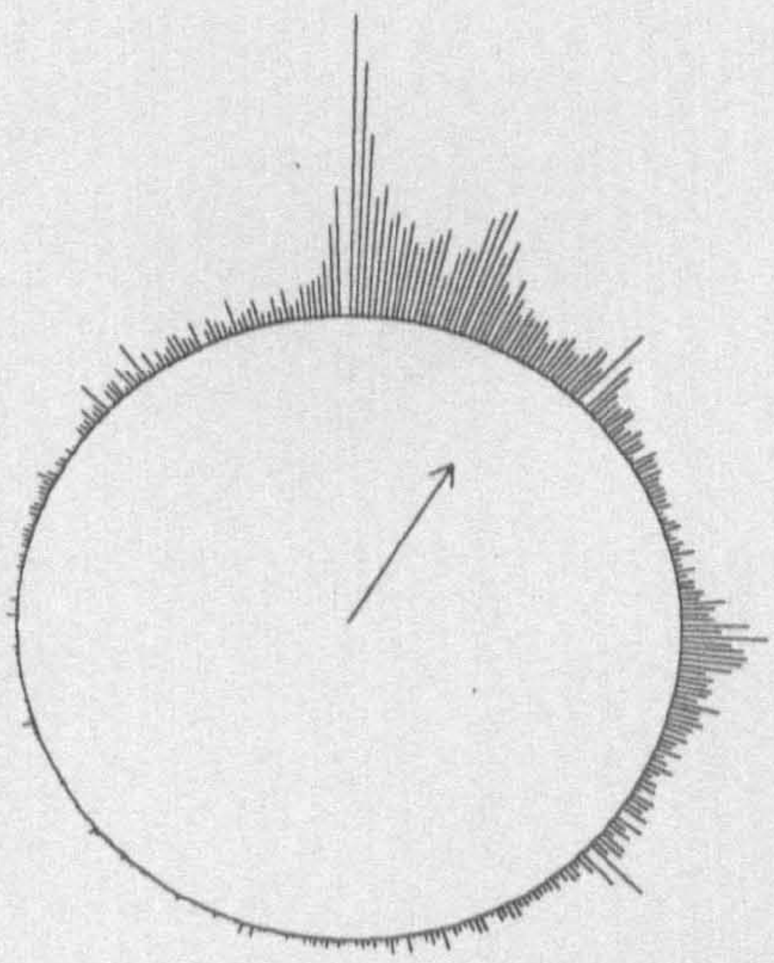

Figure 5.4d Wind direction between 18.00 and midnight (mean direction 31.8°)

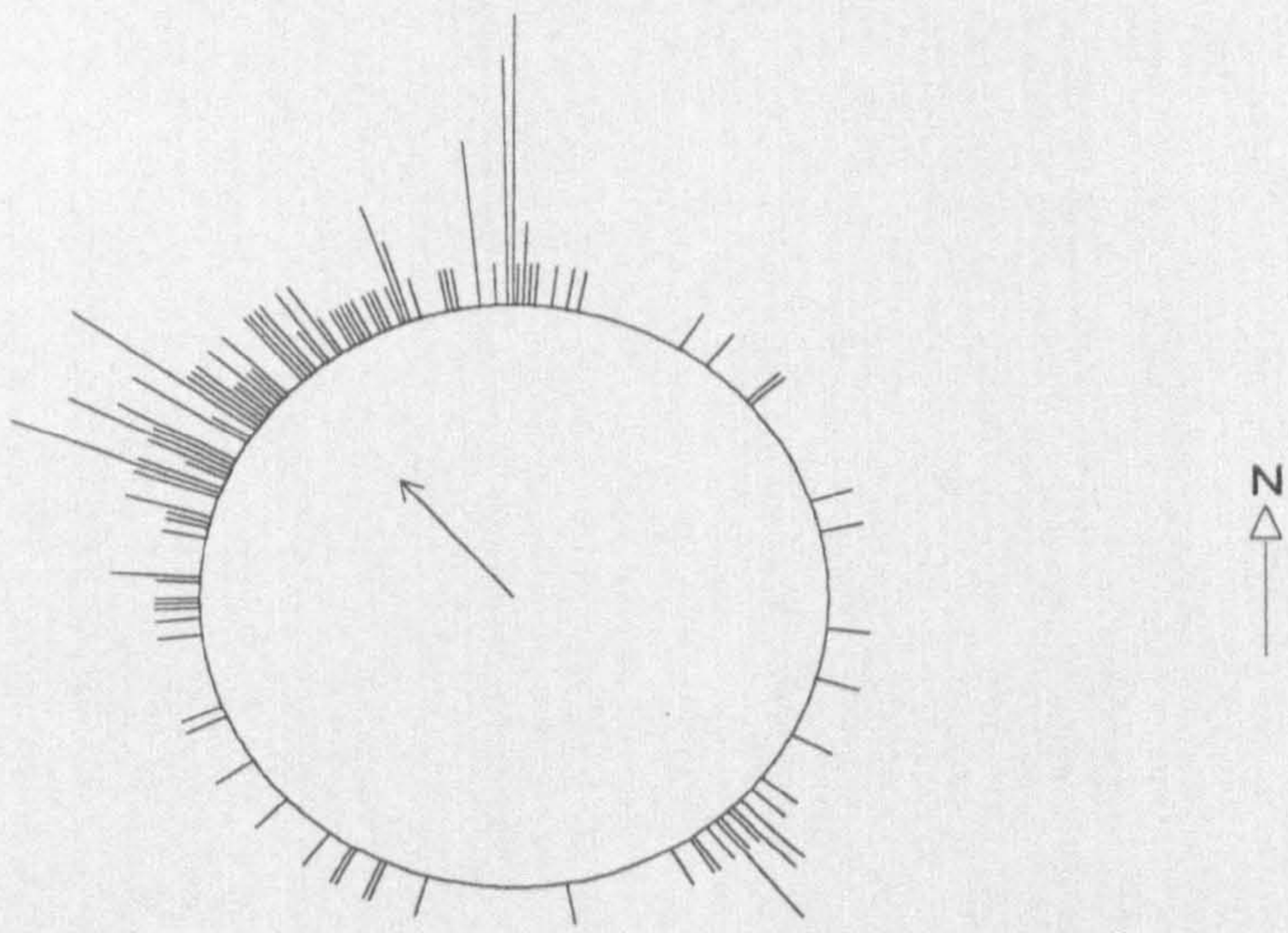

Figure 5.4e Average wind direction during all rainstorms (mean direction 318.2°)

winds (31.8°) which mainly occurs via the north. Most interesting is the fact that the average wind direction during rainfall events is from the north-west (318.2°), which corresponds to the observation that unsettled weather is dominated by low pressure disturbances penetrating eastern Jordan from the Mediterranean. In this case, it is the larger synoptic-scale circulation which controls the rainfall and wind characteristics, whereas normally they reflect local variations in pressure caused by the orographic effect of the Jebal Haurân mountains. This has important implications for west-facing slopes, because the incident angle between the rainfall and the slope is close to normal and therefore mechanical impact is much higher than on corresponding east-facing slopes. Slope position and aspect become important, therefore, in the amount of crust which can form.

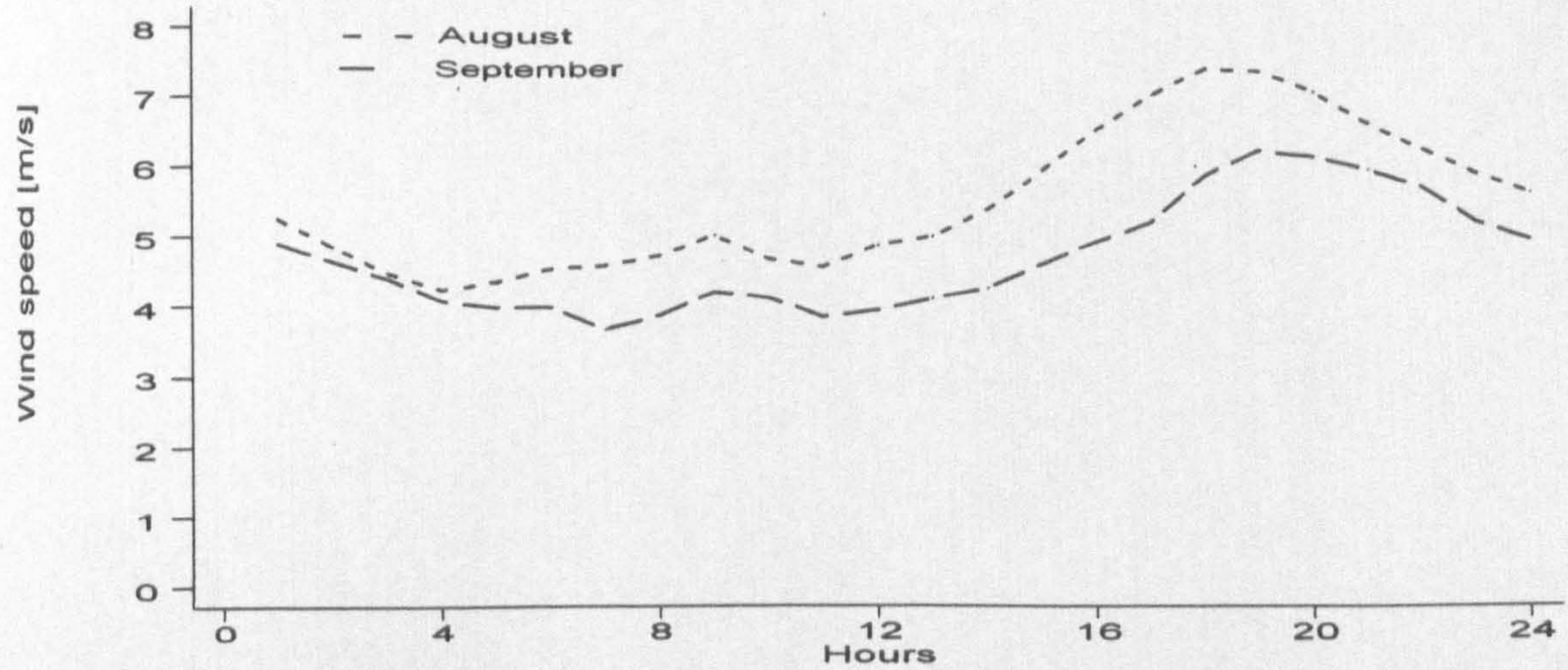

Figure 5.5: Changes in mean diurnal wind speed for different months at the AWS

The variation in windspeed is more difficult to analyse due to the lack of reliable data after October 1994, but the main trends can be seen in Figure 5.5. It is more difficult to generalise about patterns within the temporal series because of the magnitude of variation. Even averages over one hour are liable to mask significant variations in the time-series, especially gust events which may be important as geomorphological agents.

It is possible to make some useful observations. First, the highest wind speeds occur in the hours following sunset, reaching a maximum between 8 and 10 p.m. Figure 5.6 indicates that there is a strong relationship between wind strength and direction with the highest windspeeds occurring from the north and north-east. In fact, as well as there being much less wind from the southern and western quadrants, it is also much weaker.

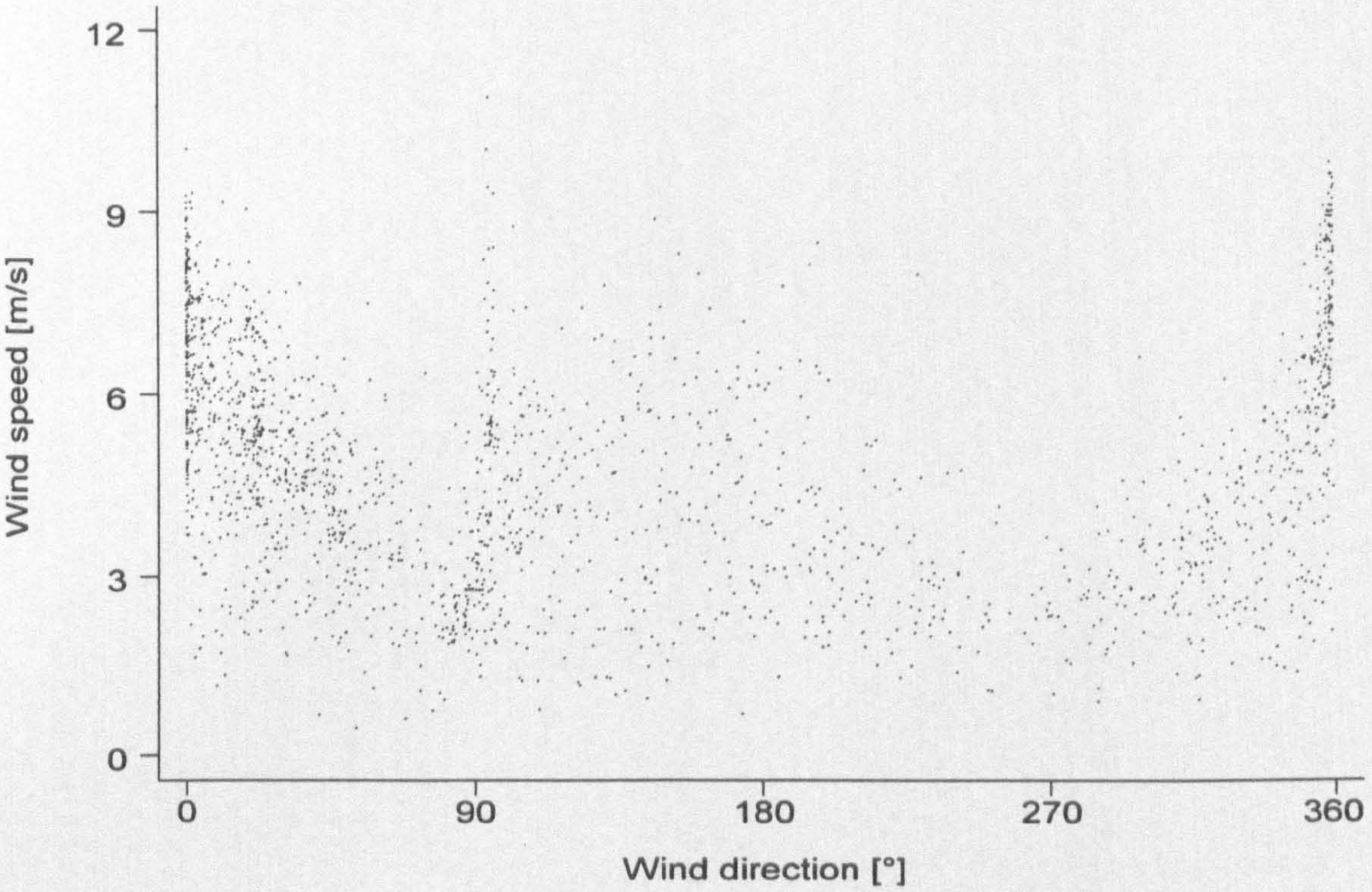

Figure 5.6: The relationship between wind direction and speed

5.2.3 Evaporation

The processes leading to the formation of a soil surface seal have a profound effect upon the net water balance within the top layers of the soil (section 3.6). Water cannot be drawn up to the surface from under the crust because of the destruction of the soil structure and specifically the conducting pores (Bresler & Kemper, 1970). In an arid environment the soil moisture flux is predominantly negative, only turning positive for brief periods after rainfall or the application of irrigation. However, if no seal is produced, the rate of water evaporation from the soil could be of an order of magnitude greater than if a seal had formed as a result of a rain event. It is therefore crucial to account for the rate of evaporation in order to model the water balance before, during and after wetting (Rose, 1996). Although a computer program was available from the Institute of Hydrology (IH) to calculate the evaporation term for periods of 24 hours using Penman's equations (Penman, 1948), it became clear that it would not provide the hourly resolution needed and so alternative calculations were

carried out. As the evaporative flux is an important term in calculating the soil water balance during and after water input and since the residence time of water in the soil is brief, hourly resolution is necessary. The Penman equation predicts evaporation from two terms, which depend on net radiation (C_1), wind speed and humidity (C_2), respectively. All of these variables can be calculated directly or indirectly from the weather station data. The full Penman equation, as approximated by Linacre (1992, p. 105), can be rewritten

$$Evaporation = \frac{\Delta}{\Delta+\gamma}(R_n) \quad + \quad \frac{\gamma}{\Delta+\gamma}\left(\frac{2.3uS}{\gamma}\right) \tag{5.1}$$

where

Δ = gradient of the saturation vapour pressure / temperature curve [hPa / C°],

γ = the psychometric constant (altitude dependent) [0.61 hPa/C° at 800 metres a.s.l.],

R_n = net solar radiation [W/m^2],

u = wind speed [m/s] and

S = saturation deficit [hPa].

In order for an hourly evaporation to be calculated, Δ and S need to be derived from the wet and dry bulb temperatures T_d and T_w.

Saturation vapour pressure

$$\delta = 6.1\, e\left(\frac{17.29\, T_d}{T_d+237}\right), \tag{5.2}$$

and vapour pressure

$$v = 6.1 e\left(\frac{17.27\, T_w}{T_w+237}\right) - \gamma\left(T_d+T_w\right), \tag{5.3}$$

with relative humidity

$$h = \left(\frac{v}{\delta}\right) \times 100 \tag{5.4}$$

and the saturation deficit

$$S = \delta - v, \tag{5.5}$$

which means that the gradient Δ can be calculated by

$$\Delta = \frac{18\delta\left(2501-\frac{12T_d}{5}\right)}{8.314\left[T_d+273\right]^2} \quad . \tag{5.6}$$

Therefore if T_d and T_w are known as well as wind speed u and net radiation R_n, their values can be substituted into the original equation to find the evaporation. Correction factors must be applied to the equations to assure that all the units compatible. In order to correct the calculations some standards have to be introduced. A net radiation of 28 W m^{-2} results in an evaporation rate of 1 mm per day (Linacre, 1992) which means that an evaporation rate of 1 mm h^{-1} or 24 mm/day would require 672 W m^{-2}. Therefore the hourly readings for the C_1 (the radiation term) should be corrected by 1/672. Similarly a wind speed of 1 m s^{-1} and a saturation deficit of 1 millibar result in 0.2 mm of evaporation per day (Linacre, 1992). If u and S are both numerically 1, the aerodynamic term C_2 would equal 3.77 mm h^{-1} or 90.49 mm/day instead of 0.2 mm/day which means that C_2 should be corrected by 452.46.

The evaporation flux calculated by the IH and revised Penman equations are summarised in Table 5.1 for the period 7th -23rd August 1994.

	The revised Penman method	IH Penman method
Period	7 Aug. at 00 h to 23 Aug. at 2400 h	
Total heat budget term (C_1)	56.76 mm	49.43 mm
Total aerodynamic term (C_2)	70.92 mm	76.51 mm
Total evaporation	127.68 mm	125.94 mm

Table 5.1: Comparison of two ways to calculate the Penman evaporation coefficients

The differences between the terms C_1 and C_2 are caused by the difference in altitude by which each term is calculated; the IH equation models evaporation according to the height of the AWS at 100 m whereas the Jordanian data come from an altitude of 800 m. Altitude has an important role to play in determining evaporation rates, as it profoundly influences the value of the psychometric constant γ. At sea-level the constant is 0.67 hPa / C°, but at an altitude of 1000 m it falls to 0.59 hPa / C° (Linacre, 1992). A decrease in γ increases the relative importance of the radiation term and reduces the influence of the wind speed and humidity terms in the evaporation equation, explaining the contrast between the two methods.

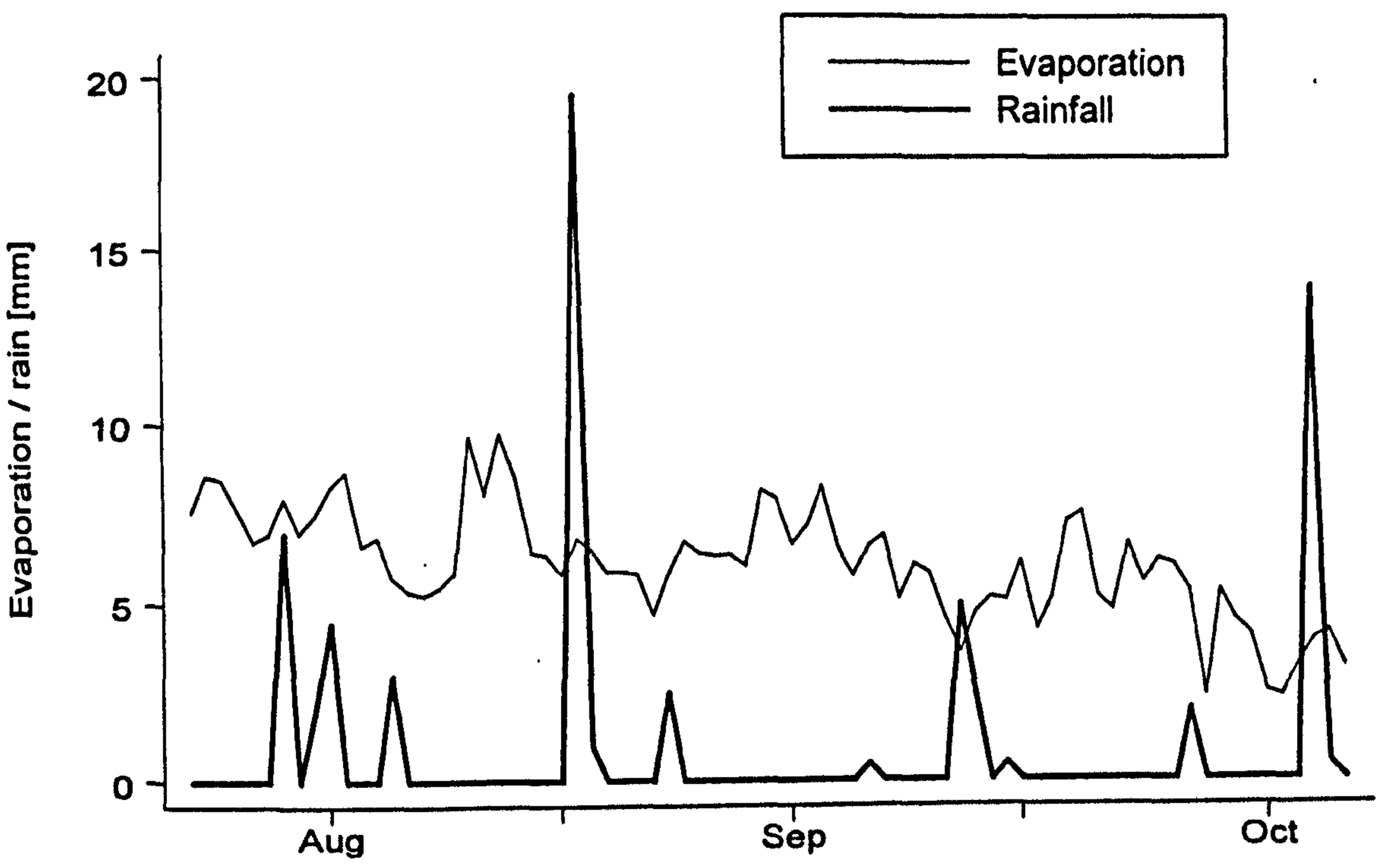

Figure 5.7: Total daily evaporation versus rainfall [7th August -20th October 1994]

From the daily totals of evaporation and rainfall (Figure 5.7), it is clear that there is a very strong negative water balance with daily evaporation rates commonly above 7.5 mm per day during the summer months. Only on days of extreme rainfall, which occasionally occur at the close of the summer season, is there a small positive water balance which only lasts for a few hours. However, by the middle of October the

evaporation rates are usually below 5 mm per day which gives a much greater potential for there to be a positive water balance, if only for a few days.

5.2.4 Rainfall

Rainfall is the key factor in soil crust formation and in the soil-water balance. The frequency, intensity and duration of rainstorms and the pattern of rain events are all factors which must be taken into account. Rainfall is the one climatic variable about which there is a reasonable amount of data at different spatial and temporal scales.

Station name	Station code	Grid Reference		Altitude in metres a.s.l.	Date established	Type of gauge [1]
		North	East			
Deir al Kahf	F4	32° 16'	36° 52'	1025	1963	D
Umm El-Quttein	F1	32° 18'	36° 39'	986	1947	D & R
Al-Aritain	F6	32° 7'	36° 59'	800	1963	D
H5 - As-Safawi	F2	32° 10'	37° 9'	715	1968	D & R
Tullul El-Khureishe	F14	32° 2'	36° 38'	550	1968	T
Azraq Evap. Station	F9	31° 58	36° 50'	533	1962	D & R

[1] D: Manual Daily ; D & R: Automated Daily and Recorder ; T: Totalizer

Table 5.2: Rainfall stations within the Azraq Basin which are within 50 km of the field site at Ash-rafia. Adapted from Water Authority, Jordan (1989)

Stations monitored by an automated system (D & R) contain the most detailed information including hourly readings of rainfall which correspond to the accuracy of the AWS information. The manual daily stations only give information about the total rainfall over a 24 hour period; these data are still useful in ascertaining the days of the year in which rain events occur. The least useful of the stations is the totalizer at Tullul El-Khureishe, which only gives an annual estimate of rainfall and can only be used for looking at long-term trends in rainfall.

The long-term variation in annual rainfall depicted in Figure 5.8 and Figure 5.9 shows a high degree of fluctuation between years and in most cases a visible decrease in the amount of precipitation from the onset of data recording in the early 1960s to the late 1980s. First, Figure 5.8 and Figure 5.9 show a large coefficient of variation between years for all stations; the standard deviation of annual rainfall totals for each station is of the order of 45% of the mean. There is a reduction of standard deviation for the data from the Umm El Quttain and Deir El-Kahf stations from the earliest years to the 1980s. The standard deviations of the annual rainfall for the whole period for the two stations are 76.7 mm and 63.4 mm respectively whereas those of the 1980-1989 period are only 34.2 mm and 51.3 mm. Safawi and Aritain do not have a significant decrease in the standard deviation and in the case of Azraq the standard deviation of the annual rainfall actually increases from 31.4 mm to 37.1 mm

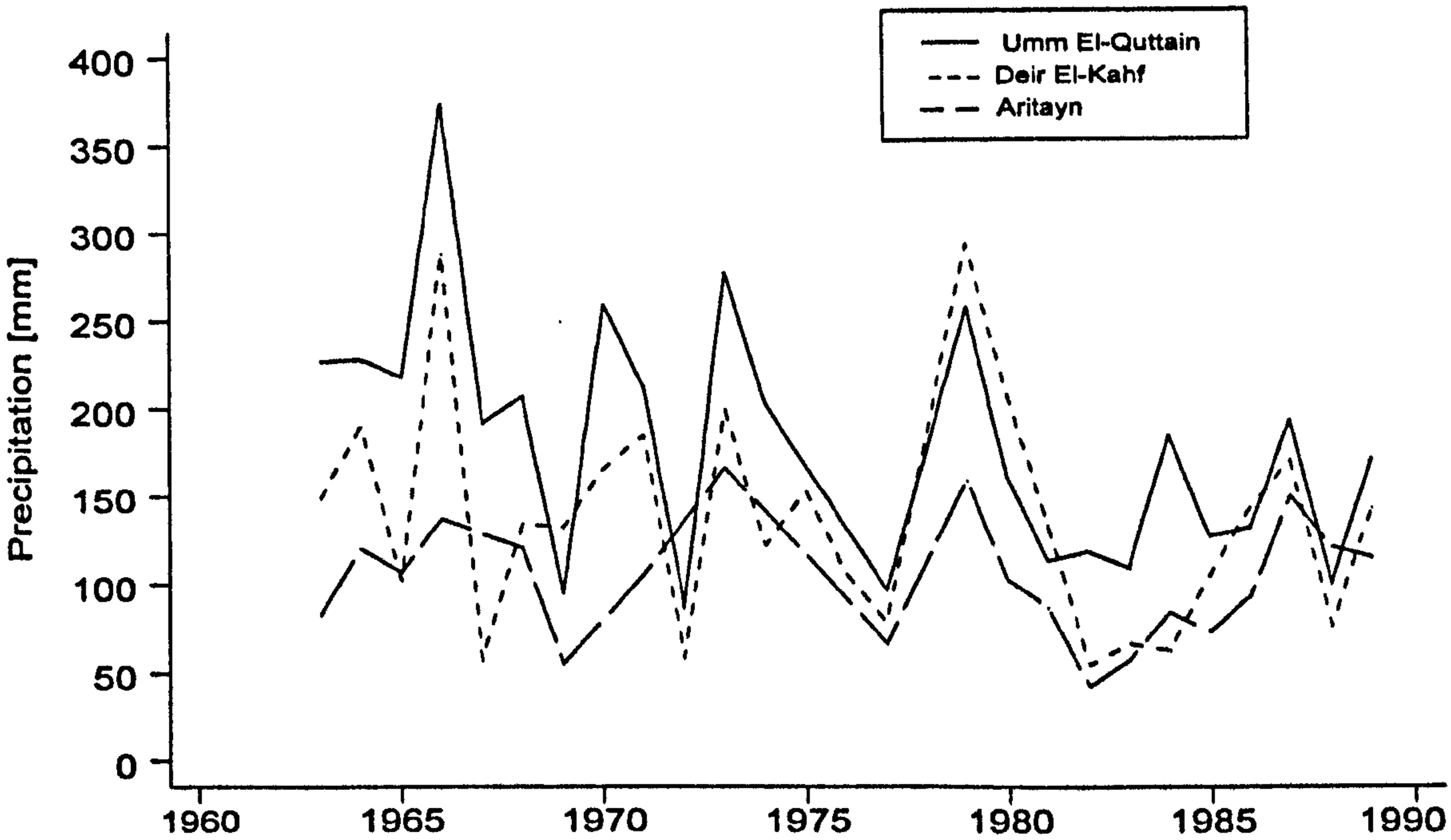

Figure 5.8: Annual change in precipitation for the Jebal Haurân sites (1963-1989)

The Jebal Haurân stations (Figure 5.8) indicate a considerable reduction in annual precipitation from the first ten years to the last ten years. The means for Umm El Quttain, Deir El-Kahf and Aritain over the whole period are 169.4 mm, 136.4 mm and 100.9 mm respectively, but the 1980-1989 means decrease to 137.4 mm, 110.1 mm and 87.6 mm. In the case of Umm El Quttain, only two years with annual rainfall significantly less than 200 mm occurred over the period 1963-1974, while in the 1980s there was not a single year when the rainfall reached 200 mm. Additional annual rainfall data for years 1992/93 and 1993/94 of 12.8 mm and 79.8 mm respectively would suggest a continuation of this trend. The Deir El-Kahf data show a similar trend and there are indications that Aritain has a reduction although the data are limited. The annual totals in 1994/95 and 1995/96 for the Menara station, which lies between the three Haurân stations, were 203.5 mm and 122 mm. The winter of 1994 was in fact the wettest since 1979, but the winter of 1995 was closer to the long-term mean.

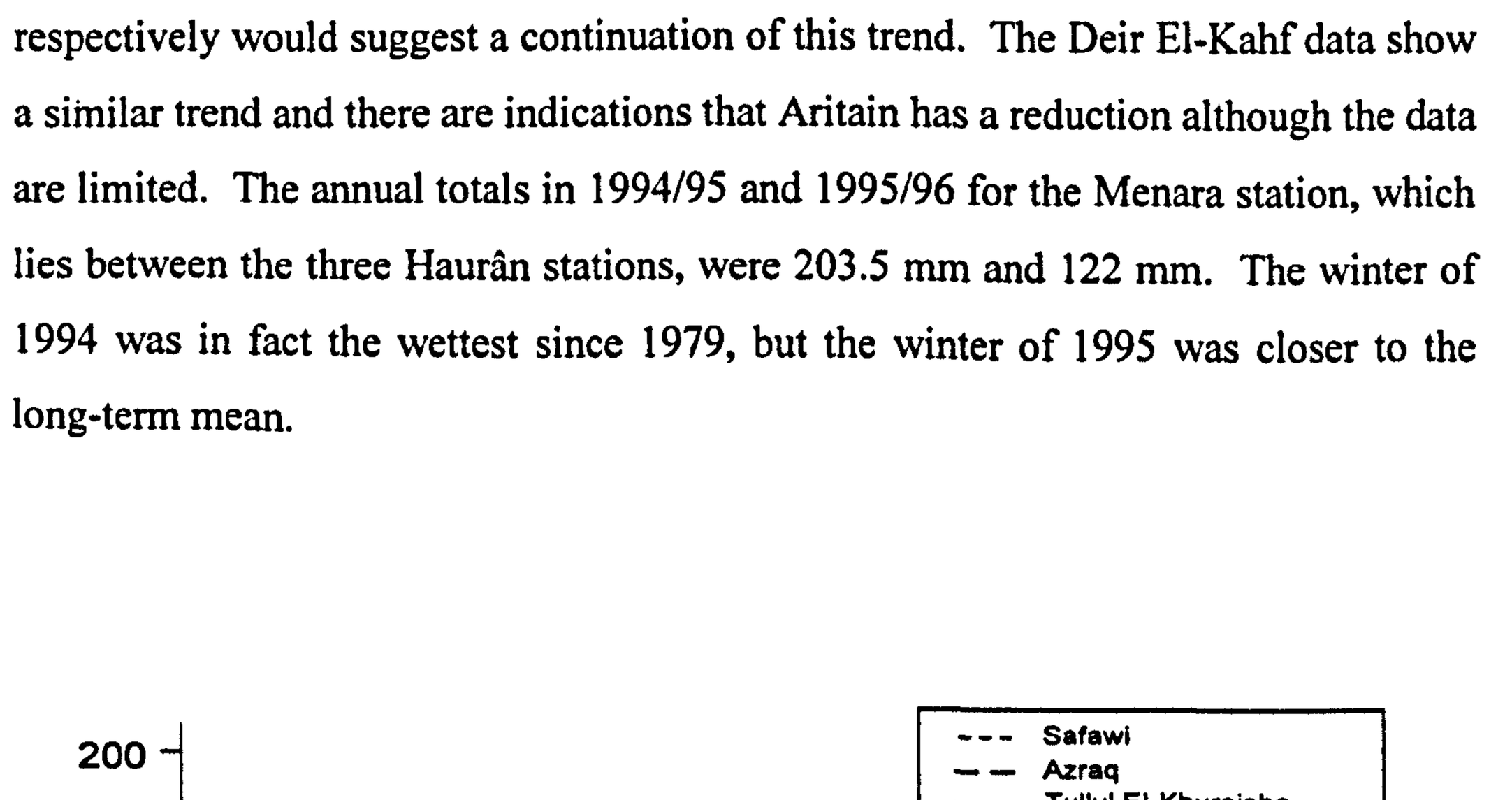

Figure 5.9: Annual change in precipitation for the non-orographic sites (1963-1989)

The sites unaffected by the orographic nature of the Jebal Haurân represent a rather different picture. The means for Azraq and Safawi for both the total series (1963-1989) and the shorter period (1980-1989) are similar: the mean for Safawi being 76.1 mm and 76.7 mm for both periods, while Azraq decreases slightly but not significantly from 70.0 mm to 67.3 mm. Data for Tullul El-Khureishe are inadequate to make any valuable comparisons.

The monthly mean rainfall data for 1980-1989 for the five rainfall stations nearest the field sites, indicate some interesting trends, which are summarised in Figure 5.10. Umm El Quttain has the highest mean annual rainfall of approximately 122 mm, with a rapid increase in rain from October to a maximum in December before decreasing slightly until March and then dropping off quickly in April leading to a negligible amount in May (<1 mm). Deir El-Kahf and Aritain show a similar pattern with annual means of 113 and 89 mm respectively with their highest monthly rainfalls in December. These three stations give credence to the idea that frontal systems that continue over the hills to the east of the Rift Valley will tend to give precipitation only as they are forced to rise over the higher ground of the Jebal Haurân. The amount of rainfall at these stations during the winter is highly dependent upon two variables: the altitude of the station and its distance eastwards. Umm El Quttain has the highest rainfall because it is the most westerly of all the stations on the Jebal Haurân, even though Deir El-Kahf has a slightly higher elevation. Umm El Quttain receives the rainfall first, whereas Deir El-Kahf, which lies on the south-eastern side of the hills, is slightly in the rain shadow and therefore receives less.

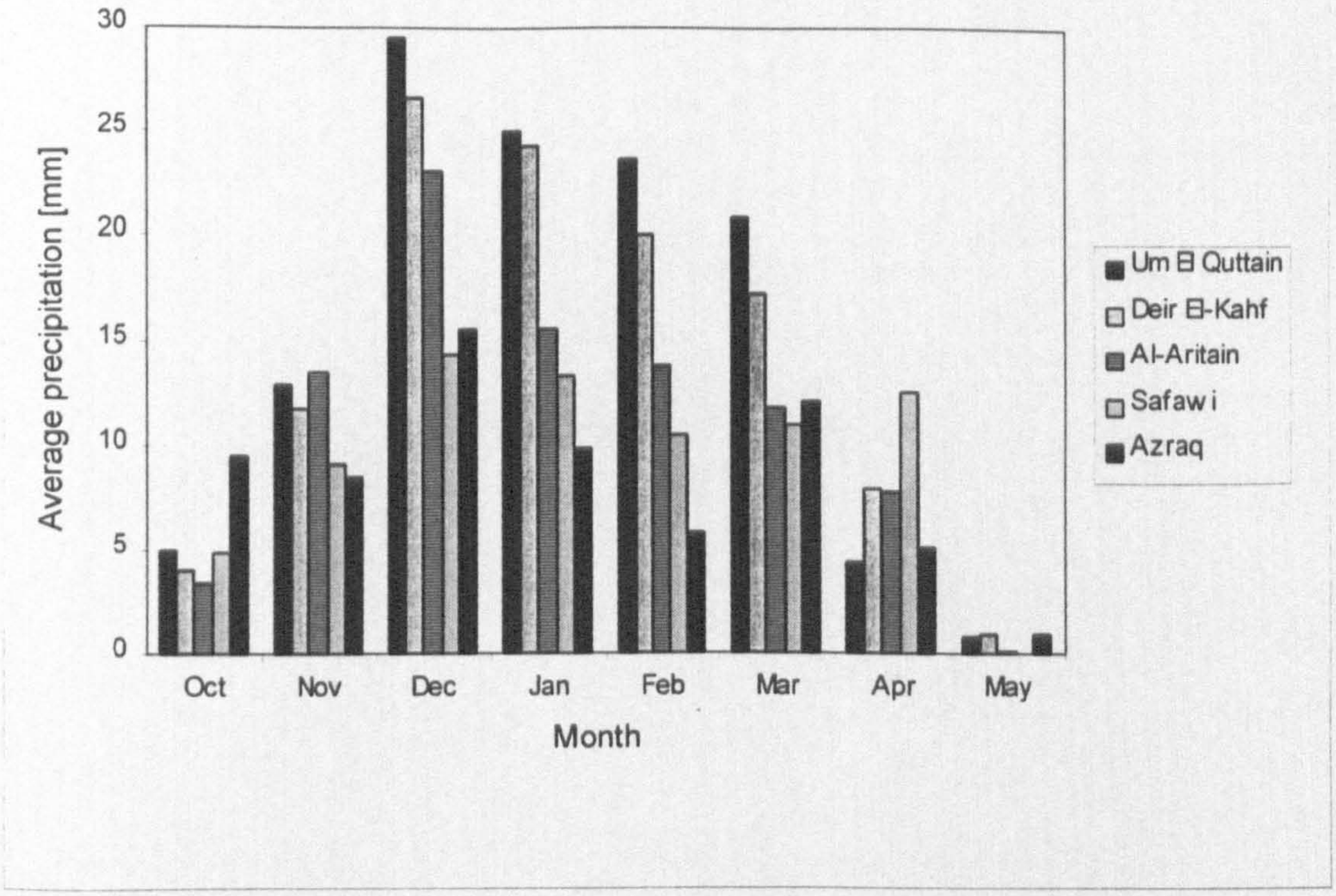

Figure 5.10: Mean monthly precipitation for stations in the area (1980 - 1990)

While the three stations on the footslopes of the Haurân mountains experience rainfall due to an orographic effect, the other stations, which lie at much lower elevations, seem to be dominated by other climatic patterns which contribute to a more random distribution in rainfall (Sharon, 1972). These stations are dominated by a rainfall pattern which bears little relation to the precipitation falling on the hills to the north and west. Azraq, for example, has an October rainfall mean which is almost double that of the other stations and is only one of three stations to experience rainfall in May. The Safawi and Azraq graphs show no distinct seasonal trends, no particular maxima, and are dissimilar to the more traditional pattern exhibited by the Haurân sites.

Further analysis shows that the rainfall pattern becomes less temporally variable the further away the site is from the Jebal Haurân. The non-orographically affected sites of Azraq and Safawi display a more consistent, if limited, pattern of rainfall throughout the winter season and over the last thirty years there has been more continuity in the amounts of rainfall. Paradoxically, the sites on the Jebal are less consistent and indeed seem to be within a variable regime whereby there are years of

plenty followed by years of relative drought. They seem, therefore, to be more profoundly affected by the larger-scale meteorological conditions that control the climate further to the west, specifically the frequency of eastward penetration of cyclones from the Mediterranean in winter.

A clear idea of the normal winter rainfall is necessary so that rainfall simulation experiments can accurately model reality. Despite a great amount of variability between years, it remains useful to investigate the nature of the rainfall using the high resolution data obtained by the AWS. As can be seen in Table 5.4, where the mean intensity used is 75 mm h^{-1}, there is a tendency for scientists to look at rainfall intensities which may have return intervals of several years (Farmer, 1973; Bryan, 1974; Riezbos & Seyhan, 1977; Roth *et al.*, 1985; Cleary *et al.*, 1987). While such an approach is suitable when looking at threshold erosion events, it is excessive when considering the formation of soil crusts on unstable soils. In the Badia, soil crusts will form annually regardless of big storm events and therefore it is more important, when considering simulation, to attempt to model typical conditions.

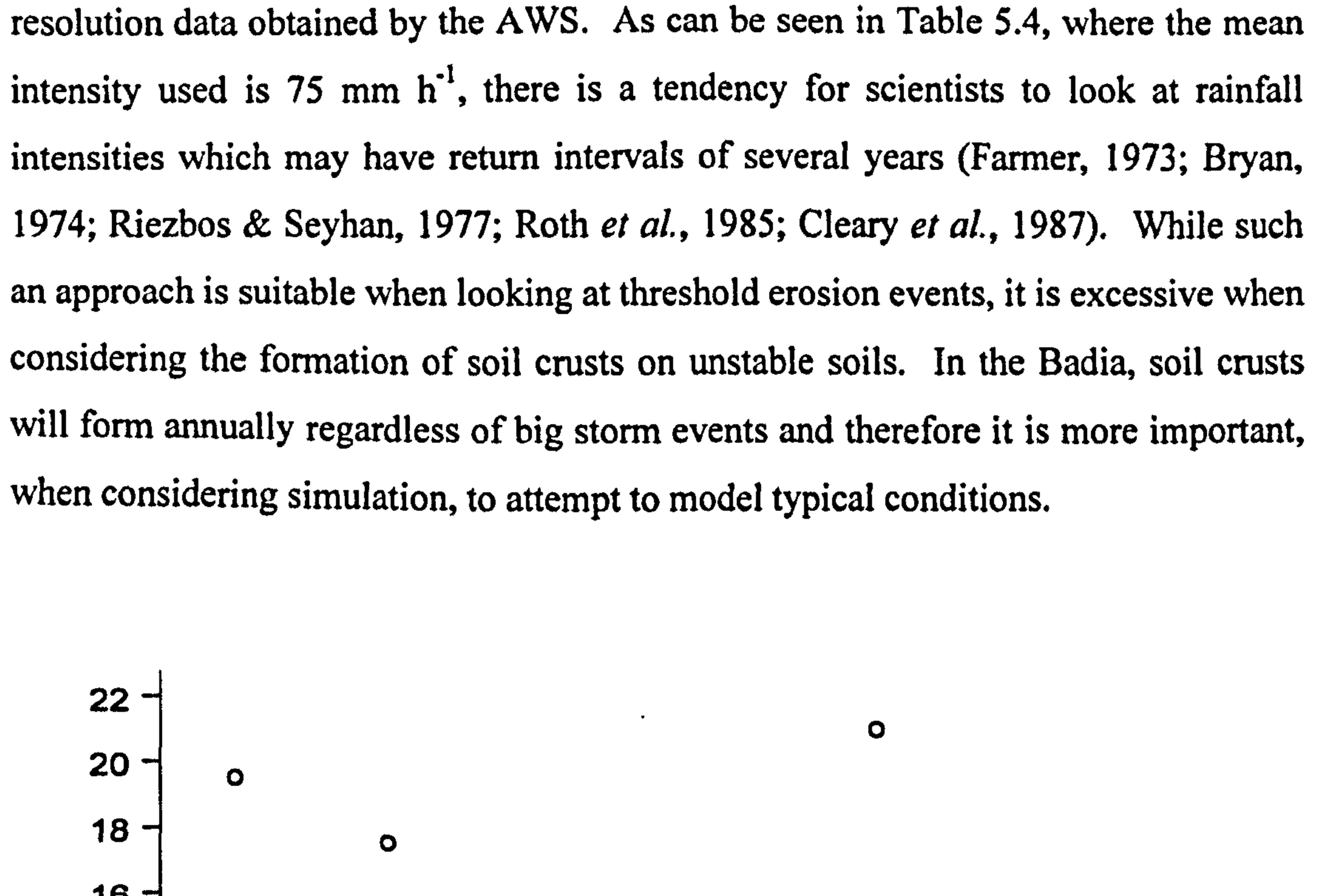

Figure 5.11: Individual rainfall events at Menara [August 1994 - May 1996]

Figure 5.11 and Figure 5.12 show the individual rainfall events which have occurred since the setting-up of the AWS in August 1994 and a calculation of the monthly rainfall respectively. Between August 1994 and August 1996 there were 190 hours of recorded rainfall which fell on a total of 75 days; 52 % of the rainfall events amounted to less than 0.5 mm of rain. The important variables which should be examined are the number of high magnitude events and the length of time over which a rainfall event lasted. There were relatively few storms with a rainfall intensity above 4 mm h^{-1}(see section 5.3.5 for further discussion), especially in the second winter season when there were only four such events (Figure 5.11). In a wet year, such as the winter of 1994/1995, when there were 12 storms (> 4 mm h^{-1}), the pattern of rainfall shows a smaller frequency of overall rainfall, but with a greater number of high magnitude events (Figure 5.13). Of the 74 hours of recorded rainfall during the 1994/5 season, only 25 had 0.5 mm h^{-1}, whereas in the following drier season there were 112 hours of recorded rainfall, of which 74 hours (66%) constituted events of 0.5 mm h^{-1}.

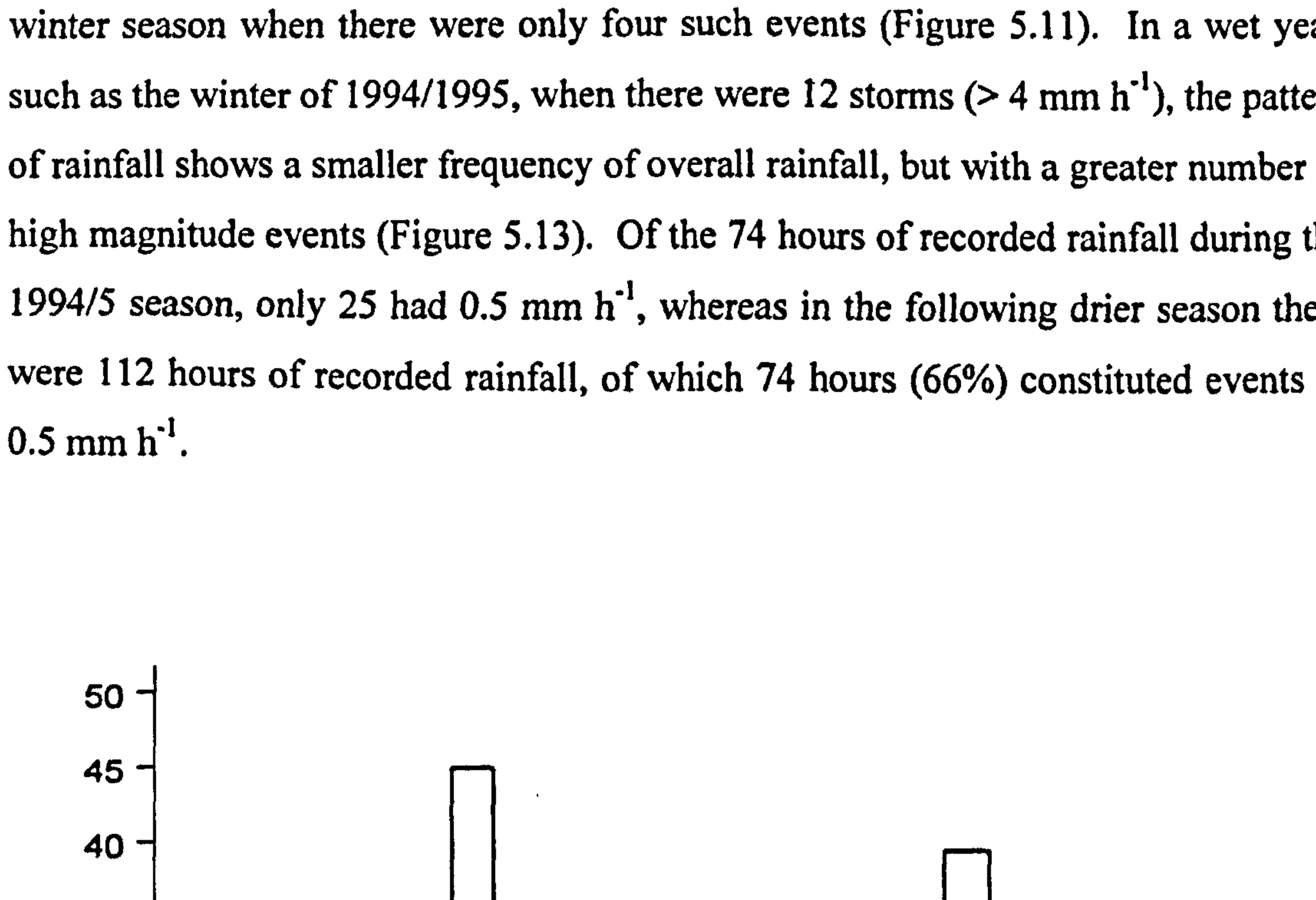

Figure 5.12: Monthly rainfall totals at Menara [August 1994 - May 1996]

This suggests that many of the rainfall events in the winter of 1995/6 were characterised by several hours of the day with a light drizzle which never exceeded 0.5 mm h^{-1} (Figure 5.14).

Considering that the majority of soil erosion processes occur at higher rainfall intensities, it is important to note that there were significant storm events at the beginning of each winter season: in the first season there was a 19.5 mm h^{-1} event at the beginning of September and in the second season there was the largest single event of the two years at 21 mm h^{-1} in November 1995.

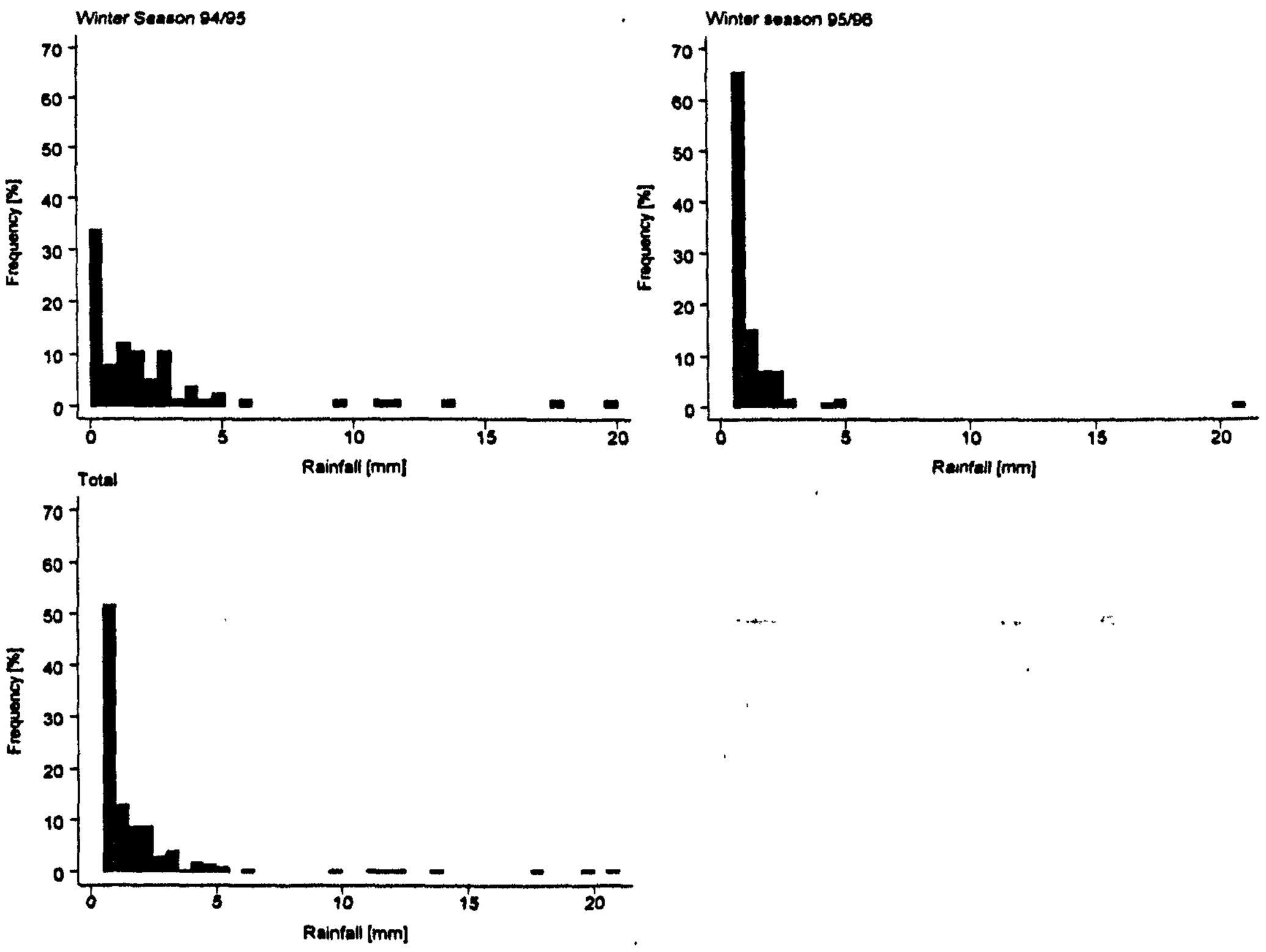

Figure 5.13: Rainfall frequency distribution at Menara [August 1994 - May 1996]

Figure 5.14: Duration of rainstorms at Menara [August 1994 - May 1996]

5.3 INTRODUCTION TO RAINFALL SIMULATION

The simulation of rainfall for studies of infiltration, surface runoff, erosion and surface crust formation is not new. Simple methods of applying rainfall using watering cans were adopted as early as 1932 (Duley & Hays, 1932). Since then, rainfall simulators have been used extensively in soil research. While in the laboratory it has been possible to refine the designs of simulators to almost any specification of drop size, intensity and energy, simulators used in the field have encountered considerable problems (Imeson, 1977; Yair *et al.*, 1980).

5.3.1 Why rainfall simulation

There are four pragmatic reasons for using rainfall simulation as a tool in soil research. Soil and soil-water interactions and processes can be measured in a relatively short time (Meyer, 1965). Simulated storms can be applied for selected periods using specific soil treatment conditions. Observations from a series of storms can indicate relative differences in those treatments. Measurements taken during simulated storms can be replicated on the same or different plots (Meyer, 1994).

In arid and semi-arid environments the need for rainfall simulation experimentation increases. Individual storms, often with intensities with return intervals of a number of years, can be the most important in modifying the landscape. For example, at the Muaq'qar experimentation station in Jordan, where the mean rainfall is 150 mm a^{-1}, five winter seasons were needed to obtain enough rainfall data to carry out adequate experimentation on the effect of different soil amendments because some years had as few as three rainstorms in the whole winter season (Abu-Sharar, 1996 - Table 5.3).

Rainfall simulators do not eliminate the need for natural rainfall experiments. In fact, such experiments are vital for long-term studies which seek to elucidate different processes caused by large amounts of low-intensity rainfall and their relationship with the high magnitude events which occur more infrequently. However, the length

of time needed to obtain satisfactory results with enough variability in the storm events which occur will often be prohibitive. The present scientific environment requires rapid answers and the questions which are asked in twenty years will probably not be those which are designed to be answered with present long-term experiments (Neff, 1979). It is important, therefore, to combine the two approaches by using longer-term and larger-scale projects to verify simulator results.

Season	Date		Total rainfall (mm)	Number of rain storms	Rain storms (mm):	
	First	Last			Maximum	Minimum
1987 / 88	17/10	19/3	114	18	20.4	0.3
1988 / 89	19/11	14/3	123	11	49.8	0.5
1989 / 90	2/1	2/4	74	8	21.2	0.9
1990 / 91	22/10	16/2	29	3	11.6	6.4
1991 / 92	13/10	31/12	76	7	22.8	2.3

Table 5.3: Selected parameters of the rainfall events in the Muaq'qar Experiment Station for the years 1987 - 1992. Source: Abu-Sharar (1996)

There is very little soil crust research which does not use some aspect of rainfall simulation to model crust formation, development and morphological characteristics. Table 5.4 gives a sample of the simulators that have been used and shows the wide variety of research which has been undertaken, although it can be noticed that much of the research is carried out in the laboratory rather than the field.

5.3.2 The characterisation of natural rainfall

It is significant that the understanding of natural rainfall is limited and therefore it is impossible to model it accurately using rainfall simulation techniques. Research has increasingly allowed the accurate simulation of individual rainfall

Type of simulator	Drop size (mm)	Velocity	Kinetic energy	Intensity (mm h^{-1})	Drop Height (m)	Field or Laboratory	Literature cited †
Drop former	2.7, 5.1	97%			11.2 m		Moss,1991a,b
Drop former	2.97	4.98	12.4 J mm^{-1}	31	1.6	Lab	Levy *et al.*, 1994
Drop former	4.6			63	4.57	Lab	Bradford *et al.*, 1986,1987 (Mutchler and Moldenhauer, 1963)
Hypodermic needles	3.5	4.0 m s^{-1}	240 J m^{-2} h^{-1}	30 ± 0.8	0.82	Lab	Ben-Hur *et al.*, 1990
	3.31-5.25	8.32-9.29			14.0	Lab	Nearing *et al.*, 1986
	1.87	92-96	160 mm h^{-1}	75-150	6.4	Lab	Farmer, 1973
Capillary	2.82-3.72	6.05-6.44 m s^{-1}	0.74 - 15.86 J m^{-2} mm^{-1}	0-185	3	Field	Roth *et al.*, 1985
Capillary		80%		20	6	Lab	Le Bissonais *et al.*, 1989
Plastic capillary tube	3.0	50%	11 J m^{-2} mm^{-1}	40-120	1.5	Field	Imeson, 1977
Polyethylene tube	3.5 & 5.0	7.2-8.4 m s^{-1}		10-200	6-10	Lab	Riezebos & Seyhan, 1977
Multiple drop	3.2	5.9	24.5 J m^{-2} mm^{-1}	40	2.5	Field	Le Bissonais & Singer, 1993 (Munn & Huntington, 1976)
Single drops	0.75 - 3.75	3.08 - 7.86 m s^{-1}	20.9 J m^{-2} mm^{-1}	n/a	2.4	Lab	Sharma *et al.*, 1995
Rainulator	4.17	6 m s^{-1}			2.4	Lab	Savat, 1977
Oscillating nozzle	2.3		28.1	64		Lab	Bradford & Huang, 1993
	2.7	>98%		30-140		Lab	Chartres & Mücher, 1989
Single nozzle	1.3	75%	0.17 J m^{-2} s^{-1}	32	6	Lab	Slattery & Bryan, 1992; 1994
						Lab	Verhaegen, 1984 (De Ploey, 1981)
Stationary nozzles	2.9-5.6			46	2.5	Lab	Young & Wiersma, 1973
Fixed nozzle	0.5-5.28	2.0-6.45	n.a.	102	2.59	Lab	Bryan, 1974
Rotating disk	1.9	6.02 m s^{-1}	470 J $h^{-1}m^{-2}$	26		Lab	Agassi, 1981 (Morin *et al.*, 1967)
Rotating disk	2.6		33 J m^{-2} mm^{-1}	100		Field/Lab	Cleary *et al.*, 1987 (Morin *et al.*,1967)
Rotating disk	2.6		25.88	81		Lab	Ekwue, 1991 (Morin *et al.*, 1967)
Rotating boom				64	2.4	Field	McIssac *et al.*, 1995 (Swanson, 1965)

Table 5.4: Rainfall characteristics used for rainfall simulation in soil crust research.
† Authors using simulators developed by others (in brackets)

characteristics (Bubenzer, 1979), and complicated simulators have been constructed with increasing control on every variable (see Table 5.5). Despite expert knowledge in the latest nozzle technology, scientists using rainfall simulators have a limited hold on the very thing they are imitating. The presupposition underlying most soil research that there is a simple relationship between the rainfall spectra and rainfall intensity over space and time is incorrect (A. Gadian, pers. comm.).

The difficulty in rainfall simulation arises because of the technical inability to measure natural rainfall adequately. Four rainfall variables are regularly cited as being fundamental to soil surface processes such as erosion, runoff and surface sealing: intensity, kinetic energy, drop size distribution and the effect of wind upon these (Hudson, 1961). An essential problem in simulating each of these variables is that they are all temporally and spatially variable during a storm event.

Rainfall intensity is important because it significantly affects the amount of infiltration, whether a crust is present (Farres, 1978) or not (Dunne, 1991). However, the recording of the mean intensity of a rain event is inadequate for modelling the impact of rainfall on the soil surface. Convective storms in semi-arid, arid and most tropical areas are often brief but with a large magnitude, which means that hourly measurements, as with the AWS at Menara, do not accurately describe the intensity unless the length of the storm is also measured. Even measurement of the storm length approximates the intensity, because storms will often increase in intensity to a maximum before decreasing again. The period of maximum intensity is the rainfall feature most significant in terms of erosivity.

Kinetic energy is connected to intensity, although there is a significant departure from a linear relationship which has been noted by various authors (Laws & Parsons 1943; Mihara, 1951; Hudson, 1961). The kinetic energy increases rapidly from low intensities, but a wide scatter is associated with these low intensities. Between intensities of 25 and 50 mm h^{-1}, the marginal rate of increase in kinetic energy falls to zero and the relationship becomes linear. At intensities greater than 100 mm h^{-1} it is suggested that there is a slight reduction in kinetic energy and the variation between storms becomes negligible (Hudson, 1961).

In any rainstorm, whether of low or high intensity, there is always a significant distribution in the size of raindrops (Figure 5.15). The minimum size of a raindrop is governed by the minimum size required to fall out of suspension in the air, while the maximum size is about 6 mm, above which drops generally become unstable (Blanchard, 1950). It is observed that there is a general increase in drop size and distribution as intensity increases. Even at high intensities, however, the number of large drops remains fairly constant. Therefore for any rain event there will be continuous spatial and temporal changes in dropsize distribution corresponding to changes in intensity.

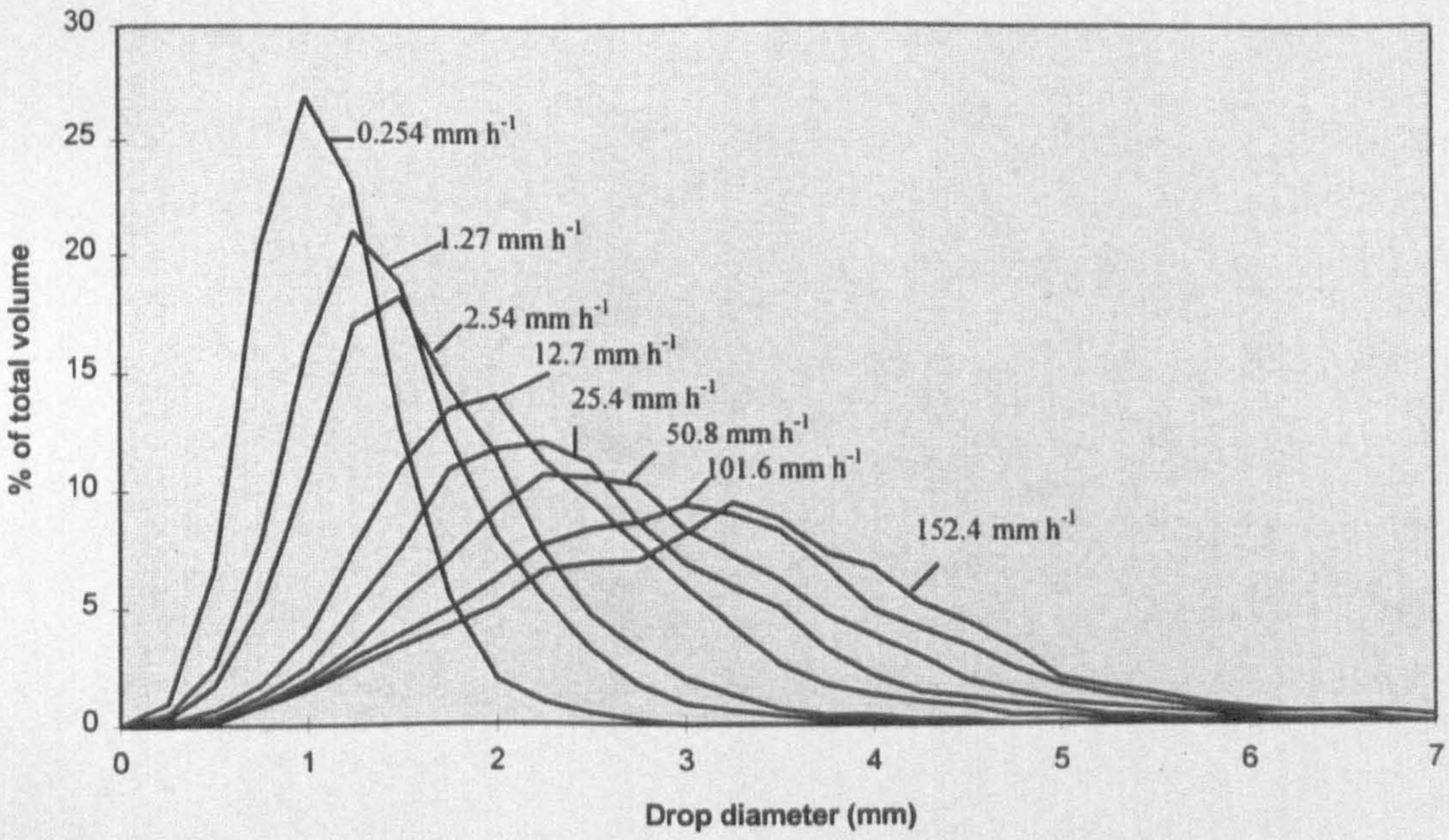

Figure 5.15: Percent of total volume contributed by simulated raindrops for eight rainfall intensities. Source: adapted from Laws & Parsons (1943)

Wind is an important secondary variable because it affects the velocity and the angle of impact of raindrops on the soil surface. Most frontal rainstorms are associated with increased wind speed which in turn increases the effective rainfall intensity (Sharon *et al.*, 1983). Associated with the impact angle of the rainfall is the slope

angle, which determines the angle at which the rain hits the surface. When these two factors are combined, there can be as much as 3:1 variation in point measurements on local slope gradients and their orientation relative to the incoming rain (Sharon *et al.*, 1983). In section 5.2.2 the correlation was made between the prevalent wind direction and rainfall which has implications for asymmetric patterns in soil crusting due to the micro-topographic slopes of furrows. In a ridge and furrow sequence there will be large variations in the erosivity of the rainfall because of such changes in local slope angle. The potential effect of these combined factors on the dislocation and splash of surface particles cannot be disregarded. Rain hitting a perpendicular surface will cause some material to be dislocated due to the development of radial jets (Al-Durrah & Bradford, 1981) and the propagation of Rayleigh surface waves causing lateral outflow sheets to form (Alder, 1979), but if a horizontal component is added to the rainfall, then there is much more potential for material dislocation and consequently erosion. In terms of crust formation, additional intensity of the rain will directly affect the vertical formation of the structural crust; with greater availability of dislocated particles, there is a greater propensity for depositional crusts to form. While a vertical rain-gauge will correctly measure quantity and intensity of inclined rain, the velocity factor must be increased by $1 / \cos \theta$ from the horizontal, which is especially important when values of terminal velocity are squared for calculating kinetic energy (Hudson, 1961).

5.3.3 Rainfall simulation techniques

Building a simulator requires a compromise among the four important variables of intensity, kinetic energy, drop size distribution and the effect of wind. It is often prudent to concentrate on one at the expense of the others depending on the focus of their research. With contemporary nozzle technology, it is possible to get close to simulating rainfall with a wide spread of drop sizes, especially at the higher rainfall intensities. Many of the devices for simulating so-called 'natural rainfall', whether of the drop-former or pressure nozzle variety, are designed to obtain a constant distribution of raindrops over a certain area for a given period of time. Although it is

possible to achieve a fairly constant distribution of raindrop size using a drip-former design, the more popular and versatile nozzles tend to give a great range of raindrop sizes approximating to the distributions of Laws & Parsons (1943). However, nozzle or sprinkler type systems tend to display an inverse relationship between median drop diameter and the applied intensity. Furthermore, depending on the type of nozzles, the fall velocities are often less than the terminal velocities of equivalent drops of natural rainfall (Riezebos & Seyhan, 1977). Whilst many simulators can simulate at different intensities, this is nearly always done between runs, rather than within runs, which does not correspond to temporal changes in intensity during a rain event (Neff, 1979). A primary consideration is whether the simulator is to be used in the laboratory or in the field. Field simulators generally have to be portable, require a large water supply and are generally limited in height which reduces the capability of getting drops falling at near-terminal velocity. It is also difficult to have any control over the wind despite elaborate sheets of metal and/or plastic. Larger-scale experiments have been undertaken (Swanson, 1965; Abrahams *et al.*, 1995), but the scale presents problems of process measurement. The small size of most plots can cause a problem when considering the disproportionate effect stones, bushes, animal burrows, etc. can have within the plot (Neff, 1979). In the laboratory it is much easier to control the rainfall and wind variables, especially with the building of towers 10 metres or more in height in order to obtain the correct velocities for the drop sizes required. Once again, the biggest limitation under these conditions is the size of plot, although the constraint is due to the size of building, rather than any field consideration. Most scientists using simulators in the field or laboratory work on plots of only a few square metres which often requires scaling-up with all the implications that involves (Kirkby *et al.*, 1996).

5.3.4 The Safawi Rainfall Simulator

The simulator used for the research in Jordan had to meet various specifications. First, the simulator had to be portable for movement over rocky ground from one plot to another. Second, efficient use of water was necessary since a regular water supply could not be guaranteed at the field site and therefore all the water had to be brought

to the site. It was therefore decided that the simulator should be approximately modelled on the simulator developed by Roth *et al.* (1985).

A nozzle system, although used in many laboratory-based experiments, is impractical for use in the field due to the amount and pressure of water needed to run such a system. Therefore, a drop-former type simulator was employed using irrigation piping and drip formers from the irrigation system. Drip formers that deliver a specific number of drops and volume of water per unit of time were purchased locally. However, since most had an application rate too large for the simulator, a set of adjustable drip-formers were purchased. These were constructed from two thin cylinders, the outer of which could be rotated by hand. Each cylinder had a hole in its side of approximately 2 mm x 4 mm; by changing the relative positions of the two holes, the flow of water could be changed. If the holes did not coincide, there would be no flow; conversely, if the holes coincided exactly, flow would be at a maximum. The drip-formers were punched into the irrigation tubing which was placed in a spiral and fixed upon a wire grid. The tubing was fixed at both ends to a two-way valve which came from the water container above to ensure that water extended all the way along the pipe, so that there was an equal supply to each drip former.

The tank was suspended 30 cm above the piping and was joined by means of a valve which regulated the flow of water out of the tank. The tank when full held 78 litres of water and had an access tube extending from the side and hatch on the top for measuring water temperature and electrical conductivity.

A completely steady water level in the tank (Roth *et al.*, 1985) was attempted by placing a second container above the first so that as the water level dropped the vacuum in the upper tank would be broken, allowing water into the lower tank and thus keeping a constant head. Difficulties in obtaining a pure vacuum in the upper tank, however, led to an alternative solution. The intensity was measured and an appropriate amount of water was added to the upper tank at 5 min intervals to keep the head, and thus the rainfall intensity, constant throughout each experiment.

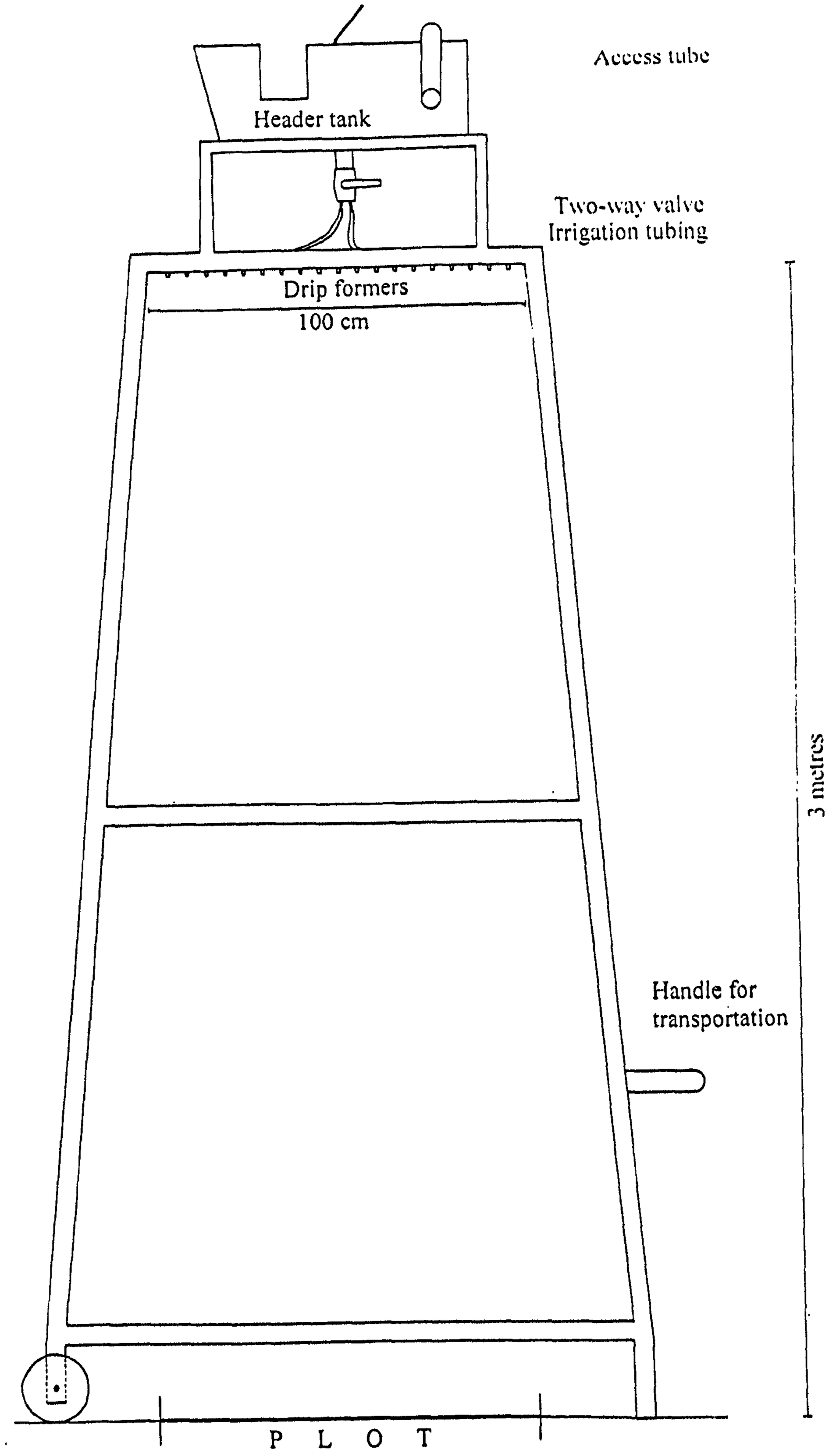

Figure 5.16: The Safawi rainfall simulator

Plate 5.2: The Safawi rainfall simulator

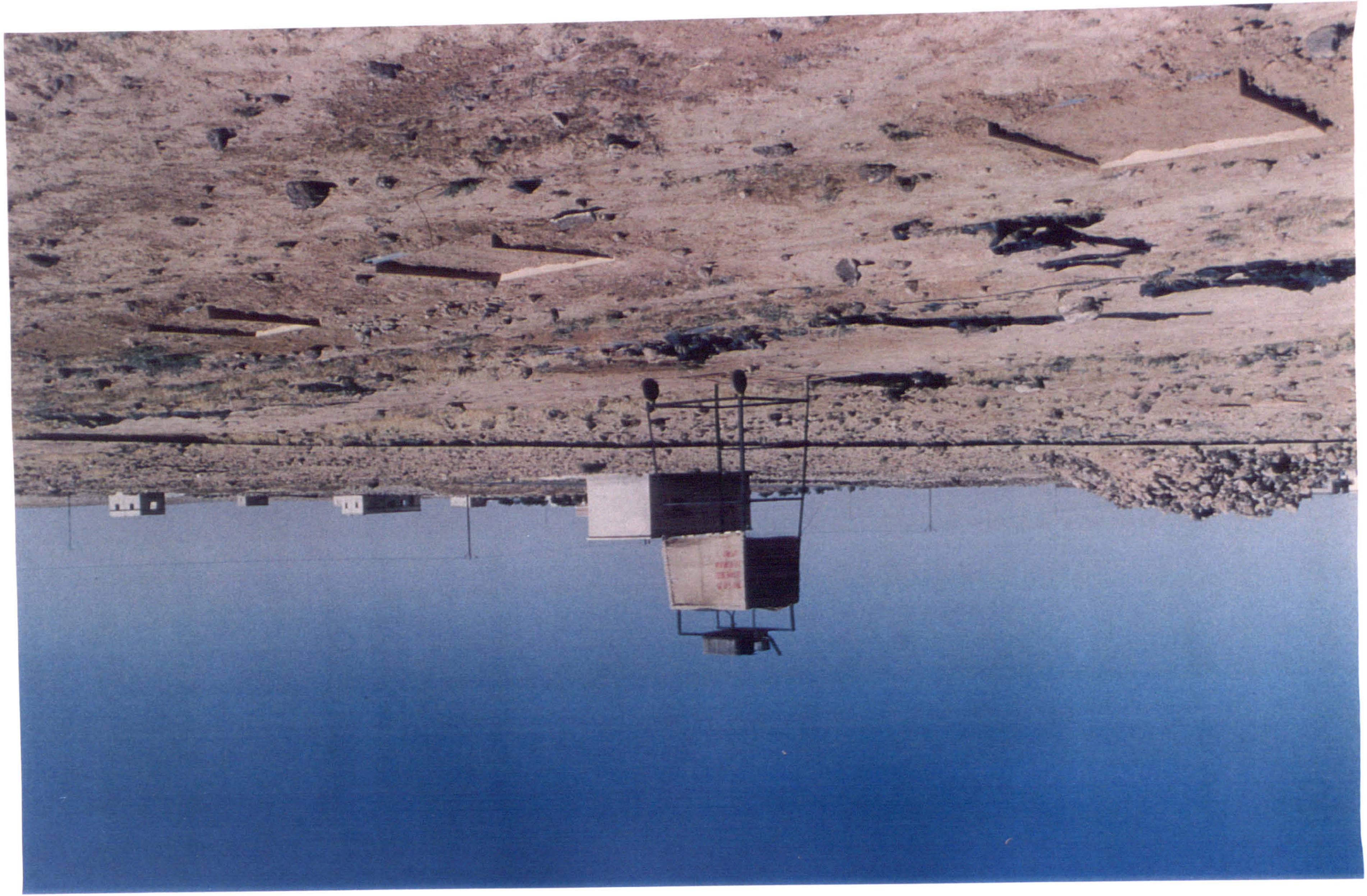

Before each experiment started, a plastic sheet was placed under the set of drip formers before the valve was opened and each former calibrated until it appeared that all the drip formers were dripping at approximately the same rate. The water level in the tank was then measured and the plastic sheeting carefully removed, marking the beginning of the experiment.

5.3.5 Rainfall parameters

None of the Jordanian rainfall data show the intensity or drop size distribution of individual storms. In addition to the hourly data from Menara, the most accurate rainfall intensity data for the Badia are 20 minute resolution for the automatic meteorological stations (Table 5.2).

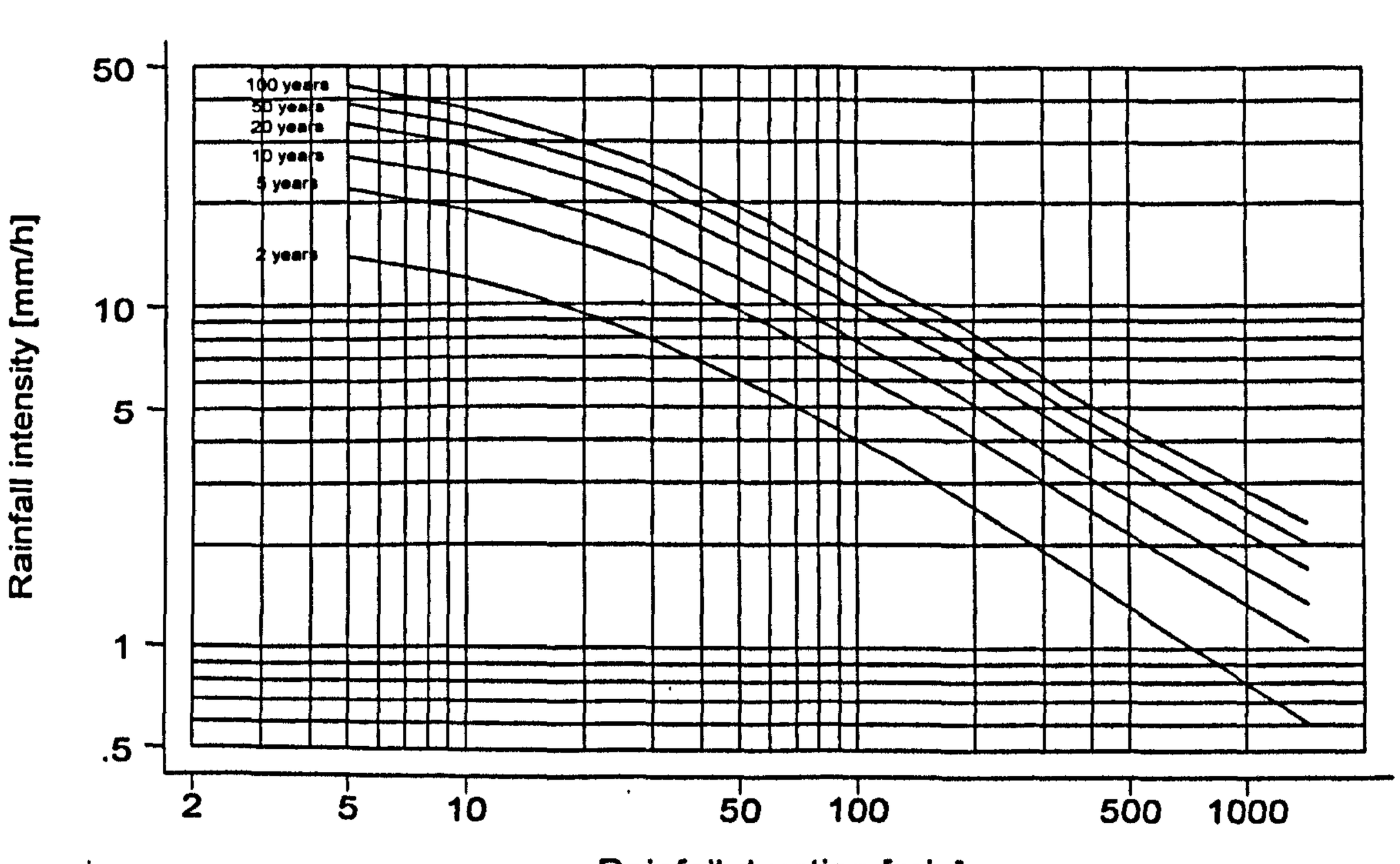

Figure 5.17: Rainfall intensity diagram for Azraq rainfall station (F9) [1965-1985]

source: Water Authority (1989)

Data from Umm El-Quttayyn from the winters of 1992/93 and 1993/94 indicate that the maximum rainfall intensities for each season were at least 42 mm h^{-1} (14 mm in 20 minutes) on 18th December 1993 and 60 mm h^{-1} (20 mm in 20 minutes) on 17th January 1994. Such data would be underestimated by the rainfall intensity graph for Azraq (Figure 5.17), only a few kilometres to the south of the field site (Water Authority of Jordan, 1989).

Data from the AWS for the winter seasons 1994/95 and 1995/96, which only give rainfall per hour (Figure 5.11a), similarly suggest that the highest storm intensities lie between 40 and 60 mm h^{-1}, but that most of the rainfall events consist of between 0.5 and 5 mm which gives intensities of between 1 and 15 mm h^{-1}. It seems that Jordan intensity graphs, such as that in Figure 5.17 for Azraq, are calculated upon rainfall amounts per hour, which result in much lower intensities because the storms rarely last more than 20-30 minutes.

From observation of rain storms in the Badia, it can be seen that there are a few short highly intense rain storms and a larger amount of longer very low intensity events. By observing the marks of the first raindrops on the soil surface, it is concluded that the drop size is usually large. It appears that, due to the very poor aggregate stability, even the smallest and least intense amounts of rain will cause mechanical breakdown of the surface soil aggregates and crust formation.

With this evidence in mind, a proposed intensity range of 10 - 15 mm h^{-1} was adopted to most closely simulate natural rainfall conditions. Although there is some debate concerning the relative importance of rainfall intensity and kinetic energy of raindrops on soil crust formation (Römkens *et al.*, 1986; Valentin, 1985; Moss, 1991a), it is generally agreed that greater rainfall intensities tend to seal the soil more quickly and hence reduce vertical development of the crust (Römkens *et al.*, 1986). Thus it is sensible to simulate rainfall at conditions which compare favourably with the majority of rainfall events in the region. There is a large body of opinion which suggests that rainfall should be simulated at high intensities (Tables 5.4 and Table 5.5), because it is often the threshold events, i.e. those with high return intervals, which are most important in modifying the landscape. From a practical point of view

it is easier to simulate at higher intensities because nozzles and drip-formers are more efficient at higher intensities and the process under examination will be activated more rapidly and responses will be more easily measured. However, it is important to realise that soil processes do occur at lower intensities, albeit over longer temporal scales. Surface crusts may well take several large storm events to develop in temperate locations, but in desert soils such as those in Jordan, there is a very high propensity to crust even with small amounts of rainfall.

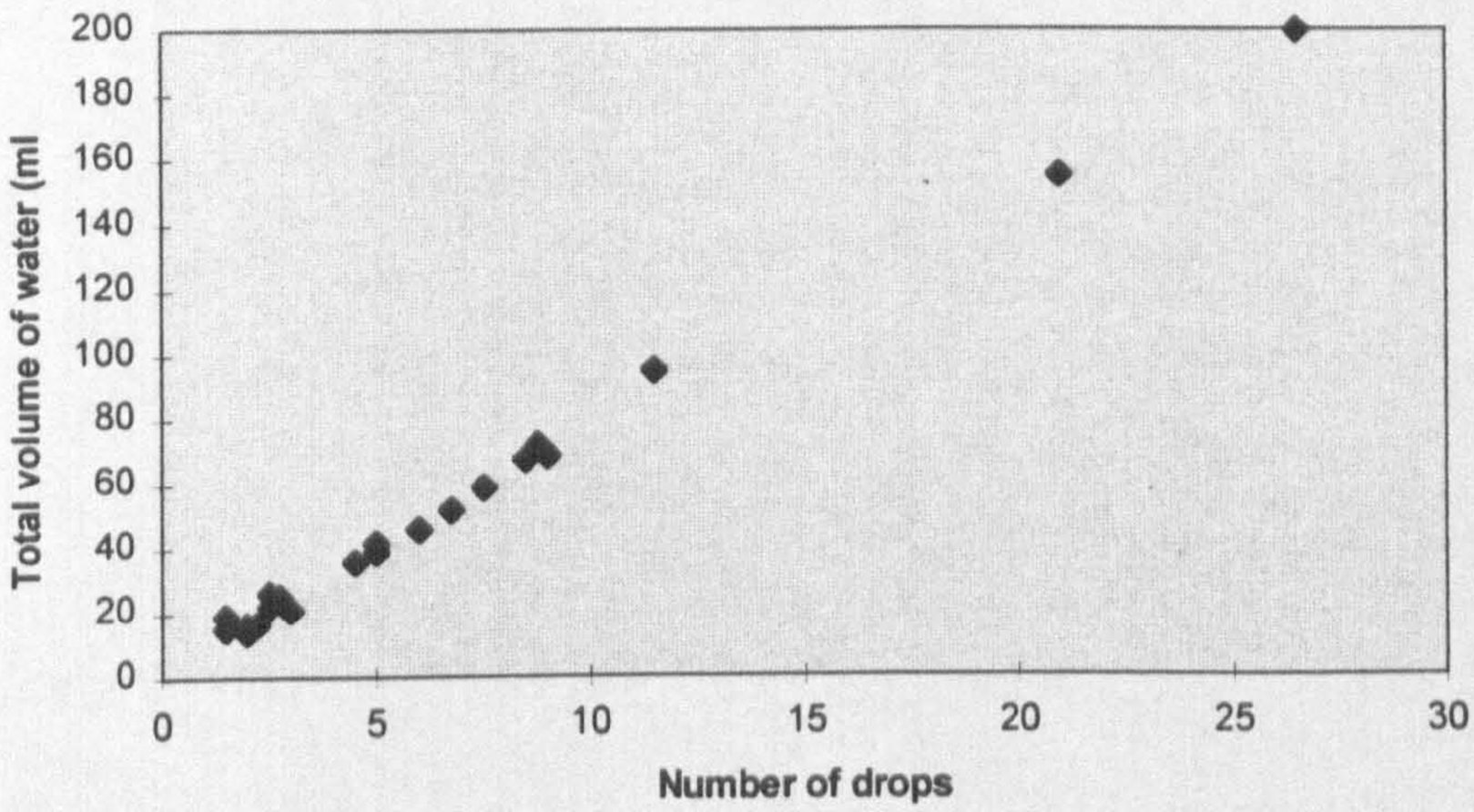

Figure 5.18: An experiment calculating the volume of drops leaving the drip-formers

In order to calculate the mean size of the raindrops falling from the simulator, the number and volume of drops falling from a random sample of drop-formers was measured over a period of one minute. Figure 5.18 shows that there is a high positive correlation between the number of drops and the total volume which indicates that there is little change in drop dimension over time or over the spatial set of drip formers. It is possible to work out the mean size of each drip by assuming each drip approximates to a sphere with volume V_d and diameter D_d, so

$$V_d = \frac{4}{3}\pi\left(\frac{D_d}{2}\right)^3 \qquad D_d = \sqrt[3]{\frac{6\,V_d}{\pi}} \tag{5.7}$$

The experimental results obtained show that the mean drop size is 6.18 mm with a standard deviation of 0.32 mm. A drop size of almost 6.2 mm is large, but if compared with the drop sizes obtained in Table 5.5 which have an mean diameter of 3.6 mm, it is consistent with the larger drop sizes simulated in Maine, Nebraska, the CSIRO in Australia and in Uganda.

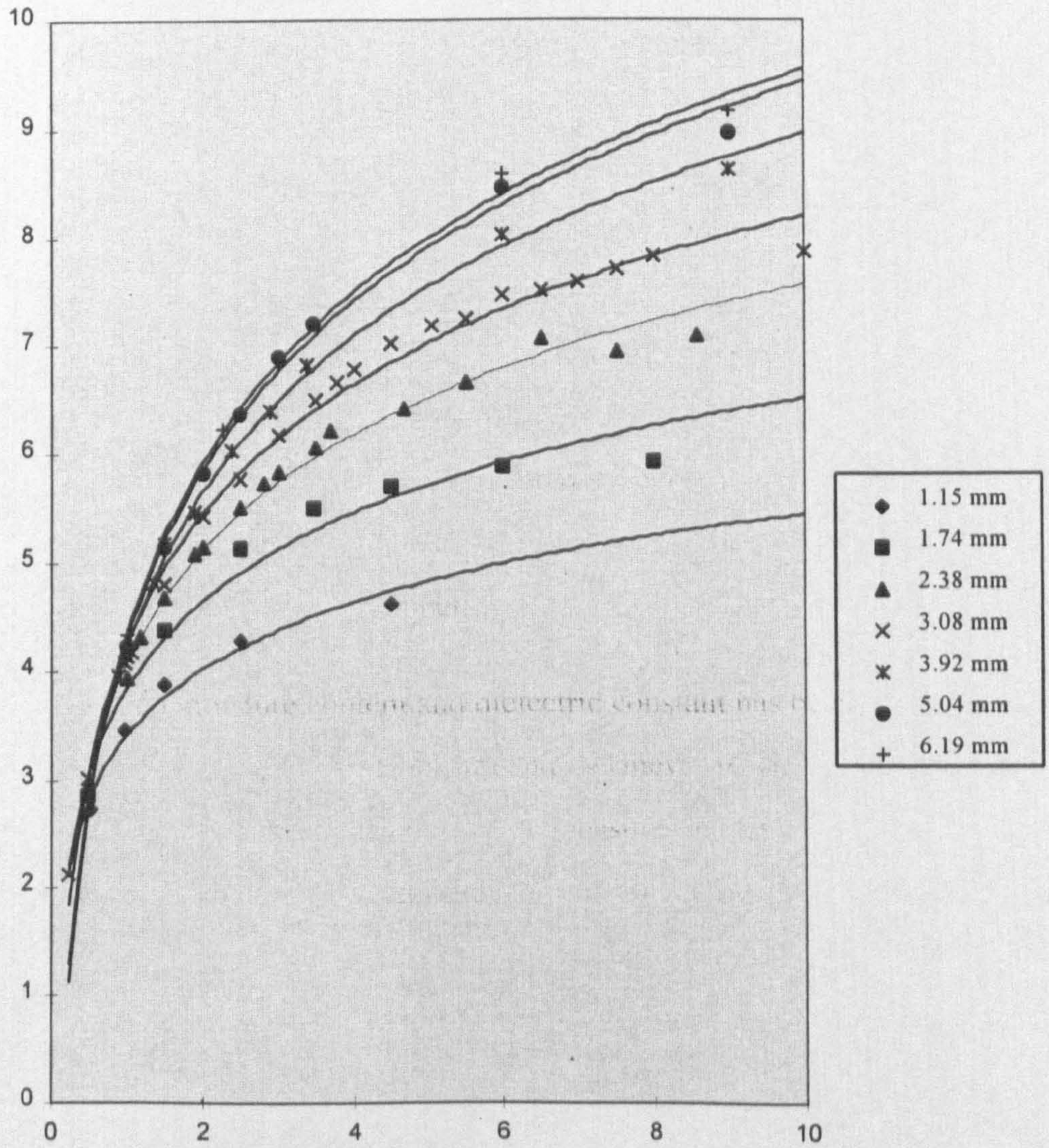

Figure 5.19: Fall velocities of waterdrops from specific heights (adapted: Laws,1941)

Rainfall simulator Location	Drop Formers	Fall Distance (m)	Drop Size (mm)	Intensity ($mm\ h^{-1}$)	Use	Reference
Mobile Infiltrometer, Wyoming	Yarn	2.6		25-152	Infiltration, Runoff	Barnes & Costel, 1957
Portable Infiltrometer, Iowa	Glass capillary tubes	1.0	5.6	101	Erosion, Infiltration, Runoff	Adams *et al.*, 1957
Laboratory Simulator, Maine	Stainless tubes	7.2	3.2 & 5.1	38-50	Erosion	Mutchler & Moldenhauer, 1963
Low-intensity Simulator, Israel	Stainless tubes		2.8	6	Infiltration	Steinhardt & Hillel, 1966
Laboratory Simulator, Illinois	Polyethylene tubes	2.7	3.2	19-33	Runoff	Chow *et al.*, 1965
Drop Tower Simulator Illinois	Hypodermic needles	8.9	2.2	10-70	Erosion and Surface Storage	Bubenzer & Jones, 1971
	Polyethylene tubes		3.4	45-350		
	Stainless tubes		4.9	100-525		
Mobile Infiltrometer, Texas	Stainless tubes	2.3	2.5	5-250	Erosion and Infiltration	Blackburn *et al.*, 1974
Laboratory Simulator, Indiana	Polyethylene tubes	2.6	2.7	13-200	Runoff	Bertrand & Parr, 1961
Laboratory Simulator, USDA	Hypodermic needles	6.7	Variable	1-250	Erosion and Infiltration	Römkens *et al.*, 1975
Tahoe Basin Simulator, CA	Polyethylene tubes	2.5	3.2	76-250	Erosion and Infiltration	Munn & Huntington, 1976
Laboratory Simulator, CSIRO	Hypodermic needles	12.3	2.5 & 5.1	20-250	Erosion	Walker *et al.*, 1977
Laboratory Simulator, Utah	Brass tubes	5.0	4.5	25-787	Erosion and Runoff	Malekuti & Gifford, 1978
	Hypodermic needles	1.6	2.5	38-250	Erosion and Infiltration	
Drip Infiltrometer, USDA	Hypodermic needles	2.6	Variable	5-102	Infiltration	Brakensiek *et al.*, 1979
Laboratory Simulator, Nebraska	Plastic rods	11.3	5.1	20-120	Erosion	Mazurak & Mosher, 1968
Laboratory Simulator, USDA	Teflon tubing	3.0	3.6	76-203	Erosion	Peterson, 1977
Laboratory Simulator, New York	Polyethylene tubes	1.0	3.2	19-33	Runoff	Black, 1970; 1972
Laboratory Simulator, Ghent	Copper tubes	2.8	Variable	4.7-64.5	Erosion	Gabriels & DeBoodt, 1975
Laboratory Simulator, CSIRO	Hypodermic needles	11.2	3.8	0-300	Erosion	Kinnell, 1974
	Plastic tubes		5.1			
Laboratory Simulator, Uganda		6.0	3.2 & 6.2	50-152	Erosion	Rose,1960
Portable Simulator, New Zealand	Wire			20-300	Infiltration	Selby, 1970

Table 5.5: Rainfall simulators and infiltrometers using drop formers to simulate rainfall. Source: adapted from Bubenzer (1979), pp. 125-126

From the work of Laws (1941), which is usually cited as the reference point for calculating the velocity of different drop sizes from different heights, it is possible to approximate the velocity of the drops impacting at the soil surface as 6.85 m s^{-1} (Plate 5.1).

Using the formula $KE = \frac{1}{2}mv^2$ to calculate the kinetic energy of raindrops and using the velocities obtained by the experimental work of Laws (1941), it is possible to calculate that the mean kinetic energy of a single drop from the Safawi simulator, hitting the soil surface from a height of 3 metres, is 3 x 10^{-3} Joules. This figure is equivilent to the kinetic energy obtained by a drop with diameter of 5 mm travelling at terminal velocity (i.e. 9.4 metres fall).

5.4 Conclusion

The study of soil crust formation lends itself to plot experimentation using rainfall simulation. However, this chapter highlights various aspects of soil crust research which are often neglected. It can be seen that the majority of soil crust research has taken place in the laboratory. As discussed in Chapter 4, the laboratory provides a location for almost all variables to be controlled, even to the extent of sieving of the soil to a specific particle size distribution (Farres & Muchena, 1996). While such experiments are undoubtedly important for determining distinct soil processes at a small scale, it nevertheless represents a gross simplification of field conditions where soil conditions are not homogeneous and where there are multiple-scale interactions.

To understand soil crust formation fully it is vital that detailed analysis of climate characteristics is carried out. Rainfall is the most important variable because of its role in forming the crust. It would seem from the analysis provided here that the majority of rainfall events are of very low intensity: 52 % of rainfall events in the two seasons monitored showed 0.5 mm of rainfall falling within an hour. In both the 1994/95 and the 1995/96 seasons there was evidence of at least one heavy rainfall event which contributed up to 20 mm in an hour and probably resulted in intensities of over 50 mm h^{-1}. Such events are very important in forming crust on newly

ploughed land at the beginning of each winter season and subsequent rainfall events would only serve to strengthen and develop that crust which was already created. The rainfall statistics also show some interesting spatial and temporal trends. Rainfall patterns divide between the Jebal Hâuran sites, (Deir El-Kahf, Umm El-Quttain and Aritain) which are dominated by relief rainfall, and the non-orographic sites (Safawi, Azraq and Tullul El-Khureishe). The former seem to have had a general decrease in annual rainfall since monitoring began in 1963, whereas the latter show no such decrease. The rainfall distribution during the winter season is also distinct with the Hâuran sites being dominated by a modal pattern, while the others display a much more random pattern showing that they are much less affected by the relief rainfall of the Jebal Hâuran.

Wind direction has a profound effect on the impact velocity of raindrops and is therefore important for describing areal extent of crust and different amounts of soil erosion on lee and windward facing slopes. There is a distinct and regular diurnal pattern to the wind direction. In the summer months there is a prevailing north-easterly wind during the evening and night, but as the temperature begins to rise in the morning there is a significant shift to a north-westerly direction. This usually occurs via north, but the data show that there are occasions, probably indicative of meteorological instability, when the wind veers via the south. The data for the winter months show a much more complicated pattern because much more of the afternoon shift veers via the south and the evening and night wind is easterly to south-easterly instead of north-easterly. The most important aspect of the data in relation to areal extent of crust formation is the direction of the wind during rainfall events. This quite clearly has been shown to come from the north west with a mean direction of 318.2°. The implications of the data on soil crust formation will be more fully explored in the following chapter.

Wind speed, temperature and radiation elements all combine to produce an understanding of the evaporative fluxes which will vary depending on the presence or absence of a crust. Evaporation during the summer months has been shown to fluctuate between 5 and 10 mm per day creating a very strong negative water

balance. However, in the winter months evaporation rates drop below 5 mm per day allowing positive water balances for several days after rainfall.

The main reason that this work requires background information on climate variables, is so that it is possible to adequately model rainfall using simulation techniques. The plot experiments carried out at Low Farm, despite difficulties in obtaining local high resolution rainfall data, are based upon real rainfall characteristics. A large number of simulators have been reviewed and it is clear that there is great disparity in the classification of rainfall variables between simulators. However, it is clear from the literature that the criteria for measuring rainfall variables is derived from the experimental set-up. In other words the raindrop characteristics which are obtained from the simulator depends upon the processes which are being observed. The Safawi rainfall simulator, which was constructed in Jordan using local materials to a similar specification to that of Roth *et al.* (1985) with a drop height of 3 metres. The use of local irrigation drip-formers meant that the mean drop size was calculated to 6.18 mm giving a velocity at drop impact of 6.85 m s^{-1}. This represents a drop size which is larger than other rainfall simulators. However, this was unavoidable and therefore the more meaningful measure of the kinetic energy would suggest a drop-size of 5 mm travelling at terminal velocity, which is a more appropriate way of comparing the Safawi simulator with others in the literature.

Soil crust research typically concentrates on either the soil processes or on the hydrological aspects although the two are intimately linked. From a good climate base, the next three chapters explore the following linkages.

1. The effect of aspect on moisture retention as controlled by differences in soil crust formation.

2. Water and wind erosion on the soil surface characteristics, at both a field and a ridge/furrow scale.

3. The micromorphological changes that accompany soil crust formation with respect to the microtopography.

6. SOIL SURFACE MOISTURE FLUXES AND THE ROLE OF THE SURFACE CRUST

The major avenue for increasing water available for crop production and aquifer recharge is to reduce the amount of water evaporating from the soil surface. (Kemper *et al.*, 1994, p. 56)

6.1 INTRODUCTION

The main focus of this chapter is to investigate the effect of the surface crust upon the moisture regime in the surface layers of the soil. The soil crust is predominantly seen as a sign of soil degradation, affecting the infiltration of water into the soil. However, the purpose behind looking at moisture changes in the soil directly below the crust is to examine the role of the crust in evaporation. This is especially important in arid environments because the moisture residency in the soil relates directly to biomass production. In order to accurately study small variations in moisture, a non-destructive method was needed. The Institute of Hydrology (IH) have been recently developing a surface capacitance insertion probe (SCIP) which is able to measure to such a resolution. This instrument has not been used in arid environments before and therefore a detailed calibration procedure needed to be carried out to make use of its capability. The first section of the chapter introduces the methodology and principles which act as a foundation to the field measurements. The data are analysed in the second half of the chapter.

6.2 THE MEASUREMENT OF FIELD MOISTURE CONDITIONS

In order to investigate the influence of the surface crust on the moisture dynamics of the near surface soil layers, a non-destructive method for moisture content determination is needed. The standard procedure calculates the weight-loss of a sample after it has been in a soil oven for at least 16 hours (Gardner, 1986; Goudie, 1990; BS1377, 1990). There are two main problems with such a method. First, there

is the practical consideration of doing research in desert environments; spatial variations in soil moisture will be small, but nevertheless important. It is vital in such cases to obtain an accurate weight as soon as possible after the sampling, which is usually impossible, given the location. Second and more important, the moisture content of soil is best monitored over time, for example after a rainfall event, and this is impossible with a destructive method. If samples are taken nearby, there is a high probability that the moisture conditions will be different because moisture content has a high spatial variability (Mason *et al.*, 1957). Sampling will alter the moisture conditions of the surrounding soil, especially when a crust structure is disrupted. To overcome these problems, various options are open, all of which rely on obtaining indirect readings for moisture content. The neutron probe has been used extensively for looking at large-scale changes down the soil profile. Neutrons emitted from the probe are scattered and slowed down by hydrogen nuclei in the soil: this transfer of energy can be measured, and the moisture content inferred. The resolution of the equipment ranges from 16 cm radius at saturation to 70 cm near zero moisture content (Van Bavel *et al.*, 1956): therefore, the instrument is not ideal for monitoring high resolution soil surface moisture variability. To obtain high resolution data, electrical methods can be used which relate the soil moisture to the dielectric constant of the soil. Two such techniques have emerged over the last twenty years: Time Domain Reflectometry (TDR) and the Surface Capacitance Insertion Probe (SCIP) (Ansoult *et al.*, 1984; Campbell, 1990).

The link between moisture content and dielectric constant has been acknowledged for many years (Smith-Rose, 1933; Hoekstra and Delaney, 1974), and yet only in the last decade has equipment been developed to measure it. Because soil is made up primarily of solid material, water and air, the dielectric constant, which is very sensitive to the amount of water, will give a ratio of water to non-water components. Time-Domain Reflectometry (TDR) is the measurement of the transit time of an electromagnetic wave propagating in the medium, so that the greater the moisture level, the slower the speed of the wave. Methods using capacitance, such as the SCIP (Figure 6.1, Plate 6.1), have two metal electrodes which measure the capacitance of the soil between. It is the soil which forms the dielectric medium. Increased

moisture levels raise the level of the bulk dielectric coefficient of the soil, which raises the capacitance and consequently alters the frequency of the oscillator current containing the capacitance (Dean, 1995).

The dielectric constant, which is a ratio and has no units, is an electromagnetic property of materials and is defined as the electric dipole moment per unit volume. In a composite material like soil, there are several contributions to the total electric dipole moment per unit volume. The dipole contribution responds to a given frequency, until a threshold frequency is reached, when it is no longer fast enough to react to changes in the electric field, and ceases to contribute to the net dielectric constant. The threshold depends on the strength of the surrounding molecular bonds and the inertia of the dipole. Water molecules have a permanent electric dipole moment and they reach the threshold of a few gigahertz, at which the dielectric constant progressively falls from a value of 80 (Dean, 1994). Further technical details concerning the functioning of the Capacitance probe can be found in Appendix 1

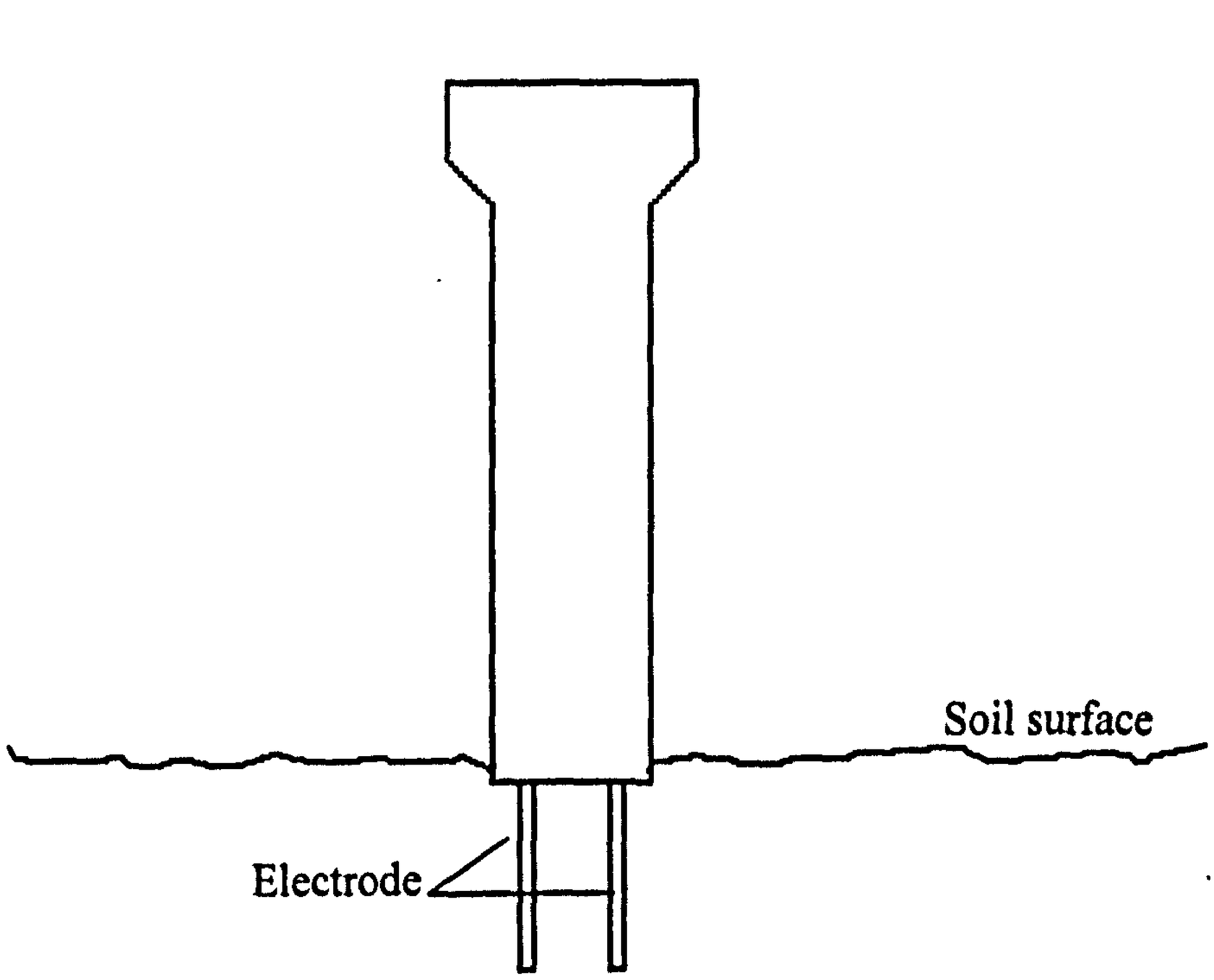

Figure 6.1: The Surface Capacitance Insertion Probe

Plate 6.1: The SCIP measuring soil moisture at a plot at Lower Farm

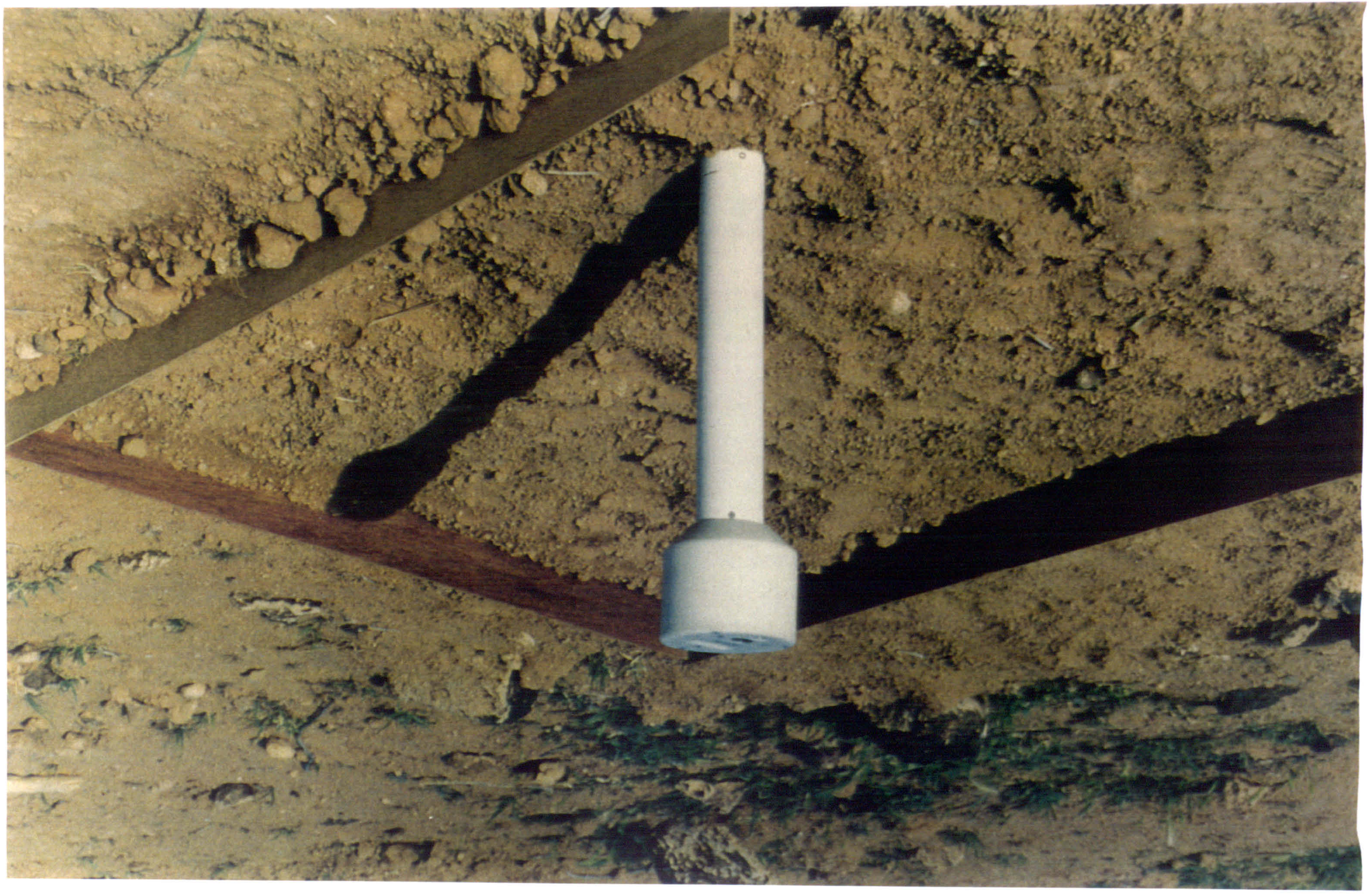

6.2.1 SCIP calibration

In order to calibrate the SCIP effectively, a method was required which compared the volumetric moisture content of a soil column with frequency readings from the probe. A plastic cylinder with a diameter of 19.9 cm and a height of 17.8 cm was placed upon a sieve with a piece of coarse filter paper in between. Assuming a soil bulk density of 1.3 g cm^{-3}, which was an average of field measurements, a calculated mass of 6065 g was put into the cylinder. The mass of the soil, cylinder, filter paper and sieve was measured to a resolution of 0.5 g. The soil was saturated from the base by placing the soil column in a larger container and filling it slowly with distilled water, forcing all the air up out of the soil. Once the soil was saturated, the probe was placed in the soil to obtain the highest dielectric constant reading. To obtain the saturated volumetric weight, the column was taken from the larger container, placed over a bucket and then weighed so that the water in the bucket could be included in the calculation. The probe stood in the soil throughout the test. There was no opportunity for preferential drying around the holes made by the probe and the difficulty of pushing the probe into the soil when it was very dry was circumvented. The core was then allowed to drain freely and the weight and dielectric constant were measured at regular intervals. For all measurements the probe was placed at a depth of 10 cm below the surface rather than 5 cm as it provided better sampling of the entire soil column. Once the core stopped dripping into the bucket, the soil was assumed to have reached field capacity (24 - 48 hours after the start of the experiment) and the contents of the bucket were discarded.

The core dried in a warm room. The probe was used every 2 days to measure the change in moisture. Once it became very dry, the core was placed in an oven set at 30 °C in order to drive off the remaining moisture. After about two months, the weight of the soil was equal to that at the start of the experiment at which point the calibration was complete.

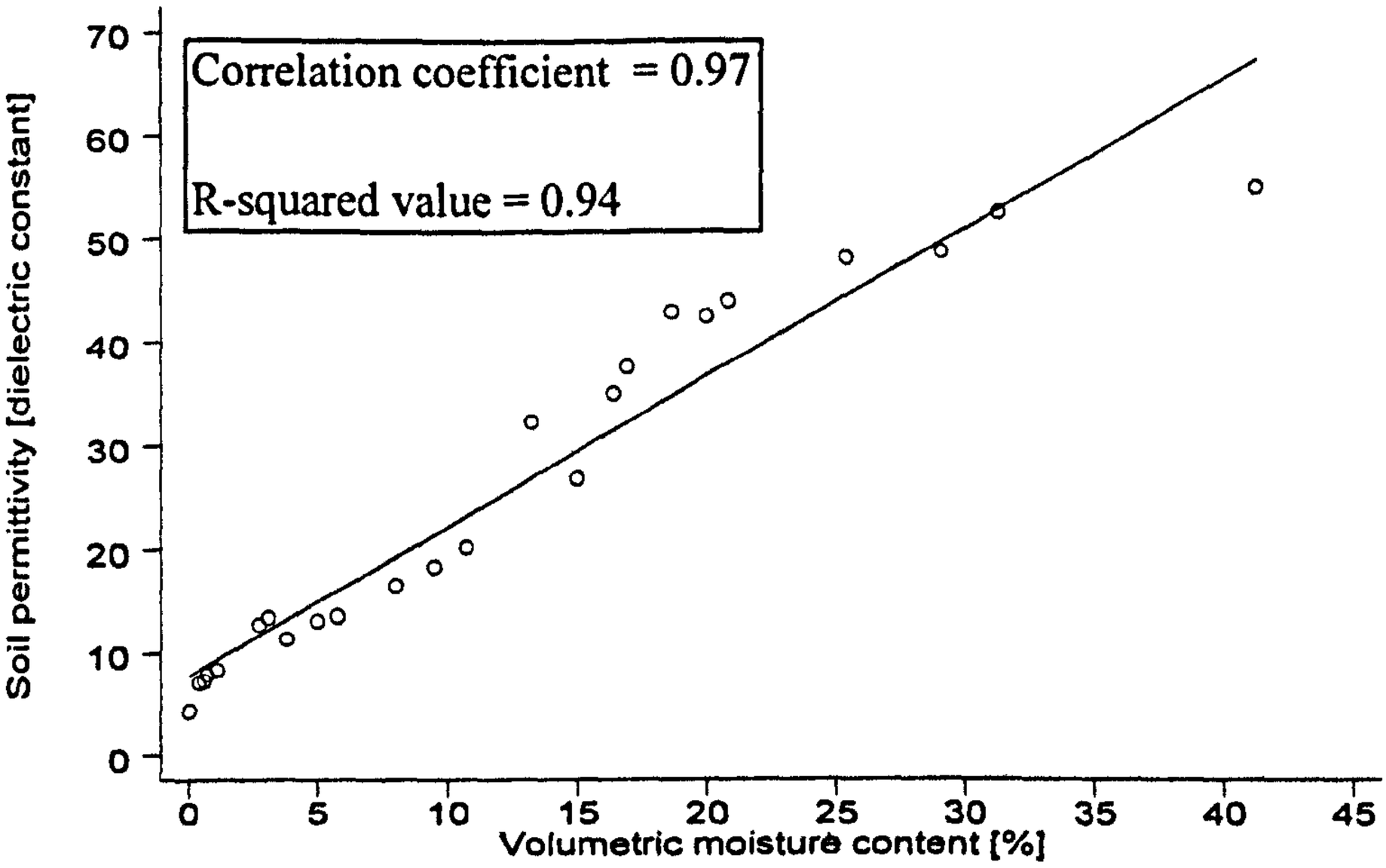

Figure 6.2: Calibration curves for the SCIP

The results of the calibration, which plots the SCIP readings against the volumetric moisture content, are shown in Figure 6.2. It shows a high degree of linearity, especially at the dry end of the scale, as shown by the high Pearson correlation and regression results. The first thing to notice is that the curve shows a certain amount of 'flattening-off' at the high moisture levels. There is a reduction in the marginal increase of permittivity after 25% moisture content and a total decline after 30%. This suggests that the SCIP is least able to distinguish between moisture variation when the soil is near to saturation.

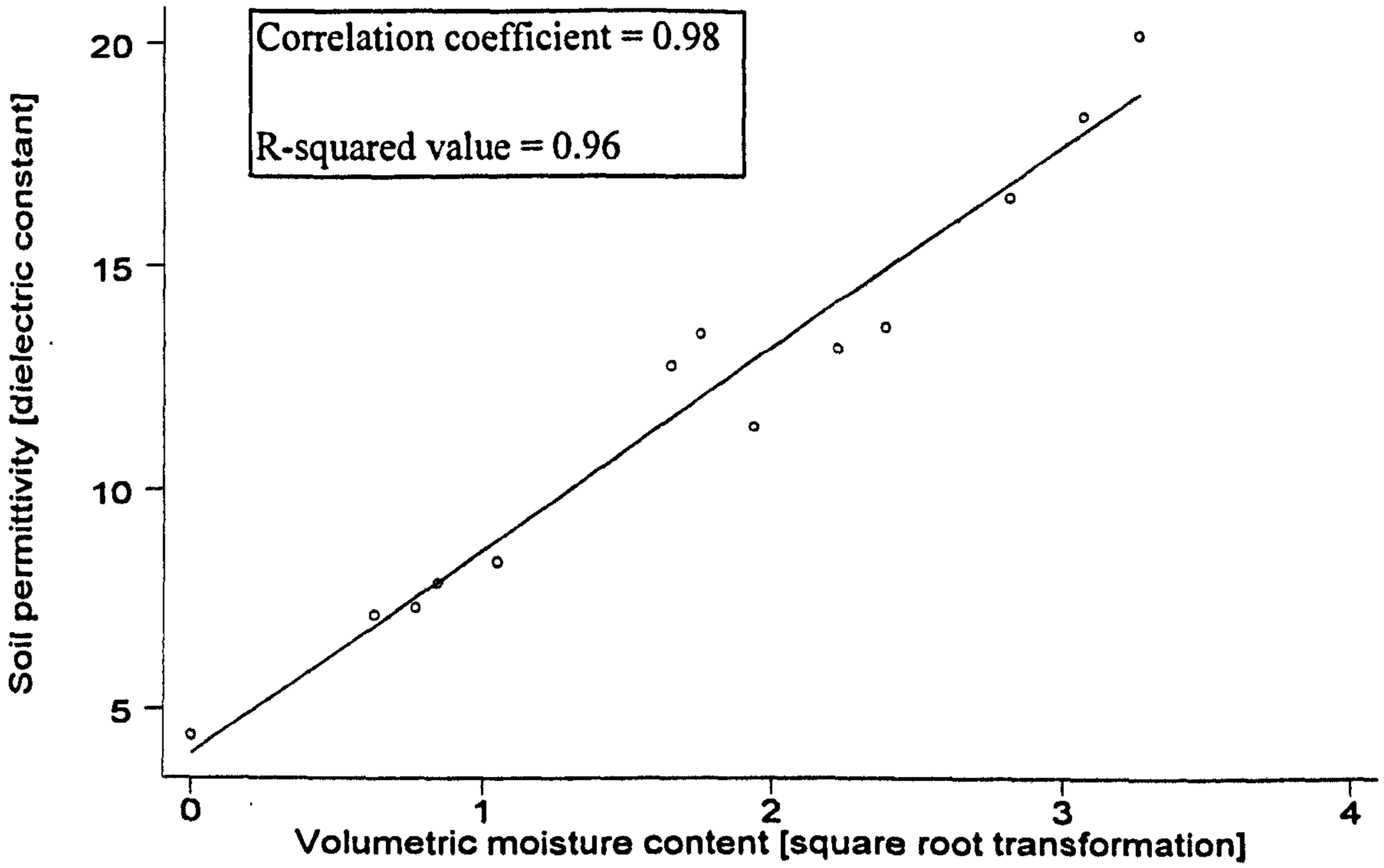

Figure 6.3: Graph to predict soil moisture from the dielectric constant

Using Figure 6.2 and the resultant regression equation $y = 1.89x + 7.69$ gives considerable problems at the dry end of the scale because the lack of linearity at the moist end affects the more accurate dry end of the spectrum. As it stands, any permittivities lower than 7.69 would be considered as a negative moisture condition. Many of the data points do fall into this category, due to the very low amounts of moisture in the Jordanian soils. However, if the higher moisture contents are ignored and the low moisture data points are transformed to increase linearity (Figure 6.3), the regression has a steeper gradient and a smaller intercept $y = 4.57x + 3.98$. This approach allows accurate prediction of the field moisture condition up to about 15% volumetric moisture which is appropriate for the dry nature of the soils under investigation.

6.3 THE RELATIONSHIP BETWEEN CRUST DEVELOPMENT AND MOISTURE STORAGE

Almost every commentator in the field of soil crust research has noted the potential for the crust to prevent the entry of water into the soil profile. Prolific numbers of studies, both using fieldwork (Morin & Benyamini, 1977; Agassi *et al.*, 1981; Trout, 1990; Fattah & Upadhyaya, 1996) and theoretical models (Hillel & Gardner, 1970; Ahuja, 1983; Brakensiek & Rawls, 1983; Ahuja *et al.*, 1989; Aboujaoudé *et al.*, 1991;), have been carried out showing that infiltration is drastically reduced by the alignment and rearrangement of surface soil particles into a dense crust. However, there is little research looking at the role of the soil crust as a barrier to evaporation. This seems to be a key issue, especially in semi-arid and arid ecosystems, where the conservation of soil moisture is essential. One problem that has made research into this area so difficult is the lack of a portable non-destructive method for measuring water content of soils and specifically a way of detecting small variations in moisture in the sub-surface layers of the soil. The following work seeks to look at moisture levels in the soil directly beneath the soil crust and consider if there are links between crust development and the storage of moisture.

6.3.1 Statistical considerations for analysing independent paired data

The research on soil moisture presented below falls into two distinct categories: first, examination of within-furrow variations, primarily relating aspects of crust type and thickness to the moisture budget and second, changes of soil moisture under specific agricultural management considerations.

In order to statistically analyse two paired datasets, it is useful to discover if one dataset is statistically different from the other. The *t*-test, which is often used in geomorphological applications (see, for example Loureiro & Coutinho, 1995), examines the difference of the means of two samples. It becomes particularly useful for investigating the difference between two matched pairs of data, such as the moisture content on one side of a furrow compared with that measured on the other side of the furrow. The approach taken here combines the statistical and visual to allow the reader to come to a fuller understanding. In the case of paired data, line

segments can be a very effective way of displaying the data (McNeil, 1992). Further information on the statistical methods used can be found in Appendix 2.

6.3.2 Correlation between rainfall intensity, crust formation and subsequent moisture conservation

The first set of experiments considered the variation of soil crust development due to aspect. Plate 6.2 shows a typical ploughed field at the site of High Farm in Al-Rafai'at during the early part of the year prior to preparation for summer irrigation. The soil was ploughed the previous autumn, in this case 1993, and left bare over the winter period. The ridge and furrows produced run roughly North to South (bearing 008°), which means that for wind coming from a north-westerly direction during the majority of rain events (see chapter 5), rainfall intensity and therefore the points of highest erosivity will occur on slopes facing north and west. If it is assumed that the effective intensity and total depth of rainfall incident on windward-facing slopes are greater than on leeward slopes (Sharon *et al.*, 1983), then there will be evidence shown both at the scale of a slope (Sharon *et al.*, 1983) and on ridges in a cultivated field (Sharon *et al.*, 1989). Although Sharon looks specifically at an erosional response to micro-topographical variations in rainfall, it is equally valid to assume that crust development will also be affected. Plate 6.2 shows distinctively the difference between the West-facing furrow flank and the East-facing flank. The crust is well developed on the former and has stabilised the flank, but on the latter a crust has not formed at all and in fact, because of its instability, there is evidence that material has slumped into the furrow base.

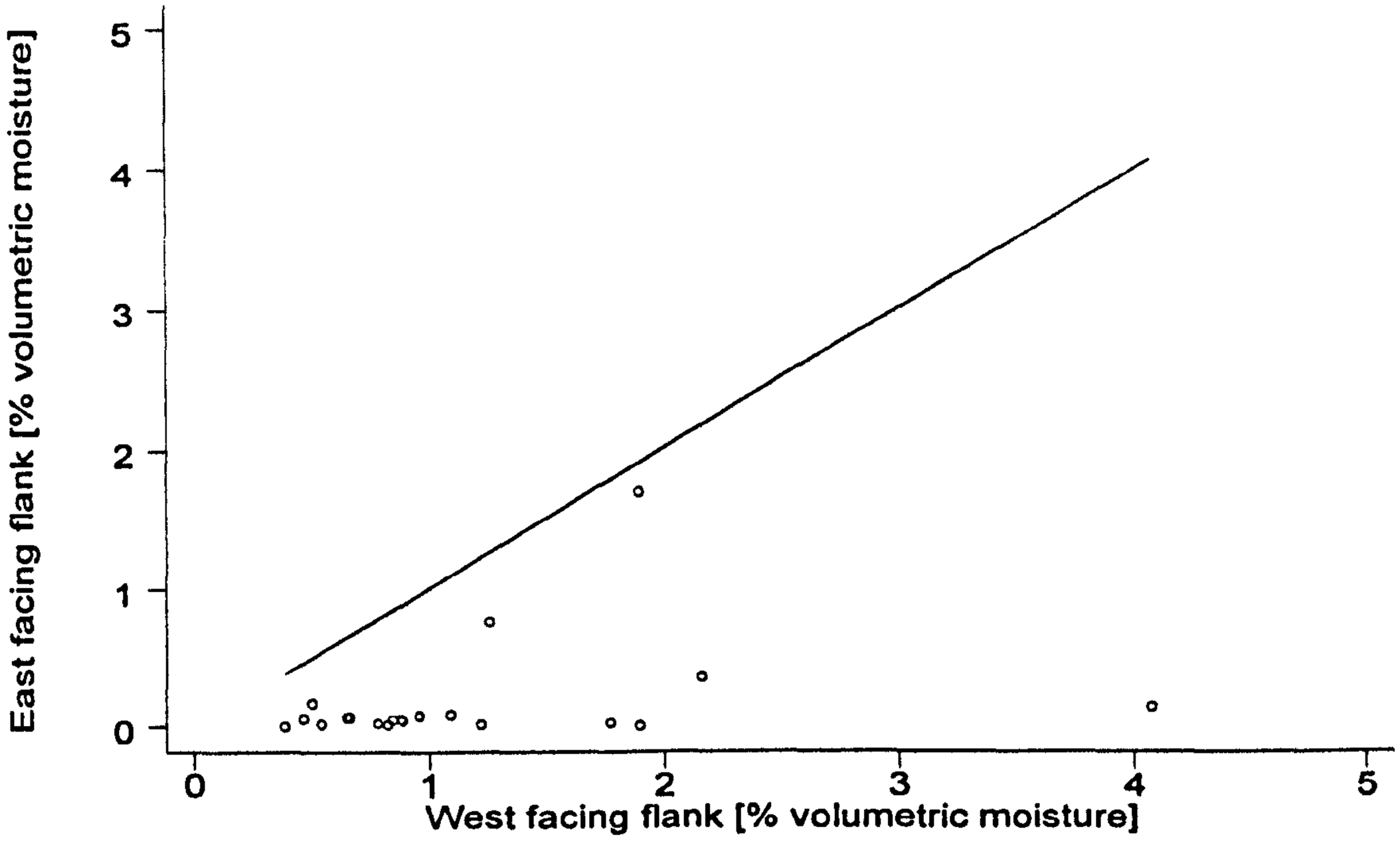

Figure 6.4 A simple plot of paired points (each point shows two measurements, one each side of the furrow) to show the relative differences in soil moisture in the top 5 cm of a ridge and furrow sequence at High Farm

The SCIP was used in conjunction with data from a shear vane in order to investigate the link between crust strength, and therefore crust development, and sub-crust moisture. The High Farm SCIP data are presented below in different forms. Figure 6.4 shows an $y = x$ line to denote equality: any point lying on it has an equal moisture distribution on both sides of the furrow. The points below the line represent places where the moisture was higher on the windward flank and all those above the line represent areas where it was lower. The further the points are from the line, the greater the difference between the wind- and leeward flanks.

Plate 6.2: The differences in soil crust development on east and west facing furrows

The west facing furrow flank is crusted and is shown by the lens cap

Site	Obs.	DC(5)	S.D.	F-test	t-test	DC(10)	S.D.	F-test	t-test
East facing 1	21	5.38	1.39	0.67	3.2×10^{-8}	8.17	3.44	0.059	2.4×10^{-4}
Furrow base 1	21	19.38	21.24			24.60	22.73		
West facing 1	21	8.73	1.54			13.20	5.44		
East facing 2	21	6.67	1.81	1.8×10^{-7}	4.6×10^{-3}	12.42	4.27	8.8×10^{-5}	1.8×10^{-3}
West facing 2	21	11.59	7.06			18.48	9.33		
East facing 3	18	4.88	0.50	5.1×10^{-5}	4.6×10^{-8}	7.42	2.64	0.078	2.3×10^{-4}
Furrow base 3	18	20.41				25.99	24.62		
West facing 3	18	8.50	1.54			11.91	4.22		
North facing 1	21	8.71	1.65	0.53	0.022	11.66	3.27	0.43	0.12
Furrow base 1	21	12.33	1.83			19.29	2.19		
South facing 1	21	8.01	1.91			11.02	4.05		
North facing 2	13	7.69	0.58	0.94	0.29	9.25	1.37	0.84	0.013
South facing 2	13	7.01	0.53			8.06	1.29		

Table 6.1 Statistics associated with the permittivity readings for furrow flanks

The set of statistics (Table 6.1) and the accompanying graphs (Figure 6.5 to Figure 6.9) reiterate the data which has been presented in Figure 6.4, but with more detail from individual furrow sets. In viewing the results for the *F*- and *t*-tests in Table 6.1 it can be seen that the majority are highly significant at the critical values, namely $F_{0.05}$ and $t_{0.05}$. In order to reject H_0 for the *F*-test, the variance of both populations needs to be taken into account and compared with the critical values for v_1 and v_2 in an *F*-test table. In all the cases in Table 6.1, v_1 and v_2 are equal and the values range from 2.46 (21 observations) to 3.12 (13 observations).

All the values for the *F*-tests are considerably lower than these values and therefore H_0 cannot be rejected. In other words, each sample set has been drawn from populations with similar or equal variance. It is therefore appropriate to test for a difference in the mean values confident that a significant outcome will reflect a difference between the means and not the variances.

Considering the *t*-test values, at a significance value of $P(0.05)$ it is possible to ascertain whether the difference of the means is significant or not. From Table 6.1 it can be seen that values for the comparison of East and West facing flanks range from 0.0046 to 4.55×10^{-8} and therefore it can be concluded that the means are significantly different and that one set is consistently higher than the other. For the North and South flank, data values range from 0.022 to 0.29 which means that in two of the four cases it is not possible to reject H_0 which says that the means are similar.

The main disadvantage with the *t*-test is that it does not estimate magnitude and although the comparison with the $y = x$ line in Figure 6.4 does give a helpful visual impression, it is better to use the vertical line plots and the tilted line segment graphs shown in Figure 6.5 to Figure 6.9.

From the three sets of graphs showing East-West data sets from High and Low farm (Figure 6.5 to Figure 6.7) a few additional points can be made which become clear using such a graphical method. First, there is a consistent increase in moisture at all three sites when comparing the westward flank with the eastward one. Second, there is an indication that the wetter the soil, the more difficult it is to distinguish between flanks. This is partly due to the plotting of the data on a log scale, but there is still a recognisable pattern at all the sites. Certainly any observation which shows a higher east-flank reading tends to be at the higher moisture levels. Third, the levels of moisture are, on average and at the upper range, higher when using the 10 cm rods, but that probably reflects higher evaporative losses from the soil closer to the surface.

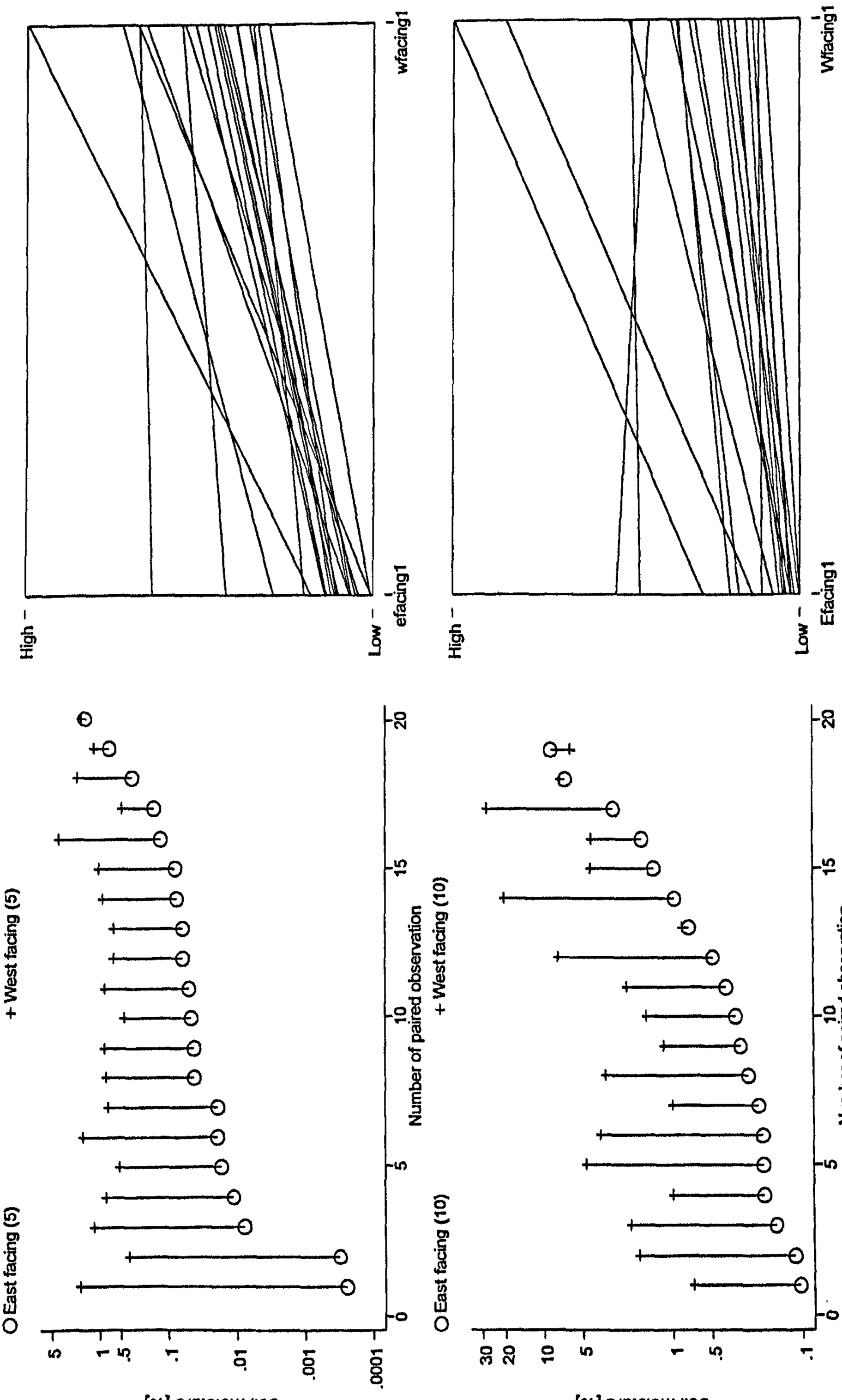

Figure 6.5 Summary of moisture levels in East/West facing furrows at High Farm

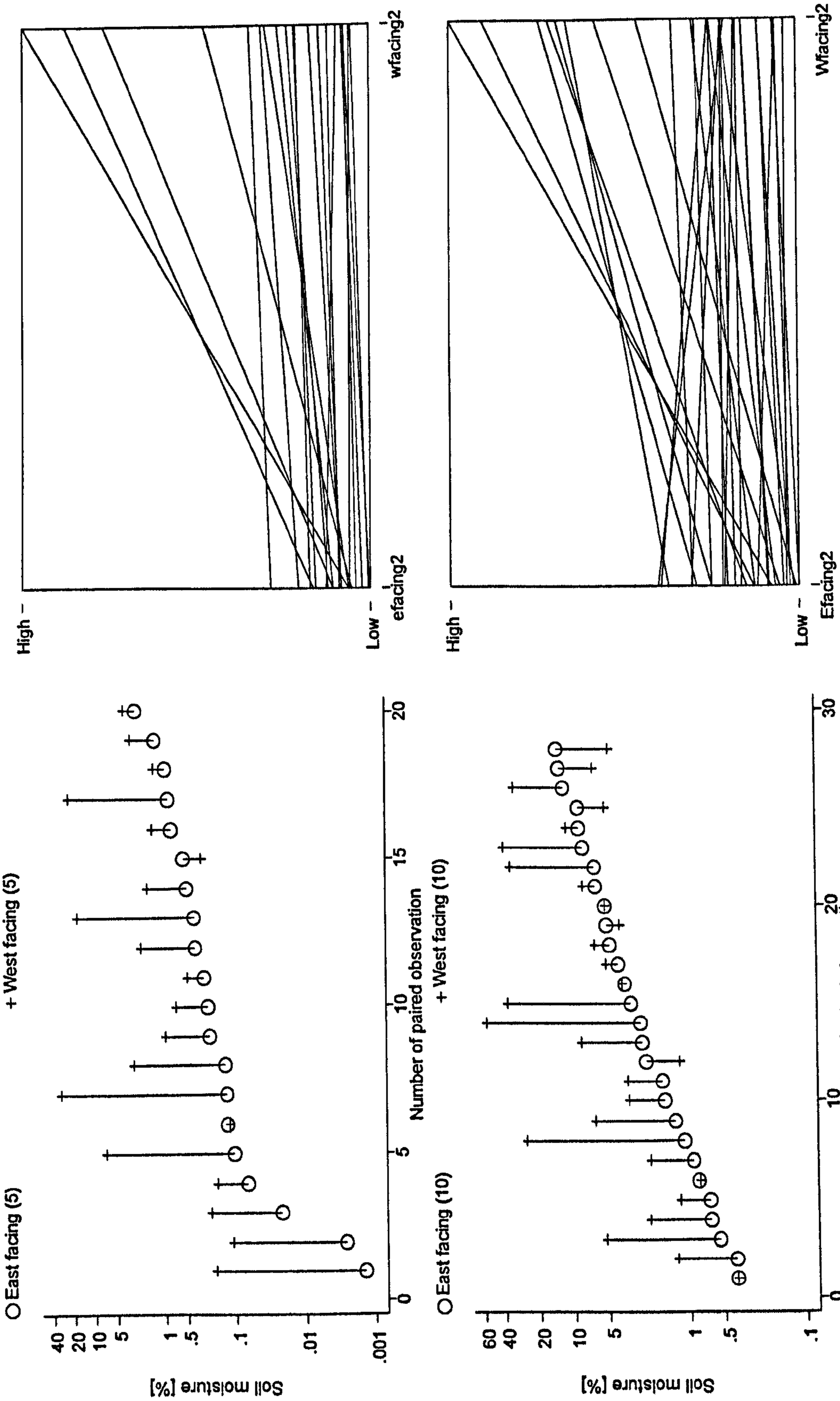

Figure 6.6: Summary of moisture levels in East/West facing furrows at High Farm

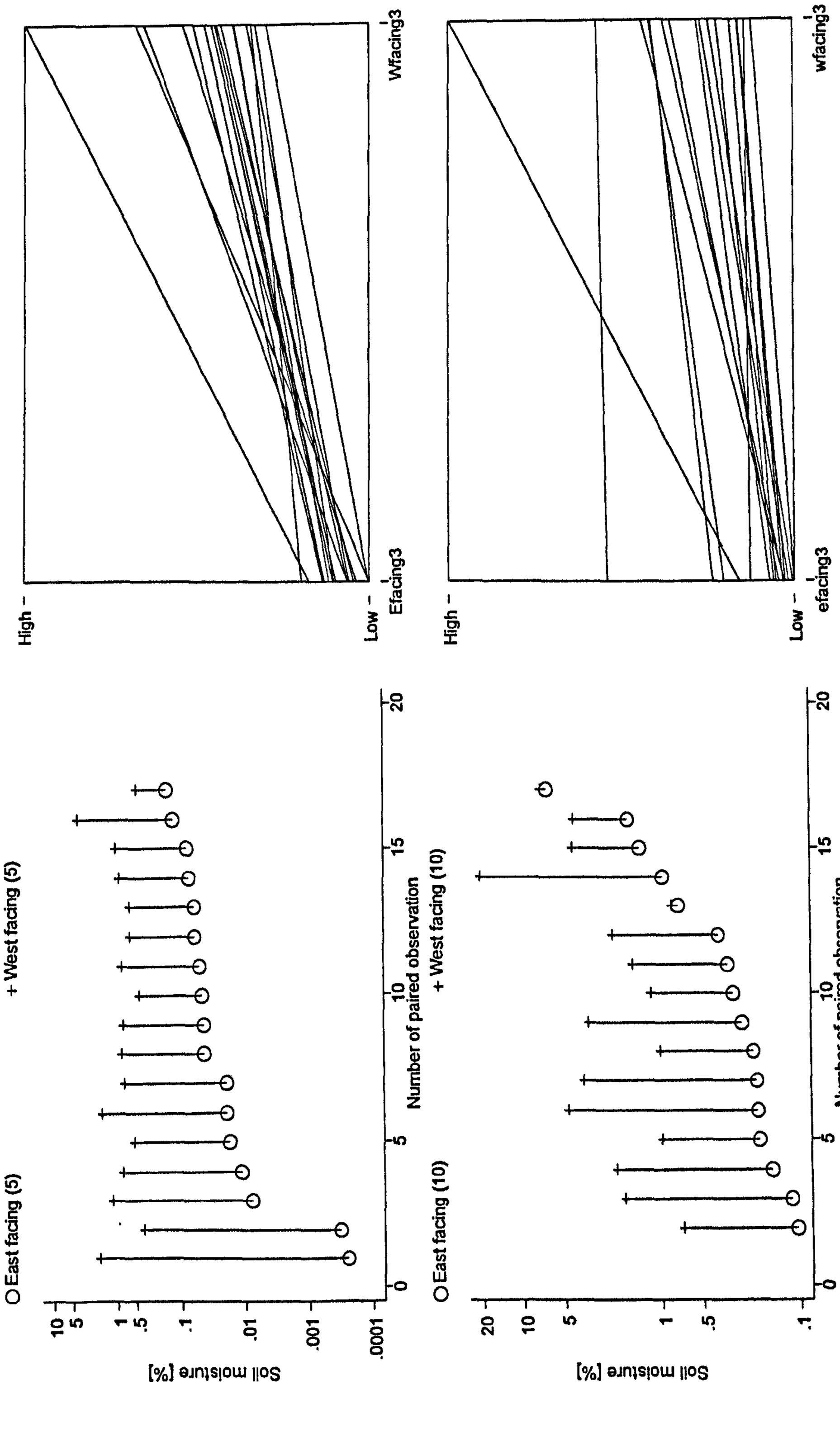

Figure 6.7: Summary of moisture levels in East/West facing furrows at Low Farm

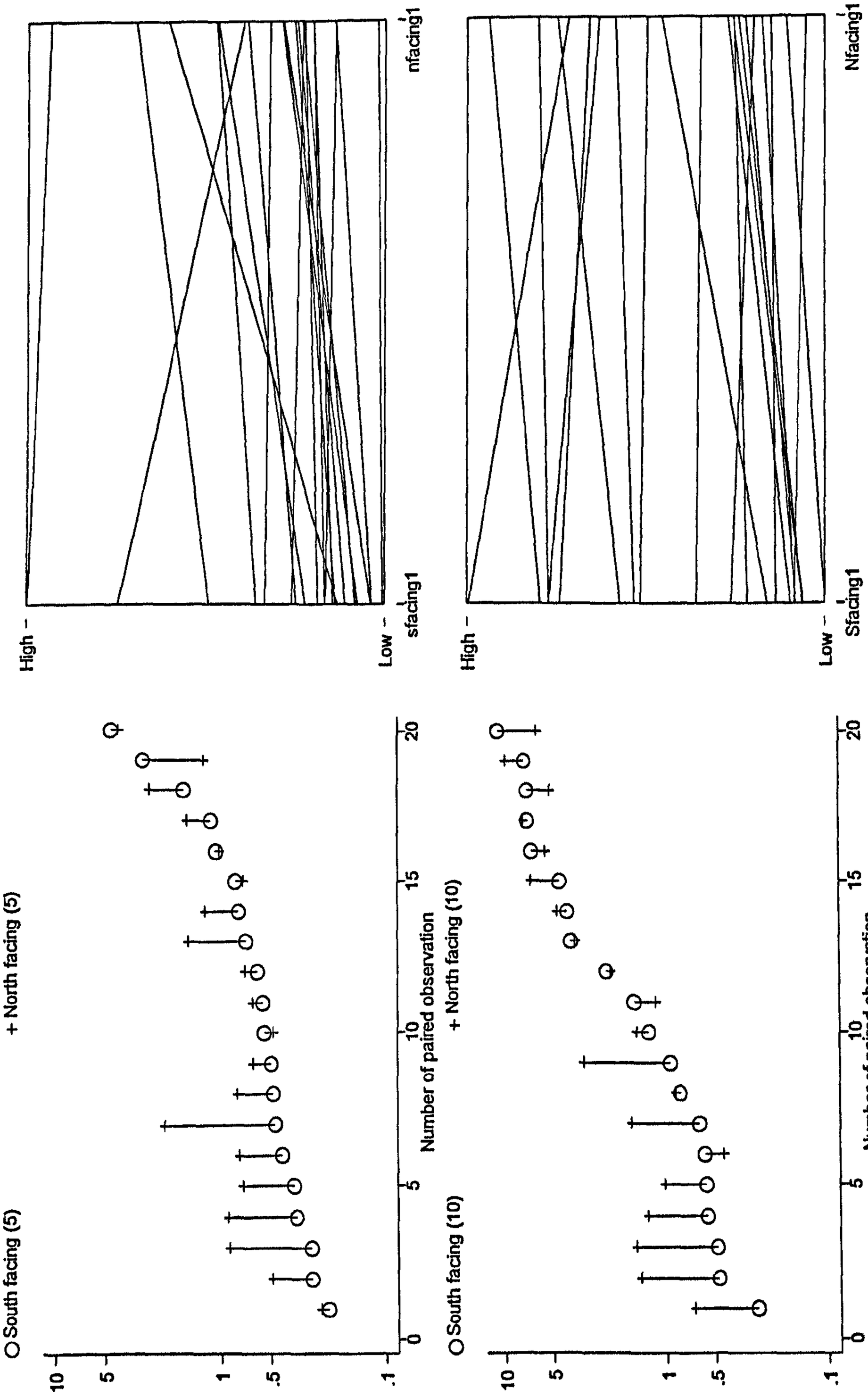

Figure 6.8: Summary of moisture levels in North/South facing furrows at High Farm

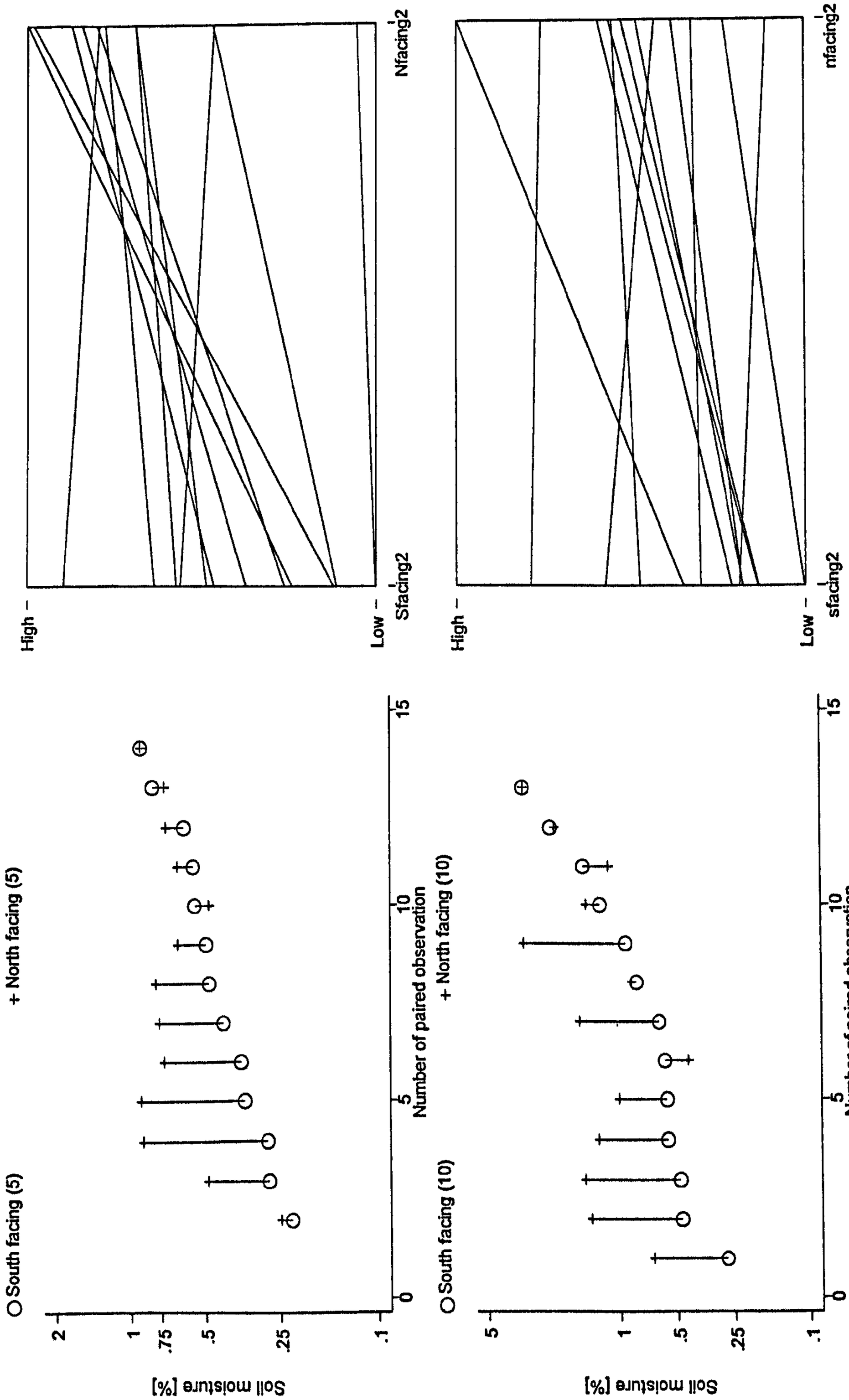

Figure 6.9: Summary of moisture levels in North/South facing furrows at Low Farm

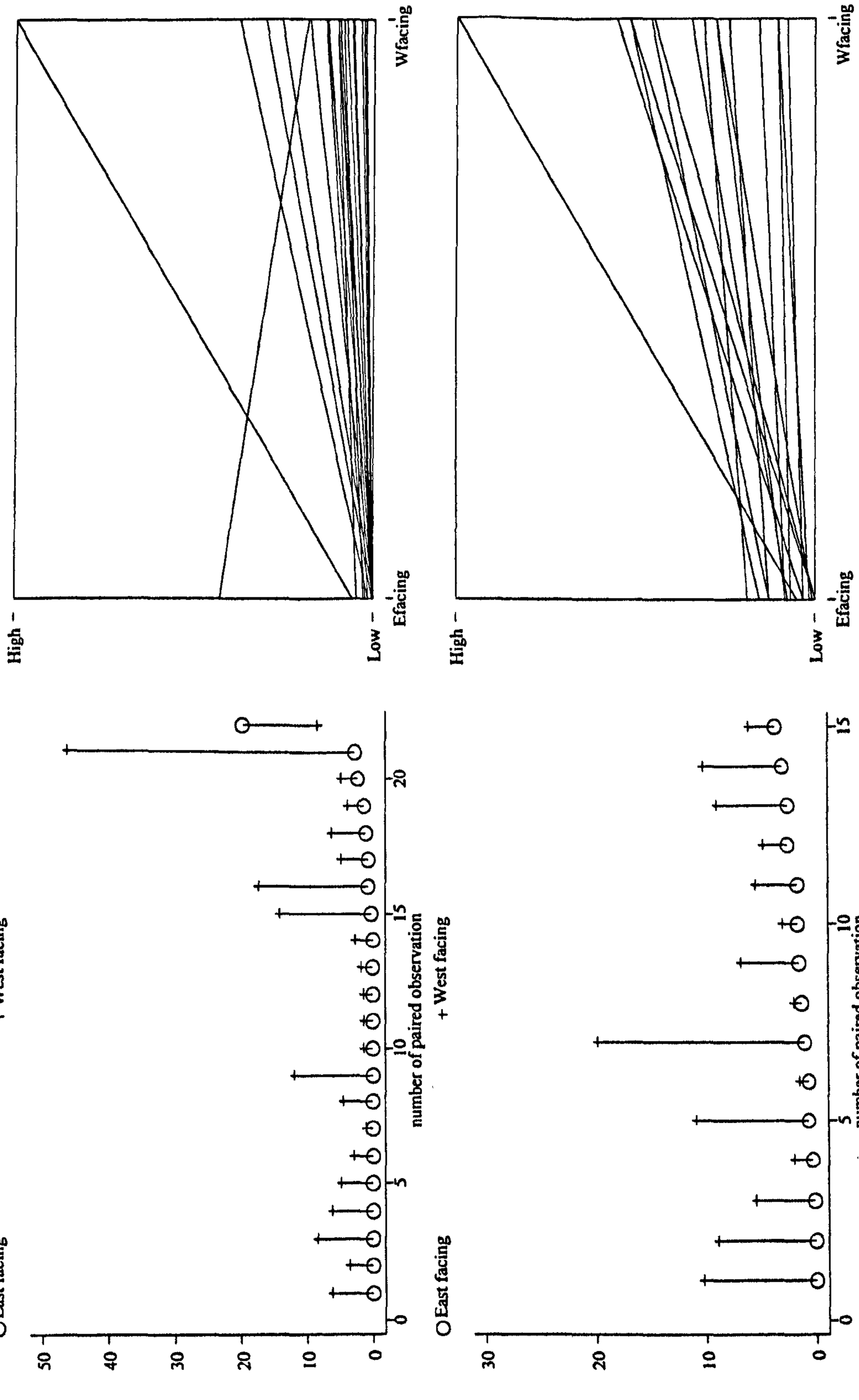

Figure 6.10: Changes in soil shear strength at 0 and 5 cm depth across a furrow at High Farm

The results from the comparison of south-north flank variations are not so compelling, although some points could be reiterated. The variation seems larger and more consistent at the dry end of the scale and most of the points which show higher levels on the southern flank are at the moister end. However, the differences on the north- facing flanks tend to be greater than the south-facing flanks, and the length of the lines descending are much less than those ascending. The less convincing results for the Low Farm example reflect the small number of observations and in fact the graph, in this case, is more convincing than the results from the *t*-test would imply. The other main difference is that the degree of moisture in the soil at 5 cm and 10 cm is much more similar and generally the values as a whole are much lower than the east-west data with permittivities rarely being greater than 12. This may be because the strongest winds come from the north, and so there is a higher uptake of water from the soil.

Figure 6.10 and Table 6.2 present data indicating the shear strength of the surface soil. From the strength characteristics, the thickness of the soil crusts can be inferred and this provides insight for the previous graphs of soil moisture. It is helpful to remember the image of Plate 6.2, which shows the physical situation illustrated by these data. Plate 6.2 shows an almost total absence of crust on the east-facing furrow flank in contrast to the developed crust seen on the west-facing flank. The shear vane is the main method for measuring shear strength of soil (BS 1377, 1975). A torque is applied to a vane of known dimensions which has penetrated the soil and when the torque is sufficient, the soil will shear. The shear strength of the soil crust correlates with crust thickness (Glancey *et al.*, 1988), although there is considerable scatter in the data which can be reduced using an automated system (Upadhyaya *et al.*, 1995). There are some obvious problems associated with this method. The vane is larger than the thickness of the crust which leads to an under-estimation of crust strength. In addition, the very penetration of the instrument into the soil before the torque is applied is likely to compromise crust strength. However, as a relative measure within datasets, it is a good link between shear strength and crust development. Figure 6.10 shows that, apart from one notable exception, there are higher strength characteristics, both at the surface and at 5 cm depth, on the west-facing flank. This

is also borne out with the *t*-test with *P*-values of 0.0086 and 0.0005 respectively. The ploughed soil has no inherent strength because of recent tillage and therefore the east-facing flank, which has practically no visible crust development, has very low values. The west-facing flank, on the other hand, shows considerable structural crust development which accounts for a mean strength of 7.45 kN m^{-2}, almost six times that of the east-facing flank. The difference at 5 cm depth is obviously not attributable to the crust, but instead signifies a wetter sub-soil which has flocculated together to form aggregates.

Site	Obs.	Mean (kN m^{-2})	S.D. (kN m^{-2})	Median (kN m^{-2})	IQR (kN m^{-2})	Skewness
East ridge	22	1.76	2.99	0.43	2.73	2.63
West-facing flank	22	7.45	9.64	4.78	5.59	3.13
Furrow base	22	16.23	16.14	9.39	19.81	1.51
East-facing flank	22	1.30	4.20	0	0.68	4.14
West ridge	22	1.93	6.04	0	1.71	4.22
5 cm depth						
East ridge	15	1.57	1.51	1.20	1.37	1.25
West-facing flank	15	7.10	4.73	6.15	7.17	1.16
Furrow base	15	9.03	10.09	5.81	6.49	2.32
East-facing flank	15	1.41	1.16	1.37	2.22	0.51
West ridge	15	1.45	0.89	1.02	1.20	0.79

Table 6.2: Summary statistics for the soil shear strength at High Farm

Table 6.2 shows that the surface crust is strongest and thickest at the base; a depositional crust has formed as material has been washed-in (Valentin & Bresson, 1992). Moisture levels are generally highest at this point as the depositional crust represents the most significant barrier to evaporation. The ridges, on the other hand, are very low in both strength and moisture, even though a structural crust has formed.

However, there is often a gap between the underside of the crust and the soil below and furthermore the crust is very friable. Such characteristics have evolved because most wind and water erosion takes place at the ridges and therefore their stability is undermined.

6.3.3 The moisture regime in the soil before and after ploughing

Table 6.3 shows a set of data at High Farm, where the farmer had recently ploughed his land (i.e. during the previous two weeks), but had missed some strips where the crust remained. In contrasting their relative moisture contents it is possible to see that as the crust is broken down or in some way removed, this promotes rapid evaporation even during the winter months. The moisture levels of the ploughed areas are consistently low, the only exception being the P(10) furrow where the probe hit the plough layer on a couple of readings and hence it gave an uncharacteristically high reading. Due to the recent nature of the tillage there is little difference between

Sample site	Ridge P(5)	Ridge P(10)	Furrow P(5)	Furrow P(10)	Ridge U(5)	Ridge U(10)	Furrow U(5)	Furrow U(10)	U(5)	U(10)
Obs.	12	12	8	8	2	2	4	4	15	15
Mean	0.05	0.25	0.09	1.18	0.33	3.06	1.98	6.72	15.67	17.29
Median	0.05	0.24	0.08	0.9*					11.44*	11.44*

P = ploughed U = unploughed (5 / 10) depth of probe * highly skewed dataset

Table 6.3: Moisture levels before and after tillage (% moisture). The readings were taken on 5th March 1995 with an air temperature of 21 °C and a ground surface temperature of 31 °C

the ridge and furrows made by the plough. The adjacent unploughed land did show a considerable difference between ridge and furrow for reasons explained in the previous section. The results from the unploughed ridges and furrows are not statistically accurate because of the low number of observations and therefore another area in the same field, which did not have an obvious ridge-furrow sequence, was measured. These data (U5 and U10) differ considerably from those of the ploughed land, and assuming that the latter had similar moisture levels prior to ploughing, it is obvious that the water evaporates rapidly once the crust has been taken away. Furthermore, there is little difference between the five and ten centimetre sampling depths, signifying that during the winter the crust acts as a barrier to evaporation. The crust plays a significant role in the storage of moisture in the soil during the winter.

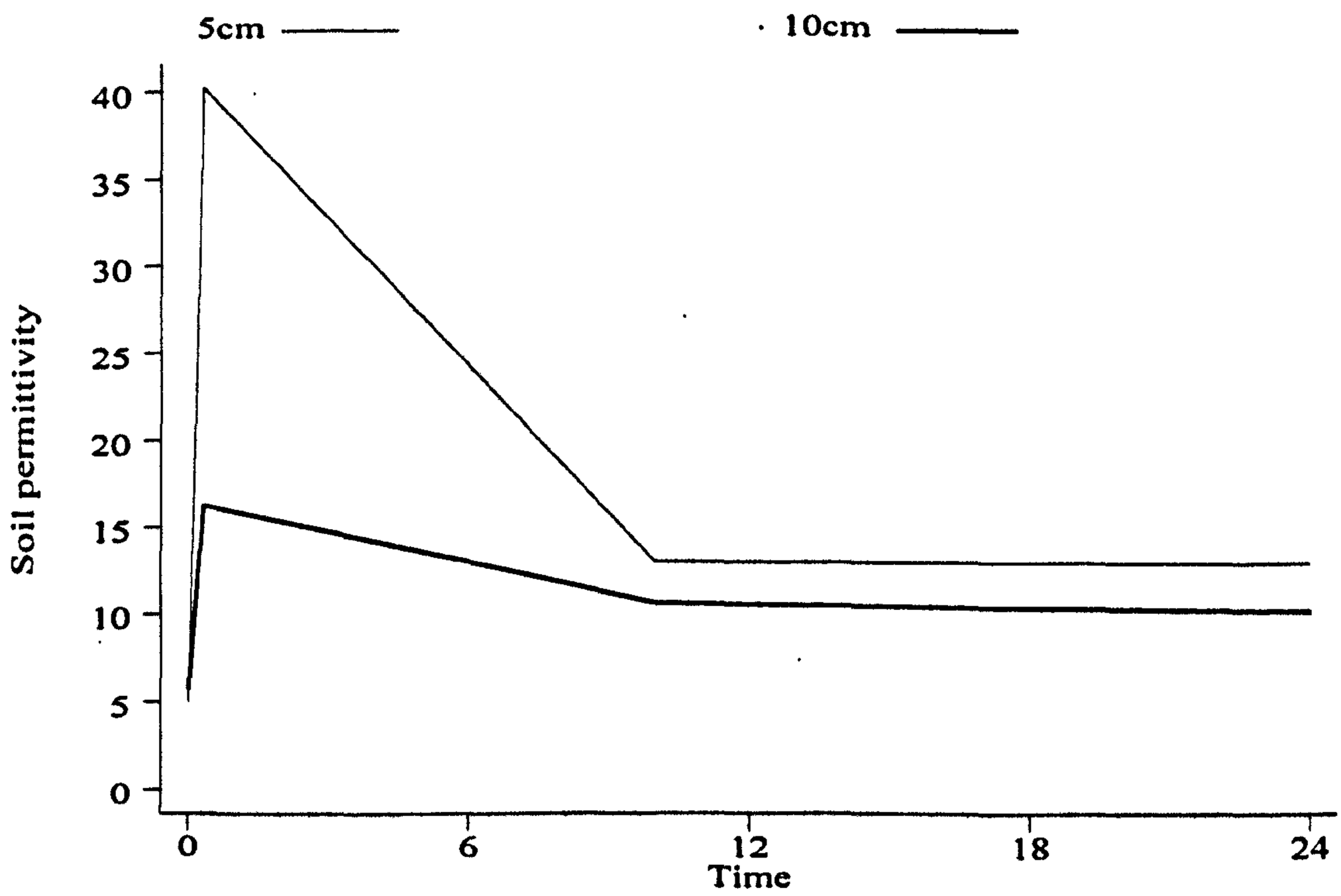

Figure 6.11: Rates of drying of a plot after rainfall simulation

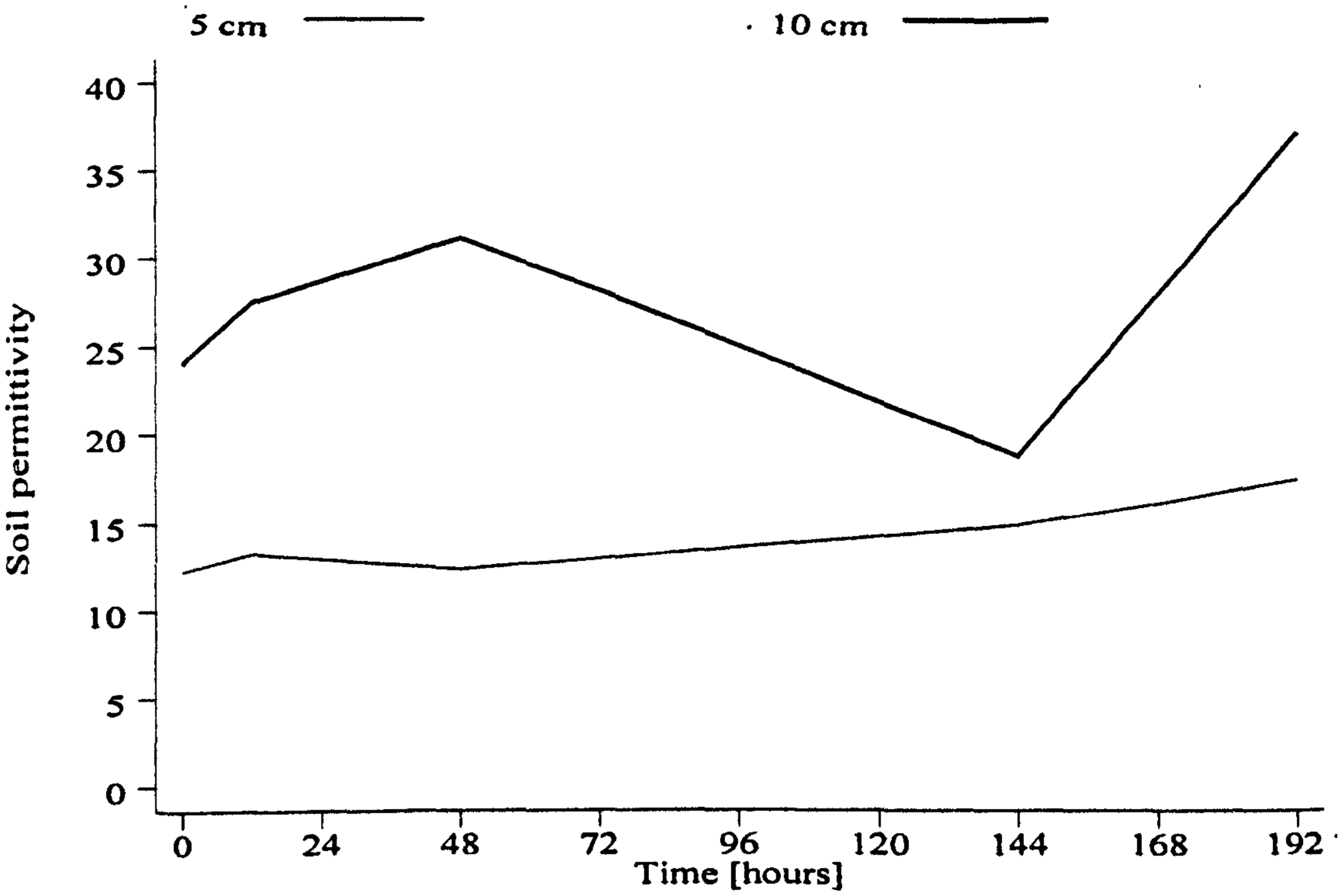

Figure 6.12: Rates of drying of a plot after natural rainfall

Figure 6.11 and Figure 6.12 show results from small plot experiments which investigate the drying of soil under a crust during May 1995. Figure 6.11 illustrates the effect after applying a rainfall event from the rainfall simulator described in chapter 5. The event consisted of a 60 minute simulation at a rainfall intensity of approximately 15 mm h^{-1}. The soil was measured at 20 points within the plot and an average taken. The graph shows that the surface layer (5 cm depth) becomes saturated during the event. Within 12 hours an equilibrium level is attained and the marginal rate of drying is much reduced. The 10 cm probe readings suggest much less saturation during the event, but a similar reduction to an equilibrium level takes place by 12 hours. Obviously these data are limited, but nevertheless show that in May, the evaporative flux is such that water evaporation from the soil, albeit crusted, is extremely rapid, especially in the short term. A more realistic graph is Figure 6.12 which presents the changing moisture regime of a similar plot during two rain events in late March 1995. The soil moisture changes, especially with regard to the two

rainfall events which occur between 120 and 144 hours after the initial readings. The 5 cm data, which seems to rise steadily throughout the period of data collection, gives problems of interpretation. If the data are correct, it must mean that moisture levels remain constant during the winter months in the region immediately below the crust and that moisture loss occurs from lower in the profile.

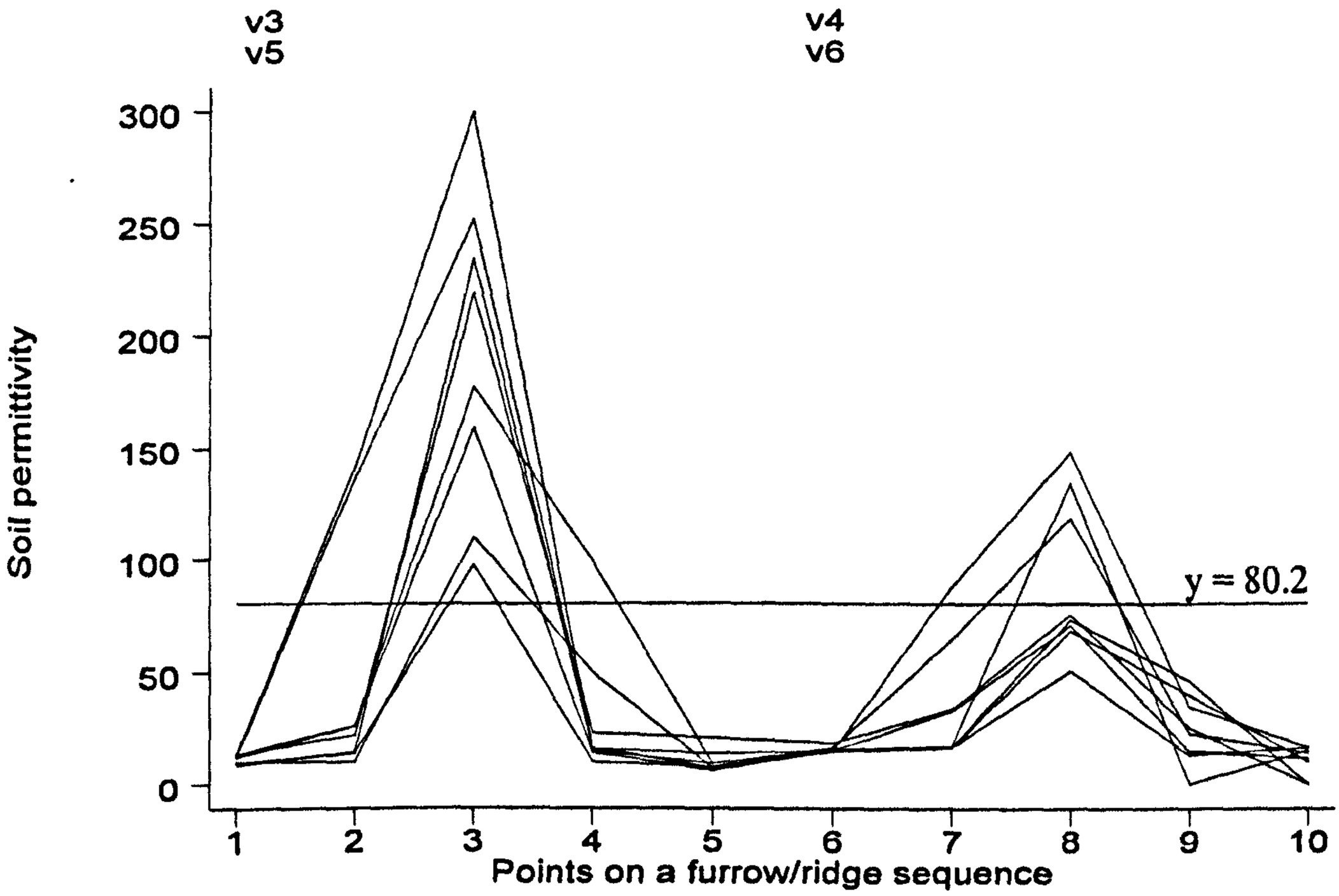

Figure 6.13: The effect of salinity on the SCIP using the irrigated ridge-furrow sequence. Points 1-5 are the data produced with the 5 cm probe while points 6 to 10 are data produced with the 10 cm probe

Lastly, Figure 6.13 shows moisture readings from an irrigated ridge and furrow sequence. This is ground which has been left fallow for a year since irrigation and the crust has developed into a thick compaction crust, although there is still evidence

Plate 6.3: Salt staining on land one year after being used for irrigation

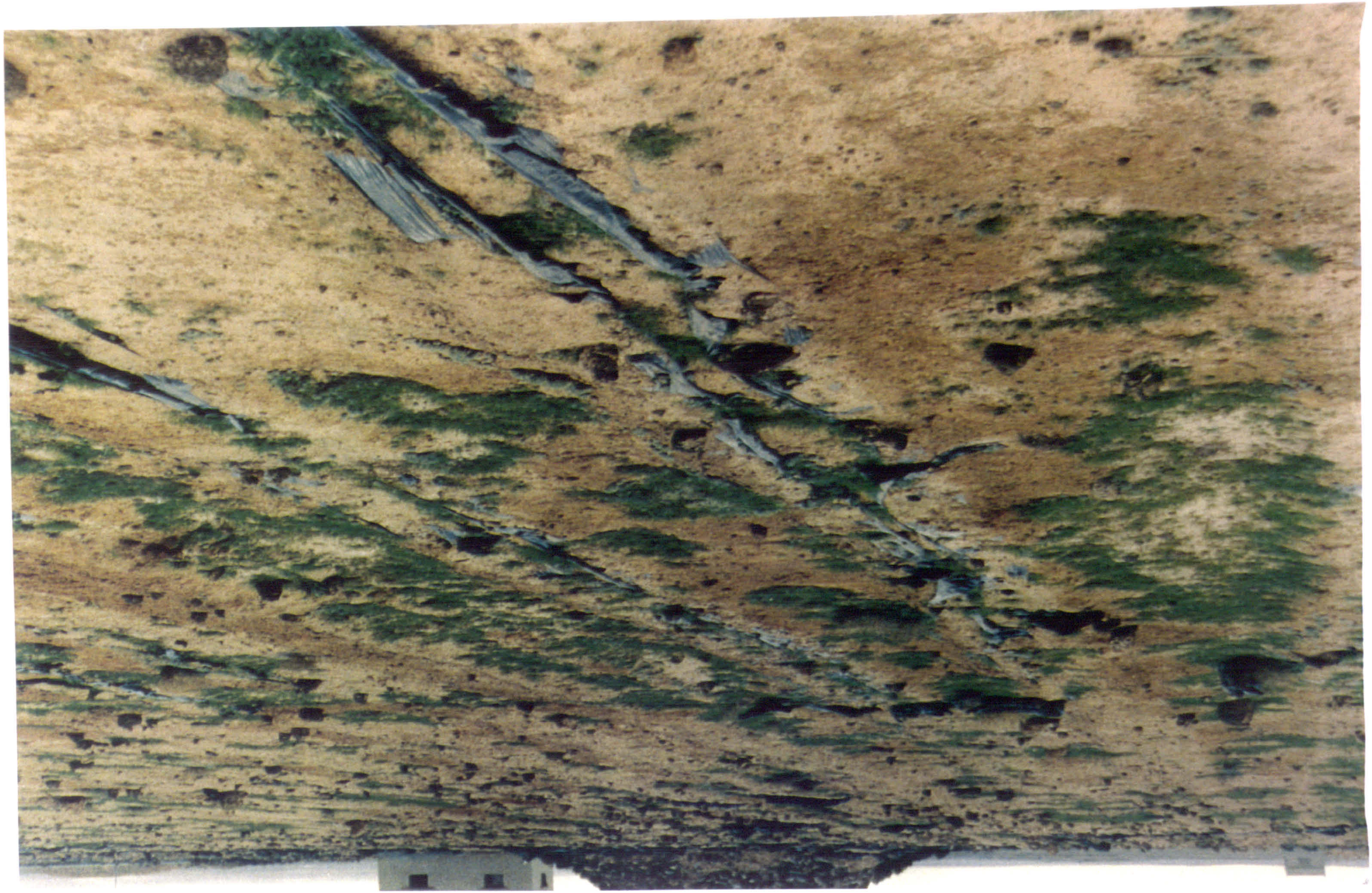

of brown staining in the centre of the furrow (Plate 6.3). This suggests that a sodium salt stain or precipitate of a mixture of salts is present at the soil surface. As the introduction to this chapter clearly states, the SCIP is unable to cope with soils with a high electrolyte conductivity. Figure 6.13 shows two sets of data across a number of ridge-furrow sequences and compares it with y = 80.2 signifying the permittivity of water. Once there is enough water to allow connection between the electrodes the salts conduct and give an exorbitant reading. If the soil was totally dry there would be no effect, but as the soil in question is under the crust there is enough soil moisture to allow it to conduct. This further illustrates the fact that it is the centre of the furrows which become most affected by increasing levels of salt. The 10 cm rod results, which are given in points 6 to 10, show the effect of depth and suggest that there are excess salts in the sub-soil as well as the surface although to a lesser extent.

6.4 Conclusion

The method of determining soil moisture using soil capacitance is new and to date only two articles have been published giving results from field measurements (Robinson & Dean, 1994; Wu, 1998). While the method is not without its problems, especially concerning the effects of electrical conductivity, it has great potential for measuring moisture at the soil surface. The problem of excessive salinity is a problem in dryland irrigated soils and therefore it has been necessary to see the effect it would have on soil permittivity. In saline soil the permittivity readings jumped to figures well in excess of that of water itself suggesting that conductivity only has an effect at a certain threshold condition. These results concur well with the theoretical approaches of Campbell (1990) and Mualem & Friedman (1991). It means that salinity has no effect until it reaches a threhold, but at that threshold the data become obviously wrong and can therefore be easily identified and discarded.

One of the biggest advantages in using the SCIP is that it is very sensitive to small changes in moisture at the driest end of the spectrum which makes it ideal for work in arid and semi-arid environments. The calibration experiment, which needs to be done with each soil type because of changes in the overall dielectric properties

associated with mineralogical make-up, shows good linearity at the dryer end of the spectrum. Only at volumetric moisture contents above 25% is there a visible 'flattening-off' of the data.

There are two important facets of the research that can be drawn out in this chapter. First, there is an important link between wind direction, rainfall, micro-topography of the land surface, soil crusting and moisture storage. Little research has followed Sharon's work in the 1980s (Sharon *et al.*, 1983; Sharon *et al.*, 1989) despite the importance of greater impact velocities of raindrops on inclined soil surfaces. His work focused upon differences in erosion, but such asymmetrical rainfall energy patterns have additional implications for the formation and development of crusts. Taking the predominant wind direction during rainfall events, calculated in Chapter 5, it was possible to hypothesise that north and west facing slopes would have a more developed crust than those facing south and east. Taking the two indirect measures of crust development, namely crust strength and sub-crust moisture content, it has been seen that there is greater crust development on west facing furrow flanks compared to east facing ones. The crust strength at the soil surface of the west-facing furrow flank was on average 5.7 times higher than the strength of its paired east-facing furrow flank. Even at 5 cm depth, the mean was still five times higher on the west-facing flank although the data at depth show the increased soil moisture rather than the thickness of the soil crust. The data show a similar pattern for north and south albeit to a lesser extent. The difference between sides of a furrow show that the variation is greater at the dry end of the scale whereas if the soil is wetter it is more difficult to distinguish between the furrow flanks. At 5 cm depth, some of the driest east- facing furrows showed volumetric moisture levels of below 0.001% compared with between 2 and 3 % on the associated west-facing furrow

The second point links the formation of crusts with the ability of the soil to store moisture. The nature of evaporation from the soil is poorly understood, especially in dryland environments (Rose, 1996). The data presented here shows that evaporation is reduced because of the presence of a crust. This is evident when different sides of a furrow having an asymmetric crust development are compared, but also when recently ploughed soil is compared with crusted soil. There was generally about an

order of magnitude difference between land which had been ploughed and land which had not been. The moisture content at 5 cm depth for ploughed soil was typically about 0.05% and 0.25% for 10 cm depth. The correspnding data for unploughed land were 0.33% and 3.06%. This shows clearly that the destruction of the crust increases evaporation rapidly and within two weeks there is almost a negligible amount of moisture in the soil. When comparing the moisture levels at 5 and 10 cm depths on furrow flanks it was found that there was a greater level of moisture at 10 cm depth indicating that, despite the presence of the crust there was still evaporation from the soil directly below the crust.

The fact that soil moisture is lost rapidly after ploughing has important implications on soil management and the balance needed between tillage techniques and optimising soil moisture in the sub surface soil. Some tillage is always needed to allow planting. In addition it is important that the crust is not too thick and well developed so as to impede seedling emergence. This has been observed as a problem since the very earliest of soil crust research (Hanks, 1960; Arndt, 1965; Rathore *et al.*, 1982; Shiel & Yuniwo 1993) because of the reduction in potential for young seedlings to push through a barrier of densely packed soil at the surface. If no ploughing takes place there is much less of a possibility for this to occur because the crust will have formed over at least one season and will be almost impenetrable. By ploughing, the newly formed crusts are relatively weak and easy for germinating seeds to push through. So while keeping crusts on cultivated land will increase the moisture storage ability of the soil, these considerations have to be offset against the ability for seeds to be planted and for their emergence.

PAGE
MISSING
IN
ORIGINAL

7. PEDOGENESIS, THE DEVELOPMENT OF SURFACE SEALS AND CONTEMPORARY SEDIMENT TRANSFER PROCESSES

To understand the spatial distribution of crusts, one needs to consider the entire history of the surface microrelief (Bielders *et al.*, 1996 p. 853)

7.1 INTRODUCTION

This chapter has several purposes. First, it seeks to elucidate the way in which the present soil has evolved by the two main processes of weathering and eolian deposition. Examining pedogenesis is necessary because it increases our understanding of why certain processes, such as aggregate breakdown, are important in the Badia environment. Furthermore, the instability of arid eolian soils leads to a greater propensity for erosion and soil degradation, which then provokes questions on the way in which the soil is managed. The previous chapter looked at the surface crust as a natural barrier to the evaporation of water from the soil and examined changes in moisture over small spatial scales. This chapter seeks to explore the role of the crust as a natural way of protecting the soil from wind erosion and investigates the nature of microtopographic differences in crust type and the resulting soil characteristics. The question of the scale of erosion and deposition within a hillslope that is undergoing agricultural activity is tackled and infiltration rates on different levels of crust development based on land usage are compared.

7.2 FINGERPRINTING LOCAL BASALT AND SOIL SIGNATURES

Most soils develop over a long period as a result of various inputs, which derive from a number of erosional, depositional and weathering processes, to produce a complex mixture of gas, water, organic and mineral matter. By looking at the mineral chemistry, the nature of the clays and the sedimentary character of the soil it is possible to gain a picture or fingerprint of the various inputs which have been instrumental in soil formation. In order to fingerprint a soil in such a way, X-ray

fluorescence (XRF) and X-ray diffraction (XRD) analyses need to be carried out to determine the geochemistry.

Site	Pyroxene	Olivine	Phillipsite	Chabazite	Faujasite	Smectite	Illite	Kaolinite	Quartz
S-3	x	x	x	tr	-	x	-	x	x
S-11	x	x	x	-	x	x	tr	x	x
S-16	x	tr	x	tr	tr	x	x	tr	tr
S-17b	x	x	x	-	tr	x	tr	tr	tr
S-26	x	-	x	-	x	x	tr	x	x
S-27	x	tr	x	-	x	x	x	tr	x
S-30	x	tr	x	-	tr	x	tr	x	x
S-46	x	tr	x	-	-	x	tr	x	x
S-54	x	tr	x	-	-	x	tr	x	x
S-57	x	x	x	tr	tr	x	tr	tr	x

Table 7.1: Occurrence of minerals after the alteration of basaltic glass adapted from Dwairi (1987). (x = abundant tr = trace)

The opinion that the soils of the northern Badia are mainly a result of the weathering of the underlying basalt (Al-Homoud *et al.*, 1995) can be tested by comparing the XRF and XRD signatures of the soil with the rock. Such an opinion is feasible given that there is evidence to suggest that weathering of the basalt core-stones beneath the soil is now taking place (Allison *et al.*, 1993).

The most comprehensive set of X-ray data on the basalt and zeolite has been collected by Dwairi (1987). The <5 μm fraction of powdered basaltic glass material taken from Jebal Aritayn was examined by Dwairi (1987) who observed two main clay peaks at 6°2θ and 12.3°2θ. The first peak corresponded with the diagnostic d-spacing of 17 Å for smectite clay, which was confirmed by its collapse after heating. The other peak was initially identified as phillipsite, but after heating it was considered to be kaolinite. Dwairi analysed the mineralogy of samples taken from Aritayn, which make up the most recent volcanic facies, and found that the predominant clay was smectite (Table 7.1).

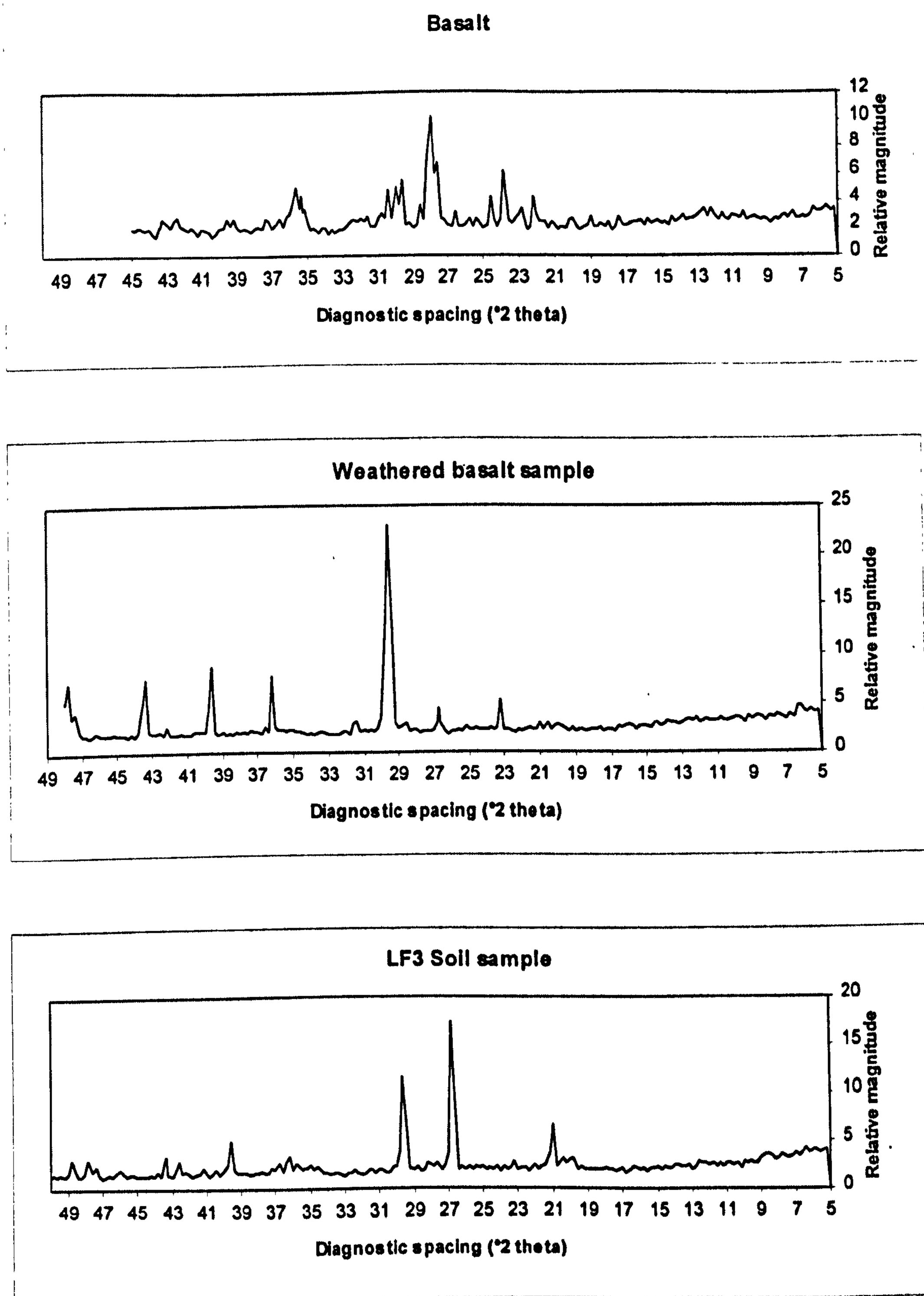

Figure 7.1: X-ray diffraction results comparing basalt,weathered basalt and soil

In both marine and non-marine palagonitic environments, it has been suggested that the formation of smectite clays is a prerequisite for phillipsite crystallisation (Arrhenius & Bonatti, 1965; Hay, 1966; Kastner, 1976). Similarly in zeolite terrains, it has been found that magnesium-rich clays, such as smectite, saponite and chlorite, precede zeolite in the alteration sequence.

7.2.1 X-ray examination of soil and rock materials at Low farm

An experiment was designed to compare the basalt and soil with Dwairi's results (Dwairi, 1987). A sample of basalt and soil was taken from Low Farm. The basalt sample was divided into two, representing pure basalt and nodules of weathered basalt. It was hypothesised that if the soil was of basalt origin, the three samples would exhibit a common mineralogy, but that they would reflect a breakdown of certain minerals and an addition of clay-forming minerals and water. However, if there was a significant change in the mineralogical character, then it would be supposed that the soil forming process was complicated by other factors.

The XRD signatures from samples taken at Low Farm suggest some interesting similarities with those obtained by Dwairi (1987). The kaolinitic peak at 12.3°2θ (Figure 7.2) is not particularly surprising, although in both cases the peak is relatively small, which is concomitant with the low-energy weathering environment found in the Badia. The smectite peak, which Dwairi describes as a extended peak, is very similar to a mixed-layered clay comprising chlorite and illite- type clays (Hardy, pers. comm.). It would be foolish to make too much of this apparent correlation because palagonitic alteration would have only taken place in proximity to the cones. However, the correlation between the clays in the soil and those associated with past vulcanism suggests that the soils are dominated by clays which have formed through the weathering of the basalt and the associated authigenic counterparts. However, the clays need to be put into the context of the overall mineralogical chemistry (Table 7.2) before such assumptions can be accepted or rejected.

Major oxides	Basalt (%)	Basalt † (%)	Weathered basalt (%)	Soil (LF3) (%)
SiO_4	40.02	44.6	18.49	43.90
Al_2O_3	15.16	16.0	5.56	13.59
Fe_2O_3	12.25	11.2	2.19	6.67
MgO	6.04	4.6	1.91	4.40
CaO	11.76	11.0	40.86	11.46
Na_2O	2.44	3.9	0.31	0.74
K_2O	1.153	2.1	1.040	1.972
TiO_2	2.309	3.6	0.293	1.188
MnO	0.214	0.1	0.051	0.180
P_2O_5	0.655	0.5	0.282	0.263
CO_2 estimate	4.0		25.00	
H_2O estimate	3.0		4.0	
Total	92.00	97.6	70.99	83.18

Trace elements	Basalt (ppm)	Weathered basalt (ppm)	Soil (ppm)
Sr	654.8	219.2	246.1
Ba	459.2	108.7	429.3
Cr	229.3	14.5	122.2
V	205.4	61.8	149.1
Ni	191.8	19.5	43.7
Zr	182.5	75.5	340.1
Zn	96.6	43.4	76.1
Cu	56.3	14.3	18.4
Nb	44.1	7.3	21.6
Ce	31.9	17.4	39.4
Nd	27.3	27.5	32.2
Ba	21.4	8.4	13.8
Y	21.2	14.3	31.7
La	17.9	25.8	30.9
Rb	11.1	22.3	45.3
Pb	8.5	13.6	15.9
Th	5.8	2.3	5.7

Table 7.2: X-ray fluorescence data for Low Farm

† Basalt XRF data from Dwairi (1987)

The basalt exhibits a regular chemical composition, although the total percentage of 92% is less than would be expected, suggesting about 4% of CO_2 and 3% structural and adsorbed water. The differences between the basalts can be explained by the fact that they are derived from different flows and that the smaller percentages of sodium, potassium and titanium relate to the acidity of the basalt. The low proportion of magnesium oxides and higher proportion of aluminium oxides suggest a basalt which is high in aluminosilicates, indicating a relatively late evolution. The high levels of calcium correlate well with the high strontium levels and come from two possible sources. First, the basalts are rich in calcium-rich aluminosilicate plagioclase feldspar which are shown by the large number of peaks of anorthite in the XRD, especially at 23.8°2θ and between 27.6 and 28.1°2θ. Second, the other possible source of the calcium is from the calcium carbonate veins within the basalt. In addition, the XRD shows that there is no quartz and that the other significant mineral present is diopside, which occurs around 30 and 35.5°2θ. Diopside is a pyroxene composed of a magnesium-calcium silicate.

The weathered basalt data, which were for material taken from nodules within the basalt, would suggest large differences in the mineralogy from that of the parent basalt. The large deficit in the total means that there is probably more than 25 % CO_2, which should be assumed to be linked with the large calcium value, creating over 73% calcite, which is evident in the XRD. The XRD suggests that there is about 10% quartz, leaving approximately 8% for clay minerals. The strontium value has decreased significantly, despite the increase in calcium, indicating that the calcium is being derived from elsewhere other than the basalt and hence diluting the strontium. It is noticeable that on the underside of many of the basalt blocks there are significant deposits of caliche. This suggests two things. First, it is possible that the large amounts of calcium within the basalt are relatively mobile and upon chemical weathering the basalt releases the calcium quickly. Second, it is possible that the calcium is derived from elsewhere. The basalt overlies large formations of limestone and it may outcrop occasionally over the Jebal Hâuran. Evidence from soil thin sections examination, in the form of calcium carbonate nodules, would support the idea of a limestone influence. In an environment with a very high evaporative flux

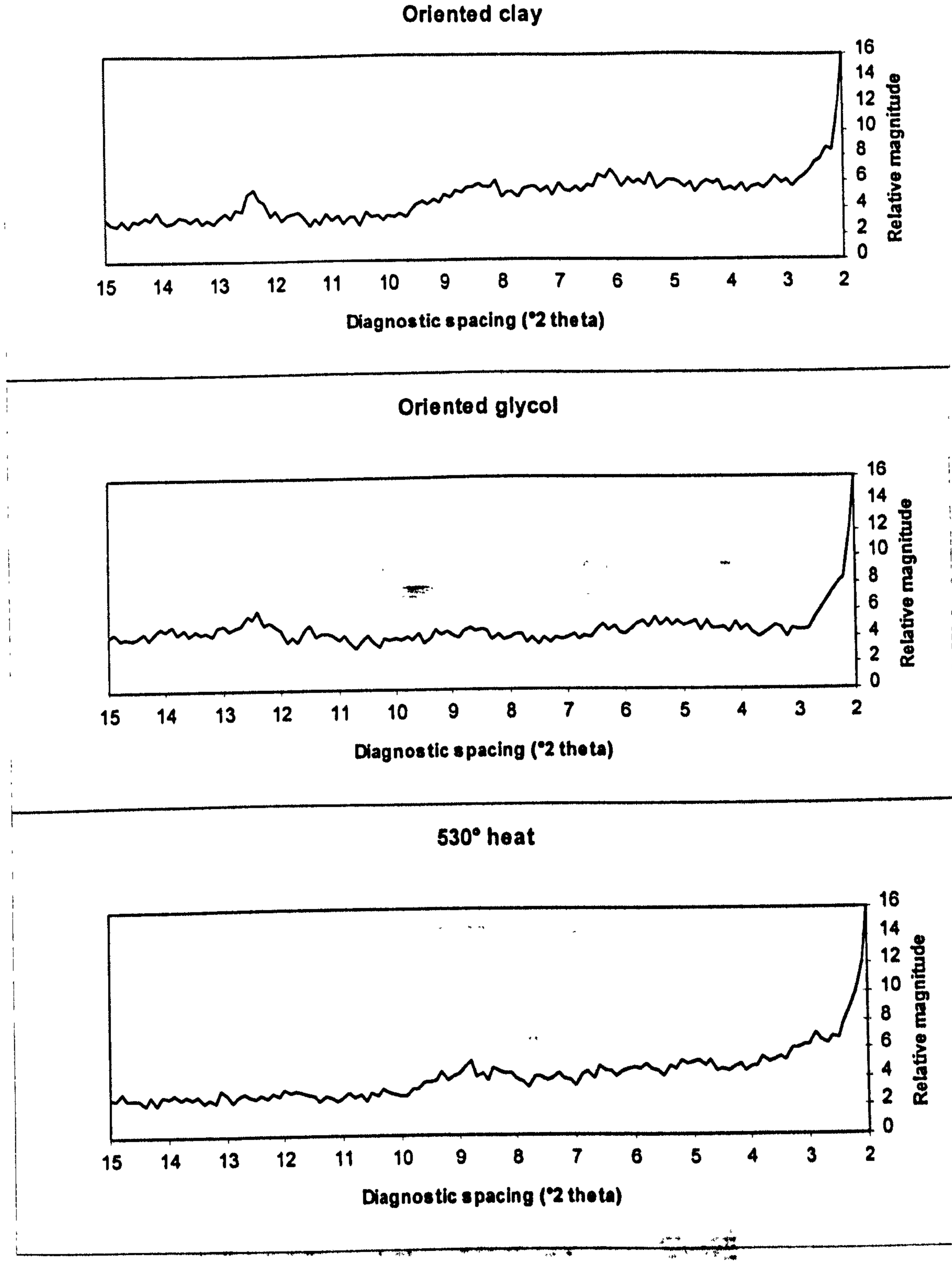

Figure 7.2: X-ray diffraction results showing the clay peaks under different treatments

for most of the year, it is possible that groundwater is forced to the surface through capillary action and as it passes through bands of limestone the water is heavily charged with calcium, which is then precipitated on the basalt blocks on or near the surface.

From the XRF data for the soil it can be seen that there has been a dramatic increase in SiO_2, but that the iron, magnesium and titanium oxides have decreased substantially. The combination of a low total value and a CaO content of 11.46% gives rise to an estimate of 25% calcite. The remainder of the total value can be explained by the presence of a greater volume of structural and adsorbed water within the soil fabric. It is evident that the influence of the basalt fraction has been vastly reduced. The anorthite and diopside have been weathered to form some of the clay minerals and are otherwise virtually unrecognisable. The dominant mineral is now quartz, which almost completely dominates the silt fraction. The quartz has obviously been incorporated into the soil profile from elsewhere, because there is no source in the vicinity as neither basalt nor limestone has quartz as a weathering product. It is likely that it is derived from an eolian process, probably originating in the Arabian Peninsula, if the evidence of Bruins & Yaalon (1979) and Ganor (1975) is taken into account (section 2.7), or alternatively from the Sahara (Yaalon & Ganor, 1973; Simonson, 1995; Yaalon, 1997).

In terms of the clay content found in the soil sample, the XRD results show that about 15% of the clay is made up of kaolinite, confirmed by the peak at 12.4°2θ, which is removed upon heating. In addition, there is evidence for a somewhat diluted peak between 8 and 9°2θ, which corresponds to approximately 30% illite mica clays, as can be seen in the XRD graph. The majority of the clays (about 55%) can only be classified as mixed-layered clays, which are randomly orientated and contain units of chlorite and illite. The mixed-layer clay may contain smectite, because there is a peak between 6.1 and 6.3°2θ, corresponding to the Dwairi results. However, there are no clear signs of change upon glycolation, which can support the idea that there is a majority of chlorite and illite. Whatever the exact composition of

the mixed-layered clays, it is likely that the clays exhibit a swelling nature similar to that of the smectites because they are very fine-grained crystalline amorphous clays.

Mineralogy	Basalt (%)	Weathered basalt (%)	Soil (LF3) (%)
Anorthite	60	0	0
Diopside	40	0	0
Quartz	0	10	45
Calcite	0	75	25
Clay	0	10	30

Table 7.3: X-ray diffraction data for Low Farm

All samples show a very high content of fine to coarse silt, clearly indicative of the eolian origin of the material (Yair & De Ploey, 1979; Gerson & Amit, 1987; McFadden *et al.*, 1987; Whalley *et al.*, 1987). The soils described by Yair & De Ploey (1979) were taken from the northern Negev south of Beer Sheva with an underlying geology of limestone. In their X-ray analysis they have 60% smectite and kaolinite, 20% calcite, 5-10% illite, 10% quartz and 5% K-feldspar and attapulgite. The last three of these were seen as indicative of eolian action. Likewise in the Badia, where the predominant wind direction is from the east (section 5.2.2) and therefore from Arabia, there is a large quantity of quartz in the soil sample which would suggest that there is a predominantly eolian origin. With the additional evidence of decreasing strontium levels and large increases in calcite, it is possible to show that the basalt is in fact a secondary contributor to the pedogenesis.

In summary, it is likely that the large silt fraction is mainly derived from eolian sources to the east and south, while the clays are a mixture of eolian origin, but with a considerable input from the local weathered basalt and associated minerals such as zeolites. This is significant because it changes opinion on the evolution of the Badia soils and is the first study where data are provided to determine the sources of the sediment.

7.3 HILLSLOPE SEDIMENT FLUXES

Having determined the origin of the soil, this can act as a foundation to look at the contemporary processes acting at various scales within the hillslope. The challenge when scaling up is to recognise the differences between local and regional signals. In the case of the field sites under observation, the relationship between these signals is complex through space and time. During the winter, when the soil has been ploughed, surface roughness is at its greatest. This invariably results in rapid crusting on one furrow flank and virtually none on the other giving rise to the differences in moisture storage discussed in Chapter 6. Wind is the dominant process at the hillslope scale especially during and after ploughing. Before a crust has formed there is a high propensity for rapid deflation of fines. Water erosion plays a lesser role causing runoff along furrows and into rills and eventually wadi systems. Such processes are only infrequently activated due to the lack of significant storm events, which means that most of the hydrological processes occur at the ridge-furrow scale and are not replicated at the larger hillslope scale.

In the summer, the soil surface is flattened and an artificial ridge-furrow sequence is produced. Water erosion can still take place at the smaller scale due to over-irrigation, but because rainfall events are very unusual during the summer there is no feedback to the larger scale. Wind erosion continues to predominate but, once the crops grow, its influence is reduced. Man-induced processes become much more important. Compaction of the already crusted soil is likely to enhance the degradation process of crust formation. In addition, irrigation during the summer has an important effect on the soil salinity, causing salt precipitation.

7.3.1 Processes acting within the scale of the hillslope

It is important to look at the sediment fluxes at different spatial scales as they will change at different rates over various temporal scales. The eolian and hydrological erosion processes will be controlled by the climatic variables discussed in Chapter 5 as well as the soil characteristics, but underpinning the natural factors, the attributes will be constrained by human activity. It is important to consider the changes in soil

chemistry and soil physical attributes within the framework of irrigation management, crop rotation and cultivation practices.

In order to evaluate the amount of erosion and deposition which has taken place, changes in particle size distributions will be examined. The results will be drawn from crust and auger samples, transect data and data from ridge-furrow sequences.

Site	Sand (%)	Coarse silt (%)	Fines (%)
Low Farm (FC)	18.9	32.6	48.5
Low Farm (FA)	12.2	31.7	56.1
Low Farm (RC)	19.3	32.5	48.2
Low Farm (RA)	14.2	30.3	55.5

FC = Furrow Crust; FA = Furrow Auger; RC = Ridge Crust; RA = Ridge Auger

Table 7.4: Average values for particle size variation at Low Farm

From the transect taken at Low Farm (Figure 4.3), which shows downslope changes in each individual size fraction, it can be seen that there are no significant trends within the data which are immediately clear, except that there is more variation in the crust samples in comparison with the auger samples and that there is more variability in the furrow crust samples than the ridge crust samples. It is more useful to concentrate on the grouped size fractions, fines, coarse silt and sand, in order to identify changes downslope more readily (Figure 7.3). As coarse silt is the dominant fraction, it is treated on its own in order to compare it with the fines, which have been defined as material below 20 μm and the sand which lies above 63 μm.

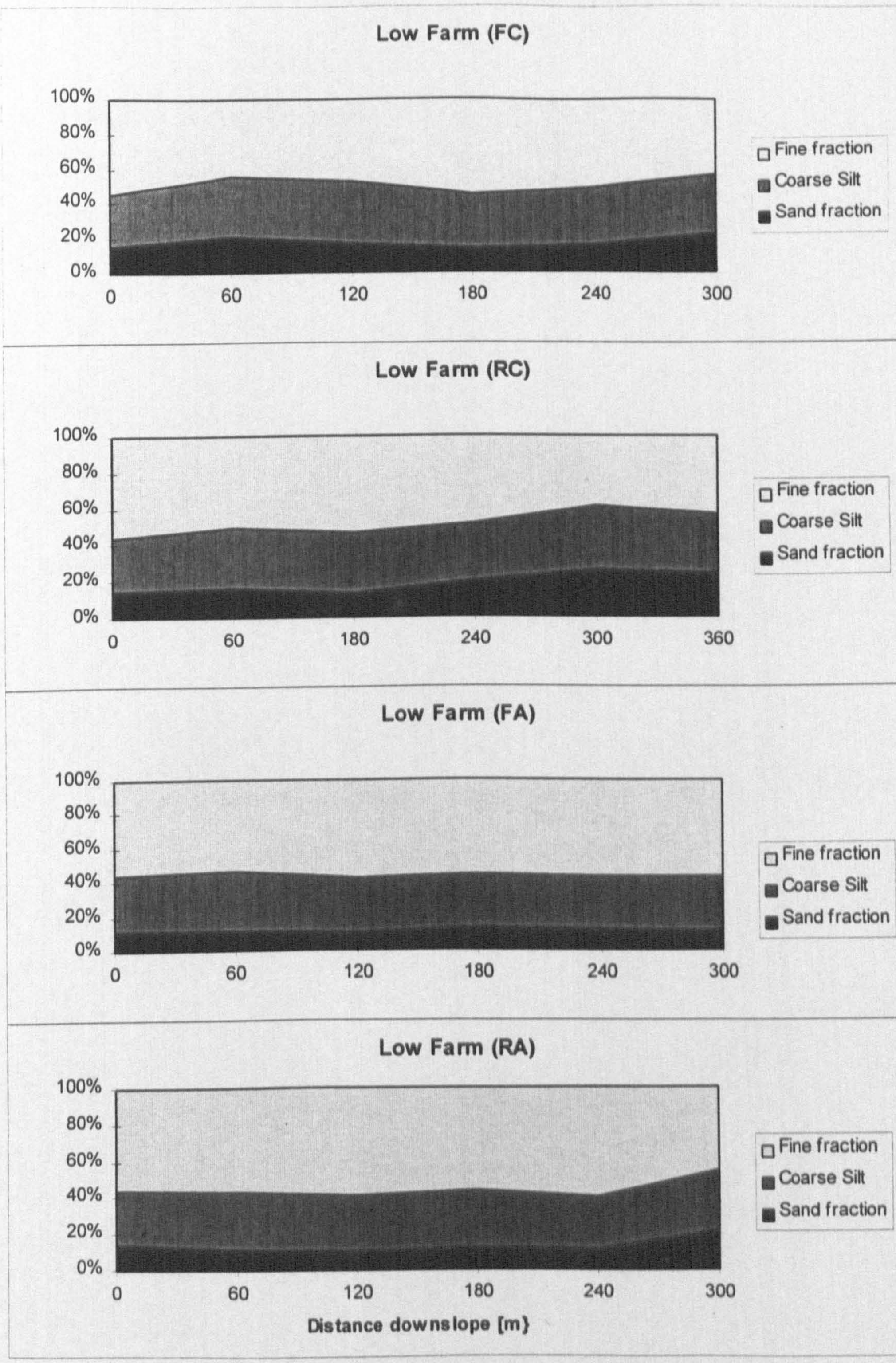

Figure 7.3: Downslope changes in particle-size distribution at Low Farm

It can be seen that the auger samples retain their characteristics downslope and there is no significant change. The furrow crust shows some variation, but it is not slope-related and can therefore be accounted for by local differences in the depositional regime. The ridge crust shows the only distinct reduction in fines and increase in sand along the transect. It can be suggested that it is the ridge which is most exposed to wind erosion and therefore is most prone to the removal of fines from the crust moving downslope. This increases the relative percentage of coarser material, which acts as a natural armouring mechanism. Although there are no visual differences in the furrow crust, Table 7.4 shows that both the ridge crust and the furrow crust have lost on average 16% of the fines and increased a similar amount in the sand fraction when compared with the auger samples.

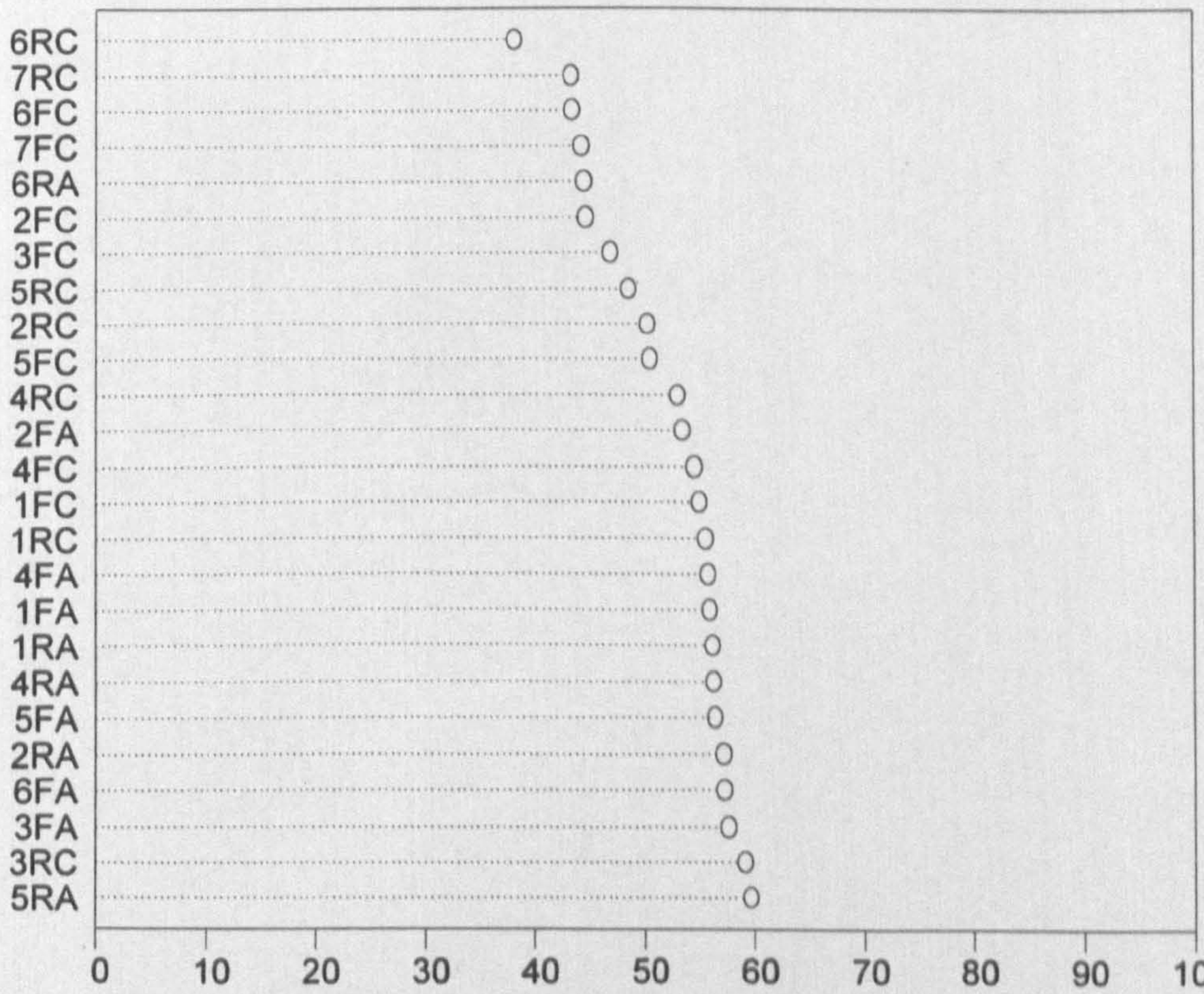

Figure 7.4: The changes in the fine fraction (<20 μm) down the slope profile at Low Farm

Figure 7.4 summarises the two main aspects of downslope changes in the particle-size distribution taken from the transect study (section 4.2.2). First, with the exception of 6RA and 3FC, there is consistently more fine material (<20 μm) in the auger samples than in the crust samples showing that there is either deflation of fines from the crust or washing-in of fines during the development of the crust itself. Second, as in Figure 7.3, there is a general increase in the amount of fines in the crust samples moving upslope, i.e. the sample numbers decrease from 6/7 to 1/2.

Site		Coarse sand (%)	Medium sand (%)	Fine sand (%)	Coarse silt (%)	Medium silt (%)	Fine silt (%)	Clay (%)
Average Furrow	Crust	6.89	3.66	8.43	32.56	15.30	13.10	20.10
Average Furrow	Auger	4.19	3.17	6.67	31.79	15.21	14.13	24.93
Average Ridge	Crust	6.06	3.59	8.41	33.26	14.39	13.90	20.44
Average Ridge	Auger	6.92	3.96	6.93	31.57	14.70	12.93	23.04
Average Uncropped	Crust	11.80	6.6	11.43	38.53	14.20	9.33	8.13
Average Uncropped	Auger	4.95	4.6	10.50	30.55	14.05	13.80	21.50

Table 7.5: Changes in particle size distribution between cropped and uncropped soil at Low Farm

Table 7.5 shows clearly that there is a distinct difference in the soil surface conditions at sites which have been cleared of basalt, but are not undergoing cultivation. For the auger samples there is very little change compared with auger samples under the land which has been ploughed and cultivated. However, the crust displays a totally different fabric. All of the sand fractions have increased so that the total sand is around 30% compared with about 19% and 18% for the average furrow and ridge crusts respectively. The coarse silt is likewise high, with about 18% more

than the newly formed crusts. The medium silt shows no apparent change, but both fine silt and clays have drastically decreased. If the auger samples represent the real particle size distribution, then there are 32% and 62% reduction in fine silt and clay respectively.

This is important. It means that the natural soil crust will develop, as long as there is no cultivation taking place, to an equilibrium stage. The finest material is relatively quickly removed and the sediment making up the crust becomes much more dominated by the sand and coarse silt fractions. The sand and coarse silt act as an armour against further wind erosion and even rainsplash erosion during precipitation events.

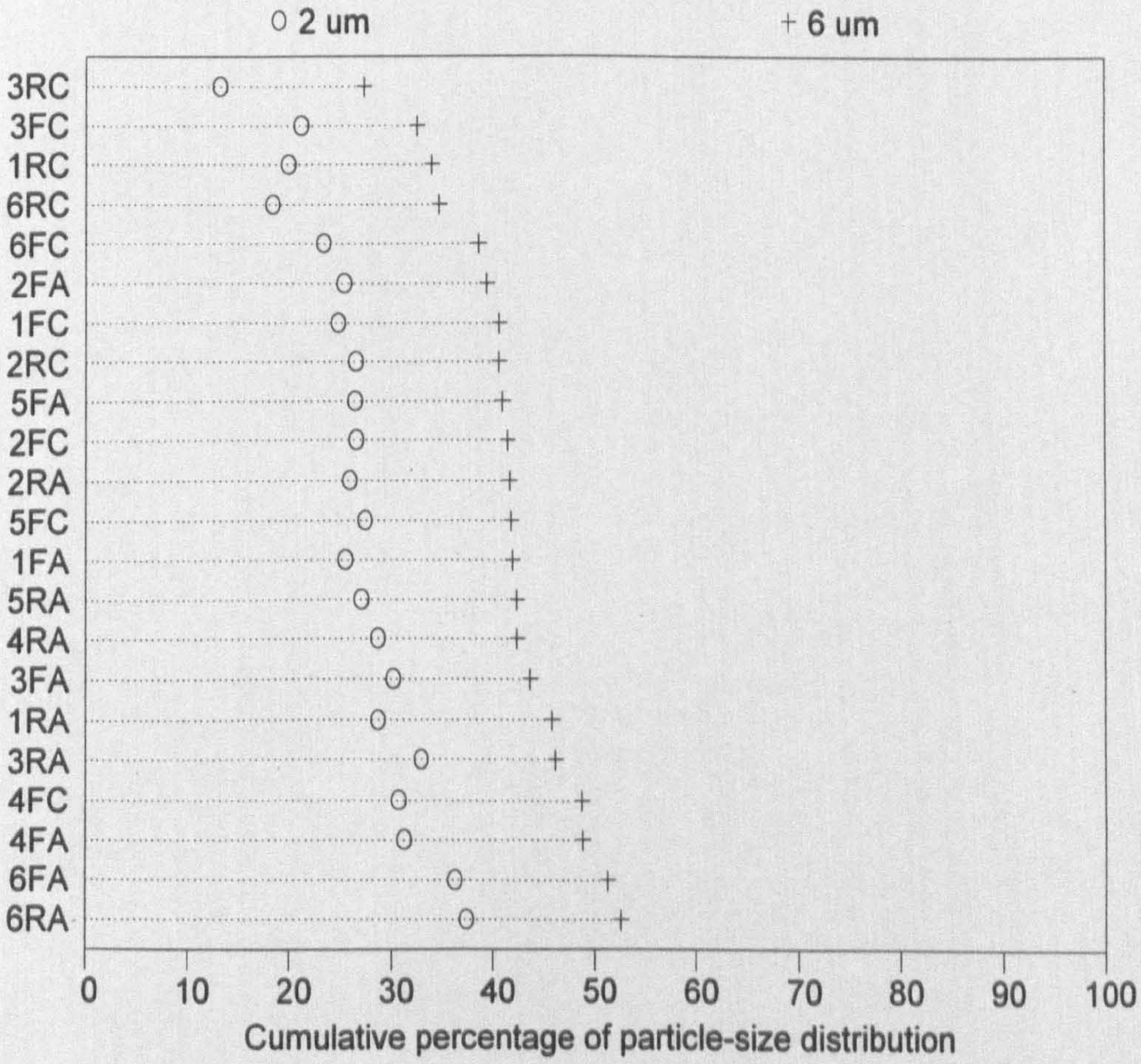

Figure 7.5: Changes in the fine fraction (<20 μm) down the slope profile at Middle Farm

These results represent a considerable change in focus from most soil crust research. Whereas much research sees a soil crust as a sign of degradation, reduction in infiltration rate and an encouragement to soil erosion, the present data seem to suggest that the formation of a soil crust provides more of a defensive mechanism. In observing the current landscape, the major wind erosion occurs as a result of ploughing at the wrong time, allowing much more fine material to be lost as the soil is turned over.

Moving to downslope changes at Middle Farm (Figure 7.5), trends are not so clear, although there is a similar discrepancy between the crust samples with less fine material and the auger samples with more. The downslope component is not marked in the same way as that of Low Farm, because it has a north-south aspect rather than a west-east. Also the samples taken from the top of the transect are on an exposed summit of a small topographic high. There is a downslope change in the auger samples: the samples at the base of the slope MF1-6 have a much higher fine content than those further up the slope. This suggests that the bulk soil, represented by the auger samples, is fining downslope as a result of longer-term slope wash, but that the surface crust is affected by short-term wind erosion.

The patterns at High Farm have two components, which are controlled by either their position on the slope or their agricultural use. Figure 7.6 and Figure 7.7 show the increasing coarse silt fraction (20 - 63 μm) and fine fraction (<20 μm) respectively. Both 3U and 4U, which were samples along the transect but had not been ploughed, behave much like the samples from the uncropped land in Low Farm (Table 7.5); they have a much lower percentage of fines, but rather more coarse silt and sand. Looking at the fine fraction from the samples, which lie on the cultivated area, there is also a reduction from the upper slope positions (1/2) to the lower ones (6/7).

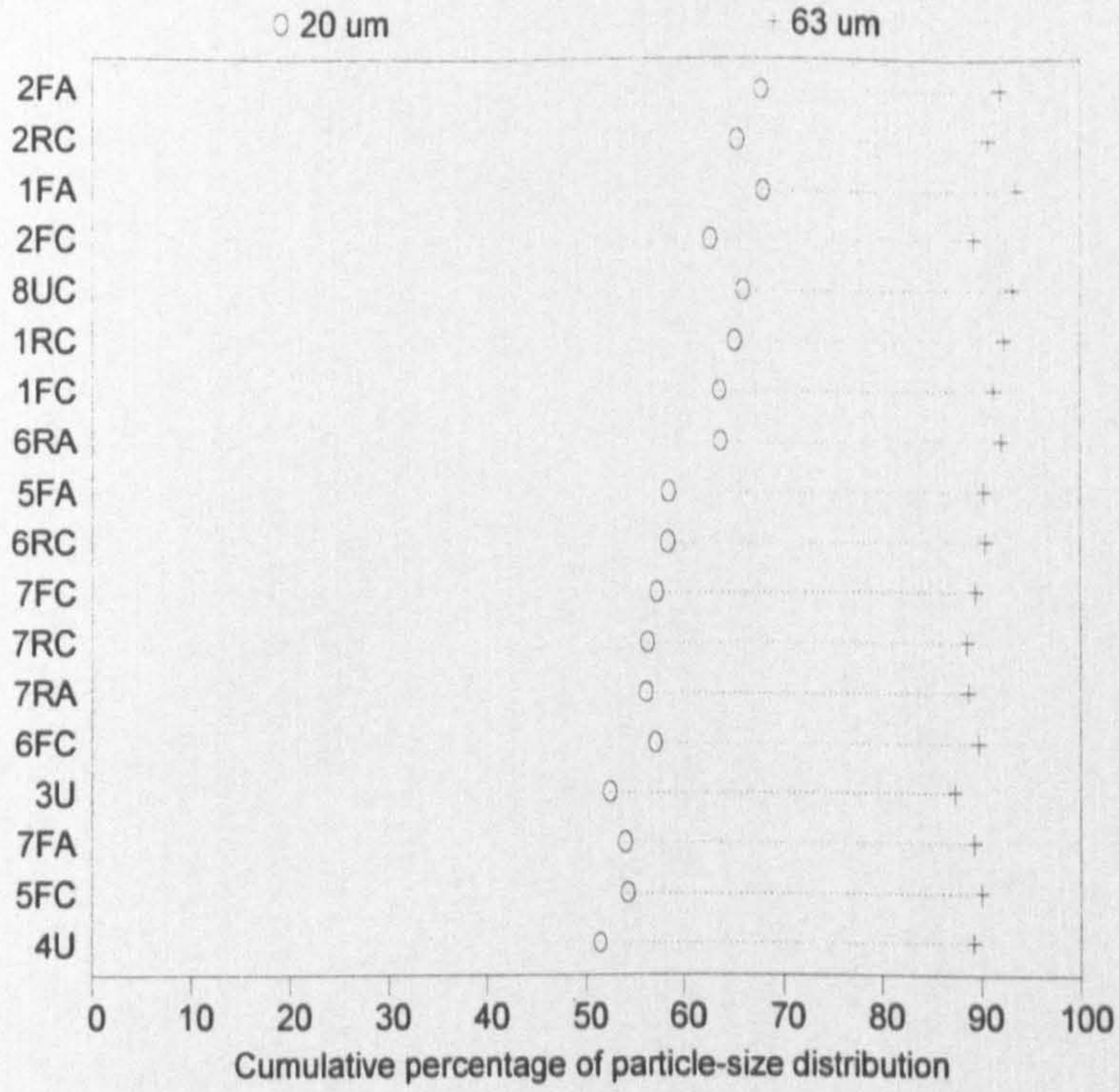

Figure 7.6: Downslope changes in coarse silt (20-63 μm) at High Farm

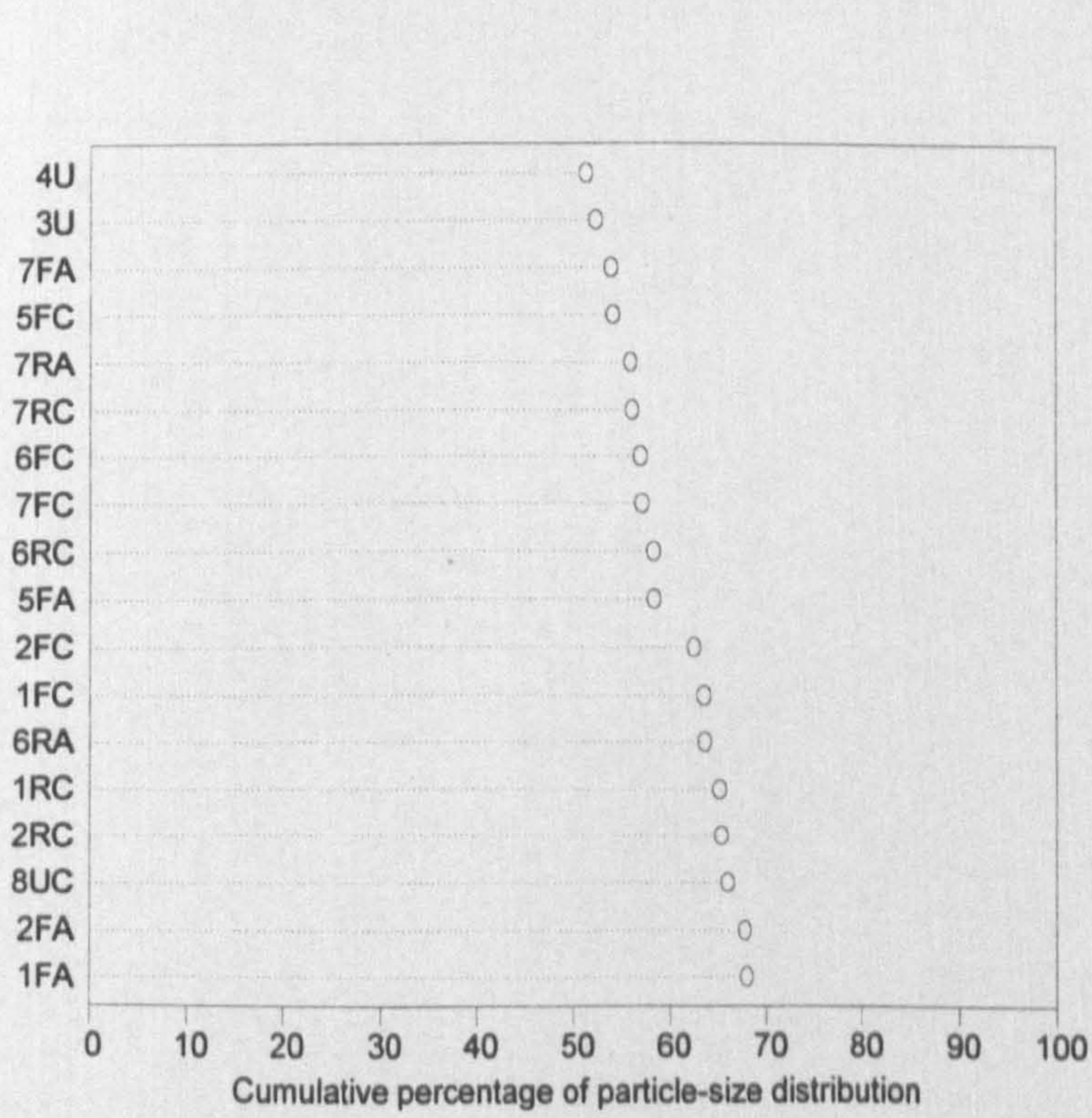

Figure 7.7: Downslope changes in fines (<20 μm) at High Farm

7.3.2 Patterns of infiltration through crusted soil with different levels of agricultural use

Both at High and Low Farms, there is a considerable difference in the physical components of the crust depending on whether the land is being used for irrigation or is uncropped. It would therefore be appropriate to see if the physical structure of the crust has an effect on the infiltration rate. The literature has concentrated upon looking at the role of the soil and water chemistry (Agassi *et al.*, 1981; Shainberg *et al.*, 1981a; Kazman *et al.*, 1983; Ben-Hur *et al.*, 1985; Shainberg, 1985), upon infiltration through the crusted layer and rather less upon the effects of particle-size distribution (Poesen, 1984; Moss, 1991a), porosity (Ela *et al.*, 1992) and clay dispersion (Amézketa & Aragués, 1995). The results presented below seek to show the effect that land-use and consequent crust formation have upon the infiltration rate.

The data are displayed in two formats (Figure 7.8 to Figure 7.10). First, the average raw data are shown with each line representing four infiltration tests carried out on a specific soil crust type: 'uncleared land', 'used land' and 'new land' which has been ploughed ready for cultivation (Section 4.2.5). The time variable in each case has been transformed to allow a greater resolution for the first 20 minutes when the majority of change in the infiltration rate occurs. The second graph shows a set of nonlinear regressions calculated by using a Hortonian-type infiltration equation,

$$i = i_0 + i_1 e^{-kt} , \tag{7.1}$$

where i_0 is the final infiltration rate (asymptote),

t is time,

and i_1 and k are constants initially derived from calculating a linear regression between log-transformed infiltration and log-transformed time.

This equation was fitted by a nonlinear least squares method: that is, the best fit equation was found by a program searching in parameter space for the set of parameter

values minimising the sum of squared deviations between observed and predicted infiltration rates.

The uncleared land has a higher infiltration rate than the other two with a relatively small initial rate. There is a crust on the soil surface, but it has developed over many years and has a better developed pore network and moisture holding ability because perennials will grow during the spring. There is enough porosity developed to allow a higher intake of water, but due to the existence of the crust, there is a natural storage to allow plants to grow. The upper soil layers are much less dense compared with those on the previously irrigated land and there are many fine root hairs from the natural vegetation which allow a higher final infiltration rate. The result for High Farm (Figure 7.8) is consistently above the corresponding curves for Middle Farm (Figure 7.9) and Low Farm (Figure 7.10), because at the latter two sites there was no uncleared land near to the farm and so the infiltration tests were carried out on land that had been cleared, but not ploughed. This explains the reduced level of the final infiltration rate. Increased grazing, compaction and a removal of the stone fragments all play a role in decreasing the overall infiltration rate and reducing soil moisture storage.

For the new land the initial infiltration rate is the highest in every case. The crust on these soils has recently developed and is comparatively thin. Therefore, as the infiltration rings are pushed into the soil, there is a considerable disruption of the crust, especially in the area next to the ring. This results in a high initial rate, which rapidly falls as the aggregates break down and fill the cracks that have developed due to the ring insertion, and the steady state is reached within about half an hour. In the case of Middle Farm and Low Farm, the final infiltration rate is the lowest, which is somewhat surprising since the soil has recently been tilled. This can be explained by the fact that there are no natural pathways, such as root hairs, to increase infiltration. Such a result brings into question the type of ploughing method used in this environment.

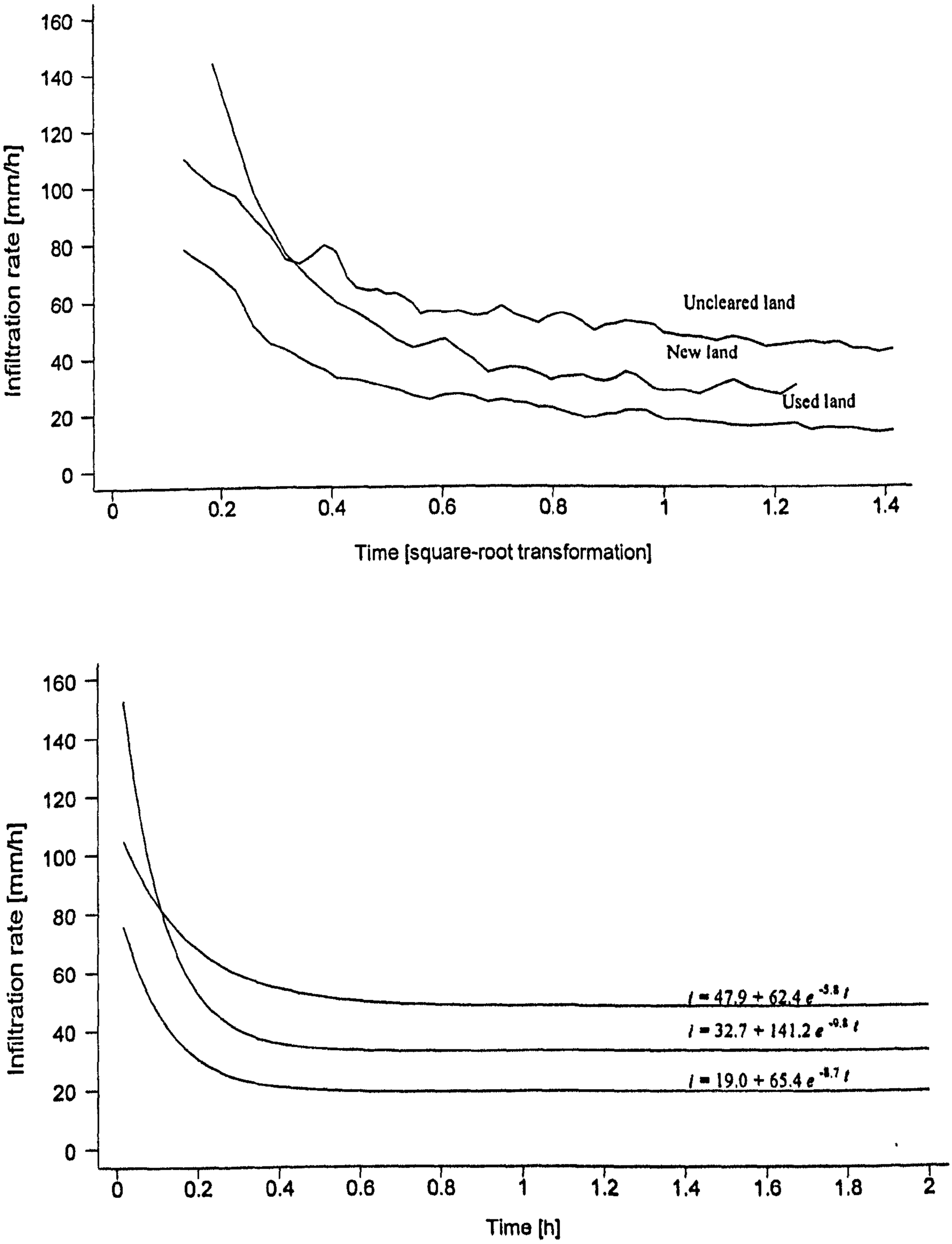

Figure 7.8: Infiltration curves at High Farm

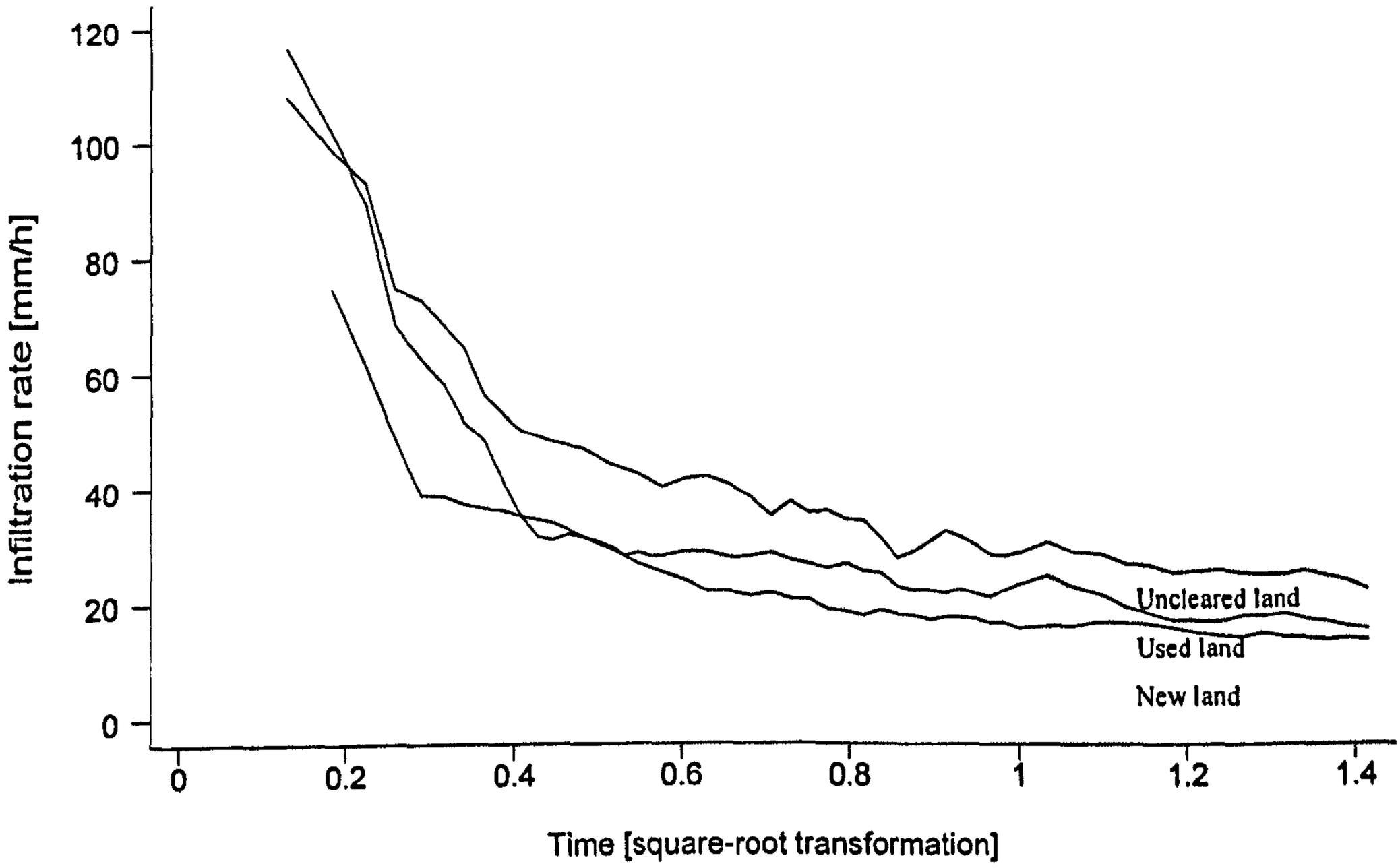

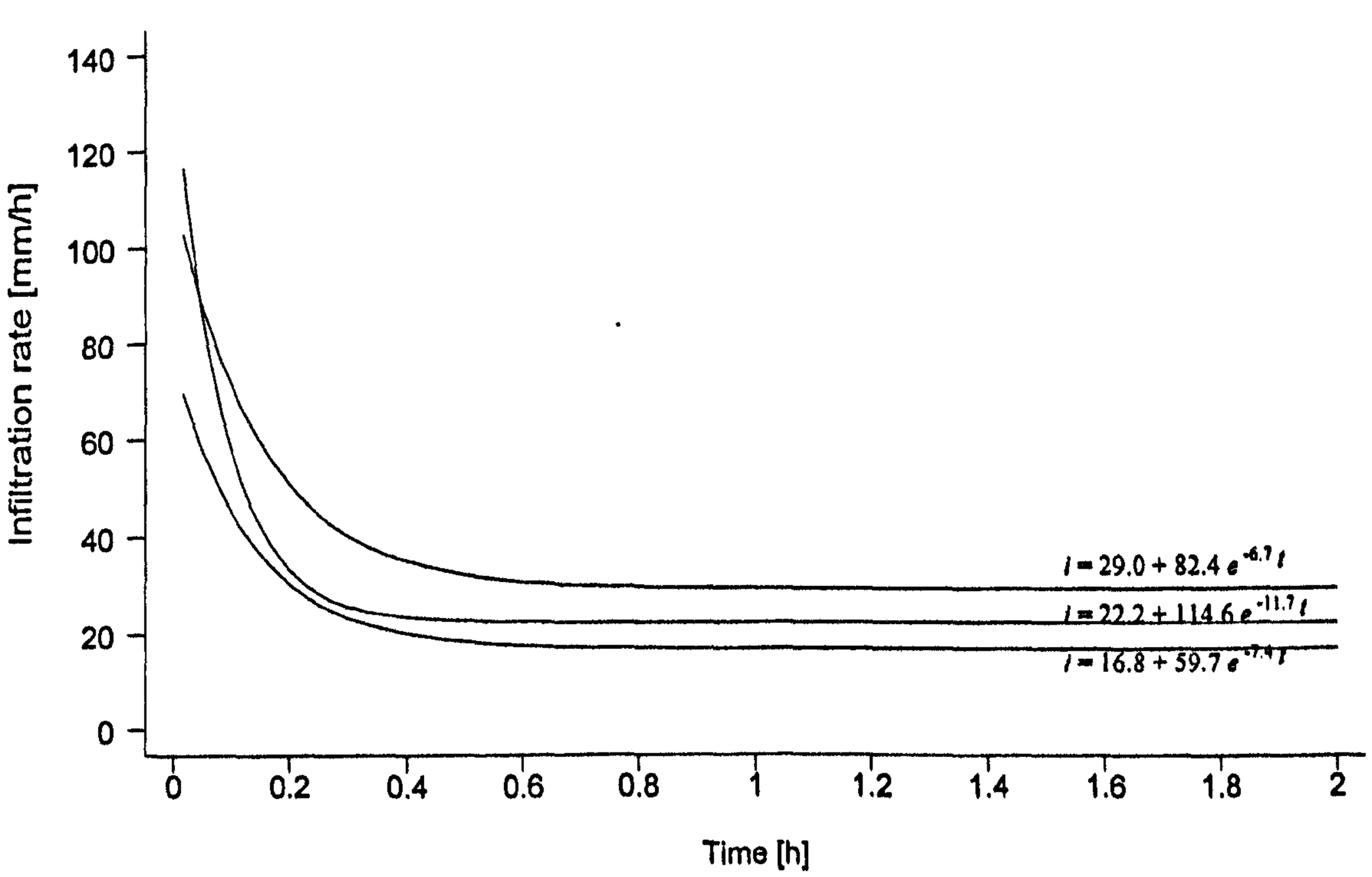

Figure 7.9: Infiltration curves at Middle Farm

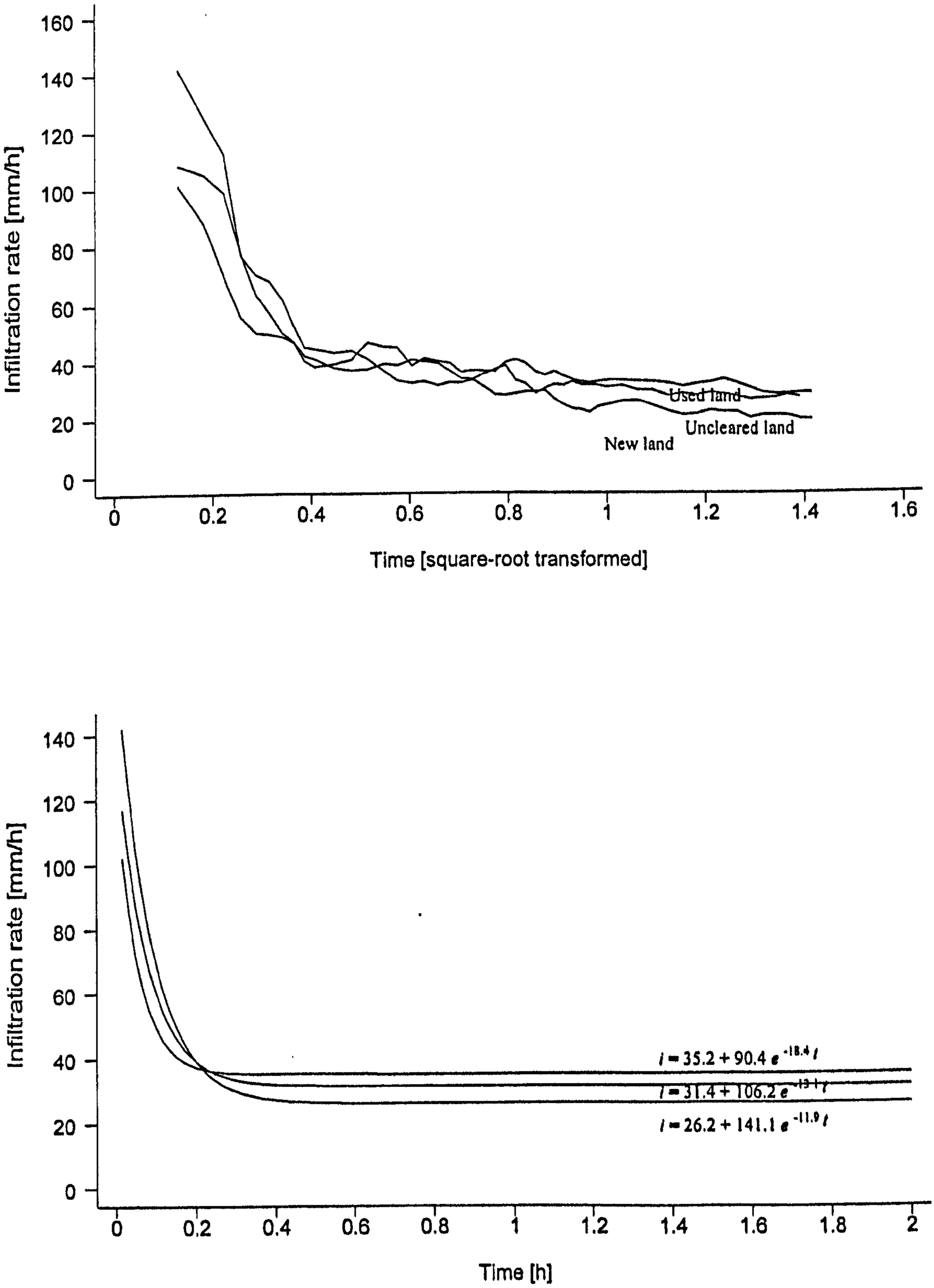

Figure 7.10: Infiltration curves at Low Farm

The previously irrigated land has a similar curve to the ploughed land but with a reduced initial rate of infiltration. The soil at the surface, which has a highly compacted thick crust developed over the previous year's cultivation, has a dramatic effect on both initial and final infiltration rates. Previous irrigation and cultivation have caused an in-washing of finer materials, which have clogged the pores in the upper soil layers resulting in a low final infiltration rate, but which is balanced by an increase in overall permeability due to an increase in the network of old root channels.

In conclusion, there is strong evidence that the intake of water into the soil is reduced as land is ploughed and then irrigated. Although all the soils show signs of crusting, the crust on the uncleared land is much less resistant to water entry. Once the soil has been tilled, however, the natural pathways which have evolved through the crust are destroyed and the new crust is significantly more resistant to water entry. After compaction and irrigation for one year the resistance is often increased but this is offset by the additional organic matter left in the upper soil layers. In the short term there is a degradation of the soil surface if infiltration rates can be used as an indicator. It is possible in the long term to postualte that if the soil is left, it will revert to a natural crust with a higher infiltration rate.

7.3.3 Spatial sediment variations within the ridge-furrow sequences

The ridge and furrow sequence used in farming in the Badia, which have already been described in Chapter 2, represent a complex set of slopes albeit at a relatively small scale in comparison with the general slope characteristics. For the purposes of the research, each position within the sequence needs to be defined. The first position is the outer ridge which is artificially formed by the farmer as he attempts to cover the plastic irrigation sheeting. The crops often lie in a slight depression on the far side of the ridge, having been encouraged to grow up through holes within the plastic. The second position is the outer furrow flank which is the slope dividing the outer ridge from the depression of the furrow. The third position is the base of the furrow and the fourth position is the centre flank. The final position is the smaller ridge which lies approximately half way between the rows of crops. As an example, Figure 7.11 shows two transects across the sequences LF3-3 and LF3-4 respectively

showing various positions which have been described above. However, it must be noted that at some sites only three or four samples were taken and that not every sequence showed exactly the same characteristics. Table 7.6 shows all the possible sequence positions with the actual samples taken at each site.

Site	Ridge under plastic	Outer furrow flank	Furrow base	Inner/ central furrow flank	Central ridge
LF3-1	D & E	C	B	A	
LF3-2	A	B & F	C & E		D
LF3-3	A		B & D		C
LF3-4	A	B & F	C & E		D
LF3-5	D	C	B	A	

Table 7.6: Compilation of sample details taken at each site

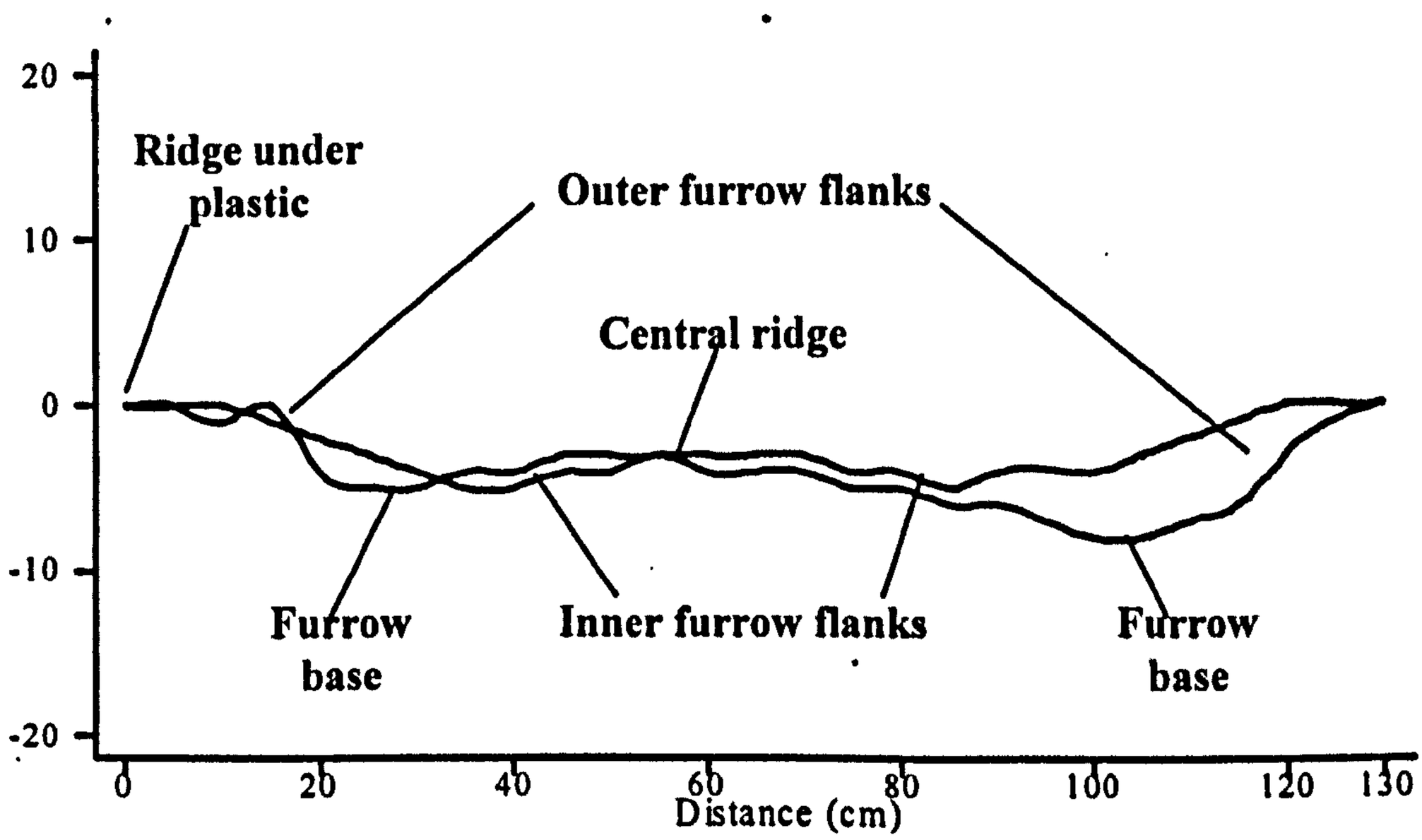

Figure 7.11: Two transects of the ridge and furrow sequence at LF3-3 and LF3-4

It can be seen that the flanks of the main furrow at points **B** and **E - F** have a much higher relief than the average slope angle of between 0.5° and 2°, often with local slopes exceeding 30° and regularly between 15° and 30°. Rainsplash erosion is least likely to affect the sequence during the first year of cultivation, because the sequence is only created in late March or early April by which time rain is unlikely. Only in subsequent seasons, while the soil is left fallow, would rainsplash erosion take place. In the short term, the more likely forms of erosion would be compaction and aggregate break-up from human activity on the one hand, and, sheet erosion caused by over-irrigation, on the other.

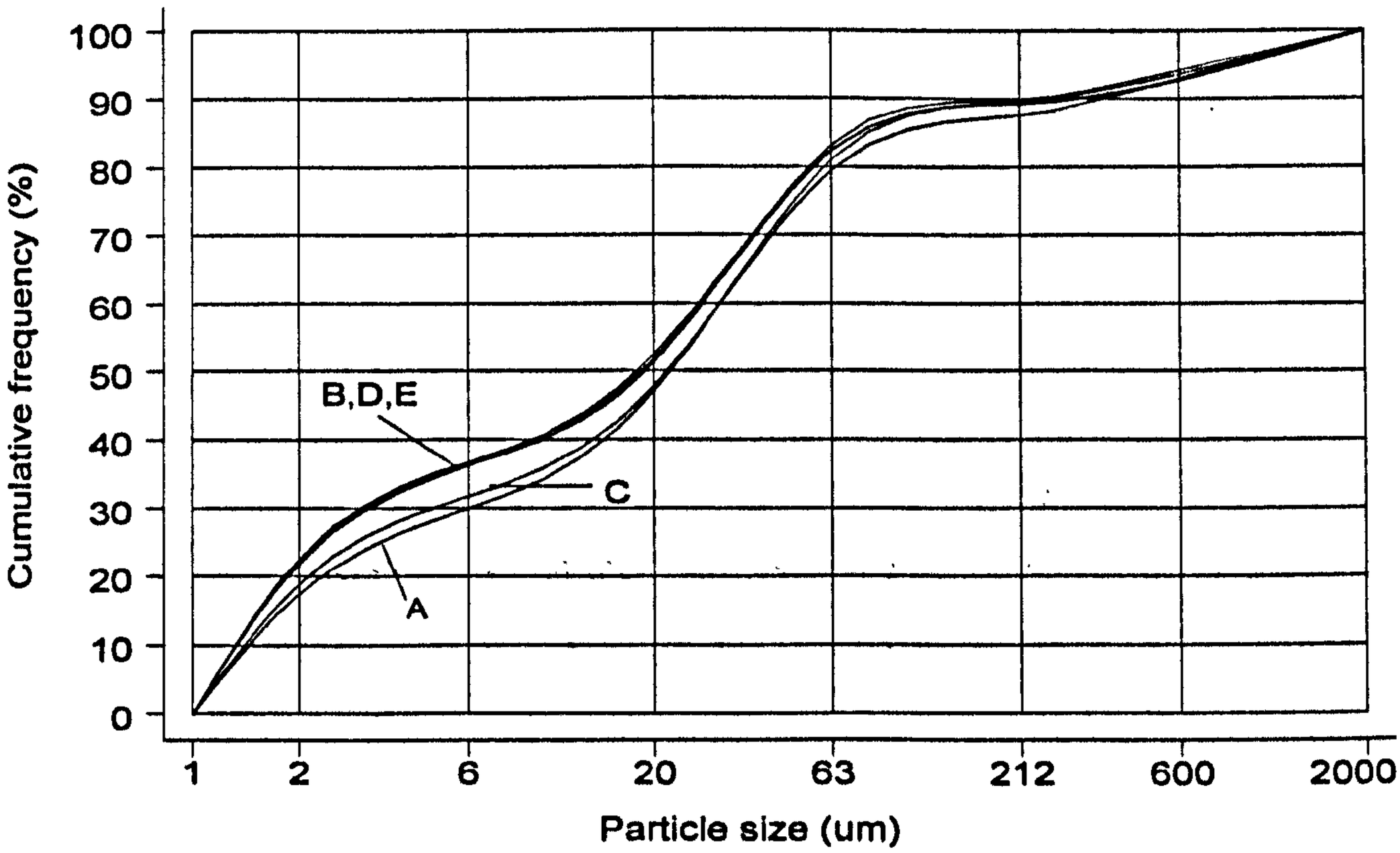

Figure 7.12: Inter-furrow variation in particle size - Furrow 1 Crust (LF3-1)

From the graphs of inter-furrow variation from Low Farm (Figure 7.12 to Figure 7.17) it can be seen that there is a considerable amount of variability. As each graph

is analysed, it is important to keep in mind the different positions within the sequence each sample occupies.

In the first example (LF3-1), samples **C** and **A** have a significant reduction in the clay and fine silt fraction compared with the other three locations. This would suggest that the fines are being preferentially removed from the flanks, but not the furrow base. If wind erosion was seen as the main potential erosive agent, it is unlikely that such a difference would occur. The control has to be the set of auger samples in Figure 7.13, which suggest that clay content should be about 21 to 24%, as there is no possibility of the auger soil being affected by wind erosion except indirectly over a long period. The furrow base must have had some deposition from the surrounding flanks, which has compensated for any wind erosion.

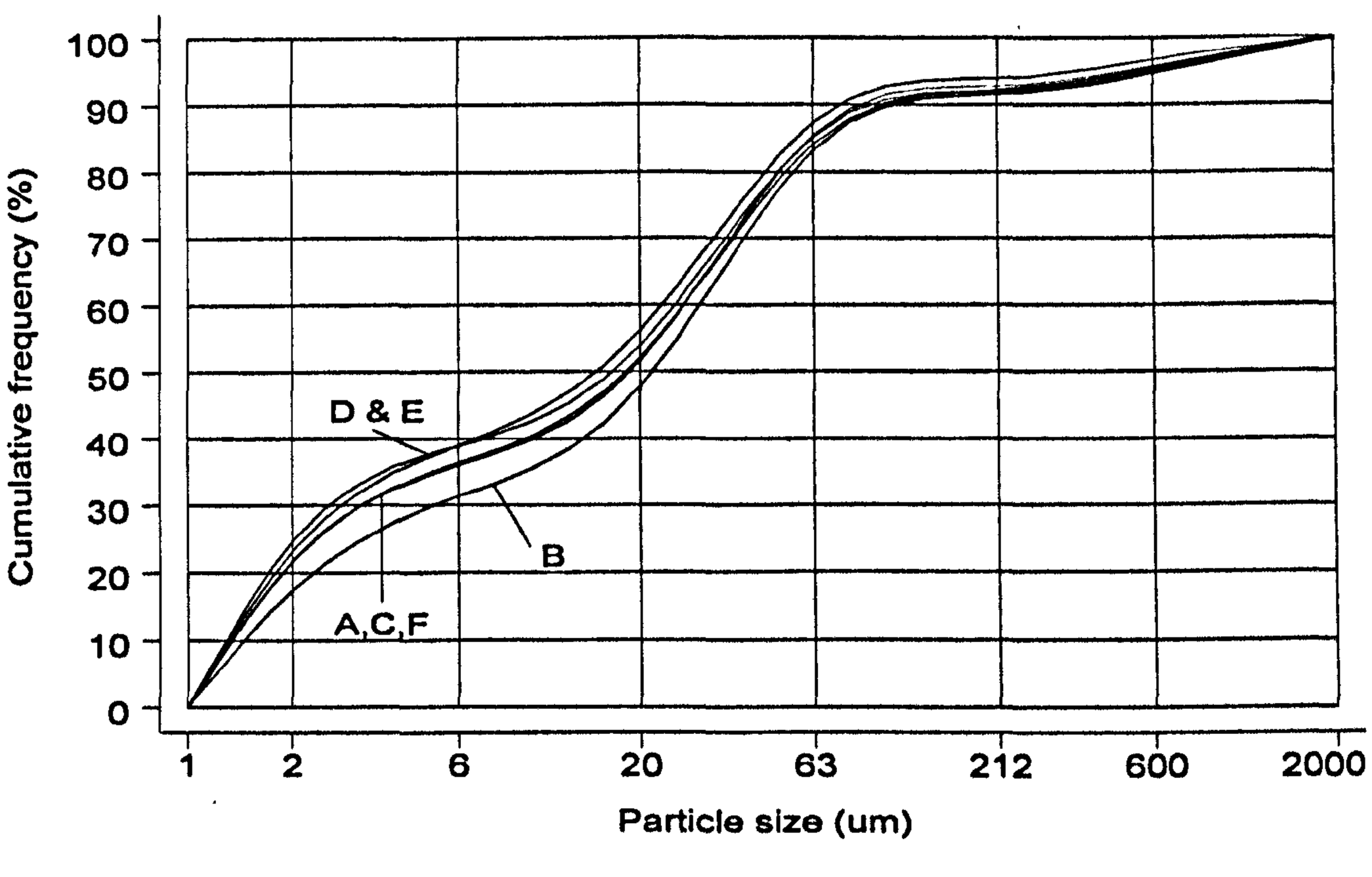

Figure 7.13: Inter-furrow variation in particle size - Furrow 2 Auger (LF3-2)

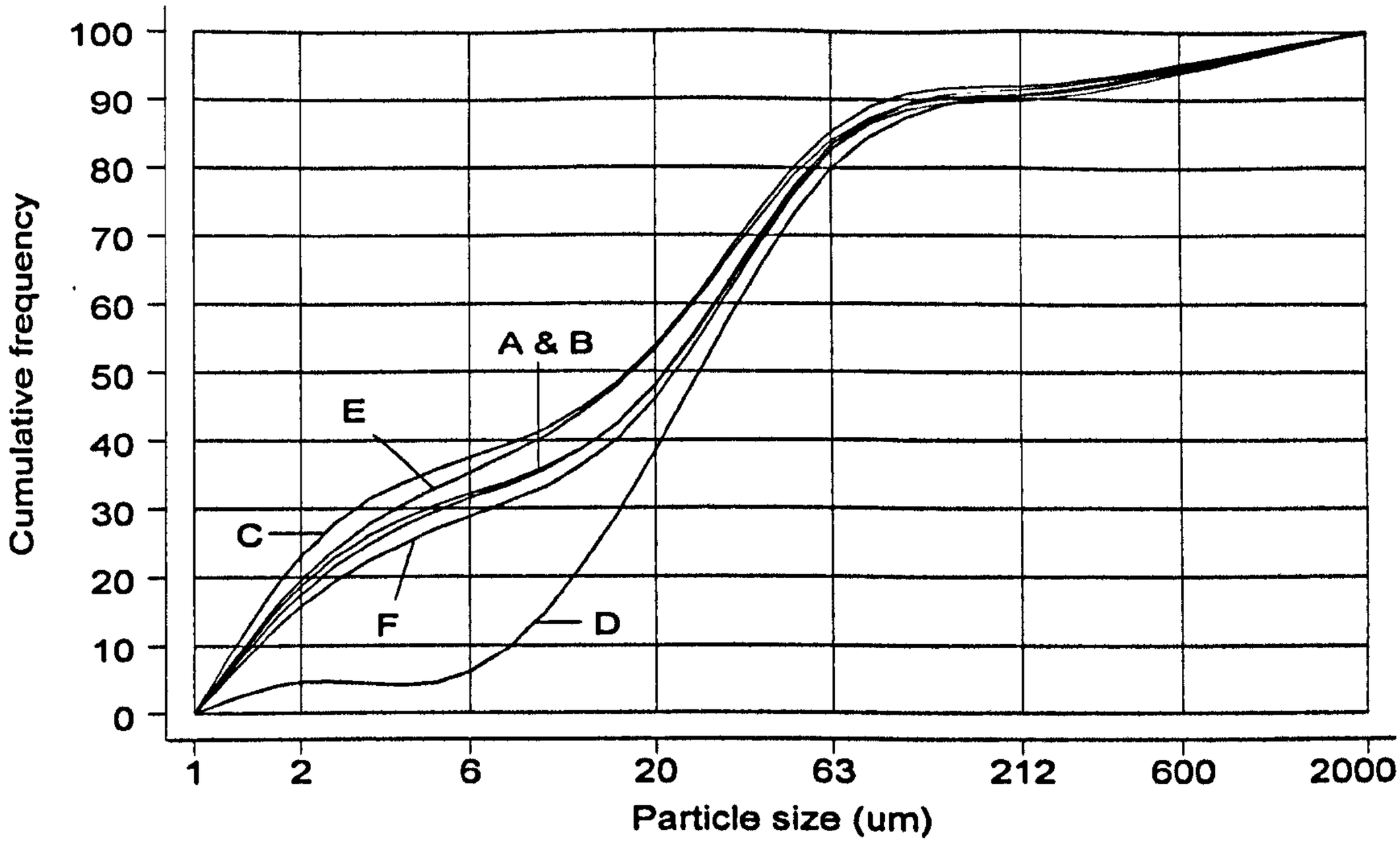

Figure 7.14: Inter-furrow variation in particle size - Furrow 2 Crust (LF3-2)

The two figures representing the auger and crust samples taken at site 2 (Figure 7.13 and Figure 7.14) should be taken together for direct comparison can be made with the control. Samples **B** and **C** are the only samples which display little change between the auger and crust samples, the latter having a similar disposition to site 1. **A** is reduced, despite being sampled under the plastic, but at 2% is not significant in relation to likely errors in sampling and analysis. Both **F** and **E** have a reduction of clay content of about 5% in the crust while **D** experiences a drastic reduction in both clay and fine silt to the order of 20 and 10% respectively. Despite a reduction of clay in **E**, both **E** and **C** remain the crust samples with the highest fines content, which correlates well with the furrow bottom sample findings from site 1. Sample **D** would seem to give the most problems in interpretation as there is so rapid a decrease in all the fine material below 6 μm.

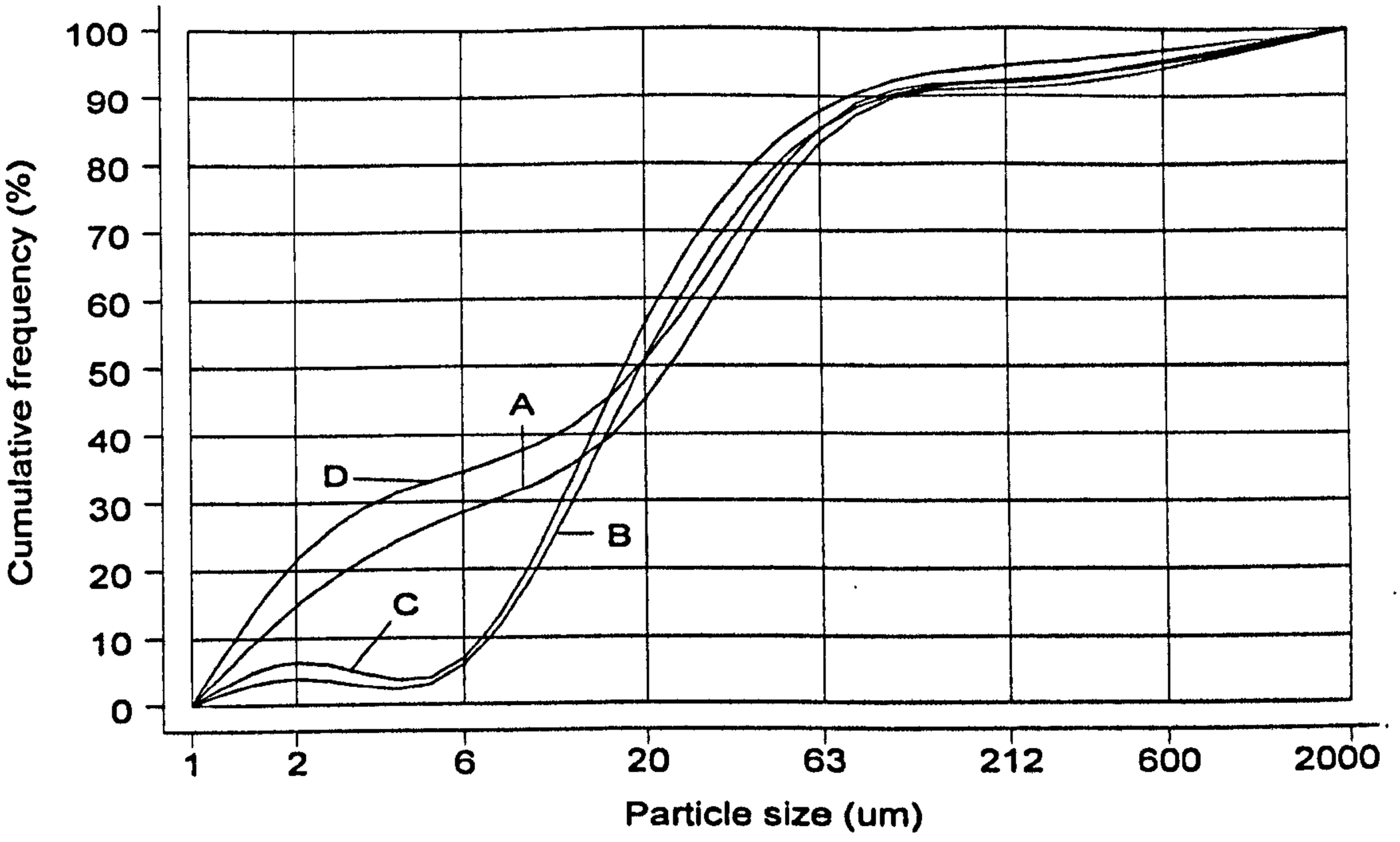

Figure 7.15: Inter-furrow variation in particle size - Furrow 3 Crust (LF3-3)

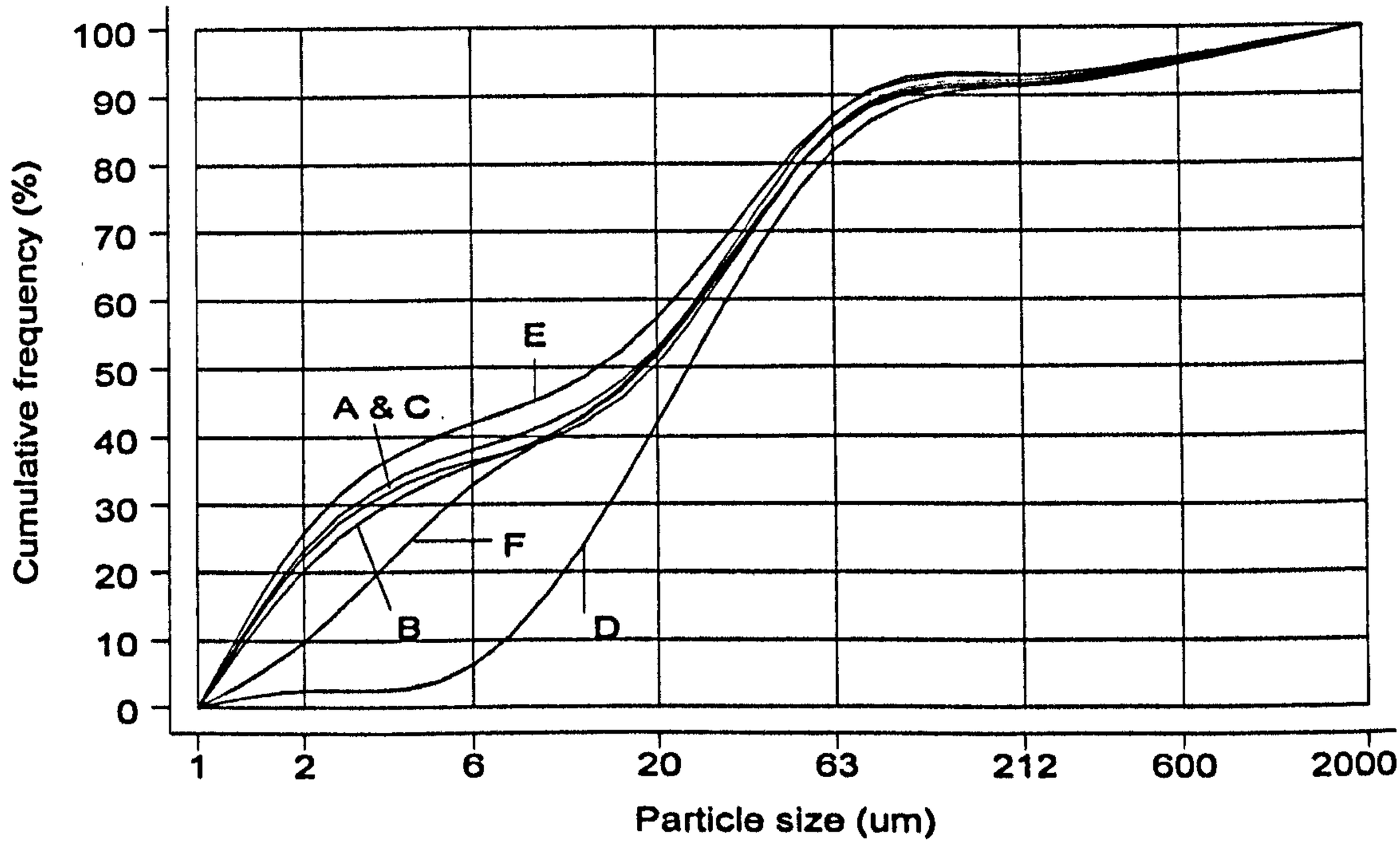

Figure 7.16: Inter-furrow variation in particle size - Furrow 4 Crust (LF3-4)

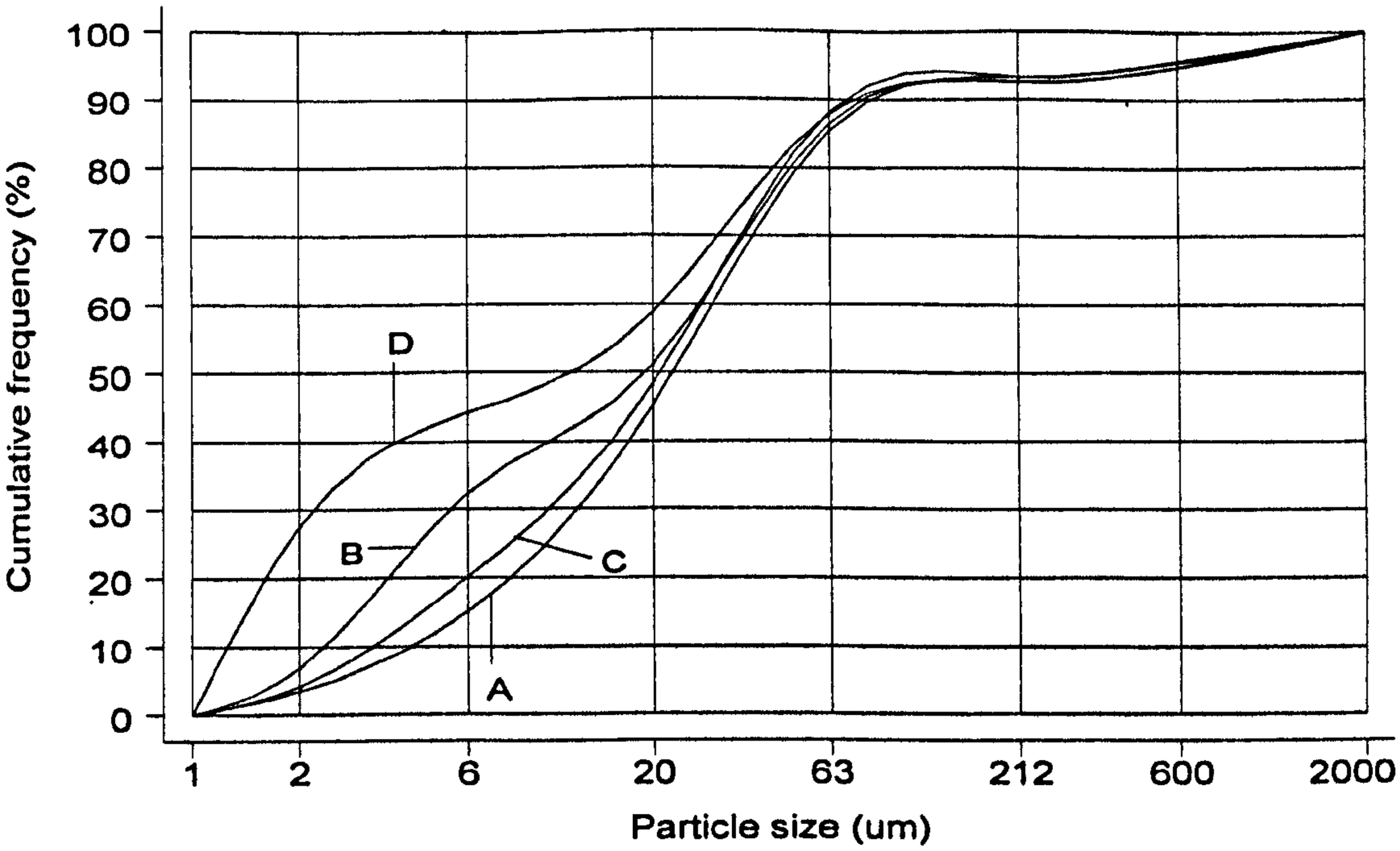

Figure 7.17: Inter-furrow variation in particle size - Furrow 5 Crust (LF3-5)

As with site 2, the furrow base **D** at site 3 has a high level of fine silt and clay fractions, although it is a little low in the medium silt fraction. All the samples are high in the coarse silt fraction. **A** is slightly lower than expected, but only by a matter of about 2% when compared with the previous sites which is not significant. The central ridge sample **C** displays similar tendencies to sample **D** in the previous example, although here the medium silt goes up to over 40% of the total sample. **B** is behaving in a similar way, which suggests that the actual position in the sequence is not primarily responsible, but rather there is a complex relationship between the irrigation input, the associated wetting bulb and their effect on the soil surface conditions. Both **B** and **C** are stained dark brown.

Six samples were taken at site 4. Here **C** and **E** remain high, with **E** showing signs that there has been some possible deposition of fines. **A** is likewise unchanged and has similar characteristics to **C**. The outer furrow flanks **B** and **F** show differing amounts of clay loss with **B** showing very little, but **F** displays a considerable reduction in clay, which is quite unlike sample **D**, because there is a relatively high

amount of fine silt, although chemically there is a similarly high amount of calcium, magnesium and sodium. **D** displays similarities with central ridge samples from previous sites.

Site five presents the largest interpretative problems. The samples come from a part of the field which had been replanted with wheat and had not been left fallow like sites 1 to 4. The original ridge-furrow sequence is unrecognisable, as the soil had been reploughed before planting, and yet the former soil chemical and physical attributes are still evident. **A, B** and **C** are all affected by high quantities of sodium, calcium and magnesium which manifests itself once again by low clay contents and for the flanks, low fine silt contents as well. Site **B**, despite a very low clay content, has a much higher level of fine silt and comparatively less medium silt. The likely explanation is that the fine silt had been redeposited due to its topographic position in the furrow base. Conversely, sample **D** shows a higher level of clay than samples in a similar position at other sites, but this can be explained by the additional soil stability and protection against wind erosion given to the soil by the wheat.

Not only does the phenomenon of sample **D** at site 2 exist elsewhere, but its occurrence is more extreme in Figure 7.15 to Figure 7.17. Another important detail to note is that all the samples reflecting this dramatic reduction in fine silt and clay were stained darker brown than the surrounding soil. Such a feature of the data, with very low clay and fine silt contents and a comparatively large medium silt fraction, cannot be fully understood within the confines of the particle size data and a simple model of erosional processes. Instead it is necessary to study the chemical data for the same samples to see if they can shed light on it.

7.3.4 Chemical changes in the ridge-furrow crust sequence

It has been observed that there is a large reduction in the fine silt and clay fractions toward the centre of the furrow and it has been suggested that there is no physical reason for such an occurrence and that the phenomenon is chemical. Figure 7.18shows the change in the three major cations in the crust samples alongside the change

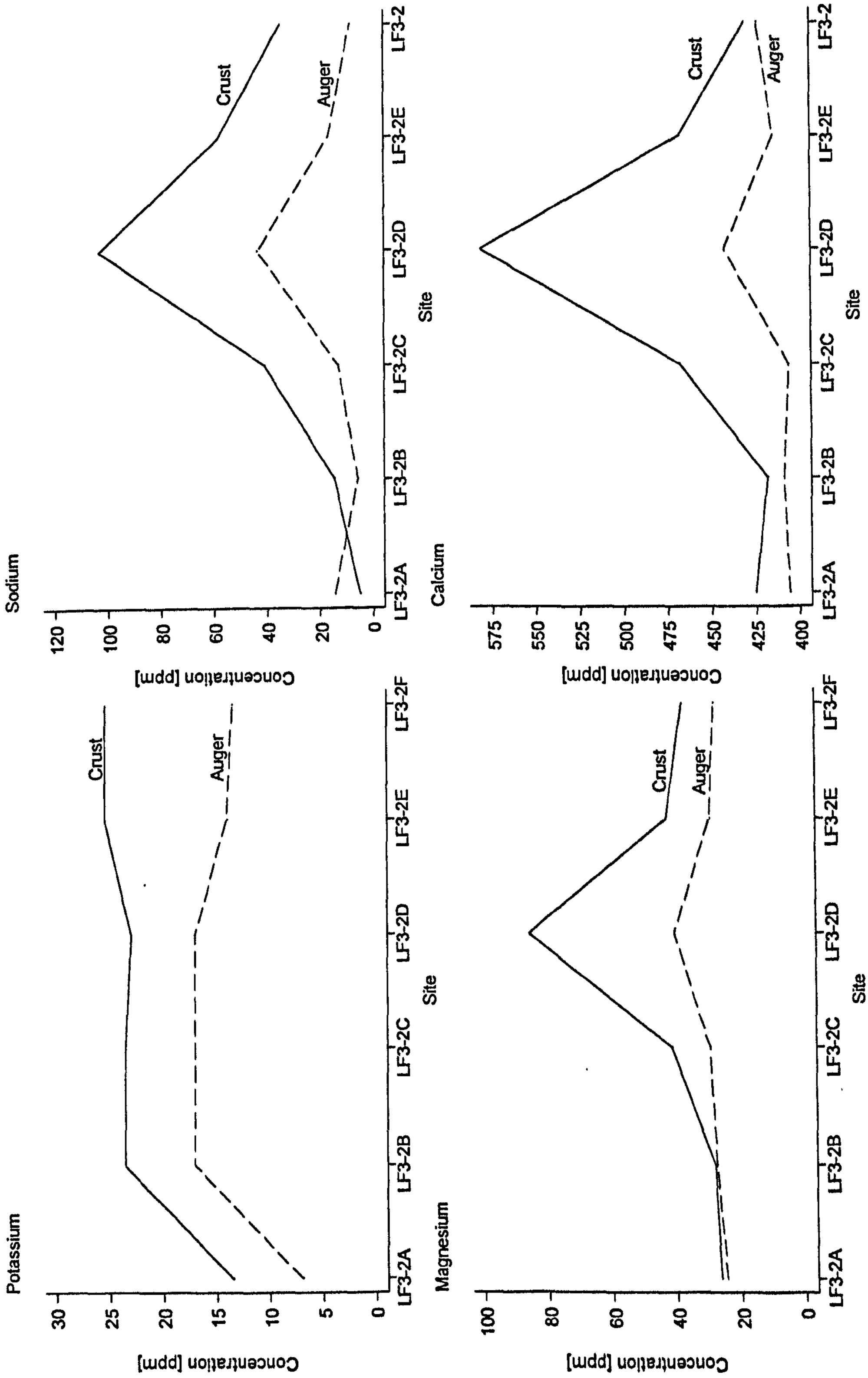

Figure 7.18: The relationship between physical and chemical characteristics at site 2

in particle size. It is quite evident that there is a significant increase in magnesium, calcium and sodium towards the centre of the furrow. The sodium is most prominent, often rising from 3-5 ppm at the edge of the ridge-furrow sequence to over 100 ppm in the centre. The magnesium shows a threefold increase, while the calcium is less variable with typical increases of about 25%. Only the potassium remains about the same across the sequence. Looking at the results for the auger sample, there are still noticeable increases in the concentrations of the three cations towards the centre of the ridge/furrow sequence, but the increase is about half that of the crust samples. With such an apparent coincidence between the soil chemistry data and the particle size data (Table 7.7), it is necessary to look for some physico-chemical process taking place at the crust surface.

	Sodium	Magnesium	Calcium	Clay	Fine silt
Sodium	1.0				
Magnesium	0.96				
Calcium	0.95	0.99			
Clay	0.71	-0.82	0.76		
Fine silt	0.76	-0.90	-0.88	0.94	
Medium silt	0.89	0.97	0.95	-0.92	-0.96

Table 7.7: Correlations between physical and chemical characteristics at site 2

7.4 LINKAGES BETWEEN SOIL PHYSICAL AND CHEMICAL CHARACTERISTICS

It has been emphasised that the physical and chemical attributes of the soil cannot be taken in isolation. Table 7.8 shows correlations between each of the particle size fractions for the whole of Low Farm. First, it must be noted that there is an in-built negative correlation between the fine fractions due to the cumulative structure of the data. In addition, the sand fraction plays a limited part in the soil, rarely making up more than 10% of the total, and does not change significantly between sites. There is

	C. sand	M. sand	F. sand	C. silt	M. silt	F. silt	clay
Coarse sand	1.00						
Medium sand	0.73	1.00					
Fine sand	0.45	0.63	1.00				
Coarse silt	0.09	0.14	0.48	1.00			
Medium silt	-0.19	-0.21	0.08	0.41	1.00		
Fine silt	-0.21	-0.27	-0.43	-0.35	-0.65	1.00	
Clay	-0.26	-0.23	-0.52	-0.82	-0.67	0.41	1.00
(obs=103)							

Table 7.8: Correlation of soil physical characteristics

	C.silt	M.silt	F.silt	Clay	Ca	Mg	Na	K
Coarse silt	1.00							
Medium silt	0.47	1.00						
Fine silt	-0.27	-0.73	1.00					
Clay	-0.80	-0.81	0.40	1.00				
Calcium	0.40	0.79	-0.47	-0.70	1.00			
Magnesium	0.46	0.91	-0.64	-0.76	0.88	1.00		
Sodium	0.41	0.76	-0.38	-0.71	0.88	0.84	1.00	
Potassium	0.38	0.57	-0.35	-0.58	0.45	0.57	0.61	1.00
(obs=42)								

Table 7.9: Correlations of selected physical and chemical characteristics for LF3

Variables	Correlation	r-squared	r-squared for transformation
Coarse silt - Clay	-0.80	0.65	n/a
Medium silt - Fine silt	-0.73	0.42	n/a
Medium silt - Clay	-0.81	0.65	0.77 ($\log_{10}$ of medium silt)
Medium silt - Calcium	0.79	0.63	n/a
Medium silt - Magnesium	0.91	0.83	0.84 ($\sqrt[3]{}$ of medium silt)
Medium silt - Sodium	0.76	0.58	0.61 ($\sqrt[3]{}$ of medium silt)
Fine silt - Magnesium	-0.64	0.41	n/a
Clay - Calcium	-0.70	0.50	n/a
Clay - Magnesium	-0.76	0.58	n/a
Clay - Sodium	-0.71	0.50	n/a

Table 7.10: Correlation and regression coefficients between the fine fraction and soil chemical attributes at LF3.

rarely a large amount of sand except, in crust samples where all the fines have been blown away, which suggests that they create stability in the soil by acting as an armouring mechanism to the soil below. It is the <63 μm fraction which is important to study in the Badia as it is the largest proportion of the soil fraction and the changing inter-relationships of the fine fractions are vital in understanding crust formation processes and the likelihood of wind erosion.

From the correlations in Table 7.10, it can be seen that the medium silt is the controlling physical variable because it has high correlations with every other attribute except potassium. Indeed if Figure 7.19 is taken into account, it can be seen that the relationship is particularly close with magnesium, which means that it could be used as a predictive tool to identify areas which have high electrical conductivities because magnesium is in turn closely related to calcium and sodium (Figure 7.20 to Figure 7.22).

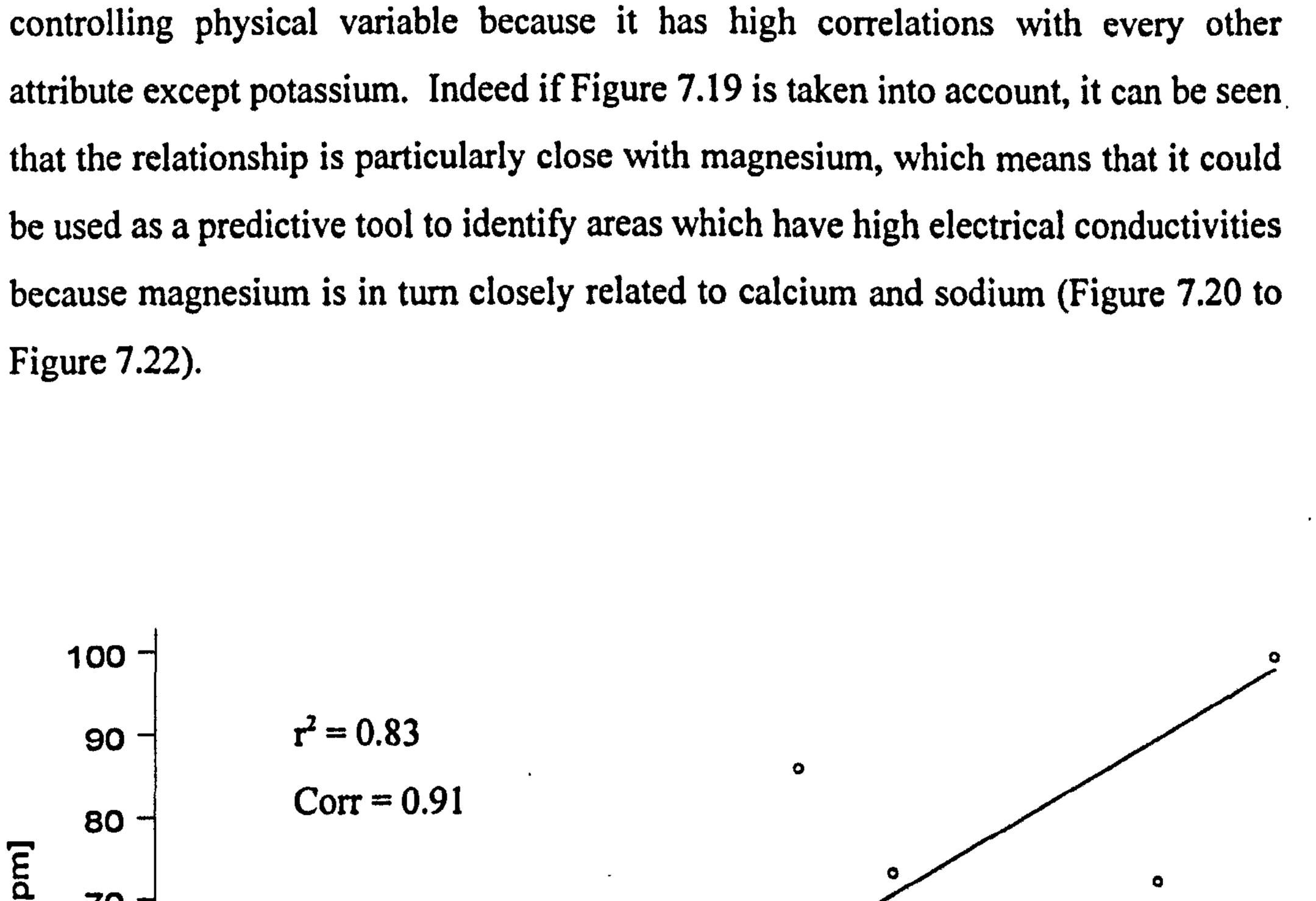

Figure 7.19: Relationship between medium silt and magnesium at LF3

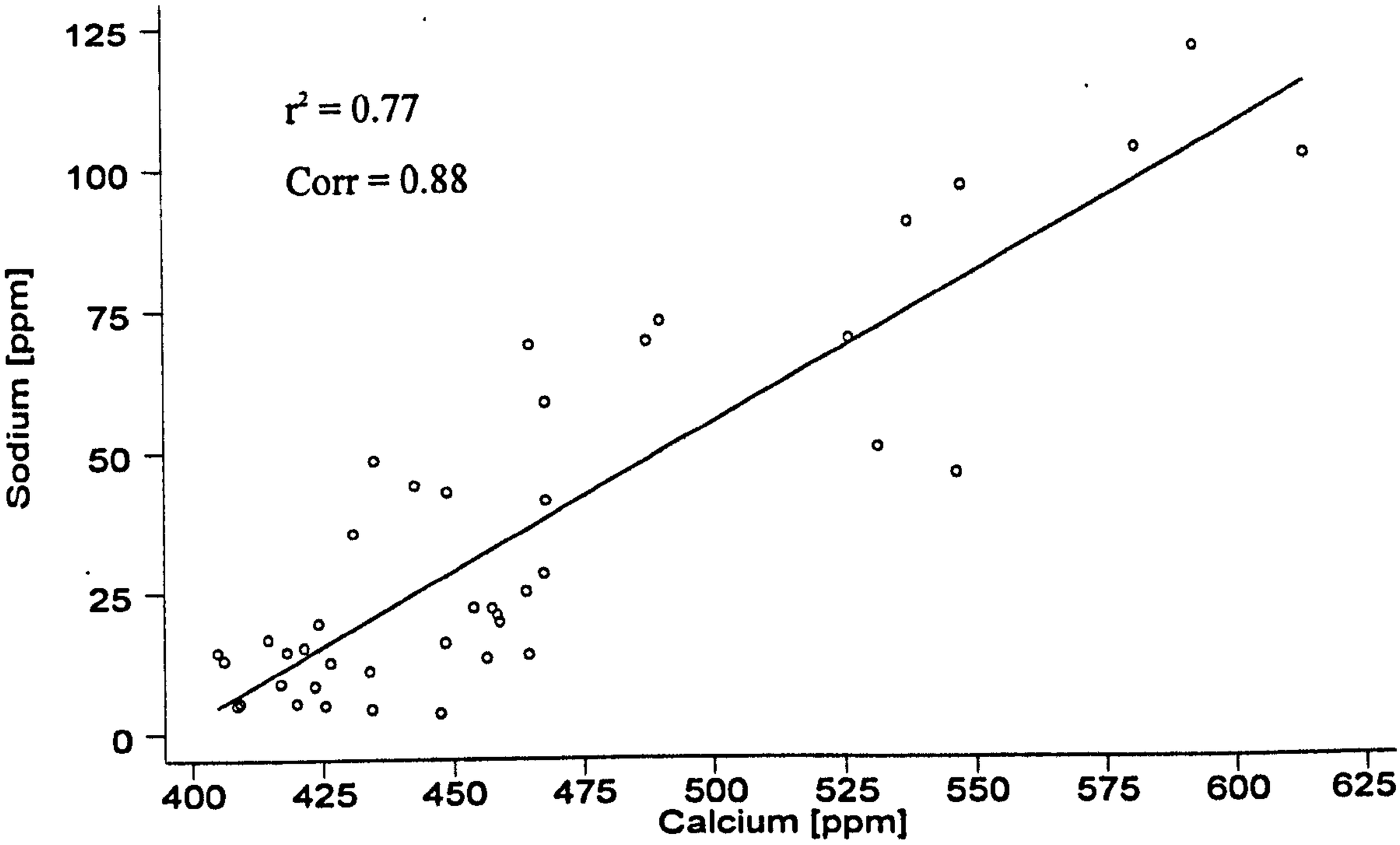

Figure 7.20: The relationship between calcium and sodium at LF3

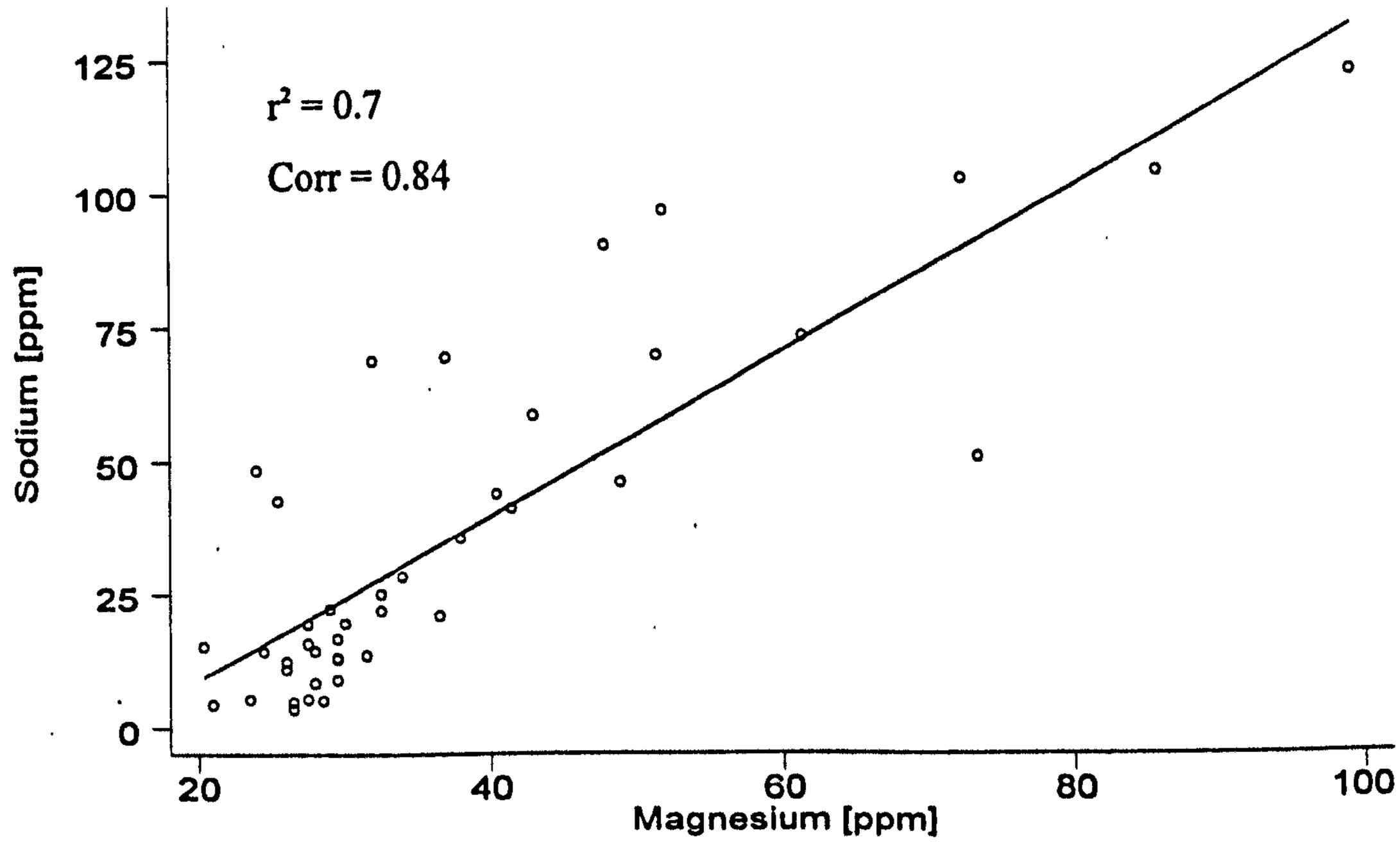

Figure 7.21: The relationship between magnesium and sodium at LF3

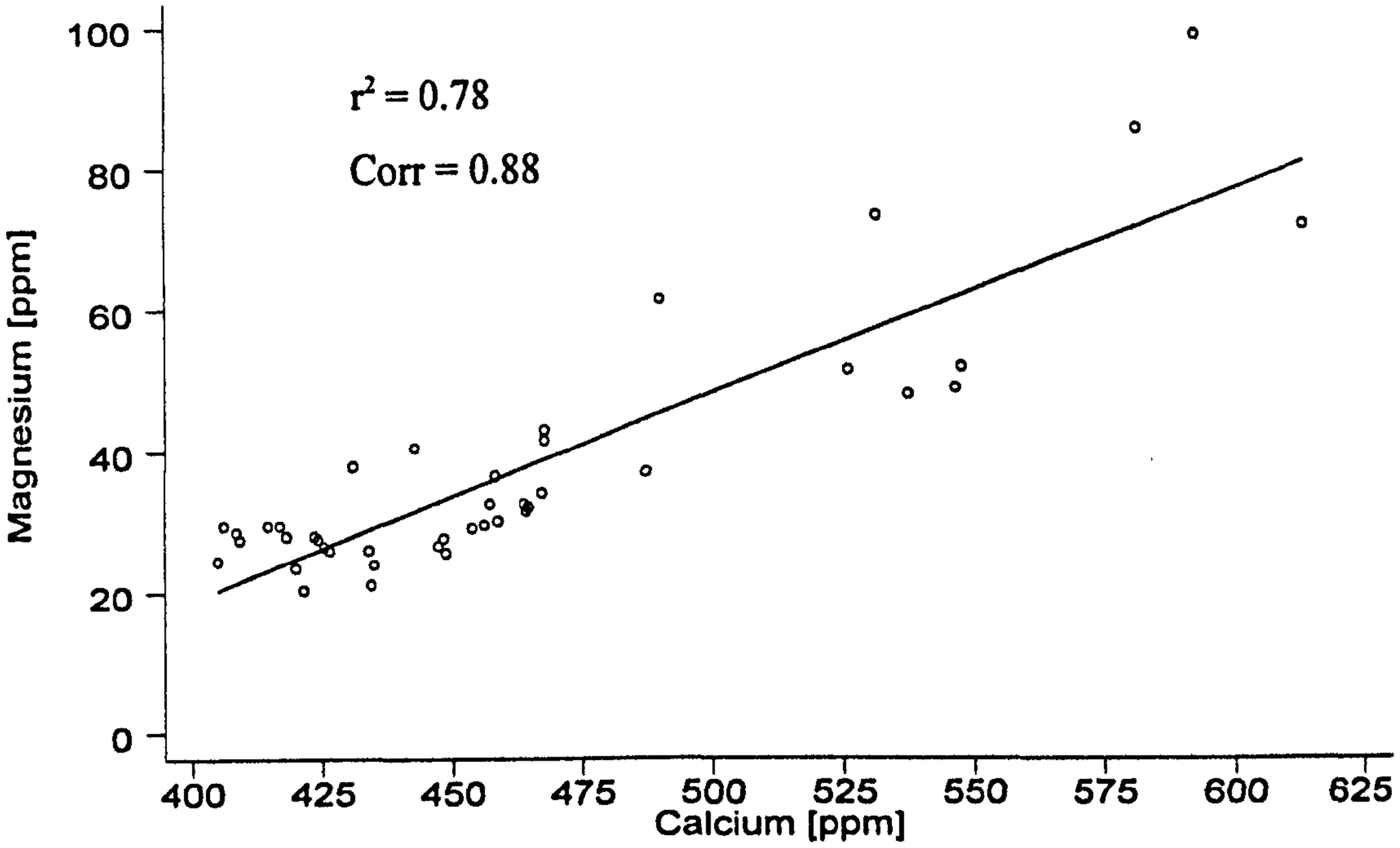

Figure 7.22: Relationship between calcium and magnesium at LF3

It is evident that there is an increase in sodium, calcium and magnesium in the middle of furrows and this leads to a decrease in the percentages of clay and fine silt and a relative increase in the proportion of medium silt. This leads to the following questions. Why is there a special case in the middle of furrows rather than closer to the irrigation water sources? Why is there no evidence of movement of potassium to the surface as there is with the other cations measured? How can the apparent paradox be solved of increasing salinity and sodicity leading to an overall weakening of the crust?

The idea of salinity increasing towards the middle of the furrow is not unusual as there has been plenty of research to show that this does in fact happen. Salinities increase towards the boundaries of the wetting bulb (Hillel, 1971, Bresler *et al.*, 1982). Evaporation is reduced closer to the plants by the layers of black plastic which cover the irrigation pipes. As the wetting front extends laterally there are changes in the evaporative regime of the soil (Gardner & Hillel, 1962). As the surface layers become progressively drier, evaporation becomes more sensitive to the heat flux in the soil (Rose, 1968). In addition, salts become more soluble in the soil

Plate 7.1: Water evaporating at the centre of the furrow

Plate 7.2: Saline deposits and brown sodium staining between irrigation lines

water as its temperature rises and therefore there is an increase in the propensity for water with high electrolyte conductivities to evaporate at the edge of the wetting bulb (Plate 7.1). The wetting bulb acts as a threshold position where the lateral movement stops and upward movement takes place by capillary action (Bresler & Kemper, 1970; Parlange *et al.*, 1993; Rose, 1996). As the water reaches the surface, the water evaporates into the atmosphere, leaving a high quantity of salts in the surface layers of the soil (Plate 7.2).

Potassium salts are the only ones which do not seem to be affected by this lateral movement of irrigation water through the soil. The previous graphs and correlations show that potassium is reasonably stable within the soil profile. Potassium is much less likely to be taken up by water for two reasons. First it has a much higher electronegativity, i.e. the amount of electron density available for binding and bonding is greater than for the other cations. Second, its atomic value is greater than the other cations (K^+ = 1.33 Å compared with Na^+ = 0.97Å, Ca^{2+} = 0.99Å and Mg^{2+} = 0.66Å). A much stronger charge of H^+ ions would be needed to cause dissolution and therefore it remains in the silicate structures of the clays and is less available for cation exchange (Sparks & Huang, 1985).

The third issue concerns the apparent paradox between stability and instability due to the contrasting effects of salinity and sodicity. It is well documented that higher Ec values of water allow soil to flocculate and its tendency to crust is vastly reduced (Shainberg, 1985). However, if the S.A.R. or E.S.P. is increased then the opposite process of dispersion occurs which causes crusts to form more rapidly (Abu-Sharar, 1988). Looking back to Figure 7.18, Figure 7.20 and Figure 7.21 it would seem that, sodium becomes the most mobile, which would lead to higher dispersion rates. This allows the freeing up of the finest fractions of the soil, which then can be entrained by the wind. The structure of the crust is actually weakened rather than strengthened, because there is no mechanical impact (Le Bissonnais, 1990). In the field the darker brown patches represent staining from the sodium salts and their structure is crumbly because the sodium has dispersed most of the clay, which has then been eroded by the wind. Such circumstances allow a relationship to be identified between the medium silt and clay because the former increases relatively as the latter is eroded.

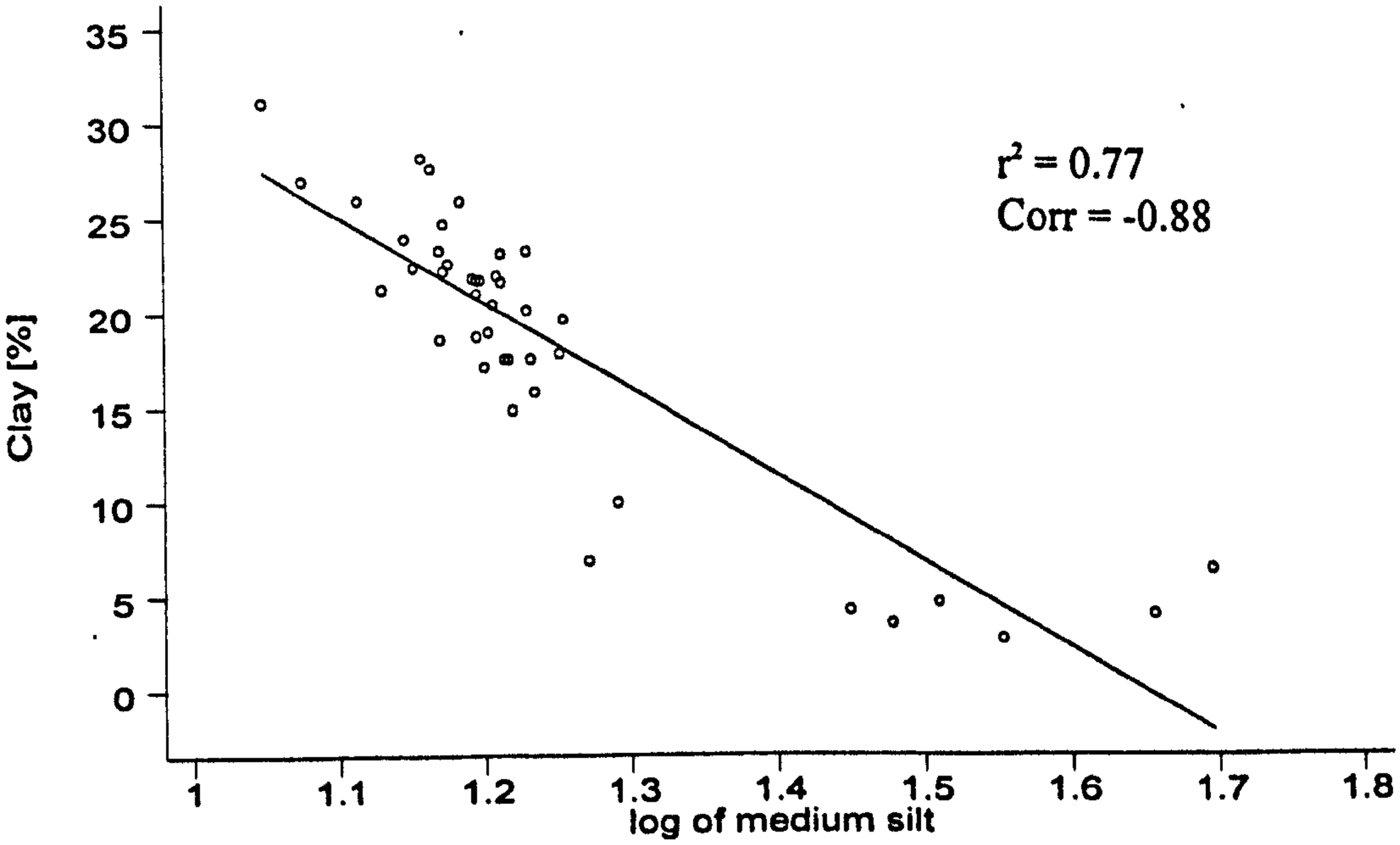

Figure 7.23: Relationship between medium silt and clay in LF3

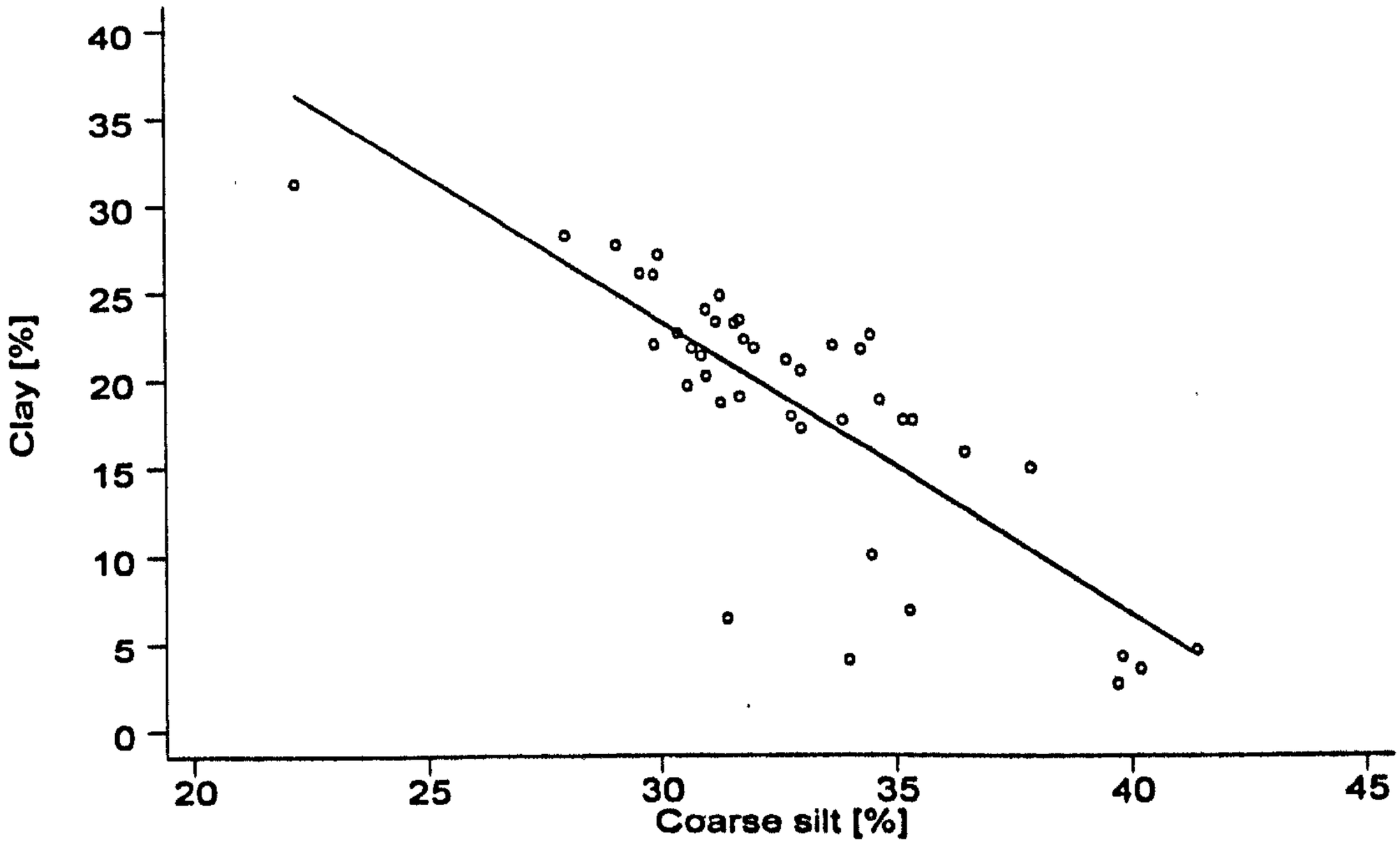

Figure 7.24: Relationship between coarse silt and clay at LF3

7.5 Conclusion

The chapter has sought to explain the different sediment fluxes which occur at different scales within the field. The soil has evolved through a complex interaction between eolian activity, erosion and deposition of local limestone-derived material as well as the weathering-out of the basalt. A combination of X-ray determination and thin section analysis allows an interpretation as to which of theses sources is important. The thin-section data, which are more fully dealt with in Chapter 8, show clearly that there is quartz in the soil which means that it cannot be completely basalt-derived because quartz is not a weathering product of basalt. The X-ray results confirm this showing that the soil contains approximately 45% quartz. In addition the X-ray results also show a considerable incorporation of calcites in the weathering products which may indicate a limestone origin although it is widely acknowledged that calcites build up naturally in desert soils. In general the X-ray results would tend to suggest that it is the eolian processes which now predominate. It has been seen that the crust plays a special role in controlling the magnitude of wind erosion. Crust samples have on average 12 to 20 % lower clay contents and up to 25 % more sand than auger samples. In areas where the crust has formed over a number of years, the clay content is almost one third of the value of soil below. This suggests that the fines are blown from the surface crust leaving the coarser sediment which armours the soil against further soil erosion.

The management of the soil is particularly important, because it influences the type of crust which forms and consequently modifies the infiltration capacity. It is evident that clearing the boulders from the surface and then ploughing the soil has a detrimental effect upon the infiltration of water into the soil. At High Farm this is particularly evident with a final infiltration rate for uncleared land of 47.9 mm h^{-1}, the rate for land which has just been ploughed, of 32.7 mm h^{-1} and the land which has already been cultivated having a final infiltration rate of only 19 mm h^{-1}. At all the sites the newly ploughed land, which has a very thin crust, has the highest initial rates of infiltration. This suggests that infiltration is not solely controlled by the initial state of the crust, but is determined by the established rootways and by the way in which the crust develops during infiltration itself. In terms of management

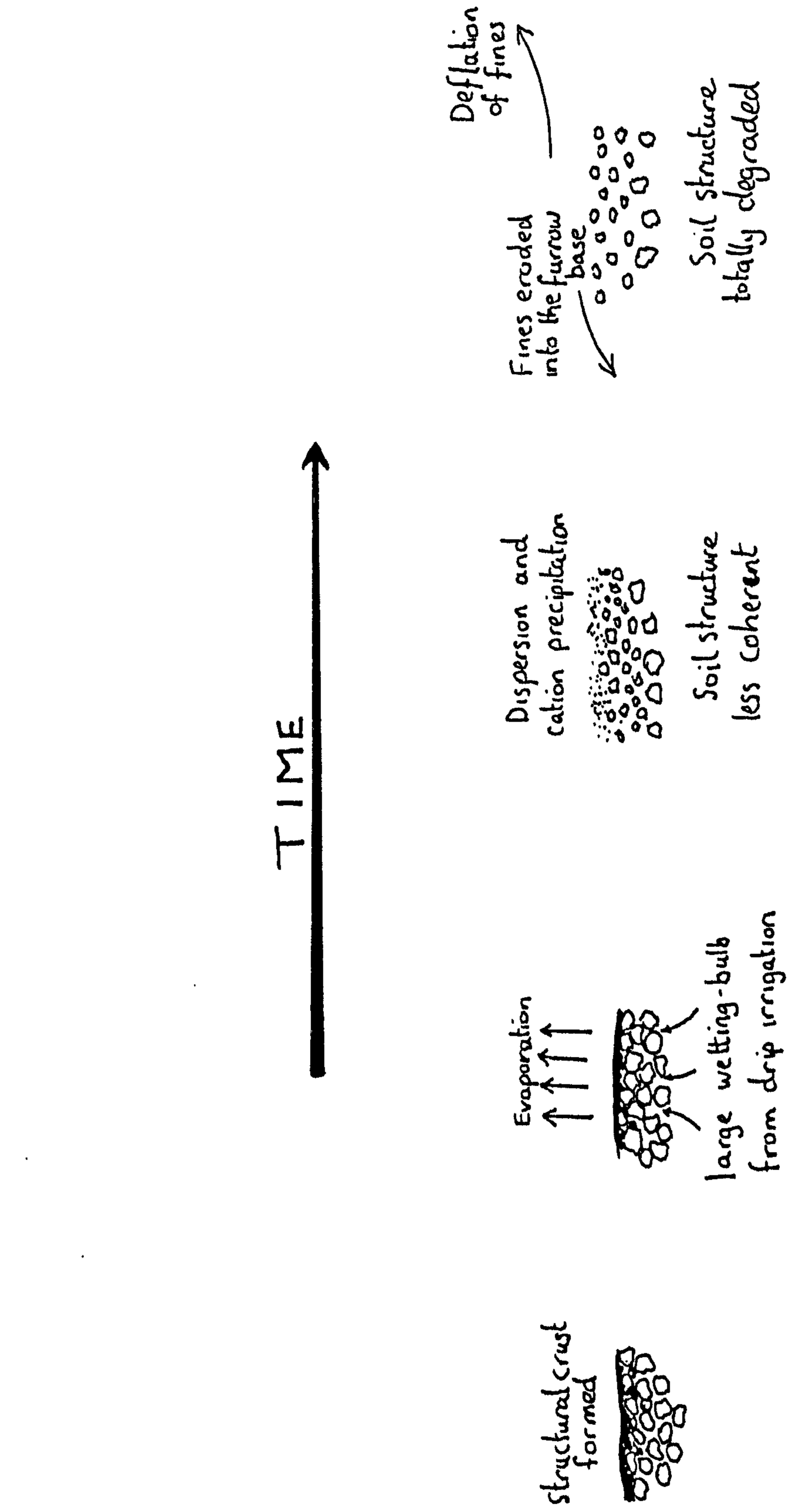

Figure 7.25: A summary of the formation of a sodic evaporation crust

practice the results suggest that the clearing of boulders degrades the surface soil layers and that conventional ploughing reduces the number of hydrological pathways by which water can infiltrate. Reducing the impact of ploughing by using seed drills and machinery which only breaks up the crust in the vicinity of the area of seedling emergence would seem to be a better way forward.

During the preparation of fields for summer irrigation there is considerable change to the soil surface characteristics which lead to the establishing of micro-topographic erosion processes and the evaporation of highly charged water from the subsurface of the soil during irrigation. An important and revealing part of the research is to see the linkages between the wetting bulb extent, evaporation and precipitation of salts on the crust surface and the subsequent modification of the crust's physical components. Previous research has confined the human impact on crusts to compaction and the effect of water chemistry upon infiltration, but here there is clear evidence that there is a complex redistribution of water and dissolution of salts after irrigation which results in a morphological restructuring of the soil crust. The result is a sodic evaporation crust (Figure 7.25), which develops from upward movement of sodic water through the crust causing clay dispersion. Normally, under infiltration conditions such clay dispersion would cause a strengthening of the crust due to pore clogging. In the present situation, however, due to the upward movement of water, clogging cannot take place and instead the clays and fine silts are eroded from the surface of the crust. This is clearly happening at the centre of most ridge-furrow sequences during irrigation and is shown by decreasing fine silt and clay contents and an increase in salts. The clay and fine silt contents commonly decrease from between 30-40% at the edge of the ridge-furrow sequence to below 8% at the centre. This decrease is negatively correlated with a 4x increase in magnesium, a 20% increase in calcium and a tenfold increase in sodium. These are considerations which have not been adequately examined by previous work and this research can thus be considered to be making a fundamental advance in this area.

Chapter 8 will consider these microtopographic changes in soil crust structure, by looking at variations in porosity and micromorphological fabric. The results of the

rainfall simulation experiments in conjunction with a physical tracer will then be examined in order to pursue a greater understanding of how fine material moves during the crust formation process.

8. THE CHARACTERISATION OF SOIL CRUST FORMATION USING IMAGE ANALYSIS AND PHYSICAL TRACING

Morphological descriptions of surface crusts are a useful tool to help explain crust behaviour and to provide direct evidence of processes that have been important to the development of the crust. West *et al.* (1992, p.89)

8.1 INTRODUCTION

The debate over the process of surface seal formation has been the key question arising from all research in this sub-discipline of soil science. From the earliest experiments, notably those of McIntyre (1958a), to the most recent research, such as that of Mermut *et al.* (1995), opinion is divided on whether there is a *washed-in* layer or the formation of the seal only represents a breaking-down and redistribution of the surface aggregates and soil particles. Such key questions in any research discipline, and especially in the earth sciences, can rarely be answered simply. The study of surface seals is no exception. There are many factors which affect the formation and development of surface seals, such as particle size distributions, aggregate stability, climatic and hydrological factors including rainfall characteristics, soil moisture conditions and evaporation fluxes, not to mention anthropogenic factors such as farming practices (Section 2.9). The question of how to characterise the various processes upon the soil surface has always been at the forefront of research (Le Bissonnais, 1990). While several scientists have used either field experiments or a laboratory approach, many have found that the only way to visualise the processes involved has been to use micromorphology.

The research of the preceding chapters has focused upon small-scale changes in the sedimentary compósition of crusts and the way that soil chemistry and micro-topography affect the distribution of fines within the crust structure. Looking at

particle-size distributions alone is not sufficient to examine the degradation of the soil surface, because the analysis inevitably means that the crust structure is destroyed. If, however, it is expected that the crust structure changes in relation to the micro-topographical position or the amount of sodium precipitated at the soil surface, then there should be evidence in the micromorphology of the thin-sections.

The chapter is divided into three parts. Initially an qualitative examination of micromorphological photographs will take place. The colour and fabric of the sections at low magnifications are invaluable for observing the differences between samples. Second, black and white photographs have been taken under UV light to obtain images which determine the pore structure. Using image analysis tools allows a quantitative picture to be constructed of how different manifestations of crust-type actually differ structurally. Third, data will be presented from the rainfall simulation tracer experiments. These involved the examination of thin sections to look at the filtration of a fine-grained hematite tracer (<63 μm) through the surface soil layers during rainfall-induced crust formation.

8.2 THE USE OF MICROMORPHOLOGY AS A TOOL FOR SOIL CRUST EVALUATION

The use of micromorphological analysis is not new in investigations of soil crust formation (Evans & Buol, 1968; Epstein & Grant, 1973; Farres, 1978; Chen *et al.*, 1980; Onofiok & Singer, 1984; Tarchitzky *et al.*, 1984; Valentin & Bresson,1992; Mermut *et al.*, 1995). Although it is possible to see a change in form of the soil surface in terms of a drastic reduction in roughness as a seal develops, it is impossible to see with the naked eye what has happened with respect to movement of particles and the redistribution of pore space. In an arid environment, where aggregate stability is very low, and especially in the eolian silty soils of the northern Jordanian Badia, slaking crusts are most in evidence and the reorganisation and reorientation of the primary silt particles can only be seen using such a technique.

Micromorphologists have spent the last twenty-five years seeking ways to quantify their results other than simple point counting. Since the introduction of Quantimet in

the early 1970s, image analyses of soil pores and aggregates have been the main areas of investigation (Jongerius *et al.*, 1972; Ismail, 1975; Murphy *et al.*, 1977a,b). More recently several image analysis techniques have been combined to provide more powerful quantitative methods at looking at the mineralogy and microfabric of the soil (Tovey *et al.*, 1992). In addition, as techniques from remote sensing have been adopted, other features can also be observed, such as different classes of matrix optical anisotropy (Terribile & FitzPatrick, 1995). The scale of the images which can be handled has increased greatly from a few cm^2 to several dm^2 (Grevers & de Jong, 1992). Instead of image analysis taking place on a single image, several arrays of the same image can be overlaid and displayed as an RGB colour composite image (Protz *et al.*, 1992; Terribile & FitzPatrick, 1992). In other words, if three photographs are taken, one under plain polarised light (PPL), one under circular polarised light (CPL) and a third under incident ultra-violet light (IUV), they can be combined to create a false colour composite which is essentially a three-dimensional image: each image or band gives a certain amount of information, but combined they allow the interpreter to observe and classify the image to a much larger extent.

At present, computerised image analysis of soil fabric is the only reliable method for investigating the size, shape, orientation, distribution, frequency, shape of the walls and morphology of pores (Bui *et al.*,1989; Mermut *et al.*,1992). Various techniques have been used on thin sections and polished blocks to enhance the contrast between particles and pore space to allow accurate image analysis to take place. The standard technique is to use an ultra-violet dye which fluoresces under a UV light source allowing the pore space to appear as white while the fabric remains isotropic (Geyger & Beckmann, 1967). However, the polyester resins which are commonly used for the impregnation of samples are often somewhat fluorescent (Altemüller & van Vliet-lanoe, 1990). This is unavoidable in most cases because, even though other resins are less fluorescent, they have poorer overall refractive properties. It is also the case that certain minerals, depending on orientation, do have fluorescent properties (e.g. phosphates and carbonates) and this can give an over-estimate of pore size (Altemüller & van Vliet-lanoe, 1990). Unlike thin sections, polished blocks require the use of epifluorescence microscopy whereby a high intensity UV source is

used as an excitation source to produce fluorescence of a longer wavelength. It must be remembered, however, whether looking at pore space distribution in thin section or using polished blocks, it is likely that there will be some under-estimation of total pore space and an over-estimation of clay, because the resolution is not good enough using optical microscopy and the medium of study is three-dimensional (25-30 μm for a thin-section) and yet it is being classified as though it were only two-dimensional (Murphy & Kemp, 1984).

The established method for measuring pore size by image analysis is the pore-chord intersection technique (Jongerius *et al.*, 1972; Ismail, 1975; Murphy *et al.*, 1977a,b; Bui *et al.*, 1989). This method systematically or randomly scans the pores using a set of horizontal transects of an image and then measures the chord lengths (the length from one side of the pore to the other along the transect), plotting them as frequency distributions. More recently this approach has been modified because measurements in one dimension are not an accurate representation of the pore size in three dimensions Unless the shortest chord length for any one pore is measured, it is impossible to extrapolate meaningful soil moisture retention data (Bui *et al.*, 1989). A technique using a multi-directional minimum chord algorithm, although still estimating in two dimensions rather than three, has been developed which will measure up to 16 directions across the pore in order to find the minimum chord length (Bouabid *et al.*, 1992). As software has advanced, so has the ability to measure more and more mineralogical and porosity parameters. The research recorded here used a variety of image processing software packages: TERRAMAR, PHOTOSHOP and GLOBAL LAB IMAGE. The last of these classifies particles primarily according to their grey level, but will weight certain particles depending on specific size and shape criterion of interest to the interpreter. Once the software has identified the particles in any particular class, it will calculate over 50 different particle attributes (see Appendix 3) using the number of pixels which make up the particle in question (Terribile & FitzPatrick, 1995, p. 41).

Company	Software	Main Application	Morphology	Multivariate segmentation	Geometric correction (warp)	3D
Ai Cambridge LTD	Perception	Opt. Micr.	*	NO	NO	NO
AMS	Optomax V	Opt. Micr.	**	NO	NO	NO
Bioscan	Optimas	Opt. Micr.	**	NO	NO	NO
Buehler	Omnimet 1	Opt. Micr.	*	NO	NO	NO
Data Translation	Global Lab Image	Opt. Micr.	**	NO	NO	NO
Digithurst	Microscale	Opt. Micr.	*	NO	NO	NO
Foster-Finday	C-images	Opt. Micr.	**	NO	NO	NO
Foster-Finday	PC-image	Opt. Micr.	*	NO	NO	NO
Kontron-Zeiss	Videoplan (manual)	Opt. Micr.	**	NO	NO	NO
Kontron-Zeiss	Vidas	Opt. Micr.	**	NO	NO	NO
Kontron-Zeiss	Ibas	Opt. Micr.	**	NO	NO	YES
Leica	Quantimet 500	Opt. Micr.	***	NO	NO	NO
Leica	Quantimet 570	Opt. Micr.	***	NO	NO	NO
Media Cybernetics	HAIL	Opt. Micr.	**	NO	NO	NO
Noesis	Visilog	Opt. Micr.	***	NO	NO	NO
Olympus	Cue 4	Opt. Micr.	***	NO	NO	YES
Quantel	Crystal	Opt. Micr.	**	NO	NO	NO
Seescan imaging	Solitaire plus	Opt. Micr.	**	NO	NO	NO
Synoptics	Semper6p	General purpose	***	YES	YES	NO

Table 8.1: Comparison between image analysis software packages.
Adapted from Terribile, pers. comm. (Opt. Micr. = Optical microscopy)

The most recent techniques to quantify 3-dimensional pore space have used consecutive slices of a polished block 40 μm thick, which have then been photographed digitally and interpreted using image analysis software (Vögel, 1997).

Although such a technique is in its infancy and various problems have arisen, such as geometric correction between photographs, it has a much greater potential for accurately describing pore shape, size and connectivity.

8.3 INITIAL OBSERVATIONS FROM THE THIN SECTIONS

Before quantitative analyses of soil fabric and pore space can be considered, it is important to look at the photographic images in order to understand the morphological change of the crust at different locations so that the processes can be explained. The terms of classification are generally taken from Bullock *et al.* (1985) or FitzPatrick (1993). The most important terms, which will be used in the following analyses, are vughs and vesicles. These refer to relatively large unconnected voids, the former defining irregular, elongated voids, while the latter defines voids with a smooth and near-spherical morphology (Bullock *et al.*, 1985).

Site	Ridge under plastic	Outer furrow flank	Furrow base	Inner/ central furrow flank	Central ridge
LF3-1	D & E	C	B	A	
LF3-2	A	B & F	C & E		D
LF3-3	A		B & D		C
LF3-4	A		C & E		

Table 8.2: The microtopographic position of the sample points at each site

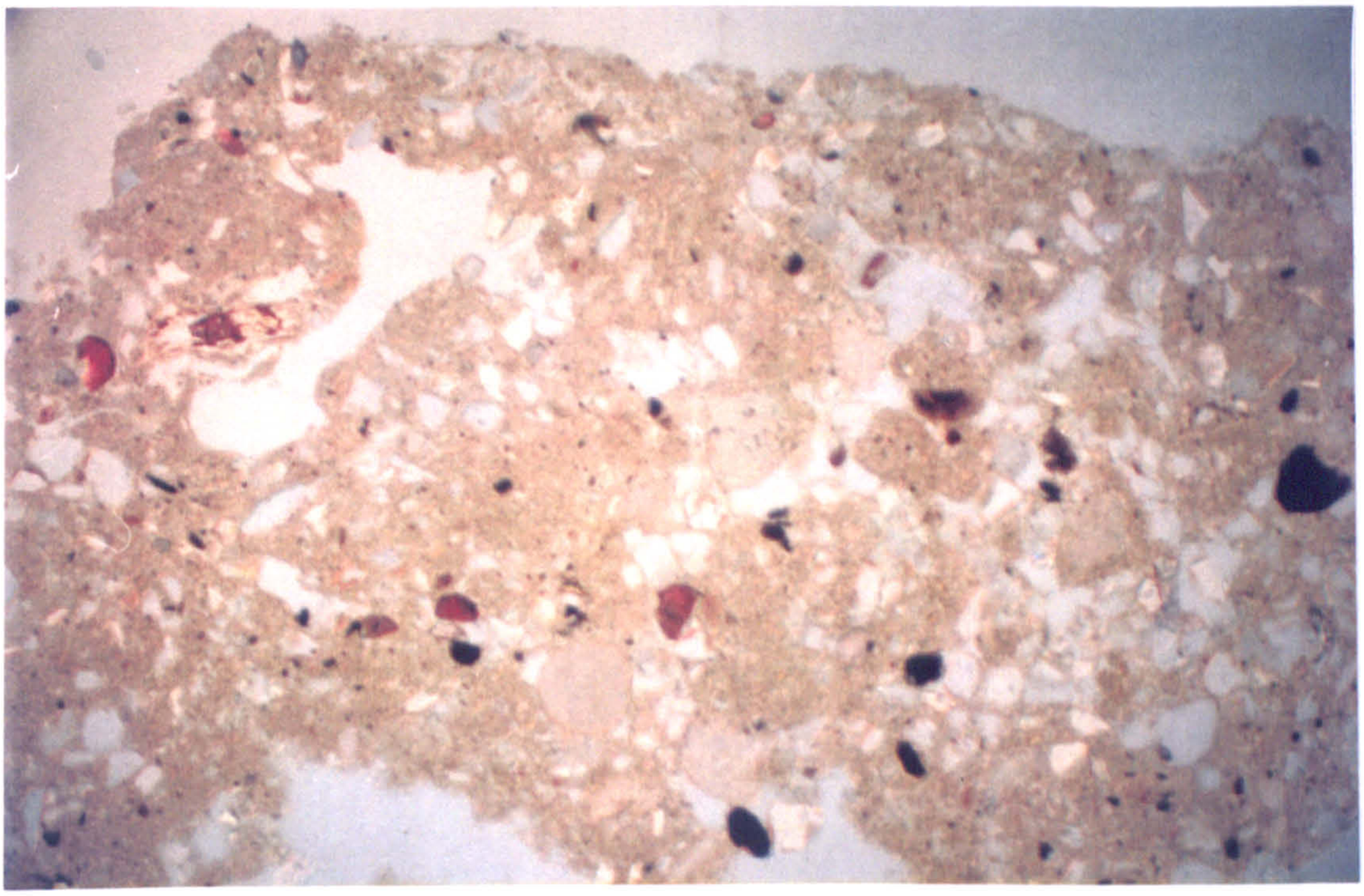

Plate 8.1a: Microphotograph of the side ridges (2A)

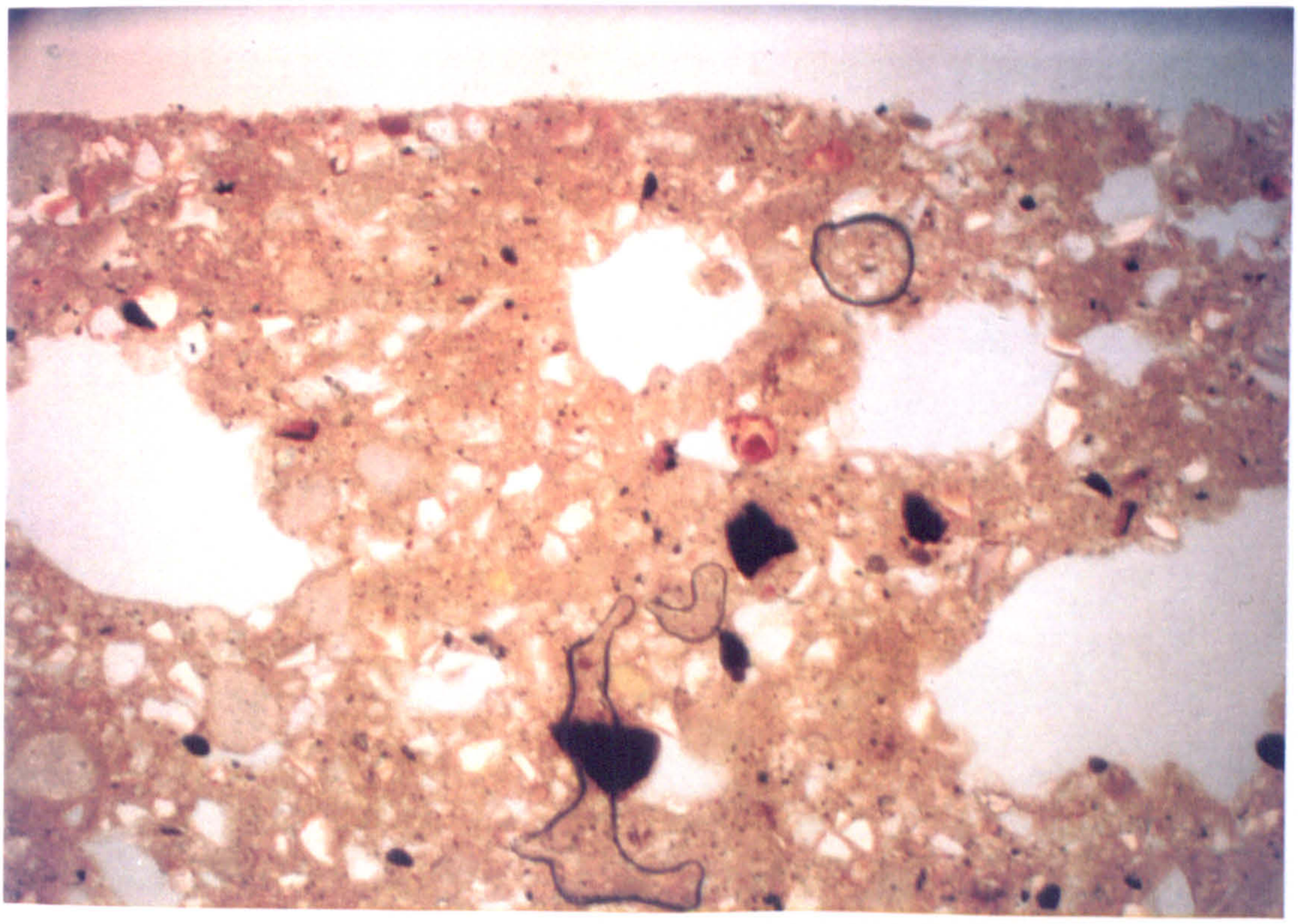

Plate 8.1b: Microphotograph of the side ridges (3A)

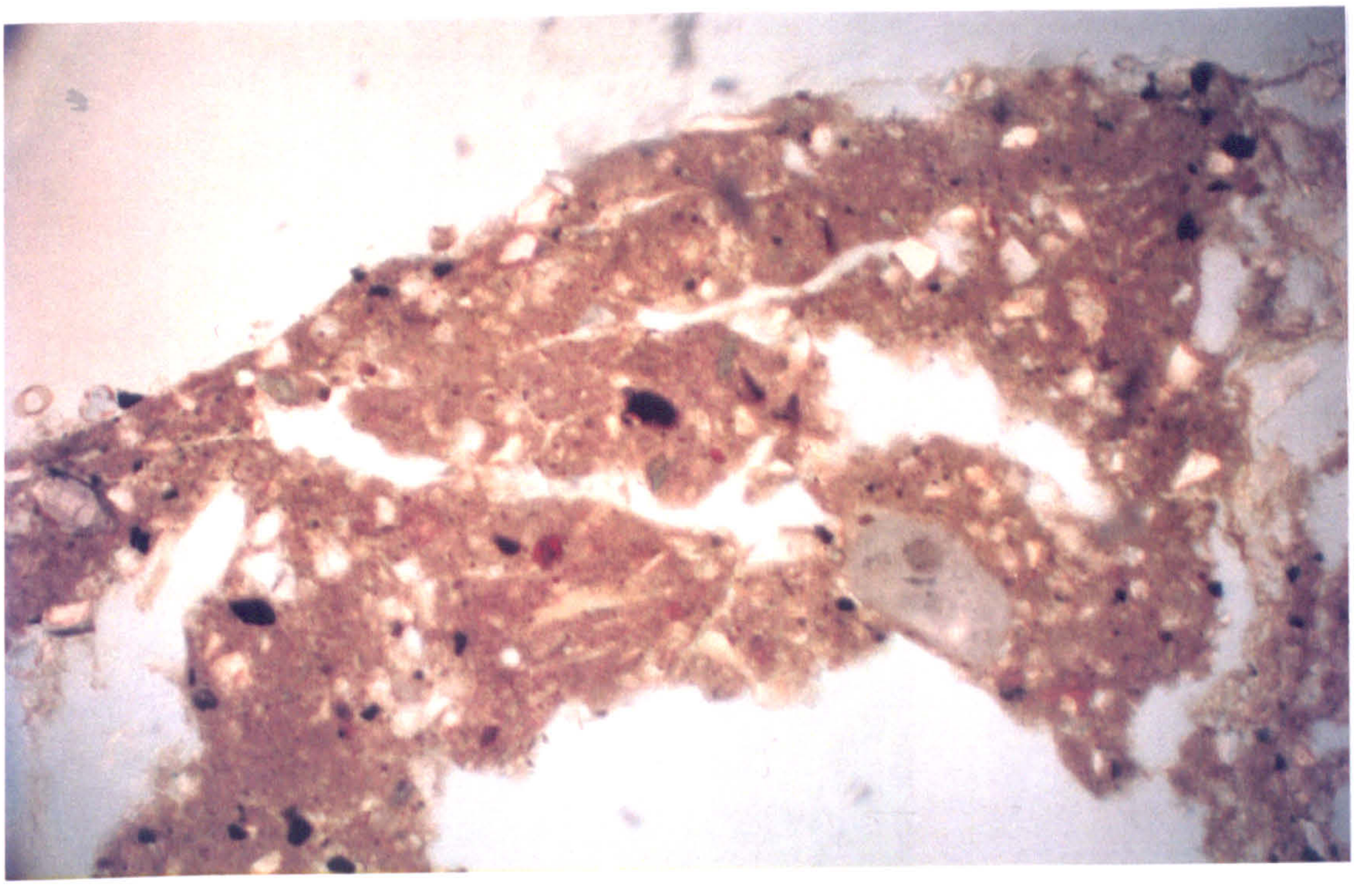

Plate 8.2a: Microphotograph of the furrow flank (2B)

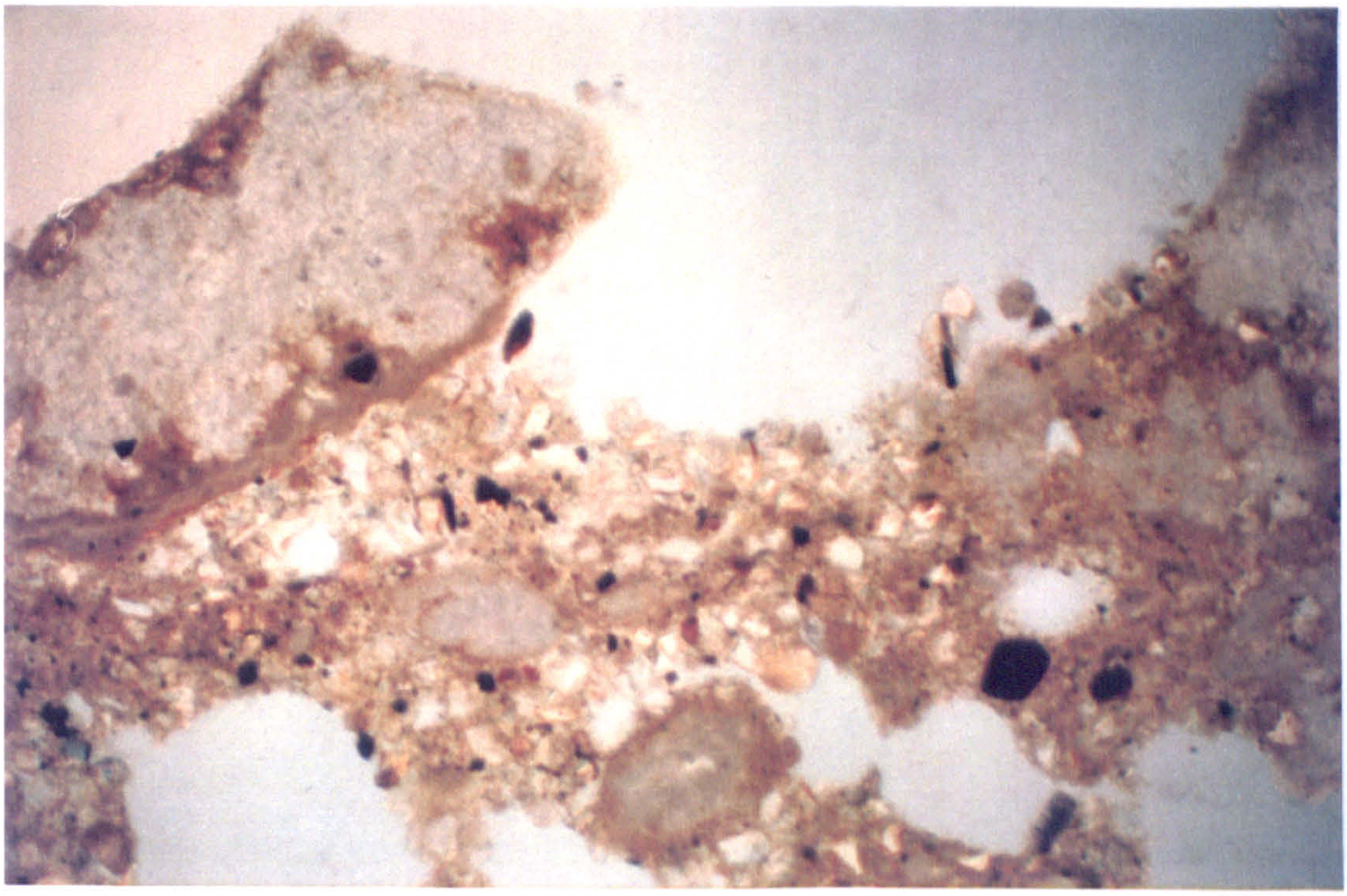

Plate 8.2b: Microphotograph of the furrow flank (2F)

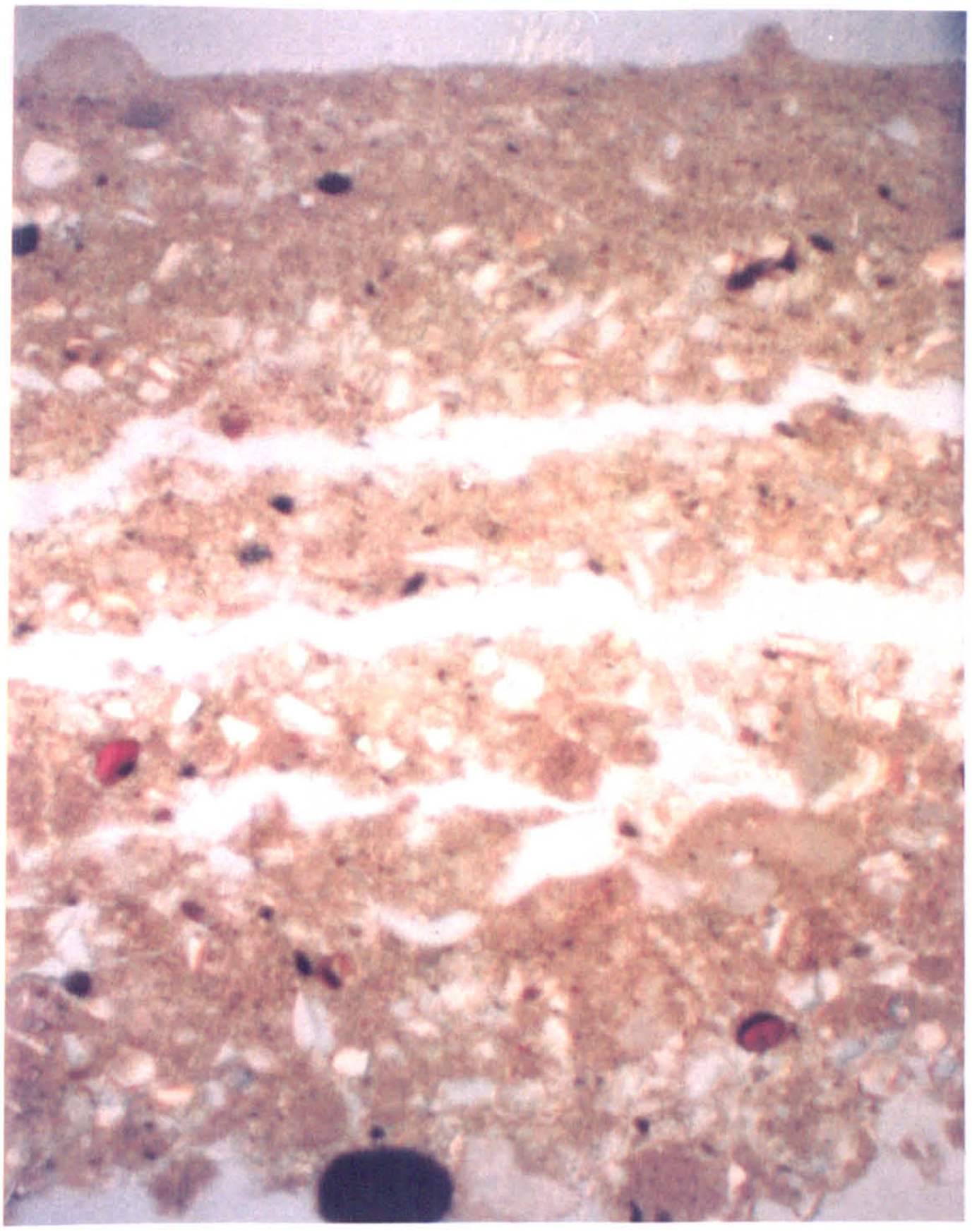

Plate 8.3a: Microphotograph of the furrow base (2C)

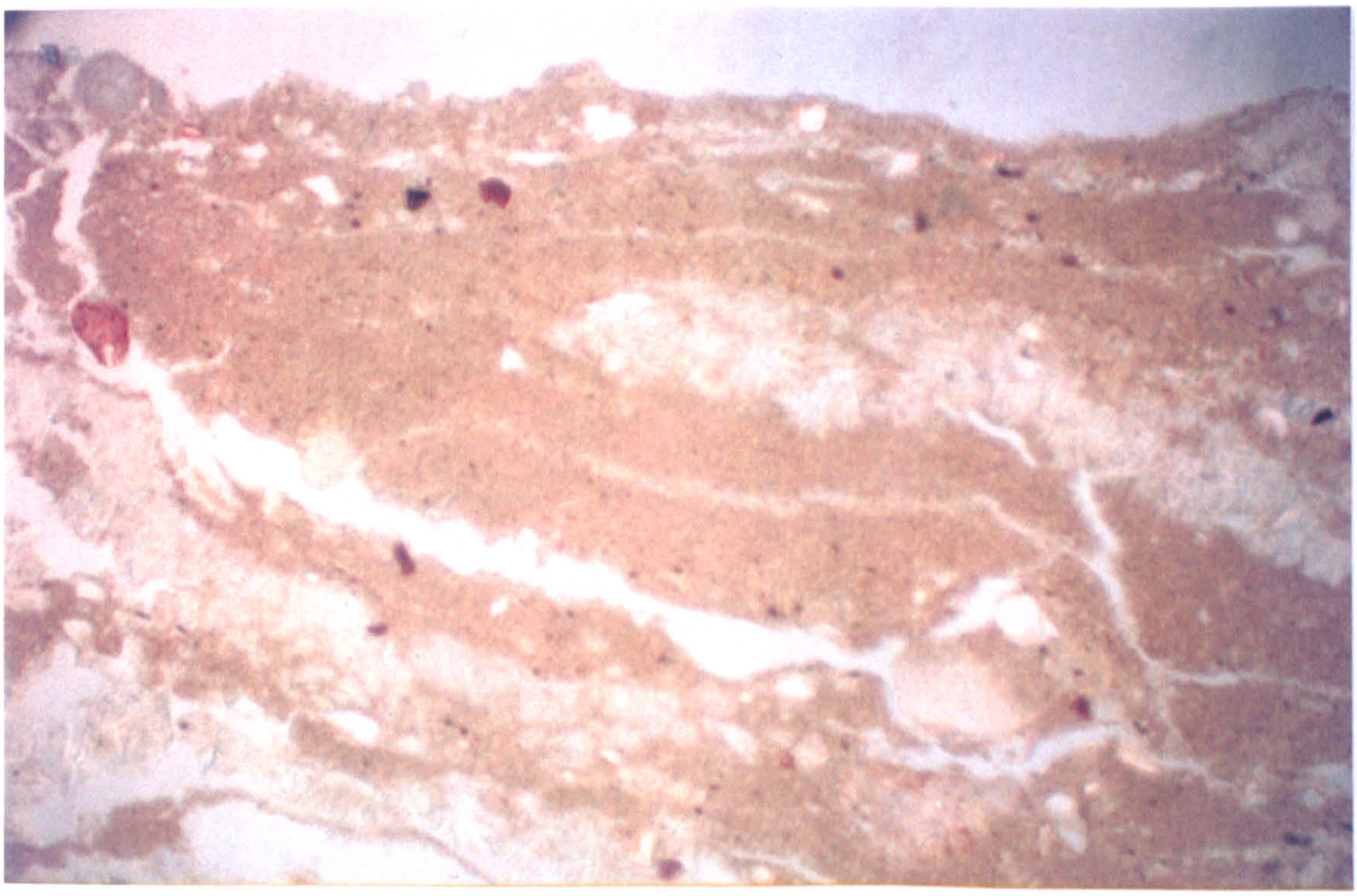

Plate 8.3b: Microphotograph of the furrow base (3B)

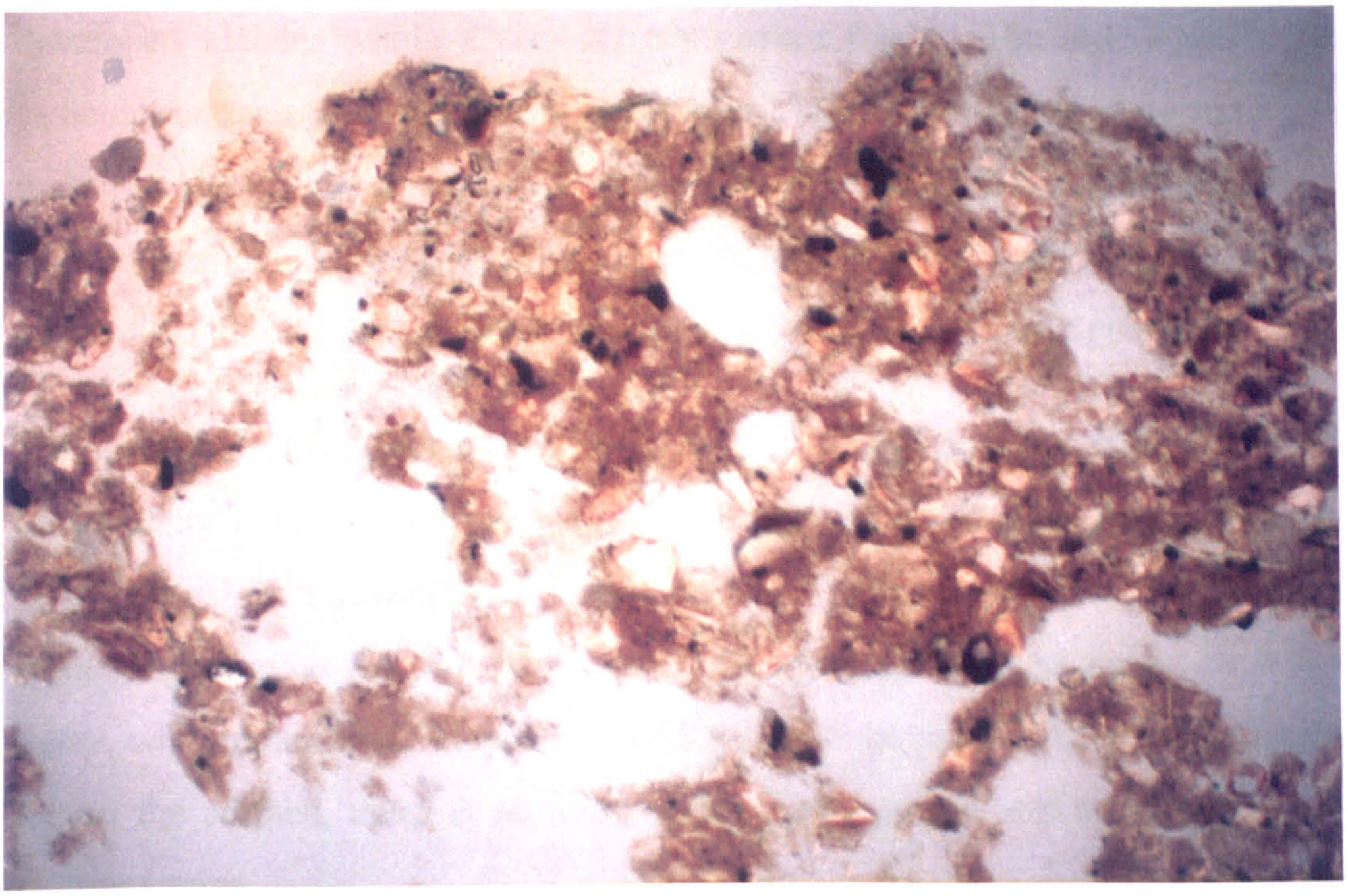

Plate 8.4a: Microphotograph of the central ridge (2D)

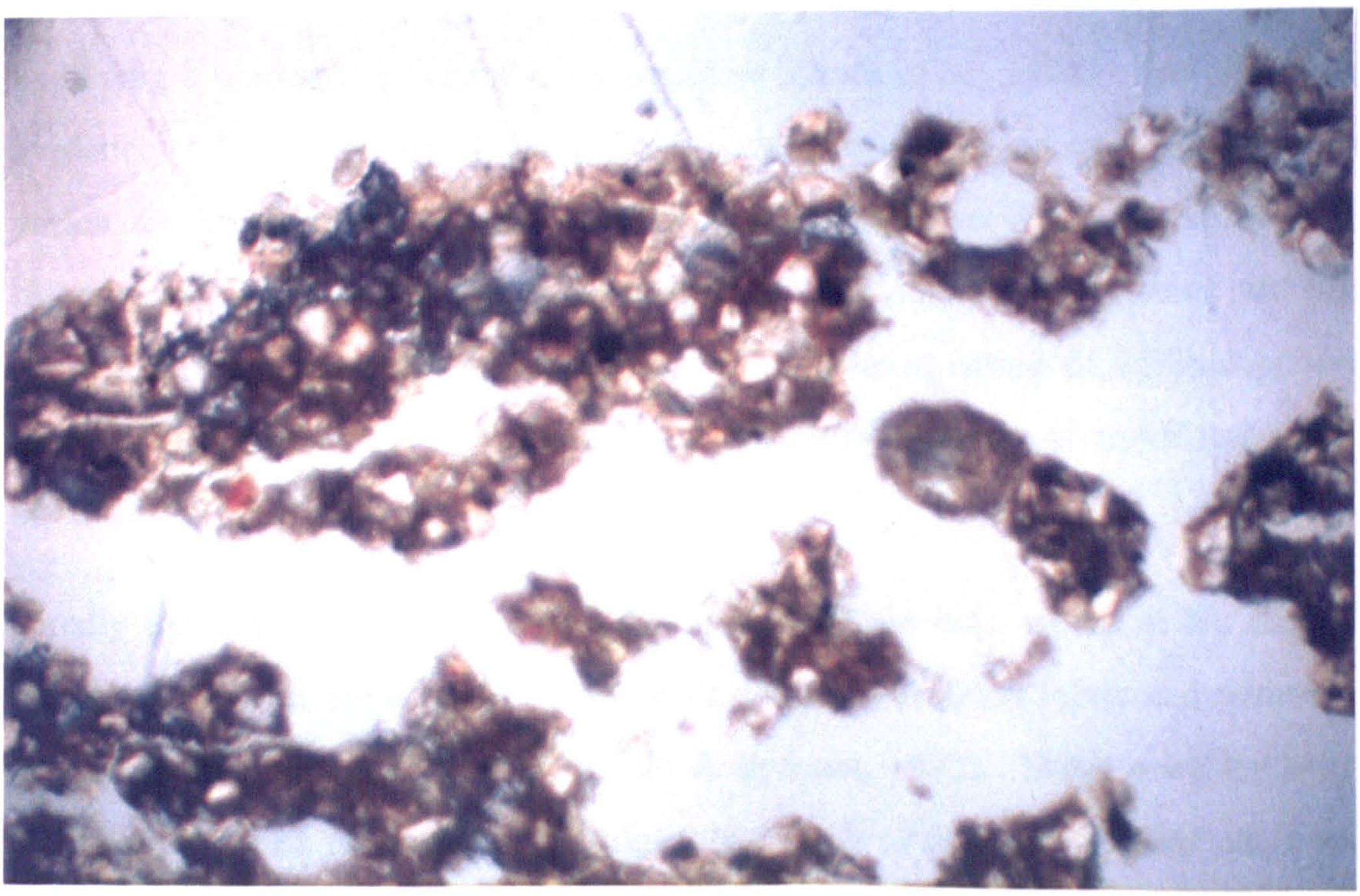

Plate 8.4b: Microphotograph of the central ridge (3C)

Plate 8.1 to Plate 8.4 show photographs which were taken at low magnification (x40) at different locations on the ridge - furrow sequence (Table 8.2). Taking sample 2A and 3A, which are the two ridge samples, it can be seen that there are some well-developed vesicles within a very densely packed fabric. The soil is poorly sorted vesicular and contains no discrete aggregates. There is no obvious connectivity and there is a layer at the surface which has no pores. The surface is dominated by very fine material, while sand-sized mineral grains tend to concentrate randomly in certain parts of the thin section, although often accumulating round the edges of vesicles.

The examples from a furrow flank, 2B and 2F (Plate 8.2), show a higher degree of connectivity with a porosity which is more vughy than vesicular. Again the fabric is poorly sorted with a weakly developed pedal structure. The surface is not developed in the same way as the ridge with some area where the seal has almost been eroded away, while other areas show some evidence of deposition. Where rock fragments lie on the surface, there is scouring of the fine material and a deposition of the coarser grains.

The furrow base sections show a very distinct type of crust formation (Plate 8.3) with a fabric which is correspondingly different. The fabric, especially in 3B, is almost entirely fine-grained and dense except for a few planar voids, and it can be classified as having a moderate to strong platy structure (Drees *et al.*, 1994). Sample 2C has evidence of several pulses of depositional activity characterised by a set of laminae which are coarse at their base and fine on their upper surface. The crust is the thickest of all the crusts under consideration. The difference between the fine-grained depositional crust of 3B and the rather coarser nature of 2C is dependent upon the type of runoff flow, with the latter being a result of more turbid flow conditions.

Finally the central ridge sections at 2D and 3C (Plate 8.4), which in the previous chapter have been named sodic crusts, have a much less dense fabric and resemble a typical slaking structural crust (Valentin & Bresson, 1992). There is evidence of a vesicular structure as on the other ridges, but much of the fine silts and clays have gone leaving a large percentage of coarser-grained material at the surface. The voids

which are not vesicles tend to be large and nondescript with a high level of connectivity.

At one level, such qualitative description is not new (Evans & Buol, 1968). However, the soil crust literature has tended to take each type of crust form and assign it a different process, rather than see that there is an inter-relationship between the position within the ridge-furrow sequence and the crust form. Past research has tended to look at crusts formed in totally different environments (Casenave & Valentin, 1992; Le Bissonnais & Singer, 1993; Valentin, 1994; Mermut *et al.*, 1995) rather than concentrating on a geomorphological approach, which seeks to look at soil crusts in the context of erosion and deposition (Bielders *et al.*, 1996). The following section will build upon the qualitative information and lead to a discussion of how the micromorphology gives an accurate picture of the process history.

8.4 THE CONNECTION BETWEEN PORE ATTRIBUTES AND SOIL DEGRADATION

The movement of water, gas and solutes through soil is controlled by its structure (Bouma & Kooistra, 1987; Vögel, 1997). The characterisation of the geometric properties of different soil crust micromorphologies can show how specific crust types and the amount of crust development affect the pathways for such movement and therefore can help in classifying the extent of degradation.

In order to gain a high-resolution image of the pore structure in a thin section, photographs have to be taken under UV light. The UV dye, which is embedded in the resin during the impregnation process, fluoresces while the soil fabric remains dark. Therefore if the UV light is allowed to shine through the section before being filtered-out and then goes up through the microscope to the camera, the resulting image will be a black and white representation of the fabric and pore space respectively. Special Kodak Tmax film is used to obtain the greatest contrast, and subjected to a maximum contrast developer. The final photographic image is then scanned and saved in a TIFF format in PHOTOSHOP. This software allowed further contrast to be obtained, because the smaller grey levels become indistinct after

scanning, and this was done by comparing the screen image with the thin section under the microscope.

The Global Lab Image software calculates pore indices (Appendix 3) based upon either upon the number of pixels or that of calibrated units. It bases its classification entirely upon grey-levels. Therefore, by specifying a certain grey-level threshold, the program will count all the particles which have values below that threshold.

There are some problems when defining the edge of a pore. There is not a sudden change from a high grey-level to a low one. Instead there is often a gradual change through some intermediate values. There is an in-built third dimension to the thin-section which is due to the fact that there is some change in the shape of the pore over a thickness of 30 μm. The amount of error is small and can usually be reduced further by the contrast features in PHOTOSHOP.

Each thin-section image can be classified and data extracted. Mean data for the whole section were produced (Table 8.3) and can be used to obtain measures of connectivity and total pore area in the section. Table 8.3 shows the mean values, but minimum and maximum values are also produced along with a measure for standard deviation. All the statistics presented have been calibrated to a millimetre scale. In all the images, except one, the calibration factor is 1 pixel:0.0071 mm x 0.0071 mm or in other words a single pixel approximates to about 50 μm^2.

8.4.1 Pore shape and the formation of vesicles and vughs

In addition to mean values for each section, Global Lab Image produces data for each pore, which allows characteristics such as the sphericity and orientation of pores to be calculated. The software is able to identify particles larger than 5 pixels in size. However, because the images have been scanned-in from photographs, there is a limited resolution, which means that the smallest pores tend to approximate spheres.

Table 8.3: Mean values for certain pore attributes measured by Global Lab Image (terms defined in Appendix 3)

Sample	LF3-1A	LF3-1B	LF3-1C	LF3-1D	LF3-1E	LF3-2A	LF3-2B	LF3-2C	LF3-2D	LF3-2E	LF3-2F
No. of particles	257	333	438	223	238	161	303	180	94	246	298
Angle (°)	-33.80	-43.42	-48.72	-59.03	-53.14	-34.33	-43.02	-44.57	-32.04	-39.95	-55.00
Area (mm^2)	0.02	0.03	0.02	0.01	0.04	0.13	0.03	0.07	0.11	0.04	0.02
Average radius (µm)	80.0	100.0	80.0	60.0	90.0	140.0	90.0	150.0	110.0	120.0	80.0
Axis Ratio	0.53	550.0	0.54	0.54	0.60	0.65	0.56	0.41	0.60	0.48	0.55
Centroid X (µm)	-720.0	-3400.0	-390.0	-140.0	10.0	0.00	-480.0	-300.0	1110.0	-500.0	-750.0
Centroid Y (µm)	-264.0	-3450.0	-3120.0	-4060.0	-3360.0	-3190.0	-1610.0	-3070.0	-2140.0	-4360.0	-3070.0
Minor axis (µm)	90.0	130.0	100.0	70.0	120.0	250.0	110.0	90.0	130.0	110.0	100.0
No. of holes	30.0	10.0	0.04	0.00	0.00	0.01	0.02	0.03	0.99	0.00	0.01
Perimeter (µm)	680.0	780.0	660.0	410.0	700.0	1160.0	660.0	1400.0	940.0	930.0	620.0
Roundness	630.0	590.0	0.57	0.64	0.68	0.69	0.63	0.49	0.59	0.58	0.62
Major axis (µm)	210.0	250.0	200.0	150.0	230.0	360.0	220.0	440.0	260.0	310.0	200.0
Hole Ratio	0.00	0.00	0.00	0.00	0.00	0.00	0.00	0.00	0.00	0.00	0.00
Maximum radius (µm)	130.0	150.0	130.0	90.0	140.0	220.0	130.0	270.0	170.0	200.0	130.0
Min radius (µm)	20.0	30.0	20.0	20.0	40.0	60.0	30.0	20.0	30.0	30.0	20.0

Sample	LF3-3A	LF3-3B	LF3-3C	LF3-3D	LF3-4A	LF3-4C	LF3-4E
No. of particles	219	162	186	278	86	239	197
Angle (°)	-45.20	-9.56	-49.13	-46.01	-37.63	-58.72	-44.29
Area (mm^2)	0.05	0.21	0.17	0.05	0.06	0.05	0.06
Average radius (µm)	110.0	150.0	130.0	110.0	130.0	80.0	150.0
Axis Ratio	0.54	0.46	0.54	0.54	0.61	0.59	0.48
Centroid X (µm)	-350.0	610.0	-810.0	-560.0	-850.0	-520.0	-390.0
Centroid Y (µm)	-3770.0	-1300.0	-3840.0	-4010.0	-3240.0	-3750.0	-3630.0
Minor axis (µm)	130.0	140.0	180.0	120.0	190.0	100.0	130.0
No. of holes	0.01	0.93	0.85	0.02	0.00	0.01	0.15
Perimeter (µm)	790.0	1710.0	1470.0	1040.0	970.0	770.0	1660.0
Roundness	0.65	0.55	0.61	0.61	0.64	0.70	0.53
Major axis (µm)	280.0	400.0	320.0	290.0	320.0	210.0	390.0
Hole Ratio	0.00	0.00	0.00	0.00	0.00	0.00	0.01
Maximum radius (µm)	170.0	260.0	210.0	190.0	200.0	140.0	250.0
Minimum radius (µm)	40.0	30.0	30.0	20.0	50.0	30.0	30.0

If they were included in the data analysis they would artificially raise the roundness values. Therefore all the single pore analysis was carried out on particles greater than 150 pixels. In addition, only the upper parts of the images were used for the single pore analysis (Sub-sample) in order to concentrate on the crust rather than the sub-soil (Table 8.4). It is clear on many images that at a certain point there was a discernible change in the porosity, either as a result of a structural threshold between crust and sub-soil, or because the base of the crust had been disturbed during transportation. Only in the cases of LF3-2C and LF3-3C was the whole image taken due to the interconnectivity of the pore system.

Site	Image dimensions Width (pixels)	Height (pixels)	Sub-sample (pixels)	Sub-Sample (mm)	No. of particles
LF3-1A	937	1270	700	5.0	102
LF3-1B	970	1256	456	3.2	58
LF3-1C	970	1256	516	3.6	117
LF3-1D	970	1256	700	5.0	43
LF3-1E	970	1256	604	4.3	74
LF3-2A	970	1256	700	5.0	65
LF3-2B	970	1256	616	4.4	167
LF3-2C	970	1256	1255	8.9	107
LF3-2D	1256	970	512	2.7	65
LF3-2E	970	1256	679	4.8	33
LF3-2F	900	1256	406	2.9	73
LF3-3A	970	1256	728	5.2	63
LF3-3B	1251	905	550	3.9	82
LF3-3C	900	1256	1251	8.9	129
LF3-3D	905	1251	700	5.0	76
LF3-4A	900	1256	660	4.7	42
LF3-4C	900	1256	730	5.2	68
LF3-4E	900	1256	730	5.2	59

Table 8.4: Image attributes for single pore analysis

The roundness coefficient is a value calculating how closely the pore resembles a circle and is calculated by 4π x Area/Perimeter^2. The values fall between 0 and 1, with a pore of circular cross-section scoring 1 and an elongated crack scoring near 0.

Dotplots clearly show the frequency distribution of pore shape between sites on the ridge - furrow sequence. Circular graphs displaying the orientation of pores within a section are calculated by taking the major axis of the pore and relating it to 0° which represents the top of the section. Sequences of orientation plots are provided to indicate whether there is prefered orientation of the pores which is often difficult to visualise.

Figure 8.1 to Figure 8.7 show comparative changes in pore roundness within the ridge and furrow sequence. In Figure 8.1 it can be seen that 1A has a bimodal distribution: the majority of pores are quite well rounded but a considerable number are angular. 1B has a generally well rounded set of pores and from Plate 8.5 it can be seen that a number of vesicles have formed directly below the seal. 1C is dominated by angular-shaped pores and from Plate 8.5 it can seen that there is a considerable amount of connectivity. The near-surface pores would be better described as vughs, due to low roundness values, rather than vesicles and are probably not formed by the sudden entrapment of air which occurs to form the vesicles. 1D is almost devoid of pores and from Figure 8.1 it can be seen that, although there are few angular pores, there is not a high frequency of well-rounded pores either. 1E has a large number of vesicles to a depth of 3-4 mm which are evident from Figure 8.1 and Plate 8.5. The majority of the pores are not connected and have been formed as a result of raindrop impact.

Sequence LF3-2 shows the greatest variability between crust types and correspondingly has a great variation in roundness coefficients (Figure 8.3 and Figure 8.4). 2C and 2E are strongly influenced by being in the base of the topographic sequence. They show a large amount of deposition which is evident in the very strong pore orientation and low roundness values. 2A is dominated by some very large near-surface vesicles, the largest measuring over 4.5 mm^2. Between 2A and 2C, there is the furrow flank which has a large number of small vughs which are not connected but their greater angularity implies that they are probably not caused primarily by raindrop impact (Figure 8.4 and Plate 8.6). Sample 2D, which is dominated by a high salt content, has a mixture of vesicles and vughs, but also has a higher amount of connectivity, which gives the impression of a less stable structure.

2F has a large variability in roundness with a few small vesicles, but rather more vughs which tend to be slightly oriented around the horizontal.

Looking at sample 3A, there is an obvious similarity to its predecessor 2A: it has several large vesicles, although unlike 2A it has a better developed set of connecting channels which link several of the large voids (Plate 8.7). Samples 3B and 3D have clearly defined depositional structures resulting in long, thin and well-oriented pores, although there are some smaller, more rounded pores (Figure 8.5 and Figure 8.6). 3C has similar characteristics to 2D with a very loose structure and a large variety of pore shapes and orientations.

The three samples from site LF3-4 are taken from the ridge nearest the irrigation lateral and the two furrow bases. 4A is a prime example of a skin layer of between 0.2 and 0.4 mm in thickness with well developed vesicles beneath. Both 4C and 4E show two horizons with a very clear deposition layer which has formed above the structural crust beneath. 4E has an especially well formed laminar structure which accounts for its low roundness and high pore orientation.

8.4.2 The characterisation of surface crusts using pore attributes

It has been recognised that tillage practice has a profound effect upon soil structure and porosity (Kooistra, 1987; Norton & Schroeder, 1987; Mermut *et al.*, 1992) and that soil management affects the resulting type of soil crust (Pagliai, 1987). The preceding analysis together with the photographic evidence leads to various fundamental implications for the study of surface crusting. The vertical development of crusts is highly variable over small spatial scales. Often this is because one crust has been overlain by another, especially in the case of depositional crusts forming above structural crusts (Boiffin & Bresson, 1987). Due to the extremely low aggregate stability of such arid soils, there is rapid reorganisation of particles which occurs until the seal has developed sufficiently to constrain further erosion.

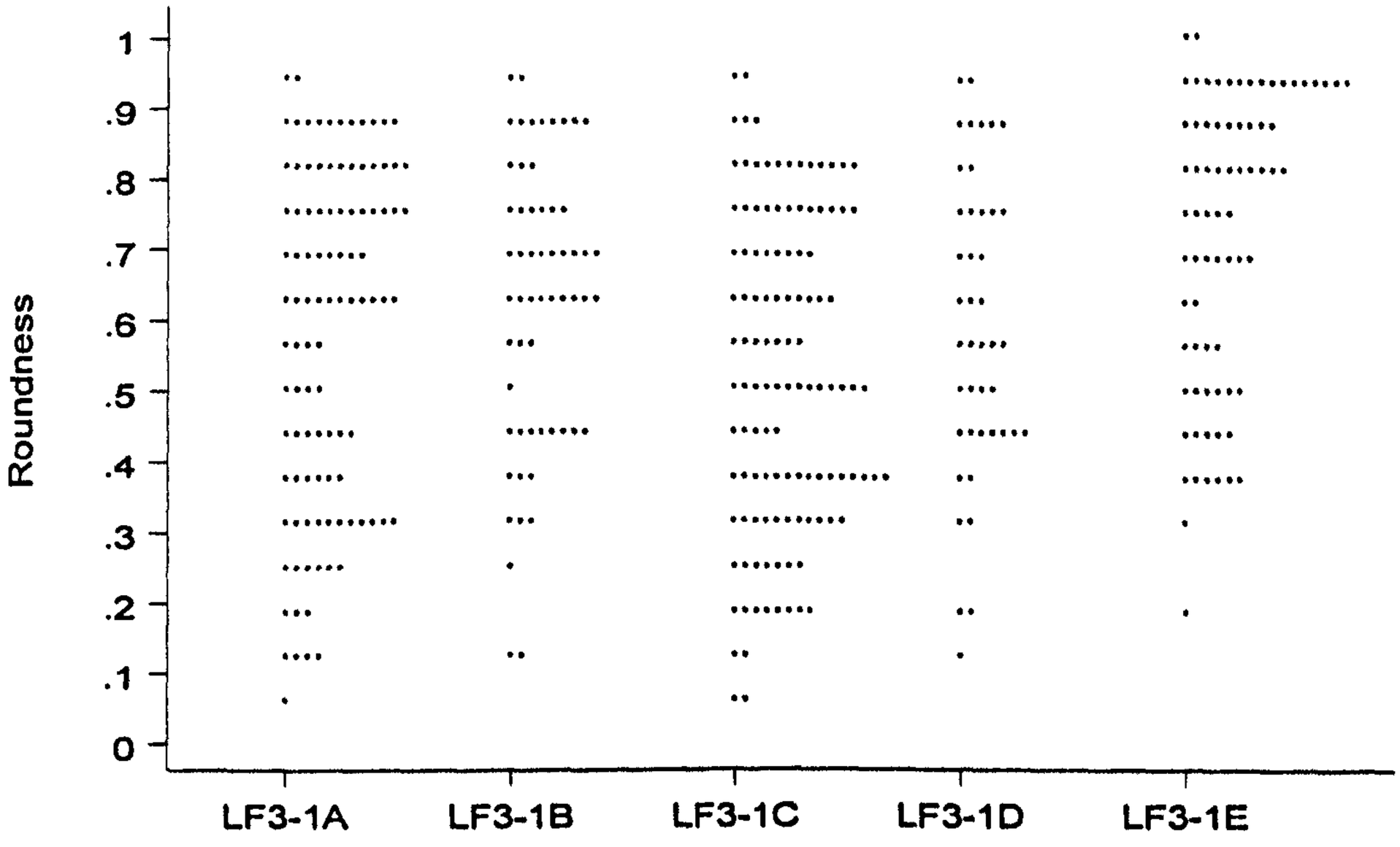

Figure 8.1: Roundness changes with microtopographic position at LF3-1

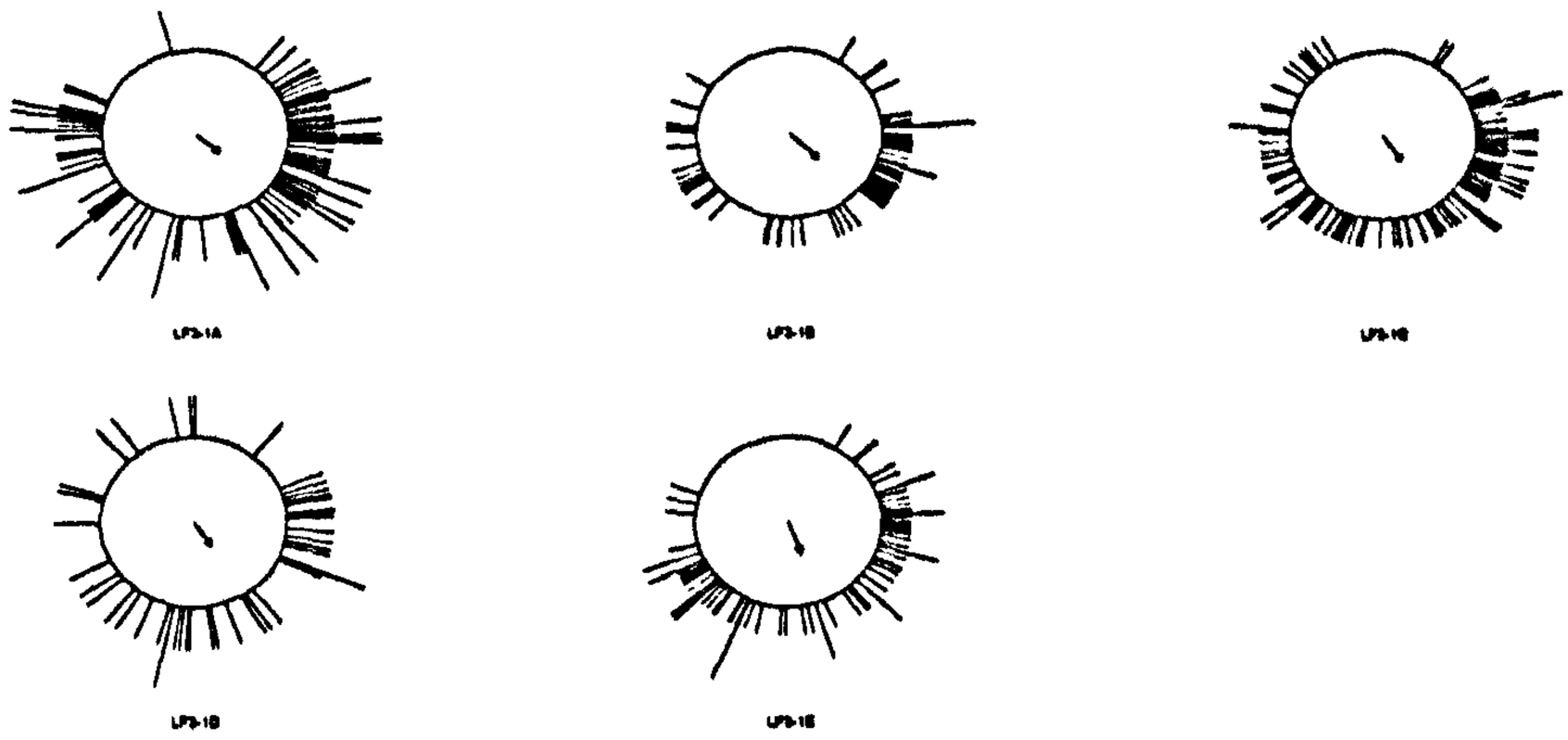

Figure 8.2: Pore orientation (°) at LF3-1

Plate 8.5: Images of porosity using UV light photography at LF3-1

LF3-1A

LF3-1B

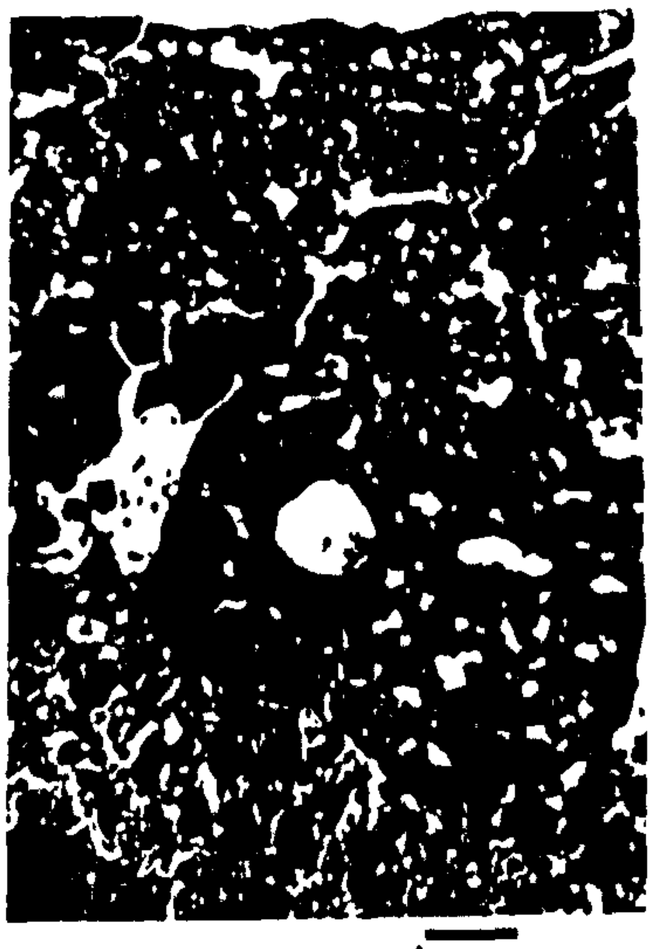

LF3-1C

LF3-1D

LF3-1E

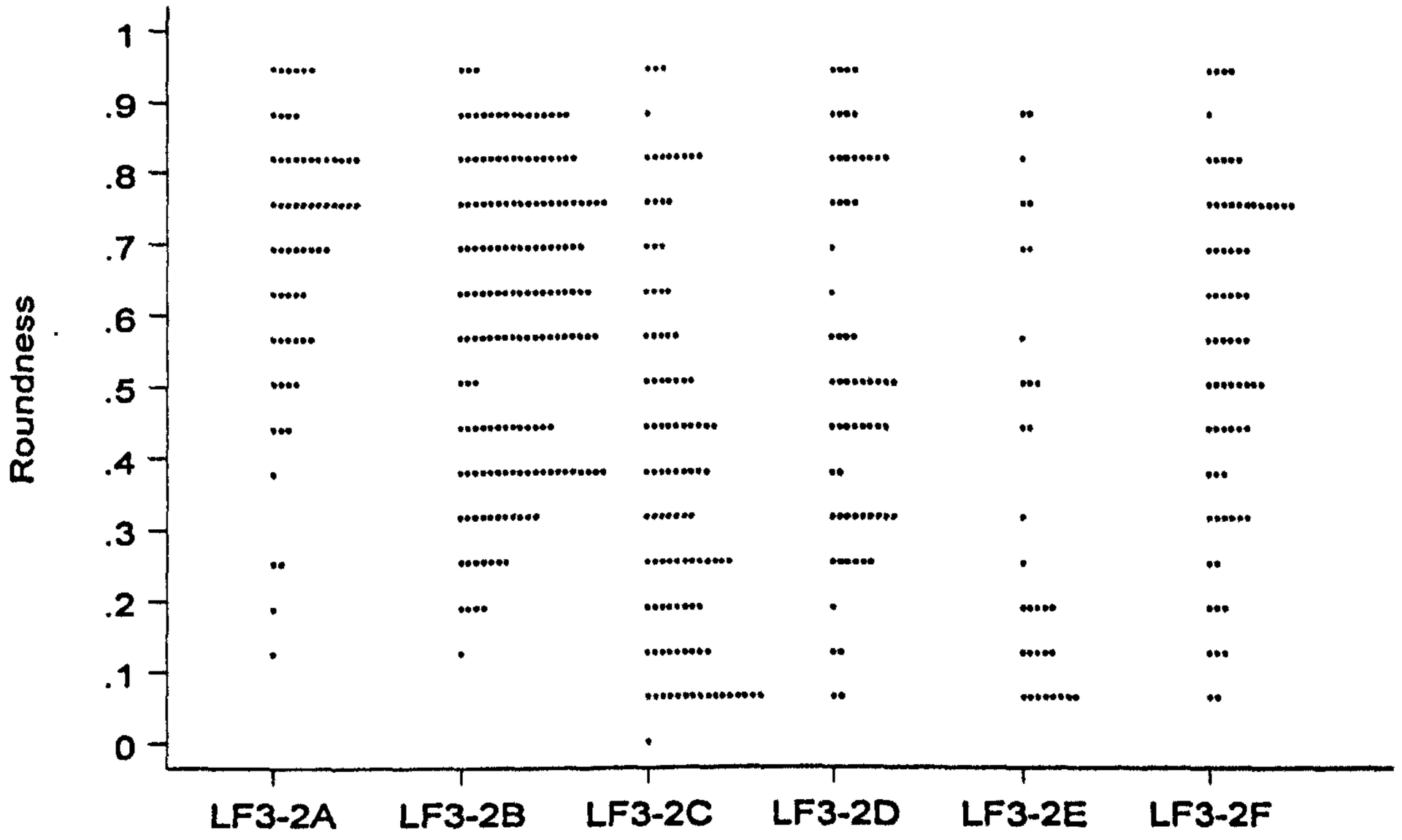

Figure 8.3: Roundness changes with microtopographic position at LF3-2

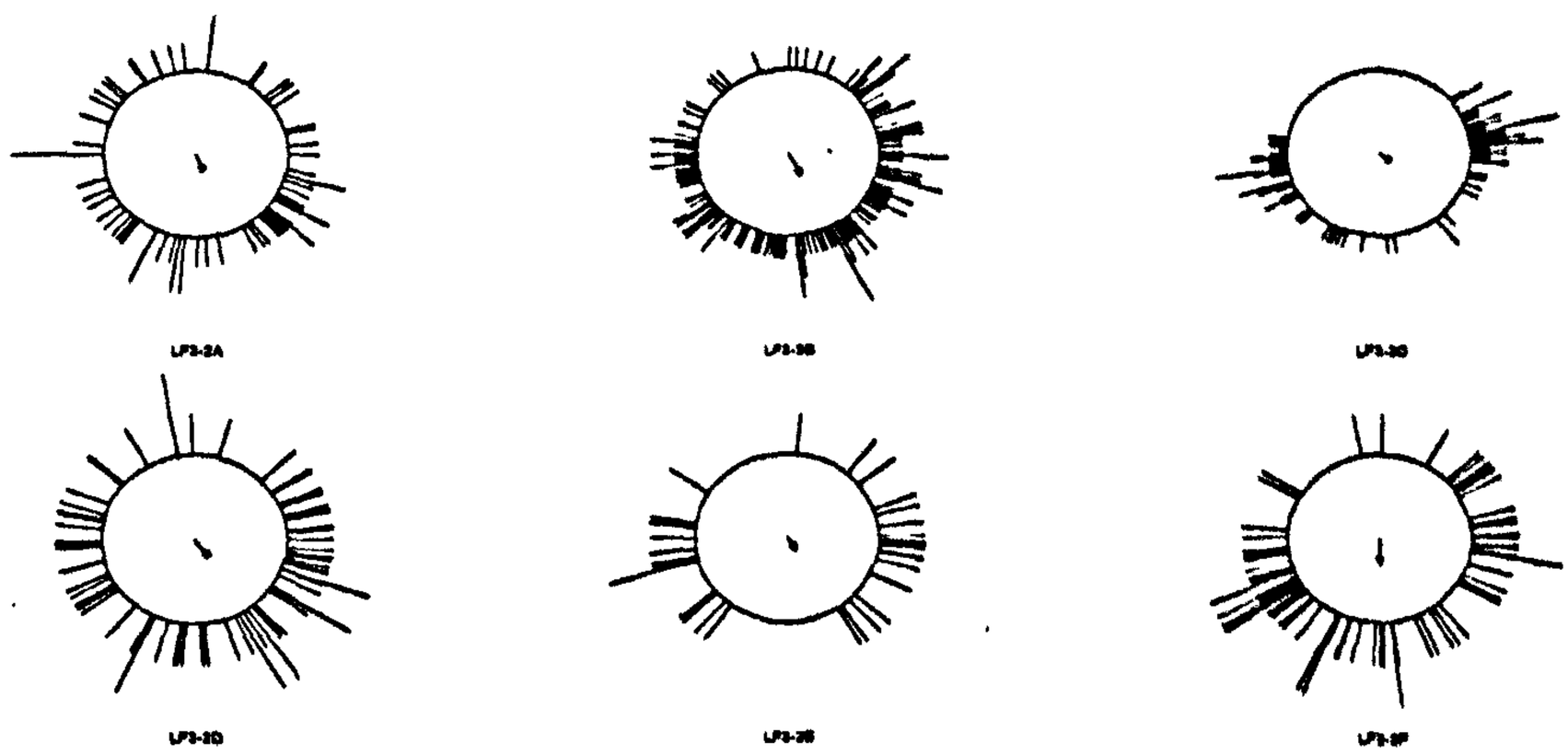

Figure 8.4: Pore orientation (°) at LF3-2

Plate 8.6: Images of porosity using UV light photography at LF3-2

LF3-2A

LF3-2B

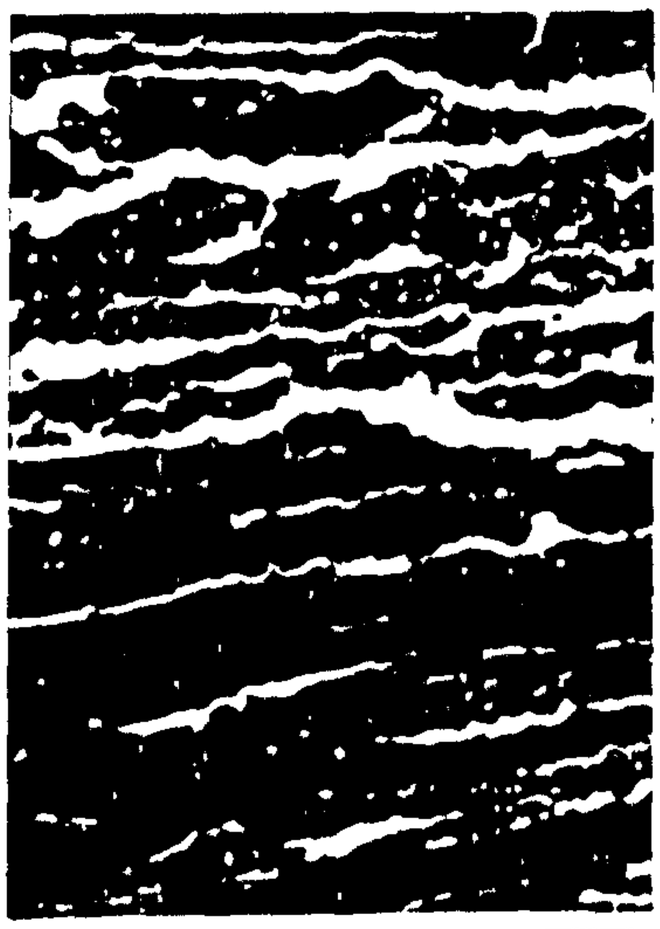

LF3-2C

LF3-2D

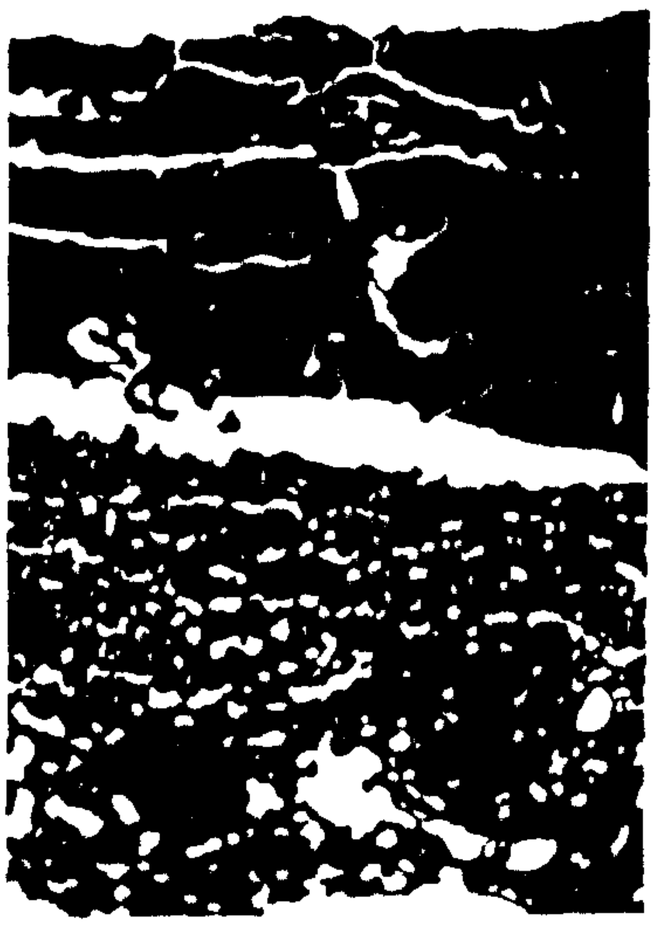

LF3-2E

LF3-2F

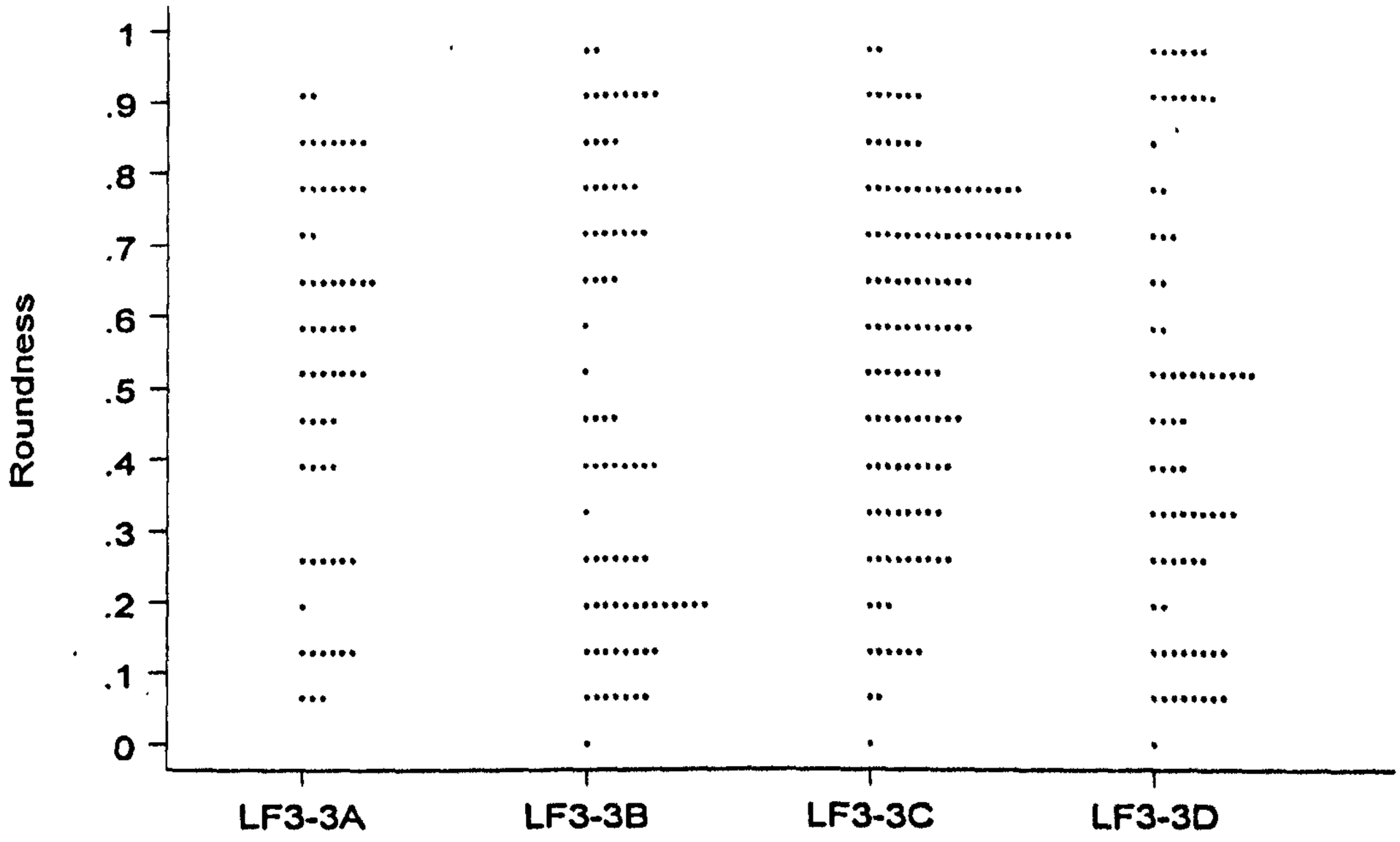

Figure 8.5: Roundness changes with microtopographic position at LF3-3

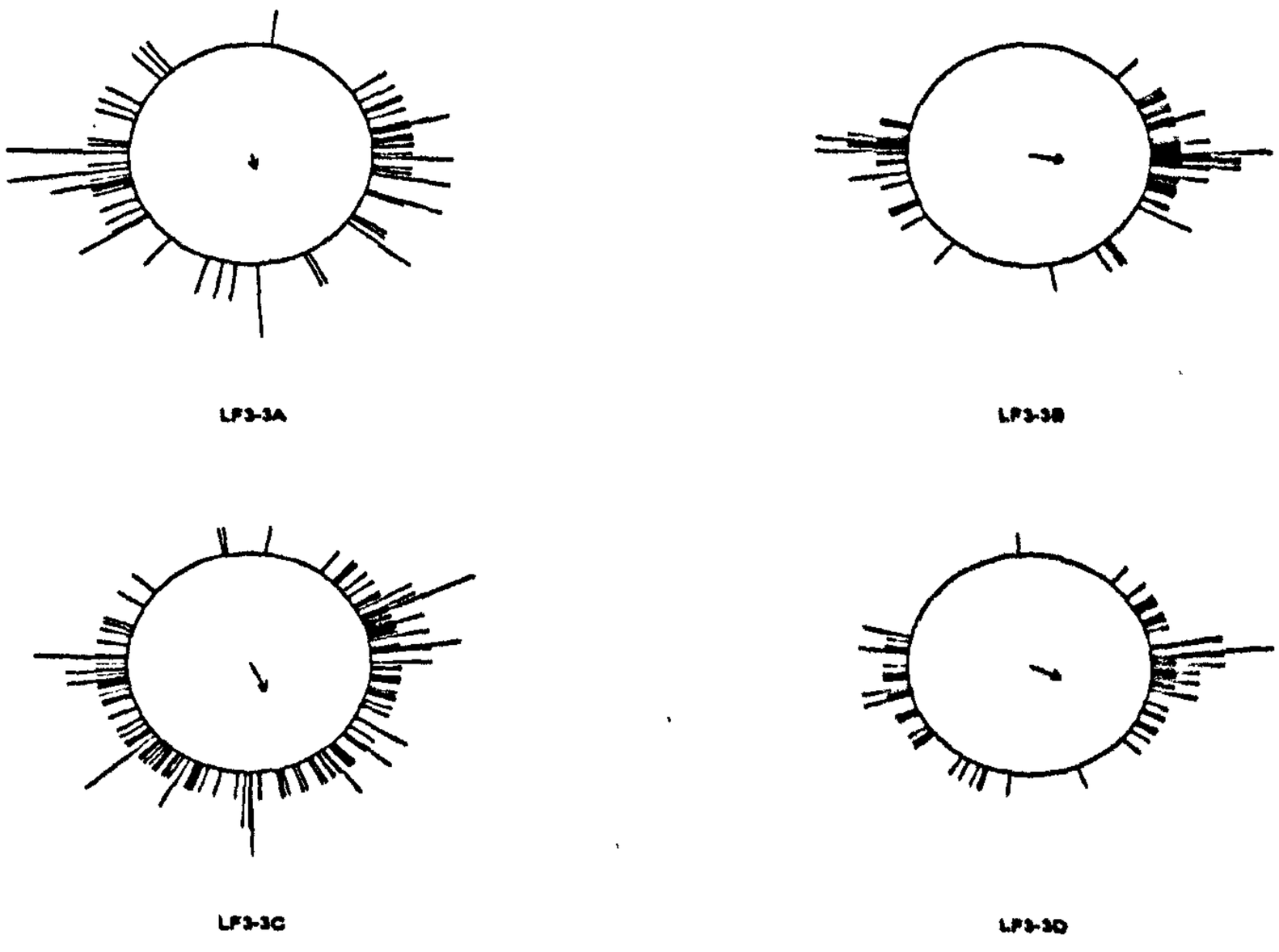

Figure 8.6: Pore orientation (°) at LF3-3

Plate 8.7: Images of porosity using UV light photography at LF3-3

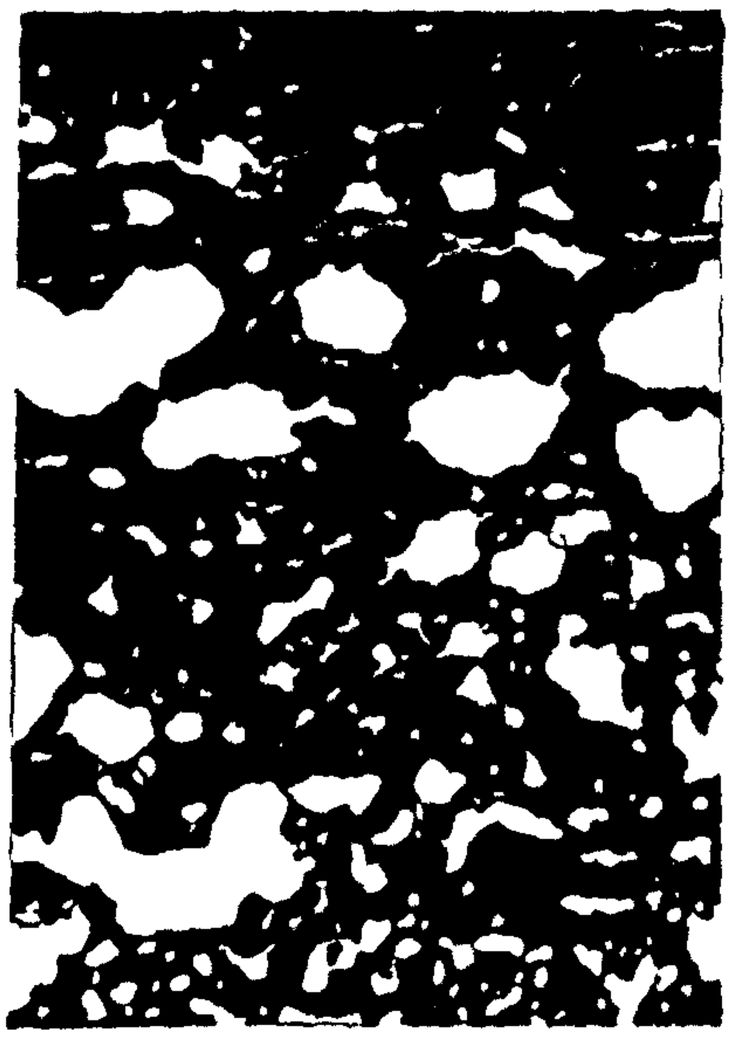

LF3-3A

LF3-3B

LF3-3C

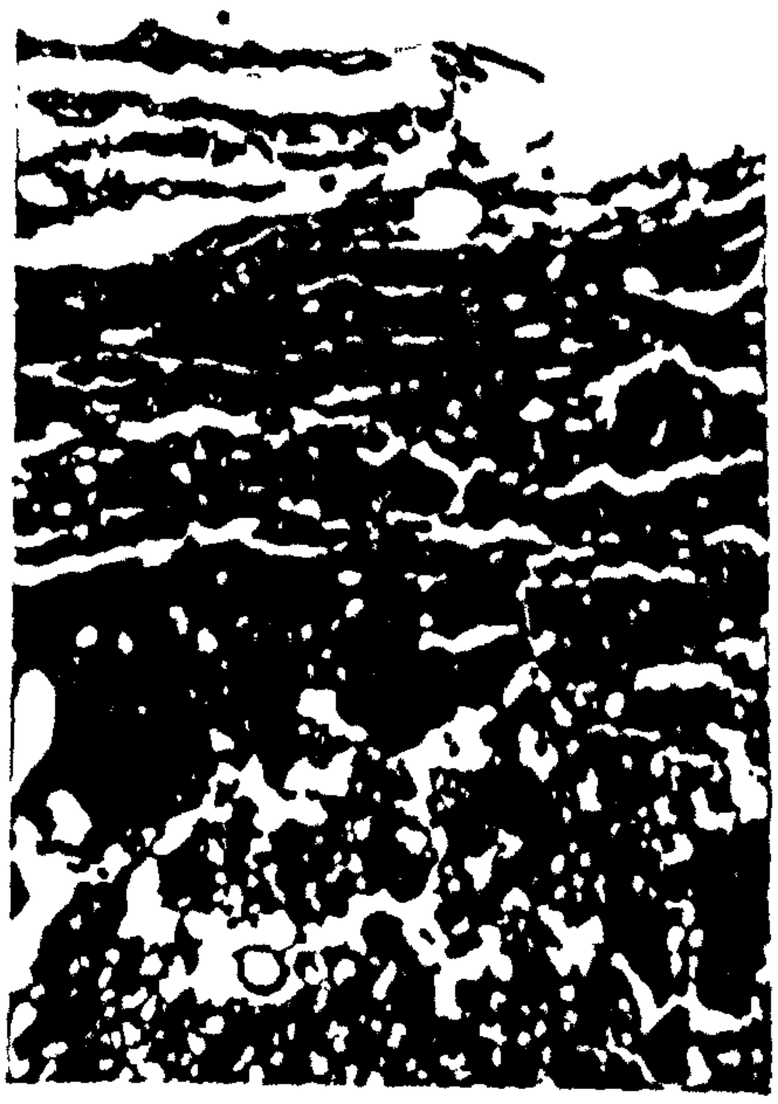

LF3-3D

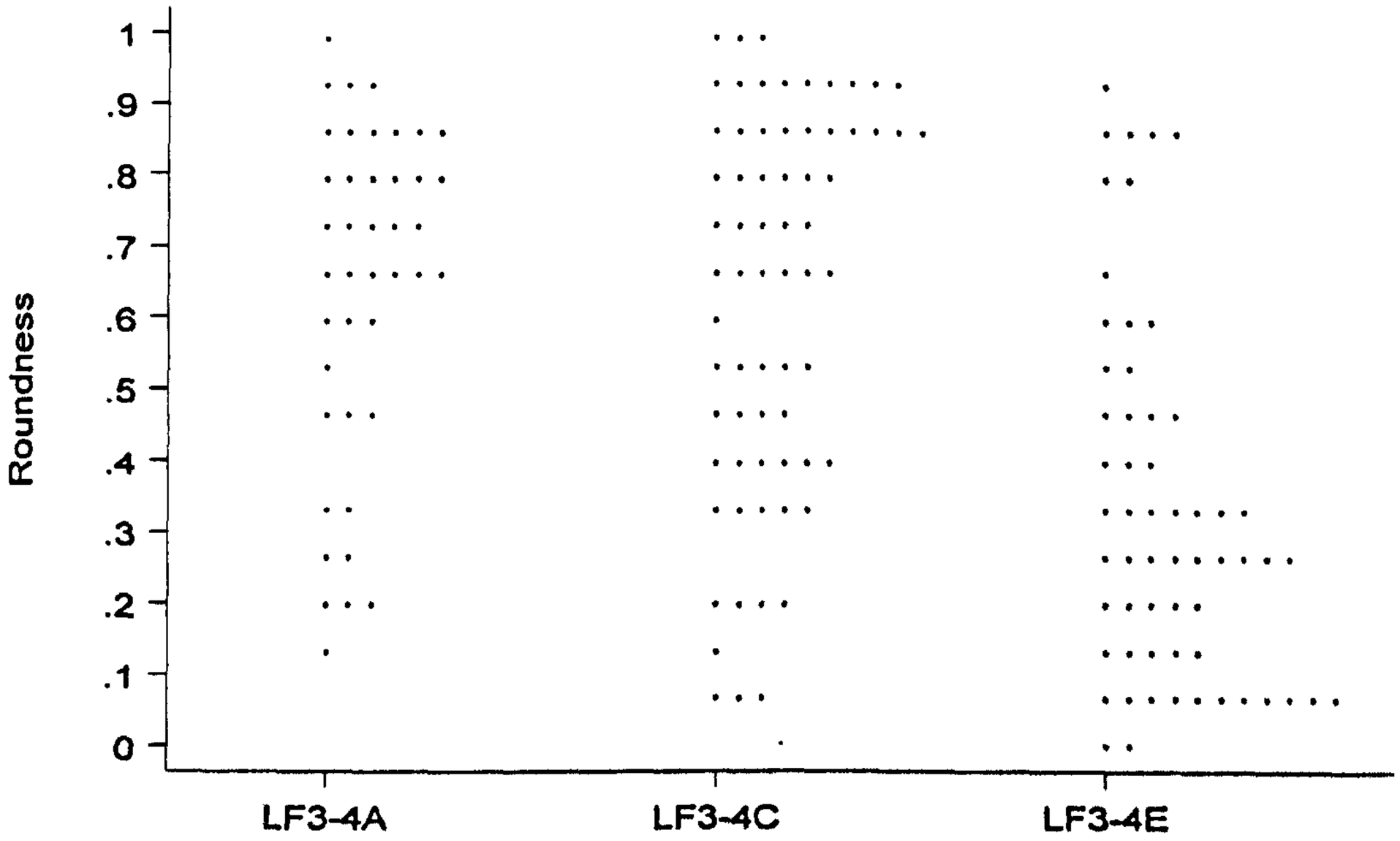

Figure 8.7: Roundness changes with microtopographic position at LF3-4

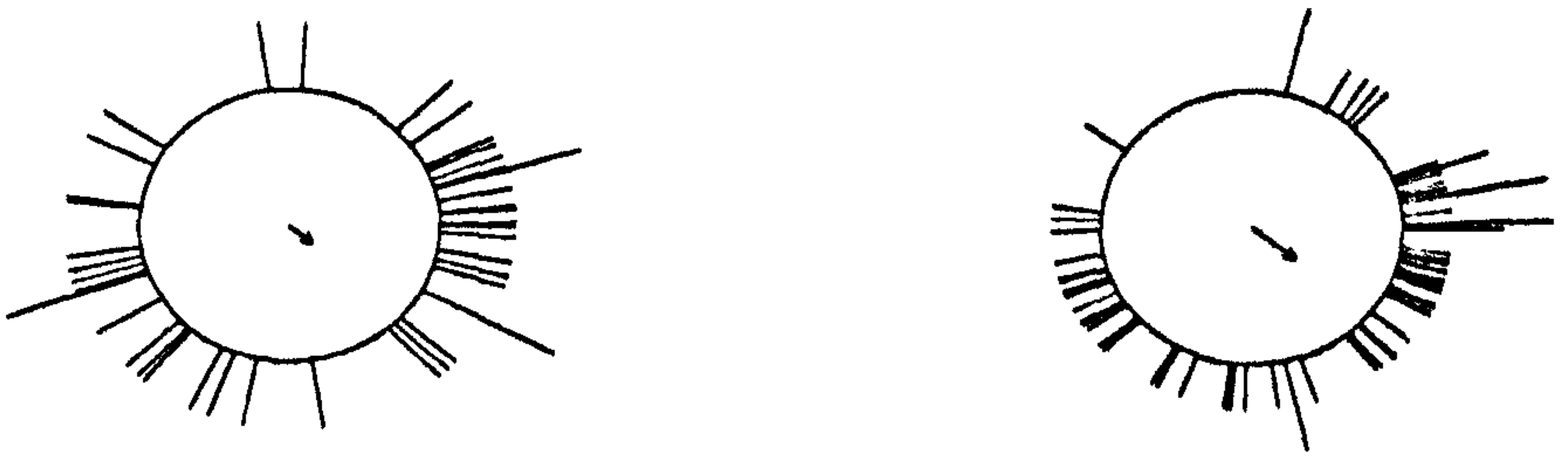

Figure 8.8: Pore orientation (°) at LF3-4

Plate 8.8: Images of porosity using UV light photography at LF3-4

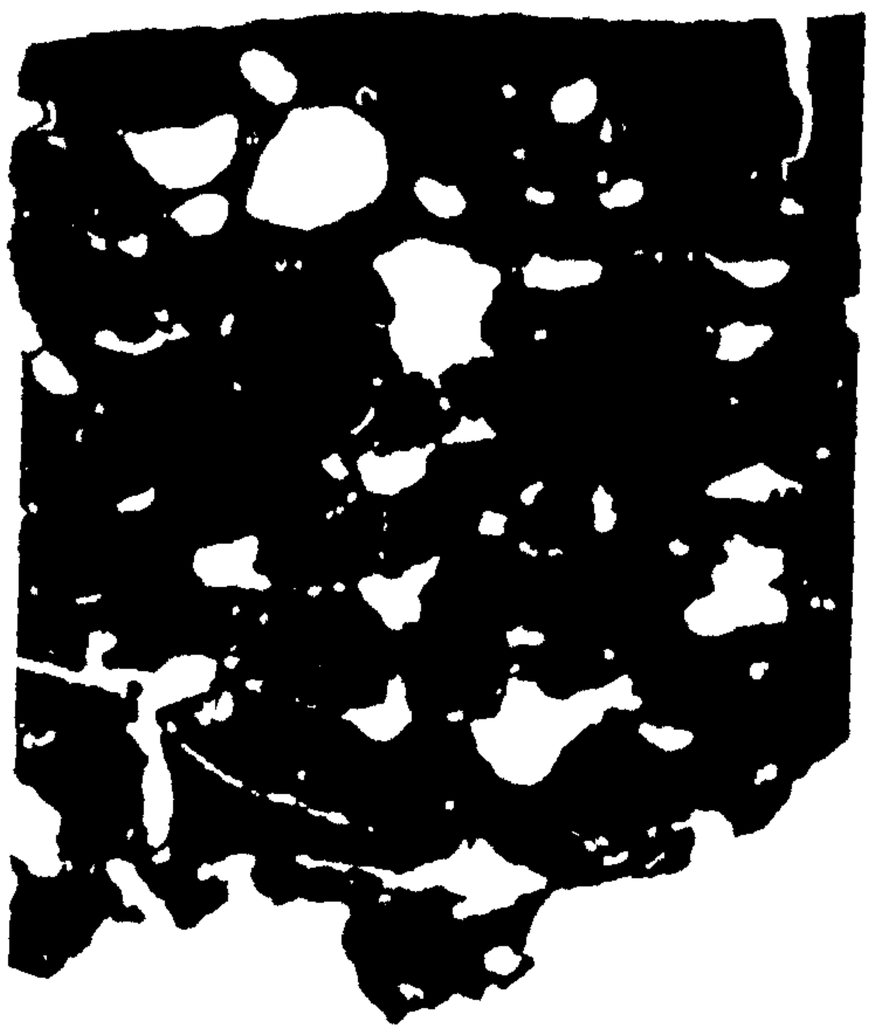

1 mm

LF3-4A

1 mm

LF3-4C

1 mm

LF3-4E

The crust samples at the base of the furrow sequences are formed initially by raindrop impact, but the process is interrupted as material is deposited from the ridges and furrow flanks. The material that is being deposited is also being reorganised as the coarser particles are laid down more rapidly than the finer material At the same time, raindrops disrupt the surface material, forming discontinuous areas of structural crusts on the surface of the depositional crust. The topography has a vital role to play in the crust formation, because in addition to its effect on the vertical development, it has been shown that it affects the areal development. The ridges next to the irrigation laterals, 1E, 2A, 3A and 4A, are all dominated by large vesicles, which is indicative of rapid entrapment of air. The surface of the crust has large embedded particles which would suggest that much of the finer material has been washed out. The furrow flanks are harder to classify as there is a complicated set of processes acting simultaneously. As the structural crust is formed, vesicles form, but then, as sheet-flow is generated from the ridges, there is erosion and the vesicles either are destroyed or become vughs. In general there is a washing-in of the finer material, which produces a much denser surface layer. It is likely that towards the base of the furrow flank vesicles are intact as the sheet flow loses energy, while nearer the ridge, vesicles are eroded or become misshapen vughs. This agrees well with the recent findings which relate the vesicular nature of the surface soil to the hillslope position (Brown & Dunkerley, 1996), albeit on a smaller scale.

The influence of the irrigation becomes apparent on the central ridge, 2D and 3C, where there is a remnant of a structural crust, but it has become structureless. Chapter 7 has shown that the central ridge is dominated by the salts precipitating on the surface causing widespread dispersion of the clay and fine silt. The loss of clay explains the lack of determinable structure, as many of the bridges between pores and larger mineral particles have been destroyed as the clay has dispersed, and then been washed away or washed further into the soil profile.

The pore roundness and orientation statistics provide a good means by which to classify the UV micromorphological images, because each topographic position has a different emphasis in relation to the different processes involved. Due to the nature of the pores produced during crust formation, i.e. vesicles, vughs or cracks between

laminae, problems of anisotropy (Vögel *et al.*, 1993) are avoided because the voids appear similar whichever direction the thin-sections are cut. The depositional crusts are dominated by well orientated cracks between each set of laminae and have very low roundness values. The structural crusts have non-orientated pores which are, in many cases, almost perfectly spherical and the furrow flanks are in between.

Finally, by observing the total porosity (Figure 8.9) it can be seen that the central ridges have almost twice as much porosity than the other samples reinforcing the suggestion that they have become unstable and structureless. The furrow flanks, on the other hand, have often become so dense, through the washing in of fine material and the destruction of surface pores, that they exhibit very low porosity.

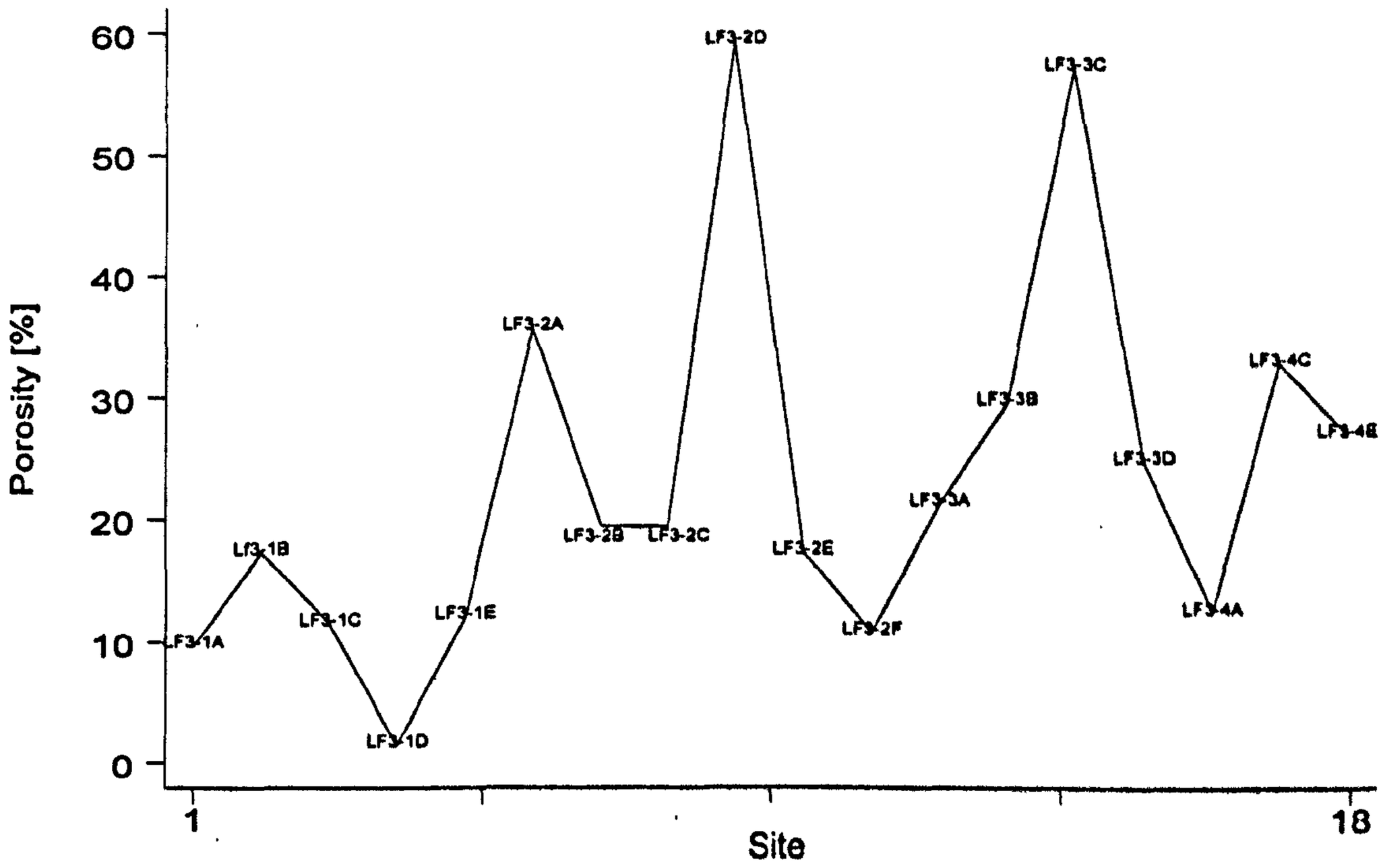

Figure 8.9: Changes in porosity at different topographical locations

8.5 METHODS FOR TRACING THE MOVEMENT OF PARTICLES DOWN THE SOIL PROFILE

If it is recognised that during a rainfall event, there is a profound change in the surface soil characteristics, in terms of both a reorganisation of particles and a redistribution of pore space, then it is important to design an experiment which will allow the observer to measure what has taken place. If field experiments are used, perhaps with a measured input of rain from a simulator, then it is impossible to see how particles have moved: there is no way of telling how far a particle has moved between rainfall initiation and the end of the experiment. If thin sections are made before and after such a rainfall event, only general trends can be observed by comparing the two images. Soil scientists have often tried to circumvent this problem by laboratory experiments on soils which have been manufactured to the criterion of the scientist. For example, Bielders & Baveye (1995a) use a mixture of 92.5% sand and 7.5% clay to gain more understanding of vertical sorting in structural crusts. Isotropic tracers have often been used to define movement of water in the surface layers of the soil (Jaynes & Rice, 1993; Philips, 1994; Curmi *et al.*, 1996; Aeby *et al.*, 1997), while physical tracers have recently been used to measure relative amounts of sediment transport during overland flow (Abrahams *et al.*, 1986; Parsons *et al.*, 1993). Image analysis has often accompanied these methods, especially in order to look at micro-scale solute pathways (Walker & Trudgill, 1983).

8.5.1 The use of physical tracers to identify particle movement

In the experiments of Parsons *et al.* (1993), it was established that magnetite was a highly effective tracer, being transported rapidly by overland flow. Although the movement of magnetite was detected by its magnetic properties, it seemed that a similar technique using hematite could be used to monitor the vertical movement of fines through the soil surface during sealing. However, instead of using the magnetic properties of the mineral tracer to observe movement, it became clear that the isotropic nature of the material in thin-section would serve as an excellent representation of particle movement. In temperate or tropical soils such a method would be inappropriate, because of the isotropic nature of the organic fraction. In

arid soils where the organic matter content is often less than 1%, this ceases to be a concern. In fact the hematite is highly visible among the light brown groundmass of the thin section.

The fact that hematite has a much higher density than the natural soil was identified as a potential problem for the determination of rates of detachability and transport by Parsons *et al.* (1993), but they overcame it by reducing the grain size about 20 μm less than material normally entrained by overland flow. Further reduction resulted in much lower detachability rates because of the relative size of the particles and the increasing likelihood that they would pass down into the interstices during rainfall. The majority of the Badia soil lies within the coarse silt fraction, 20 - 63 μm, and so it seemed prudent to crush the hematite to below 63 μm. As the main interest of the research was the movement of fines down the profile, it was necessary that there was no artificial encouragment of movement by making the particles smaller. There is therefore an implication of mass of the hematite as one would expect it to move faster and further down through the soil in comparison with the surrounding soil. Before the experiments took place, thin sections of the soil were examined and it was observed that there were considerable amounts of heavy minerals, such as rutile and garnet, in the surface layers of the soil. There was no indication that they had settled at certain layers within the soil due to their higher density; in fact their incorporation within the crust was evident. Another line of evidence concerning the relative importance of density and particle size comes from research into desert pavements (e.g. McFadden *et al.*, 1987). It is becoming more generally accepted that these landforms are produced, by not so much an upward movement of coarse material, but rather an active filtration of fine material downwards.

In order to see how much less dense material would behave under similar rainfall conditions, another plot was prepared with a surface of talc instead of hematite. Unfortunately, the talc acted as a colloidal material, as can be seen in Plate 8.16, and moved much further into the profile, but coated and joined aggregates, as would be expected of clay particles.

Plate 8.9: Filling the header tank to keep a constant head of water during rainfall simulation experiments

8.5.2 The plot experiments

The plots, already described in section 4.2.3, were left to settle for two weeks before the rainfall simulation experiments (Plate 8.9). Shortly before starting the rainfall simulation, the hematite tracer was introduced to the plot by sprinkling it evenly over the plot. Each rainfall simulation experiment lasted 90 minutes with an intensity of 15 mm h^{-1}. In order to obtain a time series to look at changes in vertical movement, a plastic sampling tin was placed over a section of soil at $t = 30$, $t = 60$ and $t = 90$ minutes (Plate 8.10). This meant that the sealing was constrained at a specific time: once the experiment had finished a sample was cut from under the sampling tin. Ideally a section would have been collected at $t = 0$, but the problem of sampling and impregnating dry soil (Section 4.4.3) meant that this could not be achieved.

8.5.3 Image analysis

Once the samples had been dried, impregnated and thin-sectioned (Section 4.4), the samples were ready to be analysed. Because the use of hematite was due to its isotropy, the distribution could be easily identified by converting the sections to 8-bit grey level images. Two methods were employed: a digital camera and an ordinary SLR camera. In the last five years camera and computer technology has enabled images to be stored digitally and it therefore represents an ideal way of analysing thin sections and polished blocks quickly and accurately (Vögel, 1997). The thin-sections were photographed under plain polarised and cross polarised light with a Kodak DCS240 digital camera mounted above a Nikon Labophot II microscope and stored as 8-bit black and white TIFF images. The images were converted to a two band image file using ARC-INFO and loaded into TERRAMAR where they could be analysed.

The traditional method of digital image acquisition involves either capturing stills using a video camera (Bouabid *et al.*, 1992; Terribile & FitzPatrick, 1995) or photographing thin-sections with a conventional SLR camera (Anderson *et al.*, 1996; Velde, 1996). Images are then scanned-in at a certain resolution to allow enough detail to be analysed appropriately. In this research, photographs were taken using tungsten film and a Canon EOS 600 SLR camera. Several attempts were needed for

each photograph because it was difficult to gauge the exposure due to the different thicknesses of thin-sections and the contrast between hematite and soil fabric. After developing the positives, they were scanned to a resolution of 300 dpi using a slide scanner and stored as TIFF images.

The first of the methods has various advantages in terms of its versatility, immediate results and the ability to take several shots under different lighting conditions without problems of geometric correction. However, its resolution, 1012 x 1524 pixels, means that it is very difficult to obtain clearly focused imagery, especially when working at magnification and with a predominantly fine-grained soil. Because the computer screen can only display 72 dpi, it is impossible to see if an image is properly focused unless it is printed out, which negates all the initial flexibility of the system. As high image resolution was the most important criterion for analysing the data, the digital photographs, despite their versatility, were rejected for the more traditional photographic method. Digital cameras are likely to become more useful for image processing as the technology improves and allows automatic focusing and higher resolutions.

The original TIFF images were converted to RAW images, which are images without a header file attached, and read into the TERRAMAR image processing software. In order to classify the images, training areas had to be set up on the image to characterise the hematite, the fabric and the pore space. Each training area included several thousand pixels in order to gain a frequency distribution of DN values for each class, which the maximum likelihood classifier then used to extrapolate to the whole image. Certain areas, such as the pore boundaries and heavy minerals, had DN distributions which did not fit into a particular class and so they were denoted as unclassified and drawn black. The classified image was then reimported to ARC-INFO and added to a specifically written header and colour file so that the final image could be transferred back to a TIFF format to allow printing.

8.5.4 Movement of fines: initial observations

The first observation is that the movement of fines is concentrated along the boundaries of gravel or rock fragments. Plate 8.11 and Plate 8.15 show that the majority of the hematite is concentrated along the boundaries of basalt fragments or calcium carbonate nodules. Plate 8.11 is particularly interesting, because the basalt fragment, which is just off the top-right-hand corner, initiates a series of laminae which flow down in to the micro-depression to create a depositional crust. The surface of the soil is probably of the order of 0.5 mm lower than the surrounding level and yet material is being washed in.

The second observation is that there is formation of vesicles, Plate 8.14, due to the rapid entrapment of air in the near-surface soil. Despite this rapid process, hematite has been able to filtrate and coat the sides of the pore.

Banding is evident at 30 minutes, with a clearly defined dense seal at the surface, above which larger sand grains and gravel lay. Then there is another distinct band approximately 250 μm below the surface. At 60 minutes, the hematite band is almost continuous and very clear and there is evidence of a band further down the section. There is a textural change below the lowest band in both cases (Plate 8.13), which looks to be size orientated; below the band it is impossible to distinguish specific particles while above it the grains look larger and less cohesive. By 90 minutes there is still a large accumulation of hematite at the surface with only the sand-sized grains above. There is a hematite-free zone which inhabits the area directly below the surface seal and then there is another set of layers between 200 and 400 μm below the surface.

Taking the structural crusts, there is an uneven boundary in the lower band of hematite as time continues. For example in the two sections taken at 60 minutes, there is a difference with one displaying a lower boundary at about 150 μm while the other section, which is within two centimetres of the first, has a lower boundary at 400 μm.

Lastly, in connection with the discussion in 8.5.1, it is interesting to note how the different sizes of hematite have moved relative to each other. The thin-sections show a variety of different shapes and sizes of hematite grains which are inevitable during the crushing process. However, it is impossible to conclude that certain sizes of particles have moved preferentially to others; there are larger particles remaining at the surface, but also some which have travelled to the base of the lower layer of hematite. Likewise with the smallest particles, there are many incorporated at the surface, but also many lower in the profile.

8.5.5 The movement of fines: explanation

Previous research into the effects of rock fragments on surface seal formation and infiltration has been inconclusive. While it is generally accepted that infiltration is increased due to the presence of rock fragments (Collinet & Valentin 1979), more recently it has been suggested that the relationship between infiltration and rock fragments in the sealed soil is not so simple (Poesen, 1986a; Poesen *et al.*, 1990). Instead the size and embeddedness of the fragment is more important (Bunte & Poesen, 1994) because they affect the neighbouring porosity (Poesen & Ingelmo-Sanchez, 1992). The results from the hematite tracer show how infiltration is affected by the presence of small rock fragments, i.e. smaller than the threshold value of 26 mm given by Wilcox *et al.* (1988). Hematite clearly flows rapidly around the edges of the rock fragments suggesting that as the surface seals, runoff is quickly generated and turbid flow into the soil is preferentially oriented to the edge of embedded fragments. This would seem to contradict the view that embedded fragments promote runoff rather than infiltration (Poesen, 1986a; Poesen *et al.*, 1990). What is more likely, especially in a fine-grained soil, is that the fines are rapidly entrained as the seal develops and runoff is initiated. The water charged with silt-sized grains preferentially infiltrates between rock fragments and the developing seal. However, the very process of turbid infiltration actually causes the plugging of the infiltration route as the silt settles out. Infiltration is therefore reduced and runoff is increased.

There is clear evidence that washing-in takes place during the formation of structural as well as depositional crusts. The surface layer of hematite seems to be already

stable by 30 minutes and does not change much in the following 60 minutes. It has been noted that the initial vertical growth of the crust is large and the rate of increase declines through time (Farres, 1978) until a threshold thickness is reached which is controlled by the aggregate size. The form of the crust resembles that of a sieving structural crust (Valentin & Bresson, 1992) which is made up of a layer of loose skeleton grains overlaying a much finer plasmic layer.

The second layer of hematite which seems to mark the base of washing-in of fines is not stable over space or time. There are some hematite particles between the plasmic layer below the surface and the base layer. This second layer has not been observed in structural crusts, although Pagliai (1987) shows microphotographs with a fine plasmic base layer separating the bottom of the crust and the subsoil, but he fails to explain the processes involved in its formation. Valentin and Bresson (1992) suggest that pavement crusts, which form in arid eolian soils, may have different textural bands due to the origin of the soil, but this is unlikely because the soil in the plots was manually tilled before experimentation. A more reasonable suggestion is that these are sieving crusts where the coarse silt grains have washed down to the base of the crust. However, the depth depends not so much on initial aggregate size, but upon the force of the drop impact (Bielders & Baveye, 1995). There is no reason to account for the difference in depth of the lower level in, for example $t = 60$, except to say that the sample with a deeper horizon of hematite had a larger number of drop impacts or drops with a higher kinetic energy within the 60 minutes.

There is great variability in crust-type depending on the interactions of the two major crust formation processes: raindrop impact and micro-scale movement of disaggregated fine material from topographic highs to lows. Our understanding of micro-scale processes is limited, but using a tracer allows greater insight into the movement of fines in an arid environment. Bielders *et al.* (1996) show how runoff and erosion crusts forming on sandy soils exhibit features dependent upon the original roughness of the soil. In silty soils, as found in the Badia, there is rapid erosion from microtopographic highs which may only be millimetres in magnitude (Plate 8.11) and yet depositional crusts with a depth of up to a millimetre form within 30 minutes of rainfall, causing a reduction in the original roughness element.

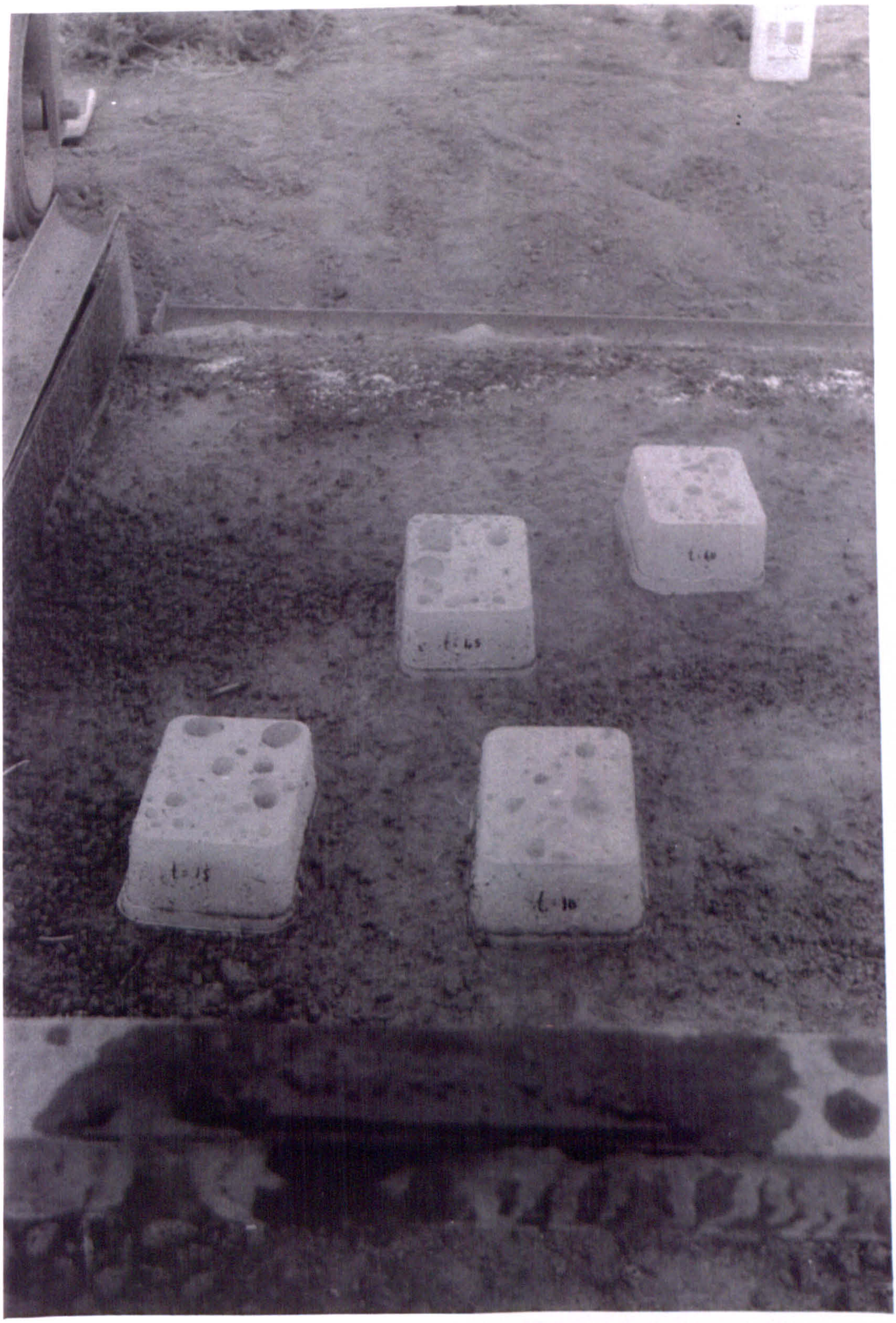

Plate 8.10: The collecting of the samples from the plot at different times

Plate 8.11: Thin-section photographs with their associated classifications at $t = 30$ minutes

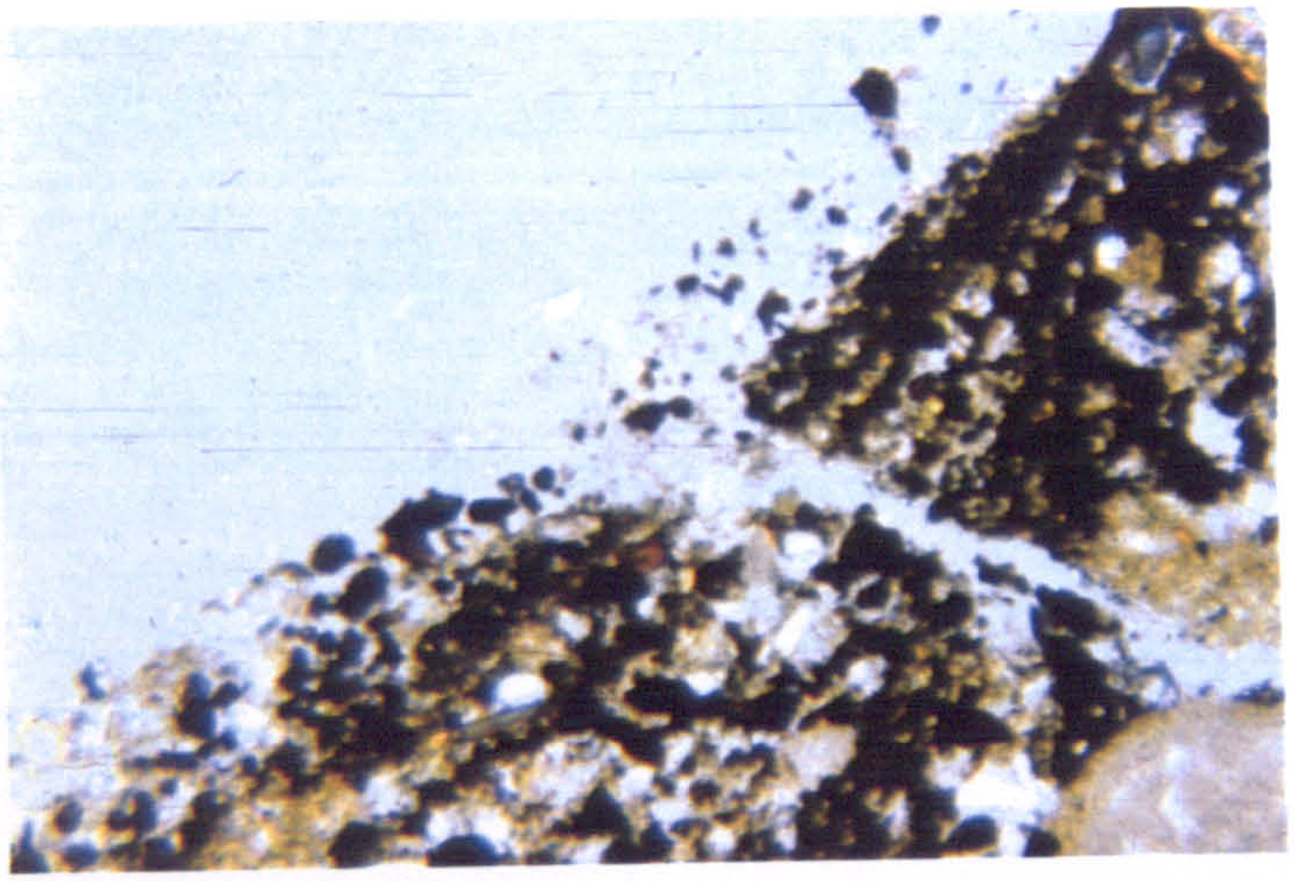

Hematite: t = 30 (a)

200 µm

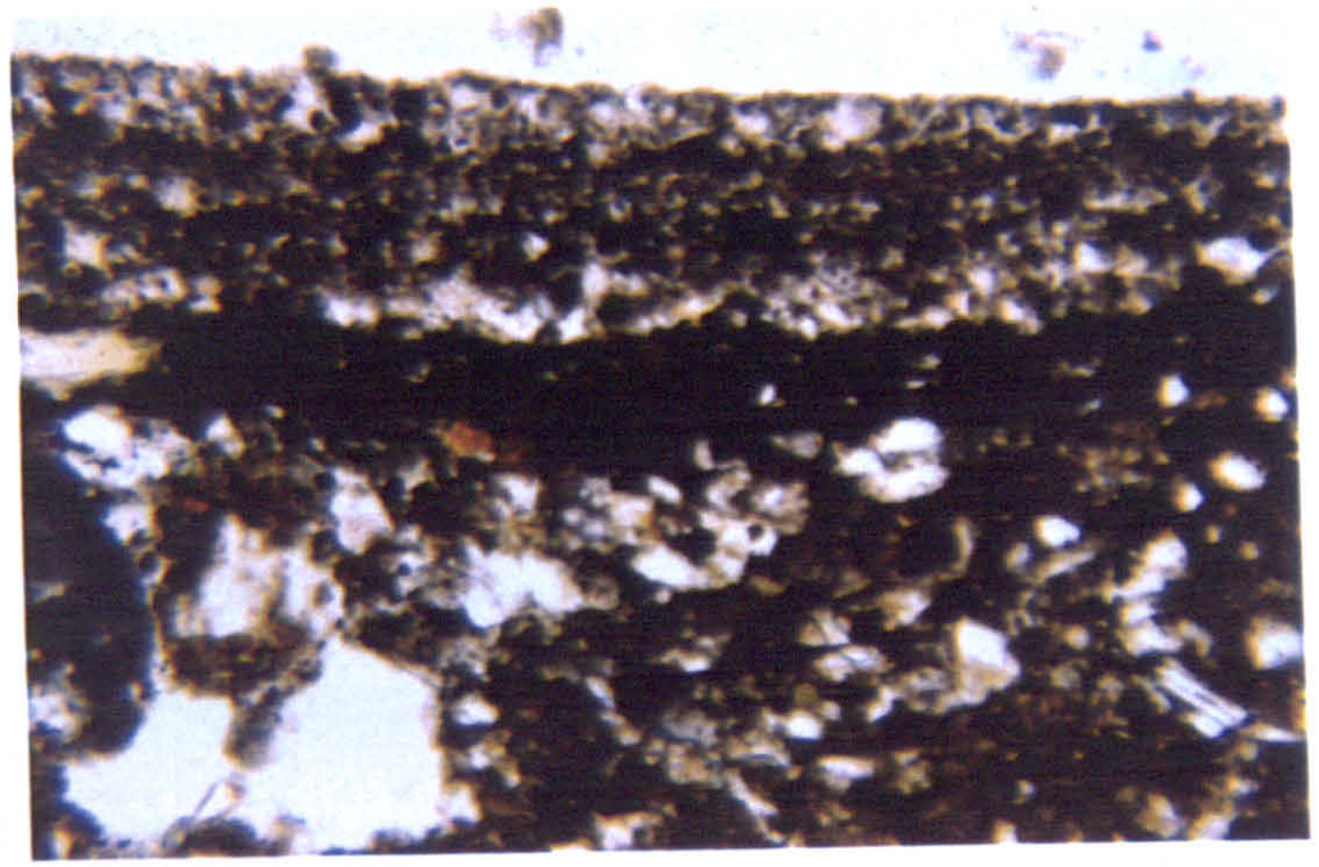

Hematite: t = 30 (b)

200 µm

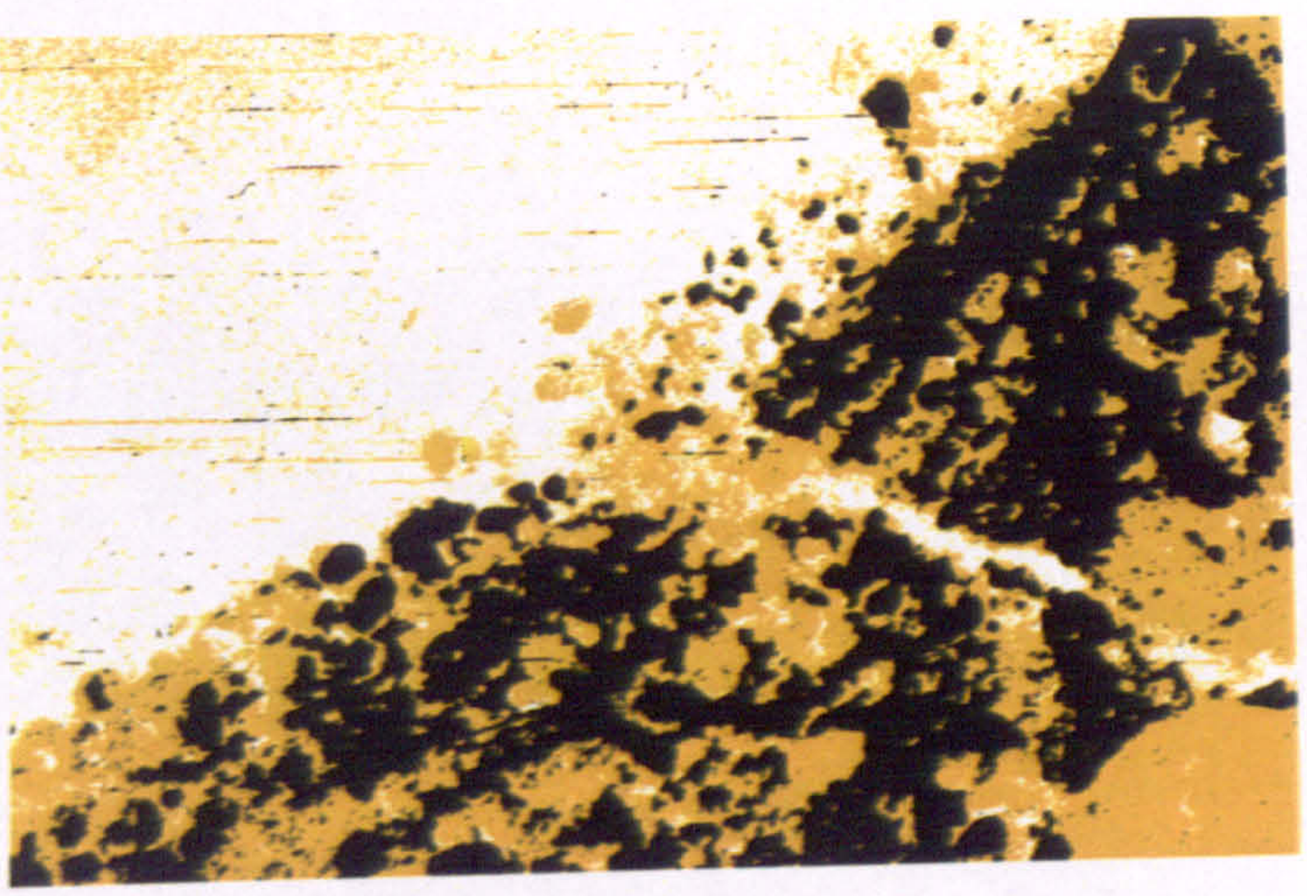

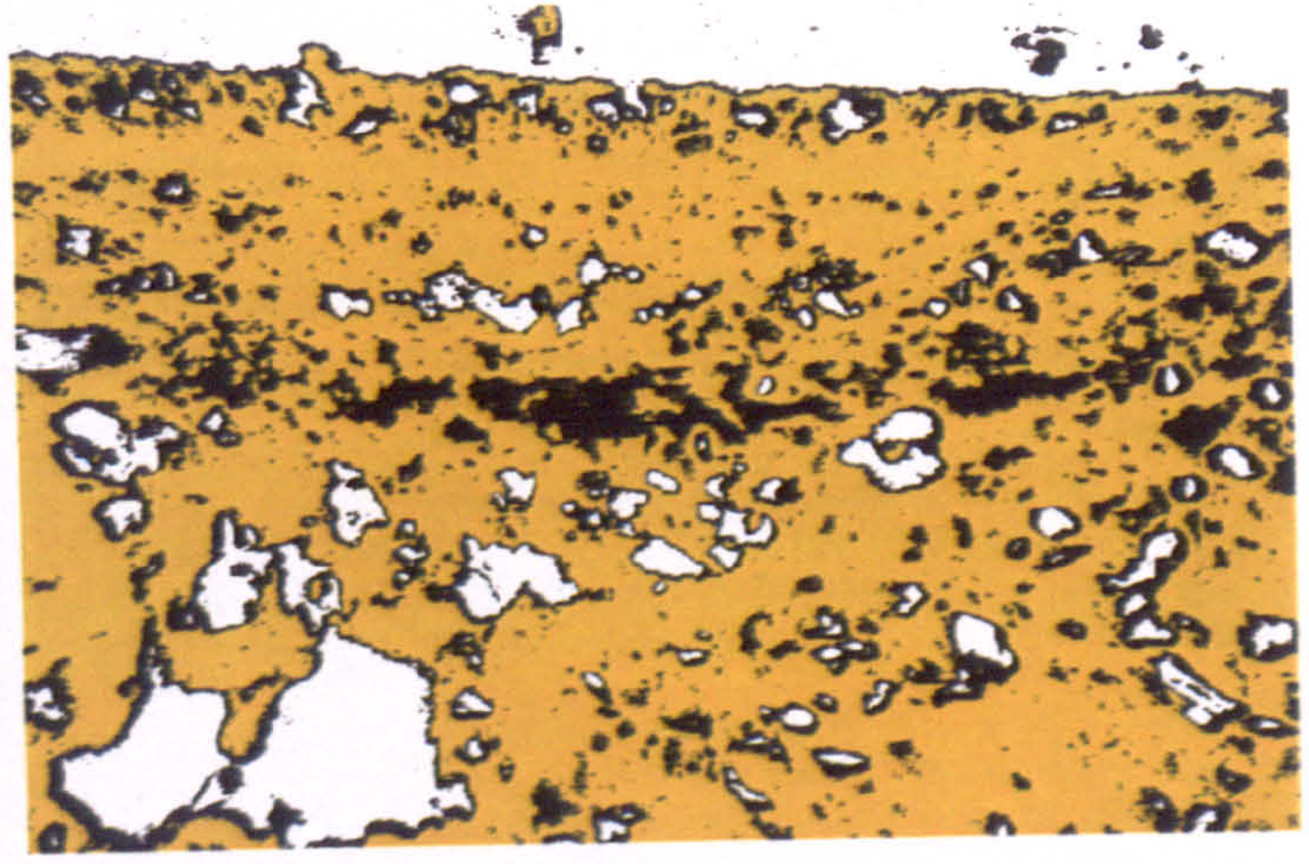

Plate 8.12: Thin-section photographs with their associated classifications at $t = 30$ minutes

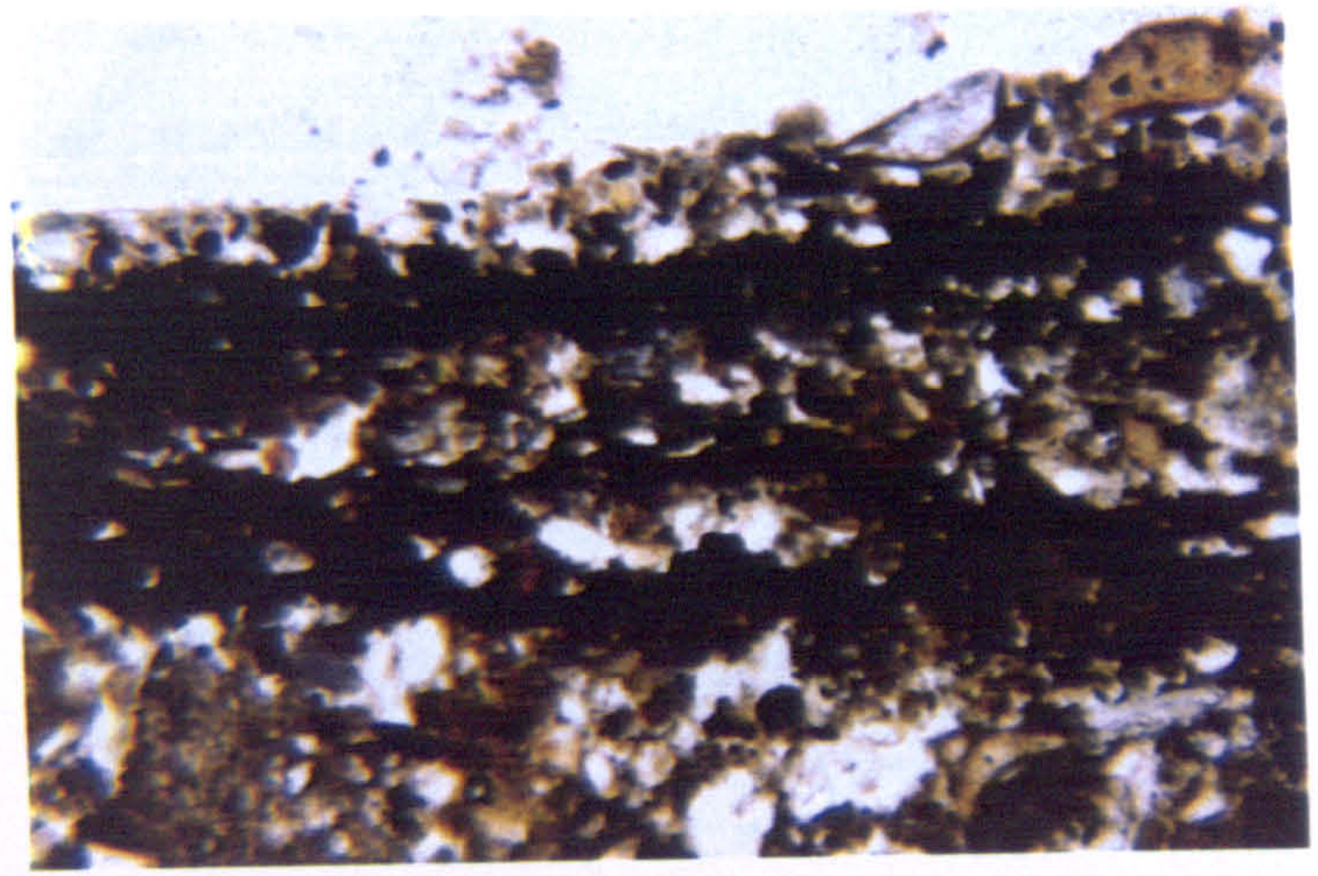

Hematite: t = 30 (c)

200 µm

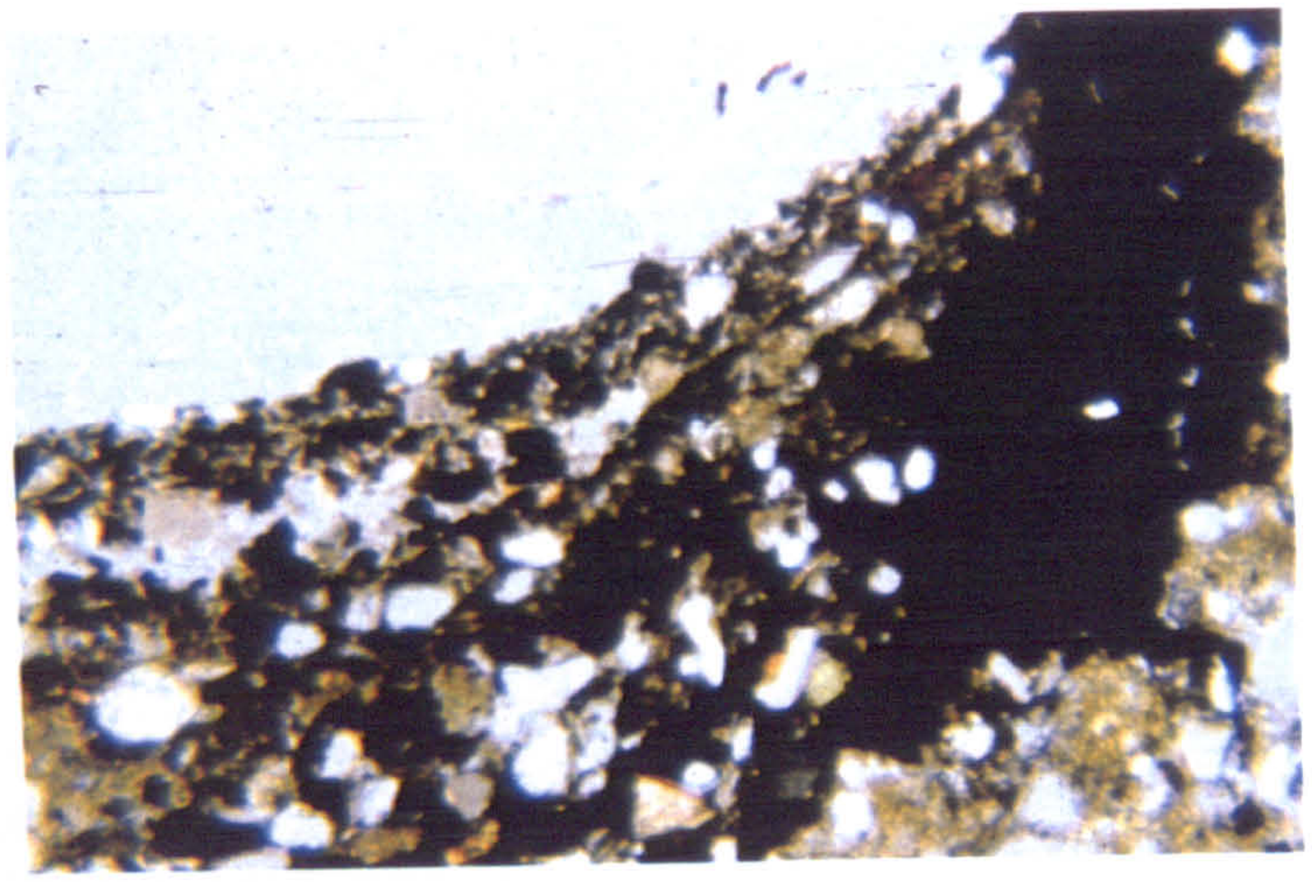

Hematite: t = 30 (d)

200 µm

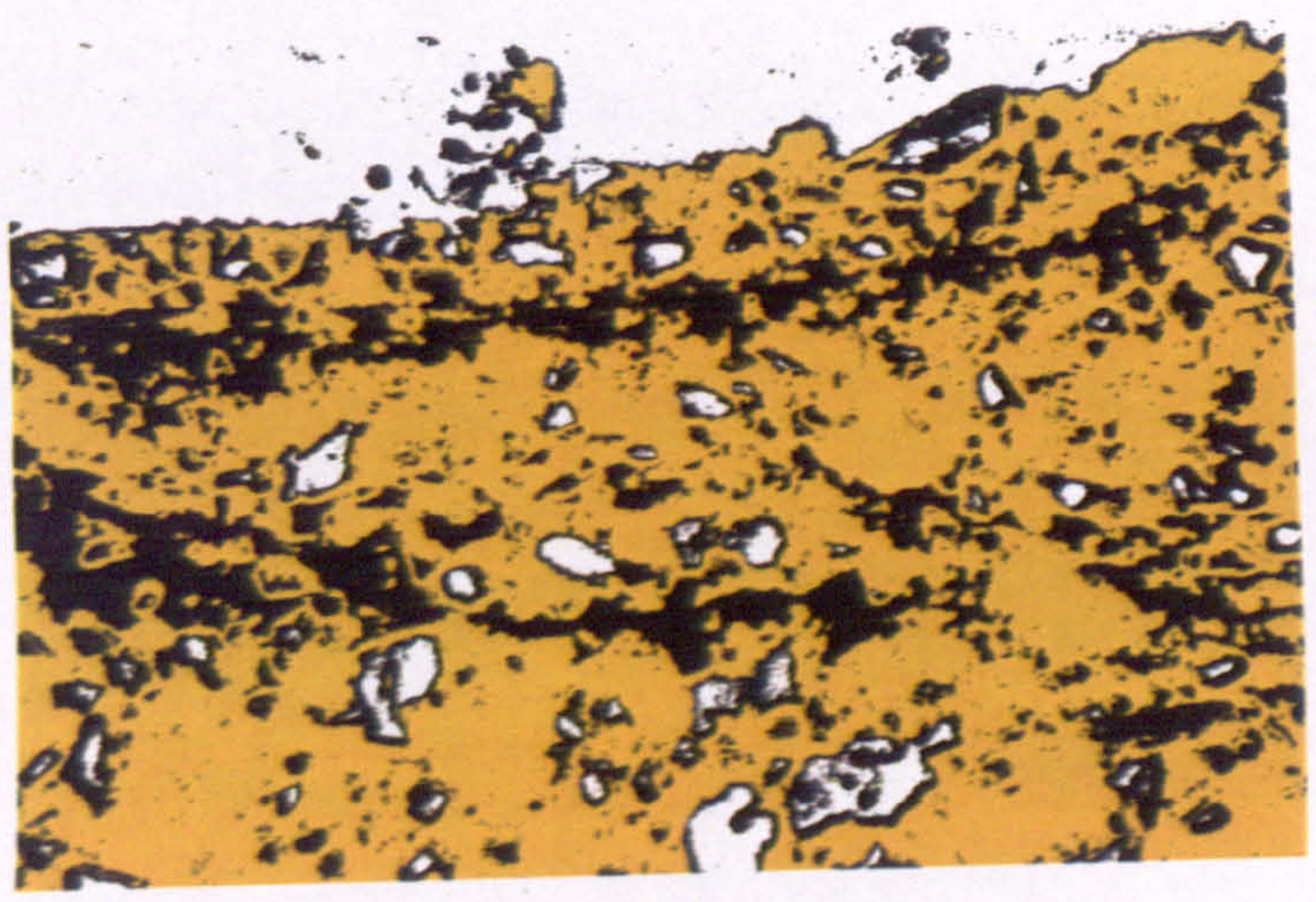

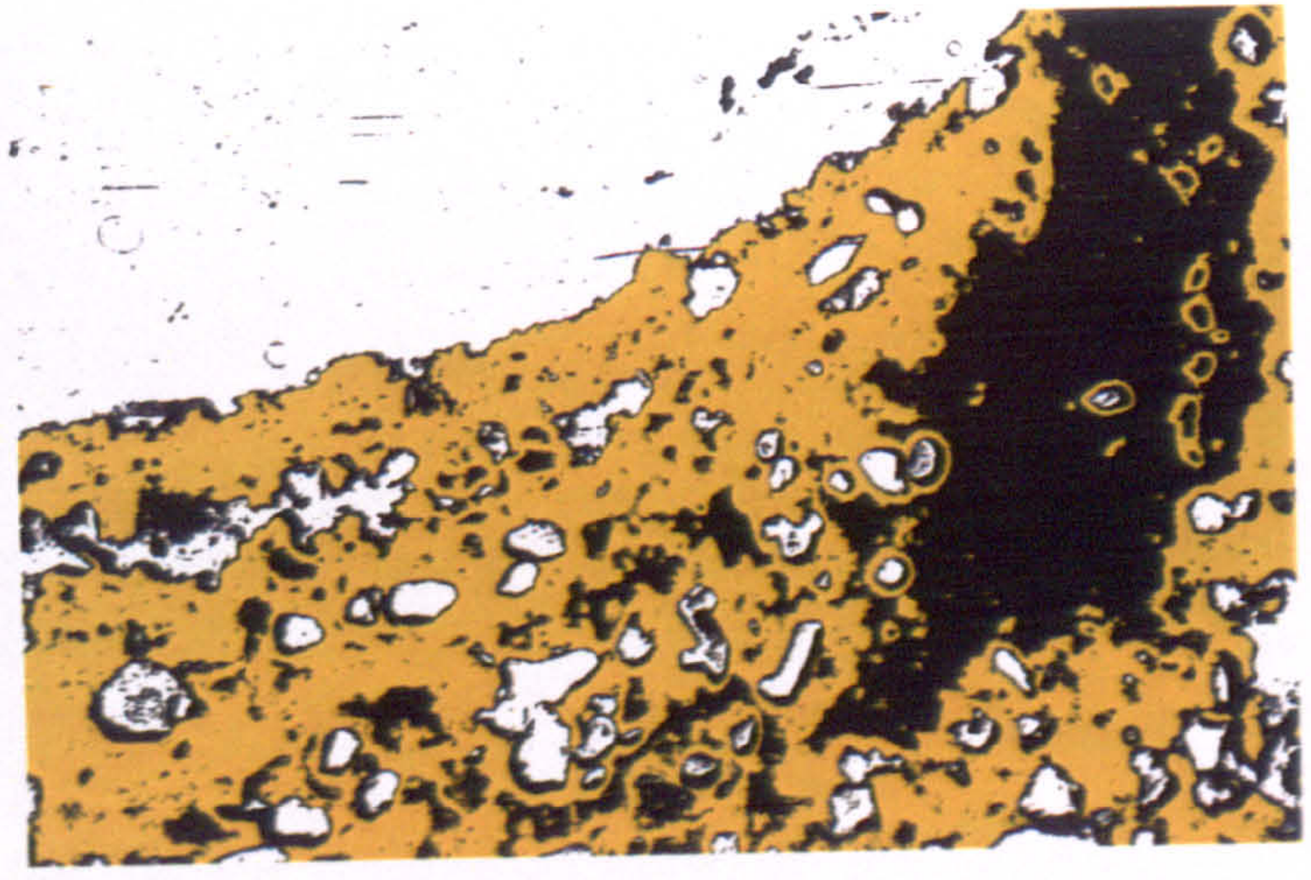

Plate 8.13: Thin-section photographs with their associated classifications at $t = 60$ minutes

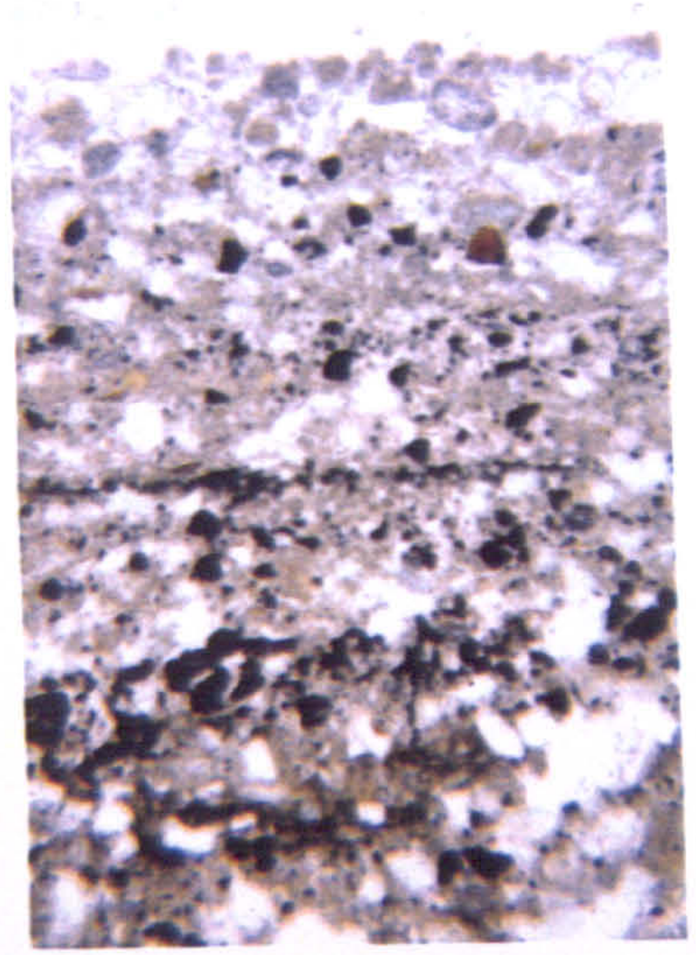

200 µm

Hematite: t = 60 (a)

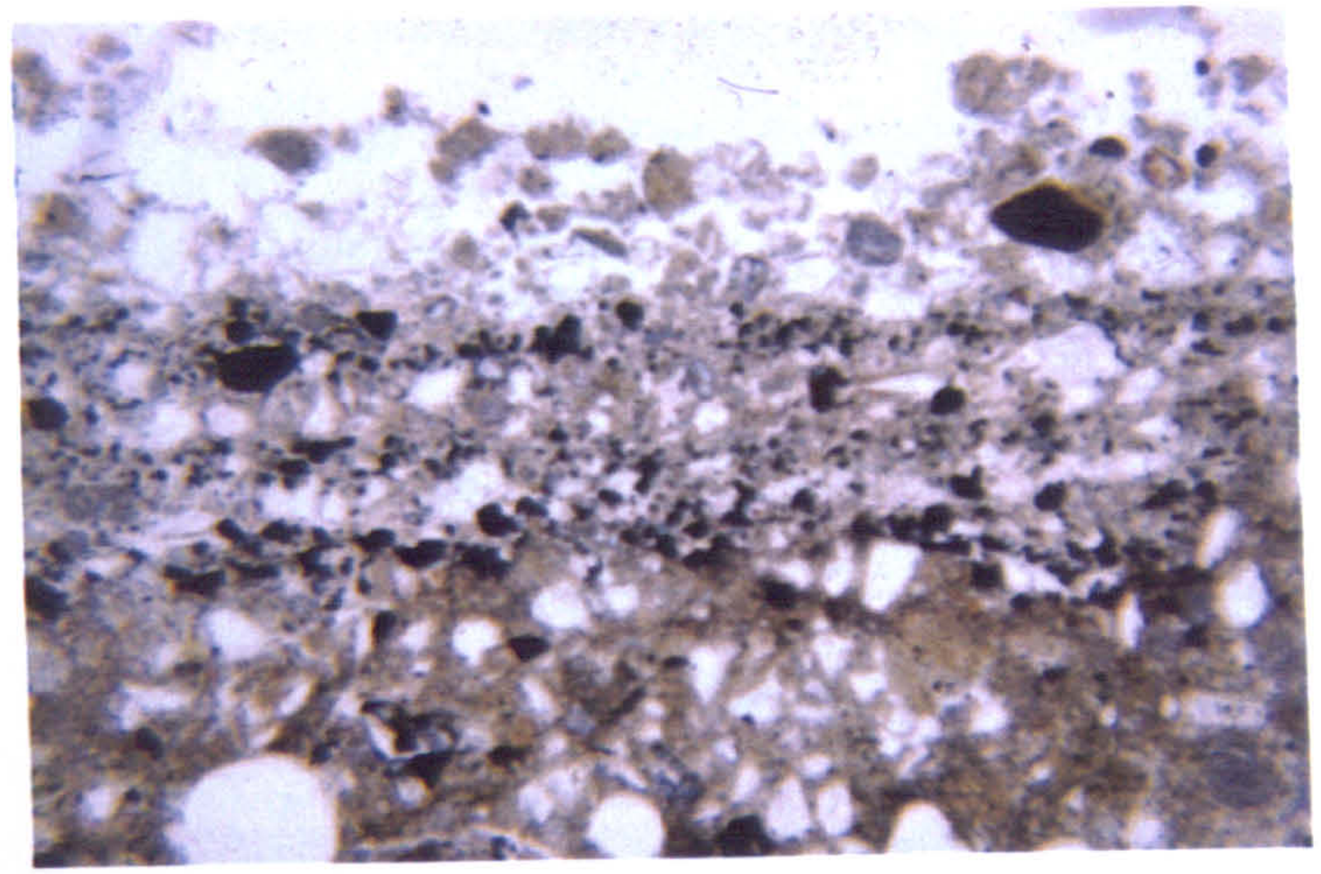

200 µm

Hematite: t = 60 (b)

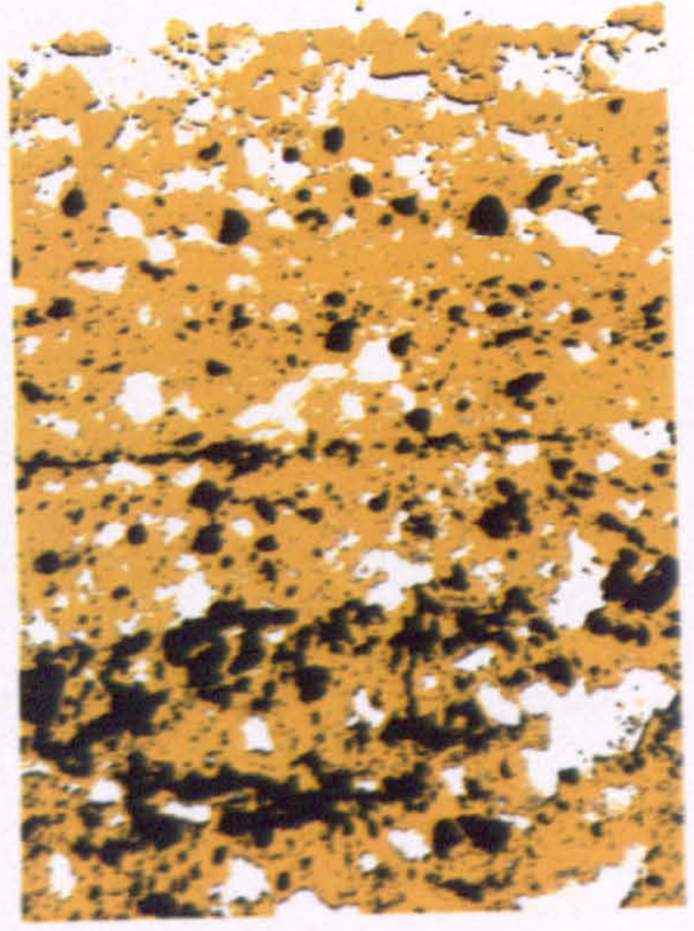

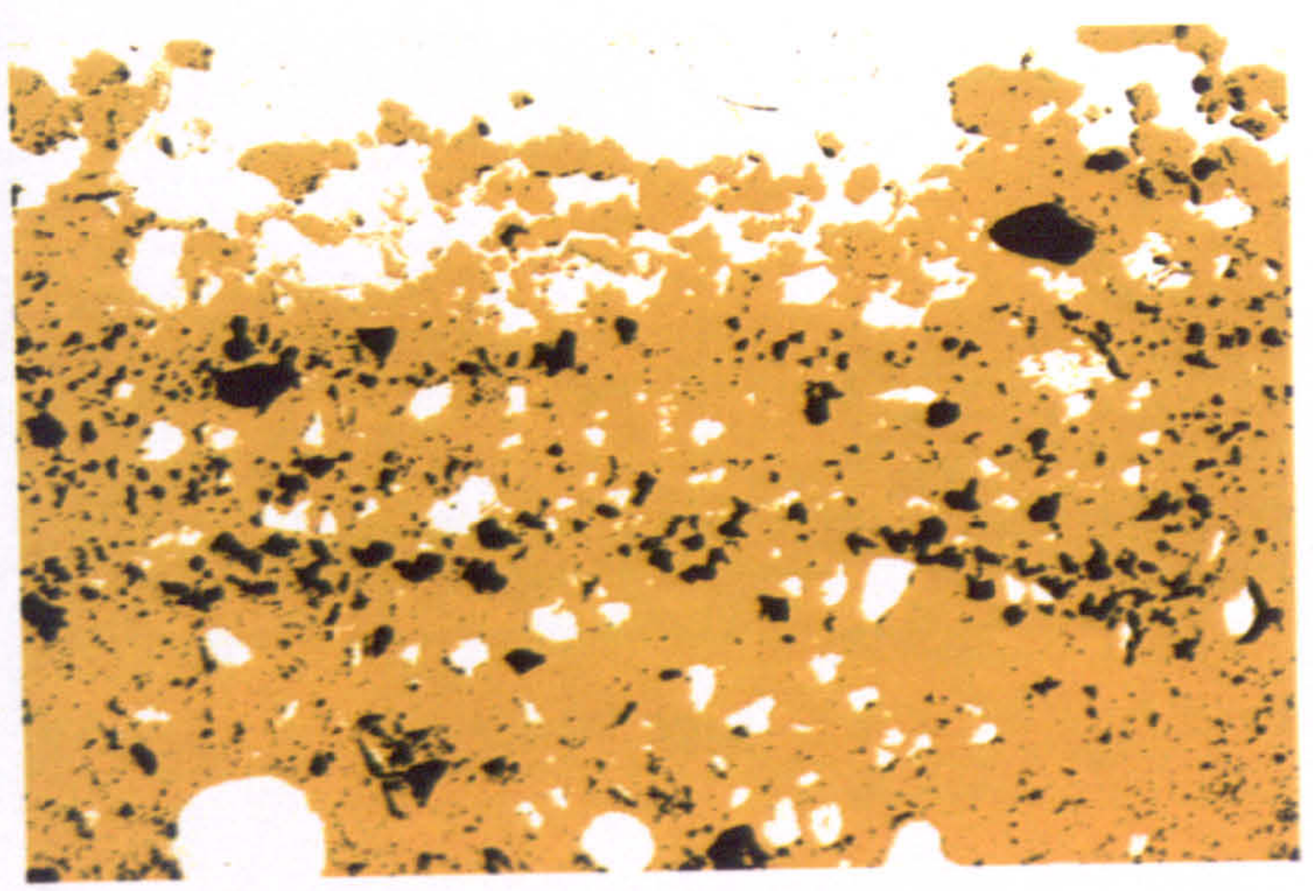

Plate 8.14: Thin-section photographs with their associated classifications at $t = 90$ minutes

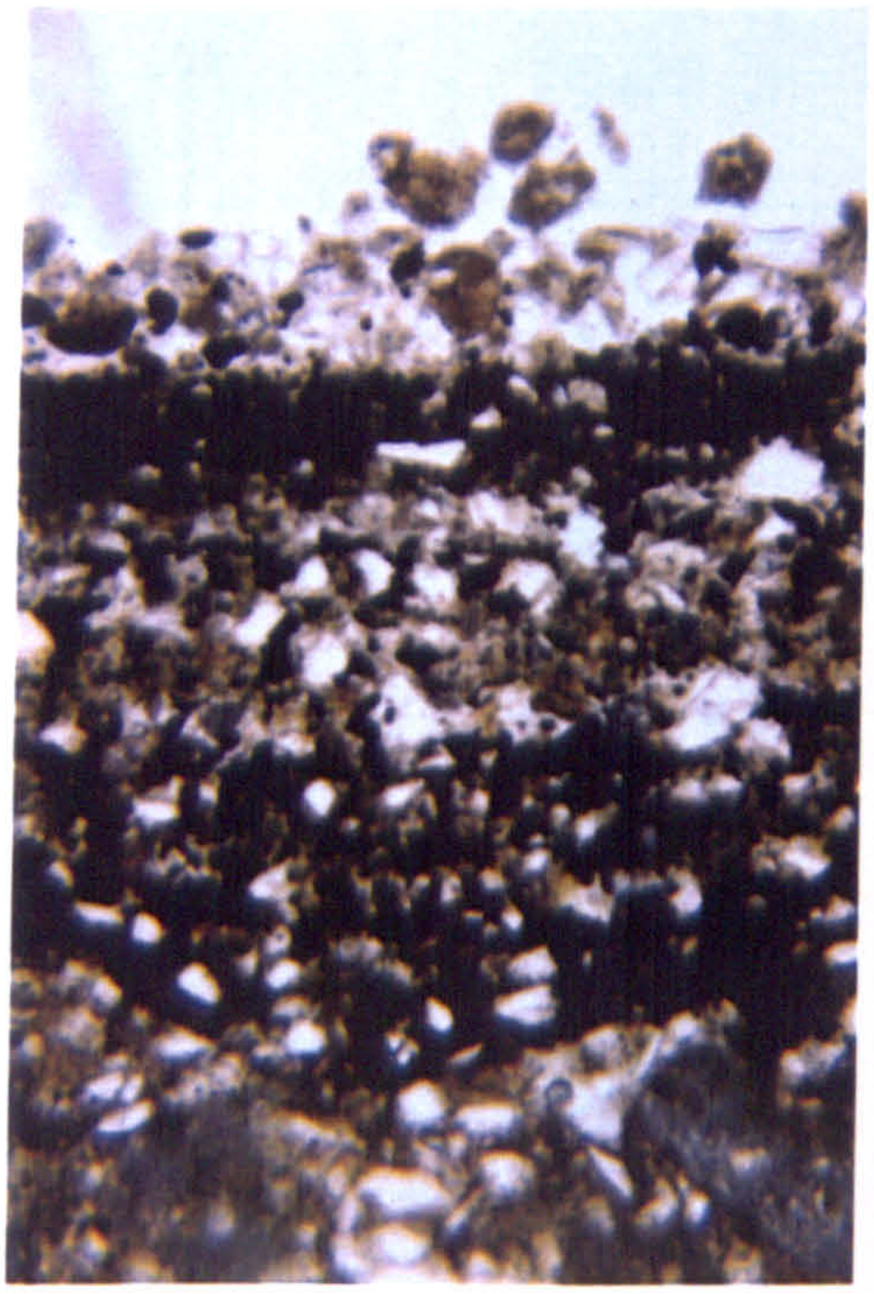

Hematite: t = 90 (a)

200 μm

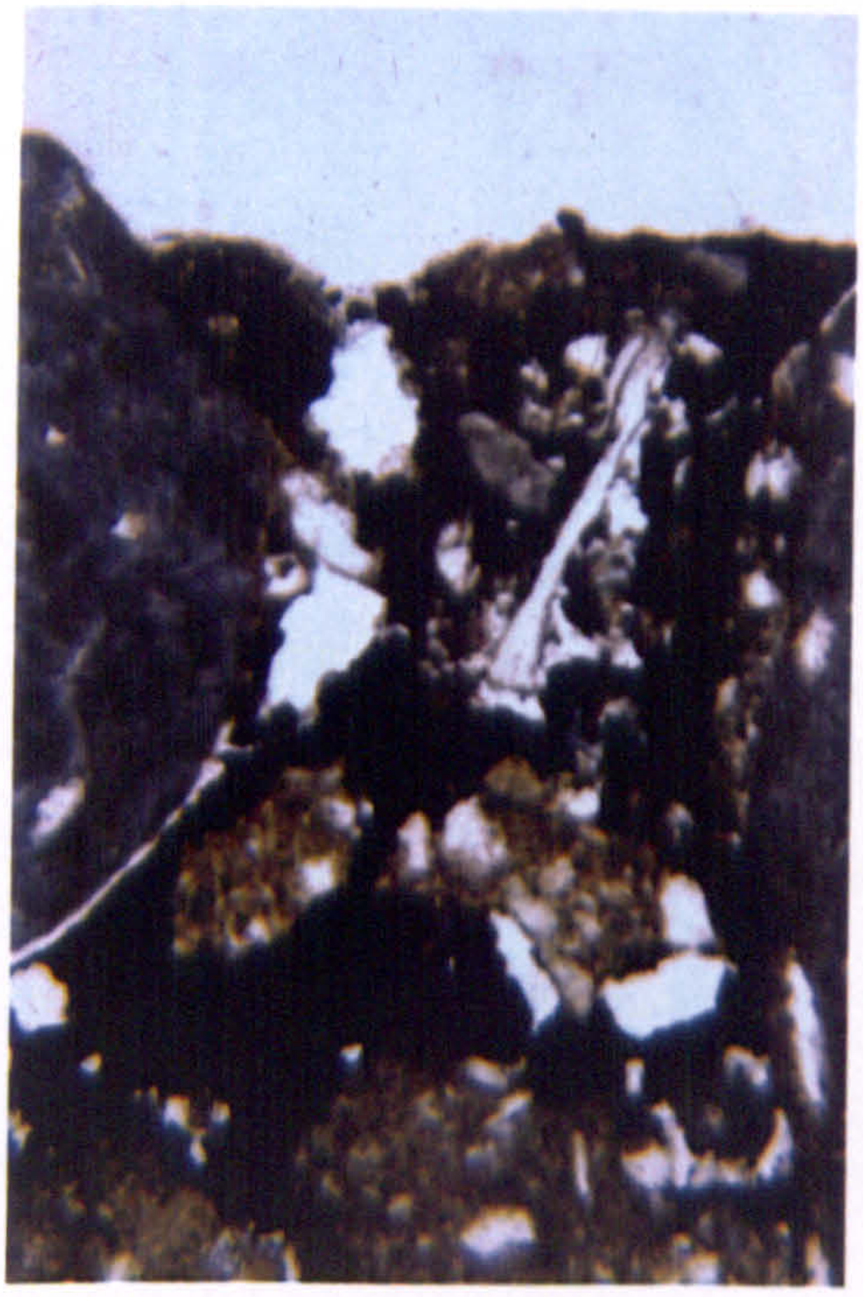

Hematite: t = 90 (b)

200 μm

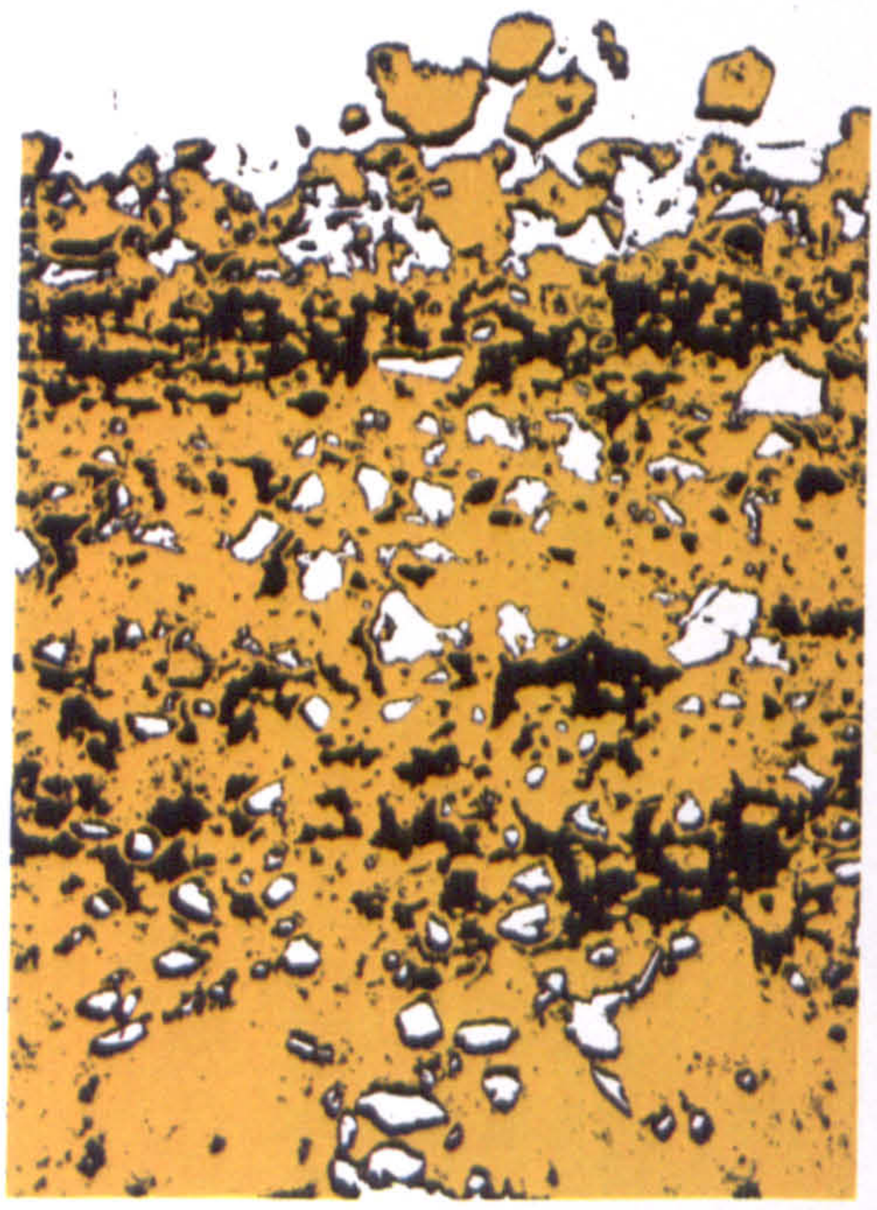

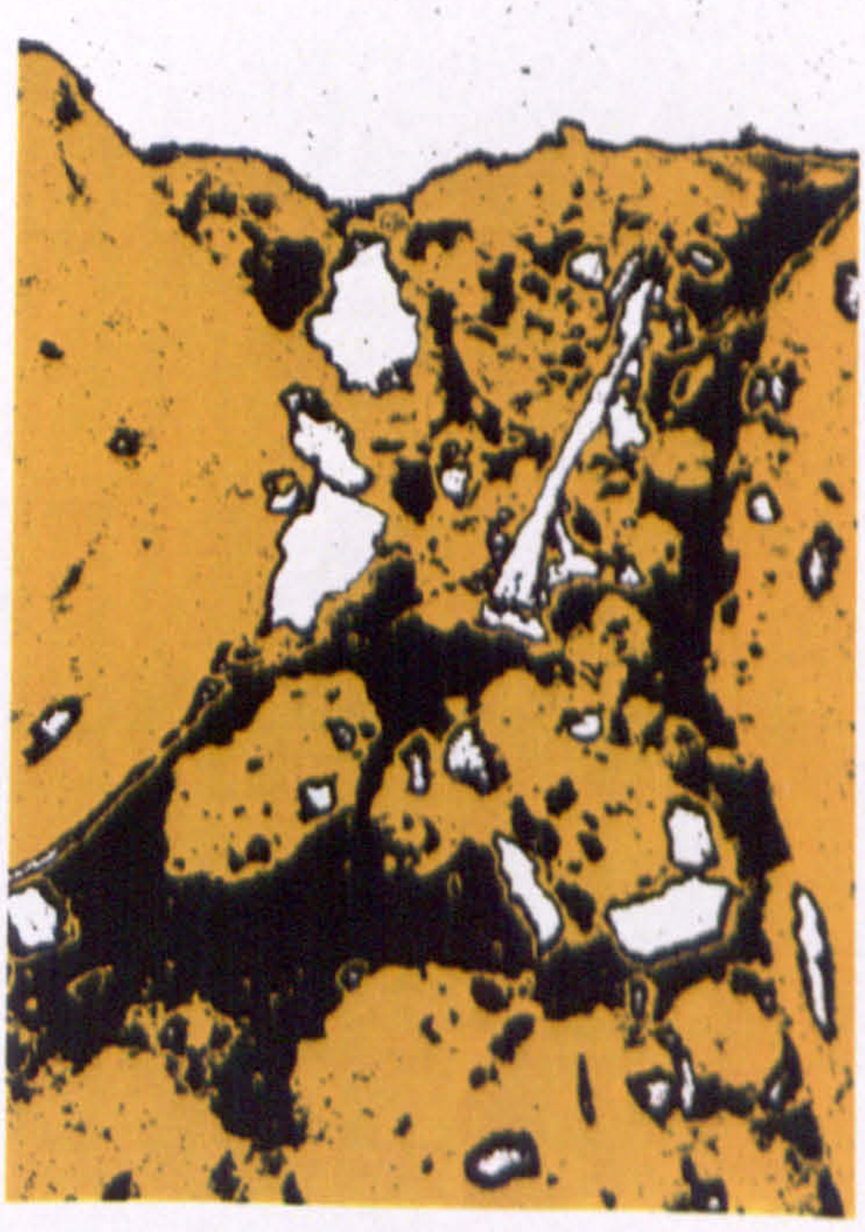

Plate 8.15: Thin-section photographs with their associated classifications at $t = 90$ minutes

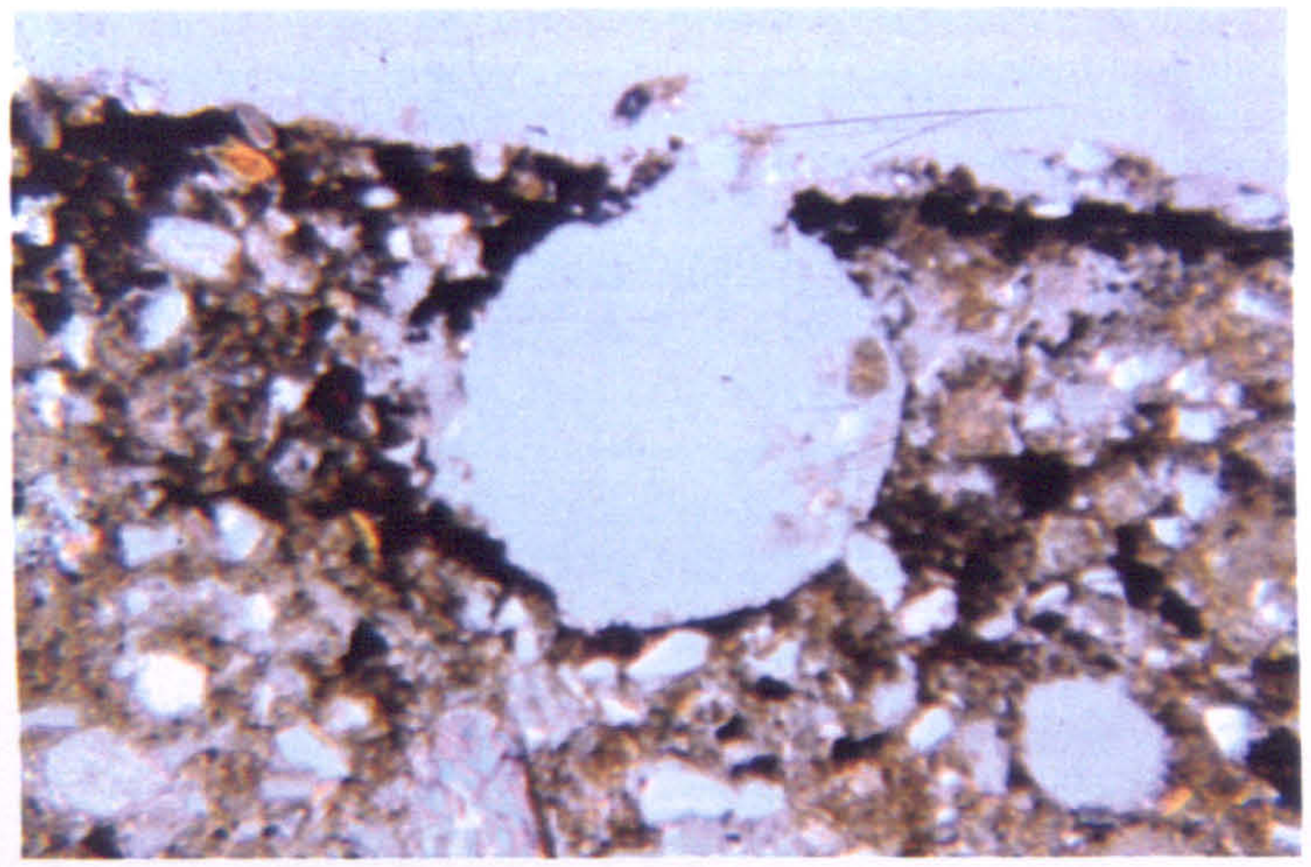

Hematite: t = 90 (c)

200 µm

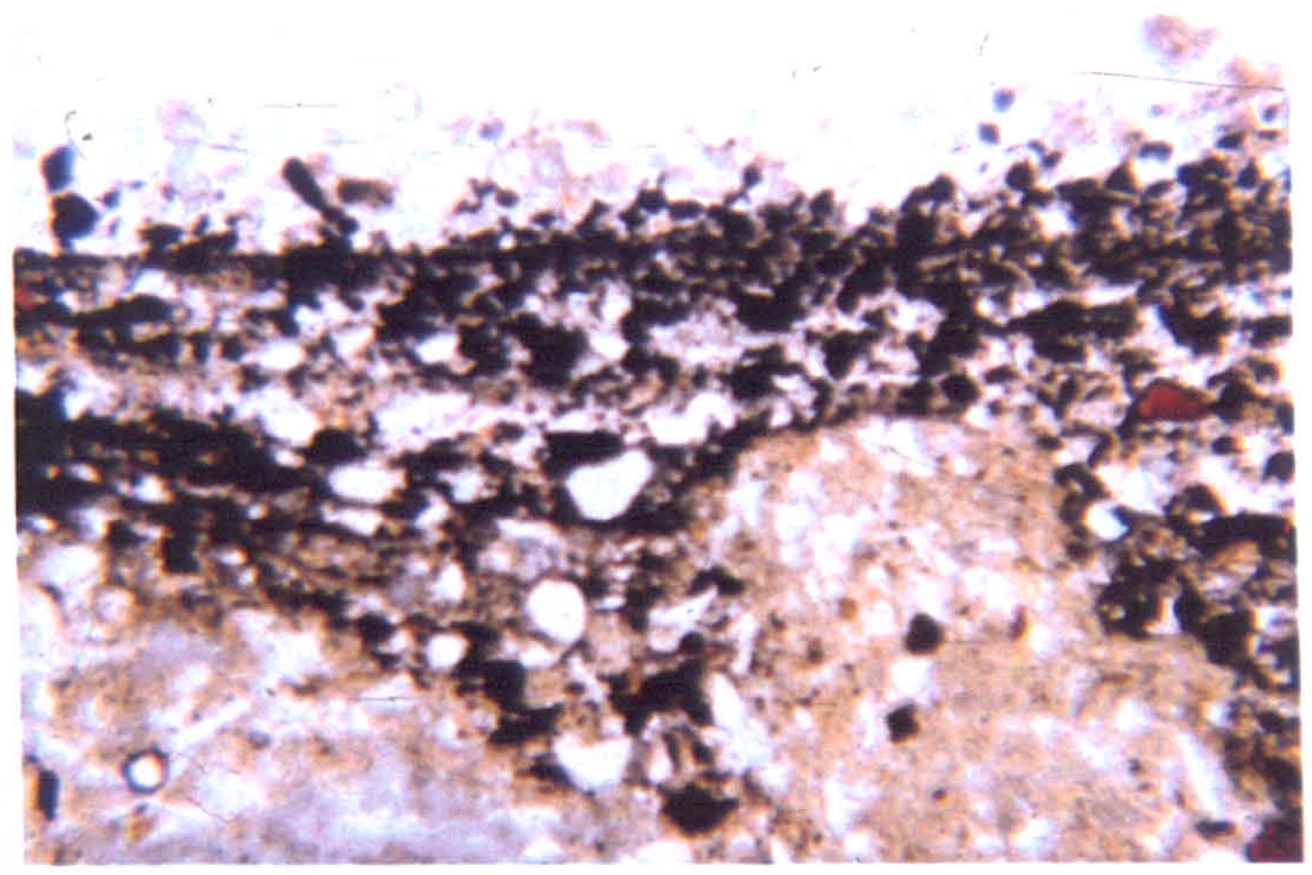

Hematite: t = 90 (d)

200 µm

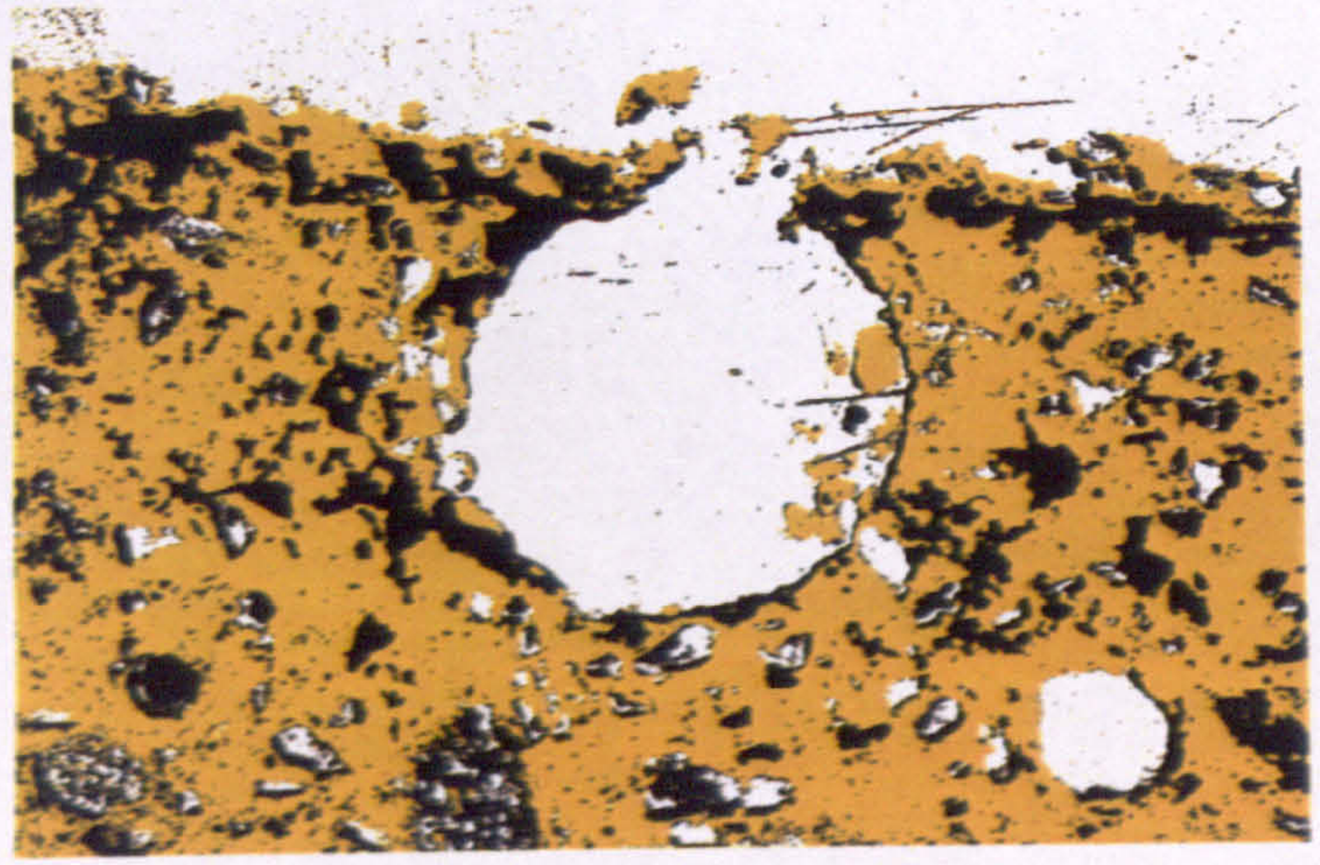

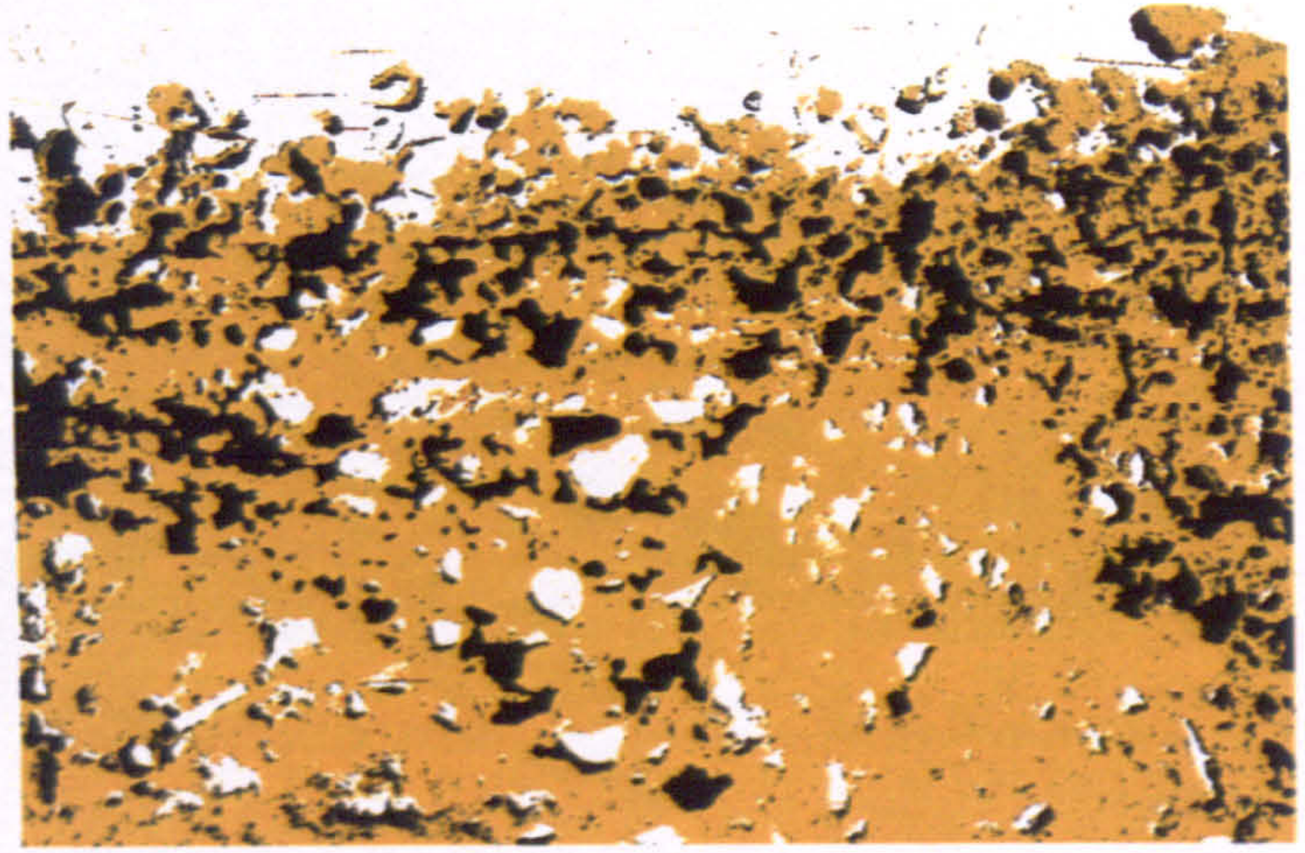

Plate 8.16: Thin-section photographs from the plot prepared with talc

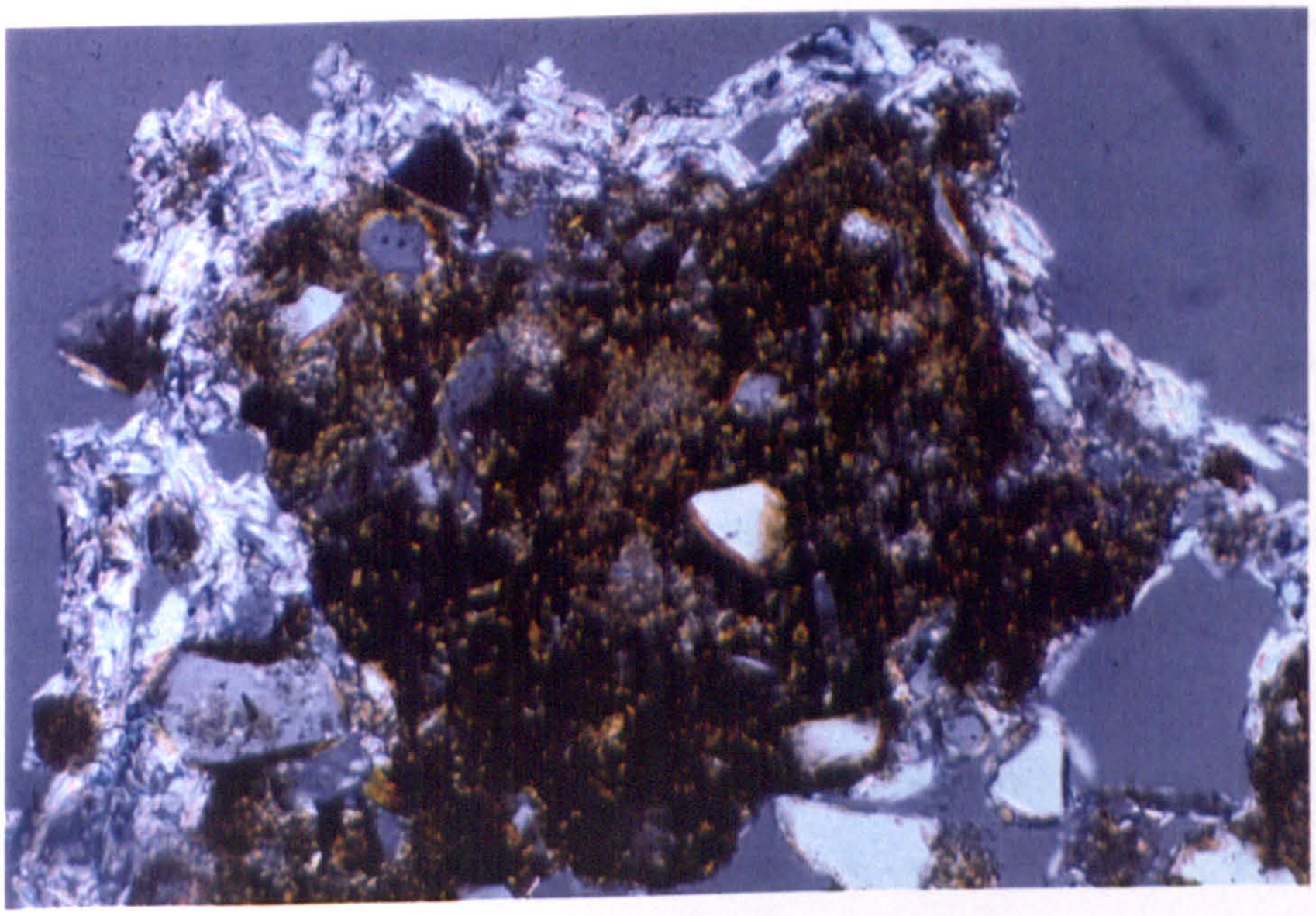

Talc: t = 15 (XPL)

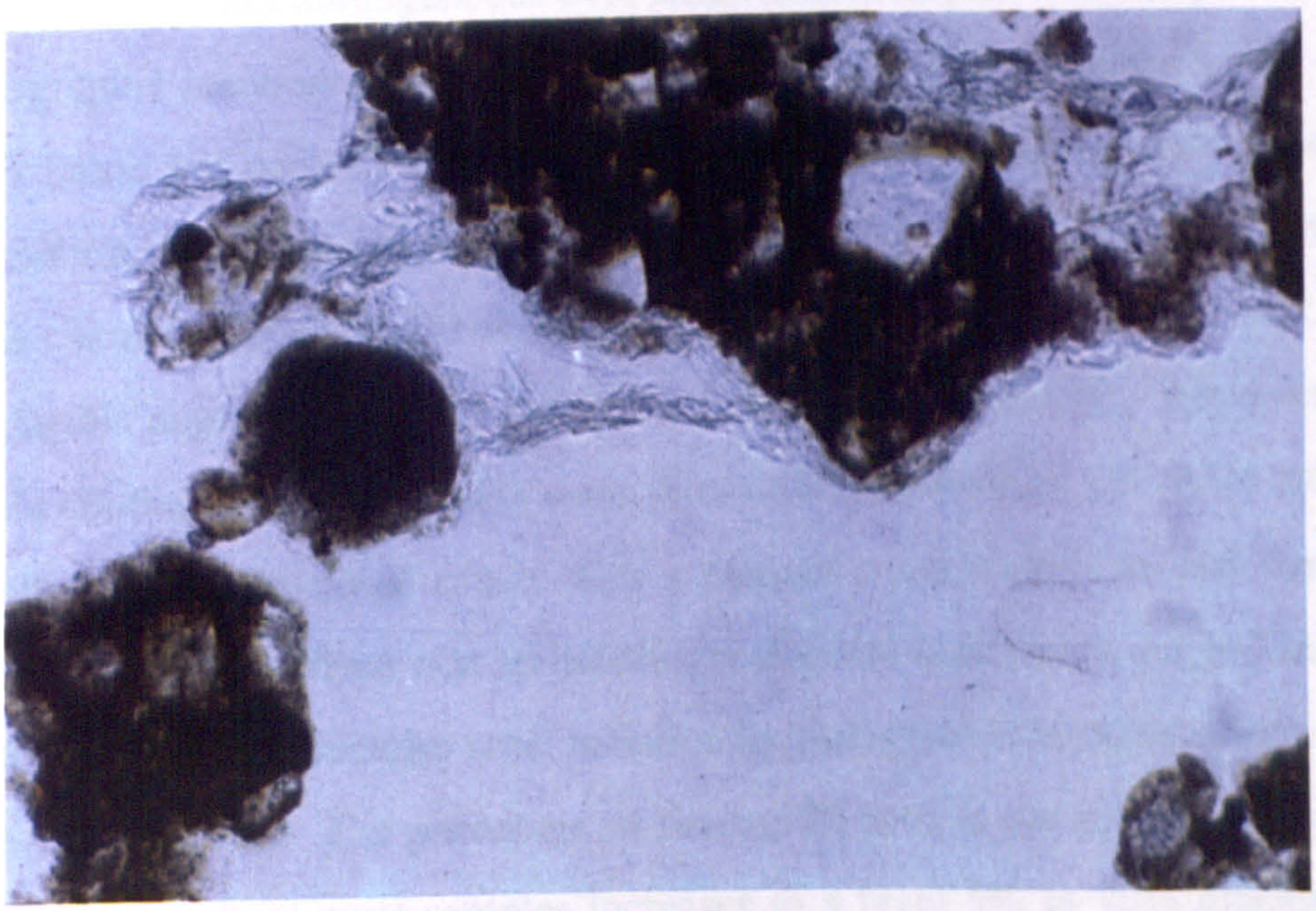

Talc: t = 30 (PPL)

8.6 CONCLUSION

Micromorphology is a technique which is under-used in geomorphology despite its ability to distinguish erosional and depositional processes. In addition, the use of physical tracers, which can be clearly identified under the microscope, can be invaluable in determining the way in which surface sediment has been transported during a rainfall event. In soil science, as Bielders *et al.* (1996) correctly observe, there is little or no account of the topographic position at any scale. The combination, therefore, of a combined geomorphological and micromorphological approach is exciting in that the spatial distribution of crusts can be explained by the micro-topography and the associated processes which are acting at that scale. The spatial distribution of crusts over small areas is of vital importance because it increases our ability to model infiltration and runoff. With an increasing move towards highly detailed DEMs and associated fractal modelling the information provided in this chapter allows a better constraint upon the process dynamics at the fine scale.

Soil crusts are not homogeneous over small spatial scales. This chapter considers the topographic location of the surface crust and its relation to fundamental changes in their fabric and porosity. Most of the differences are associated with secondary crust formation. Initially, structural crusts form at all points along the ridge-furrow profile with characteristically large vesicles and a very fine-grained surface seal. Given the negligible aggregate stability, these form almost immediately. However, as a rain event continues, or as irrigation water flows over the surface, the crusts on the furrow flanks become erosional crusts with a distinct modification in seal density and a change in porosity from non-connecting vesicles to connecting vughs. In the furrow base, the original structural crust is buried by fine-grained laminae which constitute a depositional crust. The pecentage of fines (<20 μm) in the particle size distribution of the furrow base crust samples increases to a level 5% to 10% greater than other positions on the ridge-furrow sequence. The composition of the structural crust is not necessarily destroyed, but the permeability of the surface changes as the porosity becomes dominated by cracks rather than pores.

Pore size, shape and connectivity analysis is of fundamental importance to the modelling of infiltration. High porosity does not necessarily lead to high permeability. This is clearly shown in section 8.4.1 where the ridge samples have large vesicles which are unconnected and would therefore give a low rate of infiltration. The thicker depositional crusts, despite their characteristic fine-grained nature, have a developed crack network with a much higher connectivity. The porosity is often much less, but the permeability is likely to be greater.

To observe the movement of fine material into the soil profile during crust formation, a hematite tracer ground to 20-63 μm was used. By spreading it over the soil surface, the redistribution of the tracer during a rainfall event could be monitored using micromorphological analysis. Hematite has not been used before as a tracer for the investigation of downward movement of fines, but because of its isotropy, it presents a very striking visual impact. Hematite is not without its problems, especially in terms of density, but by looking at the position of other heavy minerals within the soil profile, it is argued that its use is valid.

The results from the hematite tracer show how infiltration is affected by the presence of small rock fragments, i.e. smaller than the threshold value of 26 mm given by Wilcox *et al.* (1988). Hematite clearly flows rapidly around the edges of the rock fragments suggesting that as the surface seals, runoff is quickly generated and turbid flow into the soil is preferentially oriented to the boundaries of embedded fragments. This would seem to contradict the view that embedded fragments promote runoff rather than infiltration (Poesen, 1986a; Poesen *et al.*, 1990). What is more likely, especially in the fine-grained soil of the Badia, is that the fines are rapidly entrained as the seal develops and runoff is initiated. The water charged with silt-sized grains preferentially infiltrates between rock fragments and the developing seal. However, the very process of turbid infiltration actually causes the plugging of the infiltration route as the silt settles out. Infiltration is therefore reduced and runoff is increased.

There is clear evidence that washing-in takes place during the formation of structural as well as depositional crusts. The surface layer of hematite seems to be already stable by 30 minutes and does not change much in the following 60 minutes. The

form of the crust resembles that of a sieving structural crust (Valentin & Bresson, 1992), which is made up of a layer of loose skeleton grains overlaying a much finer plasmic layer.

The second layer of hematite which seems to mark the base of washing-in of fines is not stable over space or time. There are some hematite particles between the plasmic layer below the surface and the base layer. This second layer has not been observed in structural crusts before, and it is suggested that these are sieving crusts where the coarse silt grains have washed down to the base of the crust. The depth, however, does not depend so much on initial aggregate size, but rather upon the force of the drop impact (Bielders & Baveye, 1995). The likely explanation for the difference in depth of the lower level is not because of variability in aggregate size (Farres, 1978), but rather because of differential drop impacts or drops with a higher kinetic energy.

There is great variability in crust-type depending on the interactions of the two major crust formation processes: raindrop impact and micro-scale movement of disaggregated fine material from topographic highs to lows. Understanding of micro-scale processes is limited, but using a tracer allows greater insight into the movement of fines in an arid environment. In the silty Badia soils, there is rapid erosion from microtopographic highs and subsequently deposited as depositional crusts with a depth of up to a millimetre. Within 30 minutes of rainfall there is a rapid reduction in the original roughness element.

9. CONCLUSION

This thesis has presented results from work carried out on soil degradation in the northern Badia of Jordan taking soil crusting, and its associated effects on water movements, as an illustration of the quality of the soil.

The aims of the research were as follows:

1. To sample soil crusts in order to monitor their effect upon the equilibrium of sediment dynamics at a hillslope and ridge-furrow scale.

2. To observe the effect that the crust has upon moisture storage within the surface layers of the soil and to explain the spatial characteristics which arise due to management practice and climatic variables.

3. To monitor the effectiveness of a new, non-destructive, dielectric technique to examine moisture content in dryland soils.

4. To examine the effect of irrigation upon the surface characteristics of the surrounding soil, with special reference to the evaporation fluxes within the furrow and the associated precipitation of salts.

5. To investigate the role of small-scale topography upon the type of crust which forms in terms of both fabric and porosity.

6. To develop a new method of tracing fine material through the upper soil profile during crust formation using rainfall simulation and use it to monitor the movement of fines during crust formation and development.

9.1 ORIGINALITY OF THE RESEARCH

This thesis includes the following original contributions to knowledge.

This is the first study of surface soil characteristics in northern Jordan. Data have been provided which increase understanding on a number of issues. The pedogenesis has been elucidated using a combination of XRD, XRF and thin section mineralogy to fingerprint the soil and discover how it has evolved (section 7.2.1). It is clear that the formation of the Badia soils is not described adequately by the process of weathering of the basalt (Al-Homoud *et al.*, 1995). It is difficult to imagine how such weathering could have occurred in such a young landscape unless there was a much wetter climate in the past. The evidence for such a change in precipitation level was discussed (section 2.7) and has to be rejected. An interpretation of the environment and the data of section 7.2 lead to the conclusion that the soil has developed with contributions from the basalts and limestones of the Jebal Haurân, but the majority has clearly originated from the deserts of the Sahara or the Arabian Peninsula. This is fundamental to the research, because it explains why the general particle size distribution is dominated by the silt fraction.

Soil crusts are not homogeneous over small spatial scales. In considering the topographical location of the surface crust, not only can considerable changes in their particle size distribution be identified (section 7.3.3), but also fundamental changes in their fabric (section 8.3) and porosity (section 8.4.1) can be clearly established. Most of the differences are associated with secondary crust formation. Initially, structural crusts form at all points along the ridge-furrow profile with characteristically large vesicles and a very fine-grained surface seal. Given the negligible aggregate stability, these form almost immediately. However, as a rain event continues, or as irrigation water flows over the surface, the crusts on the furrow flanks become erosional crusts with a distinct modification in seal density and a change in porosity from non-connecting vesicles to connecting vughs. In the furrow base, the original structural crust is buried by fine-grained laminae which constitute a depositional crust. The pecentage of fines (<20 μm) in the particle size distribution of the furrow base crust samples increases to a level 5% to 10% greater than other positions on the ridge-furrow sequence. The composition of the structural crust is not necessarily destroyed, but the permeability of the surface changes as the porosity becomes dominated by cracks rather than pores.

Pore size, shape and connectivity analysis is of fundamental importance to the modelling of infiltration. High porosity does not necessarily lead to high permeability. This is clearly shown in section 8.4.1 where the ridge samples have large vesicles which are unconnected and would therefore give a low rate of infiltration. The thicker depositional crusts, despite their characteristic fine-grained nature, have a developed crack network with a much higher connectivity. The porosity is often much less, but the permeability is likely to be greater.

Research presented in this thesis has shown the effect irrigation water has upon the secondary development of crusts within the same sequence (section 7.3.4). There are important linkages between the wetting-bulb extent, the concentration of salts at the boundary of the wetting-bulb, the evaporation of water from the soil and the subsequent precipitation of salts at the surface. This process, although documented in the literature (Hillel, 1971; Bresler *et al.*, 1982), has not been taken further to identify the linkages with the secondary crust development or its ensuing effect on particle reorganisation and erosion. Such links between the physical and chemical processes occurring within the soil are often missing in the soil science literature, because of a lack of communication within the discipline, and yet it is of utmost importance that they are recognised.

There is a complex movement of water and dissolution of salts after irrigation which results in a crucial change in the crust morphology. The soil, being alkaline with a pH of more than 8, will readily exchange H^+ ions with the salts in the cation exchange sites. The dissolution of salts, and preferentially sodium, into the soil water causes salt precipitation at the soil surface as the water evaporates (section 7.3.4). The resulting crust has been classified in this work as a sodic evaporation crust. Sodium is the most destructive soil cation because it is most likely to cause clay dispersion: therefore, these types of crust characterise severe physical and chemical degradation. The physical consequence of the formation of a sodic evaporation crust is a 70% to 80% reduction in the clay and fine silt fraction of the soil. The clays, having dispersed at the soil surface, are rapidly deflated by the wind.

This thesis highlights the lack of work carried out on evaporation of water from soil crusts, because the water chemistry affects the crust structure in a totally different way from infiltrating water. Infiltrating water at specific levels of SAR and ESP is extremely well documented (sections 3.4.1 and 3.4.2), but nothing has apparently been written on the evaporation of saline water from soils and its effects on clay dispersion. Chapter 7 concludes that rather than causing pore clogging, the evaporation of sodic water causes dispersion of clay and fine silt which is then removed by erosion.

Until the completion of this work, evaporation through soil crusts was poorly understood and yet, in the context of soil moisture retention in dry land farming, it is very significant. The crust acts as a barrier to infiltration (section 3.6.1), but it has rarely been recognised that the crust can equally reduce evaporation from the soil. Various experiments were carried out to investigate how the crust affected the moisture levels of the soil beneath by developing a new method using a surface capacitance insertion probe (SCIP). Data are presented which compare the soil moisture before and after the crust is destroyed by ploughing (section 6.3.1) and it can be seen that within two weeks of ploughing, the moisture content is reduced to less than half of its value when crusted.

The relationship between micro-topography, the erosivity of rain and the wind direction was identified by Sharon *et al.* (1983) and Sharon *et al.* (1989), but the presence or otherwise of a soil crust was ignored. The ridges and furrows at the field-sites provided an ideal place to consider soil crusting. Crusts were seen to develop almost exclusively on the west-facing furrow slopes leaving the east-facing slopes uncrusted. Given that the aggregate stability is so low, the impact of drops on the east-facing furrow flanks must be negligible, which is accordant with the westerly wind direction during rain events (section 5.2.2). The fact that crusts develop on one side of the furrow allowed comparison of moisture contents across the furrow. The crusted side had a consistently higher moisture content and the difference was more evident at 5 cm depth rather than at 10 cm (section 6.3).

The SCIP has been introduced to geomorphological research and the potential advantages have been identified (section 6.1). It is a non-destructive technique for accurately measuring soil moisture, using the difference between the dielectric constants of soil and water to obtain a frequency measurement which can be calibrated to volumetric moisture content. Although the apparatus was unable to work at high soil salinities, it performed well in non-saline soils, allowing the accurate measurement of low moisture contents. In arid environments the need to discern small changes in moisture is important which means that this apparatus can be considered as a tool in equal standing with the more common Time Domain Reflectometry apparatus. The potential problem with soil salinity is easily noticeable, because it works to a threshold and then gives a very high dielectric constant, showing the operator that it has ceased to give an appropriate reading.

Rainfall simulation is an important tool for investigating the processes of soil crust formation (section 5.3). The rainfall variables, which are being modelled, often bear little relation to those of the environment under study. Therefore, a concerted effort was made to establish a good climate record for the northern Badia (section 5.2), before rainfall simulation variables were calculated (section 5.3.5). Having ascertained the likely rainfall characteristics of the region (section 5.2.4), a rainfall simulator was purpose-built and plots were located at the field site at Ash-rafiyya.

In order to observe the movement of fine material into the soil profile during crust formation, a hematite tracer was used which could be spread on the soil surface and then monitor the redistribution of the tracer during a rainfall event using micromorphological analysis. Hematite has not been used as a tracer for the investigation of downward movement of fines, but because of its isotropy, it presents a very striking visual impact (section 8.5.1). Hematite is not without its problems, especially in terms of density, but by looking at other elements in the soil micromorphology, it is argued that its use is valid (section 8.5.1). The option of changing the mean grain size, as Parsons *et al.* (1993) have done with magnetite, was thought inappropriate given the nature of the process.

The results from the hematite tracer show how infiltration is affected by the presence of small rock fragments, i.e. smaller than the threshold value of 26 mm given by Wilcox *et al.* (1988). Hematite clearly flows rapidly around the edges of the rock fragments suggesting that as the surface seals, runoff is quickly generated and turbid flow into the soil is preferentially oriented to the boundaries of embedded fragments. This would seem to contradict the view that embedded fragments promote runoff rather than infiltration (Poesen, 1986a; Poesen *et al.*, 1990). What is more likely, especially in the fine-grained soil of the Badia, is that the fines are rapidly entrained as the seal develops and runoff is initiated. The water charged with silt-sized grains preferentially infiltrates between rock fragments and the developing seal. However, the very process of turbid infiltration actually causes the plugging of the infiltration route as the silt settles out. Infiltration is therefore reduced and runoff is increased.

There is clear evidence that washing-in takes place during the formation of structural as well as depositional crusts. The surface layer of hematite seems to be already stable by 30 minutes and does not change much in the following 60 minutes. The form of the crust resembles that of a sieving structural crust (Valentin & Bresson, 1992), which is made up of a layer of loose skeleton grains overlaying a much finer plasmic layer.

The second layer of hematite which seems to mark the base of washing-in of fines is not stable over space or time. There are some hematite particles between the plasmic layer below the surface and the base layer. This second layer has not been observed in structural crusts before, and it is suggested that these are sieving crusts where the coarse silt grains have washed down to the base of the crust. The depth, however, does not depend so much on initial aggregate size, but rather upon the force of the drop impact (Bielders & Baveye, 1995). The likely explanation for the difference in depth of the lower level is not because of variability in aggregate size (Farres, 1978), but rather because of differential drop impacts or drops with a higher kinetic energy.

There is great variability in crust-type depending on the interactions of the two major crust formation processes: raindrop impact and micro-scale movement of disaggregated fine material from topographic highs to lows. Understanding of

micro-scale processes is limited, but using a tracer allows greater insight into the movement of fines in an arid environment. In the silty Badia soils, there is rapid erosion from microtopographic highs and subsequently deposited as depositional crusts with a depth of up to a millimetre. Within 30 minutes of rainfall there is a rapid reduction in the original roughness element.

9.2 THE EXTENSION OF PREVIOUS WORK

In terms of knowledge about the soils of the Badia, lying on the basalt plateau, this thesis represents the first detailed examination, beyond that of the Huntings soil surveys carried out over the past decade.

Sharon's work (Sharon *et al.*, 1983; Sharon *et al.*, 1989) on the effects of micro-climatology, and specifically incident rainfall, on soil erosivity, has been neglected in geomorphological research. The erosivity of rainfall, especially in arid environments where sediment is easily entrained, has a profound effect upon erosion, and therefore landscape evolution, at all scales. Chapter 6 takes this concept of erosivity and demonstrates its use in differential soil crust formation. Soil crusts will only develop on those slopes which are facing the wind-bearing rainfall. If the soil crust is as effective a moisture storage mechanism as the data suggest, then there are important implications for land management in terms of method and direction of ploughing.

There have been attempts to define stages of soil crust formation (Boiffin, 1986; Boiffin & Bresson, 1987; Bresson & Boiffin, 1990) and to classify the resulting forms in different environments (Bresson & Valentin, 1990) soil textures (Valentin and Bresson, 1992) and management practices (Pagliai, 1987; Bielders *et al.*, 1996). It has been acknowledged that one crust form will often develop over another (Boiffin & Bresson, 1987), but there has been no consideration of the evolution of the crust once it has formed except in terms of additional rainfall. Chapter 7 provides data on two important aspects of post-crust formation development. By comparing newly formed crusts with those that have formed during a previous season, it can be seen that the amount of fines incorporated within the crust is reduced over time by

wind action. The resulting crust becomes coarser over time and takes on the role of armouring the soil beneath. The soil crust, in this case, needs to be seen as a natural mechanism of soil protection rather than of degradation.

In addition to the effect of wind upon already established soil crusts, chapter 7 investigates the effect of changing soil and water chemistry on the soil crusts. The so-called sodic evaporation crust is a secondary development of the crust which profoundly affects the morphology and its propensity to be eroded, because of the interaction of cations and clays within the soil. Management practice, and especially the application of irrigation in arid soils, will have an important part to play in causing changes to the soil crust morphology.

Finally, the use of physical tracers has been limited (Parsons *et al.*, 1993), especially in the study of soil crusting. However, this thesis has demonstrated that such a method is extremely useful in determining the movement of specific particle size fractions. Using a tracer avoids the need to artificially produce soil crusts of a certain texture (Bielders & Baveye, 1995a; 1995b) and instead allows work to be carried out in the field. One area where this technique proves invaluable is within the debate over the effect of rock fragments at the soil surface. The hematite tracer shows that fines are rapidly entrained as the seal develops and runoff is initiated. Initially, the water charged with silt preferentially infiltrates along the rock fragment perimeter, but this very process actually causes the plugging of the route, thereby reducing infiltration over time. These observations illuminate the debate on the effectiveness of rock fragments in increasing infiltration (Collinet & Valentin, 1979; Poesen, 1986a; Wilcox, 1988; Poesen *et al.*, 1990; Bunte & Poesen, 1994).

9.3 FURTHER RECOMMENDATIONS

The following recommendations are intended to promote further research.

1. Soil formation in the Badia is a complex mixture of eolian and colluvial processes and weathering. In order to understand the genesis of the soil

further, it is necessary to conduct XRD and XRF examination on soils underlying different basalt types in order to constrain the basalt influence. SEM work would be additionally required to understand the transport mechanisms better. Opportunities to core in Qa Azraq or some other large qa would potentially combine with the soil fingerprinting to obtain a more precise picture of Holocene climate change, with special reference to increases in rainfall during past pluvials.

2. Hematite has proved to be a valuable way of tracing sediment down the soil profile during crust formation, but the use of painted quartz, which has a closer similarity to the surrounding soil, could improve the method of tracing sediment further. In addition, the experimentation could be expanded to include different rainfall intensities and a finer time resolution.

3. There is much potential to work on the modelling of evaporation through different types of soil crust. Monitoring of soil moisture below the crust, at various depths, should take place over a whole winter season coinciding with accurate rainfall data in order to increase understanding of the mechanisms involved. A mathematical model could then be constructed to describe the processes in detail. Such a model for dryland agriculture could lead to better agricultural practice, reducing the burden on the groundwater supplies.

4. Although the use of digital photography was eventually rejected in this work, there is a great potential for analysing a large number of thin sections or slices of polished blocks in a short time. As the pixel resolution of the digital cameras increase, there are possibilities of describing crust types and their associated porosity in three dimensions. In addition, as soil is increasingly viewed and described by fractal geometry (Anderson *et al.*, 1996), there is a greater need to increase the amount and resolution of data available in three dimensions to allow the modelling of the soil surface and the sub-surface and associated hydrological processes.

This thesis increases the general understanding of soil crusting processes in arid environments. Its contribution is important for the understanding of soil degradation in drylands and its conclusions bring greater clarity to the processes involved.

BIBLIOGRAPHY

Abed, A. M., Khory, H., Kruhl, J. H. 1985. On the structure of the Jebal Aritain volcano (N.E. Jordan) and the petrology of some xenoliths, *Dirasat*, **12**, pp. 109-124.

Aboujaoudé, A., Belleudy, P., Vauclin, M. 1991. A numerical study of infiltration through crusted soils: flat and other surface configurations, *Soil Technology*, **4**, pp. 1-18.

Abrahams, A. D., Parsons, A. J., Luk, S.-H. 1986. Field measurement of the velocity of overland flow using dye tracing, *Earth Surface Processes and Landforms*, **11**, pp. 653-657.

Abrahams, A. D., Parsons, A. J., Wainwright, J. 1995. Controls and determination of resistance to overland flow on semiarid hillslopes, Walnut Gulch, *Journal of Soil and Water Conservation*, **50**, pp. 457-460.

Abu-Sharar, T. M. 1988. Stability of soil aggregates as inferred from optical transmission of soil suspensions, *Soil Science Society of America Journal*, **52**, pp. 951-954.

Abu-Sharar, T. M. 1993. Effects of sewage sludge treatments on aggregate slaking, clay dispersion and hydraulic conductivity of a semi-arid soil sample, *Geoderma*, **59**, pp. 327-343.

Abu-Sharar, T. M. 1996. Modification of hydraulic properties of a semiarid soil in relation to seasonal applications of sewage sludge and electrolyte-producing compounds, *Soil Technology*, **9**, pp. 1-13.

Abu-Sharar, T. M., Bingham, F. T., Rhoades, J. D. 1987. Stability of soil aggregates as affected by electrolyte concentration and composition, *Soil Science Society of America Journal*, **51**, pp. 309-314.

Adams, J. E., Kirkham, D., Nielsen, D. R. 1957. A portable infiltrometer and physical measurements of soil in place, *Soil Science Society of America Proceedings*, **21**, p. 473.

Adler, W. F. 1979. The mechanics of liquid impact, in Preece, C. M. (Ed.), *Treatise on materials science and technology*, Academic Press, New York, pp. 127-183.

Aeby, P., Forrer, J., Steinmeier, C., Flühler, H. 1997. Image analysis for determination of dye concentrations in sand columns, *Soil Science Society of America Journal*, **61**, pp. 33-35.

Agassi, M., Shainberg, I., Morin, J. 1981. Effect of electrolyte concentration and soil sodicity on infiltration rate and crust formation, *Soil Science Society of America Journal*, **45**, pp. 848-851.

Agassi, M., Shainberg, I., Morin, J. 1985. Infiltration and runoff in wheat fields in the semi-arid region of Israel, *Geoderma*, **36**, pp. 263-275.

Agassi, M., Shainberg, I., Morin, J. 1990. Slope, aspect and phosphogypsum effects on runoff and erosion, *Soil Science Society of America Journal*, **54**, pp. 1102-1106.

Agnew, C. & Anderson, E. 1992. *Water resources in the arid realm*, Routledge, London.

Ahuja, L. R. 1983. Modelling infiltration into crusted soils by the Green-Ampt approach, *Soil Science Society of America Journal*, **47**, pp. 412-418.

Ahuja, L. R., Nofziger, D. L., Swartzendruber, D., Ross, J. D. 1989. Relationship between Green and Ampt parameters based on scaling concepts and field-measured hydraulic data, *Water Resources Research*, **25**, pp.1766-1770.

Ahuja, L. R. & Römkens, M. J. M. 1974. A similarity during early stages of rain infiltration, *Soil Science Society of America Proceedings*, **38**, pp. 541-544.

Al-Darby, A. M. 1996. The hydraulic properties of a sandy soil treated with gel-forming soil conditioner, *Soil Technology*, **9**, pp. 15-28.

Al-Durrah, M. & Bradford, J. M. 1981. New methods of studying soil development due to water drop impact, *Soil Science Society of America Journal*, 45, pp. 949-953.

Al-Durrah, M. & Bradford, J. M. 1982. The mechanism of raindrop splash on soil surfaces, *Soil Science Society of America Journal*, 46, pp. 1086-1090.

Al-Homoud, A. S., Allison, R. J., Sunna, B. F., White, K. 1995. Geology, geomorphology, hydrology, groundwater and physical resources of the desertified Badia environment in Jordan, *GeoJournal*, 37, pp. 51-67.

Al-Jayyousi, O. R. & Shatanawi, M. R. 1995. An analysis of future water policies in Jordan using decision support systems, *Water Resources Development*, 11, pp. 315-330.

Allison, R. J. 1996. Stress and strain in geomorphology, in Mäusbacher, R. & Schulte, A. (Eds.), *Beiträge zur Physiogeographie: Festschrift für Dietrich Barsch*, Heidelberger Geographische Arbeiten 104, Heidelberg, pp. 169-187.

Allison, R. J. 1997. Geomorphological processes: rates, relationships and return intervals. Plenary paper given at the *International Symposium on Engineering Geology and the Environment*, IAEG, Greece, 23-27th June.

Allison, R. J. & Higgitt, D. L. in press. Slope form and associations with ground surface boulder cover in the eastern Badia, Jordan, *Geomorphology*.

Allison, R. J., Al-Homoud, A. S., El-Sallag, M., Khattari, S., Malkawi, O., Sunna, B. F., Tuffaha, S., White, K. 1992. *Geomorphology and physical resources, Jordan Badia Research and Development Programme, Report No. 1*, Royal Geographical Society, London.

Allison, R. J., El-Rihani, A. T., Higgitt, D. L., Kirk, A. J. 1993a. *Geomorphology and physical resources - field report 11 September 1993*, Jordan Badia Research and Development Programme, Royal Geographical Society, London.

Allison, R. J., Higgitt, D. L., Longley, E. J., Warburton, J. 1993b. *Jordan Badia Research and Development Programme: Geomorphology and physical resources report No. 2, Fieldwork report 13th March to 12th April*, Royal Geographical Society, London.

Allmaras, R. R., Burwell, R. E., Holt, R. F. 1967. Plow layer porosity and surface roughness from tillage as affected by initial porosity and soil moisture at tillage time, *Soil Science Society of America Proceedings*, **31**, pp. 550-556.

Al-Omran, A. M., Shalaby, A. A., Mustafa, M. A., Al-Darby, A. M. 1990. Impact of water quality on crust strength of a gel-conditioned calcareous sandy soil, *Soil Technology*, **3**, pp. 57-62.

Altemüller, H. J. & van Vliet-lanoe, B. 1990. Soil thin section fluorescence microscopy, in Douglas, L. A. (Ed.), *Soil micromorphology: A basic and applied science*, Elsevier, Amsterdam, pp. 565-579.

Amézketa, E. & Aragüés, R. 1995. Hydraulic conductivity, dispersion and osmotic explosion in arid-zone soils leached with electrolyte solutions, *Soil Science*, **159**, pp. 287-293.

Amit, R. & Gerson, R. 1986. The evolution of Holocene reg (gravelly) soils in deserts - an example from the Dead Sea region, *Catena*, **13**, pp. 59-79.

Anderson, A. N., McBratney, A. B., FitzPatrick, E. A. 1996. Soil mass, surface, and spectral fractal dimensions estimated from thin section photographs, *Soil Science Society of America Journal*, **60**, pp. 962-969.

Andrews, I. J. 1992. *Cretaceous and Paleogene lithostratigraphy in the subsurface of Jordan*, Subsurface Geology Bulletin, Natural Resources Authority, Jordan.

Ansoult, M., De Backer, L. W., Declercq, M. 1984. Statistical relationship between apparent dielectric constant and water content in porous media, *Soil Science Society of America Journal*, *48*, pp. 47-50.

Arndt, W. 1965. The impedence of soil seals and the forces of emerging seedlings, *Australian Journal of Soil Science*, **3**, pp.55-68.

Arora, H. S. & Coleman, N. T. 1979. The influence of electrolyte concentration on flocculation of clay suspensions, *Soil Science*, **127**, pp. 134-139.

Arrhenius, G. & Bonatti, E. 1965. Neptunism and volcanism in the ocean, *Progress in Oceanography*, **3**, pp. 7-22.

Arshad, M. A. & Mermut, A. R. 1988. Micromorphological and physico-chemical characteristics of soil crust types in northwestern Alberta, Canada, *Soil Science Society of America Journal*, **52**, pp. 724-729.

Barberi, F., Capaldi, G., Gasperini, P., Marinelli, G., Santacroce, R., Scandone, R., Treuil, M., Varet, J. 1979. *Recent basaltic volcanism of Jordan and its implications on the geodynamic history of the Dead Sea shear zone*, International Symposium of the Geodynamic Evolution of the Afro-Arabian Rift System, Rome. pp. 667-682.

Bar-Matthews, M., Ayalon, A., Kaufman, A., 1997. Late Quaternary paleoclimate in the eastern Mediterranean region from stable isotope analysis of speleotherms at Soreq Cave, Israel, *Quaternary Research*, **47**, pp. 155-168.

Barnes, O. K. & Costel, G. 1957. A mobile infiltrometer, *Agronomy Journal*, **49**, p. 105.

Baruch, U. 1994. The late Quaternary pollen record in the Near East, in Bar-Yosef, O. & Kra, R. S. (Eds) *Late Quaternary chronologies and paleoclimates of the eastern Mediterranean*, Radiocarbon, Tucson, pp. 103-119.

Bar-Yosef, O. & Kra, R. S. (Eds) *Late Quaternary chronologies and paleoclimates of the eastern Mediterranean*, Radiocarbon, Tucson.

Baumhardt, R. L., Wendt, C. W., Keeling, J. W. 1992. Chisel tillage, furrow diking and surface crust effects on infiltration, *Soil Science Society of America Journal*, **56**, pp. 1286-1291.

Beaumont, P. & Atkinson, K. 1969. Soil erosion and conservation in northern Jordan, *Journal of Soil and Water Conservation*, **24**, pp. 144-146.

Beheiry, S. A. 1969. Geomorphology of central eastern Jordan, *Bulletin Société Géographie d'Egypte*, **42**, pp. 5-22.

Bender, F. 1968. *Geologie von Jordanien: Beitrage zur regionen der Erde*, Band 7, Bornträger, Berlin.

Bender, F. 1975. *Geology of the Arabian Peninsula: Jordan*, United States Geological Survey Professional Paper 560-I.

Ben-Hur, M., Shainberg, I., Bakker, D., Keren, R. 1985. Effect of soil texture and $CaCO_3$ content on water infiltration in crusted soils as related to water salinity, *Irrigation Science*, **6**, pp. 281-294.

Ben-Hur, M., Shainberg, I., Morin, J. 1987. Variability of infiltration in a field with surface seal soil, *Soil Science Society of America Journal*, **51**, pp. 1299-1302.

Ben-Hur, M., Letey, J., Shainberg, I. 1990. Polymer effects on erosion under laboratory rainfall simulator conditions, *Soil Science Society of America Journal*, **54**, pp. 1092-1095.

Bertrand, A. R. & Parr, J. F. 1961. Development of a portable sprinkling infiltrometer, *International Society of Soil Science, 8th Congress Transactions* **1**, p. 433.

Betts, A. V. G. (Ed.) 1991. *Excavations at Jawa 1972-1986*, Edinburgh University Press, Edinburgh.

Betts, A. V. G. 1992. Eastern Jordan: Economic choices and site location in the Neolithic periods, in Hadidi, A. (Ed.), *Studies in the history and archaeology of Jordan*, Department of Antiquities, Amman, pp. 111-114.

Betzalel, I., Morin, J., Benyamini, Y., Agassi, M., Shainberg, I. 1995. Water drop energy and soil seal properties, *Soil Science*, **159**, pp. 13-22.

Bielders, C. L. & Bavaye, P. 1995. Processes of structural crust formation on coarse-textured soils, *European Journal of Soil Science*, **46**, pp. 221-232.

Bielders, C. L. & Baveye, P. 1995. Vertical particle segregation in structural crusts: experimental observations and the role of shear strain, *Geoderma*, **67**, pp. 247-261.

Bielders, C. L., Baveye, P., Wilding, L. P., Drees, L. R., Valentin, C. 1996. Tillage-induced spatial distribution of surface crusts on a sandy paleustult from Togo, *Soil Science Society of America Journal*, **60**, pp. 843-855.

Biggar, J. & Nielsen, D. R. 1976. Spatial variability of the leaching characteristics of a field soil, *Water Resources Research*, **12**, pp. 78-84.

Black, P. E. 1970. Runoff from watershed models, *Water Resources Research*, **6**, p. 465-477.

Black, P. E. 1972. Hydrograph responses to geomorphic model watershed characteristics and precipitation variables, *Journal of Hydrology*, **17**, p. 309-329.

Blackburn, W. H. 1975. Factors influencing infiltration and sediment production of semiarid rangelands in Nevada, *Water Resources Research*, **11**, pp. 929-937.

Blackburn, W. H., Meeuwig, R. O., Skau, C. M. 1974. A mobile infiltrometer for use on rangeland, *Journal of Range Management*, **27**, p. 322.

Blanchard, D. C. 1950. Behaviour of water drops at terminal velocity, *Transactions of the American Geophysical Union*, **31**, pp.836-842.

Boers, T. M., Maduakor, H. O., Tee, D. P. 1988. Sheet erosion from a bare sandy soil in south eastern Nigeria, in Ijioma, C. I., Anaba, S., Boers, T. M. (Eds.), *Proceedings of the International Symposium on Erosion in S.E. Nigeria*, Federal University of Technology, Owerri, Nigeria, pp. 23-34.

Boers, T. M., van Deurzen, F. J. M. P., Eppink, L. A. A. J., Ruytenberg, R. E. 1992. Comparison of infiltration rates measured with an infiltrometer, a rainulator and a permeameter for erosion research in S.E. Nigeria, *Soil Technology*, **5**, pp. 13-26.

Boiffin, J. 1984. *La degradation structurale des couches superficielles du sols sous l'action des pluies,* Ph.D., L'institut National Agronomique, Paris-Grignon.

Boiffin, J. 1986. Stages and time-dependency of soil crusting in situ, in Callebaut, F., Gabriels, D., De Boodt, M. (Eds.), *Assessment of soil surface sealing and crusting.* ISSS/Flanders Research Center for Soil Erosion and Soil Conservation, Ghent, Belgium, pp. 91-98.

Boiffin, J. & Bresson, L. M. 1987. Dynamique de formation des croûtes superficielles: Apport de l'analyse microscopique, in Federoff, N., Bresson, L. M., Courty, M. A. (Eds.), *Micromorphologie des Sols*, L'association Française pour l'étude du sol, Plaisir, France, pp. 393-399.

Bond, J. J. & Willis, W. O. 1969. Soil water evaporation: surface residue rate and placement effects, *Soil Science Society of America Proceedings*, **33**, pp. 445-448.

Borselli, L., Biancalani, R., Giordani, C., Carnicelli, S., Ferrari, G. A. 1996a. Effect of gypsum on seedling emergence in a kaolinitic crusting soil, *Soil Technology*, **9**, pp. 71-81.

Borselli, L., Carnicelli, S., Ferrari, G. A., Pagliai, M., Lucamante, G. 1996b. Effects of gypsum on hydrological, mechanical and porosity properties of a kaolinitic crusting soil, *Soil Technology*, **9**, pp. 39-54.

Bouabid, R., Nater, E. A., Barak, P. 1992. Measurement of pore size distribution in a lamellar Bt horizon using epifluorescence microscopy and image analysis, *Geoderma*, **53**, pp. 309-328.

Bouma, A. H. 1969. *Methods for the study of sedimentary structures*, John Wiley & Sons, New York.

Bouma, J. & Kooistra, M. J. 1987. Soil micromorphology and soil water movement, in Federoff, N., Bresson, L. M., Courty, M. A. (Eds.), *Micromorphologie des sols*, L'association Française pour l'étude du sol, Plaisir, France, pp. 507-511.

Bouwer, H. 1986. Intake rate: cylinder infiltrometer, in Klute, A. (Ed.), *Methods of soil analysis. Part 1 Physical and mineralogical methods*, American Society of Agronomy, Agronomy 9, Madison, pp. 825-844.

Bowyer-Bower, T. A. S. 1993. Effects of rainfall intensity and antecedent moisture on the steady-state infiltration rate in a semi-arid region, *Soil Use and Management*, **9**, pp. 69-76.

Bradford, J. M. & Huang, C. 1992. Mechanisms of crust formation: Physical components, in Sumner, M. E. & Stewart, B. A. (Eds.), *Soil crusting: Chemical and physical processes*, Lewis, Boca Raton, pp. 55-72.

Bradford, J. M., Remley, P. A., Ferris, J. E., Santini, J. B. 1986. Effect of soil surface sealing on splash from a single waterdrop, *Soil Science Society of America Journal*, **50**, pp. 1547-1552.

Bradford, J. M., Ferris, J. E., Remley, P. A. 1987a. Interrill soil erosion processes. I: Effect of surface sealing on infiltration, runoff and splash detachment, *Soil Science Society of America Journal*, **51**, pp. 1566-1571.

Bradford, J. M., Ferris, J. E., Remley, P. A. 1987b. Interrill soil erosion processes. II: Relationship of splash detachment to soil properties, *Soil Science Society of America Journal*, **51**, pp. 1571-1575.

Brakensiek, D. L. & Rawls, W. J. 1982. *An infiltration based runoff model for a standardised 24-hour rainfall*, American Society of Agricultural Engineers, Paper No. 81-2504.

Brakensiek, D. L. & Rawls, W. J. 1982. Agricultural management effects on soil water processes. Part II: Green and Ampt parameters for crusting soils, *Transactions of the American Society of Agricultural Engineers*, **26**, pp1753-1757.

Brakensiek, D. L. & Rawls, W. J. 1994. Soil containing rock fragments: Effect on infiltration, *Catena*, **23**, pp. 99-110.

Brakensiek, D. L., Rawls, W. L., Hamon, W. R. 1979. Application of an infiltrometer system for describing infiltration into soils, *Transactions of the American Society of Agricultural Engineers*, **22**, pp. 320-325, 333.

Bresler, E. & Kemper, W. D. 1970. Soil water evaporation as affected by wetting methods and crust formation, *Soil Science Society of America Proceedings*, **34**, pp. 3-8.

Bresler, E., McNeal, B. L., Carter, D. L. 1982. *Saline and sodic soils*, Springer-Verlag, New York.

Bresson, L. M. & Boiffin, J. 1990. Morphological characterisation of soil crust development stages on an experimental field, *Geoderma*, **47**, pp. 301-325.

Bresson, L. M. & Valentin, C. 1990. Comparative micromorphological study of soil crusting in temperate and arid environments, *Transactions of the 14th International Congress on Soil Science VII, International Society of Soil Science*, pp. 238-243.

British Standards Institution 1990. *Methods of tests for soils for civil engineering purposes*, B.S.I.1377. H.M.S.O., London.

Brown, K. J. & Dunkerley, D. L. 1996. The influence of hillslope gradient, regolith texture, stone size and stone position on the presence of a vesicular layer and related aspects of hillslope hydrologic processes: A case study from the Australian arid zone, *Catena*, **26**, pp. 71-84.

Brubaker, S. C., Jones, A. J., Lewis, D. T., Frank, K. 1993. Soil properties associated with landscape position, *Soil Science Society of America Journal*, **57**, pp. 235-239.

Bruins, H. J. & Yaalon, D. H. 1979. Stratigraphy of the Neviot section in the desert loess of the Negev, *Act. Geology Academic Science of Hungary*, **22**, pp. 161-169.

Bryan, R. B. 1968. The development, use and efficiency of indices of soil erodibility, *Geoderma*, **2**, pp. 5-26.

Bryan, R. B. 1969. The relative erodibility of soils developed in the Peak District of Derbyshire, *Geografiska Annaler*, **51A**, pp. 145-159.

Bryan, R. B. 1974. A simulated rainfall test for the prediction of soil erodibility, *Zeitschrift für Geomorphologie, Supplement Band* **21**, pp. 138-150.

Bubenzer, G. D. 1979. *Rainfall characteristics important for simulation*, Proceedings of the rainfall simulator workshop, Tucson, Arizona. March 7-9, 1979. pp.22-34.

Bubenzer, G. D. & Jones, B. A. 1971. Drop size and impact velocity effects on the detachment of soils by simulated rainfall, *Transactions of the American Society of Agricultural Engineers*, **14**, p. 625.

Bui, E. N., Mazzullo, J. M., Wilding, L. P. 1989. Using quartz grain size and shape analysis to distinguish between aeolian and fluvial deposits in the Dallol Bosso of Niger (West Africa), *Earth Surface Processes and Landforms*, **14**, pp. 157-166.

Bullock, P., Fedoroff, N., Jongerius, A., Stoops, G., Tursina, T., Babel, U. (Eds.) 1985. *Handbook for soil thin section description*, Waine Research, Wolverhampton.

Bunte, K. & Poesen, J. W. A. 1994. Effects of rock fragment size and cover on overland flow hydraulics, local turbulence and sediment yield on an erodible soil surface, *Earth Surface Processes and Landforms*, **19**, pp. 115-135.

Burdon, D. J. 1959. *Handbook of the geology of Jordan*, Government of the Hashemite Kingdom of Jordan, Amman.

Burdon, D. J. 1982. Hydrogeological conditions in the Middle East, *Quarterly Journal of Engineering Geology*, **15**, pp. 71-82.

Butler, H. C. 1919. *Publication of the Princeton University Archaeological Expedition to Syria 1904-5 and 1909*, Division II, Section A, Architecture, South Syria, Leiden, .

Butzer, K. W. 1955. *Some aspects of postglacial climatic variation in the Near East considered in relation to movements of population*, M.Sc., McGill University, Montreal.

Butzer, K. W. 1958. *Quaternary stratigraphy and climate in the Near East*, Ferdinand Dümmlers Verlag, Bonn.

Butzer, K. W. 1975. Patterns of environmental change in the Near East during Late Pleistocene and Early Holocene times, in Wendorf, F. & Marks, A. E. (Eds.), *Problems in prehistory: North Africa and the Levant*, Dallas, Southern Methodist University Press, pp. 389-410.

Campbell, J. E. 1990. Dielectric properties and influence of conductivity in soils at one to fifty megahertz, *Soil Science Society of America Journal*, **54**, pp. 332-341.

Campbell, S. E., Seeler, J.-S., Glolubic, S. 1989. Desert crust formation and soil stabilisation, *Arid Soil Resource Rehabilitation*, **3**, pp. 217-228.

Carmi, I., Noter, Y., Schlesinger, R. 1971. Rehovot radio carbon measurements, *Department of Radio-Carbon*, **13**: 412-419.

Casenave, A. & Valentin, C. 1989. *Les États de Surface de la Zone Sahélienne. Influence sur l'infiltration*, ORSTROM Collection "didactiques", Paris.

Casenave, A. & Valentin, C. 1992. A runoff capability classification system based on surface features criteria in the arid and semi-arid areas of West Africa, *Journal of Hydrology*, **130**, pp. 231-249.

Chartres, C. J. & Mücher, H. J. 1989. The effects of fire on the surface properties and seed germination in two shallow monoliths from a rangeland soil subjected to simulated raindrop impact and water erosion, *Earth Surface Processes and Landforms*, **14**, pp. 407-417.

Chen, Y., Tarchitzky, J., Morin, J., Banin, A. 1980. Scanning electron microscope observation on soil crusts and their formation, *Soil Science*, **130**, pp. 49-55.

Chiang, S. C., Radclliffe, D. E., Miller, W. P. 1993. Hydraulic properties of surface seals in Georgia soils, *Soil Science Society of America Journal*, **57**, pp. 1418-1426.

Chiou, W. A., Shephard, L. E., Bryant, W. R., Looney, M. P. 1983. A technique for preparing high water content clayey sediments for thin and ultrathin section study, *Sedimentology*, **30**, pp. 295-299.

Chow, V. T. & Harbaugh, T. E. 1965. Raindrop production for laboratory watershed experimentation, *Journal of Geophysical Research*, **70**, p. 6111.

Churchman, G. J. & Tate, K. R. 1987. Stability of aggregates of different size grades in allophanic soils from volcanic ash in New Zealand, *Journal of Soil Science*, **38**, pp. 19-27.

Cleary, J. L., Loch, R. J., Thomas, E. C. 1987. Effects of time under rain, sampling technique and transport of samples on size distribution of water-stable aggregates, *Earth Surface Processes and Landforms*, **12**, pp. 311-318.

Cogo, N. P., Moldenhauer, W. C., Foster, G. R. 1983. Effect of crop residue, tillage-induced roughness and runoff velocity on size distribution of eroded soil aggregates, *Soil Science Society of America Journal*, **47**, pp. 1005-1008.

Collinet, J. & Valentin, C. 1979. Analyse des differents facteurs intervenant sur l'hydrodynamique superficielle, *Cahiers ORSTROM Série Pédologie*, **17**, pp. 283-328.

Cooke, P. 1969. *Atomic absorption spectrophotometry*, Pye Unicam Ltd.

Cousen, S. M. & Farres, P. J. 1984. The role of moisture in the stability of soil aggregates from a temperate silty soil to raindrop impact, *Catena*, **11**, pp. 313-320.

Cousin, I., Levitz, P., Bruand, A. 1996. Three-dimensional analysis of a loamy-clay soil using pore and solid chord distributions, *European Journal of Soil Science*, **47**, pp. 439-452.

Crescimanno, G., Iovino, M., Provenzano, G. 1995. Influence of salinity and sodicity on soil structural and hydraulic characteristics, *Soil Science Society of America Journal*, **59**, pp. 1701-1708.

Curmi, P., Mérot, P., Roger-Estrade, J., Caneill, J. 1996. Use of environmental isotopes for field study of water infiltration in a ploughed soil layer, *Geoderma*, **72**, pp. 203-217.

Cullen, H. 1997. North Atlantic influence on Middle Eastern climate and water supply, in *Transformations of Middle Eastern natural environments: Legacies and lessons*, a conference at the Yale Centre for International and Area Studies. October 30 - November 1.

Curtin, D., Steppuhn, H., Selles, F. 1994. Clay dispersion in relation to sodicity, electrolyte concentration and mechanical effects, *Soil Science Society of America Journal*, **58**, pp. 955-962.

Dalrymple, J. B. 1957. Preparation of thin sections of soils, *Journal of Soil Science*, **8**, pp. 161-165.

Day, P. R. 1965. Particle fractionation and particle-size analysis, in Black, C. A. (Ed.), *Methods of soil analysis, Part 1*. Agronomy 9, American Society of Agronomy, Madison, pp. 545-567.

Dean, T. J. 1994. *The IH capacitance probe for measurement of soil water content*, Report No. 125, Institute of Hydrology, Wallingford.

De Leenheer, L. & De Boodt, M. 1959. Determination of aggregate stability by the change in mean weight diameter, *Mededelingen van de Landbouwhogeschool Gent*, **24**, pp. 290-300.

De Ploey, J. 1981. Crusting and time-dependent rainwash mechanisms on loamy soil, in Morgan, R. P. C. (Ed.), *Soil conservation*, Wiley, Chichester, pp. 139-154.

De Ploey, J. & Poesen, J. W. A. 1985. Aggregate stability, runoff generation and interrill erosion, in Richards, K. S., Arnett, R. R., Ellis, S. (Eds.), *Geomorphology and soils*, Allen & Unwin, London, pp. 99-120.

De Vries, B. 1981. The Umm el-Jimal Project, 1972-1977, *Bulletin of the American Schools of Oriental Research*, **244**, pp. 53-72.

De Vries, H. & Barendsen, G. W. 1954. Measurements of age by the carbon-14 technique, *Nature*, **174**, pp. 1138-1141.

Dirksen, C. & Dasberg, S. 1993. Improved calibration of time domain reflectometry soil water content measurements, *Soil Science Society of America Journal*, **57**, pp. 660-667.

Dottridge, J., 1998. Water resource quality, sustainability and development, in Dutton, R. W., Clarke, J. I., Battikhi, A. M. (Eds.), *Arid land resources and their management*, Kegan Paul International, London, pp. 67-80.

Douglas, L. A. (Ed.) 1990. *Soil micromorphology: A basic and applied science*, Developments in Soil Science 19, Elsevier, Amsterdam.

Drees, L. R., Karathanasis, A. D., Wilding, L. P., Blevins, R. L. 1994. Micromorphology characteristics of long-term no-till and conventionally tilled soils, *Soil Science Society of America Journal*, **58**, pp. 508-517.

Drury, D. M. 1993. *Hydrogeology of the Azraq Basin*, M.Sc., University College, London.

Duley, F. I. 1939. Surface factors affecting the rate of intake of water by soils, *Soil Science Society of America Proceedings*, **4**, pp. 60-64.

Duley, F. L. & Hays, O. E. 1932. The effect of the degree of slope on runoff and soil erosion, *Journal of Agricultural Research*, **45**, pp. 349-360.

Dunkerley, D. L. 1995. Surface stone cover on desert hillslopes; parameterizing characteristics relevant to infiltration and surface runoff, *Earth Surface Processes and Landforms*, **20**, pp. 207-218.

Dunne, T., Zhang, W., Aubry, B. F. 1991. Effects of rainfall, vegetation and microtopography on infiltration and runoff, *Water Resources Research*, **27**, pp. 2271-2285.

Dwairi, I. M. A. 1987. *A chemical study of the palagonitic tuffs of the Aritain area of Jordan with special reference to nature, origin and industrial potential of the associated zeolite deposits*, Ph.D., University of Hull.

Edwards, A. P. & Bremner, J. M. 1967. Dispersion of soil particles by sonic vibration, *Journal of Soil Science*, **18**, pp. 47-63.

Edwards, W. M. & Larson, W. E. 1969. Infiltration of water into soils as influenced by surface seal development, *Transactions of the American Society of Agricultural Engineers*, **12**, pp. 463-464, 470.

Eigel, J. D. & Moore, I. D. 1983. *Effect of rainfall energy on infiltration into bare soil*, Proceedings of the National Conference on Advances in Infiltration, Dec. 12-13, 1983, Chicago, Illinois, American Society of Agricultural Engineering.

Ekwue, E. I. 1991. Effects of peat content, rainfall duration and aggregate size on soil crust strength, *Earth Surface Processes and Landforms*, **16**, pp. 485-498.

Ela, S. D., Gupta, S. C., Rawls, W. J. 1992. Macropore and surface seal interactions affecting water infiltration into soil, *Soil Science Society of America Journal*, **56**, pp. 714-721.

El-Rihani, A. 1993. *Soil morphology and analyses report for PR26 - PR30*, National Soil Map and Land Use Project, Ministry of Agriculture, Jordan.

Emerson, W. W. 1964. The slaking of the soil crumb as influenced by clay mineral composition, *Australian Journal of Soil Research*, **2**, pp. 211-217.

Emerson, W. W. & Bakker, A. C. 1973. The comparative effect of exchangeable calcium, magnesium and sodium on some properties of red-brown earth sub-soils. II. The spontaneous dispersion of aggregates in water, *Australian Journal of Soil Research*, **11**, pp. 151-157.

Epema, G. F. & Riezebos, H. T. 1983. Fall velocity of water drops at different heights as a factor influencing erosivity of simulated rain, in De Ploey, J. (Ed.), *Rainfall simulation, runoff and soil erosion,* Catena Supplementband 4, Cremlingen, pp. 1-17.

Epstein, E. & Grant, W. J. 1973. Soil crust formation as affected by raindrop impact, in Hadas, A., Swartzendruber, D. E., Rijtemo, P. E., Fuchs, M., Yaron, B. (Eds.), *Ecological studies 4: Physical aspects of soil water and salts in ecosystems*, Springer Verlag, New York, pp. 194-201.

Evans, D. D. & Buol, S. W. 1968. Micromorphological study of soil crusts, *Soil Science Society of America Proceedings*, **32**, pp. 19-22.

Falayi, O. & Bouma, J. 1975. Relationships between the hydraulic conductance of surface crusts and soil management in a typic Hapludalf, *Soil Science Society of America Proceedings*, **39**, pp. 957-963.

FAO 1962. *A study of agroclimatology in semi-arid and arid zones of the Near East*, FAO/UNESCO/WMO Interagency Report on Agroclimatology, Rome Italy.

Farhan, Y. & Mikbel, S. 1986. Applied geomorphological mapping and surveys in Jordan, *Transactions of the Japanese Geomorphological Union*, **7**, pp. 91-102.

Farmer, E. E. 1973. Relative detachability of soil particles by simulated rainfall, *Soil Science Society of America Proceedings*, **37**, pp. 629-633.

Farrell, D. A. & Larson, W. E. 1972. Dynamics of the soil-water system during a rainstorm, *Soil Science*, **113**, pp. 88-95.

Farres, P. 1978. The role of time and aggregate size in the crusting process, *Earth Surface Processes*, **3**, pp. 243-254.

Farres, P. J. 1987. The dynamics of rainsplash erosion and the role of soil aggregate stability, *Catena*, **14**, pp. 119-130.

Farres, P. J. & Cousen, S. M. 1985. An improved method of aggregate stability measurement, *Earth Surface Processes and Landforms*, **10**, pp. 321-329.

Farres, P. J. & Muchena, J. 1996. Spatial patterns of soil crusting and their relationship to crop cover, *Catena*, **26**, pp. 247-260.

Fattah, H. A. & Upadhyaya, S. K. 1996. Effect of soil crust and soil compaction on infiltration in a Yoyo loam soil, *Transactions of the American Society of Agricultural Engineers*, **39**, pp. 79-84.

Fisher, W. B., Atkinson, K., Beaumont, P., Coles, A., Gilchrist-Shirlaw, D. 1966. *Soil survey of Wadi Ziqlab, Jordan*, Department of Geography, University of Durham.

FitzPatrick, E. A. 1984. *Micromorphology of soil*, Chapman and Hall, London.

FitzPatrick, E. A. 1993. *Soil microscopy and micromorphology*, John Wiley & Sons, Chichester.

Folk, R. L. 1966. A review of grain-size parameters, *Sedimentology*, **6**, pp. 73-93.

Fowler, J. & Cohen, L. 1992. *Practical statistics for field biology*, Wiley, Chichester.

Frenkel, H. & Hadas, A. 1981. Effect of tillage and gypsum incorporation on rain, runoff and crust strength in field soils irrigated with saline-sodic water, *Soil Science Society of America Journal*, **45**, pp. 156-158.

Gabriels, D. & De Boodt, M. 1975. A rainfall simulator for soil erosion studies in the laboratory, *Pédologie*, **25**, p. 80-86.

Gal, M., Arcan, L., Shainberg, I., Keren, R. 1984. Effect of exchangeable sodium and phosphogypsum on crust structure - Scanning electron microscope observations, *Soil Science Society of America Journal*, **48**, pp. 872-878.

Ganor, E. 1975. *Atmospheric dust in Israel: Sedimentological and meteorological analysis of dust deposition (in Hebrew with English Abstract)*, Ph.D., The Hebrew University, Jerusalem, Israel.

Gardner, H. R. & Gardner, W. R. 1969. Relation of water application to evaporation and storage of soil water, *Soil Science Society of America Journal*, **33**, pp. 192-196.

Gardner, W. H. 1986. Water content, in Klute, A. (Ed.), *Methods of soil analysis, Part 1: Physical and mineralogical methods* - Agronomy monograph no. 9, American Society of Agronomy, Madison, pp. 493-544.

Gardner, W. R. 1962. Note on the separation and solution of diffusion type equations, *Soil Science Society of America Proceedings*, **26**, p. 404.

Gardner, W. R. & Hillel, D. 1962. The relation of external evaporative conditions to the drying of soils, *Journal of Geophysical Research*, **67**, pp. 4319-4325.

Garrard, A. N., Stanley Price, N. P., Copeland, L. 1975. A survey of prehistoric sites in the Azraq Basin, eastern Jordan, *Paléorient*, **3**, pp. 109-126.

Gascuel-Odoux, C., Cros-Cayot, S., Durand, P. 1996. Spatial variations of sheet flow and sediment transport on an agricultural field, *Earth Surface Processes and Landforms*, **21**, pp. 843-851.

Gee, G. W. & Bauder, J. W. 1986. Particle size analysis, in Klute, A. (Ed.), *Methods of soil analysis, Part 1: Physical and mineralogical methods* - Agronomy monograph no. 9, American Society of Agronomy, Madison, pp. 383-411.

Gerson, R. & Amit, R. 1987. Rates and modes of dust accretion and deposition in an arid region - The Negev, Israel, in Frostick, L. & Reid, I. (Eds.), *Desert Sediments: Ancient and Modern*, Geological Society Special Publication, Oxford, pp. 157-169.

Geyger, E. & Beckmannn, W. 1967. Apparate und Methoden der mikromophometrischen Structuranalyse des Bodens, in Kubiëna, W. L. (Ed.), *Die Mikromorphometrische Bodenanalyse*, Ferdinand Enke Verlag, Stuttgart, pp. 36-57.

Ghadiri, H. & Payne, D. 1977. Raindrop impact stress and the breakdown of soil crumbs, *Soil Science*, **28**, pp. 247-258.

Gibbs, B. 1993. *Hydrogeology of the Azraq Basin*, M.Sc., University College, London.

Gibbs, R. J. 1967. Quantitative X-ray diffraction analysis using clay mineral standards extracted from the samples to be analysed, *Clay Minerals*, **7**, pp. 79-90.

Gill, B. S. & Jalota, S. K. 1996. Evaporation from soil in relation to residue rate, mixing depth, soil texture and evaporativity, *Soil Technology*, **8**, pp. 293-301.

Gilley, J. E. & Finker, S. C. 1985. Estimating soil detachment caused by rain-drop impact, *Transactions of the American Society of Agricultural Engineers*, **28**, pp. 140-146.

Gilley, J. E., Woolhiser, D. A., McWhorter, D. B. 1985. Interrill soil erosion - Part I: development of model equations, *Transactions of the American Society of Agricultural Engineers*, **28**, pp. 147-153.

Glancey, J. L., Upadhyaya, S. K., Zeier, K. R., Wulfsohn, D., Chancellor, W. J. 1988. Instrumentation for measuring soil crust strength, *Transactions of the American Society of Agricultural Engineers*, **Paper 88-1021.**

Goldberg, D., Gornat, B., Rimon, D. 1976. *Drip irrigation: Principles, design and agricultural practices*, Drip irrigation scientific publications, Kfar Shmaryahu, Israel.

Goldberg, P. 1994. Interpreting late Quaternary continental sequences in Israel, in Bar-Yosef, O. & Kra, R. S. (Eds) *Late Quaternary chronologies and paleoclimates of the eastern Mediterranean,* Radiocarbon, Tucson, pp. 89-102.

Goodfriend, G. A. & Magoritz, M. 1988. Paleosols and late Pleistocene rainfall fluctuations in the Negev Desert, *Nature*, **332**, pp. 144-146.

Goudie, A. (Ed.) 1990. *Geomorphological techniques*, Second edition, Unwin Hyman, London.

Govers, G. 1991. A field study on topographical and topsoil effects on runoff generation, *Catena*, **18**, pp. 91-111.

Govers, G. & Poesen, J. W. A. 1986. A field-scale study of surface sealing and compaction on loam and sandy loam soils. Part 1: Spatial variability of soil surface sealing and crusting, in Callebaut, F., Gabriels, D., De Boodt, M. (Eds.), *Assessment of surface sealing and crusting*, ISSS/ Proceedings of the symposium at the Flanders Research Centre for Soil Erosion and Soil Conservation, Ghent, pp. 171-182.

Green, W. H. & Ampt, G. A. 1911. Studies on soil physics, *International Journal of the Agricultural Society*, **4**, pp. 1-24.

Gregorich, E. G. & Anderson, D. W. 1985. Effects of cultivation and erosion on soils of four toposequences in Canadian prairies, *Geoderma*, **36**, pp. 343-354.

Grevers, M. C. J. & de Jong, E. 1992. Soil structure changes in subsoiled solonetzic and chernozemic soils measures by image analysis, *Geoderma*, **53**, pp. 289-307.

Gribble, C. D. & Hall, A. J. 1992. *Optical mineralogy: Principles and practice*, UCL Press, London.

Guba, I. & Mustafa, H. 1988. Structural control of young basaltic fissure erruptions in the plateau basalt area of the arabian plate, N E Jordan, *Journal of Vulcanology and Geothermal Research*, **35**, pp. 319-334.

Hadas, A. & Frenkel, H. 1982. Infiltration as affected by long-term use of sodic-saline water for irrigation, *Soil Science Society of America Journal*, **46**, pp. 524-530.

Hardy, R. & Tucker, M. 1988. X-ray powder diffraction of sediments, in Tucker, M. (Ed.), *Techniques in sedimentology*, Blackwell, Oxford, pp. 191-228.

Hay, R. L. 1966. *Zeolites and zeolitic reactions in sedimentary rocks*, Special Paper of the Geological Society of America, No. 85.

Helalia, A. M. & Letey, J. 1988a. Polymer type and water quality effects on soil dispersion, *Soil Science Society of America Journal*, 52, pp. 243-246.

Helalia, A. M. & Letey, J. 1988b. Cationic polymer effects on infiltration rates with a rainfall simulator, *Soil Science Society of America Journal*, **52**, pp. 247-250.

Helming, K., Roth, C. H., Wolf, R., Diestel, H. 1993. Characterisations of rainfall-microrelief interactions with runoff using parameters derived from digital elevation models (DEM's), *Soil Technology*, **6**, pp. 273-286.

Helms, S. W. 1981. *Jawa: Lost city of the black desert*, Methuen, London.

Hemyari, P. & Nofziger, D. L. 1981. Super sluper effects on crust strength, water retention and water infiltration of soils, *Soil Science Society of America Journal*, **45**, pp. 799-801.

Hénin, S., Monnier, G., Combeau, A. 1958. Méthode pour l'étude de la stabilité structurale des sols, *Annales Agronomiques*, **9**, pp. 73-92.

Hesse, P. R. 1971. *A textbook of soil chemical analysis*, John Murray, London.

Hillel, D. 1959. *Studies on loessial crusts*, Agricultural Research Station, Beit-Dagan, Israel, Bulletin 63 [in Hebrew].

Hillel, D. 1980. *Fundamentals of soil physics*, Academic Press, San Diego.

Hillel, D. & Gardner, W. R. 1969. Steady infiltration into crust-topped profiles, *Soil Science*, **108**, pp. 137-142.

Hillel, D. & Gardner, W. R. 1970. Measurement of unsaturated conductivity and diffusivity by infiltration through an impeding layer, *Soil Science*, **109**, pp. 149-153.

Hoekstra, P. & Delaney, A. 1974. Dielectric properties of soils at UHF and microwave frequencies, *Journal of Geophysical Research*, **79**, pp. 1699-1708.

Homès-Fredericq, D. & Hennessy, J. B. (Eds.) 1989. *Archaeology of Jordan,, II Field reports*, Peeters, Leuven.

Hoogmoed, W. B. 1986. Crusting and sealing problems on West African soils, in Callebaut, F., Gabriels, D., De Boodt, M. (Eds.), *Assessment of surface sealing and crusting,* ISSS / Proceedings of the Symposium at Flanders Research Centre for Soil Erosion and Soil Conservation, Ghent, pp. 48-55.

Hooton, D. H. & Giorgetta, N. E. 1977. Quantitative X-ray diffraction analysis by a direct calculation method, *X-Ray Spectrometry*, **6**, pp. 2-5.

Horton, R. E. 1940. An approach toward a physical interpretation of infiltration capacity, *Soil Science Society of America Proceedings*, **5**, pp. 399-417.

Huang, C. & Bradford, J. M. 1990. Portable laser scanner for measuring soil surface roughness, *Soil Science Society of America Journal*, **54**, pp. 1402-1406.

Huang, C. H. & Bradford, J. M. 1992. Applications of a laser scanner to quantify soil microtopography, *Soil Science Society of America Journal*, **56**, pp. 147-221.

Huang, C., Bradford, J. M., Cushman, J. H. 1982. A numerical study of raindrop impact phenomenon: The rigid case, *Soil Science Society of America Journal*, **46**, pp. 14-19.

Huckriede, R. & Wieseman, G. 1968. Der jungpleistozäne Pluvial-See von El-Jafr und weitere Daten zum Quartar Jordaniens, *Geologica et Paleontologica*, **2**, pp. 73-95.

Hudson, N. W. 1961. An introduction to the mechanics of soil erosion under conditions of sub-tropical rainfall, *Proceedings and Transactions of the Rhodesian Scientific Association*, **49**, pp. 15-25.

Hunting Technical Services 1965. *Wadi Dhuleil investigation*, Unveröffentlicht Bericht für die jordanien Regierung, Archive of the Natural Resource Authority, London.

Ibrahim, K. 1993a. *The geological framework for the Harrat Ash-Shaam Basaltic Super-Group and its volcanotectonic evolution*, Geology Directorate, Natural Resources Authority, Amman.

Ibrahim, K. M. 1993b. *A new occurrence of zeolites in the volcanic tuff of NE Jordan*, Report for the Geology Department, Royal Holloway and Bedford College, University of London.

Imeson, A. C. 1977. A simple field-portable rainfall simulator for difficult terrain, *Earth Surface Processes*, **2**, pp. 431-436.

Imeson, A. C. & Kwaad, F. J. 1990. The response of tilled soils to wetting by rainfall and the dynamic character of soil erodibility, in Boardman, J., Foster, I. D. L., Dearing, J. A. (Eds.), *Soil Erosion on Agricultural Land*, Wiley, Chichester, pp. 3-14.

Ismail, S. N. A. 1975. *Micromorphometric soil porosity characterisation by means of electro-optical image analysis (Quantimet 720)*, Soil Survey Paper No.9, Soil Survey Institute, Wageningen, The Netherlands.

Issac, B. 1992. *The limits of empire: The Roman army in the east*, Revised Edition, Clarendon, Oxford.

Issar, A. S. & Bruins, H. J. 1983. Special climatology conditions in the deserts of Sinai and the Negev during the latest Pleistocene, *Palaeogeography, Palaeoclimatology, Palaeoecology*, **43**, pp. 63-72.

Jayawardane, N. S. 1979. An equivalent salt solution method for predicting hydraulic conductivities of soils for different salt solutions, *Australian Journal of Soil Research*, **17**, pp. 423-428.

Jayawardane, N. S. & Beattie, J. A. 1978. Effect of salt solution composition on moisture release curves of soils, *Australian Journal of Soil Research*, **17**, pp. 89-99.

Jaynes, D. B. & Rice, R. C. 1993. Transport of solutes as affected by irrigation method, *Soil Science Society of America Journal*, **57**, pp. 1348-1353.

Jeschke, W. 1990. Digital close-range photogrammetry for surface measurement, *IAPRS* **28-5**, Zürich, 1058-1065.

Johansen, J. R. 1993. Cryptogamic crusts of semi-arid and arid lands of North America, *Journal of Phycology*, **29**, pp. 140-147.

Johnson, C. B., Mannering, J. V., Moldenhauer, W. C. 1979. Influence of surface roughness and clod size on soil and water loss, *Soil Science Society of America Journal*, **43**, pp. 772-777.

Jongerius, A., Schoonderbeek, D., Jager, A., Kowalinski, S. 1972. Electro-optical soil porosity investigation by means of Quantimet-B equipment, *Geoderma*, **7**, pp. 177-198.

Kaiser, K., Kempf, E. K., Leroi-Gourhan, A., Schütt, H. 1973. Quartärstratigraphische Untersuchung aus dem Damaskus-Becken und seiner Umgebung, *Zeitschrift für Geomorphologie*, **17**, pp. 263-353.

Kastner, M. 1976. *Diagenesis of basal sediments and basalts of sites 322 and 323 leg 35: Bellinghausen Abyssal Plain*, Initial Report of the Deep Sea Drilling Program, Vol. 35. United States Government Printing Office, Washington D.C. pp. 513-518.

Kazman, Z., Shainberg, I., Gal, M. 1983. Effect of low levels of exchangeable sodium and applied phosphogypsum on the infiltration rate of various soils, *Soil Science*, **135**, pp. 184-192.

Kemper, W. D. & Chepil, W. S. 1965. Size distribution of aggregates, in Black, C. A. (Ed.), *Methods of soil analysis, Part 1*, American Society of Agronomy, Madison, WI, pp. 499-510.

Kemper, W. D. & Rosenau, R. C. 1986. Aggregate stability and size distribution, in Klute, A. (Ed.), *Methods of soil analysis, part 1*. Agronomy Monographs, 9, American Society of Agronomy, Madison, WI, pp. 425-442.

Keren, R. & Shainberg, I. 1981. Effect of dissolution rate on the efficiency of industrial and mined gypsum in improving infiltration of a sodic soil, *Soil Science Society of America Journal*, **45**, pp. 103-107.

Kheyrabi, D. & Monnier, G. 1968. Etude expérimentale de l'influence de la composition granulométrique des terres sur leur stabilité structurale, *Annales Agronomiques*, **19**, pp. 129-152.

Kinnell, P. I. A. 1974. Splash erosion: Some observations on the splash-cup technique, *Soil Science Society of America Proceedings*, **38**, p. 657.

Kirk, A. J. 1998. The effect of intensive irrigated agriculture upon soil degradation: a case study from ash-rafiyya, in Dutton, R. W., Clarke, J. I., Battikhi, A. M. (Eds.), *Arid land resources and their management*, Kegan Paul International, London, pp. 127-156.

Kirkby, M. J., Imeson, A. C., Bergkamp, G., Cammeraat, L. H. 1996. Scaling up processes and models from the field plot to the watershed and regional areas, *Journal of Soil and Water Conservation*, **56**, pp. 391-396.

Kochenderfer, J. N. & Helvey, J. D. 1987. Using gravel to reduce soil losses from minimum-standard forest roads, *Journal of Soil and Water Conservation*, **42**, pp. 46-50.

Komar, P. D. & Cui, B. 1984. The analysis of grain-size measurements by sieving and settling-tube techniques, *Journal of Sedimentary Petrology*, **54**, pp. 603-614.

Kooistra, M. J. 1987. The effects of compaction and deep tillage on soil structure in a dutch sandy loam soil, in Federoff, N., Bresson, L. M., Courty, M. A. (Eds.), *Micromorphologie des sols*, L'association Française pour l'étude du sol, Plaisir, France, pp. 445-450.

Kovda, V. 1980. *Land aridization and drought control*, Westview Press, Boulder, Colorado.

Krown, L. 1966. Approach to forecasting seasonal rainfall in Israel, *Journal of Applied Meteorology*, **5**, pp. 590-594.

Lafforgue, A. & Naah, E. 1976. Exemple d'analyse expérimentale des facteurs de ruissellement sous pluies simulées, *Cahiers ORSTOM Séries de Hydrologie* **13**, pp. 195-237.

Lamb, H. H. 1968. The climatic background to the birth of civilisation, *Advancement of Science*, **25**, pp. 103-120.

Lankester Harding, G. 1959. *The antiquities of Jordan*, Jordan Distribution Agency, Amman.

Lavee, H. & Poesen, J. W. A. 1991. Overland flow generation and continuity on stone covered soil surfaces, *Hydrological Processes*, **5**, pp. 345-360.

Lawrence, T. E. 1926. *Seven pillars of wisdom*, Penguin, London.

Laws, J. O. 1941. Measurements of the fall-velocities of water-drops and raindrops, *Transactions of the American Geophysical Union*, **22**, pp. 709-721.

Laws, J. O. & Parsons, D. A. 1943. The relation of raindrop-size to intensity, *Transactions of the American Geophysical Union*, **24**, pp. 452-460.

Le Bissonnais, Y. 1990. Experimental study and modelling of soil surface crusting processes, in Bryan, R. B. (Ed.), *Soil erosion: Experiments and models*, Catena Supplement 17, Cremlingen, pp. 13-28.

Le Bissonnais, Y. 1996a. Soil characteristics and aggregate stability, in Agassi, M. (Ed.), *Soil erosion, conservation and rehabilitation*, Marcel Dekker, New York, pp. 41-60.

Le Bissonnais, Y. 1996b. Aggregate stability and assessment of soil crustability and erodibility: 1. Theory and methodology, *European Journal of Soil Science*, **47**, pp. 425-438.

Le Bissonnais, Y. & Arrouays, D. 1997. Aggregate stability and assessment of soil crustability and erodibility: II. Application to humic loamy soils with various organic carbon contents, *European Journal of Soil Science*, **48**, pp. 39-48.

Le Bissonnais, Y. & Bruand, A. 1993. Crust micromorphology and runoff generation on silty soil materials during different seasons, in Poesen, J. W. A. & Nearing, M. A. (Eds.), *Soil surface sealing and crusting*, Catena Verlag, Cremlingen, pp. 1-16.

Le Bissonnais, Y. & Singer, M. J. 1992. Crusting, runoff and erosion response to soil water content and successive rainfalls, *Soil Science Society of America Journal*, **56**, pp. 1898-1903.

Le Bissonnais, Y. & Singer, M. J. 1993. Seal formation, runoff, and interrill erosion from seventeen California soils, *Soil Science Society of America Journal*, **57**, pp. 224-229.

Le Bissonnais, Y., Bruand, A., Jamagne, M. 1989. Laboratory experimental study of soil crusting: Relation between aggregate breakdown mechanisms and crust structure, *Catena*, **16**, pp. 377-392.

Le Souder, C., Le Bissonnais, Y., Robert, M., Bresson, L. M. 1989. Prevention of crust formation with a mineral conditioner, in Douglas, L. A. (Ed.) *Soil micromorphology: A basic and applied science*, Developments in Soil Science, 19, Elsevier, Amsterdam, pp. 81-88.

Letey, J. 1994. Adsorption and desorption of polymers on soil, *Soil Science*, **158**, pp. 244-248.

Levy, G. J., Levin, J., Shainberg, I. 1994. Seal formation and interrill soil erosion, *Soil Science Society of America Journal*, **58**, pp. 203-209.

Levy, G. J., Levin, J., Shainberg, I. 1995. Polymer effects on runoff and soil erosion from sodic soils, *Irrigation Science*, **16**, pp. 9-14.

Levy, G. J., Levin, J., Shainberg, I. 1997. Prewetting rate and aging effects on seal formation and interrill soil erosion, *Soil Science*, **162**, pp. 131-139.

Linacre, E. 1992. *Climate data and resources: a reference and guide*, Routledge, London.

Linden, D. R. & Van Doren, D. M. 1986. Parameters for characterising tillage-induced soil surface roughness, *Soil Science Society of America Journal*, **50**, pp. 1560-1565.

Lloyd, J. W. 1965. The hydrochemistry of the aquifers of north-eastern Jordan, *Journal of Hydrology*, **3**, pp. 319-330.

Loague, K. 1992. Using soil texture to estimate saturated hydraulic conductivity and the impact on rainfall-runoff simulations, *Water Resources Bulletin*, **28**, pp. 687-693.

Loch, R. J. 1994. A method for measuring aggregate water stability with relevance to surface seal development, *Australian Journal of Soil Research*, **32**, pp. 687-700.

Loureiro, N. S. & Coutinho, M. A. 1995. Rainfall changes and rainfall erosivity increase in the Algarve (Portugal), *Catena*, **24**, pp 55-67.

Low, A. J. 1967. *Measurement of stability of moist soil aggregates to falling waterdrops according to Low, West-European methods for soil structural determination*, State Faculty of Agricultural Sciences, Ghent. pp.51-78.

Luk, S. H. & Cai, Q. G. 1990. Laboratory experiments on crust development and rainsplash erosion on loess soils, China, *Catena*, **17**, pp. 261-276.

Luk, S. H., Cai, Q. G., Wang, G. P. 1993. Effects of surface crusting and slope gradient on soil and water losses in the hilly loess region, north China, in Poesen, J. W. A. & Nearing, M. A. (Eds.), *Soil surface sealing and crusting*, Catena Verlag, Cremlingen, pp. 29-46.

Maani, M., Hunaiti, H., Findlay, A. M. 1995. *Demographic change and population projections for the Badia region of Jordan, 1976-2013*, Centre for Applied Population Research, Department of Geography, University of Dundee, Research Paper Series: 95/2.

Magunda, M. K., Larson, W. E., Linden, D. R., Nater, E. A. 1997. Changes in microrelief and their effects on infiltration and erosion during simulated rainfall, *Soil Technology*, **10**, pp. 57-68.

Malekuti, A. & Gifford, B. G. 1978. Natural vegetation as a source of diffuse salt within the Colorado River Basin, *Water Resources Bulletin*, **14**, p. 195.

Malo, D. D., Worcester, B. K., Cassel, D. K., Matzdorf, K. D. 1974. Soil-landscape relationships in a closed drainage system, *Soil Science Society of America Proceedings*, **38**, pp. 813-818.

Mannering, J. V. 1967. *The relationship of some physical and chemical properties of soils to surface sealing*, Ph.D., Purdue University, West Lafayette.

Marshall, T. J. & Holmes, J. W. 1988. *Soil physics*, Second edition, Cambridge University Press.

Martin, R., Litz, P. E., Huff, W. D. 1979. A new technique for making thin sections of clayey sediments, *Journal of Sedimentary Petrology*, **49**, pp. 641-643.

Mason, D. D., Lutz, J. F., Petersen, R. G. 1957. Hydraulic conductivity as related to certain soil properties in a number of great soil groups-sampling errors involved, *Soil Science Society of America Proceedings*, **21**, pp. 554-560.

Mazurak, A. P. & Mosher, 1968. Detachment of soil particles in simulated rainfall, *Soil Science Society of America Proceedings*, **32**, p. 716.

McClure, H. A. 1976. Radiocarbon chronology of Late Quaternary lakes in the Arabian desert, *Nature*, **263**, pp. 755-756.

McNeil, D. 1992. On graphing paired data, *The American Statistician*, **46**, pp. 307-311.

McIntyre, D. S. 1958a. Permeability measurements of soil crusts formed by raindrop impact, *Soil Science*, **85**, pp. 185-189.

McIntyre, D. S. 1958b. Soil splash and the formation of surface crusts by raindrop impact, *Soil Science*, **85**, pp. 261-266.

McIsaac, G. F., Mitchell, J. K., Hirschi, M. C. 1995. Dissolved phosphorus concentrations in runoff from simulated rainfall on corn and soybean tillage systems, *Journal of Soil and Water Conservation*, **50**, pp. 383-387.

McKenna Neuman, C., Maxwell, C. D., Wayne Boulton, J. 1996. Wind transport of sand surfaces crusted with photoautotrophic microorganisms, *Catena*, **27**, pp. 229-247.

McNeal, B. L. & Coleman, N. T. 1966. Effect of solution composition on soil hydraulic conductivity, *Soil Science Society of America Proceedings*, **30**, pp. 308-312.

Mellis, D. A., Bruneau, P. M. C., Twomlow, S. J., Morgan, R. P. C. 1996. Field assessment of crusting on a tilled sandy clay loam, *Soil Use and Management*, **12**, pp. 72-75.

Mercier, N. & Valladas, H. 1994. Thermoluminescence dates for the Paleolithic Levant, in Bar-Yosef, O. & Kra, R. S. (Eds) *Late Quaternary chronologies and paleoclimates of the eastern Mediterranean,* Radiocarbon, Tucson, pp. 13-20.

Mermut, A. R., Grevers, M. C. J., de Jong, E. 1992. Evaluation of pores under different management systems by image analysis of clay soils in Saskatchewan, Canada, *Geoderma*, **53**, pp. 357-372.

Mermut, A. R., Luk, S. H., Römkens, M. J. M., Poesen, J. W. A. 1995. Micromorphological and mineralogical components of surface sealing in loess soils from different geographic regions, *Geoderma*, **66**, pp. 71-84.

Mermut, A. R., Luk, S. H., Römkens, M. J. M., Poesen, J. W. A. 1997. Soil loss by splash and wash during rainfall from two loess soils, *Geoderma*, **75**, pp. 203-214.

Merzougui, M. & Gifford, G. F. 1987. Spatial variability of infiltration rates on a semi-arid seeded rangeland, *Hydrological Sciences Journal*, **32**, pp. 243-250.

Meyer, L. D. 1965. Simulation of rainfall for soil erosion research, *Transactions of the American Society of Agricultural Engineers*, **8**, pp. 63-68.

Meyer, L. D. 1994. Rainfall simulators for soil erosion research, in Lal, R. (Ed.), *Methods in soil erosion research*, Soil and Water Conservation Society, Ankeny, pp. 83-104.

Meyer, L. D., Johnson, C. B., Foster, G. R. 1972. Stone and woodchip mulches for erosion control on construction sites, *Journal of Soil and Water Conservation*, **27**, pp. 264-269.

Mihara, Y. 1951. Raindrops and soil erosion, *Institute for Agricultural Science (Japan) - Series A*, **1**, pp. 48-51.

Miller, W. P. 1987. Infiltration and soil loss of three gypsum-amended Utisols under simulated rainfall, *Soil Science Society of America Journal*, **51**, pp. 1314-1320.

Miller, W. P. & Scifres, J. 1988. Effect of sodium nitrate and gypsum on infiltration and erosion of a highly weathered soil, *Soil Science*, **148**, pp. 304-309.

Moffat, D. T. 1988. *A volcanotectonic analysis of the Cenozoic continental basalts of northern Jordan; Implications for hydrocarbon prospecting in the block B area*, ERI Jordan EJ88-1.

Moore, D. C. & Singer, M. J. 1990. Crust formation effects on soil erosion processes, *Soil Science Society of America Journal*, **54**, pp. 1117-1123.

Morin, J. & Benyamini, Y. 1977. Rainfall infiltration into bare soils, *Water Resources Research*, **13**, pp. 813-817.

Morin, J. & Cluff, C. B. 1980. Runoff calculation on semi-arid watersheds using a rotadisk rainulator, *Water Resources Research*, **16**, pp. 1085-1093.

Morin, J. Keren, R., Benjamini, Y., Ben-Hur, M. 1989. Water infiltration as affected by soil crust and moisture profile, *Soil Science*, **148**, pp. 53-59.

Morin, J. & Kosovsky, A. 1995. The surface infiltration model, *Journal of Soil and Water Conservation*, **50**, pp. 470-476.

Morin, J. & van Winkel, J. 1996. The effect of raindrop impact and sheet erosion on infiltration rate and crust formation, *Soil Science Society of America Journal*, **60**, pp. 1223-1227.

Morin, J., Golgberg, D., Seginer, I. 1967. A rainfall simulator with a rotating disk, *Transactions of the American Society of Agricultural Engineers*, **10**, pp. 74-77,79.

Morin, J., Benyamini, Y., Michaeli, A. 1981. The effect of raindrop impact on the dynamics of soil surface crusting and water movement in the profile, *Journal of Hydrology*, **52**, pp. 321-335.

Moser, B. K. & Stevens, G. R. 1992. Homogeneity of variance in the two-sample means test, *The American Statistician*, **46**, pp. 19-21.

Moss, A. J. 1991a. Rain-impact soil crust I. - Formation on a granite derived soil, *Australian Journal of Soil Research*, **29**, pp. 271-289.

Moss, A. J. 1991b. Rain-impact soil crust. II. Some effects of surface-slope, drop size and soil variation, *Australian Journal of Soil Research*, **29**, pp. 291-309.

Moss, A. J. & Watson, C. L. 1991. Rain-impact soil crust III. Effects of continuous and flawed crusts on infiltration, and the ability of plant covers to maintain crustal flaws, *Australian Journal of Soil Research*, **29**, pp. 291-309.

Mualem, Y. & Assouline, S. 1989. Modelling soil seal as a non-uniform layer, *Water Resources Research*, **25**, pp. 2101-2108.

Mualem, Y., Assouline, S., Rohdenburg, H. 1990. Rain induced soil seal (A) - A critical review of observations and models, *Catena*, **17**, pp. 185-203.

Mualem, Y. & Friedman, S. P. 1991. Theoretical prediction of electrical conductivity in saturated and unsaturated soil, *Water Resources Research*, **27**, pp. 2771-2777.

Mücher, H. J. & De Ploey, J. 1977. Experimental and micromorphological investigation of erosion and redeposition of loess by water, *Earth Surface Processes*, **2**, pp. 117-124.

Mücher, H. J., De Ploey, J., Savat, J. 1981. Response of loess materials to simulated translocation by water: Micromorphological observations, *Earth Surface Processes and Landforms*, **6**, pp. 331-336.

Mücher, H. J., Chartres, C. J., Tongway, D. J., Greene, R. S. B. 1988. Micromorphology and significance of the surface crust of soils in rangelands near Cobar, Australia, *Geoderma*, **42**, pp. 227-244.

Munn, J. R. & Huntington, G. L. 1976. A portable rainfall simulator for erodibilty and infiltration measurements on rugged terrain, *Soil Science Society of America Journal*, **40**, pp. 622-624.

Murphy, C. P. 1982. A comparative study of three methods of water removal prior to resin impregnation of two soils, *Journal of Soil Science*, **33**, pp. 719-735.

Murphy, C. P. 1986. *Thin section preparation of soils and sediments*, A B Academic Publishers, Berkhamsted.

Murphy, C. P. & Kemp, R. A. 1984. The over-estimation of clay and the under-estimation of pores in soil thin sections, *Journal of Soil Science*, **35**, pp. 481-495.

Murphy, C. P., Bullock, P., Biswell, K. J. 1977a. The measurement and characterisation of voids in soil thin sections by image analysis. Part II. Applications, *Journal of Soil Science*, **28**, pp. 509-518.

Murphy, C. P., Bullock, P., Turner, R. H. 1977b. The measurement and characterisation of voids in soil thin sections by image analysis. Part 1. Principles and techniques, *Journal of Soil Science*, **28**, pp. 498-508.

Mutchler, C. K. & Moldenhauer, W. C. 1963. Applicator for laboratory rainfall simulator, *Transactions of the American Society of Agricultural Engineers*, **6**, pp. 220-222.

Nearing, M. A. & Bradford, J. M. 1987. Relationships between waterdrop properties and forces of impact, *Soil Science Society of America Journal*, **51**, pp. 425-430.

Nearing, M. A., Bradford, J. M., Holtz, R. D. 1986. Measurement of force versus time relations for waterdrop impact, *Soil Science Society of America Journal*, **50**, pp. 1532-1536.

Nearing, M. A., Parker, S. C. 1994. Detachment of soil by flowing water under turbulent and laminar conditions, *Soil Science Society of America Journal*, **58**, pp. 1612-1614.

Neev, D. & Emery, K. O. 1967. The Dead Sea, *Bulletin of the Geological Survey, Israel*, **41**, pp. 1-147.

Neff, E. L. 1979. *Why rainfall simulation*, Proceedings of the rainfall simulator workshop, Tucson, Arizona. 7-9 March, 1979.

Norton, L. D. & Schroeder, S. L. 1987. The effect of various cultivation methods on soil loss: A micromorphological approach, in Federoff, N., Bresson, L. M., Courty, M. A. (Eds.), *Micromorphologie des Sols*, Association Française pour l'Étude du Sol, Plaisir, pp. 431-436.

Norton, L. D., Shainberg, I., King, K. W. 1993. Utilisation of gypsiferous amendments to reduce surface sealing in some humid soils of the eastern USA, in Poesen, J. W. A. & Nearing, M. A. (Eds.), *Soil surface sealing and crusting*, Catena Verlag, Cremlingen, pp. 77-92.

Onofiok, O. & Singer, M. J. 1984. Scanning electron microscope studies of surface crusts formed by simulated rainfall, *Soil Science Society of America Journal*, **48**, pp. 1137-1143.

Oster, J. D. & Schroer, F. W. 1979. Infiltration as influenced by irrigation water quality, *Soil Science Society of America Journal*, **43**, pp. 444-447.

Page, A. L. (Ed.) 1982. *Methods of soil analysis. Part 2*, second edition,, American Society of Agronomy, Agronomy Monograph 9, Madison.

Pagliai, M. 1987. Effects of different management practices on soil structure and surface crusting, in Federoff, N., Bresson, L. M., Courty, M. A. (Eds.),

Micromorphologie des sols, L'association Française pour l'étude du sol, Plaisir, France, pp. 415-421.

Pagliai, M., Bisdom, E. B. A., Ledin, S. 1983. Changes in surface structure after application of sewage sludge and pig slurry to cultivated agricultural soils in northern Italy, *Geoderma*, **30**, pp. 35-53.

Parlange, M. B., Katul, G. G., Folegatti, M. V., Nielsen, D. R. 1993. Evaporation and the field scale soil water diffusivity function, *Water Resources Research*, **29**, pp. 1279-1286.

Parsons, A. J., Wainwright, J., Abrahams, A. D. 1993. Tracing sediment movement in interrill overland flow on a semi-arid grassland hillslope using magnetic susceptibility, *Earth Surface Processes and Landforms*, **18**, pp. 721-732.

Parsons, A. J., Abrahams, A. D., Wainwright, J. 1994. Rainsplash and erosion rates in an interrill area on semi-arid grassland, southern Arizona, *Catena*, **22**, pp. 215-226.

Penman, H. 1948. Natural evaporation from open water, bare soil and grass, *Philosophical Transactions of the Royal Society of London A*, **193**, pp. 120-145.

Perkin Elmer 1982. *Analytical methods for atomic adsorption spectrophotometry.*

Perrolf, K. & Sandström, K. 1995. Correlating landscape characteristics and infiltration - a study of surface sealing and subsoil conditions in semi-arid Botswana and Tanzania, *Geografiska Annaler*, **77A**, pp. 119-133.

Perry, A. 1981. Mediterranean climate - A synoptic reappraisal, *Progress in Physical Geography*, **5**, pp. 107-113.

Peterson, R. J. 1977. *Laboratory simulation of soil erosion*, M.S., Colorado State University, Fort Collins.

Philip, J. R. 1957. The theory of infiltration. 4: Sorptivity and algebraic infiltration equations, *Soil Science*, **84**, pp. 257-264.

Philip, J. R. 1986. Linearized unsteady multidimensional infiltration, *Water Resources Research*, **22**, pp. 1717-1727.

Philips, F. M. 1994. Environmental tracers for water movement in desert soils of the American southwest, *Soil Science Society of America Journal*, **58**, pp. 15-24.

Phillips, P. G. 1954. *The Hashemite Kingdom of Jordan: Prolegomena to a technical assistance program*, Ph.D., The University of Chicago, Illinois.

Pierson, F. B. & Mulla, D. J. 1990. Aggregate stability in the Palouse region of Washington: Effect of landscape position, *Soil Science Society of America Journal*, **54**, pp. 1407-1412.

Poesen, J. W. A. 1984. The influence of slope angle on infiltration rate and Hortonian overland flow, *Zeitschrift für Geomorphologie, Supplementband*, **49**, pp. 117-131.

Poesen, J. 1986a. Surface sealing as influenced by slope angle and position of simulated stones in the top layer of loose sediments, *Earth Surface Processes and Landforms*, **11**, pp. 1-10.

Poesen, J. W. A. 1986b. Surface sealing on loose sediments: the role of texture, slope and position of stones in the top layer, in Callebaut, F., Gabriels, D., De Boodt, M. (Eds.), *Assessment of soil surface sealing and crusting*, ISSS / Proceedings of the Symposium at the Flanders Research Centre for Soil Erosion and Soil Conservation, Ghent, pp. 354-362.

Poesen, J. W. A. 1987. The role of slope angle in surface seal formation, in Gardiner, V. (Ed.), *International geomorphology II*, John Wiley, Chichester, pp. 437-448.

Poesen, J. W. A. 1992. Mechanisms of overland-flow generation and sediment production on loamy and sandy soils with and without rock fragments, in Parsons, A. J. & Abrahams, A. D. (Eds.), *Overland flow: Hydraulics and erosion mechanics*, UCL Press, London, pp. 275-305.

Poesen, J. W. A. & Govers, G. 1986. A field-scale study of surface sealing and compaction on loamy and sandy loam soils. Part II. Impact of soil surface sealing and compaction on water erosion processes, in Callebaut, F., Gabriels, D., DeBoodt, M. (Eds.), *Assessment of Soil Surface Sealing and Crusting*, ISSS / Proceedings of the Symposium at the Flanders Research Centre for Soil Erosion and Soil Conservation, Ghent, Belgium, pp. 183-193.

Poesen, J. W. A. & Ingelmo-Sanchez, F. 1992. Runoff and sediment yield from topsoils with different porosity as affected by rock fragment cover and position, *Catena*, **19**, pp. 451-474.

Poesen, J. W. A. & Lavee, H. 1991. Effects of size and incorporation of synthetic mulch on runoff and sediment yield from interrills in a laboratory study with simulated rainfall, *Soil and Tillage Research*, **21**, pp. 209-223.

Poesen, J. W. A. & Nearing, M. A. (Eds.) 1993. *Soil surface sealing and crusting*, Catena Supplement 24, Catena Verlag, Cremlingen.

Poesen, J., Ingelmo-Sanchez, F., Mücher, H. 1990. The hydrological response of soil surface to rainfall as affected by cover and position of rock fragments in the top layer, *Earth Surface Processes and Landforms*, **15**, pp. 653-671.

Pojasok, T. & Kay, B. D. 1990. Assessment of a combination of wet-sieving and turbidimetry to characterise the structural stability of moist aggregates, *Canadian Journal of Soil Science*, **70**, pp. 33-42.

Protz, R., Sweeney, S. J., Fox, C. A. 1992. An application of spectral image analysis to soil micromorphology, 1. Methods of analysis, *Geoderma*, **53**, pp. 275-287.

Quennell, A. M. 1951. The geology and mineral resources of Trans-Jordan, *Colonial Geology and Mineral Resources* **2**, 85-115, London.

Quennell, A. M. 1956. *Geological map of Jordan (East of the Rift Valley).* Amman. Scale 1:250 000.

Quennell, A. M. 1984. The western Arabia rift system, in Dixon, J. E. & Robertson, A. H. F. (Eds.), *The geological evolution of the eastern Mediterranean*, The Geological Society, Oxford, pp. 775-789.

Quirk, J. P. 1986. Soil permeability in relation to sodicity and salinity, *Philosophical Transactions of the Royal Society of London A*, **316**, pp. 297-317.

Quirk, J. P. & Schofield, R. K. 1955. The effect of electrolyte concentration on soil permeability, *Journal of Soil Science*, **6**, pp. 163-178.

Remley, P. A. & Bradford, J. M. 1989. Relationship of soil crust morphology to inter-rill erosion parameters, *Soil Science Society of America Journal*, **53**, pp. 1215-1221.

Rhoades, J. D. 1972. Quality of water for irrigation, *Soil Science*, **113**, pp. 277-284.

Rice, M. A., Willetts, B. B., McEwan, I. K. 1996. Wind erosion of crusted soil sediments, *Earth Surface Processes and Landforms*, **21**, pp. 279-293.

Richards, L. A. (ed) 1954. *Diagnosis and improvement of saline and alkali soils*, USDA Handbook No. 60. Agricultural Research Service, Washington, DC., USA.

Riezebos, H. T. & Epema, G. F. 1985. Drop shape and erosivity Part II: Splash detachment, transport and erosivity indices, *Earth Surface Processes and Landforms*, **10**, pp. 69-74.

Riezebos, H. T. & Seyhan, E. 1977. Essential conditions of rainfall simulation for laboratory water erosion experiments, *Earth Surface Processes*, **2**, pp. 185-190.

Roberts, N. 1982. Lake levels as an indicator of Near Eastern palaeo-climates: A preliminary appraisal, in Bintliff, J. L. & Van Zeist, W. (Eds.), *Palaeoclimates, palaeoenvironments and human communities in the eastern Mediterranean region in later prehistory*, B.A.R. International Series 133, Oxford, pp. 235-267.

Roberts, N. 1995. Climatic forcing of alluvial fan regimes during the late Quaternary in the Konya basin, south central Turkey, in Lewin, J., Macklin, M. G., Woodward, J. C. (Eds) *Mediterranean Quaternary river environments*, Balkema, Rotterdam, pp. 207-217.

Robinson, A. R. 1979. *Comments - Rainfall simulator workshop*, Proceedings of the rainfall simulator workshop, Tucson, Arizona. March 7-9, 1979.

Robinson, D. A., Bell, J. P., Batchelor, C. H. 1994. Influence of iron minerals on the determination of soil water content using dielectric techniques, *Journal of Hydrology*, **161**, pp. 169-180.

Robinson, M. & Dean, T. J. 1993. Measurement of near-surface soil water content using a capacitance probe, *Hydrological Processes*, **7**, pp. 77-86.

Römkens, M. J. M. & Wang, J. Y. 1986. Effect of tillage on surface roughness, *Transactions of the American Society of Agricultural Engineers*, **29**, pp. 429-433.

Römkens, M. J. M., Glen, L. F., Nelson, D. W., Roth, C. B. 1975. A laboratory rainfall simulator for infiltration and soil detachment studies, *Soil Science Society of America Proceedings*, **39**, p. 158.

Römkens, M. J. M., Baumhardt, R. L., Parlange, J.-Y., Whisler, F. D., Prasad, S. N. 1986. Effect of rainfall characteristics on seal hydraulic conductance, in Callebaut, F., Gabriels, D., DeBoodt, M (Eds.), *Assessment of soil surface sealing and crusting*, ISSS / Proceedings of the Symposium at the Flanders Research Centre for Soil Erosion and Soil Conservation, Ghent, pp.228-235.

Römkens, M. J. M., Wang, J. Y., Darden, R. W. 1988. A laser microreliefmeter, *Transactions of the American Society of Agricultural Engineers*, **31**, pp. 408-413.

Römkens, M. J. M., Prasad, S. N., Whisler, F. D. 1990. Surface sealing and infiltration, in Anderson, M. G. & Burt, T. P. (Eds.), *Process studies in hillslope hydrology*, John Wiley, Chichester, pp. 127-172.

Rose, C. W. 1960. Soil detachment caused by rainfall, *Soil Science*, **89**, p. 28.

Rose, D. A. 1968. Water movement in porous materials III. Evaporation of water from soil, *British Journal of Applied Physics (Journal of Physics D)*, **1**, pp. 1779-1791.

Rose, D. A. 1996. The dynamics of soil water following single surface wettings, *European Journal of Soil Science*, **47**, pp. 21-31.

Roth, C. H. & Helming, K. 1992. Surface seal properties, runoff formation and sediment concentration as related to rainfall characteristics and the presence of already formed crusts, *Soil Technology*, **5**, pp. 359-368.

Roth, C. H., Meyer, B., Frede, H. G. 1985. A portable rainfall simulator for studying factors affecting runoff, infiltration and soil loss, *Catena*, **12**, pp. 79-85.

Roth, C. H., Malicki, M. A., Plagge, R. 1992. Empirical evaluation of the relationship between soil dielectric constant and volumetric water content as the basis for calibrating soil moisture measurements, *Journal of Soil Science*, **43**, pp. 1-13.

Rudolph, A., Helming, K., Diestel, H. 1997. Effect of antecedent soil water content and rainfall regime on microrelief changes, *Soil Technology*, **10**, pp. 69-81.

Sahu, B. K. 1965. Theory of sieving, *Journal of Sedimentary Petrology*, **35**, pp. 750-753.

Saleh, A. 1993. Soil aggregate and crust density prediction, *Soil Science Society of America Journal*, **57**, pp. 524-526.

Saleh, A., Fryrear, D. W., Bilbro, J. D. 1997. Aerodynamic roughness prediction from soil surface roughness measurement, *Soil Science*, **162**, pp. 205-210.

Savat, J. & Poesen, J. 1977. Splash and discontinuous runoff as creators of fine sandy lag deposits with Kalahari sands, *Catena*, 4, pp. 321-332.

Selby, M. J. 1970. Design of a hand-portable rainfall-simulating infiltrometer, with trial results from the Otutira catchment, *Journal of Hydrology*, **9**, p. 117.

Selker, J. S., Graff, L., Steenhuis, T. 1993. Non-invasive time domain reflectometry moisture measurement probe, *Soil Science Society of America Journal*, **57**, pp. 934-936.

Shainberg, I. 1985. The effect of exchangeable sodium and electrolyte concentration on crust formation, *Advances in Soil Science*, **1**, pp. 101-122.

Shainberg, I. & Letey, J. 1984. Response of soils to sodic and saline conditions, *Hilgardia*, **52**, pp. 1-57.

Shainberg, I., Goldstein, D. Levy, G. J. 1996. Rill erosion dependence on soil-water content, aging and temperature, *Soil Science Society of America Journal*, **60**, pp. 916-922.

Shainberg, I. & Singer, M. J. 1986. Suspension concentration effects of depositional crusts and soil hydraulic conductivity, *Soil Science Society of America Journal*, **50**, pp. 1537-1540.

Shainberg, I., Rhoades, J. D., Prather, R. J. 1981a. Effect of low electrolyte concentration on clay dispersion and hydraulic conductivity of a sodic soil, *Soil Science Society of America Journal*, **45**, pp. 273-277.

Shainberg, I., Rhoades, J. D., Suarez, D. L., Prather, R. J. 1981b. Effect of mineral weathering on clay dispersion and hydraulic conductivity of sodic soils, *Soil Science Society of America Journal*, **45**, pp. 287-291.

Shainberg, I., Warrington, D., Rengasamy, P. 1990. Effect of PAM and gypsum application on rain infiltration and runoff, *Soil Science*, **149**, pp. 301-307.

Shanmuganathan, R. T. & Oades, J. M. 1983. Modification of soil physical properties by addition of calcium compounds, *Australian Journal of Soil Research*, **21**, pp. 285-300.

Sharma, K. D., Singh, H., Pareek, O. 1983. Rainwater infiltration into a bare loamy sand, *Hydrological Sciences Journal*, **28**, pp. 417-424.

Sharma, P. P., Gantzer, C. J., Blake, G. R. 1981. Hydraulic gradients across simulated rain-formed soil surface seals, *Soil Science Society of America Journal*, **45**, pp. 1031-1034.

Sharma, P. P., Gupta, S. C., Foster, G. R. 1995. Raindrop-induced soil detachment and sediment transport from interrill areas, *Soil Science Society of America Journal*, **59**, pp. 727-734.

Sharon, D. 1972. The spottiness of rainfall in a desert area, *Journal of Hydrology*, **17**, pp. 161-175.

Sharon, D., Adar, E., Lieberman, G. 1983. Observations on the differential hydrological and/or erosional response of opposite-lying slopes, as related to incident rainfall, *Israel Journal of Earth Sciences*, **32**, pp. 71-74.

Sharon, D., Morin, J., Moshe, Y. 1989. Micro-topographical variations of rainfall incident on ridges in a cultivated field, *Transactions of the American Society of Agricultural Engineers*, **31**, pp. 1715-1722.

Shaw, S. H. 1947. *Southern Palestine geological map on a scale of 1: 250 000 with explanatory notes*. Government Printer, Government of Palestine, Jerusalem.

Shehadeh, N. 1985. The climate of Jordan in the past and present, in Hadidi, A. (Ed.), *Studies in the history and archaeology of Jordan*, Department of Antiquities, Jordan, Amman, pp. 35-38.

Shiel, R. S. & Yuniwo, E. C. 1993. Decreasing the impact of surface crusting on seedling emergence by spray wetting, *Soil Use and Management*, **9**, pp. 40-45.

Simonson, R. W. 1995. Airborne dust and its significance to soils, *Geoderma*, **65**, pp. 1-43.

Singer, M. J., Matsuda, Y., Blackard, J. 1981. Effect of mulch rate on soil loss by raindrop splash, *Soil Science Society of America Journal*, **45**, pp. 107-110.

Slattery, M. C. & Bryan, R. B. 1992. Hydraulic conditions for rill incision under simulated rainfall: A laboratory experiment, *Earth Surface Processes and Landforms*, **17**, pp. 127-146.

Slattery, M. C. & Bryan, R. B. 1994. Surface seal development under simulated rainfall on an actively eroding surface, *Catena*, **22**, pp. 17-34.

Smith-Rose, R. L. 1933. The electrical properties of soils for alternating currents at radio frequencies, *Proceedings of the Royal Society of London*, **140**, pp. 359-377.

Sparks, D. L. & Huang, P. M. 1985. Physical chemistry of soil potassium, in Munson, R. D. (Ed.), *Potassium in agriculture*, American Society of Agronomy, Madison, pp. 201-276.

Steichen, J. M. 1984. Infiltration and random roughness of a tilled and untilled clay-pan soil, *Soil and Tillage Research*, **4**, pp. 251-262.

Steiner, K. G. 1996. *Causes of soil degradaion and development approaches to sustainable soil management*, Deutsche Gesellschaft für Technische Zusammenarbeit GmbH, Margraf Verlag, Weikersheim, Germany.

Steinhardt, R. & Hillel, D. 1966. A portable low-intensity rain simulator for field and laboratory use, *Soil Science Society of America Proceedings*, **30**, p. 666.

Stern, R., Laker, M. C., van der Merwe, A. J. 1991. Field studies on effect of soil conditioners and mulch on runoff from kaolinitic and illitic soils, *Australian Journal of Soil Research*, **29**, pp. 249-261.

Stokes, G. G. 1851. On the effect of internal friction of fluids on the motion of pendulums, *Transactions of the Cambridge Philosophical Society*, **9**, pp. 8-106.

Sumner, M. E. 1992. The electrical double layer and clay dispersion, in Sumner, M. E. & Stewart, B. A. (Eds.), *Soil crusting: Chemical and physical processes*, Lewis, Boca Raton, pp. 1-31.

Sumner, M. E. & Stewart, B. A. (Eds.) 1992. *Soil crusting: Chemical and physical processes*, Lewis, Boca Raton.

Swanson, N. P. 1965. Rotating-boom rainfall simulator, *Transactions of the American Society of Agricultural Engineers*, **8**, pp. 71-73, 75.

Swartzendruber, D. & Olsen, T. C. 1961. Model study of the double ring infiltrometer as affected by depth of wetting and particle size, *Soil Science*, **92**, pp. 219-225.

Tackett, J. L. & Pearson, R. W. 1965. Some characteristics of soil crusts formed by simulated rainfall, *Soil Science*, **99**, pp. 407-413.

Tarchitzky, J., Banin, A., Morin, J., Chen, Y. 1984. Nature, formation and effects of soil crusts formed by water drop impact, *Geoderma*, **33**, pp. 135-155.

Ternan, J. L., Williams, A. G., Elmes, A., Hartley, R. 1996. Aggregate stability of soils in central Spain and the role of land management, *Earth Surface Processes and Landforms*, **21**, pp. 181-193.

Terribile, F. & FitzPatrick, E. A. 1992. The application of multilayer digital image processing techniques to the description of soil thin sections, *Geoderma*, **55**, pp. 159-174.

Terribile, F. & FitzPatrick, E. A. 1995. The application of some image-analysis techniques to recognition of soil micromorphological features, *European Journal of Soil Science*, **46**, pp. 29-45.

Thornthwaite, C. W. & Mather, J. R. 1955. *The water balance*, Publications in Climatology vol. 8 No. 1.

Tippkötter, R. & Ritz, K. 1996. Evaluation of polyester, epoxy and acrylic resins for suitability in preparation of soil thin sections for *in situ* biological studies, *Geoderma*, **69**, pp. 31-57.

Topp, G. C., Davis, J. L., Annan, A. P. 1980. Electromagnetic determination of soil water content: measurements in coaxial transmission lines, *Water Resources Research*, **16**, pp. 574-582.

Tovey, N. K., Krinsley, D. H., Dent, D. L., Corbett, W. M. 1992. Techniques to quantitatively study the microfabric of soils, *Geoderma*, **53**, pp. 217-235.

Towe, K. M. 1974. Quantitative clay petrology: The trees but not the forest, *Clays and Clay Minerals*, **22**, pp. 375-378.

Trout, T. J. 1990. Surface seal influence on surge flow furrow infiltration, *Transactions of the American Society of Agricultural Engineers*, **33**, pp. 1583-1589.

Trout, T. J., Sojka, R. E., Lentz, R. D. 1995. Polyacrylamide effect on furrow erosion and infiltration, *Transactions of the American Society of Agricultural Engineers*, **38**, pp. 761-765.

Truman, C. C., Bradford, J. M., Ferris, J. E. 1990. Antecedent water content and rainfall energy influence on soil aggregate breakdown, *Soil Science Society of America Journal*, **54**, pp. 1385-1392.

Upadhyaya, S. K., Sakai, K., Glancey, J. L. 1995. Instrumentation for in-field measurement of soil crust strength, *Transactions of the American Society of Agricultural Engineers*, **38**, pp. 39-44.

Valentin, C. 1981. *Organisations pelliculaires superficielles de quelques sols de région subdésertique (Agadez, Rép. du Niger). Dynamique de formation et conséquences sur l'économie en eau*, Thèse Doct., Paris VII, Paris.

Valentin, C. 1986. Surface crusting of arid sandy soils, in Callebaut, F., Gabriels, D., DeBoodt, M. (Eds.), *Assessment of Soil Surface Sealing and Crusting*, ISSS / Proceedings of the Symposium at the Flanders Research Centre for Soil Erosion and Soil Conservation, Ghent, Belgium, pp. 40-47

Valentin, C. 1991. Surface crusting in two alluvial soils of northern Niger, *Geoderma*, **48**, pp. 201-222.

Valentin, C. 1994. Surface sealing as affected by various rock fragment covers in west Africa, *Catena*, **23**, pp. 87-97.

Valentin, C. & Bresson, L. M. 1992. Morphology, genesis and classification of surface crusts in loamy and sandy soils, *Geoderma*, **55**, pp. 225-245.

Valentin, C. & Casenave, A. 1992. Infiltration into sealed soils as influenced by gravel cover, *Soil Science Society of America Journal*, **56**, pp. 1667-1673.

Valladas, H. 1992. Thermoluminescence dating of flint, *Quaternary Science Reviews*, **11**, pp. 1-5.

Van Bavel, C. H. M., Underwood, N., Swanson, R. W. 1956. Soil moisture measurement by neutron moderation, *Soil Science*, **88**, pp. 29-41.

van den Boom, G. & Suwwan, O. 1966. *Report on geological and petrological studies of the plateaubasalts in NE Jordan*, Unveröffentlich Bericht der deutschen geologischen Mission in Jordanien, Archiv Bundesanstalt für Bodenforschung, Hannover.

van der Watt, HvH. & Claassens, A. S. 1990. Effect of surface treatments on soil crusting and infiltration, *Soil Technology*, **3**, pp. 241-251.

van Olphen, H. 1977. *An introduction to clay colloid chemistry*, Second edition, Wiley, New York.

van Wesemael, B., Poesen, J. W. A., de Figueirido, T., Govers, G. 1996. Surface roughness evolution of soils containing rock fragments, *Earth Surface Processes and Landforms*, **21**, pp. 399-411.

Velde, B., Moreau, E., Terribile, F. 1996. Pore networks in an Italian vertisol: Quantitative characterisation by two dimensional image analysis, *Geoderma*, **72**, pp. 271-285.

Verhaegen, T. 1984. The influence of soil properties on the erodibility of Belgian loamy soils: a study based on rainfall simulation experiments, *Earth Surface Processes and Landforms*, **9**, pp. 499-507.

Vögel, H. J. 1997. Morphological determination of pore connectivity as a function of pore-size using serial sections, *European Journal of Soil Science*, **48**, pp. 365-377.

Vögel, H. J., Weller, U., Babel, U. 1993. Estimating orientation and width of channels and cracks at soil polished blocks - A stereological approach, *Geoderma*, **56**, pp. 301-316.

Walker, P. H., Hutka, T., Moss, A. J., Kinnell, P. I. A. 1977. Use of a versatile experimental system for soil erosion studies, *Soil Science Society of America Journal*, **41**, pp. 610-612.

Walker, P. J. C. & Trudgill, S. T. 1983. Quantimet image analysis of soil pore geometry: comparison with tracer breakthrough curves, *Earth Surface Processes and Landforms*, **8**, pp. 465-472.

Warburton, J. in press. Rapid assessment of surface water infiltration characteristics in the Northern Badia, Jordan, *Journal of Arid Environments*.

Watung, R. L., Sutherland, R. A., El-Swaify, S. A. 1996. Influence of rainfall energy flux and antecedent soil moisture content on splash transport and aggregate enrichment ratios for a Hawaiian oxisol, *Soil Technology*, **9**, pp. 251-272.

West, L. T., Chiang, S. C., Norton, L. D. 1992. The morphology of surface crusts, in Sumner, M. E. & Stewart, B. A. (Eds.), *Soil crusting: Chemical and physical processes*, Lewis, Boca Raton, pp. 73-92.

West, N. E. 1990. Structure and function of microphytic soil crusts in wildland ecosystems of arid to semi-arid regions, *Advances in Ecological Research*, **20**, pp. 179-223.

Whalley, W. B., Smith, B. J., McAlister, J. J., Edwards, A. J. 1987. Aeolian abrasion of quartz particles and the production of silt-sized fragments: preliminary results, in

Frostick, L. & Reid, I. (Eds.), *Desert Sediments: Ancient and Modern*, Geological Society Special Publication No. 35, Oxford, pp. 129-138.

Whittig, L. D. & Allardice, W. R. 1986. X-ray diffraction techniques, in Klute, A. (Ed.), *Method of soil analysis, Part 1. Physical and mineralogical methods*, American Society of Agronomy - Agronomy 9, Madison, pp. 331-362.

Wigley, T. M. L. & Farmer, G. 1982. Climate of the Eastern Mediterranean and Near East, in Bintliff, J. L. & Van Zeist, W. (Eds.), *Palaeoclimates, palaeoenvironments and human communities in the eastern Mediterranean region in later prehistory*, B.A.R. International Series 133, Oxford, pp. 3-39.

Wilcox, B. P., Wood, M. K., Tromble, J. M. 1988. Factors influencing infiltrability of semiarid mountain slopes, *Journal of Range Management*, **41**, pp. 197-206.

Williams, J. D., Dobrowolski, J. P., West, N. E. 1995a. Microphytic crust influence on interrill erosion and infiltration capacity, *Transactions of the American Society of Agricultural Engineers*, **38**, pp. 139-146.

Williams, J. D., Dobrowolski, J. P., West, N. E., Gillette, D. A. 1995b. Microphytic crust influence on wind erosion, *Transactions of the American Society of Agricultural Engineers*, **38**, pp. 131-137.

Wu, K. 1998. Measurement of soil moisture change in spatially heterogeneous weathered soils using a capacitance probe, *Hydrological Processes*, **12**, pp. 135-146.

Yair, A. 1990. Runoff generation in a sandy area - The Nizzana Sands, Western Negev, Israel, *Earth Surface Processes and Landforms*, **15**, pp. 597-609.

Yair, A. & De Ploey, J. 1979. Field observations and laboratory experiments concerning the creep process of rock blocks in an arid environment, *Catena*, **6**, pp. 245-258.

Yair, A. & Lavee, H. 1976. Runoff generative processes and runoff yield from arid talus mantled slopes, *Earth Surface Processes*, **1**, pp. 235-247.

Yair, A., Lavee, H., Bryan, R. B., Adar, E. 1980. Runoff and erosion processes and rates in the Zin valley badlands, northern Negev, Isreal, *Earth Surface Processes*, **5**, pp. 205-225.

Yaalon, D. H. & Ganor, E. 1973. The influence of dust on soils during the Quaternary. *Soil Science*, **116**, pp. 146-155.

Yaalon, D. H. 1997. Soils in the Mediterranean region: what makes them different?, *Catena*, **28**, pp. 157-169.

Yoder, R. E. 1936. A direct method of aggregate analysis of soils and a study of the physical nature of erosion losses, *Journal of the American Society of Agronomy*, **28**, pp. 337-351.

Young, R. A. 1984. A method of measuring aggregate stability under waterdrop impact, *Transactions of the American Society of Agricultural Engineers*, **27**, pp. 1351-1353.

Young, R. A. & Wiersma, J. L. 1973. The role of rainfall impact in soil detachment and transport, *Water Resources Research*, **9**, pp. 1629-1636.

Youngs, E. G. 1987. Estimating hydraulic conductivity values from ring infiltrometer measurements, *Journal of Soil Science*, **38**, pp. 623-632.

Youngs, E. G. 1991. Infiltration measurements - a review, *Hydrological Processes*, **5**, pp. 309-320.

Zar, J. H. 1984. *Biostatistical analysis*, Second Edition, Prentice-Hall, Englewood Cliffs.

Zhang, X. C. & Miller, W. P. 1996a. Physical and chemical crusting processes affecting runoff and erosion in furrows, *Soil Science Society of America Journal*, **60**, pp. 860-865.

Zhang, X. C. & Miller, W. P. 1996b. Polyacrylamide effect on infiltration and erosion in furrows, *Soil Science Society of America Journal*, **60**, pp. 866-872.

Zobeck, T. M. & Onstad, C. A. 1987. Tillage and rainfall on random roughness - A review, *Soil and Tillage Research*, **9**, pp. 1-20.

Zobeck, T. M. & Popham, T. W. 1992. Influence of microrelief, aggregate size and precipitation on soil crust properties, *Transactions of the American Society of Agricultural Engineers*, **35**, pp. 487-492.

APPENDIX 1: **Technical information concerning the working of the Surface Capacitance Insertion Probe (SCIP)**

The use of electromagnetic waves in determining soil moisture

It is well known and documented that electromagnetic systems with frequencies between 10^8 and 2×10^{10} Hz can be used in many applications in the earth sciences (Hoekstra & Delaney, 1974; Campbell, 1990; Roth *et al.*, 1992; Dirksen & Dasberg, 1993; Selker *et al.*, 1993). The dispersion and velocity of propagation of electromagnetic pulses through a medium such as soil can be derived from the dielectric constants (Smith-Rose, 1933; Hoekstra & Delaney, 1974). Time-Domain Reflectometry (TDR) and the Capacitance Probe rely on the known dielectrical properties of a soil at a certain frequency in order to calculate the percentage moisture present in the soil.

The SCIP works by setting up an oscillatory electric field between two metal electrodes. As the frequency of the electric field increases, it finds an equilibrium frequency where a charge travels between the electrodes. This frequency is inversely proportional to the permittivity, and therefore directly proportional to the dielectric constant, of the material. The real dielectric constant is the electrostatic condition, measuring the ratio of the size of the electric field in a vacuum as opposed to that in a substance. In a vacuum, the electric field cannot decay from a point charge q, but in a given substance, there will be an exponential decay because the ions or electrons in the substance act contrary to the electric field. The ratio of the rate of that decay in any substance compared with its response in a vacuum is called the dielectric constant.

If ε_0 is the dielectric permittivity of free space, equal to 8.85×10^{-12} F/m, the electric field due to a point charge q is

$$E = \frac{q}{4\pi\varepsilon_0 r^2}$$

in a vacuum and

$$E = \frac{q}{4\pi \varepsilon_0 \varepsilon_r r^2}$$

if q is embedded in a substance with dielectric constant ε_r. However, in the case of the SCIP there is not a point source, but instead an oscillatory current is set up which selects the imaginary component of the wave rather than the real part to derive the dielectric constant. The imaginary dielectric constant gives a value to the amount of variance of the electric field as it changes position within the oscillatory current.

The dielectric constant, which is inversely proportional to the dielectrical permittivity, is a function of the frequency f at which the instrument is working and the conductivity σ, which here means the electric conductivity of the soil fabric and soil water. As the frequency approaches zero, the dielectric constant becomes increasingly dominated by the conductivity effect. In other words, when the lower threshold in frequency is reached ionic movement is so slow that the conductivity effect has time to resist the electric field. However, in addition to lower frequencies, the higher the static conductivity, the more resistant are the ions to movement in the electric field; this is measured by the imaginary dielectric constant. Soil and soil water salinity are serious problems as they increase conductivity which in turn increases the measured dielectric constant, and implies that the soil is more moist than it really is.

The electrical conductivity of soil and water, both free and physically and chemically bound, influences the measurement of the absolute level of moisture. The mineralogy of the soil may be significant: for example, certain iron minerals such as magnetite affect the dielectric constant, especially when the soil is saturated (Robinson *et al.*, 1994), which necessitates prior instrument calibration for the soil type. Bound water and bulk density have been studied to investigate their effect on the dielectric properties of soils. Dirksen & Dasberg (1993) found that only soils with bulk densities exceeding 1.35 g cm^{-3} corresponded well with the standard Topp-Davis-Annan calibration equations (Topp *et al.*, 1980). Furthermore such calibration equations did not correlate well with soils with high clay contents because of the quantity of bound water, although bulk density was seen as the greater limitation.

The largest problem, however, is the soil salinity. If there is a small amount of water in the system, conductivity will not exert an effect as the ionic mobility relies upon a minimum water content. With sufficient water in the system to allow a complete pathway from one electrode to the other, i.e. long-range connectivity, a percolating threshold is reached. At this point the loss tangent, the ratio of the imaginary to the real dielectric constant, becomes constant (Campbell, 1990). Below the percolating threshold, the resistivity will be very large, but once the threshold is reached it decreases as a power law (Mualem & Friedman, 1991). So for best sampling conditions, long-range connectivity needs to be established, but must be below the percolating threshold.

In addition to visualising soil as a tripartite system of air, solid and water, Ansoult *et al.* (1984) maintain that soil should also be characterised by its electrical properties. Each of the three original soil components, if separately placed between conducting plates and submitted to a varying electric field, exhibits a specific capacitance signature characterised by the dielectric constant. The dielectric constant of air is 1, that of solid material such as the mineragenic component of soil lies around 4, although Campbell (1990) suggests a range between 2 and 14, while the dielectric constant of water equals 80. The large differences between the mineralogical and water elements indicate that the water component exerts a majority influence upon the soil dielectric properties. In response to an electric field, movement of charge from one environment to another defines a streamline (Ansoult *et al.*, 1984). In an oscillating electric field, the dielectric effect of a porous medium results from an averaging of the dielectric effects of each of the streamlines.

Obtaining the dielectric constant from field measurements of frequency

Consideration of the above limitations of soil moisture measurement using methods of capacitance, suggests that it is important to transform the frequency readings from the SCIP to a useful measure of moisture, in this case, dielectric constant (DC). First, the readings from the SCIP are converted to a frequency in MHz by

multiplying each reading by 8000. A ratio F calibrates the SCIP readings in air and deionised water. Two ratios were calculated; one for each of the probe lengths:

$$F_5 = \frac{F(air)_5}{F(water)_5} \qquad \text{and} \qquad F_{10} = \frac{F(air)_{10}}{F(water)_{10}}.$$

These ratios are combined with the constants C_1 and C_3 and the permittivity of water ε_w. The permittivity of water changes slightly with its temperature, decreasing by 0.38 per °C increase. At 15 °C ε_w = 82.2 (Dean, 1994) but as the average temperature in Jordan is closer to 20 °C a value of 80.2 is more appropriate. C_1 is a function of the spacing of the two electrodes on the probe and C_3 represents the internal capacitance of the circuit board within the SCIP itself. From C_1 and C_3, it is possible to calculate C_2, the stray parallel capacitance caused by the connections between the circuit-board and the electrodes. Once the capacitance of the SCIP is defined, an expression for L, the inductance, which is made up from a constant inductance of 0.24 microhenrys from the circuit-board and a stray inductance, can be determined. Finally, ${}_g\varepsilon_0$, which is a constant related to the probe circuitry for the 5 cm and 10 cm rods, is included to convert the frequency readings (in MHz) to permittivity readings using

$$\varepsilon(f) = \frac{\left[\left[\frac{1}{\left[\frac{f^2}{\left[\frac{1}{(2\pi)^2 \cdot L}\right]}\right] - \left(\frac{1}{15 \cdot 10^{12}}\right)}\right]\right] - (C_2)}{{}_g\varepsilon_o \cdot 10^{-12}}.$$

The final result is the imaginary dielectic constant or permittivity $\varepsilon(f)$ for the frequencies read in the field. They do not have units because permittivity is a ratio between the capacitance of the soil and that of a vacuum.

APPENDIX 2: STATISTICAL METHODS FOR DETERMINING SIGNIFICANT RELATIONSHIPS BETWEEN SOIL MOISTURE MEASUREMENTS

In order to consider two datasets in a parametric way, whether using a simple *t*-test or more complicated statistical analysis such as Anova, it is important to know whether the variances between the two are similar, although such preliminary testing is deemed superfluous by some (Moser & Stevens, 1992). The *F*-test or ratio of variance test indicates whether it is advisable to continue with the other statistical relationships; it takes two sample sets and asks if the variances of the two populations are equal (Zar, 1984; Fowler & Cohen, 1992) using

$$F = \frac{\sigma_1^2(\text{greater variance})}{\sigma_2^2(\text{lesser variance})}. \qquad (6.5)$$

Each sample set will have a critical value for a certain probability dependent on the degrees of freedom. If *F* is significant, it will be higher than the critical value and the null hypothesis is rejected as the populations have different variances. However, it is generally more important to try and prove that the variances are similar because then it is relevant to proceed to the *t*-test to see if the difference in the means is significant.

If the soil characteristics are similar on both sides of the furrow, then it is expected that moisture varies randomly depending on the natural variability of the soil and therefore a *t*-test would not prove to be significant. However, if a particular characteristic of the soil consistently influenced one side of the furrow differently from the other, it is anticipated that the *t*-test would give a significant result.

For much of the moisture data, an analysis of paired measurements is necessary. The data tend to fall into two types: either data are collected at a single point in space with readings taking place over time, or the temporal component is constant with comparison being made over space. This is particularly the case when comparing within-furrow changes in moisture. There are statistical problems in using the *t*-test alone to look at such pairs of data because of inherent assumptions within the *t*-test.

The *t*-test works best on data which are normally distributed with no covariates and are therefore sensitive to departures from the normal distribution such as skewness and the existence of outliers, but this is tested using the *F*-test. More importantly each pair should also be independent. It is better still to accompany the *t*-test with a graphical display to give weight to the analysis (McNeil, 1992).

The sum-difference plot, which is calculated by taking the sum and difference of each pair, may be used in conjunction with a $y = x$ line to observe which data point is consistently higher than the other. However, the graph may be difficult to interpret, especially in terms of the magnitude of difference between the two sets of data points. The tilted line segments can give a very good visualisation of differences. It is important to set up identical limits for each vertical axis to allow accurate comparison; however, the display can cause illusions as it is difficult to tell if near horizontal lines are descending or rising and it is still problematic to obtain an idea of magnitude. The best way to display the data is to draw the pairs of data using parallel line segments with one symbol at one end showing one data point and a different symbol at the other end signifying its pair. By retaining position along a common scale for all responses and using length rather than slope to depict response increases, this graph provides a more effective display than the equivalent graph based on parallel co-ordinates (McNeil, 1992).

APPENDIX 3: **Particle Features associated with GLOBAL LAB IMAGE**

Area: The area of the particle, excluding holes.

Average radius: The average radius from the centre of area (Centroid X, Centroid Y) to the perimeter.

Axis Ratio: A value between 0.0 and 1.0 computed by - Minor Axis / Major Axis.

Angle: The angle in degrees of the Major Axis of the particle with respect to vertical.

Box Area: The area of the bounding box oriented along the X and Y axes. This is equal to - X Difference * Y Difference.

Box Ratio: A value between 0.0 and 1.0, computed by - Area / Box Area.

Centroid X: The X centre of area for the particle, excluding hole area.

Centroid Y: The Y centre of area for the particle, excluding hole area.

CG Distance: The distance from the co-ordinate origin (0,0) to the centre of area (Centroid X, Centroid Y).

Colour: Background colour (-1) or first level particle colour (0). First level holes are background colour, second level holes are particle colour, etc.

Grey Average: The average greyscale value of all pixels within an object.

Grey Total: The sum of intensity (sum of the greyscale values of all pixels within an object).

Hole Area: The area in all holes within a particle. This includes the area of holes within holes.

Hole Ratio: A value between 0 and 1 computed by - Hole Area /(Area + Hole Area).

No. of holes: The number of (first level) holes in the particle.

Length: The length of the bounding rectangular box, oriented along the major and minor axes.

Length difference: A measure of symmetry along the major axis, computed as the displacement along the major axis of the centre of the bounding box from the centre of area. A value of 0 means that it is symmetric about the major axis. The sign of this value distinguishes left-handed and right-handed particles.

Length ratio: A value computed by - Width / Length.

Major Axis: The length of the major axis of an equivalent ellipse (an ellipse with the same second moments of area as the particle).

Minor Axis: The length of the minor axis of an equivalent ellipse.

Maximum radius: The maximum radius from the centre of area (Centroid X, Centroid Y) to the perimeter.

Maximum X: The maximum (rightmost) X co-ordinate in the particle.

Maximum Y: The maximum (bottommost) Y co-ordinate in the particle.

MaxMinRad: A value in the range -180 degrees to +180 degrees, computed by Angle at RMax - Angle at RMin.

Min X: The minimum (leftmost) X co-ordinate in the particle.

Min Y: The minimum (topmost) Y co-ordinate in the particle.

Minimum radius: The minimum radius from the centre of area to the perimeter.

Parent ID: If the particle is a hole, this value is the particle number assigned to the parent particle. If the particle is a first level particle (its parent is the background), this value is -1.

Perimeter: The length around the outside edge of the particle. This calculation is somewhat inaccurate because of the error introduced by the staircase effect, due to pixel quantization. A correction term is subtracted from the perimeter count to average out the error. The correction term assumes that half of the pixels are connected by their sides, and half are connected by their corners.

Pixel area: The number of pixels in the particle, excluding pixels that are part of holes. This value is not calibrated.

PPDA: A value computed by - Perimeter^2 / Total area.

Radius ratio: A value computed by - RMin Angle / RMax Angle.

Roundness: A value between 0.0 and 1.0 indicating how closely the shape of the particle resembles a circle. This is computed by - 4 π * Area / Perimeter^2.

RMax Angle: The angle in degrees (with respect to horizontal) of the maximum radius from the centre of area to the perimeter. The angle is computed in the range of -90 to +90 degrees in a clockwise direction.

RMin Angle: The angle in degrees (with respect to horizontal) of the minimum radius from the centre of area to the perimeter. The angle is computed in the range of -90 to +90 degrees in a clockwise direction.

Sum of X: First moment of area in X. This is the sum of the X-co-ordinates of all pixels in the particle.

Sum of XX: Second moment of area in X. This is the sum of the squared X-co-ordinates of all pixels in the particle.

Sum of XY: Second moment of area in X and Y. This is the sum of the XY product (the X-co-ordinate times the Y-co-ordinate) of all pixels in the particle.

Sum of Y: First moment of area in Y. This is the sum of the Y-co-ordinates of all pixels in the particle.

Sum of YY: Second moment of area in Y. This is the sum of the squared Y-co-ordinates of all pixels in the particle.

Total area: Total area of the particle, including holes.

Tot pix area: Total number of pixels in the particle, including pixels that are part of holes. This value is not calibrated.

Width: The width of the bounding rectangular box oriented along the major and minor axes.

Width difference: A measure of symmetry along the minor axis, computed as the displacement along the minor axis of the centre of the bounding box from the centre of area. A value of 0 means that it is symmetric about the minor axis. The sign of this value can distinguish left-handed and right-handed particles.

X at Max Y: The X pixel co-ordinate corresponding to the value of Max Y. If there are more than one, the rightmost is used.

X at Min Y: The X pixel co-ordinate corresponding to the value of Min Y. If there are more than one, the leftmost is used.

X Difference: The extent of the particle along the X axis.

X Perimeter: The X component of the perimeter, measured along the X axis.

Y at Max X: The Y pixel co-ordinate corresponding to the value of Max X. If there are more than one, the bottommost is used.

Y at Min X: The Y pixel co-ordinate corresponding to the value of Min X. If there are more than one, the topmost is used.

Y Difference: The extent of the particle along the Y axis.

Y Perimeter: The Y component of the perimeter, measured along the Y axis.